TN
269
G4

GEOPHYSICAL PROSPECTING

Official Journal of the
European Association of Exploration Geophysicists

VOLUME 4

1956

SWETS & ZEITLINGER N.V.
AMSTERDAM - 1967

Reprinted by permission of the
Europian Association of Exploration Geophysicists

MARCH

Number 1

Page
G. S. Waters and G. Phillips:
A New Method of Measuring the Earth's Magnetic Field . . . 1
W. B. Agocs and K. Isaacs:
Tunis to Lisbon Airborne Magnetometer Profile 10
V. Fritsch:
Geoelektrische Baugrunduntersuchungen in Jugoslawien und Oesterreich 24
N. A. Anstey:
Instrumental Distortion and the Seismic Record 37
A. H. Kleyn:
On Seismic Wave Propagation in Anisotropic Media with Applications in the Betun Area, South Sumatra 56
K. Helbig:
Die Ausbreitung elastischer Wellen in anisotropen Medien 70
E.A.E.G. Abstract Service 82

JUNE

Number 2

Page
G. Brinckmeier:
Team Work in Seismic Prospecting 105
S. M. Wyrobek:
Application of Delay and Intercept Times in the Interpretation of Multilayer Refraction Time Distance Curves 112
L. H. Tarrant:
A Rapid Method of Determining the Form of a Seismic Refractor from Line Profile Results 131
W. Domzalski:
Some Problems of Shallow Refraction Investigations 140
H. Richard and M. Pieuchot:
Seismic Efficiency of Explosives 167
T. F. Gaskell:
The Relation between Size of Charge and Amplitude of Refracted Wave 185
F. Šumi:
Geoelectric Exploration of Inclined Thin Beds and Ore Veins . . . 194
Book Review 205
E.A.E.G. Abstract Service 206

SEPTEMBER Number 3

Page

S. K. Runcorn:
Applications of the Remanent Magnetization of Rocks 221

A. Lundbak:
Combined Analysis of Gravimetric and Magnetic Anomalies and some Palaeomagnetic Results 226

C. Monnet:
The Use of Integrators Helps Computing Terrain Corrections in Gravimetry 236

D. S. Parasnis:
The Electrical Resistivity of some Sulphide and Oxide Minerals and their Ores 249

A. J. Hermont:
Design Principles for Seismic Reflection Amplifiers. 279

Th. Krey and K. Helbig:
A Theorem Concerning Anisotropy of Stratified Media and its Significance for Reflection Seismics 294

A. Korschunow:
On the Reliability of Harmonic Analysis of Seismograms . . . 303

Abstracts of Papers Presented at the Tenth Meeting of the European Association of Exploration Geophysicists, held in Hamburg, 16-18 May 1956 310

E.A.E.G. Abstract Service 315

DECEMBER Number 4

Page

R. W. Olson:
The Technical-Economic Aspects of Automatic Data Reduction . 335

S. H. Hall:
Scale Model Seismic Experiments. 348

A. Celmiņš:
Theoretische Fragen über Bündelung von Geophonen bei Untertage-Messungen 365

R. Bortfeld:
Multiple Reflexionen in Nordwestdeutschland 394

F. Haalck:
A Torsion-Magnetometer for Measuring the Vertical Component of the Earth's Magnetic Field 424

Book Review 442

E.A.E.G. Abstract Service 443

INDEX BY AUTHOR

	No.	Page
Agocs, W. B. Tunis to Lisbon Airborne Magnetometer Profile	1	10
Anstey, N. A. Instrumental Distortion and the Seismic Record	1	37
Bortfeld, R. Multiple Reflexionen in Nordwestdeutschland	4	394
Celmiņš, A. Theoretische Fragen über Bündelung von Geophonen bei Untertage-Messungen	4	365
Brinckmeier, G. Team Work in Seismic Prospecting	2	105
Domzalski, W. Some Problems of Shallow Refraction Investigations	2	140
Fritsch, V. Geoelektrische Baugrunduntersuchungen in Jugoslawien und Oesterreich	1	24
Gaskell, T. F. The Relation between Size of Charge and Amplitude of Refracted Wave	2	185
Haalck, F. A Torsion-Magnetometer for Measuring the Vertical Component of the Earth's Magnetic Field	4	424
Hall, S. H. Scale Model Seismic Experiments	4	348
Helbig, K. Die Ausbreitung elastischer Wellen in anisotropen Medien	1	70
——. A Theorem Concerning Anisotropy of Stratified Media and its Significance for Reflection Seismics	3	294
Hermont, A. J. Design Principles for Seismic Reflection Amplifiers	3	279
Isaacs, K. Tunis to Lisbon Airborne Magnetometer Profile	1	10
Kleyn, A. H. On Seismic Wave Propagation in Anisotropic Media with Applications in the Betun Area, South Sumatra	1	56
Korschunow, A. On the Reliability of Harmonic Analysis of Seismograms	3	303
Krey, Th. A Theorem Concerning Anisotropy of Stratified Media and its Significance for Reflection Seismics	3	294
Lundbak, A. Combined Analysis of Gravimetric and Magnetic Anomalies and some Palaeomagnetic Results	3	226
Monnet, C. The Use of Integrators Helps Computing Terrain Corrections in Gravimetry	3	236
Olson, R. W. The Technical-Economic Aspects of Automatic Data Reduction	4	335
Parasnis, D. S. The Electrical Resistivity of some Sulphide and Oxide Minerals of their Ores	3	249
Phillips, G. A new Method of Measuring the Earth's Magnetic Field	1	1
Pieuchot, M. Seismic Efficiency of Explosives	2	167
Richard, H. Seismic Efficiency of Explosives	2	167
Runcorn, S. K. Applications of the Remanent Magnetization of Rocks	3	221
Šumi, F. Geoelectric Exploration of Inclined Thin Beds and Ore Veins	2	194
Tarrant, L. H. A Rapid Method of Determining the Form of a Seismic Refractor from Line Profile Results	2	131
Waters, G. S. A New Method of Measuring the Earth's Magnetic Field	1	1
Wyrobek, S. M. Application of Delay and Intercept Times in the Interpretation of Multilayer Refraction Time Distance Curves	2	112

A NEW METHOD OF MEASURING THE EARTH'S MAGNETIC FIELD *

BY

G. S. WATERS ** AND G. PHILLIPS **

ABSTRACT

This paper describes the measurement of the Earth's total magnetic field by a determination of the frequency of free precession around this field of the protons in a sample of water. The angular frequency of precession, ω, is related to the field F by the relationship $\omega = \gamma_p F$ where γ_p is the gyromagnetic ratio of the proton.

A bottle of water is magnetised in a direction approximately at right angles to the earth's field, by passing a current through a coil wound around the bottle. The current is switched off rapidly, leaving the magnetic moment vector to precess around the earth's field direction, inducing in the coil a small alternating voltage. This voltage is amplified and its frequency measured by means of a counter. The accuracy of measurement of the total field is estimated at $\pm$ 0.5γ.

In addition to the total field value, the form of the signal voltage contains information on the field gradient across the sample.

Simple theory, experimental details and results are given.

INTRODUCTION

The method of measurement of the earth's total magnetic field by measuring the frequency of free precession in this field of protons in a sample of water was first reported by Packard and Varian (1954). We report here brief details of our investigations at Christchurch which were carried out independently.

In the earth's magnetic field the protons in a sample of water align themselves in directions approximately parallel and anti-parallel to the field. An excess number $n = \exp 2\mu F/kT$ will point along the parallel direction (the lower energy state). Here μ is the magnetic dipole moment of the proton, F the value of the earth's total field, k Boltzmann's constant and T the absolute temperature. Thus along the earth's field direction exists a small magnetic vector produced by the sum of the excess components in this direction.

If now a magnetic field H_{100} greater than the earth's total field is applied in a direction approximately at right angles to the earth's field a macroscopic magnetic moment will be produced in the direction of the resultant of this applied field and the total earth's field. If the applied field is of the order of 100 gauss, then the resultant direction will be approximately that of the 100 gauss field. The magnitude of the magnetic vector in this resultant direction will approach its maximum value exponentially with time constant T_1—the spin-lattice relaxation time—, the order producing magnetic force gradually overcoming the thermal movement disordering forces. For water the value of T_1 is approximately 3 secs. so that in 10 seconds or so after application of the 100 gauss field a magnetic vector proportional in magnitude to the value of the applied field is created, pointing in a direction at right angles to the earth's total field.

---

* Presented at the Ninth Meeting of the European Association of Exploration Geophysicists, held in London, 7-9 December 1955.

** Signal Research and Development Establishment, Christchurch, England.

If the applied magnetic field is now removed in a time τ such that $\tau < 1/\gamma_p F$ where γ_p is the gyro-magnetic ratio for the proton, the magnetic vector will not follow the decreasing resultant magnetic field, so that at time τ after commencing the removal of H_{100} the magnetic vector finds itself still at right angles to the remaining field, (the earth's field). This vector will now relax to its original value and direction in the earth's field by precessing around that field at an angular velocity $\omega = \gamma_p F$, the so-called Larmor precession frequency. This precessing magnetic vector will induce an e.m.f. in a coil wound round the water sample, and the frequency of this e.m.f. provides a measure of F. At the moment of removal of H_{100} the individual protons whose component sum produces the vector, start to precess all in phase. However, due to the fact that the magnetic field at each individual proton varies slightly due to asymmetrical magnetic field contributions from neighbours, there will occur a loss of phase as time goes on and a consequent diminution of induced e.m.f. This diminution takes place exponentially with a time constant T_2—the so-called spin-phase memory time. For water this is approximately 3 seconds, so that with an initial induced voltage signal to noise ratio of 100/1 the signal is detectable for some 12 seconds.

If the magnetic field at each proton varies by an amount more than the intrinsic value, due to the presence of a gradient in the external magnetic field, then T_2 is reduced. If the gradient is of the order of 50 γ per cm. the signal decay will be so rapid that observation would be difficult.

Also if the 100 gauss field is removed in a time τ_1 so that $\tau_1 > 1/\gamma_p F$ the magnetic vector will follow the decreasing resultant field so that after τ_1 the direction of the vector will be along the direction of the earth's field and again there will be no induced e.m.f.

The problem, therefore, is to magnetise a bottle of water—about 500 ccs. is a good quantity, using a 100 gauss field, and then to remove the magnetising field abruptly, and measure the frequency (about 2,000 cycles/sec. in England) of the e.m.f. which is induced in a coil wound around the bottle. The method which was used by us and the results obtained are described briefly below.

Apparatus

A block diagram of the apparatus is shown in Fig. 1. Essentially there are two parts to the equipment, the measuring head itself which is a relatively small passive element comprising the water sample and coil system, and the electronics consisting mainly of amplifier, frequency monitor, and if required, visual display system.

The measuring head can take two main forms either double or single coil. In the double coil system, there are separate coils for the D. C. magnetising field and for signal pick up. The D.C. coil is so designed to give a field of approximately 100 gauss over the sample, in a direction roughly perpendicular to the earth's total field direction, and with sufficiently low inductance and self capacity with associated leads to enable the current to be reduced to zero in a very short time, i.e. less than 30 μsecs. The coil in which the signal voltage is induced has a large number of turns, a good *Q* and arranged to fit closely over the water sample with axis approximately perpendicular to both *D.C.* coil axis and earth's field direction. Many variations of coil design are possible to improve the filling factor and hence signal voltage depending on practical requirements. Departure from the condition of perpendicularity does not affect the frequency of precession, but the signal amplitude will be reduced and hence the accuracy of measurement may suffer.

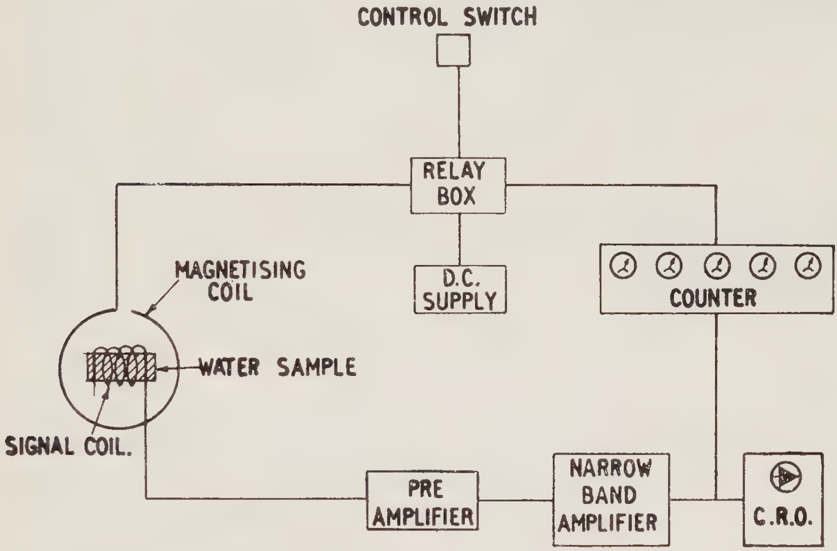

{Fig. 1. Block diagram of double coil arrangement nuclear magnetometer.

With the single coil arrangement, the water sample is at the centre of

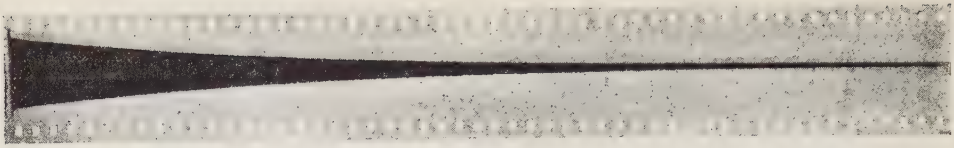

a) Distilled water

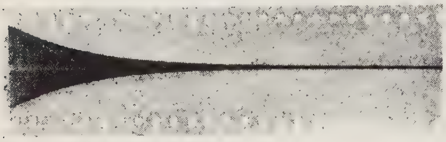

b) $\frac{1}{1000}$ N Fe $(NO_3)_3$

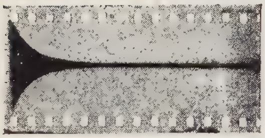

c $\frac{1}{500}$ N Fe $(NO_3)_3$

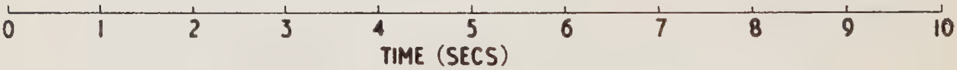

Fig. 2. Typical decay traces on free precession equipment.

a single coil which serves both purposes, initially to magnetise the sample and subsequently receive the signal from the precessing nuclei. A simple relay network is used to effect the change-over at the appropriate time. It is then necessary in design of this single coil to meet all requirements laid down for both coils in the double coil arrangement.

Both the *D.C.* current for polarising and the induced signal voltage can be transmitted over up to 100 ft. of coaxial cable and the remaining equipment can be this distance away from the measuring head if required.

The amplifier is of the straight tuned type, with narrow bandwidth centred about the expected value of $f(=\gamma_p F/2\pi)$. The bandwidth required for faithful reproduction of the decaying signal is only a few cycles, and as the signal to noise voltage ratio is inversely proportional to the square root of the bandwidth, a very narrow band amplifier is desirable. However, for practical purposes the instrument must be capable of measuring changes of field values, and hence precession frequencies, over a reasonable range. This sets a practical lower limit to the bandwidth. For instance, a bandwidth of 50 c/s centred at 2,000 c/s caters for the range of field values from 0.464 gauss to 0.476 gauss.

The output from the amplifier can be fed to the Y plates of a cathode ray oscilloscope and photographed on a film moving across the face of the tube. With a slow moving film, the 2,000 c/s are not resolved, and only the decay envelope is photographed. A typical trace from distilled water is shown in Fig. 2(a).

FREQUENCY MEASUREMENT

To determine the value of the earth's magnetic field to $\pm \frac{1}{2}\gamma$, a measurement of f to 1 part in 100,000 is necessary, and as the precession frequency is approximately 2,000 c/s, the accuracy of frequency measurement must be $\pm$ 0.02 c/s. As the signal at best only remains above noise level for a few

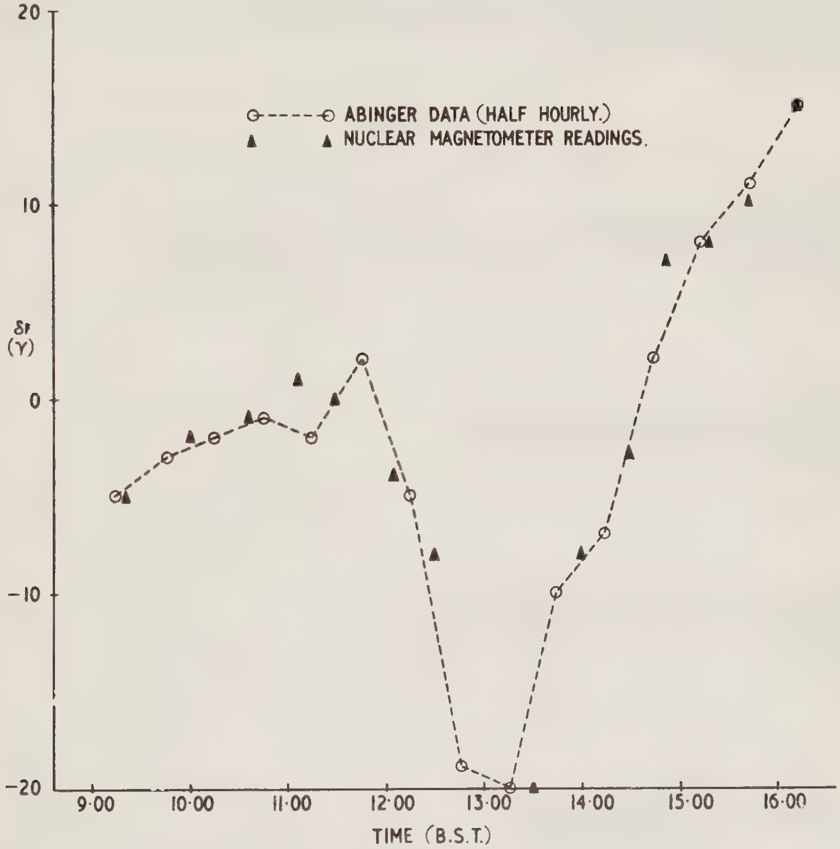

Fig. 3. Diurnal variation in earth's total magnetic field, Aug. 5th, 1955.

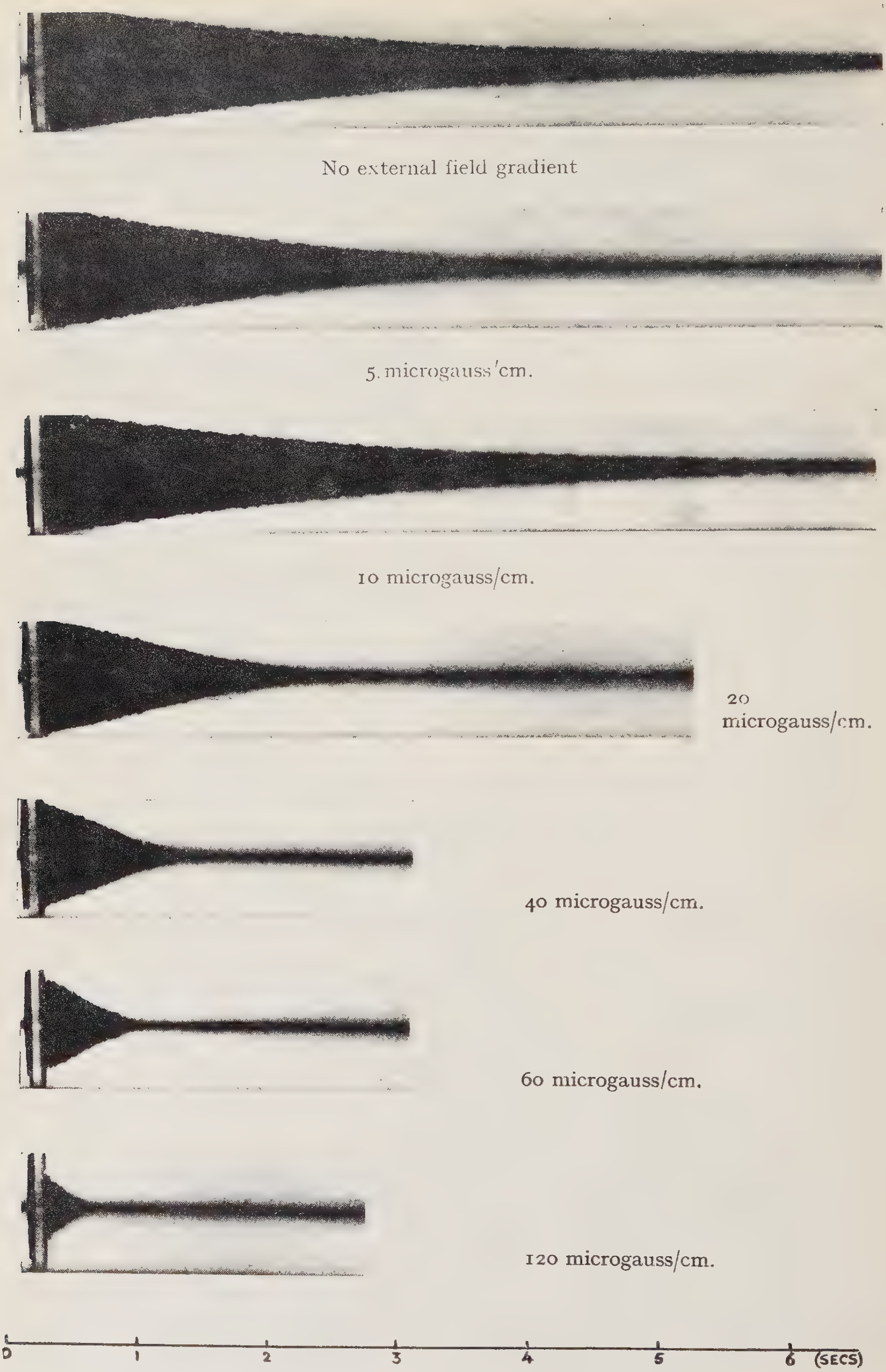

No external field gradient

5 microgauss/cm.

10 microgauss/cm.

20 microgauss/cm.

40 microgauss/cm.

60 microgauss/cm.

120 microgauss/cm.

Fig. 4. Effect of external gradient on decay time.

seconds the method used for measuring frequency can only sample the information for perhaps two seconds.

Conventional methods of counting the number of cycles during a known time interval could only give an accuracy of ± 1 c/s. To achieve the requisite accuracy, it is necessary to measure accurately the time interval for a specific number of cycles. With a signal to noise voltage ratio of better than 10 : 1, and a 100 kc/s crystal as a reference frequency for the counter, an accuracy of 1 part in 100,000 is obtainable. A beat frequency method will give comparable accuracy, but does not give an instantaneous reading (Waters 1955).

With a fixed measuring head a series of readings of F were taken throughout the day, and the variation plotted together with $\frac{1}{2}$ hourly data from Abinger magnetic station for the same period. This is shown in Fig. 3 and the close fit clearly establishes the claim of the nuclear magnetometer.

Decay Characteristics

As was mentioned earlier, a spread in field values at nuclear sites results in the decay of the signal. If this spread of values is increased, as can be done by introducing paramagnetic ions into the water sample, the decay of signal becomes more rapid, and the more the concentration the more rapid the decay. The effect of the ions in 1/1,000 Normal and 1/500 Normal Ferric Nitrate solution is shown in Figs. 2 (b) and (c). Since the accuracy of frequency measurement depends on the time over which the count can be made, this shortening of decay time (T_2) is undesirable in that accuracy is sacrificed. As we shall see later this might be worthwhile under certain practical conditions.

In the same way, an external field gradient across the sample produces slightly different precession frequencies with consequent loss of phase coherence following the initial switch off. The greater the field gradient the more rapid this loss of phase coherence and the shorter the decay time. In this case the decay time is no longer an intrinsic property of the sample liquid, and the time for the signal to fall to $^1/e$ of its initial value is referred to as T_2^*. When the field gradient reaches higher values, the decay time becomes so short that simple equipment can no longer display the signal or measure the precession frequency.

The variation of decay time with field gradient is shown in Fig. 4. The values given are, of course, dependent on the geometry of the coil system and its orientation with respect to the direction of maximum field gradient. In this particular equipment where frequency was measured by counting cycles for approx. 1 sec. of signal, measurement becomes unreliable when field gradient values exceeded 20 microgauss/cm or 60γ per foot. Over the range of perhaps 5-100 microgauss/cm the rate of decay of the signal can be measured directly, and the instrument then serves as a magnetic gradiometer.

Finally it is necessary to consider the practical consequence of the thermal relaxation time T_1, which controls the growth of magnetisation after application of the polarising field. Fig. 5 shows the state of magnetisation of the distilled water and ferric nitrate samples (as measured by the initial signal amplitude) for increasing times of polarisation. The growth in both cases is seen to approximate closely to an exponential rise with a time constant equal to the value of T_2 found from the decay curves of Fig. 2. This agrees with theory which predicts that for low viscosity liquids, $T_1 = T_2$.

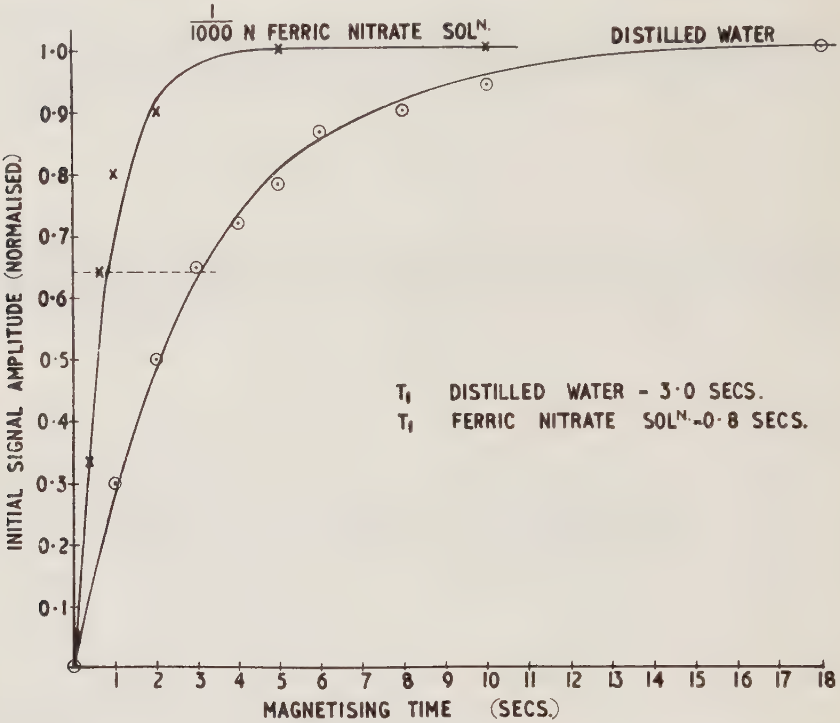

Fig. 5. Growth of magnetisation after application of the polarising field.

This means that where a sample of long T_2 is used to achieve the highest accuracy in frequency, T_1 is also long, and it is essential to leave the polarising field on for several seconds in order to ensure a good signal amplitude. Thus a complete cycle of polarisation, switch off, and frequency measurement, might take 10-15 seconds. With such a period of operation, an accuracy of $\pm \frac{1}{2}\gamma$ is possible.

However, if more frequent readings of the total field are required as might be the case with an airborne system flying at between 100 and 200 m.p.h., the distilled water could be replaced by a very dilute paramagnetic solution. With this, a good signal amplitude might be obtained with perhaps $^3/_4$ sec. of polarisation and frequency measured during the first $^1/_4$ sec. of the rapidly decaying signal.

In doing this, accuracy in frequency is sacrificed and no better than $\pm 2\gamma$ could be expected, but readings might then be taken once a second.

CONCLUSIONS

The free precession of protons in weak magnetic fields can be used to measure the absolute value of the earth's total magnetic field to an accuracy of $\pm \frac{1}{2}\gamma$. No calibration or elaborate setting up of the instrument is required. The method is not continuously recording but it should be possible to take readings as frequently as once per second with a reduced accuracy ($\pm 2\gamma$).

Over a limited range depending on coil design the instrument can be used directly as a gradiometer by measuring the signal decay time.

REFERENCES

PACKARD, M. and Varian, R., (1954) Phys. Rev. 93 941
WATERS, G.S. (1955) Nature 176, 691.

TUNIS TO LISBON AIRBORNE MAGNETOMETER PROFILE

BY

W. B. AGOCS * AND K. ISAACS *

ABSTRACT

The results of an 805-mile (1300 km) airborne magnetometer profile flown across Tunisia and Algeria, from Tunis to the coast west of Oran, across north-western Spanish Morocco and Tangier, and across south central Portugal to Lisbon are presented. The general geology of the zone over which the profile was flown is shown with the magnetic variations. Depth, structural and rock type interpretations have been made from the magnetic control. The depth values are believed to be high due to angle of the flight line with respect to the probable maximum gradient of the magnetic anomalies. However, depth values are given in all of the basins of possible interest.

INTRODUCTION

The airborne magnetometer profile which is discussed in this paper was obtained on 18 June 1950. The flight path along which the magnetic data were obtained is shown on Figure 1. No data were obtained over water between Oran, Algeria, Tangier, and the south coast of Portugal.

The purpose of this flight was to obtain regional magnetic data in North Africa and Portugal in the course of returning equipment from a project completed in Tunisia to the United States. A total of 665 linear miles (1070 kms) of magnetic data were obtained over North Africa, and 140 miles (225 kms) over southwest Portugal.

The magnetometer used for this survey was a Gulf Research and Development Company Model I. The saturable core detector was mounted in a towed "bird", and the power source, amplifiers, and recorder were mounted in a DC-3.

The flight path over land was controlled by a pre-determined course laid out on World Aeronautical Charts of the area. The actual flight path was monitored by a continuous strip film camera, and by the recording of ground check points observed by the pilot in the course of the flight. The flight altitude was maintained at a barometric level of 4000 feet above sea-level excepting for the passage over the Babor Mountains of Algeria, south of Bougie, where the

---

* Aero Service Corporation, Philadelphia, Pa.

altitude was increased, and in the section over Spanish Morocco and Tangier where the altitude was increased to 5000 feet. A further check was maintained on the terrain clearance by means of a continuously-recording radio altimeter.

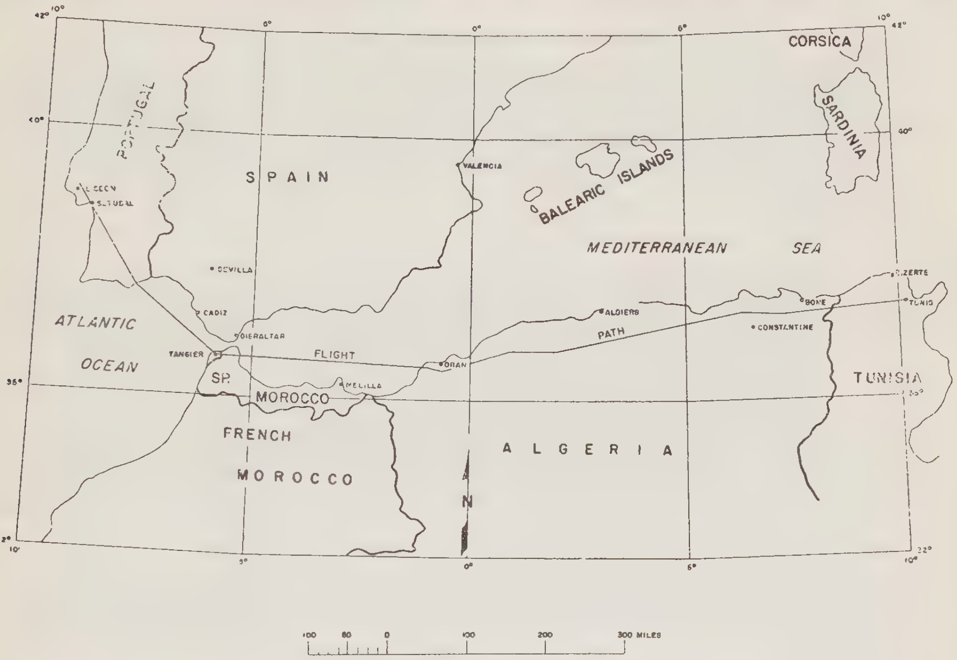

Fig. 1. Index map showing the flight path from Tunis, Tunisia, to Lisbon, Portugal, along which a continuous airborne magnetometer profile was obtained.

The correlation between the magnetic data, the continuously-recording radio altimeter, and the flight path, and their tying to ground positions is shown in Figure 2. The purpose of this illustration is to show the method of tying the data together and to the ground in an airborne type of survey.

GEOLOGY

The geology which is shown in the figures and discussed in the following was obtained from the publications of the XIX International Geologic Congress of 1952. The general references are given at the end of this paper.

Tunisia-Algeria (Figures 6 and 7)

From Tunis westward for about 125 miles, the flight crossed the Tunisian Basin, an irregular structural depression trending about north 45° east. On the east, the boundary of the basin is defined by a tectonic and topographic uplift known as the Jurassic Massif running southwestward from the Gulf of Tunis.

The basin contains sediments ranging from Triassic, or earlier, to Pliocene in age. The interior of the Tunisian basin contains a number of diapir folds. The oldest recognized rocks of the basin (Triassic) are exposed along the axes of these folds.

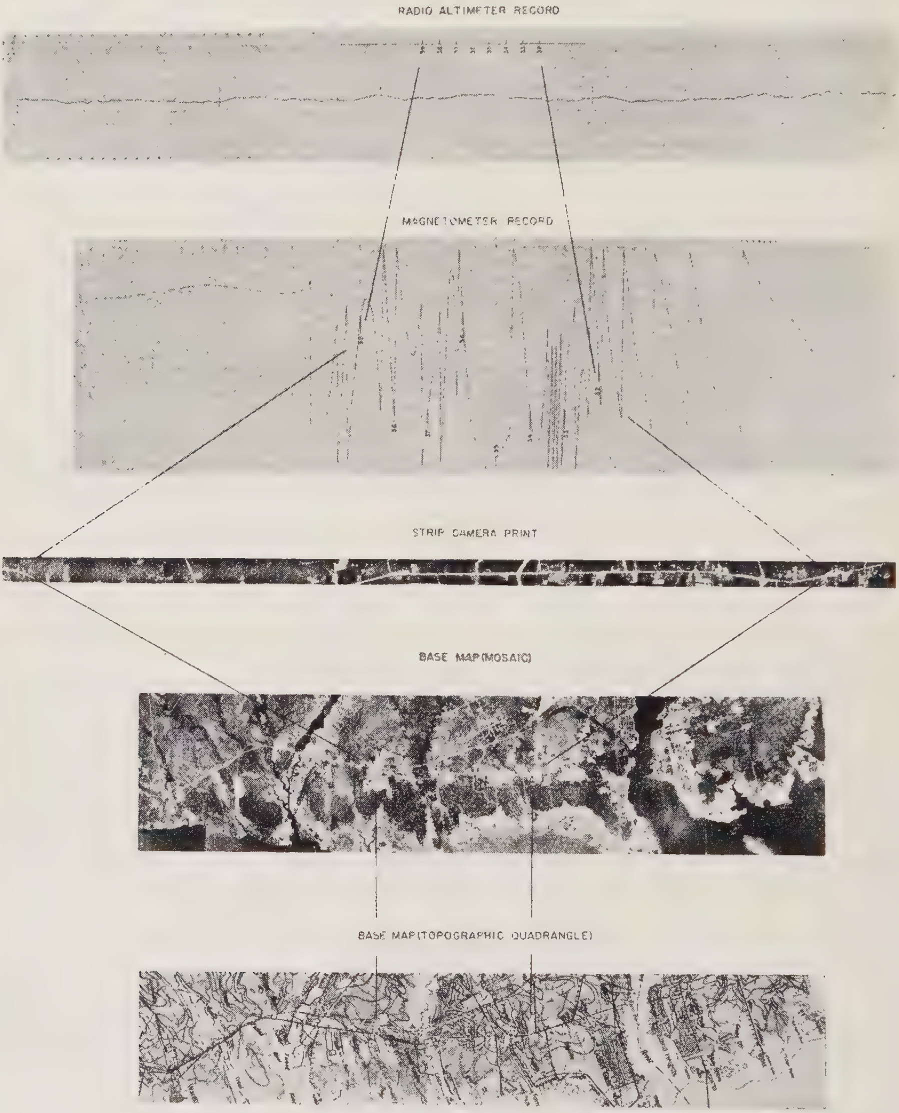

Fig. 2. Correlation of the continuous airborne data, and the tying of these data to ground positions.

A number of mines and mineral deposits of iron, lead, and zinc are present in the Tunisian Basin. Most of these are associated directly or indirectly with igneous bodies. Ore concentrations have occurred as a result of substitution and vein concentration, fissural impregnation, or combinations of these three. The fissural impregnations are unique to Tunisia, since they are associated with the previously-mentioned diapir folds. In this case, the mineralized solutions have intruded along the ruptured zones of the folds, and the ore deposits occur along the Triassic contacts. The substitution and concentration types are conventional ore bodies. Presumably, mineralization in general has occurred largely through secondary hydrothermal action associated with igneous intrusion. Two areas of dacite, an extrusive phase, are exposed in northern Tunisia and iron, lead, and zinc mines are located along the margins. This intrusion and subsequent mineralization appears to be lower Pliocene in age, accompanying the last important period of folding and mountain building in Tunisia.

The northwestern boundary of the Tunisian Basin is against the Petite Kabylie, an area of acid igneous and metamorphic rocks overlain by an irregular sedimentary veneer. This region of metamorphosed crystalline rocks extends from the east shore of the Bay of Bougie to the city of Philippeville. A smaller occurrence of igneous and metamorphic rocks, known as the Massif de l'Edough, is exposed west of Bone. The bulk of the metamorphic rocks are biotite and hornblende gneisses and schists, and the ages of these rocks are at least pre-Cretaceous and probably pre-Cambrian, or Paleozoic. The generally acidic intrusive and extrusive rocks are Tertiary, and they consist largely of granites, diorites, rhyolites, and andesites. The province is bounded on the southwest by a series of faults.

Mineral ore deposits are common in this region, chiefly small vein concentrations occurring in dikes associated with the Tertiary intrusion. The ores themselves are oxides and sulfides of iron and lead. However, at the western end of the Petite Kabylie, where the country rock is sericite and chlorite schist, tin in the form of cassiterite is mined in addition to magnetite. At Ras el Ma, mercury in the form of cinnabar is mined. The country rock here is a series of calcareous sediments.

The flight line south of the Bay of Bougie was along the axis of the Babor Mountains, a region of uplifted Jurassic and Cretaceous sediments.

Beyond the western end of the Babors, the flight crossed over the elbow of the Oued Soumman syncline, and continued along the southern and western part of this structure for twenty miles. The axis of the syncline coincides with the position of the river itself. South of it is the Biban Mountain geanticline, an important feature of the North African tectonic pattern. The Oued Soumman syncline is separated by a series of faults on its northern flank from the Grand Kabylie.

The Grand Kabylie is similar to the Petite Kabylie in structure, rock type and tectonic origin. It is an area of metamorphic rocks that have been subjected to Tertiary acidic intrusion. It occupies the coastal salient between the Bay of Bougie and Algiers.

The flight line was roughly along the axis of the Atlas Mountains. The Atlas complex is a vast uplifted, folded, and faulted structure. The area was a geosyncline during Mesozoic time, receiving at least fifteen thousand feet of sediments. It was subjected to general uplift during the Tertiary.

Beyond the Atlas Mountains the flight path crossed the Chelif Basin at an oblique angle to the axis. The Chelif Basin is at present being prospected for oil. It has a reported maximum of about ten thousand feet of Tertiary sediments with an unknown thickness of older rocks beneath them. The basin includes many subsidiary folds and faults, some of which show promise of being oil traps.

Spanish Morocco-Tangier (Figure 8)

The overall structure of the Moroccan peninsula is simple. Paleozoic metamorphic rocks outcrop along the east coast. These are overlain to the west by a series of Triassic and Jurassic calcareous sediments, which are, in turn, overlain by Jurassic, Cretaceous, Eocene, and Oligocene clastic sediments. Information relative to the thickness and attitude of the sedimentary section is unavailable.

Portugal (Figure 8)

The flight line was across the coastal plain of southern Portugal for a distance of sixty miles from the crossing of the coast. The coastal plain area is about ninety miles wide, and it consists of Devonian, Carboniferous, Jurassic, and Cretaceous sediments dipping southward toward the sea.

The flight line crossed a Tertiary basin about 80 miles northwest of the crossing of the southern coast. Information is not available regarding the nature of the basin rocks. The axis of the basin trends about north 20° east.

East of the Tertiary basin and north of the coastal plain lies an area of pre-Cambrian metamorphic rocks and igneous intrusions. This region was uplifted and intruded during the mid-Devonian chiefly by granitic rocks.

A number of iron mines are located in this region. Some of these are magmatic segregations of magnetite associated with gabbro and diorite, differentiates of the Devonian batholith. Others are metasomatic replacements along intruded zones.

MAGNETICS AND GEOLOGY

The variation in the total magnetic field intensity, the regional total magnetic field gradient, the flight path, and the geology are shown in detail on Figures 6, 7, and 8. The variations in the total magnetic field have not been corrected for the regional variation, hence the regional gradient is shown along the length of the profile.

The regional total magnetic field gradients were obtained by using Table 53 of the Carnegie Institution Publication 578. The regional values were determined at fourteen points along the flight path by linear interpolation between the published latitudes and longitudes for the points of observation. These values were plotted on the profile and connected by straight lines. The level of the regional total magnetic intensity is shown at an arbitrary level on the profiles, since its purpose is to show its relation to the observed magnetic field.

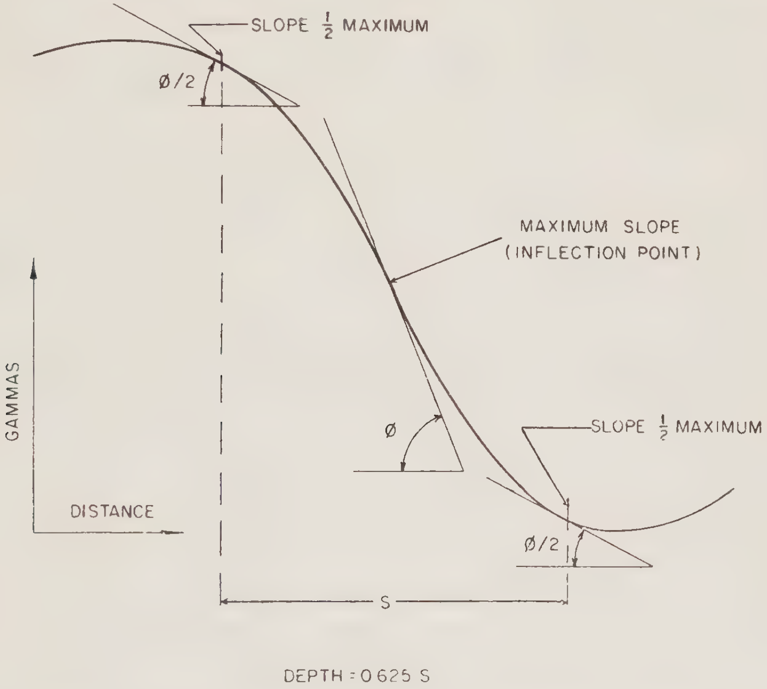

Fig. 3. Illustrative curve showing how depth determination is made from magnetic anomaly curve for elongate anomaly.

Depth determinations were made by the slope method of Peters (1949). Figure 3 shows a general illustrative curve which is used to apply this method of locating the maximum slope, and the half maximum slope tangent points. The depth to the magnetic source is roughly 0.625 times the horizontal distance between the points where the half maximum slope tangent points are located. Figures 4 and 5 show enlarged portions of the observed magnetic profile, and

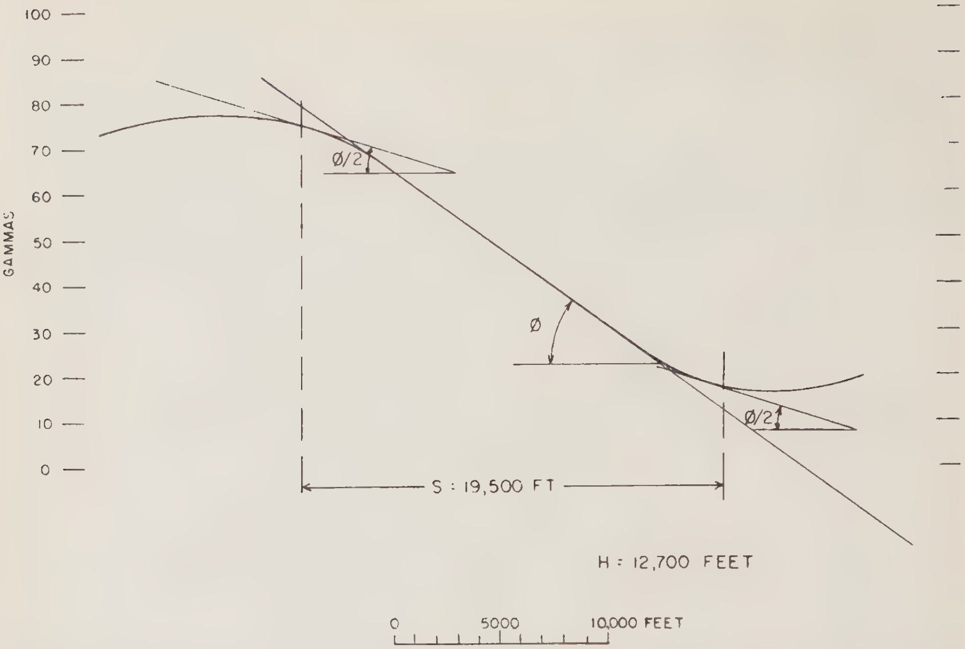

Fig. 4. Enlarged anomaly curve 9 miles west of Reference Mark 534 used for depth determination.

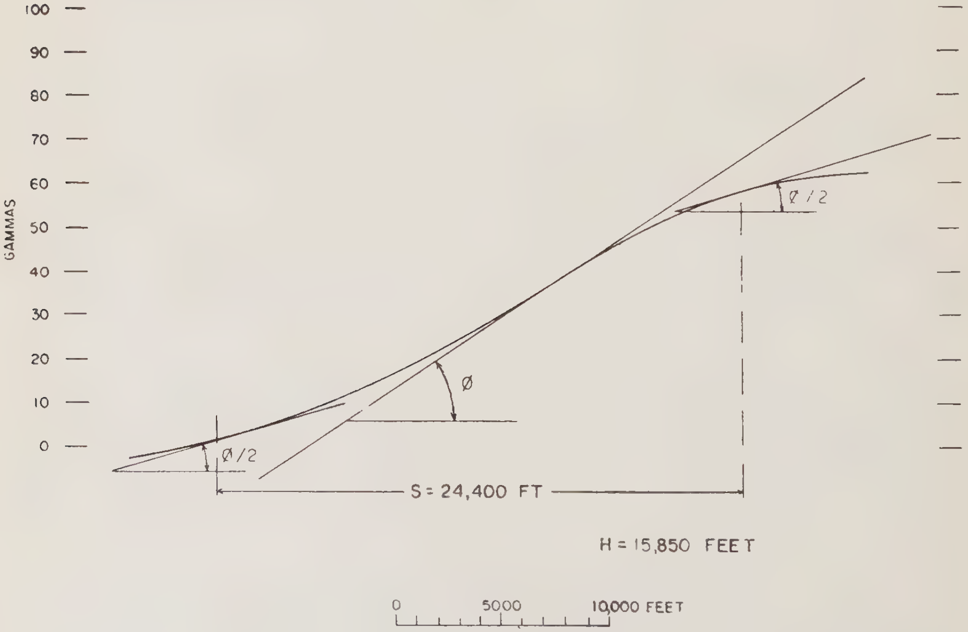

Fig. 5. Enlarged anomaly curve 30 miles east of Reference Mark 868 used for depth determination.

the determination of the horizontal distance between the half maximum slope distance from which the depth determinations were made.

The fulfillment of the following assumptions are necessary for the quantitative depth determinations of the causes of the magnetic anomalies:

1 The anomaly is caused by a susceptibility contrast rather than basement relief.

2. Polarization of the basement rocks is in the same direction as the earth's inducing field.

3. The disturbing magnetic mass has a great horizontal length in comparison to its width, and its sides are vertical and of great vertical extent.

4. The anomaly is unique and not effected by the anomalies due to adjacent masses.

Tunis, Tunisia, to Bougie, Algeria (Fig. 6)

The data shown in Figure 6 extends from Tunis to a point 50 miles (80 kms) southwest of Bougie, Algeria. The length of this section of the profile is 335 miles (540 kms).

From Tunis to reference mark 534, the magnetic data were obtained over the Tunisian Basin. In this area, depth determinations have been made at the following points: the magnetic high located between Tunis and reference mark 443; the magnetic high at reference mark 471; and the magnetic low between reference marks 510 and 534. The depths determined at these points are: 16,900 feet (5470 meters); 39,600 feet (12,100 meters); and 3,200 feet (4000 meters) respectively. If the magnetic trends are parallel to the direction of the basin's axis, and not normal to the direction of the flight line, these depths should be reduced by one-half. This latter consideration is the most probable occurrence. The minor magnetic anomaly located between reference marks 445 and 471 shows a depth range of from 2640 to 4000 feet (800 to 1220 meters) sub-flight. This indicates relatively shallow igneous rocks in this local zone.

From reference mark 534 to reference mark 561, the depth determinations for the magnetic anomalies show a depth range from 12,700 feet to 7,400 feet (3860 to 2250 meters). These depth determinations were made on the assumption that the flight line was normal to the geologic and magnetic trends.

In the interval from reference mark 561 to a point 25 miles (40 kms) west of reference mark 607, numerous small, local magnetic highs have been resolved over the outcrops of the Petite Kabylie. The complex nature of the crystallines, and the variation in structural position shows a considerable range of variation of depths. These depths range in value from 2110 feet (640 meters) sub-flight at the western extremity of the Petite Kabylie, to depths as great as 13,000 feet (3970 meters).

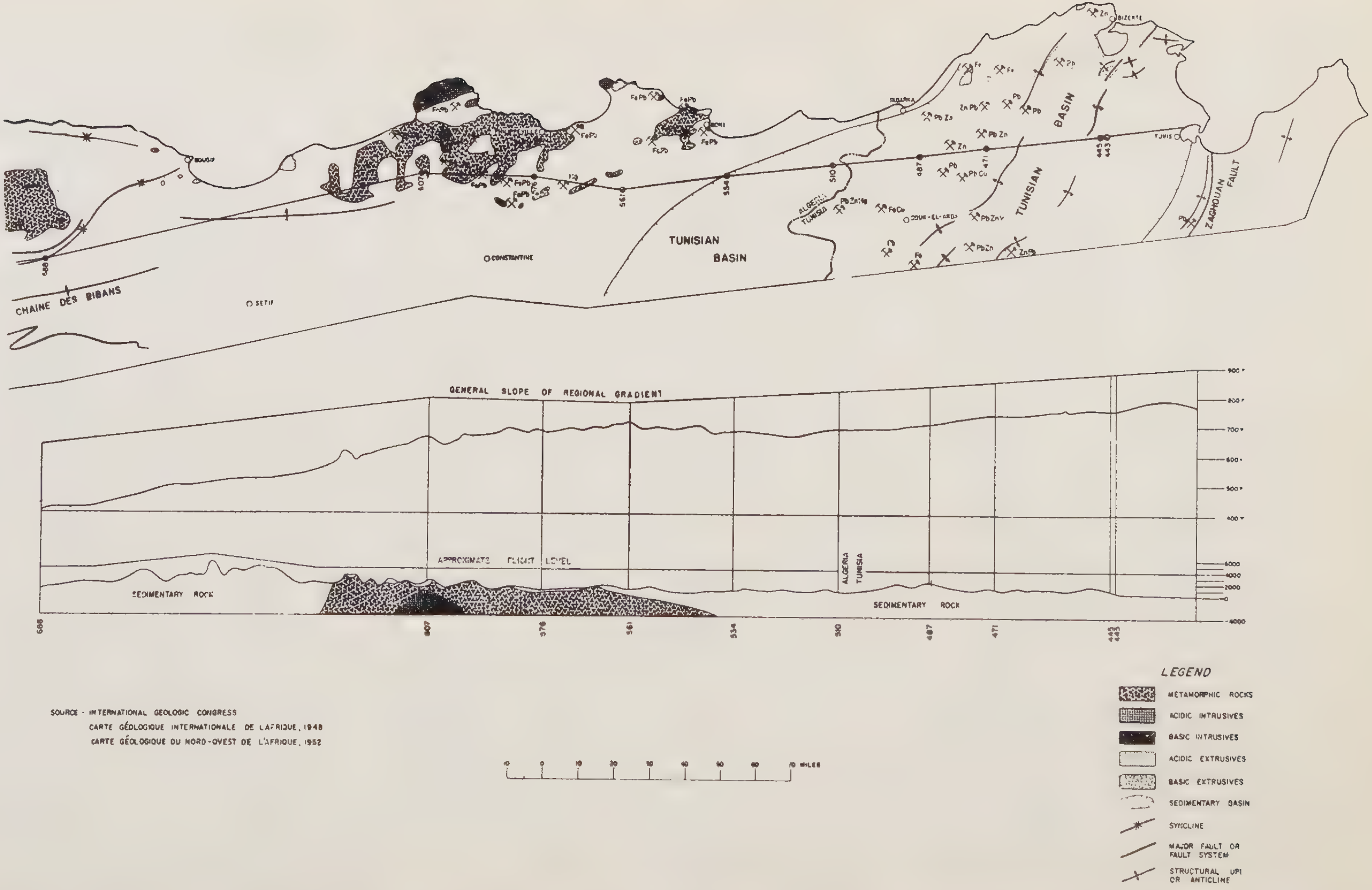

Fig. 6. Airborne magnetometer profile, geologic cross section, flight path, and geology from Tunis, Tunisia, to Bougie, Algeria.

To the west of the Petite Kabylie, west of reference 607, the profile is parallel to the Babor Mountains, and then intersects the axis of the Oued Soumman syncline at reference 688. Over both these features the magnetic control shows gentle, broad anomalies due to the great thickness of sediments and to the fact that the profile is almost parallel to the structural strike. However, between the Babor Mountains and the Oued Soumman syncline there is a 30-gamma "break" in the magnetic intensity level. This may be caused by a facies change in the basement coupled with a fault.

Northwestern Algeria (Figure 7).

The magnetic profile shown in this figure extends from reference mark 688 located 25 miles (40 kms) west of Bougie, across the remainder of Algeria to the exit at the coast 19 miles (30 Kms) west of Oran. Along the length of this section the profile traverses the Atlas Tellien Occidental, and then it crosses the Chelif Basin.

The magnetic profile follows the regional gradient closely from reference mark 688 to reference 891 which is located immediately north of Oran. A major positive magnetic anomaly of 48 gamma is observed about 44 miles (70 kms) east of reference mark 800. This anomaly lies immediately south of the axis of the Atlas Tellien Occidental. Immediately to the west of reference mark 800, over the Massif de l'Ouarsenis, a 40-gamma positive anomaly is located. Finally, between reference marks 891 and 912 a decrease of 63 gamma followed by a 200-gamma increase in the magnetic level is observed.

Depth determinations have been made at the magnetic high anomaly immediately to the west of reference mark 800, and for the high anomaly 44 miles to the east and the depth range is found to vary from 6350 feet to 25,400 feet (1930 to 7750 meters). These depth determinations were made without correction for an obtuse angle of the magnetic trends to the profile, which could reduce these depth values to one-third the values submitted.

The magnetic high zone located between reference marks 822 and 866 yielded depth values along the profile of 10,560 to 15,850 feet (3220 to 4830 meters). These magnetic highs are located in the vicinity of structural highs which may b be caused by basement uplifts. If the depth values are corrected to magnetic trends parallel to the geologic trends, they would be reduced to one-fifth the value presented above. On this latter assumption, a basement high should be located near the surface on the axis of the Chelif Basin which indicates that the basement is shallower than predicted by the geologic studies.

The relatively sharp magnetic discontinuity, and increase in the magnetic gradient between reference marks 891 and 912 indicate a possible fault zone, and a facies change in the basement. This transition zone shows a change to a

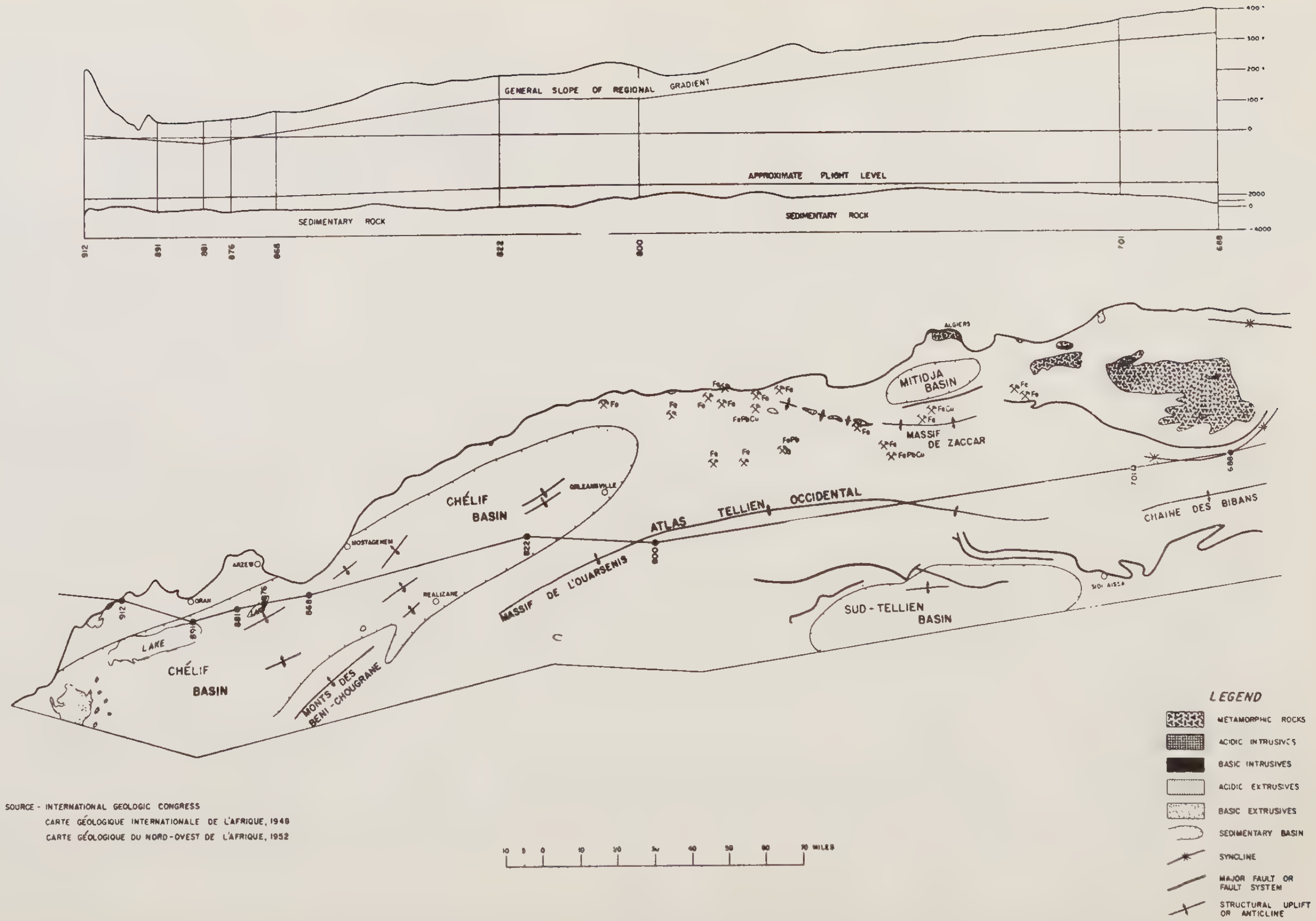

SOURCE - INTERNATIONAL GEOLOGIC CONGRESS
CARTE GÉOLOGIQUE INTERNATIONALE DE L'AFRIQUE, 1948
CARTE GÉOLOGIQUE DU NORD-OUEST DE L'AFRIQUE, 1952

Fig. 7. Airborne magnetometer profile, geologic cross section, flight path, and geology from west of Bougie, Algeria, to the coast west of Oran, Algeria.

basic igneous rock, as compared to acidic basement to the east of reference mark 891.

Spanish Morocco; Tangier; Portugal (Figure 8)

This figure shows the magnetic profile and the geology along the profile across the extreme northwestern part of Spanish Morocco, and Tangier, and from the south coast of Portugal 15 miles (25 kms) west of Ayamonte to Lisbon.

From reference marks 916 to 939 the magnetic profile crosses the metamorphic rock outcrops on the west, which are overlain to the west by Paleozoic and Tertiary sediments. The magnetic profile, however, shows minor, local sharp anomalies in the interval from reference marks 934 to 939 which are probably indicative of shallow crystalline rocks.

The magnetic profile from the south coast of Portugal to Lisbon crosses the southern coastal basin, and the Sétubal Basin. These two basin areas are separated by a high zone which probably has been intruded by acidic magmas. The magnetic profile over the southern coastal basin is dominated by a 100-gamma high which could be due to a basic facies within the basin at a depth of 10,560 feet (3200 meters). To the southeast of reference mark 002, the local, minor anomalies are indicative of shallow or surface occurrences of igneous rocks. To the northwest of reference mark 002, the Sétubal basin contact may be a faulted zone. In the vicinity of Sétubal, the basement depth is of the order of 6000 feet (1830 meters).

Conclusions

The magnetic data from this profile yield some depth values over basin areas of North Africa. These depth determinations are subject to a large margin of error due to the lack of control on the relation between the magnetic trends to the known geologic trends. However, the data shown on this profile should be of general aid in correlating known structure with their basement indications, and the reported depth determinations should yield some measure of the sedimentary thickness in the basins, if the expected range as pointed out in the paper, is considered.

Acknowledgements

The authors wish to express their thanks to Mr. Virgil Kauffman, President of Aero Service Corporation, for permission to publish this paper, and to the personnel of Aero Service Corporation for their aid in assembling these data, particularly to Mr. F. X. McWilliams, pilot on this flight; Mr. Frank Morgan, Magnetometer Operator; and Mr. J. Ardiff, Magnetometer Division.

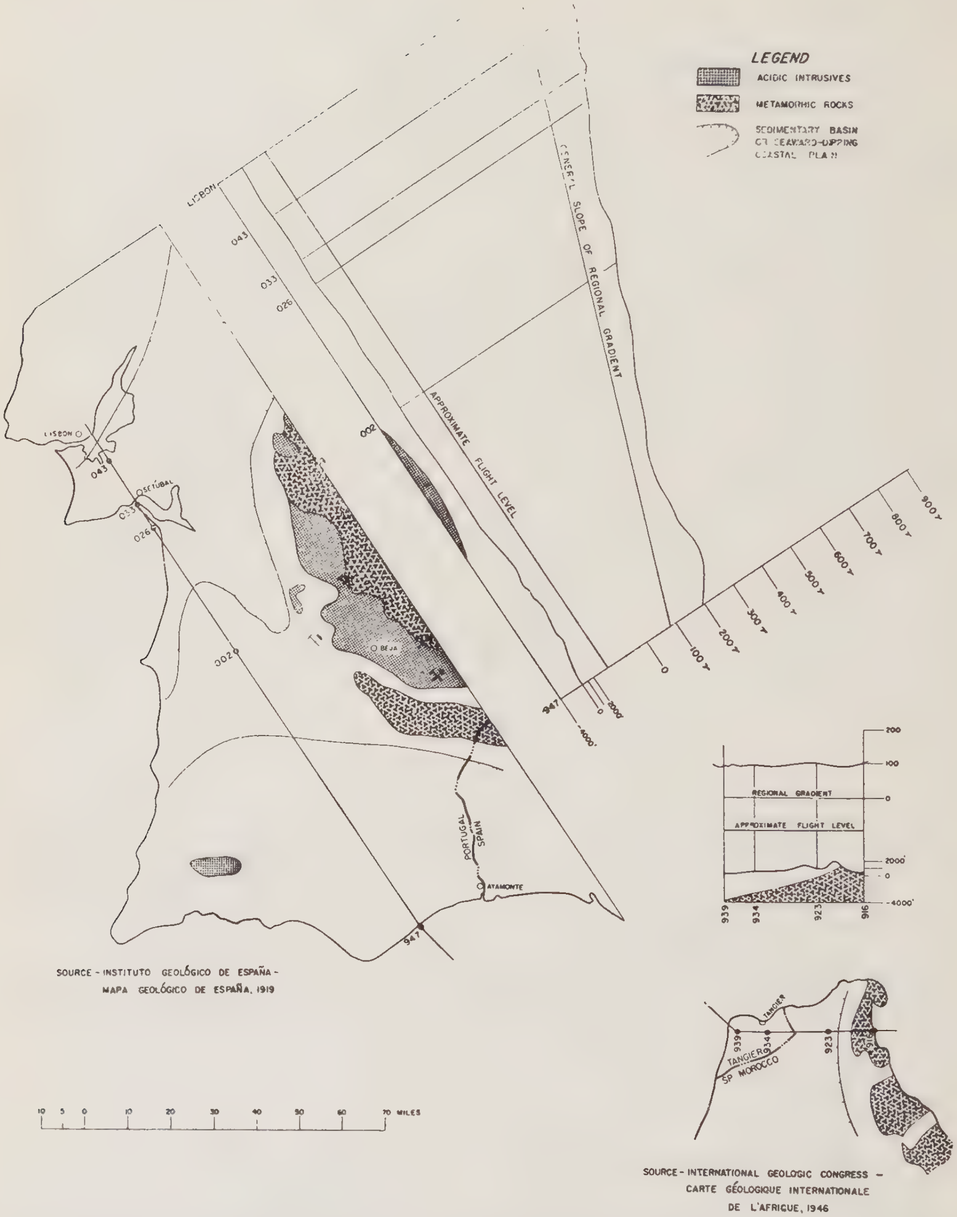

SOURCE - INSTITUTO GEOLÓGICO DE ESPAÑA - MAPA GEOLÓGICO DE ESPAÑA, 1919

SOURCE - INTERNATIONAL GEOLOGIC CONGRESS - CARTE GÉOLOGIQUE INTERNATIONALE DE L'AFRIQUE, 1946

Fig. 8. Airborne magnetometer profile, geologic cross section, flight path, and geology from across northwestern Spanish Morocco and Tangier, and from the south coast of Portugal to Lisbon.

Pertinent Literature (not cited in the text)

All of the following are Regional Monographs of the XIX International Geologic Congress, 1952:

Tunisia-Algeria

1. Bolfa, J., Hilly, J., and Roubault, M., Massifs Cristallins du Nord, Constantinois, 1re Serie, No. 23.
2. Bolze, J., Burolollet, P. F., and Castany, G., Le Sillon Tunisien, 2eme Serie, No. 5.
3. Castany, G., Paleogeographie, Tectonique, et Crogenese de la Tunesie, 2eme Serie, No. 1.
4. Dalloni, M., L'Atlas Tellien Occidental, 1re Serie, No. 24.
5. Duplan, L., La Region de Bougie, 1re Serie, No. 17.
6. Flandrin, J., La Chaine du Djurdjura, 1re Serie, No. 19.
7. Glangeand, L., and others, Histoire Geologique de la Province d'Alger, 1re Serie, No. 25.
8. Gottis, Ch. and Sainfelf, P., Les Gites Metalliferes Tunisiens, 2eme Serie, No. 2.
9. Sadran, G., Les Roches Cristallines du Littoral Oranais, 1re Serie, No. 18.
10. La Société Nationale de Recherches et d'Exploitation des Pétroles en Algérie, Le Bassin Neogene du Chelif, 1re Serie, No. 16.
11. ——, Regions Sud-Telliennes et Atlas Saharien, 1re Serie, No. 20.
12. Betier, G., et al., Etudes sur les Gisements de Fer de l'Algerie, Symposium sur les Gisements de Fer du Monde, Tome I, XIX International Geologic Congres, 1952.

Spanish Morocco-Tangier

1. Choubert, G., and Marçais, J., Geologie de Maroc, Regional monograph, International Geologic Congres, 3eme Serie, No. 6.

Portugal

1. De Jèsus, A. M., and Cotelo Neiva, J. M., Informations sur les Minerais de Fer Portugais, Symposium sur Les Gisements de Fer du Monde, Tome II, 1952, International Geologic Congres.

General

1. Peters, L. J., 1949, The Direct Approach to Magnetic Interpretation and its Practical Application, Geophysics, V. 14, p. 290-320.
2. Vestine, E. H., et al, 1947, Description of the Earth's Main Magnetic Field and Its Secular Change, 1905-1945, Carnegie Institution of Washington publication 578, Washington, D.C.

GEOELEKTRISCHE BAUGRUNDUNTERSUCHUNGEN IN JUGOSLAWIEN UND OESTERREICH *

VON

VOLKER FRITSCH **

Abstract

Examples are given illustrating the application of geo-electrical methods to engineering problems in Austria and Yugoslavia. A large number of these examples deal with dam problems. In this field, resistivity methods are used for bedrock investigations, to check the efficiency of cement injections into the rock, and to investigate the seepage of water underneath the dam. In the building and maintenance of roads, resistivity methods are used for the detection of cavities underneath the road. On the Vienna air port, a radio method was used for the same purpose.

Seit dem Ende des zweiten Weltkrieges hat die Geoelektrik in Jugoslawien und Oesterreich einen sehr raschen Aufschwung genommen. Zur Zeit sind in diesen beiden Ländern ständig 6 bis 8 Messtrups mit geoelektrischen Aufschliessungsarbeiten beschäftigt. Einen starken Impuls erhielten diese Arbeiten durch den Bau der grossen Staumauern, bei denen die Untersuchung des Untergrundes oft dem Geoelektriker übertragen wurde.

Da die wirtschaftlichen, geologischen und technischen Voraussetzungen in beiden Ländern sehr ähnliche sind, so kam auch eine sehr enge Zusammenarbeit der beiderseitigen Fachleute zustande. Aus diesen Gründen ist eine zusammenfassende Darstellung gerechtfertigt.

Die Anwendung der Geoelektrik umfasst im wesentlichen folgende Gebiete:

a) Baugrunduntersuchungen bei der Planung von Talsperren,
b) Kontrolle der mechanischen Bodenverfestigung durch Zementinjektionen,
c) Baugrunduntersuchungen im Zuge von Strassen, Rollfeldern und Eisenbahnen,
d) Baugrunduntersuchungen bei der Planung von Hafenanlagen,
e) Sanierung von Rutschhängen,
f) Elektrohydrographische Messungen.

Dazu kommen noch verschiedene Arbeiten, insbesondere beim Bau von Gebäuden.

---

* Presented at the Eighth Meeting of the European Association of Exploration Geophysicists, held in Paris, 18-20 May 1955.

** Elektrotechnisches Institut der Technischen Hochschule, Vienna.

In technischer Hinsicht umfassen die bisher geleisteten Arbeiten:

a) Sondierungen nach dem Vier- und Fünfpunktverfahren mit kommutiertem Gleichstrom oder niederfrequentem Wechselstrom,
b) Sondierungen mit Hochfrequenz,
c) geoelektrische Rammsondierungen,
d) geoelektrische Injektionskontrolle,
e) elektrohydrographische Messungen.

Im Versuchsstadium befinden sich:

a) Bohrlochuntersuchungen in Bohrlöchern ohne Spülung,
b) Ermittlung des K-Wertes aus geoelektrischen Untersuchungen,
c) geoelektrische Bodenverfestigung bei gleichzeitiger elektrischer und mechanischer Verfestigung.

Aus dem bisher zu Stande gekommenen Messmaterial, das an die 15.000 Sondierungen umfasst, seien einige interessante Beispiele herausgegriffen:

Beim Bau der Nikola-Tesla-Stufe Lokvarka (bei Rijeka) wurden geoelektrische Sondierungen herangezogen. Der Staudamm hat eine Kubatur von

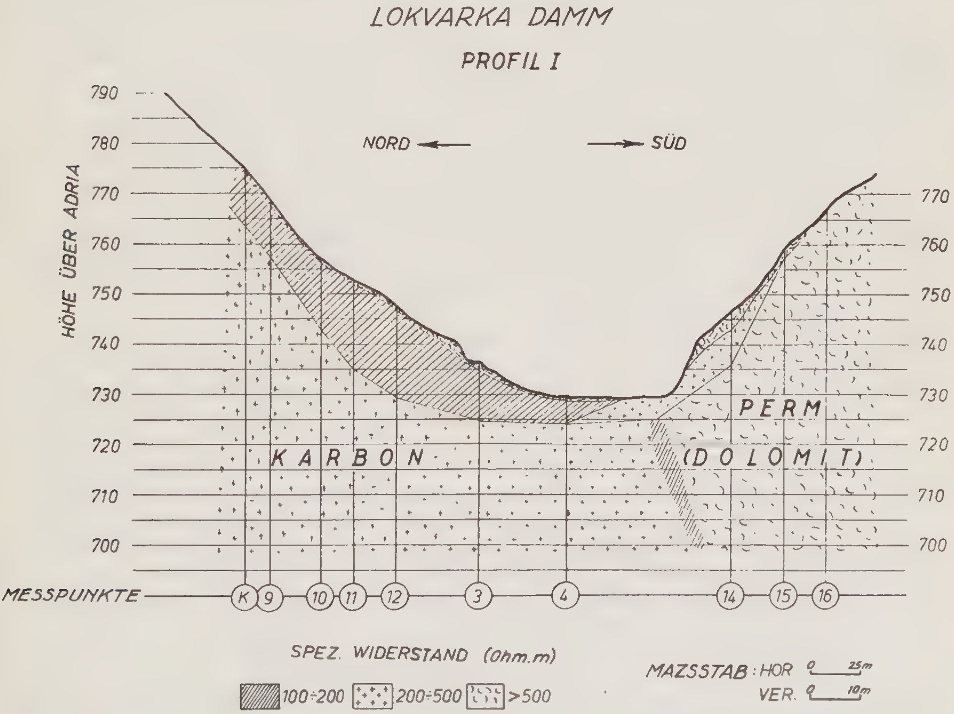

Fig. 1. Geoelektrische Untersuchungen Lokvarka. — Geo-electrical survey Lokvarka.

560.000 m^3, bei einer maximalen Höhe von 47 m und einer Kronenbreite von 276 m. Es ist ein Kontrollgang vorgesehen. Im Bereiche des Staudammes liegt, wie Fig. 1 zeigt, der Kontakt zwischen dem Dolomit und dem Karbon. Das Gestein ist in diesen Bereichen sehr klüftig und man befürchtete daher grosse Wasserverluste. Es wurde daher ein 20 m tiefer Injektionensschleier gezogen, der in beiden Flanken durch Betonkerne fortgesetzt wird. Die geoelektrische Untersuchung erfolgte durch Oberflächensondierung und durch Kontrolle der Bohrlöcher während der Zementverpressung. Man erhielt folgende Durchschnittswerte für den spezifischen Widerstand:

Karbon: Glimmerschieffer und Phyllit	225 Ohm m
Konglomerat aus Quarz und Sandstein	190 Ohm m
Dolomit und Schiefer	650 Ohm m

Es war daher eine Unterscheidung der beiden Formationen möglich. Der geringe spezifische Widerstand des Karbons ist vor allem durch die Kittsubstanz bedingt. Der relativ niedrige Widerstand des Phyllites deutet auf eine hohe Klüftigkeit hin. Die Messungen wurden vor und nach der Verpressung der Injektionsbohrlöcher ausgeführt. Aus den Widerstandsunterschieden und Vergleichsmessungen im Laboratorium wurde berechnet, dass das mittlere Hohlraumvolumen nach der Injektion noch 15‰ im Mittel beträgt. Ein solches Gebirge ist als „kompakt" oder „schwach porös" zu bezeichnen.

Die Messungen haben in praktischer Hinsicht gezeigt, dass der Bau eines Dammes in diesem Gelände richtig ist und sie haben weiter die notwendigen Unterlagen für den Ansatz der Injektionen und die richtige Festsetzung des Injektionsdruckes gegeben. Es sei bemerkt, dass zu hohe Injektionsdrucke während der Bauzeit des Dammes eine Auflockerung des Untergrundes bedingten, die geoelektrisch an einer Erhöhung des spezifischen Widerstandes deutlich zu erkennen war.

Beim Bau der Limbergsperre im Kapruner Tale wurden über Veranlassung des Baudirektors Dipl. Ing. Böhmer in der Zeit von 1948 bis zum Abschluss der Arbeiten im Jahre 1951 die Injektionen laufend geoelektrisch kontrolliert. Das Verfahren ist an anderen Stelle genauer beschrieben (V. Fritsch, 1953 and 1954). Im wesentlichen wird die Aufnahme an Injektionsgut aus der Verringerung des Gebirgswiderstandes berechnet. Diese ist beträchtlich, weil der spezifische Widerstand des Injektionsgutes nur 1-2 Ohm m beträgt.

Die Höhe der Beton-Staumauer beträgt 120 m und ihre Kubatur ungefähr 450.000 m^3. Das Volumen des durch Injektionen verfestigten Felsraumes beträgt ungefähr 500.000 m^3. In diesem verlaufen 13.200 m injizierte Bohrlöcher. Von diesen wurden 72% geoelektrisch kontrolliert. Die Anfangsklüftigkeit des Gesteines (Kalkglimmerschiefer) betrug 20-40‰. Von diesen Klüften dürften allerdings nur 30-50% offen gewesen sein, sodass die ,,offene Anfangsklüftigkeit'' ungefähr 10-20‰ betragen dürfte. Nach der Verfestigung fiel das ,,offene Kluftvolumen'' auf Werte von 5-10‰. Das Gestein durfte also als völlig verfestigt bezeichnet werden. Die Messungen wurden dann bei den Sperren der Oberstufe (Mooser- und Drossensperre) bis zum Jahre 1954 fortgesetzt. Es wurden dort systematische Vergleiche mit den Kontrollen ausgeführt. Diese zeigten deutlich, dass die bisher üblichen Wasserabpressungen allein nicht ausreichen, um das Gebiet einwandfrei zu beurteilen. Dagegen können beide Verfahren zusammen einen sehr hohen Grad von Zuverlässigkeit verbürgen. Aus den geoelektrischen Messungen wird die Verfüllung des offenen Kluft volumens berechnet. Ausserdem ist aber auch die tätsächlich eingepresste Menge des Injektionsgutes bekannt. Durch Vergleich dieser beiden Angaben kann man nun erkennen, ob noch offene Klüfte existieren, oder ob das Injektionsgut ausgeflossen ist. Auch ist zu erkennen, ob durch den Injektionsdruck Klüfte erweitert worden sind, da in diesem Falle der gemessene spezifische Widerstand grösser wird, oder ob die Klüfte oberflächlich verlegt sind und daher bei dem zulässigen Druck kein Injektionsgut aufnehmen können. Es wurde ein Klassifikationssystem ausgearbeitet und dieses bei der Planung der Verteilung der Injektionsbohrlöcher ausgewertet.

Jede der beobachteten Injektionserscheinungen wird nach einem — den besonderen Bedingungen der Baustelle angepassten — Schema bewertet und die einzelnen Bewertungspunkte werden dann zusammengezählt. Stellen, die besonders viele Bewertungspunkte aufweisen, werden bei der zweiten Injektion noch einmal injiziert. Dadurch ,dass man aber diese Stellen geoelektrisch ermitteln kann, muss man die 2. Injektion nur dort anwenden, wo sie wirklich notwendig ist und erspart daher beträchtlich an Bohrlänge gegenüber einer rein schematischen Sekundärinjektion.

In Fig. 2 ist ein Ausschnitt aus einem Diagramm gezeigt, in dem die einzelnen Bohrstufen nach dem erwähnten Klassifikationssystem bewertet sind. Je höher die berechnete Ziffer ist, desto schlechter ist der Injektionserfolg. Er war auf diese Weise möglich ,beträchtliche Einsparungen an Bohrlängen zu erzielen.

Eine grosse Untersuchung dieser Art läuft derzeit auf der Baustelle Peruča (Cetina) in Dalmatien. In diesem stark karstifizierten Gelände sind die Injektionen besonders wichtig, ja ihre richtige Durchführung schafft überhaupt erst die Voraussetsung für die Anlage einer Sperre. Im vergangenem Herbst wurde dort mit einer Grossinjektion begonnen, die zur Zeit noch läuft. Zunächst wurden 2 Felder mit insgesamt 86 Sonden gemessen. Im ersten Felde wurden 34 Sonden nach durchgeführten Injektion gemessen, im zweiten Felde mit 52 Sonden werden die Injektionen laufend, also auch während des Injektionsvorganges selbst, kontrolliert. Der Vorgang weicht von jenem in Kaprun in

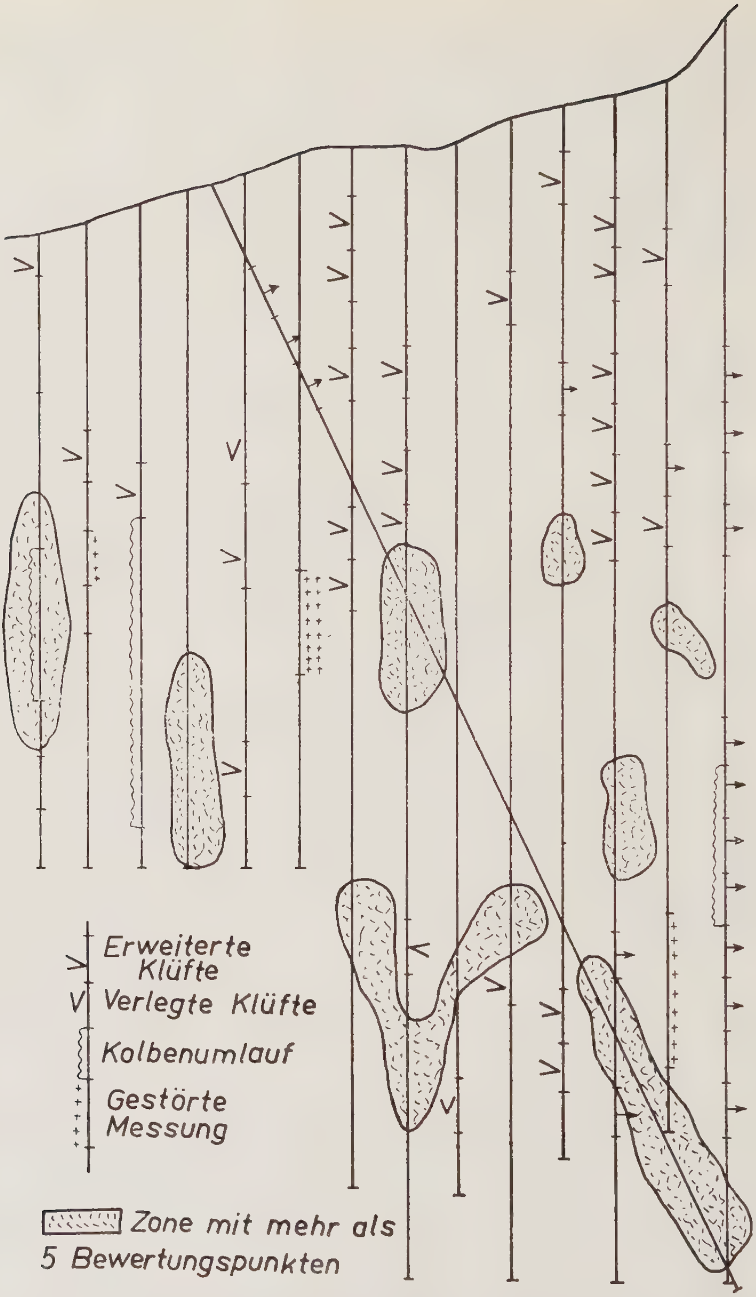

Fig. 2. Ausschnitt aus einem Diagramm, in dem der Injektionserfolg auf Grund geoelektrischer Widerstandsmessungen durch ein Punktesystem dargestellt ist (Messungen Kaprun). — Part of a diagram in which the efficiency of injections, as found by resistivity measurements, is shown by a system of evaluation points (measurements at Kaprun).

zweierlei Hinsicht ab. Zunächst wird auf der Cetina ein Injektionsgut verwendet, das einen starken Lehm-und Tonzusatz hat und dessen spezifischer Widerstand etwas höher ist (4-5 Ohm m). Weiters wurde die Injektion von oben nach unten durchgeführt, also entgegengesetzt jener, die in Kaprun praktiziert wurde. Das ergab gewisse Verschiedenheiten in der Methode. Der spezifische Widerstand des Gebirges (Kalkstein, Sandstein, Einlagerungen von Ton und Terra rossa) lag je nach dem Grade der Verwitterung zwischen 300 und 2000 Ohm m. Die Überprüfung des Injektionserfolges durch blosse Wasserabpressung führte in vielen Fällen zu ganz unrichtigen Resultaten, wie das in Fig. 3 dargestellte Diagramm in einem Beispiel zeigt. Die einzelnen Messungen streuen so stark, dass kein klarer Zusammenhang zwischen dem Wasserverlust und der Aufnahme an Injektionsgut gefunden werden kann. Eine systematische Überprüfung der Messergebnisse bewies, dass in vielen Fällen die Wasser-

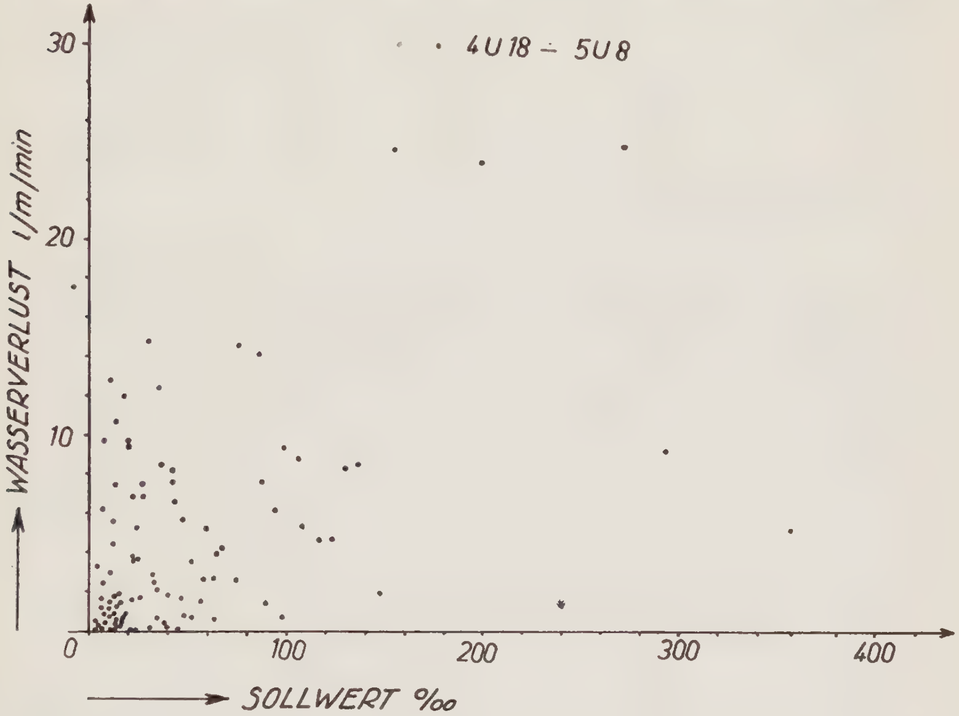

Fig. 3. Resultate der Wasserabpressung. Ordinate: Wasserverlust in l/m/min; Abscisse: Aufnahme an Injektionsgut, dargestellt durch den Sollwert. Sollwert = $= \frac{\text{Injiziertes Gut } (l)}{\text{Injiziertes Volumen } (l)}$ 1000 ‰ — Results of water ejection. Ordinate: water loss in l/min/m; Abscissa: absorption of injected material, represented by the ratio $\frac{\text{injected material } (l)}{\text{injected volume } (l)}$ 1000 ‰.

abpressung und der Injektionsbefund einander völlig widersprachen. Es war deshalb die geoelektrische Kontrolle mit den anderen Kontrollverfahren zu kombinieren. Die Widerstandsunterschiede waren deutlich ausgeprägt. In der folgenden Tabelle sind einige Werte zusammengestellt.

	Spezifischer Widerstand in Ohm m			
des Grundgebirges *vor* der Injektion	des Gebirges *nach* der Injektion bei einer Verfüllung von			
	0,5%	1%	3%	5%
1000	590	370	155	105
500	350	270	140	95
300	240	200	120	85

Spezifischer Widerstand des Injektionsgutes = 4 Ohm m.

Durch zahlreiche Untersuchungen wurde der spezifische Widerstand des Grundgebirges vor der Injektion ermittelt. Aus diesen Werten konnte die Klüftigkeit vor der Injektion ermittelt werden. Aus den nach der Injektion gemessenen Werten konnte die Abnahme der Klüftigkeit und das noch offene Kluftvolumen ermittelt werden. Die Unterschiede wurden in einem Diagramm dargestellt, das Fig. 4 im Ausschnitt zeigt. Die Stellen, an denen noch unverfüllte Klüfte existieren, können nunmehr festgestellt und nachinjiziert werden.

Durch die Widerstandsmessung während der Injektion kann man mit ziemlicher Sicherheit Zonen erkennen, aus denen das Injektionsgut nach entfernten Räumen ausfliesst, die verlegte Spalten und Klüfte enthalten, oder deren Klüfte durch den hohen Injektionsdruck erweitert wurden. Die Verfahren sind also auch dazu geeignet, den maximal zulässigen Injektionsdruck zu beurteilen.

Geoelektrische Verfahren werden auch nach der Fertigstellung von Talsperren eingesetzt, um zu konstatieren, ob Wasser durch Spalten und Klüfte unter der Sperre hindurch sickert. Das durchsickernde Wasser setzt den spezifischen Gebirgswiderstand herab. Um diesen zu messen ,wurden, wie Fig. 5 zeigt, auf der Sohle des Kontrollganges der Limbergsperre 51 Elektroden eingesetzt, zwischen denen im Vierpunktverfahren der spezifische Gebirgswiderstand bei verschiedenen Konfigurationen gemessen wurde. Es wurde dann wieder das wassererfüllte Klüftvolumen berechnet. Bei dieser Berechnung musste natürlich auch die Änderung des spezifischen Widerstandes des Betonkörpers der Staumauer berücksichtigt werden. Zu diesem Zweck wurden in die Staumauer an mehreren Stellen Elektroden eingesetzt, zwischen denen der Widerstand bestimmt wurde. Der Betonwiderstand steigt von ganz geringen Werten (3-5 Ohm m) allmählich an und erreicht — je nach der Ausdehnung des Körpers —

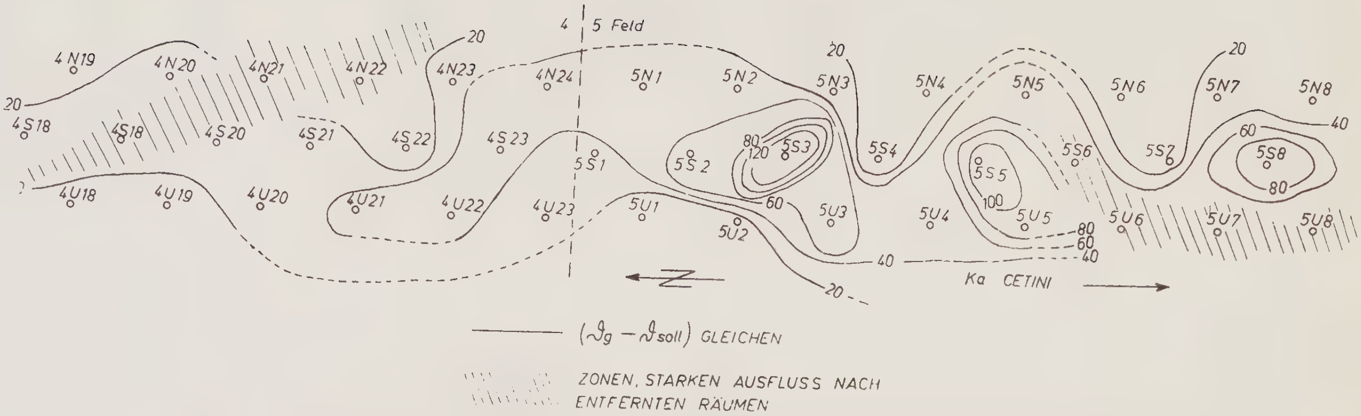

Fig. 4. Geoelektrische Messungen Cetina. Nachweis klüftiger Zonen. — Geo-electrical measurements at Cetina; demonstration of fissured zones.

nach einigen Monaten, oder selbst Jahren, den Endwert (400-700 Ohm m). In der folgenden Tabelle sind die Messorte angegeben (in % aller Messorte), an denen der Anteil des eindringenden Kluftwassers mehr als 5‰ des Gesamtvolumens betrug.

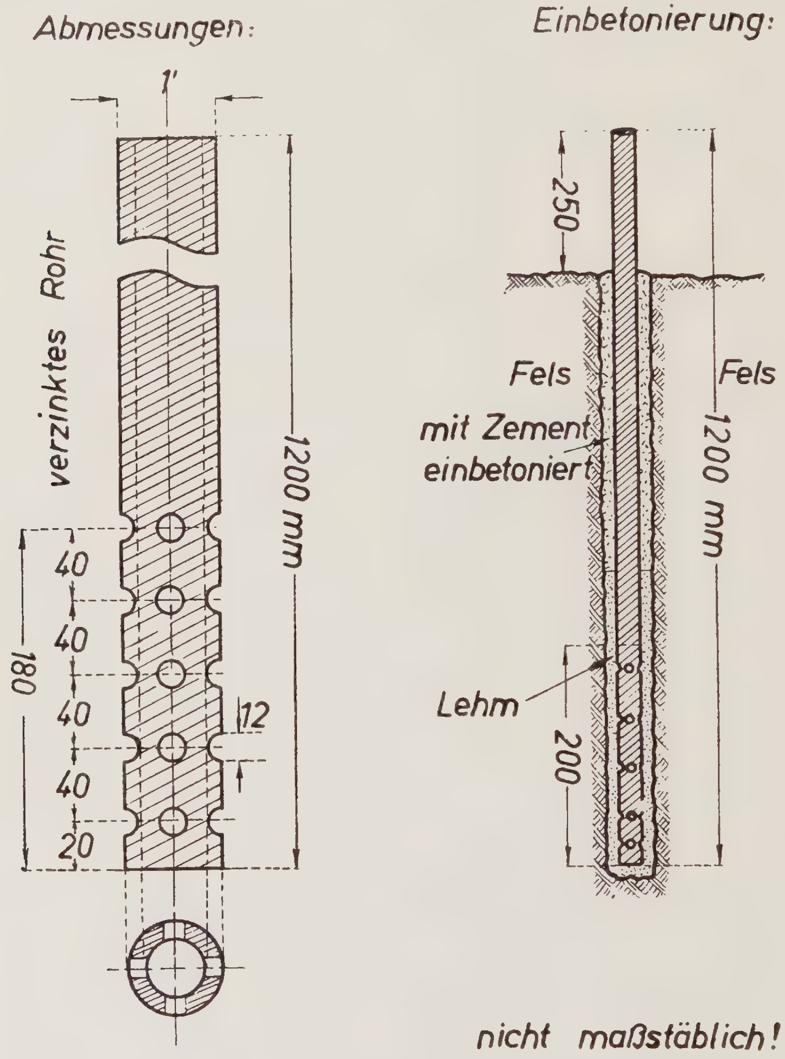

Fig. 5. Einbau von Elektroden im Kontrollgang der Limbergsperre Kaprun. — Method of building in electrodes in the control passage of the Limberg dam at Kaprun.

Jahr	Monat	Stauhöhe *) (über Adria)	Anteil der Messorte mit mehr als 5%
1950	Dezember	1631-1639 m	15%
1951	Juli	1618-1628 m	37%
1951	November	1656 m	33%

* Kronenhöhe 1672 m

Die Arbeiten wurden im Sommer 1951 fertiggestellt. Man erkennt, dass trotz der Erhöhung des Staues die Zahl der Messorte mit stärkerem Wassergehalt etwas zurückgegangen ist. Die geoelektrischen Messungen zeigen also, dass die Kluftfüllungsverhältnisse sich rasch stabililiert haben.

Eine umfangreiche geoelektrische Vermessung fand im Mündungsgebiet des Flusses Neretva bei Ploče statt, wo ein neuer grosser Hafen gebaut wird. Der Felsuntergrund besteht aus Sandstein, dessen Oberfläche aber stark verwittert sein dürfte. Darüber lagert Sand, Schotter und schliesslich Schlamm, der stellenweise von Meerwasser überspült ist. Die Aufgabe der Untersuchungen war die Feststellung der Felsoberfläche. Es handelte sich hier um die Behandlung eines Vierschichtenproblems. Die oberen drei Schichten (Schlamm. Geschiebeschichten, Verwitterungsschichte) haben sehr kleine spezifische Widerstände (1-25 Ohm m). Der feste Fels hat dagegen wesentlich höhere spezifische Widerstände (einige hundert Ohm m). Die Kurven zeigen in erster Annäherung den typischen Charakter einer Zweischicht. Trotzdem ist die genaue Bestimmung der Felshöhe deshalb schwer, weil zwischen der Oberfläche des festen („gesunden") Felsens und der unteren Grenzfläche der Sedimente eine Verwitterungszone liegt, deren spezifischer Widerstand meist mit der Tiefe ansteigt. Vom bautechnischen Standpunkt aus ist dies allerdings kein Nachteil. Den Bautechniker interessiert nicht die geologisch definierte Felsoberfläche, sondern die Begrenzung des festen Felsens, auf dem er die Molen fundieren kann. Diese Angabe aber liefert recht genau die Geoelektrik. Eine weitere Komplikation war durch das schräge Einfallen der Schichten gegeben. Durch Vergleichmessungen im aufgeschlossenen Gelände wurden Korrekturfaktoren ermittelt. Die Messungen wurden im wesentlichen während einer Saison ausgeführt. Wäre es notwendig gewesen die Aufgabe durch Bohrungen zu gewältigen, so wären mit Rücksicht auf das sumpfige, umwegsame Gelände, mehrere Jahre notwendig gewesen.

In den letzten Jahren wird an der weitgehenden Modernisierung des Wiener Strassennetzes gearbeitet und an die Stelle der alten Pflasterstöckel- und Asphaltstrassen tritt die moderne Betonstrasse. Der Baufortschritt ist nun wesentlich davon abhängig, dass die schweren und komplizierten Baumaschinen gleichmässig eingesetzt und fortbewegt werden können. Da nun die Wiener Hauptstrassen im Zuge meist uralter Strassenzüge liegen, so kam es des öfteren vor, dass die Fortsetzung der Arbeit durch den plötzlichen Einbruch alter Hohlräume (Keller, Kanäle etc.) behindert wurde. Auch bildeten sich unter den Betonplatten durch Wassererrosionen Hohlräume, die durch Verpressungen unschädlich gemacht werden müssen. Aus diesem Grunde werden Strassenzüge, die solche Komplikationen befürchten lassen, vor dem Umbau geoelektrisch untersucht. Gemessen wird stets nach dem Vierpunktverfahren mit kommutiertem Gleichstrom oder niederfrequentem Wechselstrom. Bei diesen Messungen kommt es vor allem auf rasche Durchführung an. In der Regel werden die Punkte in drei Reihen und in Abständen von 5 m gesetzt, sodass auf einen Kilometer Strassenlänge 600 Messpunkte entfallen. An die Stelle des sonst bei solchen Messungen üblichen Kompensators tritt daher meist das Röhrenvoltmeter, das bei konstantgehaltenem Aussenelektrodenstrom direkt die Sondenspannung angibt, die bloss mit einer Konstante multipliziert werden muss, um den scheinbaren spezifischen Widerstand zu erhalten. An jeder Stelle werden Sondierungen mit den Elektrodenabständen 2 × 1,5...2 × 2,5...2 × 3,5... ...2 × 4,5...2 × 5,5 m und fallweise bis zu 2 × 20 m ausgeführt. Die Diagramme, in die die berechneten Werte eingetragen werden, lassen, wie Fig. 6 zeigt, folgendes erkennen:

a) Schichtung des Untergrundes mit besonderer Berücksichtigung der älteren Strassendecken.

b) Lage von Hohlräumen, wie Kellern, Kanälen, Mauerwerk etc.,

c) Lage aufgelockerter Zonen und alter verfüllter Gräben,

d) Wassererrosionen.

Bei älteren Betonstrassen lockert sich der Boden unter den Fugen der Platten auf. Die Platten beginnen dann bei Belastung zu pendeln und brechen oft in der Mitte. Auch zum Nachweis dieser Fugenauflockerungen, die an einer Erhöhung des spezifischen Bodenwiderstandes zu erkennen sind, wird die Geoelektrik verwendet.

Die wichtige Eisenbahnlinie vom Adriahafen Rijeka nach Zagreb wird schon seit Jahrzehnten beim Dorfe Zalezina von einem mächtigen Erdrutsch bedroht. Um diesen zu sanieren, war die Entwässerung der Gleitfläche notwendig. Um die Lage und Beschaffenheit der Gleitfläche festzustellen, wurden geoelektrische Sondierungen durchgeführt. Diese gestatten die Darstellung eines Profiles und damit auch die Berechnung der in Bewegung befindlichen Massen. Da dieser Rutschhang sehr empfindlich ist und eine Störung des Bahnbetriebes auf jeden Fall vermieden werden muss, so konnten weder Bohrungen noch seismische Untersuchungen die geoelektrische Untersuchung ersetzen.

Zum Schlusse sei noch die Untersuchung der Betonpiste des Wiener Flughafens Schwechat besprochen, die deshalb bemerkenswert ist, weil sie mit Hochfrequenz durchgeführt wurde. Die Betonpiste ist mit einer Asphaltschichte überdeckt, die ein sehr schlechter Leiter ist. Aus diesem Grunde konnte nicht mit galvanischen Elektroden gearbeitet werden. Für die Messung

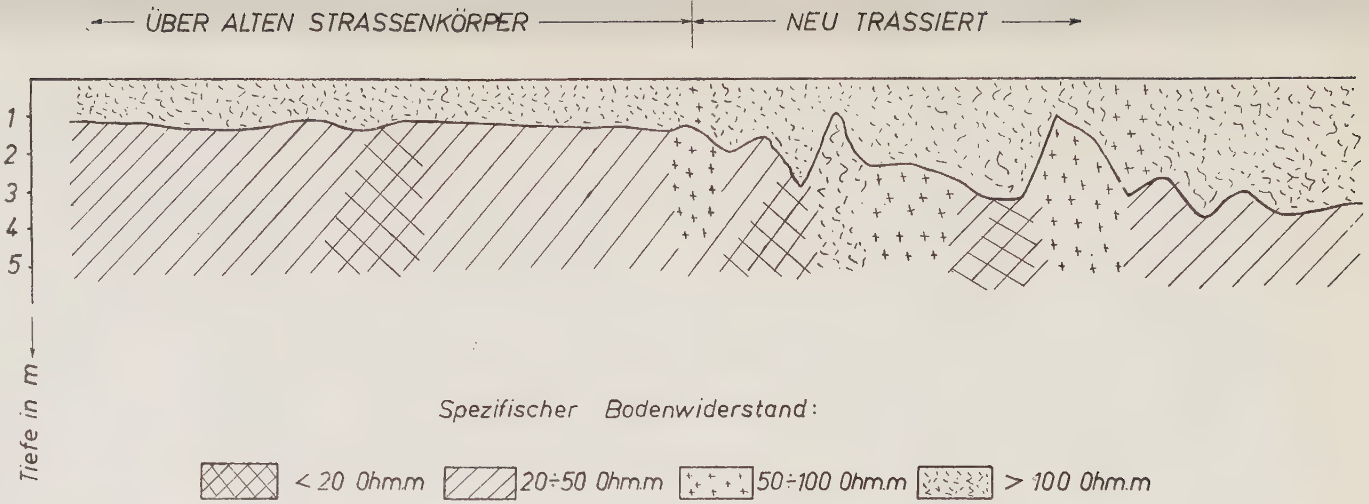

Fig. 6. Geoelektrisches Profil entlang einer Strassenachse. — Geo-electrical profile along a road.

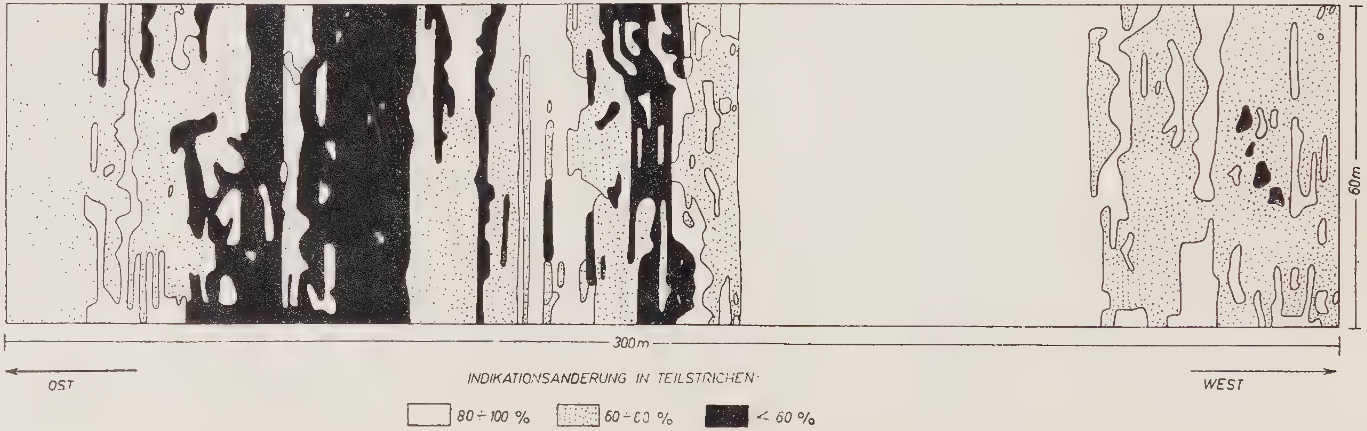

Fig. 7. Geoelektrische Messung and der Flugpiste Wien. — Geo-electrical measurements on Vienna air port.

mussten vielmehr kapazitive Elektroden verwendet werden, die rasch an die Oberflächenschichte angelegt werden konnten. Die Verwendung solcher Elektroden ist aber nur bei Hochfrequenz möglich. Die Aufgabe der Messung war die Feststellung von kleinen Hohlräumen und Auflockerungszonen unter der Betondecke, die durch ungleichmässiges Absetzen des Untergrundes entstehen. Zu diesem Zweck wurde ein kleiner Sender mit einer Wellenlänge von ungefähr 5 m verwendet, an dessen Schwingungskreis die beiden kapazitiven Elektroden angeschlossen wurden. Jenachdem diese auf Stellen aufgesetzt wurden, unter denen fester Boden oder Hohlräume lagen, war auch die Verstimmung des Kreises grösser oder geringer. Die entsprechende Anzeige bildet daher ein Mass für die Beschaffenheit des Untergrundes. Das Gerät wurde zunächst über Punkten der Piste getestet, an denen die Untergrundbeschaffenheit bekannt ist. Das Ergebnis ist in der folgenden Tabelle festgehalten.

Untergrund über	Anzeige in Teilstrichen	
Unverletzte Asphaltschichte	63 ± 4	100%
Beton mit geringer Asphaltauflage (Rand des Rollfeldes)	38 ± 5	∾ 60%
Beton mit geringer Asphaltauflage (Mitte des Rollfeldes)	38 ± 4	∾ 60%
einem bekannten Hohlraum	21 ± 2	∾ 33%

Die Anzeigen wurden wieder in das Diagramm eingetragen, aus dem Fig. 7 einen Ausschnitt zeigt. Die Messung zeigte, dass die Piste am stärksten an den Stellen unterhöhlt war, an denen die Flugzeuge die Motorenprobe vornehmen oder starten. Der übrige Teil der Rollbahn zeigte kaum ein Veränderung.

Die wenigen hier gezeigten Beispiele sollen darlegen, dass in Jugoslawien und Oesterreich die angewandte Geoelektrik heute bereits ein wertvoller Helfer des Bautechnikers geworden ist und dass ihre Bedeutung ständig zunimmt.

LITERATUR

FRITSCH, V., 1953. Geoelektrische Uberprüfung der Baugrundverfestigung durch Zementinjektionen, Geofisica pura e appl. 25, 207.

FRITSCH, V., 1954. Geoelektrische Baugrunduntersuchung, Bautechnik 31, 318-322.

INSTRUMENTAL DISTORTION AND THE SEISMIC RECORD *

BY

N. A. ANSTEY **

ABSTRACT

This paper is presented to the geophysicist concerned with the interpretation of seismic records. Those instrumental factors which can affect the validity or accuracy of the records are detailed. Inferences are drawn relating to the picking, timing and grading of reflections, and the shooting of records in the field.

It is recognized that an important function of the seismic channel is the introduction of a controlled transformation of the input signal. This desirable distortion, chiefly in the filters and automatic gain control, makes legible a seismic record which would otherwise have a range of amplitudes of between one thousand and one million to one, and on which noise signals from many sources might obscure the reflections almost completely. However, in conventional seismic equipment the desired signal distortion is always accompanied by further distortion which, far from being desirable, may, in some cases, seriously reduce the amount of useful information which can be derived from the record. This undesirable distortion, according to its type, may affect the amplitude, time, or character of a reflected pulse, or it may introduce new components into the records which are not a part of the original ground motion.

While the sources and nature of these undesirable distortions have been known to instrument designers for many years, and while their magnitude is customarily stated in instrument specifications, the manner and extent of their effect on the validity of the seismic records themselves may require some clarification to the field geophysicist. Accordingly it is the purpose of this paper to describe, and more particularly to illustrate, the harmful effects on the record of unwanted distortion in the seismograph channel.

Such effects arise from the following causes:

1. Character distortion, particularly in the filters.
2. Time distortion, also particularly in the filters.
3. Distortion of character and relative amplitudes in the automatic gain control.

---

* Presented at the Ninth Meeting of the European Association of Exploration Geophysicists, held in London, 7-9 December 1955.

** Seismograph Service Limited, London.

4. Harmonic and intermodulation distortion, particularly at high signal levels.

The first two of these effects are inter-related; nevertheless this artificial division assists the illustration of the effects.

For those concerned with the interpretation of records, any illustration of distortion should conform as nearly as possible to the practical case observed on the record. On the other hand, there must be some idealisation, for otherwise it would not be possible to infer generalisations from the results. One of the most satisfactory idealisations of the seismic record is a random succession of primary seismic wavelets superimposed on a background of random noise and single-frequency ground roll. The form of the seismic wavelet to be used in this discussion is the symmetrical velocity wavelet postulated and experimentally established by Ricker (1951).

There can be no doubt that the ideal mathematical entity represented by such a wavelet approximates closely to the observed fact; *it will be seen in the following discussion that any minor variations in the form of the pulse will not jeopardise the illustrations.*

There is, of course, a major variation in the form of the pulse at travel times too short to be of normal interest to the oil prospector. This fact should be borne in mind when considering weathering and extremely shallow reflection problems, as should the general point that the form of the wavelet used is that derived from a velocity-sensitive (electromagnetic) geophone.

The discussion now turns to the four major manifestations of instrumental distortion; the illustrations presented have been taken on various conventional equipments commercially available, and do not represent effects peculiar to the equipment of one manufacturer.

CHARACTER DISTORTION

It is well known that if a sharp electrical impulse is applied to a filter, the resultant output is characteristic of the filter. It is also well known that when the form of this transient response has been established, the response of the filter to any other form of excitation can be decuded (Washburn, 1937, Born and Kendall, 1941, Piety, 1942). Accordingly instrument specifications often include details of the transient response of the amplifier with different filter settings.

However, the field geophysicist, while readily appreciating that the appearance of a reflection on the record will be in some way a combination of the input pulse and the characteristic transient response of the filtering, still needs to know exactly what this appearance will be for the pure primary seismic pulse. He then knows precisely the "units" from which his record is synthesised.

The interaction between pulse and filter are therefore to be illustrated.

Figure 1 shows the effect of varying the peak frequency of the pulse relative to a fixed, wide, filter pass-band. The frequency spectrum of the primary seismic pulse is quite wide relative to filters conventionally used, and even a band as wide as any normally employed in the field cannot embrace it sufficiently to reproduce it without distortion. (To do this completely, of course, no filters at all can be used, except in so far as the wavelet contractor (Ricker, 1953) constitutes a filter.) Accordingly the best possible pulse, for the filter response shown, is considerably distorted, while the output corresponding to the broadest pulse contains no fewer than seven half-cycles in place of the original three. It will be evident from the spectrum diagram that multiple differentiation of the lower frequencies is occurring; consequently the filtering at this end of the spectrum will introduce an additional half-cycle for each additional 6 dB/octave of filter slope. It is to be noted that the increased distortion introduced by the double-section filters, on the third trace, does not appear serious in this case; it should also be noted that, in the case of the single-section filters, on the second trace, the maximum amplitude registered in the filtered pulse remains in the early part of the waveform.

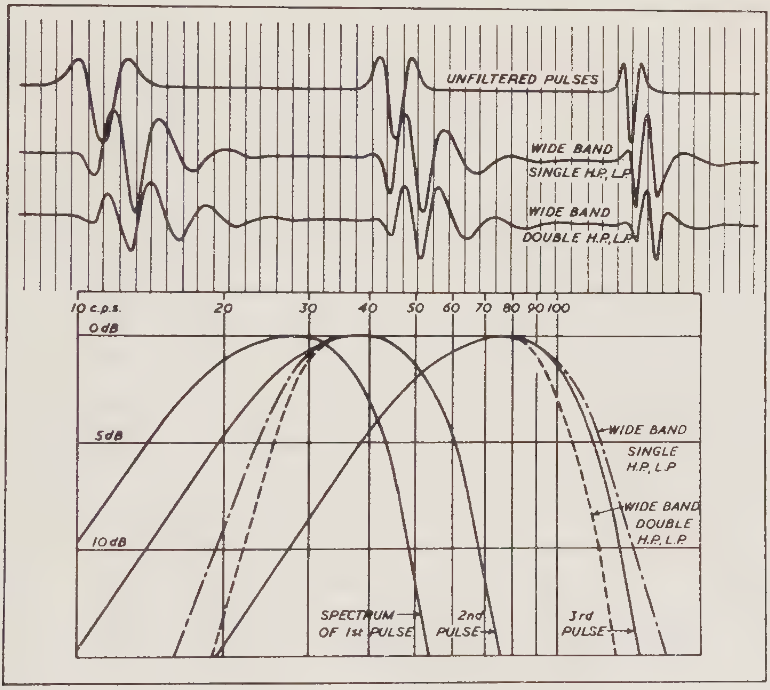

Fig. 1. Showing the effect of varying the peak frequency of a pulse relative to a fixed filter.

Figure 2 demonstrates the effect of varying the filter bandwidth relative to a fixed pulse spectrum. In particular, it shows that a highly tuned circuit, i.e., a narrow, steep-sided filter pass-band, destroys completely the character of the original pulse (Jakosky, 1952).

Figure 3 depicts the effect of varying the slope of the two filters within the pulse spectrum. It will be seen that the effect of increased slope in the high-pass filter is the addition of more half-cycles to the waveform, while that of increased slope in the low-pass filter is to make the pulse envelope more nearly symmetrical about the maximum amplitude.

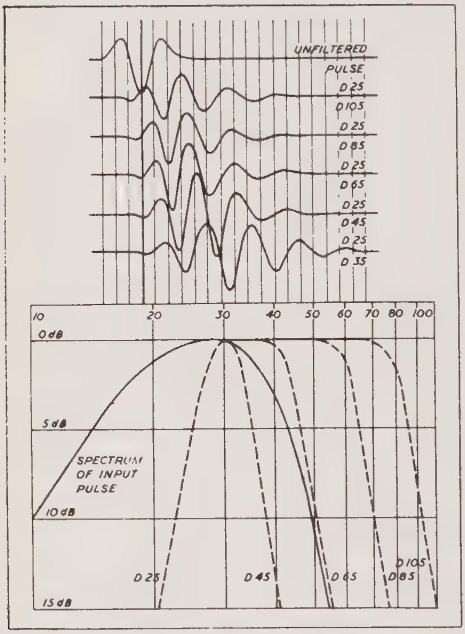

Fig. 2. Showing the effect of varying the filter bandwidth relative to a fixed pulse spectrum.

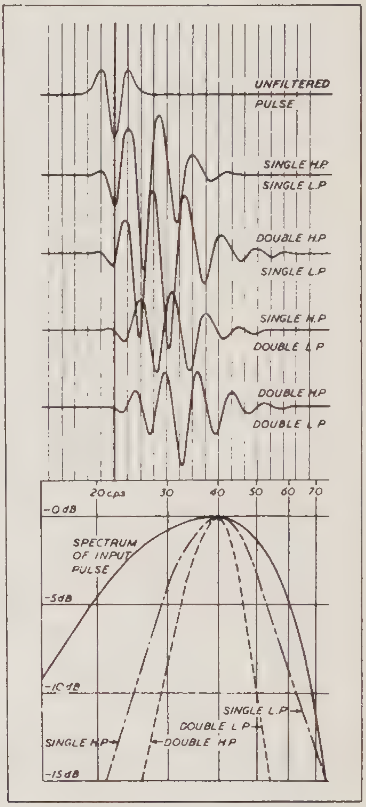

Fig. 3. Showing the effect of varying the slope of the filters within the pulse spectrum.

It is clear that character distortion of the form and extent discussed can have a serious effect on the resolution of two closely-spaced reflection wavelets. Figure 4 shows two such wavelets after they have passed through a wide-band filter and a narrow-band filter; in the latter case the second pulse is not separable from the first.

Another form of distortion is illustrated in Figure 5. This is a consequence of poor filter design, rather than being fundamental to the type of filter in use (as are the effects quoted above). If the frequency response in the pass band of a wide-band filter is not flat, but drooping, then the output waveform shown in the lower trace can result.

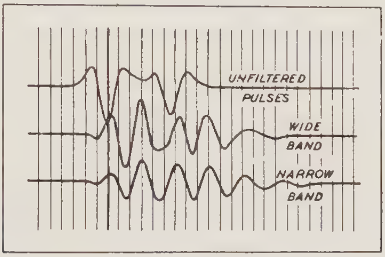

Fig. 4. Showing the effects of different filters on two successive pulses.

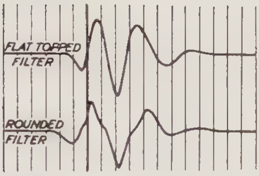

Fig. 5. Showing the effect of a rounded filter.

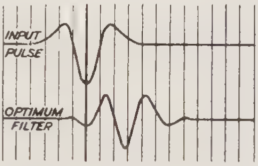

Fig. 6. Showing the distortion caused by an optimum filter.

In a previous paper read before this Association (Muir and Hales, 1955) it has been shown that the optimum filter for a criterion of maximum of peak reflection amplitude to r.m.s. noise has a frequency response identical to the spectrum of the input pulse, and that such a filter also satisfies a criterion of minimum distortion. The distortion which does occur in such an optimum filter is shown in Figure 6; the output waveform is seen to retain the symmetry of the input pulse, while small cycles have been added before and after. The illustrations of Figures 1-5 represent the behaviour of constant-K filters, which are the type normally employed in seismic amplifiers. The term "optimum" in connection with the filter of Figure 6 refers to the given criterion when the input is a Ricker velocity wavelet; a different optimum filter would result from different criteria or a different pulse. In particular, these "optimum" filters should not be confused with so-called "ideal" filters.

It is clear from the given illustrations that the apparent time of a reflected event may vary by tens of milliseconds from one filter setting to another —it is well known, of course, that a change of filter response during a prospect is unwise. This applies particularly to changes from single-section to double-section filters.

Before we pass on to the consideration of time distortion, it is perhaps worth pointing out that when the waveform of a pure pulse through a certain filter is compared with a field record shot with that filter, the exactness of the duplication between such waveform and the good reflections is remarkable.

TIME DISTORTION

On the seismic record everything must be interpreted in terms of *time*, and the time relation is the one which should remain completely specified. Time distortion of a symmetrical pulse occurs when the phase-frequency curve of the amplifier is not linear and does not intercept the phase axis at zero or an integral multiple of π; it represents the extent to which the delay between input pulse and output pulse varies with the peak frequency of the input pulse.

Time distortion is, of course, a feature of all resonant systems at some part of the frequency range. Thus, quite apart from the amplifier, both geophone and galvanometer exhibit this form of distortion; it is normally minimised over the frequency range of interest by choice of suitable natural frequencies and of a suitable damping factor.

For the illustrations of this effect in the amplifier fitted with constant-K filters we return to the pure primary seismic pulse, noting that the part of the pulse which travels with the velocity characteristic of the transmitting material is that point at which all the component frequencies are in phase, i.e., the centre peak (or trough, if the phase is inverted on reflection). Ideally this point of maximum amplitude should always be picked for a reflection time, and it should also be picked when determining average velocities to depth. The position of the first peak or trough relative to the centre of the pulse varies, of course, with the shot-point conditions, the travel time, and the geophone-ground coupling. Thus, with a *distortionless* seismograph, the picking of the first leg causes mis-ties of correlation between records shot with different shot-hole conditions, mis-alignments from differently planted geophones, and errors of time interval between reflections on the same record.

When filtering of the input signal must be introduced in order to reduce the noise, and character distortion of the form just discussed occurs in the filters, it is customary to pick the first trough of the resultant waveform. This is because the time of the first significant trough approximates to that of the centre of the input pulse (or, at least, it did before filter slopes became as steep as those now in use); consequently it is reckoned wiser to associate the pick with a travel time which is nearly correct than to accept a later pick which might yield better correlation. There are two other points which must be recognized when the picking is done on first troughs: that one can pick only the first *visible* trough (this is often actually the second, since the first may be small), and that there will be many reflections from interfaces where the velocity contrast will be such as to invert the pulse – the pick will then be, in fact, on the first peak.

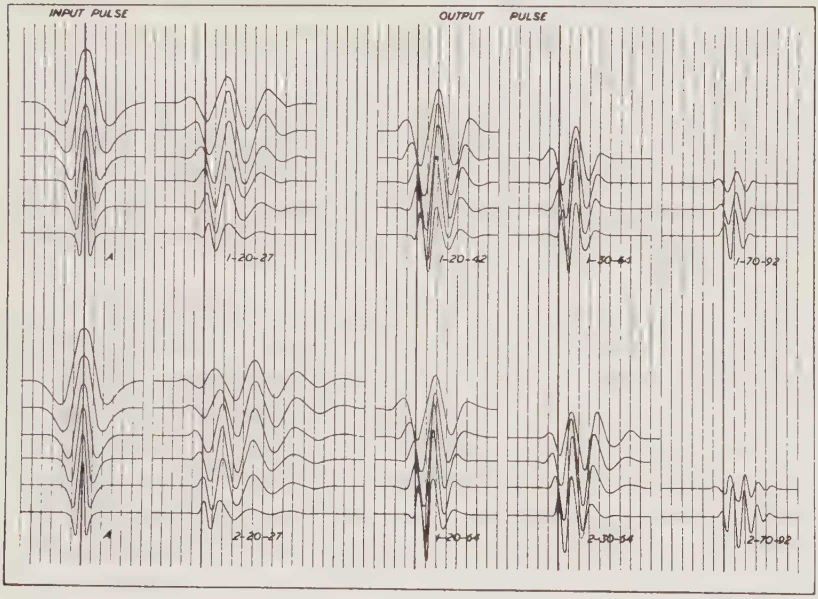

Fig. 7. Showing the effect of the filter response on pulses of varying breadth.

Figure 7 shows, for each of eight filter settings, the effect of the filter response on primary pulses of varying breadth. The peak frequencies of the six pulses range from 17 to 71 c.p.s.; the time of the pulse centre is represented by a heavy line for each filter illustration. All the pulses are inverted, relative to the previous illustrations, in order to accord with the convention of downward-breaking first arrivals. Features which emerge form a consideration of this figure are as follows:

(a) For each filter setting, a phase can be specified for which there is a substantially constant time delay from the centre of the input pulse, whatever the breadth of the latter. Thus for the 1-20-27 filter setting the second peak of each waveform occurs 23 milliseconds after the centre of the pulse, for the 2-20-27 filter the phase is the second trough and the delay is 33 milliseconds, for the 1-20-42 the phase is the second peak and the delay is 19 milliseconds, and so on.

(b) The phase of constant time delay, with constant-K filters, is not always associated with the maximum amplitude of the pulse. If the filter pass-band cuts across the high-frequency side of the pulse spectrum the maximum amplitude follows the phase of constant time delay, if it cuts the low-frequency side the maximum amplitude precedes the phase of constant time delay. The maximum amplitude of the filtered pulse has restricted significance if it cannot be guaranteed that the filter setting is approximately correct for the pulse spectrum This guarantee cannot always be given, since, if the noise spectrum should be peaked for any reason, the "best" filter setting may be to one side of the pulse spectrum.

(c) Although the use of double-section low-pass filters is not illustrated in Figure 7, it is clear from Figure 2 that the delays then associated with the phase of constant time delay may be of the order of 70 milliseconds.

(d) The time relation between the first troughs of input pulses of different breadth is not preserved in the first troughs of corresponding filtered pulses. In fact, it is not preserved anywhere.

All this places the reflection seismologist in a quandary: where should a reflection pick be made? It also provides the reason for the great current interest in different forms of filtering, particularly in correlation and selective sampling methods (Jones, 1954 and 1955, MIT Geophysical Analysis Group, 1954 and 1955, Swartz, 1954, Wadsworth, 1953) and to a lesser extent in constant time-delay electrical filters. Perhaps at this point a digression would be warranted, to show what can be done when the unfiltered seismogram is recorded on magnetic tape. First, is it clear that if, on a good reflection, the form of the output pulses on a number of different filter settings can be compared, then it is possible to reconstruct the pure input pulse from them, completely specified in time and breadth. Second, without this procedure it is possible to eliminate the time error altogether by playing the tape once forward and once backward, through appropriate filters, or twice forward with an inverted filter operator the second time. The object of a constant time-delay electrical filter should perhaps be mentioned also; this ensures that the maximum amplitude of the output pulse *does* bear a fixed time relation to the maximum amplitude of the input pulse.

But many reflections are yet to be picked on records shot with conventional filters. There are four courses open: to pick the first trough, to pick the peak or trough nearest to the maximum envelope amplitude and to subtract a filter correction from the observed time, to pick the phase of constant time delay and to subtract that delay, or, lastly, to attempt to fit a tracing of the filter response to a pure pulse, upright or inverted, on top of the observed reflection, and thence to deduce the arrival time of the input pulse peak. Of these the fourth would probably take too long for a regular field procedure, though it may be the only method when small structures, faults and stratigraphic traps are being investigated. (It is noteworthy that this method allows positive identification of the erect or inverted nature of a reflection.) Instrumental considerations affecting the choice between the first three are as follows:

(i) If the noise is serious and, with any particular filter setting, only one and a half cycles of the reflection pulse are visible, then a pick on the first visible trough may be several cycles (perhaps 70 milliseconds) in error. Accordingly the average velocity used in computing the pick, and the spread correction, are in error. If the velocity information was obtained from the *first breaks* of a well geophone, the average velocities used are too high, and this last error is increased again when the return time is assumed equal to the downward time. Fortunately, the time errors introduced by considering first breaks for weathering velocity determinations and for weathering corrections on the record tend to nullify each other, and usually do to a few milliseconds. Nevertheless the total of the above errors can be considerable; it should be noted that the picking of the first visible trough causes the greatest time error that can arise in the picking operation.

(ii) Approximately the same considerations apply to the picking of the phase of constant time delay, which is normally the second or third peak or trough. Such a pick, when the constant time delay is subtracted, can be accurate only if the initiation of the pulse is clearly visible on at least one trace. However, it should be pointed out that if this last requirement is met (as it probably is on many good records) the method of picking the phase of constant time delay is exactly accurate. It is, of course, important that the *direction* of the initiating break should be clear in order to tell whether the pulse has been inverted on reflection; otherwise an error of one half-cycle may occur. As noted before, if the direction of initiation is not itself apparent, it can be inferred by fitting a trace of the filter pulse response on top of the reflection.

(iii) If the maximum amplitude is picked, however, the picking error is unlikely to be more than one half-cycle *whatever the noise level*. The only problem then is the accuracy of the delay correction applied. When the noise spectrum is flat and the filter is suited to the pulse spectrum, the delay correction will be exact; if not, an error of one half-cycle may occur with shallow-cut filters and one cycle (or rather more in unlikely extreme cases) with steep-cut filters.

(iv) Under noisy conditions, therefore, the time error occurring when maximum amplitudes are picked and time-corrected is less than when the pick is made on first troughs. Further, the maximum-amplitude method has all the advantages associated with time measurements on the centre of the pure pulse.

(v) The maximum-amplitude method is also best suited to conditions where two reflections are closely spaced. Thus a first-trough method requires that two reflections should be seperated by an obvious change of phase before there is any assurance that the second pick is anywhere near the centre of the second wavelet; with narrow filters this change of phase will, of necessity, be smoothed out. Thus some geophysicists are driven to picking every trough; this results in geological confusion and depth information which is of little value. On a maximum-amplitude picking method, however, a train of waves need show only a maximum amplitude, then a slight decrease, and then another maximum, to warrant just two clear-cut picks, neither of which can be greatly in error when time-corrected. If a train of waves longer than the known single-pulse response shows no decrease in amplitude, then a pick when it attains the maximum and another just before it decreases will furnish a good working approximation to the truth.

It must be mentioned here that the recognition of maximum amplitudes can be correct only when there is no distortion of relative amplitudes in the a.g.c.; this will now be discussed.

DISTORTION OF CHARACTER AND RELATIVE AMPLITUDES IN THE A.G.C.

It is well known that the amplitude of any signal reproduced through a conventional amplifier fitted with a.g.c. is determined partly by its own magnitude and partly by the preceding signal, rectified and integrated over past time. Newcomers to seismograph techniques are often puzzled by this. In brief explanation it may here be said that the characteristic required of the amplitude-controlling device is that it shall preserve the amplitude difference between a reflection and the noise on either side of it (thereby assisting identification of the reflection) while contriving to eliminate the enormous amplitude difference between the two ends of the record. This cannot be done by an operation actuated by the instantaneous amplitude; the result of such an operation would be either "clipping" (in which excursions beyond a certain amplitude are cut off, thus destroying their character completely) or a trace on which the character is preserved but there still exists a marked difference in amplitude between the ends of the record. By varying the *actual gain* of the amplifier, however, according to the signal level integrated over a duration of past time short relative to the length of a record but long relative to the time of a reflected pulse, this rather stringent control requirement can be met.

The factors affecting the duration over which the integration is made (i.e., the speed of the a.g.c. action) may be discussed in the light of the following considerations.

(a) The concept of controlling the gain of an amplifier by the signal level integrated over past time implies two variables—the a.g.c. attack time, which is a measure of the rate at which the gain decreases to its equilibrium value when the signal increases, and the a.g.c. release time, which is a measure of the rate at which the gain increases when the signal decreases.

(b) If the a.g.c. attack time is very short, the gain of the amplifier will be reduced very quickly when the signal level is increased by the advent of a reflection, and after the first half-cycle or so the reflection will be reduced to the amplitude of the preceding noise. It is therefore apparent that if amplitude contrasts are to be maintained the attack time must be of the same order as the time of a reflection pulse. From the foregoing remarks on character distortion it is evident that a difficulty exists here in deciding what is the time truly involved. If the pure primary pulse is observed, then the answer is straightforward; if the pulse is longer by reason of interference between primary pulses then the attack time should be longer also, but if the pulse is longer by reason of character distortion in the filters then it may be that the attack time should not be longer. This point is discussed further under (j) and (k) below.

(c) A short attack time is essential if the a.g.c. alone is to compress high amplitudes adequately in the very early part of the record. With modern presuppression techniques, of course, this is not so important. A short attack time is also indicated if a reflection pulse has very high amplitude; otherwise the output amplitude will be such as to cause traces to overlap to the point of illegibility.

(d) If the a.g.c. release time is very short, the gain of the amplifier will be increased very quickly as the last cycle of a reflection pulse dies away, and so no amplitude contrast will exist between the reflection and the noise which follows it. Therefore the release time must be long compared to the time from the peak to the end of a reflection pulse. If it is too long, however, the gain of the amplifier will still be materially reduced when the next reflection is recorded and so the two reflections will not be reproduced in their correct amplitude relationship.

(e) It is therefore apparent that considerable distortion of relative amplitudes can occur in the a.g.c. if the attack and release times are not optimum for the circumstances.

(f) The optimum attack time (determined by the length of the reflection pulse) then depends, in the simple case, on the travel time and the characteristics of the shot point; in the complex case, it also depends on the nature of those small reflector separations which can yield reinforcing reflected pulses. The optimum release time (determined, above a certain minimum, by the time separation of reflections) depends largely on the stratigraphy. There is therefore no intrinsic connection between these optimum times, and ideally they should be independently variable. In practice they are usually linked, being variable together; while this is adequate for the general case, special applications may demand greater flexibility.

(g) Since the a.g.c. is essentially a non-linear device, its speed of operation must depend on the signal level. This means that both a.g.c. times will be less at the beginning than at the end of a record; since the reflection pulse breadth changes in the same way this variation is desirable in the case of the attack time and often tolerable in the case of the release time. It still remains true, of course, that different parts of the record may be best suited by different settings of the a.g.c. time controls.

(h) All the foregoing remarks apply to the case where there is a considerable signal-to-noise ratio, i.e., the reflection amplitudes (after filtering, normally) are high relative to the noise which precedes and follows them. If this is not so, and the reflections in the filtered but uncontrolled signal are recongnisable solely by alignments, then a change in the attack or release times will produce little or no effect (provided they are long relative to the longest wave period on the record, which is normally so).

(i) It should also be pointed out that, even when a short attack time reduces the reflection amplitude to the level of the preceding noise, the signal-to-noise ratio *within the reflection pulse* is unaltered by the a.g.c.

(j) In many conventional amplifiers with only one a.g.c. loop, the low-pass filter is between the a.g.c. take-off point and the control point. In such cases, the attack time will depend (to an extent which may be significant if a very fast attack is desired) on the time delay occurring in the filter and, consequently, on the filter setting and slope. For normal attack-time requirements, however, this effect is self-compensating; the longer delay in the filter will produce a pulse which requires a long attack time, and this will be automatically furnished.

(k) On the other hand, a narrow filter band-width will, as we have seen, lengthen the reflected pulse considerably; the effect of this on the a.g.c. is to increase the *apparent* release time.

There is some difficulty in illustrating all these effects in a manner which is not artificial; particularly is it difficult to illustrate what is happening to the noise. Probably the best method is to use a noise source of very high frequency and a galvanometer whose response is down to about one quarter at this frequency; the effect of the a.g.c. on the noise would then be represented by the thickness of the galvanometer trace, while the noise itself would not distort the form of the pulse used. However, for the present illustrations the effect on the noise is not shown; the noise used is of a very high freqeuncy, so that it does not show at all on the record, and is employed at a level equal to the maximum pulse amplitude for the records showing low signal-to-noise ratio and at a level one-third of the minimum pulse amplitude for those showing high signal-to-noise ratio.

Figure 8 then shows that an attack time which will allow substantially correct reproduction of a single pulse may be far too short for a double pulse, the second being practically eliminated.

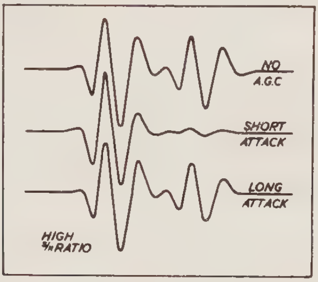

Fig. 8. Showing the effects of a short and of a long attack time of the automatic gain control on a double pulse.

Figure 9 demonstrates the effect of variations in the release time; it will be noted that a reflection pulse can suffer on account of a strong reflection which preceded it by a considerable period. On the basis of this figure, it might be thought that a very short release time is always desirable; this is not necessarily so, since the noise (as well as subsequent reflections) is thereby quickly elevated to a level near to that at which the strong reflection is recorded.

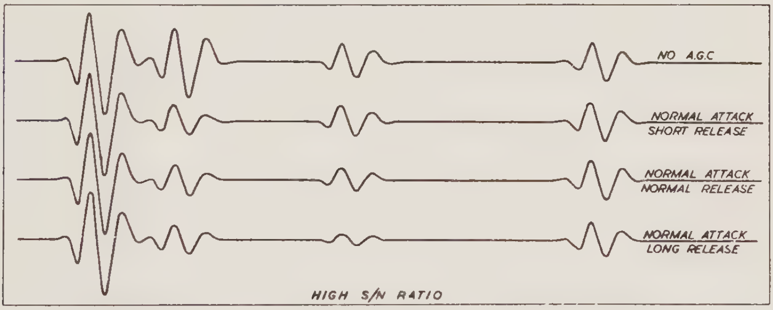

Fig. 9. Showing the effect of variations of the release time of the automatic gain control.

Figure 10 illustrates, on the second trace, the distortion of relative amplitudes which occurs early in the record when the signal-to-noise ratio is high; it will be noted that both attack and release times are short. The third trace shows the same signal-to-noise ratio as it would appear at the end of the record; both attack and release times are long. If the signal-to-noise ratio is low, however, as on trace 4, the relative amplitude reproduction is practically correct.

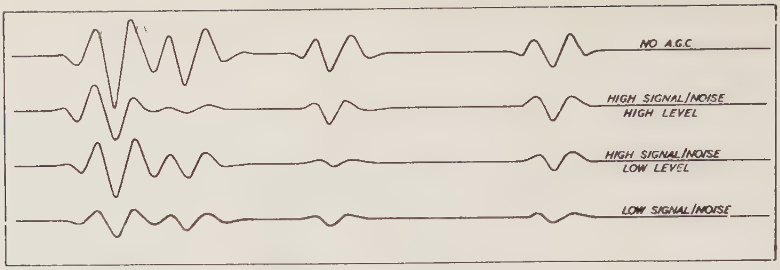

Fig. 10. Showing the distortion of relative amplitudes.

Figure 11 demonstrates the effects referred to in (j) and (k) above. The first trace shows the output with a wide-band filter; both attack and release times are short. The second trace represents the same state of affairs except that a narrow ringing filter is used; both attack and release times are lengthened.

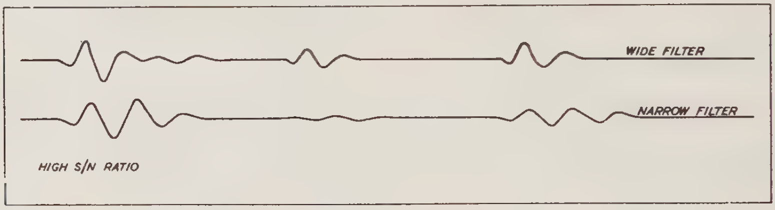

Fig. 11. Showing the effect of the filter bandwidth on the attack and release times.

A note should be appended here relating the discussion of distortion of relative amplitudes in the a.g.c. to that of picking reflections. It may appear that the case for the picking of maximum amplitudes is vitiated by the remarks above. This is not so; while care should be taken to ensure that the attack time is always adequately long, it should be noted that these amplitude distortions occur only when the signal-to-noise ratio is high, and under these conditions it is possible to pick the phase of constant delay. It is when the signal-to-noise ratio is low that it is necessary to pick maximum amplitudes, and then distortion in the a.g.c. is small.

HARMONIC AND INTERMODULATION DISTORTION

It is a well known fact that an ordinary electronic amplifier exhibits harmonic distortion when large signals are applied to it—that is to say, the output signal becomes distorted as though new signals, whose frequencies are integral multiples of that of the input signal, had been added in the amplifier. The magnitude of this effect is customarily stated in terms of the total harmonic content of the output as a percentage of the fundamental output; in a conventional seismic amplifier this may be mainly second harmonic or mainly third harmonic, according to the type. Figures of more than 5% are encountered in some early seismic amplifiers for low frequency inputs of the order of 100 millivolts.

It is evident that the addition of a small fractional component of frequency 120 c.p.s. to a reflection of peak frequency 40 c.p.s. is not likely to cause any trouble; nevertheless harmonic distortion can become exceedingly important in areas where there is serious ground roll. Riggs (1954) has reported cases where the measured particle velocity occasioned by ground roll was 0.05 ins./sec., while that associated with reflections was between one-fifth and one-hundredth of this. In the extreme case, and assuming a ground roll frequency of 10 c.p.s., a reflection peak frequency of 40 c.p.s., and a single conventional geophone of natural frequency 10 c.p.s. damped to 0.7 of critical, the input to the amplifier will consist of ground roll of peak amplitude 50 millivolts and reflection signal of peak amplitude 0.75 millivolts. The use of a multiple geophone pattern designed to optimise the reflected signal (Muir and Hales 1955), may increase the corresponding electrical signal to perhaps 3 millivolts but will increase the ground roll signal to perhaps 150 millivolts, while the use of one designed to minimise ground roll may be seriously unfavourable to the reflected signal (Hales and Edwards, 1954). It is noted that in this quoted case a high-pass filter of slope 24 dB/octave will satisfactorily eliminate the steady ground roll from the record, but it is also noted that if third harmonic distortion to the extent of 5% at 150 millivolts input occurs before this filtering, the reflections will be seriously obscured by 30 c.p.s. signals which constitute no part of the original ground motion.

Fortunately, the harmful consequences of ground roll from the point of view of harmonic distortion are more easily rendered negligible than those from the point of view of character distortion. The modern seismic amplifier, by suitable distribution and protection of those units wherein harmonic distortion can arise, is capable of handling an input of the order of 1 volt without the introduction of appreciable harmonics. However, many seismograph systems now in use do not have this facility, and so the effects of harmonic distortion on the record are here illustrated. Figure 12 (a) shows the output of a conventional amplifier (which would be quite adequate for areas where ground roll is not a problem) when the input is a signal of 15 c.p.s. at a level of 100 millivolts; the distortion is mainly second harmonic. Figure 12 (b) shows another conventional amplifier into which is injected 10 c.p.s. at 100 millivolts; the distortion is mainly third harmonic.

In some areas where ground roll is particularly severe, it is associated with quite low frequencies. This gives rise to an effect which, in removing the obvious periodicity of the harmonic signal, may make this form of distortion even more difficult to detect on the record. If the amplitude of the ground roll signal after filtering is sufficient to contribute materially to the a.g.c. action, and its frequency is of the same order as the time constant of the a.g.c. at that signal level, then both the reflected energy and the harmonics of the ground roll will be amplitude modulated by the ground roll itself. The effect is illustrated in Figure 12 (c); a steady signal which is well into the a.g.c. is suddenly augmented by a high-amplitude signal of 10 c.p.s., and the pattern of the resultant distortion is evident. Since these high ground-roll amplitudes may persist only for a few cycles, and since this illustration is extreme, the change in the nature of the trace may not be obvious despite the fact that the trace has become substantially worthless. It is clear that this form of distortion is serious only when the ground-roll amplitude is high and when either its frequency is very low or the a.g.c. action is fast.

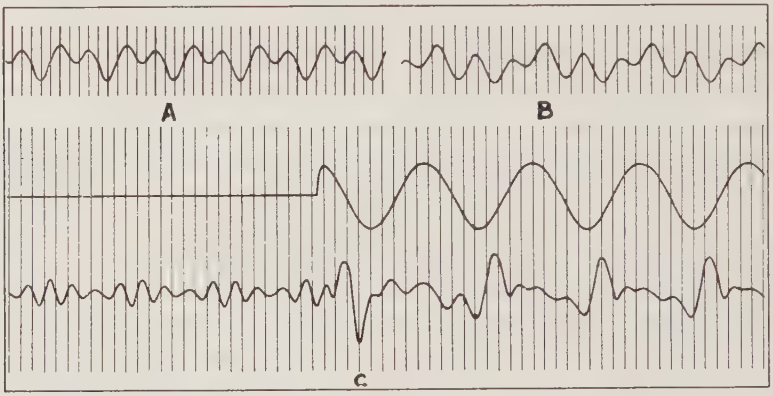

Fig. 12. *a*. Showing second harmonic distortion. — *b*. Showing third harmonic distortion. — *c*. Showing amplitude modulation caused by the ground roll.

On account of the limited frequency range normally of interest in a seismic amplifier, intermodulation distortion and distortion involving harmonics higher than the third or fourth are not ordinarily important. This is not the case, however, when the frequency range is extended; in modern reflection amplifiers covering as much as five octaves care must be taken, by suitable positioning of the high-pass filters and the manual and automatic gain control points, to eliminate the generation of harmonics as high as the ninth.

CONCLUSIONS

The inferences which can be drawn from this discussion affect the picking of reflections, the grading of reflections, and the actual shooting of records in the field. We turn now to the grading of reflections.

Grading systems can follow two schemes: they can attempt to compensate for instrumental distortion and thereby to grade the original earth motion, or they can ignore all such distortions and grade the record as it is observed. Bearing in mind that the object of seismic exploration is to obtain information of *geological* significance, there can be little doubt that, ideally, a grade on the original ground motion is desirable. However, while such a grading is perfectly feasible by electronic means it is practically impossible by eye. With such a grading system, the criteria on which the value of the event would be graded are:

(i) peak reflection amplitude relative to r.m.s. noise (or some similar amplitude criterion),

(ii) correlation, i.e., the exactness with which *an entire pulse* on one trace can be found on another, and

(iii) alignment.

It might be argued that the first and third of these are interrelated, that good alignment cannot exist unless there is good elevation. While this is true (over a considerable number of traces) it is also true that the absolute amplitude of a reflection pulse observed with a velocity-sensitive geophone, multiplied by the travel-time raised to the power of five-halves, represents valuable geological information. Although the elevation of the reflection over the noise does not quite give this information, the amplitude criterion should be retained. The second criterion, correlation, has no visual equivalent to the exact information-theory expression, and so the complete solution to the grading problem is to be found, with that of the time distortion problem, in the future use of electronic record computers.

If then, at the moment, we are not able to grade the earth motion strictly according to these criteria, should we attempt to compensate for the instrumental distortion visually? On the question of elevation it is feasible, using an a.g.c. level indicator; on the question of character correlation it is at best extremely difficult. Therefore no attempt to compensate for instrumental distortion fully could represent a practical field grading method.

Consequently we are reduced to grading the record as it is observed. The question then arises: are the above criteria still valid?

Elevation, or reflection amplitude relative to noise, remains a valid criterion provided that the record has been shot with adequately long a.g.c. attack and release times.

Correlation, however, in its approximate visual forms of character, essential copy, envelope and duplication (Gaby, 1947), has very much less significance with modern steep-cut filters than it had in years past. Indeed, with a narrow, steep filter a wide variety of input pulses, provided they had amplitude, could appear much the same on the record.

Alignment, on the other hand, represents the one reflection attribute which can never be distorted, but only improved, by the instruments. It therefore retains the fullest significance as a grading criterion, and it is necessary only to caution concerning over-mixing and its geophone-pattern equivalent.

In any system designed to grade the record as it stands, therefore, the major emphasis should be on the criterion of alignment and a minor emphasis on that of elevation. No stipulation should be made concerning the length of the reflection pulse, for valid reflections from two interfaces may interfere to produce a waveform which consists, substantially, of one cycle only (Ricker, 1953). Through a very wide filter this may appear in its original form, while through a narrow, steep filter it may be reproduced as four or five complete cycles. Further, such a stipulation would demand a different grading system, as well as a different picking system, when the geophone is of piezoelectric or capacity type.

One other point concerning grading should be mentioned: that with a picking system using maximum amplitudes or phases of constant delay it becomes feasible to allot a *time certainty* grade to a reflection.

Finally, the inferences of this discussion on the shooting of records in the field should be stated. The wide flexibility of modern reflection instruments may tempt the operators to experiment with all manner of settings, but it should be clearly understood that the presence of more controls does not necessarily indicate that their use is justified. The precepts of reflection shooting laid down in the early years of the art apply now as fully as ever they did; ground roll should be eliminated as far as possible by correct charge and depth conditions (rather than by steep-cut filtering), short a.g.c. attack and release times should not be used indiscriminately, and filter settings narrow enough to impair resolution should be avoided. Records should, in the general case, be shot for *the maximum information*; a certain minimum criterion of reflection acceptance should be established, and instrumental settings used which will furnish on the record the maximum number of these minimally acceptable reflections. In particular, the settings used should not be specifically chosen to improve reflection grades associated with a criterion of envelope duplication, for this will inevitably lead to narrow filters and thereby to a loss of real information. An even greater mistake, of course, is to design instruments around such a grading system; the instruments should be designed to maximise the information obtainable, and the grading system should be designed after the performance of the instruments is known.

ACKNOWLEDGMENTS

The author takes pleasure in recording his indebtedness to the directors of Seismograph Service Limited, for permission to publish this paper, to Mr. G. Harbron and Mrs. G. Whittle, who prepared the illustrations, and to Mr. Francis Muir, for the benefit of many stimulating discussions.

REFERENCES

Born, W. T. and Kendall, J. M., 1941, "Application of the Fourier Integral to some Geophysical Instrument Problems", Geophysics, VI, 2, p. 105.

Gaby, P. P., 1947, "Grading System for Seismic Reflections and Correlations", Geophysics, 1947, XII, 4, p. 590.

Hales and Edwards, 1955, "Some Theoretical Considerations on the Use of Multiple Geophones Arranged Linearly along the Line of Traverse", Geophysical Prospecting III, 1, p. 65.

Jakosky, J. J., 1952, "Frequency Analysis of Seismic Waves", Geophysics, XVII, 4, p. 721

Jones, H. J. and Morrison, J. A., 1954, "Cross-correlation Filtering", Geophysics, XIX, 5, p. 660.

Morrison, J. A., Sarrafian, G. P. and Spieker, L. J., 1955, "Magnetic Delay Line Filtering", Geophysics, XX, 4, p. 745.

MIT Geophysical Analysis Group, 1954, Report No. 6.

——, 1955, Report No. 9.

Muir, F., and Hales, F. W. ,"A Rational Approach to the Design of Electrical Filters and of Shothole and Geophone Patterns in Seismic Reflection Prospecting", Geophysical Prospecting, III, 4, p. 350.

Piety, R. G., 1942, "Interpretation of the Transient Behaviour of the Reflection Seismograph", Geophysics, VII, 2, p. 123.

Ricker, N., 1951, "The Form and Laws of Propagation of Seismic Wavelets", Proc. Third World Petroleum Congress.

——, 1953, "Wavelet Contraction, Wavelet Expansion, and the Control of Seismic Resolution", Geophysics, 1953, XVIII, 4, p. 769.

Riggs, E. D., 1954, "Field Measurements of Reflection and Surface Wave Amplitudes", read at 8th Annual Midwestern Meeting of S.E.G.

Swartz, C. A. and Sokoloff, V. M., 1954, "Filtering Associated with Selective Sampling of Geophysical Data", XIX, 5, p. 402.

Wadsworth, G. P., Robinson, E. A., Bryan, J. G. and Hurley, P. M., 1953, "Detection of Reflections on Seismic Records by Linear Operators", Geophysics, XVIII, 5, p. 539.

Washburn, H. W., 1937, "Experimental Determination of the Transient Characteristics of Seismograph Apparatus", Geophysics, II, 3, p. 243.

ON SEISMIC WAVE PROPAGATION IN ANISOTROPIC MEDIA WITH APPLICATIONS IN THE BETUN AREA, SOUTH SUMATRA*

BY

A. H. KLEYN **

ABSTRACT

An analytical solution of refraction problems in anisotropic media is based on the expression for the refraction angle in an uniaxial anisotropic medium with vertical axis and elliptic anisotropy. The theory is applied to a test on the anisotropic behaviour of the sedimentary section in the vicinity of Betun, South Sumatra, employing the results from a refraction profile, a well velocity survey and a radial well survey. It is concluded that, in the Betun area, the anisotropy factor is variable with depth. Its maximum value may be as high as 1.15 in the middle part of the section.

INTRODUCTION

During recent years experimental studies of elastic anisotropy have been made by several investigators. The results of those studies indicate that elastic anisotropy plays an important part in sedimentary rocks of various ages and that, as a rule, seismic wave velocities are higher parallel to the stratification of bedded formations than at right angles thereto.

As to the nature of this velocity anisotropy, it can be concluded from field observations by Ricker (1951) and Cholet and Richard (1954) that, in sedimentary sections, the functional relationship between velocity and direction is an elliptical one. Ricker (1951) showed that horizontal velocities in Cretaceous shales in Colorado are 15 to 18% higher than the corresponding vertical velocities, whereas according to Cholet and Richard (1954) the anisotropy factor of Cretaceous sands and shales in the Sahara region amounts to 1.09.

The present paper is concerned with some theoretical aspects of refraction problems in anisotropic sections and with an analysis of the anisotropic behaviour of the sedimentary section near Betun, South Sumatra.

The refraction theory developed in the subsequent paragraphs is based on the assumptions that the velocity stratification is horizontal and that the successive strata are uniaxial anisotropic media with elliptic anisotropy. In this case the influence of the anisotropy of a layer can be expressed by means of the relation:

---

* Presented at the Ninth Meeting of the European Association of Exploration Geophysicists, held in London, 7-9 December 1955.

** Standard Vacuum Petroleum Company, Sungei Gerong.

$$V_\theta^2 = V_h^2 V_v^2 (V_h^2 / \cos^2\theta + V_v^2 \sin^2\theta \quad . \; . \; . \; . \; . \; . \; . \; . \quad (1)$$

where V_h and V_v are the horizontal and vertical velocities and V_θ is the velocity in the direction θ (θ being the angle between the wave path and the vertical).

THEORETICAL CONSIDERATIONS

Refraction angle

It can be demonstrated with the aid of Fermat's principle of least travel time that the critical refraction angle θ_a in an anisotropic medium, defined by equation (1), is given by the relation:

$$\tan\theta_a = KV_h / (V_a^2 - V_h^2)^{\frac{1}{2}} \quad . \; . \; . \; . \; . \; . \; . \quad (2)$$

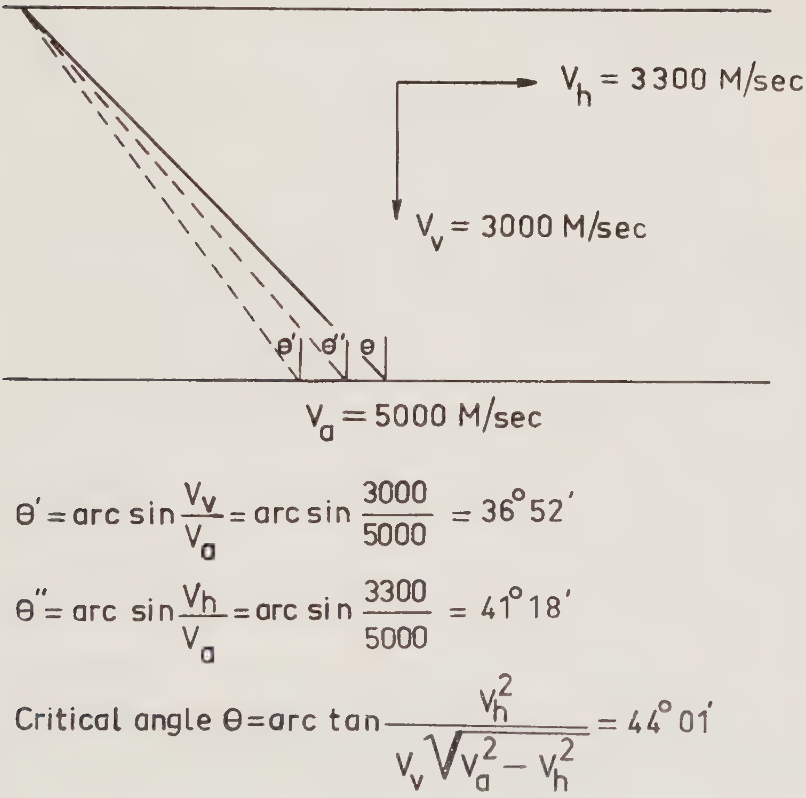
$V_h = 3300$ M/sec
$V_v = 3000$ M/sec
θ'
θ''
θ
$V_a = 5000$ M/sec
$\theta' = \arcsin \frac{V_v}{V_a} = \arcsin \frac{3000}{5000} = 36°52'$
$\theta'' = \arcsin \frac{V_h}{V_a} = \arcsin \frac{3300}{5000} = 41°18'$
Critical angle $\theta = \arctan \frac{V_h^2}{V_v \sqrt{V_a^2 - V_h^2}} = 44°01'$

Fig. 1. Critical angle in an anisotropic medium overlying a high velocity refractor.

where V_a is a parameter representing the apparent refractor velocity and K is the anisotropy factor, defined by: $K = V_h/V_v$.

Figure 1 illustrates the effect of anisotropy on the obliqueness of a refracted path in an anisotropic medium overlying a non-dipping high velocity refractor.

Horizontal displacement

Consider a series of n layers with thicknessess dz_i, horizontal velocities V_{ih} and anisotropy factors K_i. From equation (2) it follows that the horizontal component dx_i of a wave path segment in a layer i can be expressed by;

$$dx_i = K_i \, dz_i \, V_{ih}/(V_a^2 - V_{ih}^2)^{\frac{1}{2}} \quad . \; . \; . \; . \; . \; . \; . \; . \; . \quad (3)$$

where V_a is the apparent velocity associated with a particular wave path. Accordingly, the horizontal displacement from the shot point of a point at a depth $z = \sum_{i=1}^{n} dz_i$ and on a wave path characterized by an apparent velocity V_a can be expressed by:

$$x = \sum_{i=1}^{n} dx_i = \sum_{i=1}^{n} K_i \, dz_i \, V_{ih} / (V_a^2 - V_{ih}^2)^{\frac{1}{2}} \quad . \; . \; . \; . \; . \quad (4)$$

Travel time

Using the same notations as in the previous paragraph, it can be demonstrated with the aid of equations (1) and (2) that the travel time dt_i along a wave path segment in a velocity layer i is given by:

$$dt_i = K_i \, dz_i \, V_a \, / \, V_{ih} \; (V_a^2 - V_{ih}^2)^{\frac{1}{2}} \quad . \; . \; . \; . \; . \; . \; . \; . \; . \quad (5)$$

From equation (5) it follows that the travel time along a wave path, characterized by an apparent velocity V_a, to a point at a depth $z = \sum_{i=1}^{n} dz_i$ equals:

$$t = \sum_{i=1}^{n} dt_i = \sum_{i=1}^{n} K_i \, dz_i \, V_a \, / \, V_{ih} \, (V_a^2 - V_{ih}^2)^{\frac{1}{2}} \quad . \; . \; . \; . \; . \; . \quad (6)$$

Equations (4) and (6) constitute the parametric equations for either a time depth curve related to a well velocity survey or a travel time curve related to a radial well survey. In the first case the depth z is a variable and the distance x is constant. In the second case the distance x is the variable and the depth z is constant. The parameter V_a corresponds to the apparent velocities on the travel time curve from a radial well survey.

Refraction profiles

With the aid of equations (4) and (6) analytical expressions can be derived for the various segments of the travel time curve over an anisotropic section with a certain number of horizontal velocity discontinuities. Thus, the general expression for the surface-to-surface travel time of a wave that has penetrated to a layer n can be written as:

$$t_n = x/V_{nh} + 2 \sum_{i=1}^{n-1} K_i \, dz_i \, (V_{nh}^2 - V_{ih}^2)^{\frac{1}{2}} / V_{ih} V_{nh} \quad \ldots\ldots (7)$$

Accordingly, the zero intercept or delay time, relative to the refractor n becomes:

$$t_{on} = 2 \sum_{i=1}^{n-1} K_i \, dz_i \, (V_{nh}^2 - V_{ih}^2)^{\frac{1}{2}} / V_{ih} V_{nh} \quad \ldots\ldots\ldots (8)$$

Equations (7) and (8) show that the thickness of a certain velocity layer i, computed by neglecting anisotropy, equals the true thickness of this velocity layer times its anisotropy factor K_i. It is obvious that when K_i is unknown the refraction problem becomes ambiguous and that an infinite number of anisotropic velocity distributions may satisfy the same travel time curve.

Continuous variation of velocity with depth

A quantitative evaluation of the problem of seismic wave propagation in anisotropic media with a continuous change of velocity with depth requires the choice of two smooth velocity functions, namely one for the horizontal and one for the vertical velocity. For the linear case it is not too difficult to develop a curved path theory by integrating the expressions for the differentials of travel time and horizontal displacement (equations (3) and (5)), after inserting linear velocity functions for both the vertical and the horizontal velocities. The analytical expressions that can thus be derived for travel time, displacement, travel time curves and time depth curves are considerably more complicated than corresponding expressions valid for isotropic media. A simplification can be effected by considering sections with a constant anisotropy factor. In that case, when the horizontal and vertical velocity functions are represented by: $V_{zh} = V_{oh} + bz$ and $V_{zv} = V_{ov} + az$ respectively, the following relation obtains: $K = V_{oh} / V_{ov} = b/a$, or: $bV_{ov} = aV_{oh}$.

With the supposition of a constant anisotropy factor and a linear velocity distribution the functional relationship between horizontal displacement and depth becomes:

$$x = 1/a \left[\sqrt{V_a^2 - V_{oh}^2} \pm \sqrt{V_a^2 - (V_{oh} + bz)^2} \right] \quad \ldots\ldots (9)$$

Equation (9) shows that the wave paths in an anisotropic section with a linear velocity distribution and a constant anisotropy factor are parts of ellipses.

Under the conditions such as specified above the travel time curve over an anisotropic section can be represented by the following relation:

$$t = 2/a \sinh^{-1} (ax/2V_{oh}) \quad \ldots\ldots\ldots\ldots \quad (10)$$

which expression is precisely the same as the one derived by Slotnick (1936) for the travel time curve over an isotropic section with a linear velocity distribution.

When the relation $bV_{ov} = aV_{oh}$ does not hold, then the travel time curve cannot be satisfied by a linear velocity distribution in an isotropic section. However, it can be demonstrated that for $bV_{ov} \approx aV_{oh}$, the travel time curve can still be approximated very closely with the aid of a linear velocity distribution in an isotropic section.

It is found by experience that travel time curves over sedimentary sections in Tertiary basins can often be approximated closely with the aid of linear velocity functions. This would imply that in these cases the vertical, as well as the horizontal, velocity increases linearly with depth. A different situation occurs in the vicinity of Betun, South Sumatra. Here, though the velocity survey of the well Betun No. 1 shows that the vertical velocity in the Tertiary section increases linearly with depth, any attempt to interpret the Betun travel time curves with the aid of a linear velocity function fails completely. It will be shown in the next section that the shape of the Betun travel time curves can be explained satisfactorily through the conception of an irregular change of the horizontal velocity with depth and a linear increase of the vertical velocity with depth.

ANISOTROPY STUDIES IN THE BETUN AREA, SOUTH SUMATRA

Vertical velocities—geological cross section

The sedimentary section in the Betun No. 1 well consists for the greater part of shales and sandy shales of Neogene age. The top of the igneous pre-Tertiary lies at 2075 meters below sea-level. The total depth of the well is 2085 meters. The time depth curve from the well velocity survey shows that, on the whole, the vertical velocity increases steadily with depth. This smooth increase of the vertical velocity is interrupted by a low velocity brown coal bed, approximately 120 meters thick at 650 meters below sea-level, and a high velocity limestone, approximately 65 meters thick at 1800 meters below sea-level. The vertical velocities of the brown coal and of the limestone amount to 1530 and 5000 m/sec respectively. In approximating the time depth relation with the aid of a smooth velocity function the appropriate corrections have been applied to account for the effects of the brown coal and limestone layers.

During the analysis of the data it became evident that even though one linear velocity function could give a fairly accurate description of the time-depth values, a better approximation of the time-depth curve could be obtained through the use of two linear velocity functions, each valid for a particular range of depths. Thus the best approximation of the time-depth relation was acquired by employing:

$$V_{zv} = 1645 + 1.00z \quad \text{for } z < 625 \text{ meters below sea-level} \quad (1a)$$

and:

$$V_{zv} = 1424 + 0.98z \quad \text{for } z > 625 \text{ meters below sea-level} \quad (1b)$$

On Table I are listed the observed and computed time values from top to bottom of the well, applying the velocity functions 1*a* and 1*b*.

Table I

Betun No. 1 well velocity survey. Comparison of observed and computed time values.

depth meters below sea-level	observed time millisec.	computed time millisec.	difference millisec.
126	074	074	000
226	131	129	002
326	182	181	001
426	232	230	002
526	277	277	000
625	321	322	001
725	386	387	001
825	431	436	005
920	478	478	000
1020	522	521	001
1120	561	561	000
1218	599	599	000
1318	636	637	001
1418	673	673	000
1508	705	704	001
1608	739	738	001
1716	776	774	002
1851	806	808	002
1951	840	839	001
2075	877	875	002

From the above analysis it can be concluded that the vertical velocity at sea level is about 1650 m/sec. The elevation in the area of the Betun No. 1 well is in the order of 10 meters above sea-level. The first breaks on reflection seismograms in the Betun area indicate a horizontal velocity of 1640 m/sec for the first consolidated layer, whereas refraction surveys indicate 1670 m/sec. Therefore it follows that, near the Betun No. 1 well, there is a very small difference, if any, between horizontal and vertical velocities near the ground surface.

During the analysis of a Betun refraction profile and the data from the Betun No. 1 radial well survey, described in the subsequent paragraphs, use has been made of a layered shale section (Table II) with a vertical velocity distribution that is commensurate with the linear velocity functions 1a and 1b. This velocity distribution also roughly conforms with the interval velocity graph from the well velocity survey.

Betun refraction profiles

Figure No. 2 depicts an observed travel time curve across the Betun No. 1 well. This refraction profile is, as far as the shale velocities are concerned, very nearly identical with other refraction profiles along traverses near or through the Betun No. 1 well. Therefore, it can safely be concluded that there is very little dip, if any, in the velocity layers of the sedimentary section in the vicinity of the Betun No. 1 well.

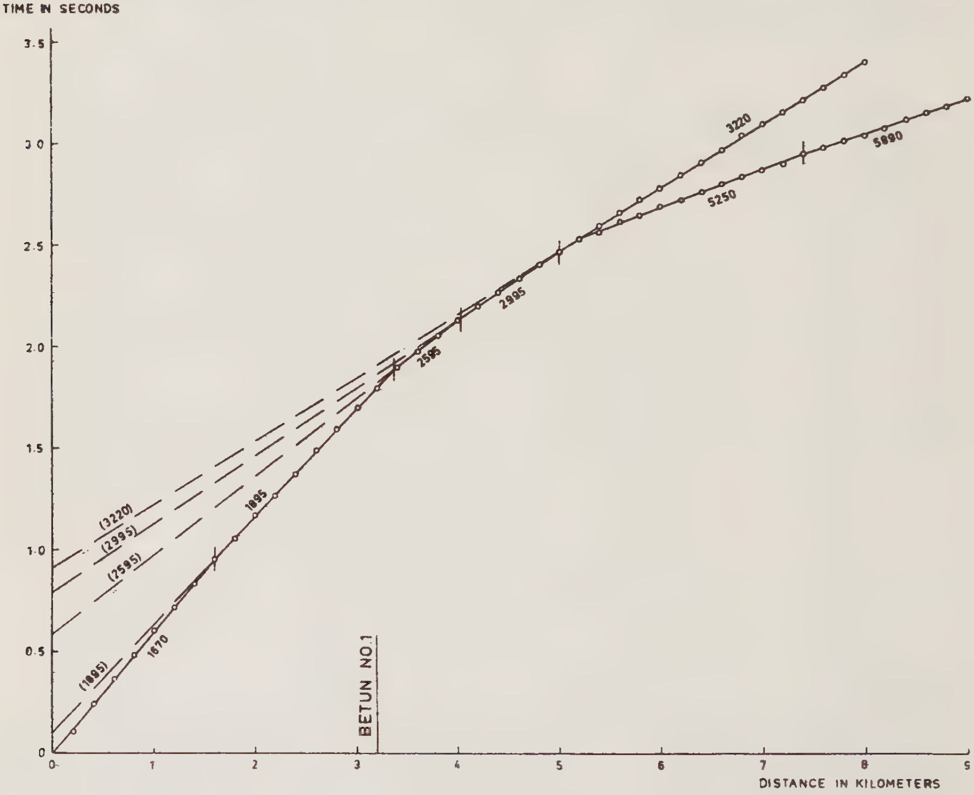

Fig. 2. Typical example of a refraction profile in the Betun area.

The observed apparent velocities relative to the sedimentary section range from 1670 to 3220 m/sec. The 3220 m/sec velocity segment is based on secondary time picks. Shale velocities higher than 3220 m/sec could not be detected with certainty.

The shape of the Betun travel time curves is characterized by the fact that the shale velocities are represented by a few straight line segments only. This condition indicates that although the vertical velocity increases continuously with depth, there is no continuous refraction of energy. It seems that, in the Betun area, critical refraction of energy occurs only at a few interfaces.

The observed arrival times of energy that has traveled along wave paths associated with apparent velocities of 2595, 2995 and 3220 m/sec are considerably smaller than the corresponding arrival times computed from the vertical velocity distribution. This indicates that the 2595, 2995 and 3220 m/sec refractors are located higher in the section than would follow from the results of the well velocity survey.

It has been shown by Hagedoorn (1954) that under favorable circumstances (clearly defined velocity layers, each represented by a straight line segment of the travel time curve) the anisotropy factors of the successive sedimentary layers can be determined through a direct comparison of refractor velocities with the corresponding vertical velocities from a well velocity survey. It is obvious that in the Betun area such favorable circumstances do not exist.

Towards solving the Betun refraction problem, it can be stated that by choosing appropriate values for the anisotropy factors of the successive velocity layers (Table II) the observed refraction data can be satisfied by several anisotropic velocity distributions. These interpretations can be obtained through the application of equations (7) or (8).

Despite the ambiguous character of the present problem it is believed that the solution presented in the upper part of Table II is a reasonable approximation of actual subsurface conditions. This solution is based on the following considerations:

1. The near surface layers are isotropic. The value of 1.00 for the anisotropy factor of the layers immediately below the weathered zone was estimated from a comparison of the apparent velocity of the first segment of the travel time curve with the vertical velocity near the top of the section.

2. The 2595 m/sec refractor is probably located below the brown coal layer. Placing the 2595 m/sec refractor higher in the section would introduce values of 1.18 or more for the anisotropy factor of the layers above the brown coal. Such values are considered too high in the upper part of Tertiary sections.

3. An assumption had to be made as to the value for the anisotropy factor of the brown coal and the layers immediately above and below thereof. By assigning a priori the value 1.06 a solution could be obtained that is characteri-

zed by an overall increase of the anisotropy factor with depth. Moreover, the interpretation in Table II suggests that the anisotropy factor between two successive refractors is constant. Thus the tentative hypothesis is advanced that, at least in the middle part of the Betun sections, critical refraction of energy occurs where the horizontal velocity, and the anisotropy factor, increase abruptly.

There is, admittedly, no satisfactory explanation regarding the lack of energy return from the layers immediately above the brown coal. Poor transmission properties of those layers may be the cause for the absence of velocity segments of apparent velocities between 1895 and 2595 m/sec.

In computing time and depth values with the aid of equation (8) calculations can conveniently be carried out by employing a set of graphs giving values for the factor $2\,(V_{nh}^2 - V_{ih}^2)^{\frac{1}{2}} / V_{ih}$ for any set of values of V_{ih} and V_{nh}. Formula (8) can then be written as:

$$t_{on}\, V_{nh} = \sum_{i=1}^{n-1} K_i\, dz_i\, A_{in}$$

where A_{in}, the "delay time" factor, equals $2\,(V_{nh}^2 - V_{ih}^2)^{\frac{1}{2}}/V_{ih}$.

Example: computation of the depth of the 2595 m/sec refractor. $t_{on} = 0.586$ sec., $V_{nh} = 2595$ m/sec.

$$t_{on}\, V_{nh} = 1521 = 1.00 \sum_{i=1}^{4} dz_i\, A_{in} + 1.06 \sum_{i=5}^{8} dz_i\, A_{in} + 1.06\, dz_9\, A_{9n}$$

$$= 794 + 631 + 1.06\; 0.84\, dz_9$$
$dz_9 = 108$ meters.

Depth of the 2595 m/sec refractor: $\sum_{i=1}^{9} dz_i = 908$ meters ≈ 900 meters.

At this depth the vertical velocity is: 2355 m/sec and the anisotropy factor is: 2595/2355 or 1.10.

A depth of 900 meters for the 2595 m/sec refractor corresponds to a value of 0.584 for the associated zero intercept time. Therefore, the above approximation results in a time error of 2 milliseconds. It is clear that this type of error can be kept arbitrarily small by using a layered section with sufficiently small depth intervals.

The upper part of Table II presents a possible solution of the Betun refraction problem. A value of 1.06 was assigned for the anisotropy factor of the brown coal and the layers immediately above and below it.

Table II

Possible interpretation of the data from a Betun refraction profile (Fig. 2) and the Betun radial well survey (Fig. 3)

depth interval meters	vertical velocity m/sec	horizontal velocity m/sec	anisotropy factor	actual zero intercept time sec	computed zero intercept time sec
0- 100	1695	1695	1.00		
100- 200	1795	1795	1.00		
200- 300	1895	1895	1.00	0.100	0.088
300- 400	1995	1995	1.00		
400- 500	2095	2221	1.06		
500- 630	2207	2339	1.06		
630- 750'	1530	1622	1.06		
750- 800	2184	2315	1.06		
800- 900	2257	2392	1 06		
900-1000	2355	2595	1.10	0.586	0.584
1000-1100	2453	2703	1.10		
1100-1200	2551	2811	1.10		
1200-1300	2649	2995	1.13	0.797	0.799
1300-1400	2747	3107	1.13		
1400-1500	2845	3220	1.13	0.908	0.913
1500-1600	2933	3050	1.04		
1600-1700	3031	3152	1.04		
1700-1750	3105	3229	1.04		
1750-1815"	5000	5000	1.00		
1815-1900	3234	3363	1.04		
1900-2000	3325	3458	1.04		
2000-2075	3410	3346	1.04		

' Brown coal " Limestone

The writer had also computed an alternative solution, obtained through the assumption of isotropic properties of the section between the ground surface and the depth of the 2595 m/sec refractor. This depth would then amount to about 800 meters and the anisotropy factors for the intervals from 800-1200 and 1200-1500 meters would be approximately 1.15 and 1.13 respectively.

Both of the above solutions indicate that, in the Betun area, the amount of anisotropy is variable with depth and that relatively high values for the anisotropy factors of the layers in the middle part of the section are necessary in order to explain the shape of the observed travel time curves.

The Betun No. 1 radial well survey

The radial survey of the Betun No. 1 well was carried out by placing a geophone on top of the pre-Tertiary basement (2075 meters below sea-level) and shooting at various distances ranging from 100 to 4500 meters in four directions from the surface location of the well. The four observed hyperbola-like travel time curves, relating to the arrival of the direct energy, are very nearly identical, indicating that in the immediate vicinity of the well the velocity stratification is practically horizontal.

The travel-time curve shown in Figure 3 was obtained by averaging the four observed travel-time curves. The portion of the travel-time curve beyond a distance of about 1500 meters from the well consists of several straight line segments, the first of which ought to be tangential to the curve shown. This portion, representing arrival times of energy that has been refracted at the high velocity basement, has no bearing on the present study and has therefore been omitted from Figure 3.

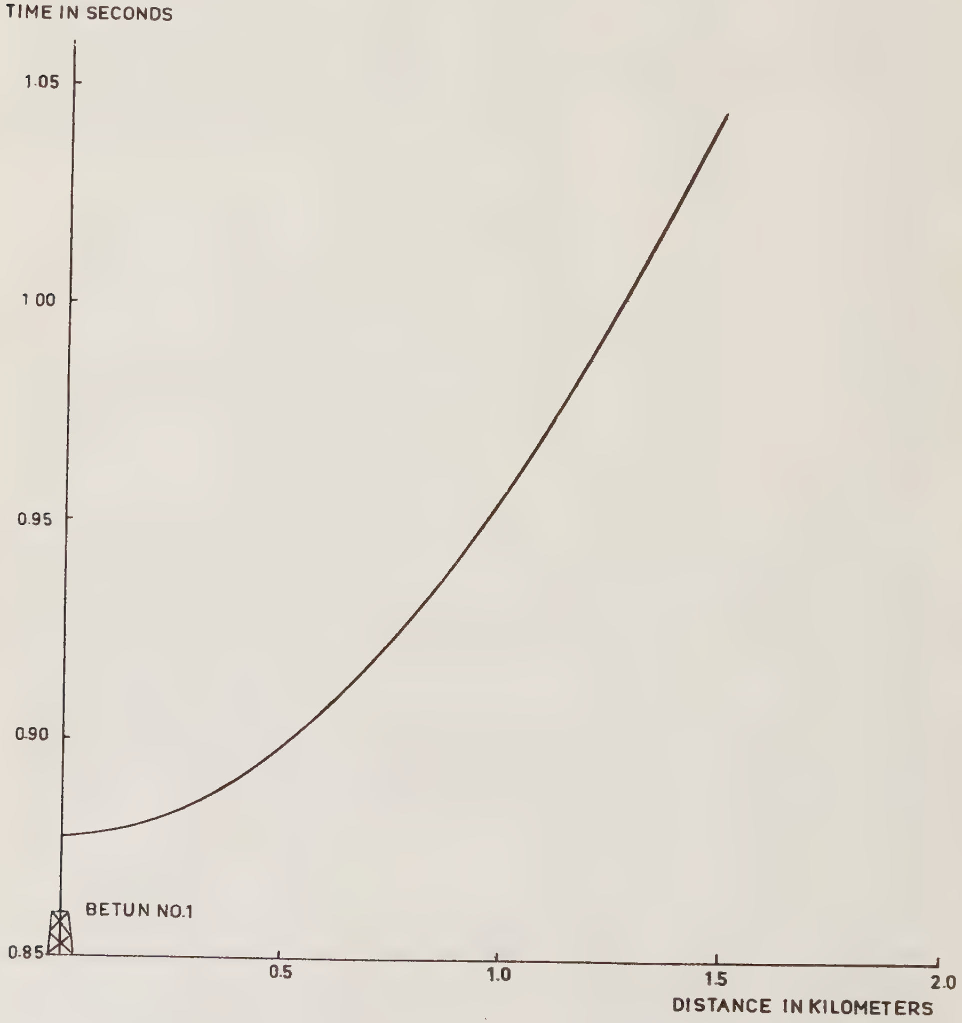

Fig. 3. Average travel time curve from the Betun No. 1 radial well survey. Curve indicates arrival times of direct energy.

In the present case the general problem is to find a horizontal velocity distribution that matches the given vertical velocity distribution in such a way that arrival times and distances computed from equations (4) and (6) will conform with the travel time curve in Figure 3. Although theoretically there is only one solution, it will be demonstrated below that the problem is ambiguous in a practical sense. This ambiguity arises partly from the insufficient accuracy of seismic field observations and partly from the fact that beyond a rather short distance from the well energy refracted at the high velocity basement masks the direct energy that has traveled along wave paths with large emergence angles.

Below are indicated three different interpretations, each resulting in nearly equally good approximations to the travel-time curve in Figure 3.

Interpretation I

Constant anisotropy factor of 1.06 *throughout the sedimentary section.*

distance meters	computed time seconds	observed time seconds	difference seconds
0	0.877	0.877	0.000
585	0.905	0.905	0.000
880	0.939	0.939	0.000
1085	0.970	0.969	0.001
1180	0.985	0.986	0.001

Interpretation II

Linear increase of the difference between horizontal and vertical velocities with depth in the shale section. Isotropic brown coal and limestone layers. Isotropic near surface layer. Anisotropy factor at bottom of sedimentary section 1.08.

distance meters	computed time seconds	observed time seconds	difference seconds
0	0.877	0.877	0.000
470	0.895	0.896	0.001
1070	0.969	0.967	0.002
1255	0.997	0.997	0.000
1420	1.028	1.028	0.000

Interpretation III (see Table II)

Below 1500 *meters below sea-level an overall value for the anisotropy factor in the shale section of* 1.04. *Isotropic limestone. Above* 1500 *meters an anisotropic velocity distribution such as is indicated on Table II.*

distance meters	computed time seconds	observed time seconds	difference seconds
0	0.877	0.877	0.000
486	0.897	0.897	0.000
1099	0.972	0.972	0.000
1327	1.011	1.011	0.000

Only the third of the above interpretations satisfies both the data from the refraction profile across the Betun No. 1 well (Fig. 2) and the travel time curve from the radial well survey (Fig. 3). Accordingly, it is believed that the last interpretation conforms closest to the real conditions.

Referring to Interpretation III the question may arise what the outcome will be if the alternative interpretation of the Betun refraction profile, such as sketched in the previous paragraph, is used instead of the one indicated above. It may suffice to mention here that, in that case also, the relatively low value of 1.04 for the anisotropy factor in the shale section below 1500 meters is sufficient to allow a good approximation to the travel-time curve from the radial well survey.

CONCLUSION

An analysis of all the available seismic data in the vicinity of the Betun No. 1 well leads to the conclusion that the sedimentary section in the Betun area must be considered as anisotropic. The results from a refraction profile across the Betun No. 1 well indicate that the anisotropy factor is one or very close to one immediately below the ground surface and that it probably increases to a maximum value of 1.13 or possibly 1.15 at a depth of about 1300 meters below sea-level. The travel-time curve from the Betun No. 1 radial well survey, by including the information obtained from the refraction profile across the well, can be matched closely by assigning an overall value of only 1.04 for the anisotropy factor in the scale section below 1500 meters below sea-level. Consequently, the anisotropy factor may even be lower than 1.04 near the bottom of the sedimentary section.

The results of this study disclose the possibility that at great depths, through a decrease of the anisotropy factor, the horizontal velocity may locally decrease or remain constant even though the vertical velocity increases with depth. This phenomenon might partly explain the lack of energy return from deeper parts of sedimentary sections, as often experienced in refraction surveys.

ACKNOWLEDGEMENTS

The author is indebted to the Standard Vacuum Oil Company for the permission to publish the contents of this paper. He also wishes to thank Mr. E. G. Jones of the Exploration Department in Sungei Gerong, Indonesia, for his friendly advice in preparing the manuscript.

REFERENCES

CHOLET J. and RICHARD H., 1954, A test on elastic anisotropy measurement at Berriane (North Sahara), Geophysical Prospecting, 2, 232-246.

HAGEDOORN J. G., 1954, A practical example of an anisotropic velocity-layer, Geophysical Prospecting, 2, 52-60.

RICKER N., 1951, The form and laws of propagation of seismic wavelets, Proceedings of the Third World Petroleum Congress, section 1, 514-536.

SLOTNICK M. M., 1936, On seismic computations, with applications, Geophysics, 1, 9-22.

DIE AUSBREITUNG ELASTISCHER WELLEN IN ANISOTROPEN MEDIEN *

VON

K. HELBIG **

Abstract

In seismic underground surveys carried out by Seismos GmbH in siderite mines of Siegerland (Germany) anomalies in velocities have been found which could be explained only by the assumption of slates being aeolotropic. In this paper some of the peculiarities connected with the propagation of elastic waves in aeolotropic media—especially those consisting of thin beds of isotropic material—are discussed. Schlieren-pictures of wave-fronts are presented, which show the validity of the theory.

Die Seismos G.m.b.H. führte in den letzten Jahren reflexionsseismische Messungen auf Spateisensteingruben des Siegerlandes durch. Das Nebengestein ist Devonschiefer mit im allgemeinen sehr unruhiger Lagerung. An einigen Stellen mit ruhiger Lagerung und steilem Einfallen wurde beobachtet, dass die Geschwindigkeit der seismischen Wellen senkrecht zur Schieferung kleiner, parallel zur Schieferung grösser ist als die mittlere Geschwindigkeit, die an Stellen mit unruhiger Lagerung beobachtet wird. Das bedeutet, dass der Schiefer anisotrop ist. Aus Symmetriegründen muss es sich dabei um "Transversalisotropie" (Love 1944) handeln: alle Richtungen senkrecht zur Symmetrieachse sind gleichwertig.

Die durch die Anisotropie entstehenden Komplikationen wurden zunächst theoretisch untersucht [1]). Auf Vorschlag von T. Krey wurden zu diesen Überlegungen Modellversuche an einem aus dünnen Schichten bestehenden Material vorgenommen, das in seinem elastischen Verhalten gewisse Ähnlichkeiten mit Schiefer aufweist.

Besonderheiten elastischer Wellen in anisotropen Medien

In der Kristalloptik tritt Doppelbrechung auf, d.h. zu jeder Richtung gibt es anstelle der einen Welle in isotropen Medien deren zwei mit verschiedenen Polarisationsrichtungen und im allgemeinen verschiedenen Ausbreitungsgeschwindigkeiten. Entsprechend gibt es in anisotropen Körpern drei Typen von elastischen Wellen anstelle der zwei in isotropen Körpern (longitudinal und transversal). Die drei zu einer Richtung gehörenden Ausbreitungsgeschwindigkeiten sind — abgesehen von besonderen Richtungen — voneinander verschieden. Die drei zugehörigen Verrückungsrichtungen sind zueinander orthogonal (Kelvin 1904), jedoch nicht mehr rein longitudinal (und rotationsfrei) bezw. rein transversal (und divergenzfrei). Die Verhältnisse in transversalisotropen Medien zeigt Abb. 1: eine der drei Verrückungen (1) ist rein transversal und steht senkrecht auf dem Hauptschnitt (Ebene durch Symmetrieachse und Wellennormale), die andern beiden liegen im Hauptschnitt. Bei nicht zu starker Anisotropie sind die Abweichungen gegen die longitudinale und transversale Richtung gering, die Welle 2 ist „quasi-transversal", Welle 3 „quasi-longitudinal". In allen schichtungs-anisotropen Medien hat die Welle 3 die grösste Ausbreitungsgeschwindigkeit. In der Regel ist diese parallel zur Schichtung grösser als in Richtung der Symmetrieachse, doch ist auch das umgekehrte Verhältnis möglich (im Gegensatz zu der von Riznichenko (1949) vertretenen Ansicht).

---

* Presented at the Ninth Meeting of the European Association of Exploration Geophysicists, held in London, 6/10. Dezember 1955. This paper is part of a Doctors Thesis of Göttingen University, which will be published in 1956.

** Seismos G.m.b.H., Hannover.

[1] Die mathematischen Ableitungen sind hier nicht wiedergegeben worden, da der zur Verfügung stehende Raum nicht ausreicht. Hierfür sei auf die zitierte Literatur sowie auf meine Dissertation verwiesen.

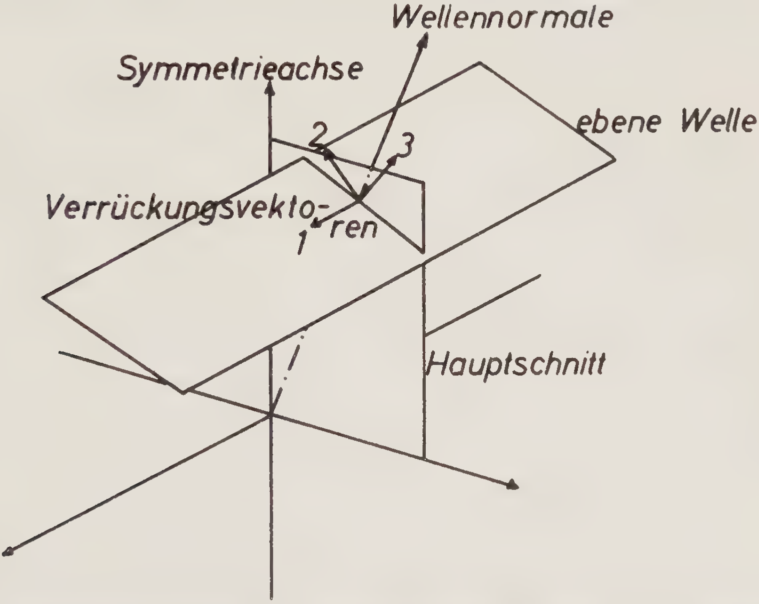

Abb. 1. Verrückungsrichtungen in transversalisotropen Medien: 1. senkrecht zum Hauptschnitt, transversal; 2. im Hauptschnitt, „quasi-transversal"; 3. im Hauptschnitt, „quasi-longitudinal". — Displacement directions in transverse isotropic media: 1. Perpendicular to principal section, transverse; 2. In principal section, "quasitransverse"; 3. In principal section, "quasilongitudinal".

Aus Symmetriegründen sind die Ausbreitungsgeschwindigkeiten der Wellen „2" und „3" in Richtung der Symmetrieachse gleich. Ebenso gross ist die Geschwindigkeit der Welle „2" (quasi-transversal, im Hauptschnitt polarisiert) in der Richtung parallel zur Schichtung. Die rein transversale Welle „1" läuft in dieser Richtung stets schneller als die quasitransversale Welle „2".

In isotropen Medien muss man — wenn Dispersion vorliegt — zwischen Phasen- und Gruppengeschwindigkeit unterscheiden. Dabei ist die Phasengeschwindigkeit die Ausbreitungsgeschwindigkeit ebener Wellen fester Frequenz (z.B. aus dem Abstand der Knoten stehender Wellen berechnet), die Gruppengeschwindigkeit die Ausbreitungsgeschwindigkeit endlicher Wellengruppen (z.B. seismischer Impulse). In anisotropen Medien sind diese beiden Geschwindigkeiten nicht nur der Grösse, sondern auch der Richtung nach voneinander verschieden, und zwar auch dann, wenn keine Dispersion vorliegt, die Geschwindigkeit also nur von der Richtung, nicht aber von der Frequenz abhängt. (Definitionsgemäss hat die Phasengeschwindigkeit die Richtung der Wellennormale, die Gruppengeschwindigkeit die Richtung der Strahlen, man spricht daher auch von Normalengeschwindigkeit und Strahlgeschwindigkeit.) Die Zusammenhänge werden in Abb. 2 erläutert. Die eingezeichneten ebenen Wellen schreiten von unten nach oben fort. Die Phasengeschwindigkeit v erhält man aus den Abständen der Flächen gleicher Phase, die Gruppengeschwindigkeit durch Ausblenden eines seitlich scharf begrenzten Strahles.

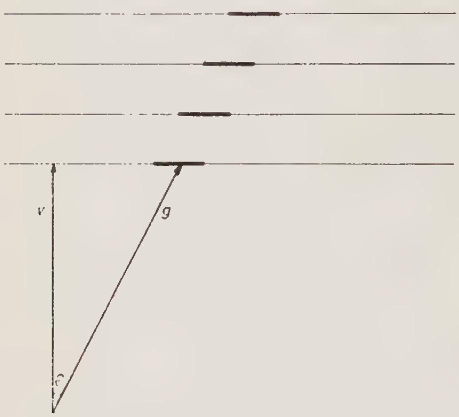

Abb. 2

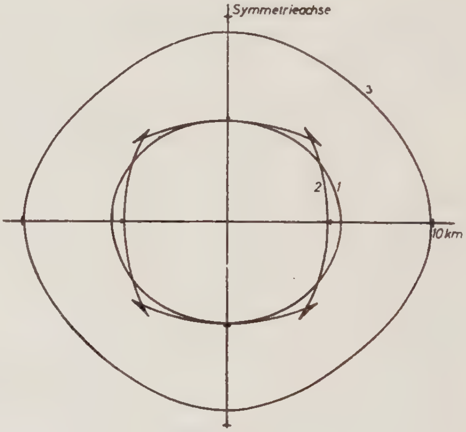

Abb. 2

Abb. 2. Phasen- und Gruppengeschwindigkeit in anisotropen Medien bei Fehlen von Dispersion. — Phase and group velocities in non-dispersive anisotropic media.
Abb. 3. Meridianschnitt der dreiblättrigen Wellenfläche von Beryll. — The meridional section of the three sheets of the wave surface in beryl.

Aus dem Gesagten folgt unmittelbar, dass in anisotropen Medien die Strahlen keine orthogonalen Trajektorien der Wellenfronten sind (vgl. auch Abb. 2).

Die charakteristischen Flächen der Wellenausbreitung

Für die Seismik ist es wichtig, das Verhalten von elastischen Wellen an Diskontinuitätsflächen zwischen anisotropen Medien — also eine Verallgemeinerung des Brechungsgesetzes — zu kennen. Diese Verallgemeinerung lässt sich auf verschiedene Weise vornehmen. (Die Ergebnisse sind selbstverständlich physikalisch identisch und nur formal verschieden.) Am übersichtlichsten ist die von Hamilton (1837) angegebene Form, die hier ohne strenge Ableitung angegeben werden soll. Dazu müssen noch einige Begriffe definiert werden.

Bei punktförmiger Erregung breiten sich in isotropen Medien Kugelwellen aus. In anisotropen Medien sind die Wellenfronten wesentlich komplizierter. Die Wellenfront zur Zeit $t = 1$ heisst Wellenfläche, sie ist charakteristisch für die Wellenausbreitung in dem betreffenden Medium (z.B. treten sie bei sinngemässer Anwendung des Huygensschen Prinzips an die Stelle der Kugelflächen). Man erhält die Wellenfläche, indem man vom Ursprung aus alle Strahlgeschwindigkeitsvektoren aufträgt. Eine implizite Darstellung der Wellenflächen elastischer Medien gab zuerst Kelvin (1904) an, eine Parameterdarstellung für transversalisotrope und rhombische Medien Rudzki (1911) (allerdings sind sowohl die Formeln als auch die Zeichnungen bei Rudzki nicht fehlerfrei). Als Beispiel sei hier die Wellenfläche von Beryll angegeben (Abb. 3). Entsprechend den drei Wellentypen besteht die Wellenfläche aus drei Schalen. Der Meridianschnitt der Fläche „1" ist eine Ellipse, der der Fläche „2" eine Kurve mit zwei Rückkehrspitzen und einem Doppelpunkt in jedem Quadranten, der der Fläche „3" ein ellipsenähnliches Oval. (Die Wellenfläche ist selbstverständlich rotationssymmetrisch und die kristallographische Achse). Es ist sehr schwierig, allgemeine Aussagen über die geometrischen Eigenschaften von Wellenflächen zu machen. Bei Beschränkung auf den Spezialfall der aus dünnen Schichten bestehenden Medien jedoch gilt: die Schale „1" ist immer ein abgeplattetes Rotationsellipsoid, die Schale "3" immer ein glattes Oval ohne Spitzen, während der Meridianschnitt der Schale „2" gleiche Hauptdurchmesser aufweist und in jedem Quadranten höchstens vier, in der Regel zwei oder keine Spitzen besitzt. Man erkennt, dass das Geophon je nach Orientierung zwei- bis fünfmal von einer Welle getroffen werden kann. Die drei zur Welle „2" gehörigen Einsätze sind jedoch nur bei stark ausgeprägten Spitzen zu trennen.

In isotropen Medien bezeichnet man als Brechungsindex die Grösse v_0/v, wo v die Phasengeschwindigkeit und v_0 eine beliebige feste Geschwindigkeit ist. In anisotropen Medien ist der Brechungsindex von der Richtung abhängig.

In sinnvoller Verallgemeinerung definiert man den "Indexvektor" als einen Vektor von der Richtung der Wellennormale und vom Betrage des zu dieser Richtung gehörenden Brechungsindex. Die Gesamtheit dieser Indexvektoren wird repräsentiert durch die Indexfläche, die man gewinnt, indem man vom Ursprung aus alle Indexvektoren aufträgt. Die Indexfläche ist dann der geometrische Ort der Vektorspitzen. Auch die Indexfläche ist für die Ausbreitung elastischer Wellen in dem betreffenden Medium charakteristisch. Auch sie besteht im Falle elastischer Wellen wegen der drei verschiedenen Wellentypen aus drei Schalen.

In ganz entsprechender Weise gewinnt man die Normalenfläche, indem man in jeder Richtung die zugehörige Normalengeschwindigkeit (Phasengeschwindigkeit) aufträgt.

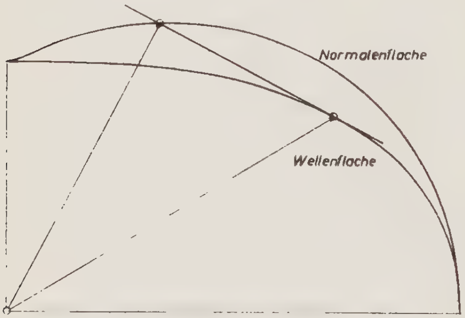

Abb. 4

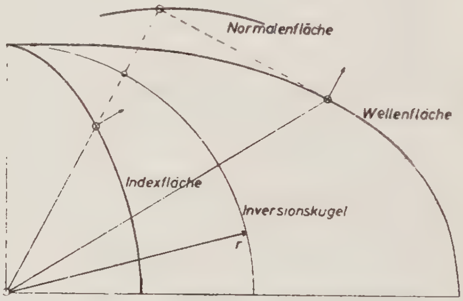

Abb. 5

Abb. 4. Zusammenhang zwischen Wellenfläche und Normalenfläche. — The relation between wave surfaces and normal surfaces.

Abb. 5. Zusammenhang zwischen Wellenfläche und Indexfläche. — The relation between wave surfaces and index surfaces.

Zwischen diesen drei Flächen bestehen geometrische Beziehungen, die es erlauben, aus jeder die beiden anderen zu gewinnen. In Abb. 4 ist der Zusammenhang zwischen Wellenfläche und Normalenfläche dargestellt. Ausser den Schnittkurven der beiden Flächen ist ein Teil der Abb. 2 eingezeichnet: eine ebene Welle und die zugehörige Normalen- und Strahlgeschwindigkeit. Es ist unmittelbar zu sehen, dass der Fusspunkt des Lotes vom Ursprung auf die Tangentialebene der Wellenfläche auf der Normalenfläche liegt. In Abb. 5 ist dieselbe Situation nocheinmal gezeichnet, nur ist zusätzlich die Indexfläche eingetragen. Der Zusammenhang zwischen Normalenfläche und Indexfläche ist unmittelbar klar: die Vektoren haben gleiche Richtung, ihre Beträge sind zueinander reziprok. Besonders wichtig ist der Zusammenhang zwischen Wellenfläche und Indexfläche: die Flächennormale der Wellenfläche und der Indexvektor sind parallel, da sie beide auf der gestrichelten Tangentialebene senkrecht stehen. Darüber hinaus sind aber auch Strahlrichtung (Ortsvektor der Wellenfläche) und Flächennormale der Indexfläche untereinander parallel.

DAS BRECHUNGSGESETZ

Mit Hilfe der im vorigen Abschnitt gebildeten Begriffe lässt sich das verallgemeinerte Brechungsgesetz formulieren. Ausgangspunkt ist die in isotropen Medien übliche Form $n . \sin \varphi = \text{const}$, wo n der Brechungsindex und φ der Winkel zwischen Wellennormale und Einfallslot ist. $n . \sin \varphi$ ist nichts anderes als die Projektion des Indexvektors auf die Diskontinuitätsfläche, es gilt also:

„Die Projektionen der Indexvektoren auf die Trennfläche sind gleich lang und gleich gerichtet".

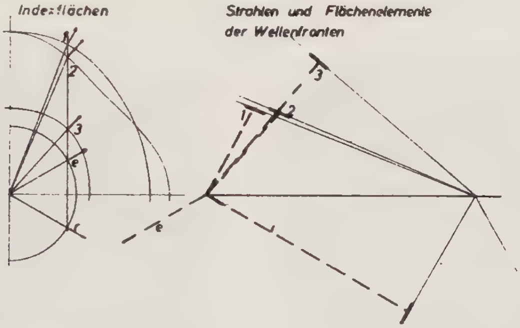

Abb. 6. Brechung und Reflexion an der Grenzfläche zwischen Beryll (oben) und einem isotropen Material (Ausbreitungsgeschwindigkeit 12000 m/sec). — Refraction and reflection at the boundary surface of beryl overlying an isotropic material.

Diese Aussage führt zu der in Abb. 6 erläuterten Konstruktion: damit die Projektionen identisch sind, müssen die Spitzen der Indexvektoren auf einer gemeinsamen Senkrechten zur Trennfläche liegen, nach der Definition liegen sie aber ausserdem auf der Indexfläche. Die Konstruktion verläuft so, dass man von der Spitze des Indexvektors der einfallenden Welle das Lot auf die Trennfläche fällt. Die übrigen Schnittpunkte dieses Lotes mit den verschiedenen Schalen der beiden Indexflächen (entsprechend den beiden Medien, die an der Trennfläche zusammenstossen) ergeben die Indexvektoren aller der Wellen, die mit dem Brechungsgesetz in Einklang stehen. Ob diese Wellen wirklich auftreten, hängt im Einzelnen von den physikalischen Bedingungen ab. Die Strahlrichtungen der sekundären Wellen sind wegen des oben beschriebenen Zusammenhangs zwischen Index- und Wellenfläche die Richtungen der Flächennormalen in diesen Punkten. Wie in isotropen Medien gilt, dass die Wellennormalen aller gebrochenen und reflektierten Wellen mit der Wellennormale der einfallenden Welle und dem Einfallslot in einer Ebene liegen. Die Strahlen liegen im allgemeinen nicht in dieser Ebene, ausgenommen dann, wenn diese Ebene zugleich die Symmetrieachse (bei transversalisotropen Medien) enthält. Diese Bedingung ist bei den unten beschriebenen Modellversuchen stets erfüllt.

Bei der Reflexion treten eine Reihe ungewohnter Erscheinungen auf. So wird z.B. ein senkrecht auf eine Trennfläche fallender Strahl nur dann in sich reflektiert, wenn Normalen- und Strahlrichtung zusammenfallen.

MODELLVERSUCHE

Bei den Modellversuchen wurde das folgende Prinzip verwendet: aus dem zu untersuchenden Material wird ein Zylinder geschnitten (mit der Symmetrieachse in einem Durchmesser des Zylinders). Auf der Zylinderachse springt ein Unterwasserfunken über, der eine elastische Welle erregt. Der Weg vom Erregungszentrum bis zum Umfang des Zylinders ist in jeder Richtung gleich lang. Ist das Material isotrop, so wird die Welle überall zur gleichen Zeit in das umgebende Wasser austreten, ist es anisotrop, so wird die Welle an verschiedenen Stellen des Umfangs zu verschiedenen Zeiten eintreffen. Die in das umgebende Wasser ausgetretene Welle wird mit Hilfe eines zweiten Funkens fotografiert. Die verwendete Apparatur stimmt bis auf einige Veränderungen (Güth 1955) mit der überein, über die E. Müller im Dezember 1952 auf der Tagung der EAEG berichtet hat (vgl. Müller 1954).

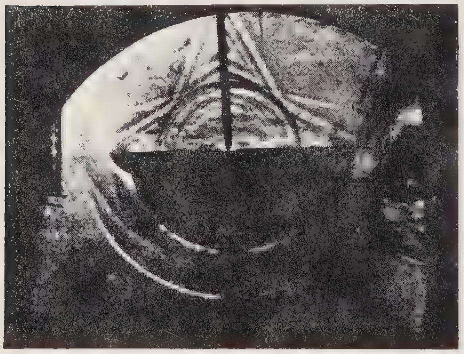

Abb. 7

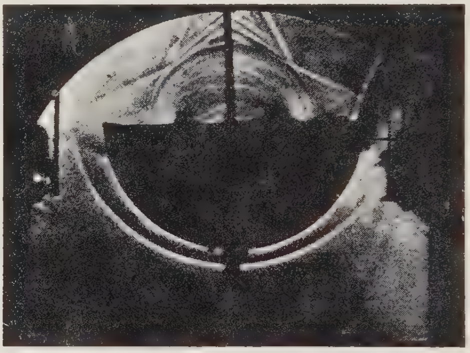

Abb. 8

Abb. 7. Wellenfronten in der Umgebung eines durch Unterwasserfunken angeregten Aluminium-Halbzylinders nach 9 μsec. — Wave fronts, in the neighbourhood of an aluminium half cylinder excited by an underwater electric spark, after 9 μsecs.
Abb. 8. Wellenfronten in der Umgebung eines durch Unterwasserfunken angeregten Pertinax-Halbzylinders nach etwa 11 μsec. — Wave fronts, in the neighbourhood of pertinax half cylinder excited by an underwater electric spark, after about 11 μsecs.

In einem Vorversuch bestand der (Halb-)Zylinder aus isotropem Material (Aluminium). Abb. 7 zeigt das Wellenbild in seiner Umgebung. Oberhalb erkennt man die geführten Wellen, die von den Longitudinal- und Transversalwellen erregt worden sind. Im unteren Teil des Bildes sind alle Wellen als konzentrische Kreise abgebildet, mit Ausnahme der Front, die die ersten beiden konzentrischen Wellen miteinander verbindet. Diese ist von einer "inneren geführten Welle" verursacht worden, die von der Longitudinalwelle an der ebenen Oberfläche erregt wird und im Innern des Materials als ebene Welle (genauer Kegelwelle) die transversale Wellenfront berührt. Dass diese Front im Wasse gekrümmt erscheint, liegt an der "Linsenwirkung" der gekrümmten Trennfläche Wasser-Aluminium.

Abb. 8 ist eine ebensolche Aufnahme, mit dem Unterschied, dass der Halbzylinder aus Pertinax (einem aus Papierschichten aufgebauten Isoliermaterial) besteht. An den verschiedenen Abständen der (in Abb. 7 kreisförmigen) Wellenfront vom Umfang des Zylinders erkennt man unmittelbar, dass die Ausbreitungsgeschwindigkeit parallel zur Schichtung (also parallel zur ebenen Oberfläche) um rund 25% grösser ist als die in Richtung der Symmetrieachse. Ausser der zu der longitudinalen Welle gehörenden Front und den von ihr geführten Wellen ist auch die von der inneren geführten Welle herrührende Front zu sehen. Von Transversalwellen geführte Wellen sind nicht zu erkennen, da die Welle „1" nur schwach erregt wird und auch nur schwach mit der

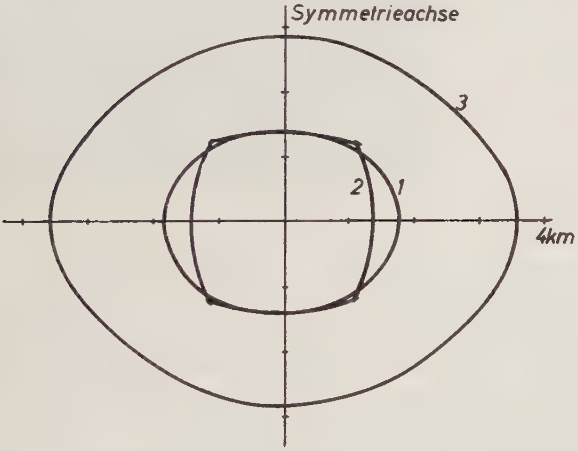

Abb. 9

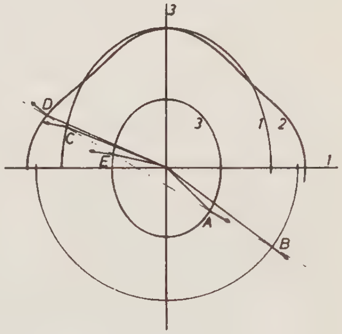

Abb. 10

Abb. 9. Meridianschnitt der dreiblättrigen Wellenfläche von Pertinax. — The meridional section of the three sheets of the wave surface of pertinax.

Abb. 10. Konstruktion des gebrochenen und der reflektierten Strahlen an der Grenzfläche Pertinax-Wasser. — Construction of the refracted and reflected rays at a pertinax-water boundary.

Flüssigkeit gekoppelt ist und die Geschwindigkeit der Welle „2" kleiner als die Wellengeschwindigkeit in Wasser ist.

Mit Hilfe dieser und ähnlicher Aufnahmen lassen sich die charakteristischen Flächen von Pertinax bestimmen. Abb. 9 zeigt die Wellenfläche. Auffallend ist die starke Abweichung des quasilongitudinalen Blatts von der Kugelform. Das quasitransversale Blatt besitzt Spitzen, die allerdings sehr schwach ausgeprägt sind.

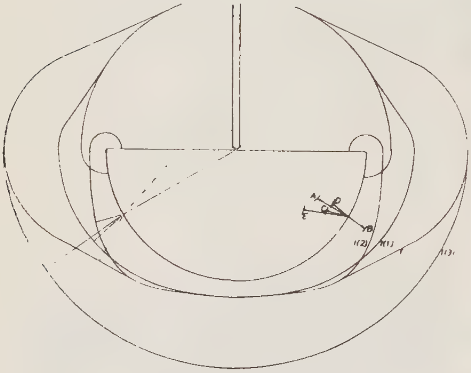

Abb. 11

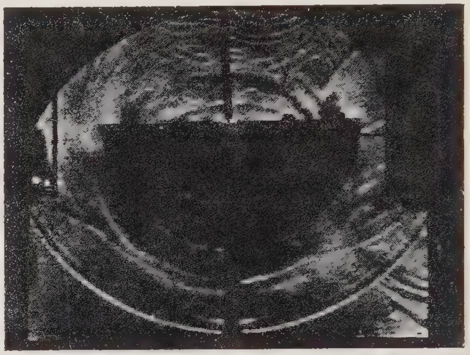

Abb. 12

Abb. 11. Teil des Wellenbilds in der Umgebung eines Pertinaxzylinders nach 20 µsec. Die Front „f" ist durch eine innere geführte Welle verursacht. Links die zu den einzelnen Fronten gehörenden Strahlen, rechts (für einen früheren Zeitpunkt) die zu einer einfallenden quasilongitudinalen Welle gehörenden sekundären Strahlrichtungen und Wellenfront-Elemente. — Part of the wave system in the neighbourhood of a pertinax cylinder after 20 µsecs. The front "f" is produced by an internal guided wave. On the left, the rays belonging to the several fronts. On the right (for an earlier time) the secondary ray directions and wave front elements belonging to an incident quasilongitudinal wave.
Abb. 12. Schlierenaufnahme des Wellenfelds in der Umgebung eines Pertinaxzylinders nach 20 µsec.. Die Aufnahme entspricht den Abb. 11 und 13. — Schlieren-picture of the wave pattern in the neighbourhood of a pertinax cylinder after 20 µsecs. The picture corresponds to figures 11 and 13.

In Abb. 10 ist dargestellt, wie sich mit Hilfe der Indexflächen von Pertinax und Wasser die reflektierten und gebrochenen Wellen bestimmen lassen (oberhalb der Trennlinie die drei Blätter der Indexfläche von Pertinax, unterhalb das zur quasilongitudinalen Welle gehörige Blatt und die Indexfläche von Wasser, die wegen der Isotropie eine Kugel ist). Im Bild ist die Ermittlung derjenigen sekundären Wellen gezeigt, die eine unter 60° Neigung gegen die Symmetrieachse laufende Welle beim Auftreffen auf den Zylinderumfang erregt. Bei A befindet sich die Spitze des Indexvektors der einfallenden Welle. Da der Strahl senkrecht auf die Trennfläche auffällt, haben die Flächennormale der Indexfläche (Strahlrichtung) und die Grenzflächennormale (Einfallslot) gleiche Richtung. Bei B liegt die Spitze des Indexvektors der im Wasser erregten Welle, bei C, D, und E die Spitzen der Indexvektoren der reflektierten Wellen. Mit Hilfe dieser Konstruktion lässt sich das Wellenfeld im Prüfstück und in seiner Umgebung zu jedem Zeitpunkt bestimmen. Durch Vergleich mit entsprechenden Schlierenaufnahmen kann dann die Gültigkeit der Theorie gezeigt werden.

In Abb. 11 sind rechts die Strahlrichtungen sowie die Elemente der Wellenfronten der verschiedenen Wellen (einfallende, reflektierte und durchgehende) eingetragen. Es ist augenscheinlich, dass trotz senkrechten Einfalls die reflektierten Wellen nicht in sich zurücklaufen. Aus solchen Wellenfront-Elementen ist das Wellenbild in der Umgebung des Zylinders bestimmt worden, und zwar für einen Zeitpunkt 20 μsec nach der Erregung der Wellen. Abb. 12 ist eine Schlierenaufnahme, bei der die Verzögerung etwa ebensoviel beträgt. Die beiden Wellenbilder stimmen weitgehend überein, sofern man von den aus der Umgebung kommenden Wellen absieht, die nichts mit dem eigentlichen Vorgang zu tun haben. Nicht in den Rahmen der Theorie passen die beiden ausgeprägten Fronten zwischen der longitudinalen und transversalen Front in der unteren Bildmitte. Sie verdanken ihre Entstehung dem Umstand, dass — entgegen der Voraussetzung — die Schichtdicke nicht hinreichend klein gegenüber der Wellenlänge ist.

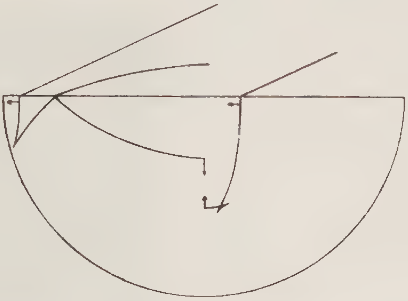

Abb. 13. Teil des Wellenbildes innerhalb und ausserhalb eines Pertinaxzylinders, rechts nach 13 μsec, links nach 20 μsec. — Part of the wave pattern inside and outside a pertinax cylinder. To the right after 13 μsecs, to the left after 20 μsecs.

In Abb. 7 war oberhalb des Prüfstücks nur das System sich kreuzender geführter Wellen zu sehen. Abweichend davon tritt in Abb. 12 eine gekrümmte Wellenfront oberhalb des Prüfstücks auf. Zum Verständnis ihrer Entstehung ist es notwendig, den weiteren Verlauf der quasilongitudinalen Wellenfront im Innern des Prüfstücks zu verfolgen. In Abb. 13 entspricht die rechte Seite etwa der Abb. 8, die linke der Abb. 12. Ganz offensichtlich muss bei Pertinax ausser der geführten Welle eine solche gekrümmte Front auftreten.

In Abb. 14 und 15 ist versucht worden, nach einer weiteren Reflexion konstruiertes und beobachtetes Wellenbild zu vergleichen. In einigen typischen Zügen stimmen die beiden Bilder noch überein, insbesondere in den stark ausgeprägten Kreisen an den Ecken des Halbzylinders. Auch die Aufhellungen unterhalb dieser Kreise sind reelle Wellenfronten, wie sich durch Vergleich aufeinanderfolgender Aufnahmen ergibt. Besonders an dieser Front erkennt man jedoch, dass eine weitere Verfolgung keinen Sinn mehr hat, da die Wellen zu verwaschen werden.

Das Problem war hier, aus den bekannten Anisotropie Eigenschaften des Materials und der bekannten Lage der reflektierenden Fläche die Form der Wellenfronten zu bestimmen. Für das Problem der angewandten Seismik, aus der beobachteten Form der Wellenfronten auf die unbekannten Diskontinuitäten zu schliessen, gibt es bislang keine exakte Methode. Im Falle nicht zu starker Anisotropie kann man z.B. Index- und Wellenflächen durch Ellipsoide ersetzen (M. Oks 1938) und die für isotrope Medien üblichen Verfahren entsprechend abwandeln. In jedem Fall wird man jedoch zu untersuchen haben, ob ein solcher Ersatz zulässig oder zweckmässig ist.

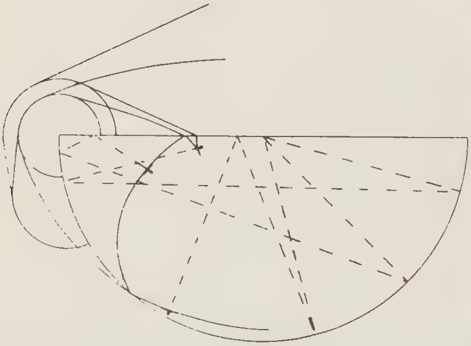

Abb. 14

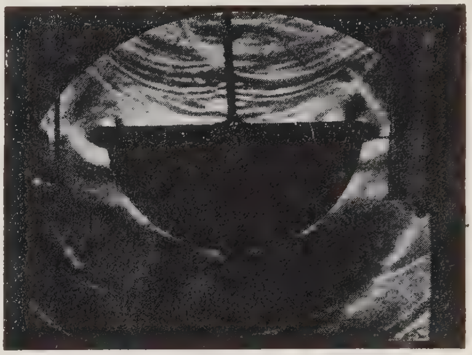

Abb. 15

Abb. 14. Teil des Wellenbildes in der Umgebung eines Pertinaxzylinders nach 26 μsec. Im Innern des Prüfstücks ein Teil der quasilongitudinalen Wellenfront und drei zugehörige Strahlen. — Part of the wave pattern in the region of a perinax cylinder after 16 μsecs. Inside the sample part of the quasilongitudinal wave front and part of three associated rays.

Abb. 15. Schlierenaufnahme des Wellenbilds in der Umgebung eines Pertinaxzylinders nach 26 μsec. — Schlieren-picture of wave pattern in the neighbourhood of a pertinax cylinder after 26 μsecs.

Ich möchte Herrn T. Krey für wertvolle Anregungen sowie der Seismos G.m.b.H. für die Unterstützung der Arbeit danken.

LITERATUR

GÜTH, W., 1955, Die Leitung von Schallimpulsen in Metallstäben, Acustica 5, S. 35.

HAMILTON, W. R., 1837, Trans. Roy. Irish Acad. 17, S. 144.

KELVIN, W., 1904, Baltimore Lectures, Cambridge.

LOVE, A. E. H., 1944, A treatise on the theory of elasticity, Dover Publications, New York.

MÜLLER, E., 1954, Experimente über Wellenausbreitung in Gesteinsproben, Geologisches Jahrbuch 70, S. 127.

OKS, M., 1938, Influenca de la anisotropia elástica de los estratos en los cálculos sismográficos de refráccion, Boletin de informaciones petroleras 15, S. 109.

RIZNICHENKO, J. W., 1949, Über seismische Quasi-Anisotropie (russisch), Isw. Akad. Nauk. SSSR, Serija geogr. i geof. 13, S. 518.

RUDZKI, M. P., 1911, Parametrische Darstellung der elastischen Welle in anisotropen Medien, Anz. d. Akad. d. Wiss. Krakau 1911, S. 503.

E.A.E.G. ABSTRACT SERVICE

EXPLORATION — GENERAL

1. *A Geological and Geophysical Study of Pilot Knob (South), Travis County, Texas.*
F. Romberg & V. E. Barnes, Geophysics, Vol. 19, No. 3, pp. 438-454, July, 1954.

Pilot Knob is an exhumed volcano of Cretaceous age, composed of "serpentinized" pyroclastics and minor amounts of basalt in both intrusive and extrusive masses. The geology of Pilot Knob was re-examined, and gravity and magnetic observations made and interpreted, in order to present a complete picture of the feature itself, its history, its relation to the region and the area surrounding it, and the resemblances between it and the serpentine plugs in the neighbourhood, to which it is geologically related. Some of these plugs have been found by geophysical methods, and some so discovered have produced oil; the application of gravity and magnetic data to such discoveries is analyzed.

The extrusive masses are here reported for the first time, and other evidence is given for the age and volcanic nature of Pilot Knob. The observations reveal (1) strong gravity and magnetic anomalies over the central basalt mass, (2) a pattern of weaker anomalies probably caused by flows and dykes and suggesting that Pilot Knob is situated neat the intersection of two sets of fractures, and (3) evidence that "serpentinized" pyroclastics show weak magnetic anomalies and (in the local setting) no visible gravity anomalies.

(Author's Abstract)

2. *Geophysical History of Mamou Field, Evangeline Parish, Louisiana.*
D. R. Dobyns, & W. B. Roper, Geophysics, Vol. 19, No. 3, pp. 490-508, July, 1954.

This paper presents a chronological historical record of the geophysical activity in the area near the town of Mamou, Louisiana which subsequently led to the discovery of the Mamou oilfield. The successive stages of geophysical exploration were:

(1) Mechanical seismograph refraction survey by North American Exploration Co. (German) in 1926 for Magnolia-Union Sulphur- H. Hanszen.
(2) Torsion balance survey by Shell Oil Co. in 1934.
(3) Magnetometer survey by Atlantic Refining Co. in 1936.
(4) Torsion balance survey by Atlantic Refining Co. in 1936.
(5) Gravity survey by Magnolia Petr. Co. 1942-43.
(6) Three weeks' seismic work by Petty Geophysical Engineering Co. for Magnolia Petro. Co. in 1943
(7) A few weeks' work by General Geophys. Co. for Cities Service Oil Co. in 1943.
(8) Detailed seismic survey by Independent Expln. Co. for Magnolia Petr. Co., 1943-45.

(Author's Abstract)

3. *Exploration Problems and Procedures in the Williston Basin.*
R. A. Pohly & S. H. Harris, World Oil, Vol. 139, No. 1, pp. 119-124, July, 1954.

The various geophysical and geological methods which have been employed in the Williston Basin are described generally and briefly. The methods included are: surface mapping, photogeology, magnetic, gravity, seismic and core drilling. Their application to the exploration programme is evaluated and discussed in some detail under the subheadings of 'unglaciated area' and "glaciated area".

4. *Public and Private Activities in the Uranium Industry on the Colorado Plateau.*
Q. L. Brewer, Mines Mag., Vol. 44, No. 8, pp. 25-28, 1954.

Methods employed in the search for uranium ores on the Colorado Plateau include the use of airborne scintillation counters, portable scintillation and Geiger counters, radiometric well-logging equipment, and other more conventional geophysical means. The development of this activity is reviewed.

5. *Examples of Geophysical Exploration for Uranium, Colorado Plateau Area.*
D. Wantland, Mines Mag., Vol. 44, No. 8, pp. 18-24, 1954.

A description of uranium prospecting carried out by the U.S. Atomic Energy Commission and the U.S. Geological Survey includes the use of airborne radiation surveys and drill-hole radioactivity-logging. A number of uranium areas have been surveyed by the resistivity method which was first used on the Colorado Plateau in 1941.

6. *Geophysics and the Study of the Subsurface.* (In Italian).
C. Morelli, Industr. Min., Anno 5, No. 4, pp. 193-196, 1954.

The geophysical methods used in mineral prospecting and engineering are reviewed. They include the gravimetric, magnetic, seismic, electric, and radioactive methods. The search for natural gas and natural sources of heat in Italy is also discussed.

SEISMIC — GENERAL

7. *Seismic Studies on Fletcher's Ice Island*, T-3.
A. P. Crary, Trans. Am. Geophys. Un., Vol. 35, No. 2, pp. 293-300, 1954.

8. *Elastic Waves in Arctic Pack Ice.*
J. Oliver, A. P. Crary, & R. Cotell, Trans. Am. Geophys. Un., Vol. 35, No. 2, pp. 282-292, 1954.

9. *Study of the Velocities of Seismic Waves on the Inland Ice Cap of Greenland.* (In French)
A. Joset & J. J. Holtzscherer, Ann. Geophys., Vol. 9, No. 4, pp. 330-344, 1953.

10. *Geophysical Investigations in the Emerged and Submerged Atlantic Coastal Plain.* Part. VIII. *Grand Banks and Adjacent Shelves.*
F. Press & W. Beckmann, Bull. Am. Geol. Soc., Vol. 65, No. 3, pp. 299-314, 1954.

11. *Geologic and Geophysical Investigations in the Meppen Region, West of the Ems.* (In German).
J. J. Fabian & H. Helms, Erdöl u Kohle, Jahrg. 6, Heft 10, pp. 601-604, and Heft 11, pp. 726-729, 1953

A discussion of the geophysical investigations of the area between the border of the Netherlands and the Ems in northwestern Germany made before 1949 In this region of about 300 sq. km., geophysical exploration for oil was begun in 1935; the first surveys were by magnetic and gravity methods, and since 1946 seismic reflection and refraction methods have been used. The results are presented as parallel seismic and geologic profiles.

Results of the investigations since 1949 by seismic reflection and refraction methods are presented in the second paper. Several sites were explored and geologic profiles constructed on the basis of the travel time curves.

(From Geophysical Abstracts 157, U.S. Geol. Survey).

12. *Shallow Exploration for Iron Ore with the Reflection Seismograph.*
W. B. Beatty, Explosives Engineer, Vol. 31, No. 6, pp. 172-174, 1953.

A description of Stanford Research Institute's shallow reflection experiments in Minnesota.

13. *Geophysical Investigations in the Emerged and Submerged Atlantic Coastal Plain, Part VII. Continental Shelf, Continental Slope and the Continental Rise South of Nova Scotia.*
C. B. Officer & M. Ewing, Geol. Soc. Am. Bull., Vol. 65, No. 7, pp. 653-670, 1954.
The results of a series of refraction profiles made over the continental shelf south of Nova Scotia and extending down to the adjacent deep basin are reported

14. *Shooting for Oil in the Gulf of Mexico*
W. Richardson, Explosives Engineer, Vol. 31, No. 5, pp. 135-153, 1953.
An account of present activity over the Gulf continental shelf, using the seismic reflection method of prospecting for oil.

15. *Muskeg Buggy Aids Canadian Exploration.*
Petroleum Engineer, Vol. 26, No. 8, pp. B. 106-B. 108, August, 1954.
A tractor has been devised which will operate successfully over the Canadian muskeg in both summer and winter. It incorporates two tandem wheel tracks, each 29 ins wide, which present approximately 5,000 sq. ins. of surface to the ground, this preventing sinking. A range of four bodies has been designed: a seismic drilling unit; a water unit; a seismic instrument unit; and a general utility and supply unit.

SEISMIC — INTERPRETATION

16. *A Process of Seismic Reflection Interpretation*
J. G. Hagedoorn, Geophysical Prospecting, Vol. 2, No. 2, pp. 85-127, June, 1954.
A process is described whereby the interpretation of seismic reflection data is carried out by a preliminary two-dimensional plotting procedure followed by a three dimensional migration. The concept of a surface of maximum convexity is introduced as an integral part of the process of migration. The procedures for deriving the necessary charts of curves are considered and a number of serviceable charts presented.
(Author's Abstract)

17. *On the Determination of Wave-Velocity in Seismic Reflection Measurements* (In German.
H. Dürbaum, Geophysical Prospecting, Vol. 2, No. 2, pp. 151-167, June, 1954.
Seismic velocities can be determined from borehole data to an accuracy of about 1%. Without boreholes, however, one must rely on refraction and reflection measurements. The procedure for the evaluation of reflection seismograms for velocity data is given.

18. *Calculation of Depth and Dip of Several Layers by Refraction Seismic Method.*
J. C. Dooley, Australian Bur. Min. Resources Geol. & Geophys. Bull., 19, 1952.
A graphic calculation of the depth and dip of several layers from seismic refraction data is described. The following assumptions are made: all interfaces are continuous plane surfaces; the seismic velocity does not vary in each layer; each layer has a higher velocity than the layers above it; all layers have enough thickness and velocity contrast to be recorded; the traverse lies approximately in the direction of maximum dip of all interfaces.
(From Geophysical Abstracts 156, U.S. Geol. Survey).

19. *Computation of Anticlinal Data from Refraction Travel-Time Curves.* (In Hungarian)
G. Kilczer, Magyar Allami Eötvös Lorand Geofiz. Intezet Geofiz. Közlemenyek, Kötet 2, Szam 3, pp. 25-32, 1953
This study gives a graphoanalytical method of analyzing results obtained from seismic refraction exploration of anticlinal structures in search for oil or coal deposits. By this procedure the depth of the refracting layer, angles of the inclination of the flanks, and the velocity of propagation of the seismic waves may be determined

with sufficient accuracy. Both symmetrical and asymmetrical anticlines are considered. The suggested procedure may be extended to more than two layers, as, for example, a salt dome covered by two layers.

(From Geophysical Abstracts 156, U.S. Geol. Survey).

20. *Diffraction Phenomena in Seismic Reflection* (In Italian).
C. Contini, Ann. Geofis., Vol. 6, No. 1, pp. 73-112, 1953.

Following the methods used in geometrical optics, Contini applies the principles of Huygens-Fresnel and Kirchhoff to the study of the path of seismic waves meeting a reflecting surface in their propagation through the ground. The results vary from the familiar ones obtained in geometrical optics, because of the great length of seismic waves. Thus discontinuities of the reflecting plane do not produce abrupt variations in the shape of the wave fronts reaching the surface as predicted by the principles of geometric optics, but the shape is changed gradually, both in amplitude and phase angle. These results are important in the interpretation of seismograms.

Several examples of correlations between the details of subsurface structure and the seismograms are analysed.

(From Geophysical Abstracts 156, U.S. Geol. Survey).

21. *Improvement of Seismic Data by Computing Procedures*
R. F. Beers & C. F. Casey, Paper read at the Annual Meeting of the S.E.G. at St. Louis, Missouri, April, 1954. (Not yet published).

A simple transcribing device is used to place conventional seismic records on magnetic tape. In this form studies have been made of various computing procedures to determine their effect on signal-to-noise ratio. The observed improvements may also be accomplished in direct recording of seismic data on paper or magnetic tape.

22. *Correlation Analysis of Seismic Exploration Data*
H. J. Jones & J. A. Morrison, Geophysics, Vol. 19, No. 4, pp. 660-683.

Correlation analysis techniques may be applied to seismic data already subjected to standard recording and analysis procedure in an effort to extract additional information. These techniques involve determination of certain parameters which provide a quantitative measure of the correlation between two sets of data. Among the most useful of these parameters are the auto- and cross-correlation coefficients and functions long used by statisticians in time series analysis and recently applied to filtering and prediction problems in the field of communications. This paper discusses some applications of correlation analysis in interpretation of seismograms. The use of auto-correlation to identify repetitive patterns on complex seismograms is described. Examples of the determination of the power spectrum from the auto-correlation function are presented. The use of cross-correlation analysis to identify weak messages masked by high noise is illustrated for several problems. Equivalence of correlation analysis procedures to filtering operations is stressed. Special analog computing equipment facilitating computation of correlation coefficients and power spectra directly from oscillograms or graphs is described.

23. *Method for the Construction of Continuous Reflecting Horizons on Steep Flanks Taking into Account the Refraction Effect.* (In German).
H. Lorenz, Gerlands Beitr. Geophysik, Band 63, Heft 2, pp. 99-107, 1953.

This paper presents a method of correcting seismic reflection data, obtained on the steep flanks of salt domes, for the effect of refraction. It is shown that the true co-ordinates of a reflecting point L_n can be obtained by interpolating between those of L^*_n the point obtained by the tangent method (that is, neglecting the tangent effect), and those of L_n°, obtained by the method of path differences. Formulae and diagrams are given for the calculations by each method, and a practical example for 3 layers is worked out.

(From Geophysical Abstracts 156, U.S. Geol. Survey).

24. *Filtering Associated with Selective Sampling of Geophysical Data.*
C. A. Swartz & V. M. Sokoloff, Geophysics, Vol. 19, No. 3, pp. 402-419, July 1954.

Geophysical data are often subjected to a variety of selective sampling operations in order to render their interpretation easier. The filtering effects of a number of commonly employed selective sampling procedures are discussed in detail in this paper.

Curves are given showing the frequency selectivity characteristics of several arithmetic sampling processes including simple averaging, successive differences, and residual curves and maps.

Instrumental sampling such as geophone mixing and electric filtering is also considered. The equivalence of electric filtering to an arithmetic sampling process is pointed out and illustrated by an example.

A recently developed statistical method of detecting seismic reflections is discussed as a sampling procedure and curves are presented to show the filtering action for two special cases under restricted conditions.

(Author's Abstract)

25. *An Example of the Identification of Multiple Reflections on the Basis of the Velocity.* (In German).
R. Garber, Erdöl u Kohle, Jahrg. 7, Heft 4, pp. 197-199, 1954.

Seismic exploration in the province of Limburg, Netherlands, included a region where the subsurface consisted of several parallel, almost-horizontal strata. This made it necessary to distinguish on the seismograms the arrivals of the once-reflected waves from those belonging to multiple-reflected waves. The analysis of seismograms was made in the following manner: Travel times were computed for a number of waves reflected from various layers with increasing depth and on the basis of these times the curve representing the variation of the velocity with depth was drawn. On this curve it was possible to see clearly sharp deviations from the expected shape each time a multiple reflected wave was picked.

(From Geophysical Abstracts 157, U.S. Geol. Survey)

26. *Mean Error of Seismic Reflection Measurements.* (In Hungarian with Summaries in English and Russian).
K. Posgay, Magyar Allami Eötvös Lorand Geofiz. Intezet Geofiz. Közlem., Kotet 3, Szam 4, pp. 41-54, 1954.

A method of finding the mean error in seismic-reflection arrival times rapidly is presented in which the correction equations are deduced from equations for propagation times measured with symmetrically located seismometers. Practical examples of its application are included.

(From Geophysical Abstracts 158, U.S. Geol. Survey).

27. *On the Determination of the Reflected Plane.* (In German).
A. Tarczy-Hornoch, Geofis, Pura e Appl., Vol. 27, pp. 87-97, 1954.

Adjustment of seismic-reflection data by conversion to equal geophone altitudes is a cumbersome method. A simpler way to increase the accuracy of determination of reflection planes is to use indirect observations to obtain the most probable values of the velocity and the co-ordinates of the image of the shot point. Mean-square errors of the unknown quantities may be calculated from the adjustment. The approximate value needed for the adjustment can best be calculated from the linear equations.

(From Geophysical Abstracts 158, U.S. Geol. Survey).

28. *On the Seismic Reflection Interpretation of a Fault Structure.* (In German).
R. Bading, Geol. Jahrb., Band 67, pp. 73-82, 1953.

Under favourable conditions it is possible to determine structure from seismic reflection data even in complexly faulted regions. Many examples of seismograms are given, showing the effect of vertical layers and the angles of faults.
(From Geophysical Abstracts 158, U.S. Geol. Survey).

29. *Determination of Propagation with the Seismic Reflection Method.* (In Hungarian with Summaries in English and Russian).
A. Tarczy-Hornoch, Magyar Allami Eötvös Lorand Geofiz. Intezet Geofiz. Közlem., Kötet 3, Szam 5, pp. 55-69, 1954.
A formula is derived for more precise determination of velocity for three seismometers, equally spaced along a line .For velocities graeter than 1,500 m/sec. and depth greater than 1,000 m, wider spacing is necessary.
(From Geophysical Abstracts 158, U.S. Geol. Survey).

30. *On Reflected Refraction Impulses.* (In German).
H. Reich, Geol. Jahrb., Band 67, pp 135-142, 1953.
Certain impulses appearing in refraction seismograms and travel-time curves are obviously caused by reflections of the refracted waves, which may occur in the case of well-defined boundary planes that act as effective reflecting planes as well as "conductors" for the refracted impulse. Such contracts may be recognized in the Donau region, namely the upper surface of the crystalline basement, and the contact of the Malm Limestone with the underlying Mesozoic rocks.
(From Geophysical Abstracts 158, U.S. Geol. Survey).

31. *Possibilities of Application of Combined Reflection and Refraction Measurements Especially to the Determination of Average Velocities.* (In German).
H. Helms, Geol. Jahrb., Band 67, pp. 115-126, 1953.
By means of calculations for the cases of two horizontal layers and two inclined layers and by practical examples, the usefulness of combined reflection and refraction measurements is demonstrated. Where true average velocity is known, the layer velocity of individual reflecting horizons, which also appear in the refraction travel-time curve, can be determined and from this, often, their stratigraphic position. Where the true average velocities are not known, but where it is reasonable to assume that horizons appear simultaneously in reflection and refraction (as in the Oberkante of the Upper Cretaceous of north-western Germany, for example), a satisfactory approximation of the average velocity can be determined by direct measurement. Depth determinations in reflection as well as refraction measurements can be made precise in this way. (From Geophysical Abstracts 158, U.S. Geol. Survey).

32. *Geometric Problems in the Evaluation of Underground Seismograms.* (In German).
H. Linsser, Geol. Jahrb., Band 67, pp. 127-134, 1953.
There are geometrical problems in the interpretation of seismic records made underground. The usual method of construction of the image point is not applicable. Reflections must be calculated at each seismograph individually. From these a group of ellipsoids of rotation is obtained to which the reflection plane is tangential. When the ellipses are projected upon a level, the reflecting plane appears in a zone of aggregation. This method is valid only if the reflecting plane is perpendicular; otherwise a correction must be introduced in the construction of the ellipses. The case of very genlte dip and the evaluation of surveys on several levels are also discussed.
((From Geophysical Abstracts 158, U.S. Geol. Survey).

SEISMIC — THEORY & RESEARCH

33. *The Initial Propagation of Spherical Blast from certain Explosives.*
F. J. Berry & M. Holt, Proc. Roy. Soc., A, Vol. 224, No. 1157, pp. 236-251, 22 June, 1954.

The initial disturbance due to the detonation of an uncased spherical charge of explosive, initiated at its centre, is analysed in full. The equations of unsteady spherical motion are solved in the neighbourhood of the singularity at the origin of the air blast wave in the timedistance plane. Expansions are used in series of half-powers of the radia distance from this origin, with coefficients depending on the transverse co-ordinate. Two singular characteristics are found to start at this origin, and it is shown that the inner of these develops into a shoch wave. This is identified as the secondary blast wave previously observed in experimental and numerical work. The wave is very weak at first with a strength which is zero initially and then begins to grow in proportion to the radial distance.

In this paper the explosive gas is assumed to be polytropic, with $\gamma = 3$, but the method developed here can be extended to apply to any type of gas at the cost of additional labour.

(Author's Abstract)

34. *A Test on Elastic Anisotropy Measurement at Berriane* (North Sahara).
J. Cholet & H. Richard, Geophysical Prospecting, Vol. 2, No. 3, pp. 232-246, September, 1954.

The geophysicists who attempted to evaluate elastic anisotropy of some bedded formations often gave but little information about recording and interpreting the measurements. Maybe they did not lay enough stress on the fact that any determination of the anisotropy factor is a critical operation and that, to have some certainty, it must be made under good conditions and then discussed.

Due to the very favourable conditions offered, undisturbed tectonics and topography and relatively regular series, the Berriane district in Northern Sahara is rather well suited to accurate measurements and to an anisotropy study down to 1,250 meters. Since measurements have been carried out in the wildcat drilled at Berriane by S. N. Repal, it seems interesting to communicate the results obtained and and to discuss them according to the influence of high velocity layers.

It can be noted in the clay and sand series that have been investigated, anisotropy coefficient amounts to 1.09 or so.

To conclude, it seems desirable that determinations made by numerous operators should allow a more accurate knowledge of the anisotropy factor in the main types of rocks.

(Author's Abstract)

35. *Seismic Model Study of Refractions from a Layer of Finite Thickness.*
F. Press, J. Oliver, & M. Ewing, Geophysics, Vol. 19, No. 3, pp. 388-401, July, 1954.

Two-dimensional model experiments on refractions from layers of finite thickness are described. Refractions can be unreliable for velocity and depth determinations when they occur with wavelengths which are large compared to the layer thickness. Discrepancies reported between refraction velocities and borehole velocities can be partially accounted for in this manner. Even simple two- and three-layer models can show such effects as misleading second arrivals, echeloning of travel time curves, masked layers, and selective absorption in the overburden.

(Author's Abstract)

36. *Energy Distribution in Explosion-Generated Seismic Pulses.*
B. F. Howell, Jr., Geophysics, Vol. 20, No. 1, pp. 33.

Three separate pulses were recognized on a group of seismograms of ground motion resulting from explosions measured at distances ranging from 10 to 1,172 feet from the shot point. It is believed that the first pulse represents primarily body waves, the second pulse coupled waves formed by internal reflections in the low-velocity surface layer, and the third pulse Rayleigh and Love waves arriving simultaneously. The ratios of the energies of the various pulses are given for several distances. The rates of attenuation of the three pulses are expressed as exponential functions and also as inverse power functions.

37. *On the Propagation of Elastic Waves in an Inhomogeneous Sphere.*
Y. Nomura & K. Takaku, Tohoku Univ. Sci. Repts., Ser. 5, Vol. 4, No. 1, pp. 31-41, 1952.

The velocities of elastic waves propagating in a large inhomogeneous spehre are assumed to be functions of distance from the centre. From the rigorous solutions of wave equations are calculated various modes of reflection at the free surface, resulting in curved geometrical ray waves and surface waves, From these, intensities of various seismic waves are calculated.

(From Geophysical Abstracts 157, U.S. Geol. Survey).

38. *On the Propagation of Elastic Waves in an Inhomogeneous Sphere.*
Y. Nomura & K. Takaku, Tohoku Univ. Sci. Repts., Ser. 5, Vol. 5, No. 1, pp. 22-33, 1953.

The mathematical study of elastic wave propagation has been extended to the case of an elastic sphere of large radius having a concentric spherical fluid core whose radius is also large. The media of both shell and core are inhomogeneous, and their respective velocities are proportional to r^{-m} and r^{-s}, where m and s are arbitrary numbers larger than -1. Using values of elastic constants taken from seismological observations, reflection and refraction at the inner fluid boundary are calculated for the value $m = 0.3$, which takes into account waves far from the source.

(From Geophysical Abstracts 158, U.S. Geol. Survey)

39. *On the Reflection and Refraction of the Explosive Sounds at the Ocean Bottom.*
H. Honda & K. Nakamura, Tohoku Univ. Sci. Repts., Ser. 5, Vol. 4, No. 3, pp 125-133, 1953.

Reflection and refraction at a solid sea bottom of explosive sounds originating in a point source in the water have been treated mathematically. When the velocities of the longitudinal and transverse waves of the floor are greater than the velocity of the sound waves in water, both kinds of waves are refracted back into the water from the bottom, after travelling some distance along the bottom surface at horizontal distances from the source larger than some definite critical values. Expressions of reflected and refracted waves are obtained for periodic as well as aperiodic cases. Some numerical examples are given.

(From Geophysical Abstracts 158, U.S. Geol. Survey).

40. *Crustal Structure from Seismic Exploration.*
M. A. Tuve, H. E. Tatel & P. J. Hart, J. Geophys. Research, Vol. 59, No. 3, pp. 415-422, 1954.

The exploration of the earth's crust with seismic waves has an accuracy limited by conversion-scattering and the scattering of surface and interior irregularities. These scattering effects produce signals masking the smaller signals which might be present from minor structural features. Consequently, only the broader aspects of crustal structure may be observed with the seismic method. Our data in the form of travel-time plots may be fitted with a family of theoretical curves derived from a group of velocity vs depth relationships of a somewhat similar nature. These show that the wave velocity is greater at greater depths within the crust .The demarcation between crust and mantle (where the compressional velocity is 8 km./sec.) may be abrupt — less than 250 m. — or, as an extreme, may be gradual — within several kms. More complex velocity vs depth functions may be made to fit the data, but these require more complex assumptions. For example, it is not necessary to assume the existence of discrete systematic intermediate layering to fit the data; smooth continuous functions suffice and, in addition, no systematic reflections have ever been observed from such intermediate layers. (Author's Abstract).

41. *On a Case of Propagation of Sound in a Non-Homogeneous Medium.* (In Russian).
L. M. Brekhovskikh, Dokl. Akad. Nauk SSSR, 87, No. 5, pp. 715-718, 1952.
The acoustic field is analysed in a non-homogeneous stratified medium in which the velocity of sound depends as follows on the co-ordinate $z : c = c_0$ for $0 \leqslant z \leqslant h$, and $c = c_0 / [1 + 2a(z - h)]^{\frac{1}{2}}$ for $h \leqslant z \leqslant \infty$, remaining contsant in planes at right angles to the z axis. The boundary $z = 0$ is assumed to be totally reflecting, and the source has a point form.

42. *Surface Motion due to a Point Source in a Semi-Infinite Elastic Medium.*
E. Pinney, Bull. Seismol. Soc. Am., Vol. 44, No. 4, pp. 571-596, October, 1954.
The theory of the motion of the surface of a semi-infinite elastic solid due to an impulsive point source is developed, both for P-wave and S-wave point sources. The resulting motions have been computed numerically for the case $\lambda = \mu$ and are presented both in tabular form and graphically.

43. *Wave Propagation in a Visco-Elastic Medium.*
E. J. Scott, Q. Appl. Maths, Vol. 12, No. 3, pp. 300-306. Oct. 1954.
By combining Maxwell and Voigt spring-and-dashpot units in various ways-it is possible to describe the complex behaviour of real materials. The stress-strain laws obtained have been used to study the physical properties of high polymers and wave propagation in a visco-elastic medium.
This article considers the propagation of longitudinal waves in a medium confined between two parallel planes and whose physical behaviour is representable by a linear mechanical model consisting of two Maxwell units coupled in parallel.

44. *Microseism Ground Motion at Palisades and Weston.*
M. Blaik & W. L. Donn, Bull. Seismol. Soc. Am., Vol. 44, No. 4 ,pp. 597-612, Oct., 1954.
Statistical and individual wave studies of microseism ground motion at Palisades and Weston are analysed, using data from three-component seismographs. Results show that the microseisms are either pure Rayleigh waves or combinations of Rayleigh waves approaching from different directions. Some relationship is indicated between microseism parameters and local geology.

45. *Attenuation of Seismic Waves Near an Explosion.*
B. F. Howell, Jr. & E. K. Kaukonen, Bull. Seismol. Soc. Am., Vol. 44, No. 3, pp. 481-491, July 1954.
The energies of the first recorded pulses of seismic waves generated by a series of buried explosions is plotted as a function of distance from the shot point. At short distances the first pulse is a combination of the direct compressional wave, surface waves, and other pulses. Beyond 800 feet it is a pulse refracted at the bottom of the weathered layer. The refracted pulse has about 1/600 the energy of the direct pulse. The rate of attenuation of the two pulses is examined in an attempt to determine whether all the energy loss can be reasonably attributed to normal exponential absorption.

46. *Dispersive Properties of a Fluid Layer Overlying a Semi-Infinite Elastic Solid.*
I. Tolstoy, Bull. Seismol. Soc. Am., Vol. 44, No. 3, pp. 493-512, July 1954.
The dispersive properties of wave propagating in a system consisting of a fluid layer overlying a semi-infinite elastic body are investigated by means of new formu-

lae for the group velocity. The distribution of stationary values of the group velocity is examined in the light of these formulae and of numerical results. Also it is shown that the minimum group velocity of the fundamental mode may belong either to the normal-mode branch or to the Stonely-wave branch, depending on the contrast in wave velocities between the two media.

47. *Measured Response of a Structure to an Explosive-Generated Ground Shock.*
D. E. Hudson, J. L. Alford & G. W. Housner, Bull. Seismol. Soc. Am., Vol. 44, No. 3, pp. 513-527, July 1954.

Measurements were made of ground accelerations and the resulting building accelerations at a point very near a large quarry blast. It is shown that, in the case of simple buildings, the building acceleration may be calculated with satisfactory accuracy from a knowledge of the ground acceleration.

The response of the test building to the ground acceleration of a typical strong-motion earthquake was computed, and it was found that the resulting accelerations were in excess of those usually provided for in earthquake-resistant design. It is concluded that the satisfactory performance of well-designed structures during strong earthquakes may have two explanations: first, that vibration energy is dissipated by stresses in excess of the elastic limited, with the result that hidden damage may occur; and second, that ordinary buildings may have sources of strength which are not taken into account in their design.

GRAVITY — GENERAL.

48. *Gravitation — Still a Mystery.*
P. R. Heyl, Sci. Monthly, Vol. 78, No. 5, pp. 303-306, 1954.

A review of concepts and experiments concerning the force of gravitation from earliest times to the present, concluding with a brief mention of the practical applications of gravity to geodesy and petroleum prospecting.

(From Geophysical Abstracts 157, U.S. Geol. Survey)

49. *Comparison between a Geologic and Geophysical Study (by Gravimetry) in the Basin of Blanzy.* (In French).
J. Louis, Soc. Geol. France Comptes Rendus, No. 7, pp. 141-144, 1954.

A gravimetric study was made in 1952 of the basin of Blanzy, in west-central France, and compared with a geologic study made in 1947. In general ,agreement was found to be satisfactory. The gravimetric measurements do not show details such as minor dislocations, and intersections of faults.

(From Geophysical Abstracts 157, U.S. Geol. Survey).

50. *Gravity and Magnetic Anomalies Associated with Basic Rocks of New Caledonia.*
Y. Crenn, Ann. Geophys., Tome 9, No. 4, pp. 291-299, 1953.

A discussion is given of the major gravimetric and magnetic (vertical component) anomalies of New Caledonia. Values are given of specimen densities and susceptibilities. A Bouguer anomaly map with 10-mgal contour interval and a magnetic map with significant anomalies indicated by (+) and (—) signs are presented. On the northwest coast of the island there is a positive gravity gradient of 10-mgal per km. This is interpreted as indicating a large intrusion of peridotite and the source of the apparently thinner peridotites covering the south of the island. A zone of peridotites and basalts extends along the northwest coast of the island. This zone seems to persist in depth, at least to a few kms. In one place the peridotite appears to overlie the basalt.

Isostatic balance seems to be realized, on an average, at a depth of 60 km., but there may be a partial local equilibrim under the island at a lesser depth.

(From Geophysical Abstracts 157, U.S. Geol. Survey).

51. *Report on the Gravimetric Measurements in the Basic Gravimetric Network During* 1950.
J. Picha, Czechoslovak J. Phys., Vol. 1, No. 3-4, p. 210, 1952.

During 1950 the work on the basic gravimetric network of Czechoslovakia was continued. Using the Nørgaard gravimeter, 181 stations of the first and second order were occupied, forming 8 triangles and a loop around the city of Praha. The base stations were Jested and Petrin.

(From Geophysical Abstracts 157, U.S., Geol. Survey).

52. *A Gravitational Survey over a Concealed Portion of the Warburton Fault near Lymm, Cheshire.*
W. Bullerwell, Bull. G. B. Geol. Survey, No. 6, pp. 1-12, 1954.

53. *A Gravimeter Survey over the Tilmanstone Fault, Kent Coalfield.*
W. Bullerwell, Bull. G. B. Geol. Survey, No. 6, pp. 13-20, 1954.

54. *A Gravimeter Survey of the Ston Easton-Harptree District, E. Somerset.*
W. Bullerwell, Bull. G. B. Geol. Survey, No. 6, pp. 36-56, 1954.

55. *Gravimetric Anomalies in the Grand Duchy of Luxembourg.* (In French).
A. Gloden, Ciel et Terre, 70^e Annee, Fasc. 5-6, pp. 185-187, 1954.

56. *Gravimetric Anomalies in the Little Danubian Lowland and Adjacent Regions.* (in Czech. with summaries in English and Russian).
R. Behounek, Czech., Ustredni Ustav Geol. Sbornik, Svasek 19, pp. 273-284, 1952.

57. *Gravimetric Profile between the Tyrrhenian and the Ionian Seas along the 40th Parallel.* (In Italian).
G. Boaga, Accad. Naz. Lincei Atti, Cl Sci. Fis., Mat. e nat., Rend., Vol. 14, No. 2, pp. 175-178, 1953.

58. *Gravity Measurements along the Lines of Precise Levels over Whole Japan by means of a Worden Gravimeter. I. Skikoku Island.*
C. Tsuboi, A. Jitsukawa, & H. Tajima, Proc. Acad. Japan, Vol. 29, No. 6, pp. 235-238, 1953.

59. *Gravity Measurements along the Lines of Precise Levels over Whole Japan by means of a Worden Gravimeter. II. Chugoku District.*
C. Tsuboi, A. Jitsukawa & H. Tajima, Proc. Acad. Japan, Vol. 29, No. 7, pp. 311-315, 1953.

60. *Gravity Measurements along the Lines of Precise Levels over Whole Japan by means of a Worden Gravimeter. III. Kinki District.*
C. Tsuboi, A Jitsukawa & H. Tajima, Proc, Acad. Japan. Vol. 29, No. 7, pp. 316-320, 1953.

61. *Gravity Measurements along the Lines of Precise Levels over Whole Japan by means of a Worden Gravimeter. IV. Tohoku District.*
C. Tsuboi, A. Jitsukawa & H. Tajima, Proc. Acad Japan, Vol. 29, No. 9. pp. 503-508, 1953.

62. *Gravity Measurements along the Lines of Precise Levels over Whole Japan by means of Worden a Gravimeter. V. Chubu District.*
C. Tsuboi, A. Jitsukawa & H. Tajima, Proc. Acad. Japan. Vol. 29, No. 10, pp. 550-555, 1953.

63. *Gravity Measurements along the Lines of Precise Levels over Whole Japan by means of a Worden Gravimeter. VI. Kanto District.*
C. Tsuboi, A. Jitsukawa, & H. Tajima, Proc. Acad. Japan, Vol. 29, No. 10, pp. 556-560, 1953.

64. *Gravity Anomalies in the Portuguese Part of Island of Timor.* (In Portuguese).
C. Teixeira, Garcia de Orta, Vol. 1, No. 2, pp. 211-217, 1953.

65. *On the Gravity Field of the Sunda Region, West Indonesia.*
B. J. Collette, Geol. en Mijn., Jaarg. 16, No. 7, pp. 271-300, 1954.

66. *On the Gravity Field of the Sunda Region, West Indonesia-A Postscript.*
B. J. Collette, Geol. en Mijn. Jaarg. 16, No. 8, pp. 335-338, 1954.

GRAVITY — INSTRUMENTAL

67. *A Gsi Pendulum Apparatus for Gravity Measurements*
K. Muto, Acad. Japan Proc., Vol. 29, No. 8, pp. 439-445, 1953.
The GSI instrument consists of three quartz pendulums and a recording device. Laboratory and field measurements indicate an accuracy of 0.2 milligal for the mean of several readings at a single station.
(From Geophysical Abstracts 158, U.S. Geol. Survey).

68. *The Basic Principles of Gravimeters Especially Adopted for Observations on Unstable Ground.* (In Spanish).
L. Lozano Calvo, Rev. Geofis. ano 12, No. 46, pp. 101-117, 1953.
Two new gravimeters, one torsional and the other differential, are described. They are both designed to overcome the difficulties of levelling and eliminating vibrations on unstable or marshy ground.

69. *Remote Control Gravimeters for Gravimetric Exploration in Marine Areas.* (In Spanish).
G. Sans Huelin, Rev. Geofis. ano 12, No. 47, pp. 234-237, 1953.
Two remote-controlled gravimeters for marine exploration are described. Each is mounted in a bell-shaped vessel and has a heater, a thermostat, and a motor for levelling and adjusting. The vessel is lowered to the sea bed. Limitations to accurate use are 400 m in depth and 15 km out from the shore.

70. *Study of Periodic Changes of the Force Of Gravity.* (In Russian).
Y. S. Dobrokhotov, Akad. Nauk SSSR Vestnik, No. 4, pp. 85-87, 1954.
To observe diurnal and other changes of gravity due to lunisolar effect and the resulting deformations of the earth, a special gravimeter of high sensitivity was constructed. With this instrument it is possible to measure and to record photographically the relative value of gravity and simultaneously to determine the deviations of the vertical at the station. The sensitivity of the instrument is such that the amplitude of the diurnal variation is 10 mm for visual observations and greater if photoelectric recording is used. The drift is linear with time and can be made very small. The main element of the gravimeter is a quartz fibre horizontally stretched and twisted by an eccentrically attached weight.
(From Geophysical Abstracts 158, U.S. Geol. Survey).

GRAVITY — INTERPRETATION

71. *On an Analytical Method of Calculating the Regional Anomaly.* (In French).
V. Baranov, Geophysical Prospecting, Vol. 2, No. 3, pp. 203-226, September, 1954.
The common notion that the regional anomaly must be as regular as possible, can be translated into mathematical language by requiring that the regional anomaly

shall be represented over a not too large area by a surface of the second or of the third degree. The residual anomaly is commonly defined by the requirement that its horizontal dimensions must be as small as possible. This implies that also its amplitude should be small. This requirement may be moulded into a mathematical form by stating that the square of the distance between the Bouguer anomaly and the regional anomaly, integrated over a certain area, must be a minimum. On these two definitions an analytic method is based for deriving the regional anomaly. Practical computation procedures are presented.

(Author's Abstract).

72. *The Regular Parts of the Gravity Field, with an Application to Central Europe.* (In German).

A. Berroth, Geofis. Pura e Appl., Vol. 28, pp. 1-35, 1954.

The regular parts of the gravity field means the continental and the regional ones. The residuals are the local parts. The regional parts certain a too large area, as to establish them by a single rate, they demand two rates. The separation of all 4 parts can be obtained by two different methods: the one demands calculation point by point by means of theoretical gravity functions and therefore allows application only in particular cases. The other one permits derivation area by area with a method of practical adjustment. Several gravity maps are the result of those calculations.

(Author's Abstract).

73. *Divergence of the Normal Gravitational Field* (In Italian).

A. Marussi, Geofis. Pura e Appl., Vol. 25, p. 5, 1953.

In some modern procedures for the study of gravity anomalies, the divergence of the surface gradient of gravity (second differential parameter of Beltrami) on a level surface is considered. Such divergence is connected with the geometrical and dynamical elements of the filed by simple relations, in particular with second derivatives of gravity along the lines of force. In the present paper the general formulae are applied to Somigliana's field referred to its intrinsic co-ordinates, and the values of the surface divergence and other elements of the normal field are given for latitudes from 0° to 90°.

74. *Numerical Computation of the Variation of Gravity with Time for a Rigid Earth.* (In German).

H. G. Reinhardt et al., Bergakademie, Jahrg. 5, No. 5, pp. 187-195, 1953.

The complete derivation of the correction to gravity measurements for the tidal effects of the sun and the moon on a rigid earth by the methods of spherical astronomy is given. Numerical results are presented in the form of graphs, and auxiliary tables to facilitate computations are also given. By comparing these corrections with actual values recorded at a station for a sufficiently long period of time, it is possible to determine the additional correction for the deformation of the earth.

(From Geophysical Abstracts 157, U.S. Geol. Survey).

75. *On the Determination of Deviations of the Vertical by means of the Gradient* U_{zzs}. (In German).

W. Sand, Geofis. Pura e Appl., Vol. 27, pp. 30-34, 1954.

This paper shows how the difference between the verticals at two points in the earth's gravitational field can be calculated from U_{zzs} ($U_{zzs} = \pm\sqrt{U_{zzx}^2 + U_{zzy}^2}$) without using astronomic or geodetic measurements.

76. *The Least Squares Method of Determining Regional Contours.*

L. H. Tarrant, Bull. G. B. Geol. Survey, No. 6, pp. 33-35, 1954.

In determining regional effects, the general problem is one of producing a set of smooth contours approaching as nearly as possible the original contours. Such a set can be represented by equations of the form $V = A + Bx + Cy + Dx^2 + Ey^2 + Fxy$, where V is the contour value at any point with co-ordinated x and y, and A to F are numerical coefficients. By determining A to F by least squares, the condition of near approach to original contours is satisfied. If the points are chosen in a symmetrical array, many coefficients become zero, and if the scale is adjusted to make the points of the array unit distance apart, the remainder is easily calculated. A similar approach to the problem has been developed by Agocs.

(From Geophysical Abstracts 158, U.S. Geol. Survey).

77. *The First and Second Vertical Derivatives of Gravity.*
C. Tsuboi, J. Physics of the Earth, Vol. 1, No. 2, pp. 95-96, 1952.

A method is shown for calculating the distribution of $\delta g / \delta z$ from that of g. The first power quantities are less sensitive to local horizontal gravity variations and observational errors than the second derivative $\delta^2 g/\delta z^2$, and are preferable where the object is merely to get a quantity reasonably sensitive to small irregularities in gravity distribution.

(From Geophysical Abstracts 158, U.S. Geol. Survey).

78. *Anomalies of the Vertical Gradient of Gravity Assiciated with Anomalies of Gravity.*
C. Tsuboi, J. Physics of the Earth, Vol. 1, No. 2, pp. 97-100, 1952.

The relation between the anomalies of the vertical gradient and total gravity anomalies are investigated mathematically and it is concluded that the former are sometimes too large to be neglected in the free-air reduction of gravity. A difference of 20 milligals is possible in the free-air reduction for an altitude of 3,000 m.

(From Geophysical Abstracts 158, U.S. Geol. Survey).

79. *Curvature of Equipotential Surfaces, Gradients, and Horizontal Components of Gravity.* (In Mexican).
O. Schneider, Interamericana Recursos Minerals, Primera Convencion, Mem,. pp. 191-199, 1952.

A method of calculating differential curvature of the gravitational equipotential surface from gravimetric (Bouguer) maps. Formulae for north and east components of differential curvature are derived. The resulting values are free of the regional effect and require no latitude correction.

80. *Computations of Spatial Distribution of Potential Fields and their Utilization in Geophysical Exploration, Part* 4. (In Russian).
B. A. Andreyev, Akad. Nauk SSSR Izv. Ser. Geofiz., No. 1, pp. 49-64, 1954.

This paper deals primarily with gravitational and magnetic anomalies and their interpretation by matching the curves obtained in a survey with potentional field patterns produced by bodies of different geometric shapes. Several examples of sharply localized anomalies and of anomalies produced by extended horizontal layers are included.

(From Geophysical Abstracts 157, U.S. Geol. Survey).

81. *Calculation of Density in Gravimetry.* (In Mexican).
O. Schneider, Interamericana de Recursos Minerales, Primera Convencion, Mem. pp. 200-201, 1952.

A method of calculating density which eliminates the personal equation. An equation is derived for the free-air Bouguer correction, then the density may be calculated from the formula $k = (0.3086 — 0.04185\ \sigma)$ mg/m. An example is given.

82. *On the Determination of Altitudes and Gravimetric Corrections.* (In Spanish).
A. Coloma Perez, Rev. Geofis., ano 12, No. 47, pp. 182-216, 1953.

A discussion of the determination of Faye and Bouguer corrections and the reverse problem, or the determination of the altitude of a point above base level from the measured difference in gravity. Results are presented in a general table, in convenient form for use in computations.

(From Geophysical Abstracts 158, U.S. Geol. Survey).

83. *A Simple Method of Reduction of Geophysical Anomalies to a Given Altitude.* (In Russian).
B. A. Andreyev, Vses. Nauchno-issled. Inst. Razved. Geofiz. Trudy, Vypusk 3, pp. 6-9, 1950.

In two-dimensional problems, values of the potential function U (gravitational or magnetic) on the surface of the earth and on a plane at elevation *h* can be compared by using the formula

$$U\ (x'_1 - h) = h/\pi \int U\ (x,0)\ dx/\ (h^2 + (x - x')^2)$$

where x is the co-ordinate of a point on the earth's surface and x' the point at height h above it.

The integration is simplified by introducing a new variable, and a chart is presented for graphic determination of the integral. The accuracy of these procedures is sufficiently high.

(From Geophysical Abstracts 158, U.S. Geol. Survey).

84. *On the Conditions of Applicability of the Formulae Derived for Two-Dimensional Problems in the Interpretation of Magnetic and Gravitational Anomalies.* (In Russian).
B. A. Andreyev, Vses. Nauchno-issled. Inst. Razved. Geofiz. Trudy, Vypusk 3, pp. 3-5, 1950.

In interpretation of magnetic and gravitational anomalies, it is often assumed that the disturbing body is infinitely extended in one direction, which reduces the problem to just two co-ordinates and simplifies the analysis. Andreyev discusses cases where such an assumption is admissible and computes the error committed by such simplification. The assumption is valid, for instance, in the case where the disturbing body is an ellipsoid of revolution with the ratio of long axis to transverse greater than 5. The resulting error in such a case is less than 2 per cent.

(From Geophysical Abstracts 158, U.S. Geol. Survey).

85. *Interpretation of the Gravity Field of the Eastern Alps.*
M. H. P. Bott, Geol. Mag., Vol. 91, No. 5, pp. 377-383, September 1954.

It is demonstrated that a deficient mass reaching within 10 km of the surface is responsible for the central belt of negative gravity anomalies in the Eastern Alps. Hypotheses for explanation of the deficient mass are discussed and it is concluded that the presence of unexposed granite in addition to crustal downwarp is the most satisfactory of these. The position of part of the mass deficiency is irreconcilable with existing isostatic hypotheses and an alternate hypothesis is proposed. The development of the granite mass deficiency is briefly discussed.

(Author's Abstract).

GRAVITY — THEORY & RESEARCH

86. *Possible Maximum Variations in the Force of Gravity as may be Observed at the Earth's Surface.*
V. G. Gabriel, St. Louis Acad. Sci. Trans., Vol. 31, No. 7, p. 9.

The earth and its ideal mathematical representation, a spheroid of revolution, are briefly defined in terms of radii and other parameters. The force of gravity at the earth's surface is defined by means of Newton's law of universal gravitation, and free-air, Bouguer, and isostatic corrections are briefly explained. By applying generally accepted furmulae, the combined effect of theoretical gravity values referred to the International Ellipsoid and the maximum deviations from it due to the necessary corrections are evaluated and plotted as a curve having latitude against possible maximum gravity in gals.

(From Geophysical Abstracts 157, U.S. Geol. Survey).

87. *A Laboratory Investigation of the Second Order Corrections to Gravity Measured at Sea.*
J. C. Harrison, Mon. Not. Roy. Astronom. Soc., Geophys, Suppl., Vol. 7, No. 1, pp. 22-31, October 1954.

A Vening Meinesz pendulum apparatus was subjected to simple harmonic accelerations and the changes in the periods of the pendulums caused by the motion were measured. The second order corrections were investigated for vertical accelerations with periods between 5.9 and 12.8 seconds and for horizontal accelerations with periods between 3.30 and 6.85 seconds. These corrections were always found to be consistent with Browne's expressions. The long-period pendulums, added to the main apparatus in 1938 in order to record its horizontal accelerations, were found to give satisfactory results.

MAGNETIC — GENERAL

88. *Rock Magnetism as a Temperature Indicator.*
H. Manley, J. Geomagnetism & Geoelectricity, Vol. 6, No. 1, March, 1954.

The magnetic properties of a suite of Scotch dykes are given briefly and the results afford a good correlation with their degree of metamorphism. The intensity of remanent magnetisation falls rapidly with increase of metamorphism. The unaltered dyke material described here is believed to be a case of remanent magnetism in the oldest rocks yet mentioned in literature.

(Author's Abstract)

89. *Aeromagnetic Survey and Geologic Reconnaissance of Part of Piscataquis County, Maine.*
J. R. Balsley & E. P. Kaiser, U. S. Geol. Surv. Geophys. Inv. Map GP 116, 1954.

An aeromagnetic survey, followed by geologic reconnaissance of part of Piscataquis County ,Maine, was made in an effort to locate masses of gabbroic rock similar to that containing the deposit of massive pyrrhotite at the Katahdin Iron Works. No direct evidence of previously unknown sulfide deposits was found. Thirteen anomalies are discussed and recommendations are made for further work.

(From Geophysical Abstracts 157, U.S. Geol. Survey).

90. *Geophysical Surveys in Salt Lake Valley, Utah.*
K. G. Books, Science, Vol. 119, No. 3094, pp. 513-514, 1954.

Anomalies observed on an aeromagnetic survey in the southern part of Salt Lake Valley, subsequently detailed by ground magnetometer and gravimeter surveys, are attributed to a cylindrical body 500 feet in radius, buried less than 1,000 feet deep, with a susceptibility of 12350×10^{-6} cgs units and a density contrast of 0.25. The sources of the anomaly may be an instrusion.

(From Geophysical Abstracts 157, U.S. Geol. Survey).

91. *Aeromagnetic Surveys in the Aleutian, Marshall and Bermuda Islands.*
F. Keller, J. L. Meuschke & L. R. Alldredge, Trans. Am. Geophys. Un., Vol. 35, No. 4, pp. 558-572, 1954.

92. *Gravity and Magnetic Anomalies associated with Basic Rocks of New Caledonia.*
Y. Crenn, Ann. Geophys., Tome 9, No. 4, pp. 291-299, 1953

A discussion is given of the major gravimetric and magnetic (vertical component) anomalies of New Caledonia. Values are given of specimen densities and susceptibilities. A Bouguer anomaly map with 10-mgal contour interval and a magnetic map with significant anomalies indicated by (+) and (—) signs are presented. On the northwest coast of the island there is a positive gravity gradient of 10-mgal per km. This is interpreted as indicating a large intrusion of peridotite and the source of the apparently thinner peridotites covering the south of the island. A zone of peridotites and basalts extends along the northwest coast of the island. This zone seems to persist in depth, at least to a few kilometers. In one place the peridotite appears to overlie the basalt.

Isostatic balance seems to be realized, on an average, at a depth of 60 km, but there may be a partial local equilibrium under the island at a lesser depth.

(From Geophysical Abstracts 157, U.S. Geol. Survey).

93. *Geologic Investigations of the Boyertown Magnetite Deposits in Pennsylvania.*
H. E. Hawkes, H. Wedow, & J. R. Balsley, U.S. Geol. Survey Bull., 995-D, pp. 135-149, 1953.

94. *A Vertical Force Magnetic Survey of the Coalisland District, Co. Tyrone, Northern Ireland.*
W. Bullerwell, G. B. Geol. Survey Bull., No. 6, pp. 21-32, 1954.

MAGNETIC - INSTRUMENTAL

95. *Note on a Proposed Three-Component Aeromagnetometer.*
V. B. Gerard, New Zealand J. Sci. Tech., Sec. B, Vol. 35, No. 1, pp. 1-3, 1953.

For observation by this instrument, flying is restricted to clear nights, and star photographs are taken by a non-magnetic camera mounted on the fluxgate gimbal mechanism of a total-force aeromagnetometer. The camera's optical axis is parallel to the total-force fluxgate, and, by identifying the stars photographed, the orientation of the total-force fluxgate is determined and the magnetic declination and dip calculated. Tests made on the ground, with an experimental camera, indicated that this proposed method is feasible, and that the expected error would be about ± 0.2° in both declination and dip.

(Author's Abstract).

96. *The Magnetic Field Mill.* (In German).
K. Burkhart, Geofis, Pura e Appl. ,Vol. 24, pp. 37-53, 1953.

A detailed description is given of a new instrument for exploration of magnetic fields. Operation is based on intermittent opening and screening of horizontally placed coils thus producing of electromotive force in them by the vertical component of geomagnetic field. The induced alternating voltage of about 2 volts is electronically amplified. The instrument is well adapted to absolute measurement of the vertical component of the geomagnetic field. The compensation of the vertical vector necessary for the calibration of the instrument is made, as usual, by a Helmholz coil. Using an amplification ranging from 30 to 50 it is possible to measure the minimum intensity of the field with an error of ± 0.6 gamma.

(From Geophysical Abstracts 157, U.S. Geol. Survey).

97. *This Mobile Magnetometer Accurately Maps these Contacts.*
N. S. Morrisey, Oil & Gas J., Vol. 53, No. 19, pp. 120, September 13, 1954.

A truck-mounted magnetometer measures anomalies as small as 25 gammas. It is a suitable medium between the airborne magnetometer and the station-reading hand instrument.

Total field intensity is continuously recorded at speeds up to 30 m.p.h. along the profile. The detector is automatically oriented to receive maximum intensity, and data is simultaneously recorded graphically.

MAGNETIC — INTERPRETATION

98. *Computations of Spatial Distribution of Potential Fields and their Utilization in Geophysical Exploration, Part* 4. (In Russian).
B. A. Andreyev, Akad. Nauk SSSR Izv. Ser. Geofiz., No. 1, pp. 49-64, 1954.

This paper deals primarily with gravitational and magnetic anomalies and their interpretation by matching the curves obtained in a survey with potential field patterns produced by bodies of different geometric shapes. Several examples of sharply localized anomalies and of anomalies produced by extended horizontal layers are included.

(From Geophysical Abstracts 157, U.S. Geol. Survey).

99. *On the Conditions of Applicability of the Formulae Derived for Two-Dimensional Problems in the Interpretation of Magnetic and Gravitational Anomalies.* (In Russian).
B. A. Andreyev, Vses. Nauchno-issled. Inst. Razved. Geofiz. Trudy, Vypusk pp. 3-5, 1950.

In interpretation of magnetic and gravitational anomalies it is often assumed that the disturbing body is infinitely extended in one direction, which reduces the problem to just two co-ordinates and simplifies the analysis. Andreyev discusses cases where such an assumption is amissible and computes the error committed by such simplification. The assumption is valid, for instance, in the case where the disturbing body is an ellipsoid of revolution with the ratio of long axis to transverse greater than 5. The resulting error in such a case is less than 2 per cent.

(From Geophysical Abstracts 158, U.S. Geol. Survey).

100. *Geologic Interpretation of Magnetic Survey Results.* (In Russian).
V. I. Bauman, Vses. Nauchno-issled. Inst. Razved. Geofiz. Trudy, Vypusk. 2, pp. 3-58, 1950.

Bauman calculates the magnetic effect produced by a single pole; by an infinitely small dipole; by a thin infinite horizontal line of magnets having a magnetic intensity of $+\sigma$ per unit length; by two similar lines infinitely close and parallel, with magnetic intensities of $+\sigma$ and $-\sigma$ respectively; by two infinite parallel lines separated by a distance of 2λ; by an infinite horizontal slab having a thickness of 2b and intensity of $+\sigma$; by two infinite horizontal slabs, infinitely close, having a thickness of 2b and intensities of $+\sigma$ and $-\sigma$ respectively; and finally, by two parallel inclined slabs. Illustrations include the anomalies produced in each case as seen in the horizontal and vertical planes.

(From Geophysical Abstracts 158, U.S. Geol. Survey).

101. *When should the Vertical Magnetic Intensity be Recorded in a European Measuring Area.* (In German).
A. Schleusener, Geol. Jahrb., Band 67, pp. 361-365, 1953.

The most suitable interval between field measurements of vertical intensity, which are to be corrected for diurnal variations against observatory records in European areas, depends on the accuracy desired. For very precice work (limit of error ± 2 to $\pm 5\gamma$), readings should be made every 2 to 4 hours in the field and at the base station, and within 100 km of an observatory. For surveys (± 5 to $\pm 10\gamma$), field registration is not absolutely necessary but desirable, for by referring to observatory records, measurements made during rather strong disturbances (over 40γ) can be repeated. Base station readings should be made at the beginning and end of the work day and possibly once or twice during the day; maximum distance from an observatory should be 500 km. For coarse measurements ($\pm 15\gamma$ or more), such as over magnetite deposits, reference to observatory records is not necessary except to avoid large disturbances. Base station readings are necessary only in morning and evening.

(From Geophysical Abstracts 158, U.S. Geol. Survey).

MAGNETIC — THEORY & RESEARCH

102. *Rock Magnetism.*

T. Nagata, Tokyo, Maruzen Co., p. 236, 1953.

This is a review of present knowledge of the magnetism of rocks. The topics covered are: magnetic properties of rock-forming ferromagnetic minerals and of rocks, instruments and methods of measuring the magnetic properties of rocks, the remanent magnetization of igneous and sedimentary rocks, and such "geophysical problems" as paleomagnetism inverse remanent magnetization, and the relation of rock magnetism to magnetic anomalies and local variations in the geomagnetic field.

(From Geophysical Abstracts 156, U.S. Geol. Survey).

103. *Total Intensity Magnetic Anomalies of Three-Dimensional Distributions by means of Experimentally derived Double Layer Model Fields.*

I. Zietz & R. G. Henderson, Science, Vol. 119, No. 3088, pp. 329-330, 1954.

A series of experimental measurements of the total magnetic intensity in the direction of the inducing field has recently been completed for a series of models as part of a programme to devise rapid methods for the interpretation of total-intensity aeromagnetic maps. Experiments were conducted in a building of nonferrous material in which a Helmholz coil is used to simulate the field of the earth, and models composed of uniform mixtures of 1 part magnetite and 2 parts plaster of paris and of several different dimensions were studied. Experimentally derived field maps will be made available in a form independent of the susceptibility of the model and the strength of the inducing field and dependent only on the geometry of the model so that complicated bodies may be built up by proper combinations of blocks and the total normalized field computed arithmetically.

(From Geophysical Abstracts 156, U.S. Geol. Survey).

104. *About Possibilities and Limitations in Aeromagnetic Surveying* (In German).

A. Lundbak, Geofis. Pura e Appl., Vol. 27, pp. 110-115, 1954.

Aeromagnetic surveys of the past 20 years are reviewed. The outstanding development during this period is the airborne-fluxgate-magnetometer which has become very popular. This instrument measures the total intensity of the magnetic field. However, for prospecting purposes measurements of the separate components of the magnetic field are desired. These may be obtained either by direct measurement or by mathematical processes which are based on total-intensity measurements. The difficulties of each method are discussed and some solutions presented.

105. *The Remanent Magnetism of some Sedimentary Rocks in Britain.*

J. A. Clegg, M. Almond & P. H. S. Stubbs, Phil. Mag. ,Vol. 45, No. 365, pp. 583-598, 1954.

The remanent magnetism of nine sandstones from the Keuper Marl series was determined, and the polarization was found to be consistent in an approximately NE-SW direction with dips significantly less than that of the present earth's field; in some the direction of magnetization was reversed. Samples of the Pennant Sandstone (Upper Coal Measures) and Lower Old Red Sandstone also showed the same general axis of magnetization; the first showing a north-westerly declination with downward dip, and the second polarized in the reverse direction. Tests showed the rocks had a high degree of magnetic stability when exposed to alternating fields, but were easily changed by direct-current fields, suggesting that the rocks contain two magnetic components of different properties. Experimental deposition of powdered rocks suggests the rocks acquired their magnetization on deposition. The most likely explanation of origin of observed magnetization is said to be that the whole of the land mass which now constitutes England has rotated clockwise through 34° relative to the earth's geographical axis, since deposition of the rocks. The reversed magnetization is attributed to a reversal of the earth's field, although the effect of chemical and physical changes in the rocks since compaction is not ruled out.

(From Geophysical Abstracts 157, U. S.Geol. Survey).

106. *Reversals of the Main Geomagnetic Field.* I.
J. Hospers, Proc. K. Ned. Akad. Wetensch. B, 56, pp. 467-476, November 1953.

Data on the history of the geomagnetic field was sought from measurements of the direction of permanent magnetization of igneous and sedimentary rocks. Many instances of igneous rocks show permanent magnetization approximately opposite in direction to the present field. This may be due to a property of the igneous rocks which on cooling produces reverse magnetization in a normal field, or ordinary thermo-remanent magnetism acquired in a reversed field. Preliminary results are given of measurements of datable sediments around the volcano Hecla (Iceland) from approximately 5 × 10^7 years ago to 1947-48. These include (1) historic, (2) postglacial, (3) early quarternary, (4) tertiary plateau, and (5) sediments. For (1) the vertical component is downwards and for (3) upwards. Those of (2) show the magnetic pole centred on the geographical pole. In (4) there are alternate zones of normal and reserved magnetization. The results are tabulated and a stratigraphic column for Iceland is given.

(From Physics Abstracts, September 1954).

107. *Reversals of the Main Geomagnetic Field.* II.
J. Hospers, Proc. K. Ned. Akad. Wetensch. B, 56, pp. 477-491, November 1953.

From examinations of samples of various groups of lava it is concluded that the mean duration of permanent magnetization is consistently more in agreement with the dipole and for normally (N) magnetized Tertiary specimens it originated before the tectonic movements. It has been stable in direction for several million years. It is of thermoremanent origin, was acquired during the initial cooling, and has been stable ever since. For reversed (R) natural magnetization Neel's proposed mechanisms with changes in the lattice for tetrahedral and octahedral types, with later selective chemical changes, are examined and checked by laboratory tests. It is concluded with reservations that only the assumption of a repeatedly reversing magnetic field is satisfactory and thus is confirmed by striking similarities between N and R magnetization.

(From Physics Abstracts, September 1954).

108. *Reversals of the Main Geomagnetic Field.* III.
J. Hospers, Proc. K. Ned. Akad. Wetensch. B, 57, pp. 112-121, January 1954.

Icelandic rocks have preserved a record of a repeatedly reversing magnetic field. The reversal is through 180° and apparently worldwide with a reversal of the polarity of the earth's magnetization in a way not yet known. The period of reversal is given as 2.5 to 5 × 10^5 years with the change occurring in 2 to 20 × 10^3 years. Four reversals of field are known but it has apparently occurred since at least Miocene times, 2 × 10^7 years ago. In examination of other works the views are not in serious disagreement. In relation to continental drift theories, Iceland appears, within the limits of experimental accuracy, to have suffered no rotation and no changes in latitude since Miocene times. The position of the geographic pole in Miocene times given by workers on polar wandering is outside possible limits and the theory of polar wandering is not supported.

(From Physics Abstracts, September 1954).

109. *The Thermo-Magnetic Properties of the Tholeiite Dykes of Britain.*
H. Manley, Geofis. Pura e Appl., Vol. 29, pp. 57-70, 1954.

Some results are given of the thermo-magnetic behaviour of typical dolerites. It includes some work on the stability of their thermo-remanent magnetism and their variation in susceptibility, with temperature up to the Curie point, which was, also, determined for a number of samples. (Author's Abstract).

110. *On the Origin of Inverse Remanent Magnetization in Rocks.* (In Russian).
M. A. Grabovskiy & A. N. Pushkov, Akad. Nauk SSSR Izv. Ser. Geofiz., No. 4, pp. 320-329, 1954.

Experiments indicate that induced magnetization of a ferromagnetic rock cannot give rise to a magnetization of opposite polarity and of an intensity greater than that of the external field producing the induced magnetization; a ferromagnetic substance undergoing thermo-remanent magnetization can produce a magnetic field of resersed polarity and of an intensity greater than that of a constant magnetic field in which the rock is cooling; in the thermo-remanent magnetization of two rocks of different coercivity and different Curie points it is possible for one specimen to become magnetized with polarity opposite to that of the earth's field.
(From Geophysical Abstracts 158, U.S. Geol. Survey).

111. *Magnetic Correlation in Volcanic Districts.*
J. Hospers, Geol. Mag., Vol. 91, No. 5, pp. 352-360, September 1954.

Alternating zones of normal and reverse natural permanent magnetization, each comprising about twenty-five flows, have been found in the Tertiary and Quarternary plateau basalt series of Iceland. The techniques for measuring this permanent magnetization are discussed and some results shown. It is suggested that zones of normal and reverse magnetization may be useful for correlation purposes in volcanic districts. Some other possible applications of rock magnetism are mentioned.
(Author's Abstract)

112. *The Natural Permanent Magnetization of the Lower Basalts of Northern Ireland.*
J. Hospers & H. A. K. Charlesworth, Mon. Not. Roy. Astronom. Soc., Geophysical Suppl., Vol. 7, No. 1, pp. 32-43, October 1954.

The natural permanent magnetization of the Lower Basalts of Northern Ireland is investigated. Lava flows, on cooling, become permanently magnetized in the direction of the local magnetic field, thus studies can reveal the direction of magnetic fields in the past. All lava flows studied here possess reverse magnetization. Results of this work are compared with similar studies in Iceland.

ELECTRICAL

113. *Geo-Electrical Investigations of Manganese Ore Bodies in India.*
K. D. Jensen, Geofis. Pura e Appl., Vol. 28, pp. 91-108, 1954.

The manganese ore bodies in India are producing certain electrical potential fields on the surface, which are typical for these deposits and which can exactly be surveyed by combined potentiometer and resistivity method. The range of the relative potentials recorded so far are generally varying between 150 to 200 millivolts; near deeper buried deposits accordingly lower but not lower than 100 millivolts the relative resistivities vary from 50 to 400 megohms. The electrical surface indications are so clear that the respective position of an ore body can be located with an evident exactness as it is proved in this paper. Furthermore it is demonstrated how vast geological areas can be prospected in a minimum of time by this method for the benefit of the mining industry. (Author's Abstract).

114. *Electromagnetic Prospecting of some Lead-Zinc Deposits.* (In Jugoslav).
S. Jankovic, Glasnik Prirod. Mus. Srpske Zemlje, Ser. A, Kniga 5, pp. 159-170, 1952.

Lead-zinc deposits were located at Mazhic, near Trepca, and Ajvalija, near Pristina in Jugoslavia in Februari 1952 by the "Turam" method. In this method the in-phase and quadrature components of electromagnetic fields are measured;

the field is induced by a long grounded cable. Important anomalies of phase angles and out-of-phase components of the vertical field vector were found, making possible the exact delineation of ore bodies. The maximum gradient of the phase angle amounts to 3° per 10 m. Where the curves of phase angles and of the quadrature components did not show anomalous changes, the position of ore-bearing masses was determined by the equiphase curves of inphase components. The results of the measurements are presented on four maps of surveyed areas with characteristic curves traced in.

(From Geophysical Abstracts 157, U.S. Geol. Survey).

115. *On a Fundamental Geomatrans Problem.* (In Italian).
A. Belluigi, Geofis. Pura e Appl.; Vol. 28, pp. 57-65, 1954.

A solution to a 'geomatrans' problem for a homogeneous earth with deep horizontal stratification (good conductor). The magnetic field (matran) is particularly examined for indications to further prospecting by surface geomatran methods.

116. *On some Geoelectrical Investigations of Mineralized Zones.* (In Italian).
F. Mosetti, Observatory of Geophysics, Trieste Pub., No. 35, p. 4, 1953.

This paper describes in brief test surveys which use the resistivity method for identifying deposits of ores such as bauxite, blende, galena or pyrite. The extent of the deposit may also be determined.

117. *A Field Evaluation of the Electromagnetic Reflection Method.*
A. Orsinger and R. Van Nostrand, Geophysics, Vol. 19, No. 3, pp. 478-489, July 1954.

Previous publications have outlined the general theory of electromagnetic wave propagation along an interface such as the air-earth boundary and described model experiments in which this theory was verified. Equipment similar to that described for the laboratory experiments has been adapted for field use. Two large loops, one for transmitting and the second for receiving, are laid on the surface of the ground and a current square wave is passed through the transmitting loop. A similar arrangement of loops is placed on the surface of a metallic model. The signals from the two receiving loops are mixed in opposition. The layering in the model is then manipulated until the difference signal is a minimum, which condition signifies that the actual earth has been approximated in the model, after account is taken of the appropriate scaling factors. At five stations in Dallas County, Texas, this technique was used to determine the depth of the Austin chalk—Eagle Ford shale contact, which varies from 50 to 400 feet, within an average accuracy of about 5%.

(Author's Abstract).

118. *Interpretation of Resistivity Depth Curves.* (In Hungarian with Summaries in English and Russian).
K. Sebestyen, Magyar Allami Eötvös Lorand Geofiz. Intezet Geofiz. Közlem. Kotet 3, Szam 3, pp. 31-39, 1954.

A discussion of the practical use of the differential, the cumulative curve methods, and the master curves.

(From Geophysical Abstracts 158, U.S. Geol. Survey).

119. *On the Use of Elliptic Polarization of the Magnetic Field in Exploration.* (In Russian).
I. K. Ovchinnikov, Vses. Nauchno-issled. Inst. Razved. Geofiz. Trudy, Vypusk 3, pp. 39-49, 1950.

The magnetic field produced in the ground by e.m. induction is ellipsoidal in shape. In the case of acoustic frequency the phase angle of this vector is strongly influenced by the electrical conductivity of the ground, making the phase angle a sensitive indicator usable in prospecting.

Ovchinnikov presents tables of computed components of the magnetic vector from which the phase angle can be readily determined. The tables give the normal fields of loop conductor and cable conductor and of the same fields disturbed by a conducting sphere and cylinder, respectively.

(From Geophysical Abstracts 158, U.S. Geol. Survey).

120. *Underground Water Investigations by means of Geophysical Methods (Particularly Electrical) in the Central Anatolia.*
M. Y. Dizioglu, Maden Tetkik ve Arama Enstitüsü Mecmuasi, No. 44-45, pp. 63-70, 1953.

OTHER METHODS

121. *Airborne Radioactivity Surveys for Phosphate in Florida.*
R. M. M xham, U.S. Geol. Survey Circ. 230, 1954.
Airborne radioactivity surveys were carried out in 10 areas which were geologically favourable for uraniferous phosphate. Abnormal radioactivity was recorded in 8 of the 10 areas. Two of the anomalies were investigated on the ground. One resulted from a deposit of river-pebble phosphate, samples containing an average of 0.013 per cent equivalent uranium. The other anomaly resulted from outcrops of leached phosphatic rock containing as much as 0.016 per cent equivalent uranium.

122. *Airborne Scintillometer Survey of Radium Hill Area, South Australia.*
W. H. Cross, Canadian Min. Metall. Bull., Vol. 47, No. 505, pp. 348-350, 1954.
An airborne scintillometer survey of the Radium Hill area in South Australia indicated a number of areas with higher-than-normal radioactivity. The measurements were made from an aircraft travelling at a speed of 80 m.p.h., at a height of 250 feet. Traverses were spaced 500 yards apart.

123. *How to Use a Counter.*
W. Bilicke, Mines Mag., Vol. 44, No. 6, pp. 40, 90-92, 1954.
A description of how to use Geiger and scintillation counters in prospecting for uranium.

124. *Prospecting for Uranium with Car-Mounted Equipment.*
J. M. Nelson, U.S. Geol. Survey Bull., 988-I, pp. 211-221, 1953.
The basic principles of the car-traverse technique are simple. Rocks and soils of abnormally high uranium or thorium content are surrounded by an equivalenty high gamma radiation field. This field can be detected at relatively high speeds by a vehicle equipped with a Geiger-Müller counter. Once detected the area may be examined in more detail with portable equipment.

TEAM WORK IN SEISMIC PROSPECTING *

BY

G. BRINCKMEIER **

Professor Bentz *** has given a clear picture, and indeed a fascinating one, of the geological significance of the geophysical exploration in Northwest Germany beginning with the very first general exploration with magnetic methods, gravimetry, and refraction seismology, progressing to the refined detailed investigations now in use. Therefore I don't need to dwell on the objective side of our science, but I wish rather to deal with the men executing geophysical, and especially seismic exploration.

I am not going to report on those outstanding individuals who have made the most impressive contributions to the progress of our science and our practical work, but I prefer to speak primarily about the great number of those who carry out the surveys and investigations, and who make the interpretations.

At the heroic time, the pioneer time of Applied Geophysics when Eötvös, Conrad Schlumberger, Mintrop, Schweydar, to mention only a few, carried out their ideas and started the epoch of geophysics in prospecting not only for oil, but for useful minerals deposits in general; in those days it was possible that one man could master the entire extent of a geophysical survey. In the course of approximately 35 years, during which period I have been actively engaged in applied geophysics, I had the privilege to become very well acquainted with one of the pioneers just mentioned, Mintrop, the creator of the refraction seismic method who passed away only a few months ago. I myself saw him when he crept into the recording tent, mounted his self-designed seismic equipment, gave the necessary orders for placing the charge, gave the shooter the command for the shot, recorded the explosion, developed the film, interpreted the seismogram on the spot, drew the geological profile, and made the arrangements for the next shot.

No doubt the other pioneers of applied geophysics did their work in a similar manner. They had the idea for their method, they could construct their own equipment, they went out into the field, they themselves made the recording, they interpreted the results, they knew the problems and tasks, and in the event of a break-down they knew how to rectify it with the most primitive equipment.

---

* Presidential Address delivered at the Tenth Meeting of the European Association of Exploration Geophysicists, held in Hamburg, 16-18 May, 1956.

** Gewerkschaft Elwerath, Hannover.

*** Opening Address delivered at the Tenth Meeting of the E.A.E.G.

Apart from these theoretical and practical abilities they had properties of character which enabled them to select suitable coworkers, who were in fact their pupils, and then to inspire them with their own enthusiasm and pleasure in the work, and to show them the problems. Even in those days this circle included physicists, geologists, surveyors, precision mechanics, electrical engineers, in fact a collection of many professions and trades which were somehow connected, but without specialisation, with the geophysical objectives, equipment or field-technique. During an investigation each person had to be able to do every job by himself.

The general development and refinement of the equipment and the methods, and the steadily increasing demand on the part of the industry account for the fact that it is now rare to find combined in one person the gamut of different qualities and abilities associated with the whole field of applied geophysics. It is even unusual to find that one man possesses all the knowledge and experience required in the complete application of a single geophysical method, ranging from its field operations to the interpretations and theoretical considerations of highly qualified scientists.

The tasks which we now have to face have been so greatly refined and complicated since the heroic days of applied geophysics that a single man, even if he did possess all the outstanding qualities of the pioneers, would no longer have the ability to master and to control all the detailed problems alone.

First of all, there is the problem proper. In the heroic period it would suffice to find a salt dome, i.e. a huge quantity of rock of high elasticity within a layer of low elasticity (this is not the proper definition but the shortest one) or of low density within rocks of high density, or to locate the position and strike of a large anticline or large fault. These problems could be solved with simple methods, and the geological problems involved were well-known, not only to the geologists, but also to the physicists and geophysicists, and even to the observer. The problems prevailing to-day call for a combination of knowledge of all the geological possibilities, such as alterations in the facies, reef formations, and small faults, together with a knowledge of the physical properties of such formations, in order to enable the scientist to define the problem in such a way that a practical solution can be reached. It is very seldom that such an ability is possessed by one man, and frequently a whole team of geologists, physicists and geophysicists is required to plan a survey correctly.

On the other hand, the geologist will be rather lost if the reflection of a distinct interface is to be emphasized in the seismogram. This task very often requires the combined art both of the physicist and of the operator working in the field.

The representation of the position of the planes of reflection of any transverse events of the seismograms again calls for the abilities of an expert in applied mathematics.

All these efforts will, however, be in vain if, for example, the drilling crew fails or the explosives are blasted at too high, or too low a level.

The work of the surveyor, too, may be of decisive importance if the levellings have not been carried out with the necessary care. Slight inaccuracies in levelling may eliminate or simulate meaningful or false structures, respectively, which even though small, may be of sufficient magnitude to decide on the success or failure of a well.

The correct operation of the party chief, too, is of the greatest importance, whether he be a scientist or an engineer. His ability to organise will affect the economical efficiency of the crew, although economising in its proper sense can hardly be considered in geophysical work. The party chief's ability to get on with his men is another important factor.

It is very difficult to separate clearly the functions of each individual in a geophysical department. The chief geophysicist, for example, when allotting to a party a certain field of operation, must not only recognise and understand the possibilities allowed by reconciliation of the technical and geological aspects of the problem, but must also select the men best suited for the job. Moreover, the supervisor as well as the crew leader are expected to have this ability to a high degree. The supervisor has to plan the surveying programme in such a way, that it will do justice to all the aspects named, and the party chief must know whether, where, and how he may alter the planned programme for the sake of an easier realisation of the task without neglect of the real aim. Furthermore, he should know where the project will involve the tackling of greater technical difficulties. In many cases, however, the crew leader, in judging the extent of the technical difficulties in relation to the task proper, has to rely on the judgement of the man who controls the field work on the spot, perhaps in the jungle or in swampy and marshy districts, in rocky mountains, in arctic regions or under the glare of the tropical sun. Here again, despite all technical resources, the readiness to work, and the physical ability of even the last hand are decisive and essential factors.

There is no doubt that the best method to carry out our work to the extreme limit of technical perfection—apart from good material conditions—is to give everybody concerned a clear idea of the importance of his function in the framework of combined efforts. Similar conditions as in the technical realisation and the organisation of our work hold good for the scientific evaluation of the results. The geologist who, in the end, is given the contour maps and cross sections for the planning of a well must be able to feel fully confident that the submitted interpretation and computations correspond exactly with what is contained in the seismograms.

This is attained by a long path which leads from the observer to the computing staff, the crew leader, the supervisor and the computer in the central office, and to the interpreters. Even though the observer did his best, and gave the computers in the crew the best seismograms obtainable under existing conditions, and even though the maps and the information supplied by the surveyor were correct, and that the computers were competent to handle the seismograms correctly, the correct appraisal and interpretation of the seismograms still requires that the senior computer or the party chief should possess a knowledge which by far exceeds a mere elementary acquaintance with the potential geological conditions in the field of operation. In addition, the recognition and treatment of all the seismic complications such as reflected refractions, multiples, and lateral effects, requires a thorough knowledge of the possible paths of vibration waves. It is, of course, simply absurd to explain any seismic event of the seismogram as a multiple or a lateral effect, without stating sufficient reasons—a practice which, unfortunately, occurs again and again. True, we are well on the way towards eliminating human insufficiency by mechanising the computing process, but machines must be operated by man, and these machines must be operated intelligently. Otherwise the machines, too, would give faulty results, and there is no doubt that, for a long time to come, perhaps for ever, the human brain will serve as the basis for the geological interpretation of the survey.

In order to eliminate human insufficiency, the general procedure to-day is to obtain as many completely independent interpretations of the same seismograms as possible. First of all, there is the party chief, who, if a scientist, will examine the work of his computers. This, however, will not suffice, as the party chief, in addition to his scientific work, has to cope with many other problems, such as organisation, inspection of the field crew and the like, and, consequently, does not always have enough time to devote himself sufficiently to his scientific task.

And there is the supervisor. He either checks the results of the crew on the spot, or he receives an independent computation made by the computers in the central office from copies of the seismograms, or he has the results of the crew checked in the central office. He can then, in case of discrepancies, try to make the results correspond with the views of the men in the crew, or he can try to find other possibilities for a solution.

At this point, the results should have already been subject to sufficient criticism based on the established geological facts and dealing with the question whether or not the proposed solution is possible, or whether it is more or less probable. This criticism calls for a thorough knowledge of the geological possibilities in the area concerned, as well as of the appearance which geological facts may take in seismograms, and in the maps and sections derived from them. However, it is sometimes necessary to step boldly from the normal path of geological thinking and to give way to the power of imagination—to a limited degree, of course,—for many an idea which was far from normal has often proved prolific. I know of cases where notoriously wrong interpretations of geophysical surveys led to the discovery of an oil field. True, our final aim is to discover oil or other useful mineral deposits, but we can and must be contented if our drilling prognoses prove right and if one single drilling test can decide whether the investigated area must be considered unproductive or still hopeful.

New imaginative ideas, however, should be introduced in the interpretation only in such cases where they can be reasonably and constructively criticised by experienced colleagues.

The last link in the chain is then the discussion of the derived geological interpretation (and there are often several possibilities for the interpretation) with the geologists, who, from the point of view of technical realisation, have to decide on the drilling. Here, all the possibilities permitted by the interpretation will have to be clearly defined, and arranged according to their probability and their limits of error.

We have now considered the tasks which the surveying crew and the other staff of a geophysical department have to face from the commission of the operation, during its performance, after the time when the seismogram becomes available, and until the drilling is started (similar conditions hold good for any kind of geophysical investigation). But there is still one gap open. We have not yet mentioned the recording of the seismogram and the men who carry out this work. These men form the field crew, which consists of the labourers, the drillers, operators, the surveyors, the shooter, the field manager, the drivers and the party chief. Even pilots and ship's captains and others may be numbered among these men. These men, in fact, are the very nucleus of the geophysical department, since their work will decide the availability, usefulness, and usability of the seismograms. The correct planting of the seismographs which will ensure the exact recording of the vibrations of the earth depends on the care with which the labourers do their job. The driver, if careless, may land in a ditch with the whole equipment, and thus cripple the work of the crew for days, or even longer. The surveyor may make mistakes when spotting the points or be careless when making the levellings. The shooter may wrongly load the charge, the drillers may do a bad job, the operator may use the wrong filters or may make other mistakes in the handling of the highly complicated equipment. The field manager, too, may fail and upset the whole organisation. So many men and functions, so many sources of error. A certain guarantee is given by the fact that almost every function of any one man in the crew is controlled by the function of another man. But far too often the one will rely on the other, so that several simultaneous errors will arise in several places and make the efforts of the others futile. There is only one means of protection: a careful selection of the most reliable men. This is of particular importance, of course, in the case of the operator, who must have a precise knowledge of his equipment and of its operation. As a consequence, this responsible job—particularly at the time when the number of crews was smaller than to-day—was given to a theoretically qualified man or at least to an expert technician.

True, the industry has been endeavouring (successfully, by the way) to make instruments which are extremely foolproof, but these endeavours were again obstructed by the refinement of the task calling for more complicated equipment with a wider range of possibilities. We have to-day reached a stage where we want to record vibrations from 2 cps up to 500 cps with only one set of equipment and with one single blast only, a requirement which led to the introduction of the magnetic tape equipment.

The method of the magnetic tape recording, after having been generally applied, will, however, necessitate a reorganisation of the operations which is entirely different from the orthodox method. The man who has the most important function will then sit in the central computing office transforming the magnetic tapes into readable seismograms. This, indeed, is anything but an easy task as it requires the excellent operation of an electrical machine with many hundreds of possibilities.

All this again shows that, no matter which part of a seismic investigation or geophysical investigation in general is being dealt with, we shall never be able, in spite of the high degree of mechanisation, to do away with the work of qualified men. All participants, from the simple labourer up to the men in the "brains trust" who will eventually have to decide on the site of the drilling, and including the men who, retrospectively, starting from the result of the drilling operation will have to revise the preceding interpretations in order to eliminate potential errors and to avoid them in future investigations—all these men make up one great team doing responsible work. It is absolutely absurd that any of the groups in this chain of different functions should consider themselves inferior—a fact which can be repeatedly stated. A geophysical investigation constitutes teamwork in which no single link in the chain is permitted to fail even though the utmost degree of safety and security has been provided.

The enlarged team for a geophysical investigation comprises other groups of men who supply us with the means to carry out our investigations. There are the instrument makers who must understand the requirements and who must be well conversant with the most intricate ideas and methods of electronics. Another group is that of the geophysicists proper, who supply the computers, interpreters and geologists with the mathematical and physical means, by which the mere physical surveys can be transformed in such a way that they can be read and interpreted by the geologist and drilling engineer, and even by such laymen as for example, the managing directors.

The tasks which, in the times of the pioneers, could be handled by one single man, such as Eötvös, or Schlumberger, or Mintrop, had, with the increasing requirements, to be distributed among a steadily growing number of individuals. Each of these men, in his special capacity, whether he be an observer, a party leader, a chief geophysicist, an interpreter, a surveyor or a geologist, is as important in the chain of a geophysical investigation as his colleague. He is given his place, not only in accordance with his special knowledge and training, but also according to his human properties, which, in many respects, may be even more important.

APPLICATION OF DELAY AND INTERCEPT TIMES IN THE INTERPRETATION OF MULTILAYER REFRACTION TIME DISTANCE CURVES *

BY

S. M. WYROBEK **

Abstract

The well known quantities, delay and intercept times, can be made fully useful in the interpretation of multilayer refraction problems dealing with small undulating dips.

The identification of the individual refractors is made by the use of reciprocal and intercept times and by applying an additional and useful relationship, namely that the delay time profile between two shot-points should match the half-intercept time profile when calculated using the true velocity of the refractor.

With a suitable arrangement of shot-points this relation permits us to obtain the true horizontal velocity of a refractor from one direction of shooting only.

Presentation of the refraction results in the form of time sections, similar to those used in reflection surveys, is often desirable. These sections can be converted easily into depth sections, once the overburden velocities are defined.

The use of the method is limited not only by the dip, but also by the depth of the refractor. Deep refractors can be, however, worked out by this method, by reducing a multilayer problem to that of two layers, using again the delay times.

Introduction

There are many ways in which refraction time distance curves can be interpreted, but when dealing with problems in which a number of refracting layers of varying horizontal velocities have to be considered, the computations can become rather involved.

It is proposed in this paper to describe a method which we have found useful in our work and which we hope may be of use to others. In this technique we employ the quantities known as intercept and delay times.

Though the fundamentals of refraction interpretation are well known, for the sake of clarity it may be advisable first to recall what these quantities are.

---

*) Presented at the Ninth Meeting of the European Association of Exploration Geophysicists, held in London, 7-9 December 1955.

**) The British Petroleum Co. Ltd.

Part I

Delay and Intercept times for horizontal refractor

When a refractor of true velocity V_R is at the surface then the travel time of the seismic event from the shot point to the station at distance L will be

$$\mathrm{T}_o = L/V_R$$

When the same refractor is below the surface and the overburden velocity is V_o ($< V_R$), then the travel time T of the refracted wave from the same shot point to the same station will be longer, due to the presence of the overburden. The difference between these two times is called therefore the overburden delay time

$$T_D = T - T_o = T - L/V_R$$

If the depth of a horizontal refractor is h, and the critical angle is given by $\sin i = V_o/V_R$, then the algebraical expression for the overburden delay time can be given as:

$$T - L/V_R = 2\,h \cos i/V_o = 2\,h/V_R \tan i \,. \quad . \quad . \quad . \quad . \quad . \quad . \quad (1)$$

This leads us to the well known formula for the depth:

$$h = \tfrac{1}{2}\,(T - L/V_R)\,V_R \tan i = \tfrac{1}{2}\,T_D.F$$

i.e. the depth of a refractor below the datum is the product of half the delay time and the conversion factor, and this formula is similar to the expression for the depth of a reflector:

$$h = \tfrac{1}{2}\,T_v\,.\,V_a\ (T_v = \text{normal time, } V_a = \text{average velocity})$$

By setting $L = O$ in equation (1) we obtain the expression for the intercept time of the time-distance curve with the time axis:

$$I = 2\,h/V_R \tan i \quad . \quad . \quad . \quad . \quad . \quad . \quad . \quad . \quad . \quad . \quad . \quad . \quad (2)$$

which for horizontal beds is equal to the delay time, equation (1).

Delay and Intercept times for an inclined refractor

The delay time for a shot from A into a seismometer at B, or conversely, (see fig. 1) is defined by:

$$T - L/V_R = (AC + BD)/V_o + CD/V_R - L/V_R$$

putting:

$$h_2 = h_1 + \Delta\,h \qquad\qquad \text{and remembering that}$$
$$p_1 = h_1 \cos\alpha \qquad\qquad \sin i = V_o/V_R$$
$$p_2 = h_2 \cos\alpha \qquad\qquad \Delta\,h = L\,.\,\tan\alpha$$

and introducing the trigonometrical relations from fig. 1, we obtain after appropriate grouping:

$$T - L/V_R = \frac{\cos\alpha}{V_o}\left[2\,h_1 \cos i + \frac{L}{\cos\alpha}\left\{\sin\,(i+\alpha) - \sin i\right\}\right]$$

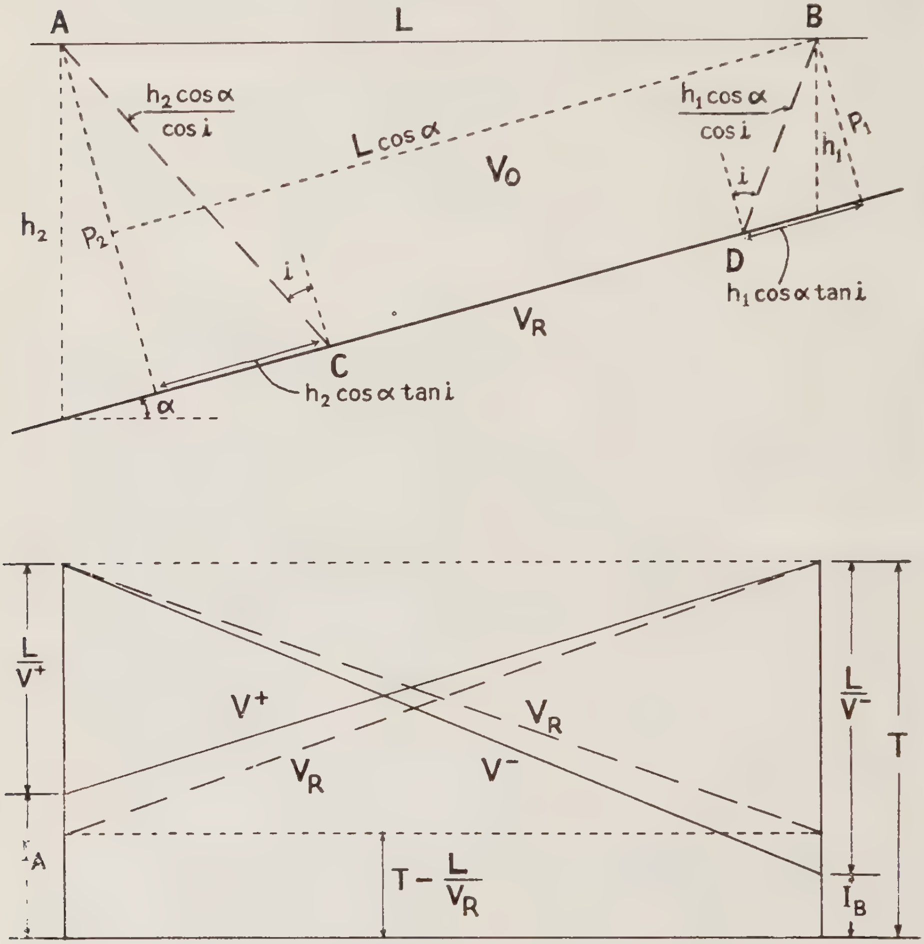

Fig. 1. Delay and intercept times for an inclined refractor.

The last equation leads us to:

$$T - L/V_R = (2\,h_1 \cos\alpha \cos i)/V_o + L\,(1/V^- - 1/V_R) \quad . \; . \; . \quad (3)$$

where V^- is the apparent velocity recorded shooting down-dip.
In the opposite direction we obtain similarly:

$$T - L/V_R = (2\,h_2 \cos\alpha \cos i)/V_o - L\,(1/V_R - 1/V^+) \quad . \; . \; . \quad (4)$$

where V^+ is the apparent velocity shooting up-dip.

Since $V_R = 2 \cos \alpha \dfrac{V^- V^+}{V^- + V^+}$, we may write for small α that

$$2/V_R = 1/V^+ + 1/V^- \text{ or } 1/V^- - 1/V_R = 1/V_R - 1/V^+$$

Taking this into account, the numerical values of the second terms on the right hand sides of equations (3) and (4) are equal for small angles of dip. They will be referred to as the "delay time difference" and denoted by ΔT_D. They represent the difference between the delay times of horizontal and inclined refractors .This delay time difference for a shot from A to B is equal and opposite to that for a shot from B to A.

Since the first term on the right in equations (3) and (4) is the intercept time (for $L = 0$) then these two equations can be written:

$$T - L/V_R = I_B + |\Delta T_D| \quad \dots\dots\dots\dots \quad (5)$$

$$T - L/V_R = I_A - |\Delta T_D| \quad \dots\dots\dots\dots \quad (6)$$

where the symbol || indicates "numerical value of".

The graphical equivalent of (5) and (6) is given in the lower part of fig. 1. Adding (5) and (6) we have:

$$T - L/V_R = \tfrac{1}{2}(I_A + I_B) \quad \dots\dots\dots\dots \quad (7)$$

$$\therefore V_R = L/[\mathrm{T} - \tfrac{1}{2}(I_A + I_B)] \quad \dots\dots\dots \quad (8)$$

which gives the true velocity of the refractor if the refractor does not change its dip and the velocity is constant between the shot-points. Subtracting (5) from (6), we obtain:

$$|\Delta T_D| = \tfrac{1}{2}(I_A - I_B) \dots\dots\dots\dots \quad (9)$$

i.e. the numerical value of the delay time difference between two shot points is equal to half the difference between the intercept times at these two points.

Graphical expression of the results

Plotting underneath the seismometer stations the values of the delay times for shots from A and B into one spread, we obtain two lines (fig. 2a), the lower representing the delay time profile from SP. A and the upper from SP. B. These lines are parallel to each other when the delay times have been computed using the correct value for V_R, and in this case their spacing is equal to the delay time difference for a shot from A to B. They will therefore coincide when the bed is horizontal.

Following equation (9) we plot (fig. 2b), half of I_A under $SP.A$ and half of I_B under $SP.B$ and the connecting line will be parallel to the two lines of fig. 2a. On the vertical under $SP.A$ we have the depth of the refractor under A expressed in time (strictly speaking the normal depth of the refractor divided by the conversion factor), on the vertical under $SP.B$ is the depth of the refractor under B expressed in time, and the slope of the line represents the slope of the refractor between A & B, expressed in time. This profile will be called therefore, the half-intercept time profile, similar to the vertical time profile used in reflection surveying.

Equations:

$$V_R = L/\left[T - \tfrac{1}{2}(I_A + I_B)\right] \text{ and } \Delta T_D = \tfrac{1}{2}(I_A - I_B)$$

are significant in pointing out a simple way in which the true velocity of a refractor can be determined graphically. It follows from them, that if we draw a delay time profile of the refractor between two shot-points using an arbitrary velocity and applying an approximate offset, match this profile by tilting to coincide with the half-intercept time profile obtained for these shot-points, then the velocity for which the coincidence occurs is the true velocity of the refractor.

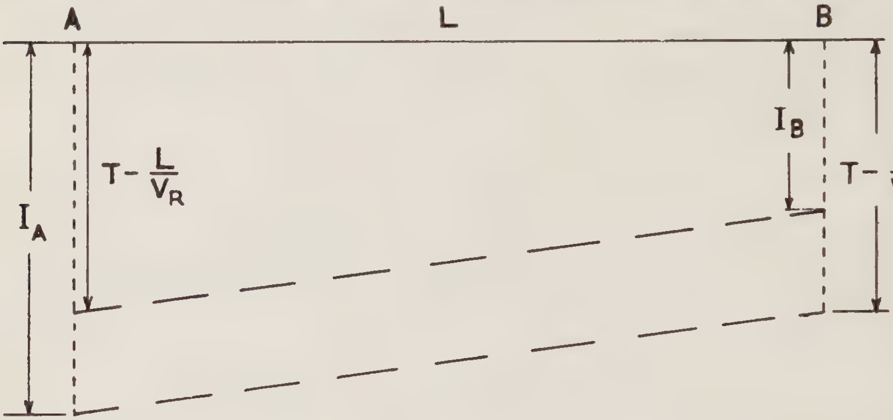

Fig. 2a. Delay time profiles from S.P.A. and S.P.B.

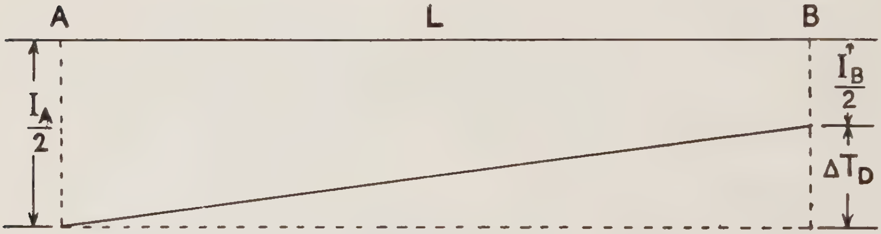

Fig. 2b. Half-intercept time profile between S.P.A. and S.P.B.

From the above it follows that with a suitable arrangement of shot-points, shooting in one direction only can be sufficient to secure the true velocity of the refractor.

From fig. 1 it is seen that instead of shooting profile AB from A and B, we can observe it in one direction only, say from shot-point A, and from shot-point B we observe a further profile to the right of B. Thus we shall have intercept time values for each shot-point and a profile between A and B, which according to equations (8) and (9) is sufficient for positioning the refractor under the datum and to obtain its true velocity. This will be readily seen in the example given below.

Example (*fig.* 3).

Suppose that we have observed in one direction only a single refractor along a line from seven more or less evenly spaced shot-points (A to G). On each spread the refractor is continuously covered along the length of the spread: this is obtained by overlap shots which cover the refractor from the critical distance back towards each shot-point. The overburden velocity was assumed to be 5,000 ft./sec., the refractor velocity 15,000 ft./sec. on the left side, and 16,000 ft./sec. from between shot-points E-F towards the right hand side of the figure.

The construction based on the foregoing is as follows:

1. Using formula $V = L/[T - \frac{1}{2}(I_A + I_B)]$ we compute the approximate value (V) of the refractor velocity between any 2 shot-points, or we can use a mean value from the time-distance graph, and for this value we compute delay time profiles for each shot-point separately, applying the formula $T_D = T - L/V$, (a value $V = 15{,}500$ ft./sec. was used in the example).

2. These delay times are plotted under the relevant seismometer stations and separate delay time profiles are obtained, one for each shot-point.

3. We construct a continuous delay time profile, usually on a separate tracing. (In the example it is based on the delay time segment from SP.B).

4. We determine the intercept time values for each shot-point on the time distance curves, or on the delay time profiles, by extrapolating each segment back towards its shot-point, parallel to the segment overlapping it, or by placing the tracing with the continuous delay time profile on each individual delay time segment, and reading the intercept of the profile with the vertical at each shot-point.

5. Half of these intercept time values are plotted below the corresponding shot-points.

6. The tracing with the continuous delay time profile obtained in (3) is now placed on the plot of half-intercept times (5), displaced parallel to itself by an approximate offset and matched by tilting to coincide with the values of the half-intercept times. This procedure is shown in the bottom drawing of figure 3. The part of the drawing with a time scale on both sides and small circles refers to the plot of half-intercept times. A separate tracing containing the continuous

delay time profile is shown as an overlay. It will be noted that from *A* to *E*, we shall have to tilt the tracing anticlockwise and from *F* to *G* in the clockwise direction.

7. From the amount of tilt we compute the velocity gradient and using this, the velocity for which the profile was drawn may be corrected to obtain the true velocity of the refractor. In our case the tilt amounts to —20 millisec per 10,000 ft. for the left side, and +20 millisec per 10,000 ft. for the right side, which represents a decrease of 500 ft./sec. and an increase of 500 ft./sec. respectively on the value chosen.

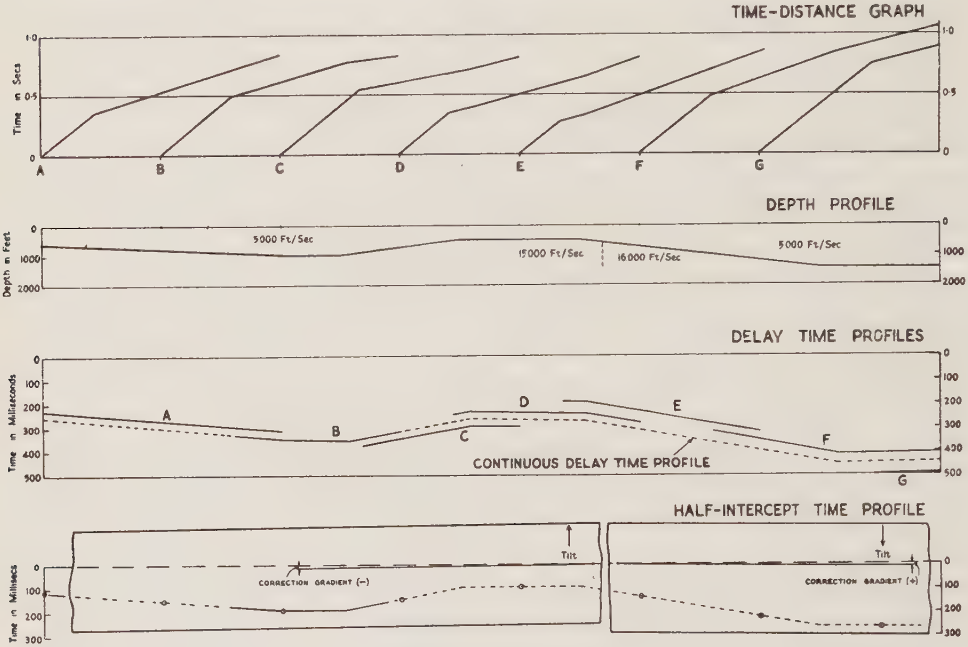

Fig. 3. Interpretation of results — shooting from one direction only.

8. If the tilt is small, then the individual station values, as copied on the tracing, can be pricked through on to the half-intercept time profile underneath, thus obtaining a completed half-intercept time profile with all the outstanding features which are picked up along the profile in the direction of shooting.

9. The time value under each station on the half-intercept time profile needs to be multiplied by the relevant conversion factor, to obtain its depth value in feet. With values converted into depth we draw arcs from each station, and the envelope to those arcs constitutes the final depth profile.

PART II

In the continuous profiling by the reflection method, a reflection is correlated from record to record or from spread to spread by the use of its vertical time value at the shot-point and of its reciprocal (interlocking) time values between two successive shot-points, the impulses across the record serving to follow the reflection continuously from one shot-point to another. Furthermore, it is general practice to plot vertical times of each reflection below shot-points and with the use of the reciprocal times, obtain time profiles or time sections of the reflectors with reference to an assumed datum. If the average velocity distribution is known for the area, these time sections can easily be converted into depth sections. As they are, these time sections constitute, in certain circumstances, a final conversion of record and other field data into a usable section on which further interpretation can be carried out, often without further reference to the records and preliminary computations.

Our aim is similar in continuous refraction surveys, that is, to have all field data from a continuous refraction line converted into a time section in which the vertical scale is expressed in delay times below the datum, and each refracting interface is distinguished from another by its true value of horizontal velocity. To obtain such delay time sections for several refractors, we have to carry out continuous profiling along the line, normally observing in two directions. The interval between two consecutive shot-points should be continuously covered by impulses from each refractor considered. After a time-distance curve is produced, one has to identify the individual refractors. This, as we have seen, is done by the reciprocal and intercept times between any two shot-points. Confirmation of the identification of the impulses from any one refractor is obtained by comparing reciprocal times (which should be equal), and intercept times at each shot-point which should match in the two directions of shooting. Also, one of the important factors in identification is obtained from the relation introduced in Part I, i.e. that the delay time profile of each refractor drawn between any two shot-points should match the appropriate half-intercept time profile in both directions of shooting for the same velocity. This procedure applied to a multilayer problem will be illustrated by a numerical example.

Numerical example (*Fig.* 4).

A 3-layer case was chosen with refractor velocities of 7,000 ft./sec., 14,000 ft./sec. and 20,000 ft./sec. The first interface between the 7,000 ft./sec. and 14,000 ft./sec. layers forms a gentle anticlinal surface with a depth varying from 1,500 ft. to 4,000 ft. with a maximum dip of about 7° on the left flank.

The second interface between 14,000 ft./sec. and 20,000 ft./sec. at a minimum depth of about 4,000 ft. forms a saddle between two highs of the same depth.

The left high is slightly broader and has a steep flank of more than 10° on its left. The other flank gently passes into a straight profile. Note that the inside flanks have dips up to about 8°. The time distance graph has been constructed assuming 11 shot-points (*A* to *L*) at 5,000 ft. intervals, giving satisfactory continuous cover for both shallow and deep refractors. For the sake of space at both ends of the graph, second events were constructed.

Interpretations of this time distance graph will consist of the following steps:

1. A preliminary identification of the refractors is carried out first on the graph, with the use, as far as possible, of intercept and reciprocal times. The branches of individual refractors can be marked with colours. In Fig. 4 overburden velocity is marked with a thin line, the shallow refractor with a thick line, the deep refractor again with a thin line. The second events are in a dashed line, station values are marked by circles and crosses according to the direction of shooting .We assume that the top layer has a constant velocity of 7,000 ft./sec.

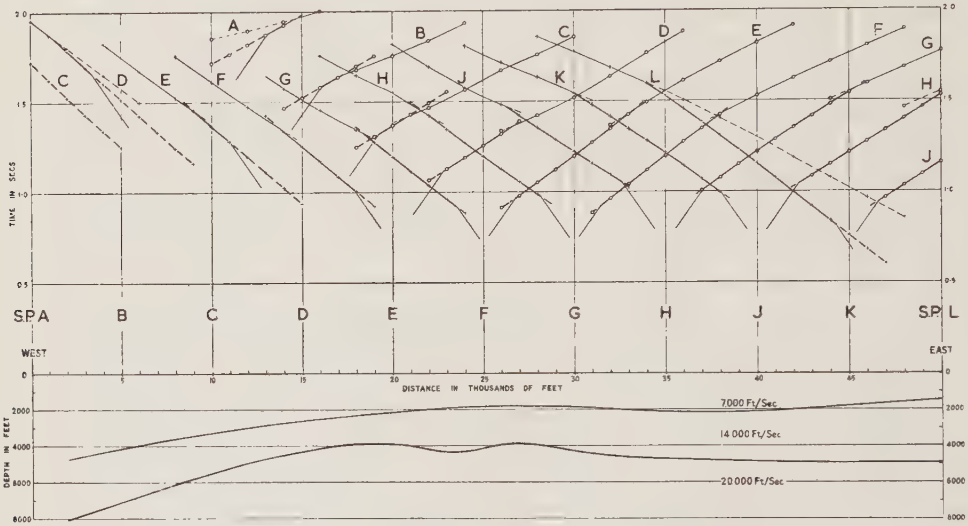

Fig. 4. Continuous time-distance graph over two refractors.

2. We proceed now with the preparation of the delay time profiles, separately for each refractor and for each individual shot-point within the refractor. For a velocity, assumed initially to be constant along the line, and chosen to approximate to the probable true velocity of the refractor on which we are working, we convert each segment of the shallow refractor in the time distance graph into a delay time profile by the use of the formula $T_D = T - L/V$.

By plotting the computed values below the station positions, using an appropriate time scale, we obtain a set of curves (fig. 5), which refers to the velocity segments in the time distance graphs in the direction of shooting from left to right (from *W* to *E*).

3. If we deal only with one well-defined refractor, we may proceed in the manner described in Part. I. However, in more complicated areas, a refractor may be preceded by a shallower one and followed by a deeper one, and the impulses will interfere with those from the refractor under consideration making further discrimination necessary. This is obtained by producing a similar set of delay time profiles in the opposite direction of shooting and in this case as shown in Fig. 5 we obtain a second set of delay time profiles referring to the direction of shooting from right to left, (or from *E* — *W*).

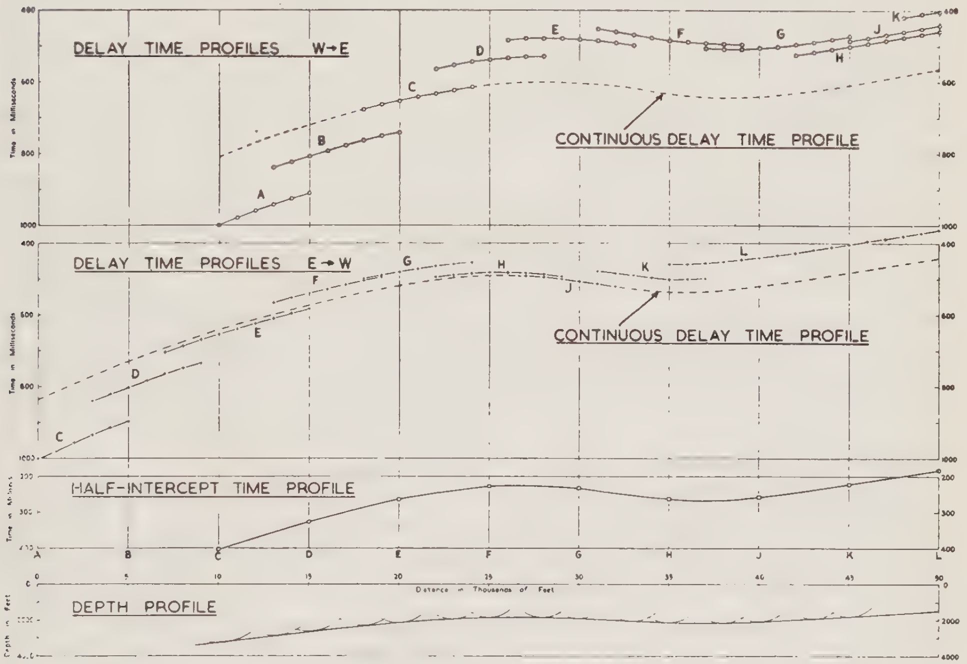

Fig. 5. Interpretation of the results of the shallow refractor in fig. 4.

4. Having these two sets of delay time profiles from *W* — *E* and from *E* — *W* we may check whether these two sets belong to the same refractor. We can do it directly on the time distance curve by checking the individual reciprocal times. It is much easier, however, to carry this out on the delay time profiles checking the reciprocal delay times. Thus we check that, for instance, a segment from *S.P. H* towards *E* cuts the vertical at *S.P. K* at the same delay time as the

segment from *S.P. K* towards *W* cuts the vertical at *S.P. H*. Similarly, the delay time from *S.P.* E on *S.P. G* (*W* — *E*) should be the same as that from *S.P. G* on *S.P. E* (*E* — *W*), and so on.

5. After this preliminary check we proceed with the construction of two continuous delay time profiles one in each direction of shooting. We base the first profile in *W* — *E* direction say on shot-point *C*, and the second profile, in *E* — *W* direction say on *S.P. J*. These two continuous time profiles are best constructed on two independent tracings.

They are essential for a final check of the reciprocal delay times, for computing the intercept times and for obtaining the combined time profile. In more complicated instances they form the basis of conversion of time profiles into depth profiles.

The final check of the reciprocal delay times is carried out in practice in the following manner:

The traced continuous delay time profile (say from *W* — *E*) is placed on to the delay time segment from shot-point *C* (as in figure 5) and delay time values are read off at all other shot-points (at the intersection of the continuous delay time profile with a vertical from each shot-point). Now the tracing with the reverse continuous profile is placed in turn on all delay time segments from *E* — *W* direction, and the reciprocal delay times are read off at the intersection with the vertical from shot-point *C*. Corresponding times read with the use of the first tracing and their reciprocals read with the use of the second tracing should be equal.

6. Now we determine and check the values of the intercept times in a similar manner. We place the tracing of the continuous delay time profile in the *W* — *E* direction on a particular delay time segment shot in the same direction. The time value of the continuous profile at the shotpoint, from which the particular segment has been shot, is then equal to the intercept time at that shotpoint. We now repeat the same procedure with the reverse delay time profile and check that the two intercept times derived from direct and reverse profiles for each shot-point are the same.

7. Discrepancies in both reciprocal delay times and intercept times are expected. The tolerable discrepancy is governed by the general accuracy of the survey and especially by the quality of the records and impulses obtained. It may vary up to 10-15 m.sec. If the discrepancies are greater, check that there was no error committed when constructing continuous time profiles. A fairly large discrepancy in the intercept times may prove that wrong impulses were chosen (and one has to go back to the records) or that we have come across a small fault or a marked change of dip under the shot-point considered, or that we deal with a diffraction and not a refraction.

8. Determination of the true velocity of the refractor is made in the manner

indicated in Part. I The intercept times under each shot-point are averaged and half of their values are plotted under the relevant shot-points. After applying an appropriate offset, we match the direct delay time profile to them by tilting, then we repeat the same procedure with the profile in the opposite direction, and determine the average of the values obtained. Both profiles, theoretically should show the same true velocities. If this is not so, and the discrepancies are large, we should re-check the work, as it may transpire that we are not working on the same refractor in each direction of shooting.

It is expected that we may come across changes in the horizontal velocity of the refractors, and when we observe changes in one direction, the same changes should be observed in the reverse direction, if the impulses in both directions of shooting arrive from the same refractor.

Determination of the continuous half-intercept time profile for the first refractor can be made directly from time distance curves or from two continuous delay time profiles.

By virtue of their definitions the total delay time value for a station, or a shot-point, in the case of a horizontal or nearly horizontal refractor, is equal to its intercept time. These times can be obtained by the known method of differential summation. If T is the reciprocal time between two shot-points A and B, and T_1 and T_2 are the readings at any station K on the time distance curves from shotpoints A and B respectively, then the intercept time for this station will be:

$$I_K = T_1 + T_2 - T$$

When the time-distance curves for the refractor under consideration are converted into continuous delay time profiles (in both directions of shooting) then the delay time values for any station K between two shot-points A and B, for a velocity V will be:

$$T_1 - L_{AK}/V = a$$
$$T_2 - L_{BK}/V = b$$

and the delay time value for the shot from A to B is

$$-T + L_{AB}/V = 1\text{-}c$$

adding these three equations we obtain:

$$I_K = a + b - c$$

For the shallow refractor in the example, we add the delay times of the continuous profiles from C and J at each station and subtract from the sum the delay time from C on J = from J on C. A plot of half of each of the values so obtained under the corresponding station, will give us the same profile as is obtained by matching the delay time profiles into the half intercept time values of the shot-points, provided the initial assumptions of small dips and small offsets are justified.

9. No fit, however good, should be considered correct where the dip of the refractor exceeds 10°, for in such a case the true velocity cannot be obtained with accuracy by this method. Such segments or parts of the line should be profiled by other methods.

10. The final depth profile of the shallow refractor may be obtained in the manner given in Part. I. Each time value of the completed half intercept time profile will be multiplied by the appropriate conversion factor. Here $F = 14{,}000 \tan (\sin^{-1} 7{,}000/14{,}000) = 8{,}080$ ft./sec., and arcs with radii equal to $F.I/2$ are drawn from each station position. A smooth line tangent to all these arcs will give the depth profile.

Presentation of refraction results in the form of time sections.

Before discussing the interpretation of the deep refractor in our example, let us consider a general case of several nearly horizontal shallow refractors. If the upper refractor drawn in the way indicated shows only slight variations in dip, the procedure for the next refractors is the same and for each of the refractors we obtain its individual half-intercept time profile. If we plot all these half-intercept time profiles in one section below the station positions we obtain what could be called a time section, where the vertical scale is expressed in seconds.

The top horizon in such a section would have been profiled at the velocity of the first consolidated layer and each of the profiles below would represent a refractor whose velocity would be marked underneath. It may vary laterally, and all these changes should be marked clearly. A time section of this kind will constitute the basis for the next step, which is the conversion into a depth section.

Before attempting depth profiling by any method at least three alternative possibilities referring to vertical velocities in virgin territory should be considered when the horizontal velocities fluctuate:

(a) The vertical velocity of a refractor may vary independently of any lateral changes of the velocity along the refractor.

(b) The velocity along the refractor may change laterally but the vertical velocity may have a certain mean value throughout.

(c) Changes of velocity occur in "Blocks" which are isotropic.

Depth of Refractors

The time section gives us the half-intercept time from the datum to the top of the refractor. These half-intercept times are, in the case of horizontal or nearly horizontal beds, equal to delay times which in turn are the sum of the delay times in each overlying refractor with reference to the refractor considered. Thus:

$$I_n/2 = (T - L/V_n)/2 = h_1/V_n \tan i_1 + h_2/V_n \tan i_2 + \ldots\ldots\ h_r/V_n \tan i_r + \\ + \ldots\ldots\ h_{n-1}/V_n \tan i_{n-1}$$

where $\sin i_r = V_r/V_n$

This equation may be written simply as

$$I_n/2 = \sum_{r=1}^{r=n-2} (h_r/V_n \tan i_r) + h_{n-1}/V_n \tan i_{n-1}\,.$$

It shows the way in which the depths of successive refractors are computed from the half-intercept time profiles. In the numerators we have the successive thicknesses of the horizons and in the denominators the conversion factors. The latter are obtained usually from a special nomogram. By dividing the known thicknesses by the relevant conversion factors and adding the results we determine the delay time due to all the layers above the one whose thickness is required. Thus the value of h_{n-1} is easily obtained, and by summing the thicknesses, the required depth follows.

Nomograms for conversion factor

The normal equation for the conversion factor:

$$F = V_R \tan i \qquad \text{where } \sin i = V_0/V_R$$

can be expressed in the form:

$$1/F^2 = 1/V_o^2 - 1/V_R^2$$

for which a nomogram consisting of 3 parallel straight lines can be prepared.

A simpler way to read F for a given set of values of V_o and V_R is based on the equations $F = V_R \tan i$ and $V_o = V_R \sin i$; this is easy to see in the right-angled triangle in Fig. 6. A practical device may have the shape of a half cross of perspex, the long arm of which will cut the scales of F and V_R placed at right angles to each other, whereas the shorter arm on which we plot V_o (of the same scale as F and V_R) will pass through the origin of F and V_R.

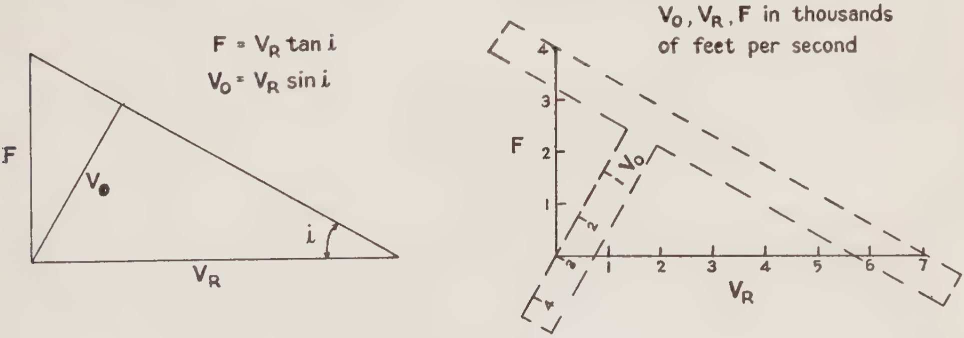

Fig. 6. Conversion factor.

Deep Refractors

The procedure involved in the practical use of the method can be adapted easily to all refracting interfaces and is particularly useful when the horizontal refractor velocities are not constant.

The direct use of the method, however, is limited not only by the dip of the refractor, but also by its depth. The method requires that along a segment of an interface equal to the double offset distance, the refractor does not suffer any large changes in dip. For deep refractors, the double offset distance is large enough for such changes to be expected and if only half-intercept values are used, these will have a smoothing effect on the depth profiles, i.e. highs will be lower and the lows less accentuated, and the delay time profiles can be matched into half-intercept values only along long and flat portions of the refracting horizon.

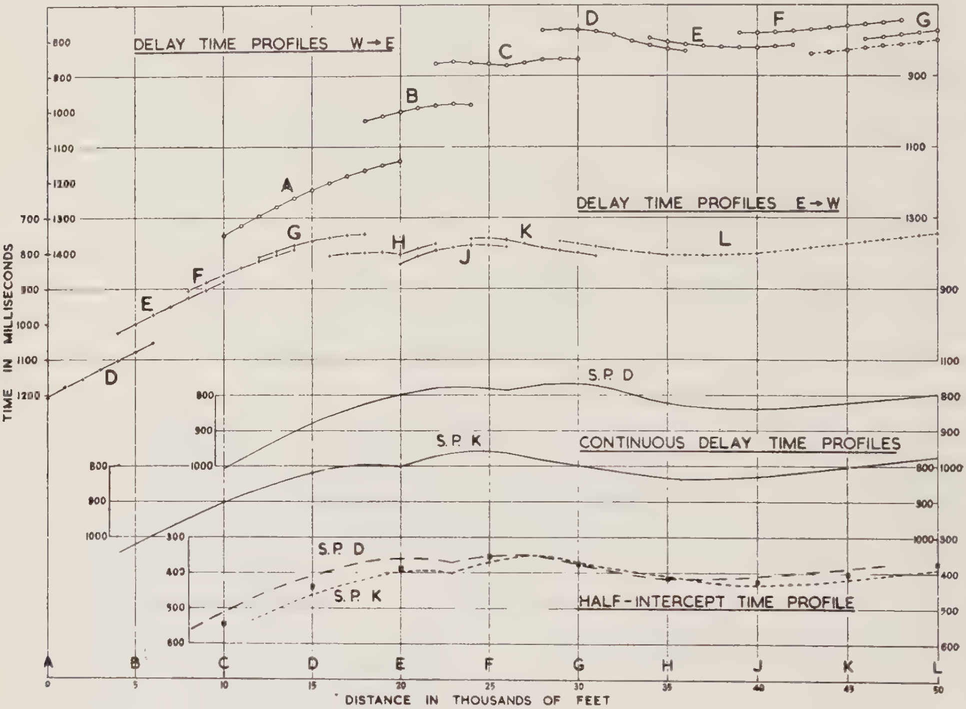

Fig. 7. Interpretation of the results of the deep refractor in fig. 4.

Determination of the true velocity and of the true shape of the interface will have to be made in a modified way by reducing a multilayer problem to that of two layers, and the method is described in the following:

From the time-distance graph (fig. 4) we compute the delay time profiles of the deep refractor and draw two continuous delay time profiles based on shot-point *D* for direct (*W* to *E*) shooting and on shot-point *K* for reverse shooting (fig. 7) .In addition we construct the half-intercept time profile and we notice that though we have used the true velocity, both delay time profiles will not match each other and will not match the half-intercept time profile either. The discrepancies are due, partly to the upper refractor as far as the delay time profiles are concerned, and partly to the large double offset on the deep refractor which at the end points of the offset cone displays different dip. Hence the half-intercept time values will not always lie on the refractor. We may notice however, that over the left high and flatter portion of the refractor, the matching of the mean delay time profile appears to be fairly satisfactory, and we may assume that the velocity chosen is sufficiently close to that of the true value so that further work can be done on these two continuous delay time profiles from shot-points *D* and *K*. We choose now a new datum (—2,800 ft.)

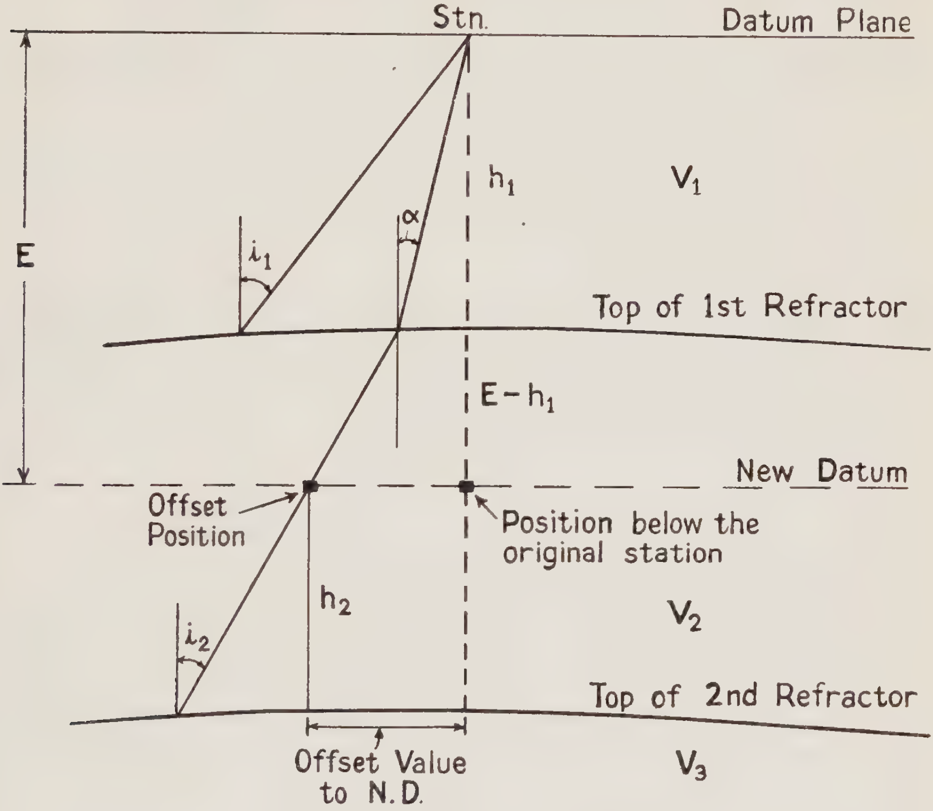

Fig. 8. Reduction to a new datum.

and the reduction of each point of the delay time profile will be carried out as shown in Fig. 8. Considering the ray-path from any point on the previous datum to the second refractor, reduction to the new datum will involve the delay time within the upper bed, i.e.

$$h_1/F_{13} = h_1/V_3 \tan\alpha \qquad \text{where } \sin\alpha = V_1/V_3$$

and the delay time between the first interface and the new datum,

$$(E - h_1) \,/\, F_{23} = (E - h_1)/V_3 \tan i_2 \quad \text{where } \sin i_2 = V_2/V_3$$

and E is the difference in elevation between the original datum and the new one.

Thus the correction for a station to the new datum will be:

$$t_{ST} = h_1/V_3 \tan\alpha + (E - h_1)/V_3 \tan i_2$$

$$\text{But } 2h_1 = I.V_2 \tan i_1 \text{ and } \sin i_1 = V_1/V_2 = \sin\alpha /\sin i_2$$

$$\therefore \quad t_{ST} = (I/2) \sin (i_2 - \alpha)/\cos i_1 \sin i_2 + E \cos i_2/V_2$$

$$\text{or} \quad t_{ST} = C_1\,(\mathrm{I}/2) + C_2$$

where $I/2$ is the half-intercept time value for the first refractor and is given by the half-intercept time profile in fig. 5. C_1 and C_2 are constants for the given set of velocity values along the whole line. Each station will have additionally a correction at the shot-point end, computed in the same way, so that the total correction for each station along the profile will be

$$t_S = t_{ST} + t_{SP}$$

and in our particular case

$t_S' = t_{ST} + t_{SP(D)}$ for the time profile from shot-point D,

$t_S'' = t_{ST} + t_{SP(K)}$ for the time profile from shot-point K.

These corrections will have to be substracted from the total delay times of each station (read on the delay time profiles from shot-point D and shot-point K in fig 7) and the results can be plotted either below each station, in which case no further calculation is needed, or at the offset position on a new datum. The latter case is preferable to the former as will be seen later, and the calculation of the offset position is also simple:

$$\begin{aligned}\text{Total offset } &= h_1 \,.\, \tan\alpha + (E - h_1) \tan i_2 \\ &= h_1 \,.\, \sin(\alpha - i_2)/\cos\alpha \cos i_2 + E \,.\, \tan i_2 \\ &= h_1 \,.\, C_3 + C_4\end{aligned}$$

where h_1 is the depth of the first refractor below the previous datum and is given by the depth profile in fig. 5, and C_3 and C_4 are constants for the line, depending on the velocities and the distance between the two datum levels.

At the top of fig. 9 we have the corrected time profiles with reference to the new datum, as plotted below the original station position. It is noticeable that the delay time profiles are now of nearly the same shape, but still the fit into the half-intercept times is not satisfactory particularly over the left high.

The second set of curves in fig. 9 shows the delay time profiles plotted below their offset positions on a new datum with their half-intercept time profile, computed by differential summation.

i.e. $I = a + b - c$, where

a = delay time value for the station on the profile from shot-point *D*.

b = delay time value for the same station on the profile from shot-point K.

c = the reciprocal delay time of profile *D* at shot-point *K* which should be equal to that of profile *K* at *SP.D*.

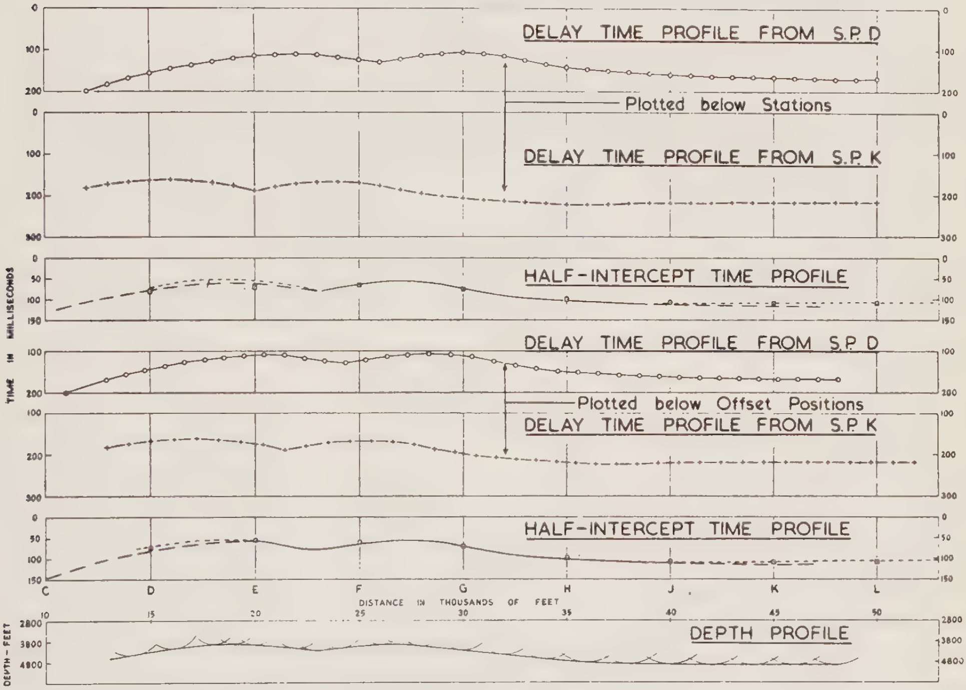

Fig. 9. Continuity of interpretation on the deep refractor Reduction to new datum (—2800 feet).

We notice now that both delay time profiles, after an offset in the proper direction, afford a very good fit into the half-intercept time values; this fit confirms that the choice of velocity was correct. The combined delay time profile is now drawn into the half-intercept time values thus obtaining a continuous half-intercept time profile.

The depth profile is obtained by multiplying each half-intercept time value by the relevant conversion factor for velocities of 14,000 ft./sec. and 20,000 ft./sec. and the depth is plotted from the new datum with arcs of radii equal to the computed depth; the envelope to these arcs will give the depth profile.

Comparing the final depth results of fig. 9 with the original ones in fig. 4, we notice that the shape and depth of the second refractor is within the accuracy of the drawing. The actual numerical figures confirm this very satisfactorily except for the depth of the saddle, which appears about 80 feet shallower than originally; there are a few points on the right flank of the structure also at a slightly shallower depth. This inaccuracy is to be expected, since in this method we assume parallelism of all refracted rays and the largest deviations in this parallelism occur where the horizons display largest unconformity. Shallower depths will also be expected over the left flank of the refractor when the dip exceeds 10°.

Acknowledgments

The author wishes to express his thanks to the Chairman, Board of Directors, and Chief Geophysicist of The British Petroleum Co. Ltd. for permission to publish this paper.

A RAPID METHOD OF DETERMINING THE FORM OF A SEISMIC* REFRACTOR FROM LINE PROFILE RESULTS

BY

L. H. TARRANT **

Abstract

A set of refraction line arrival times can be readily converted into a set of delay-times providing the refractor velocity is known. If we then subtract the delay-time at the shot-point end, we arrive at a set of delay-times representing the refractor depths at the receiving end .This paper is concerned with the conversion of such a set of delay-times into a profile of the refractor.

The method is semi-graphical and very easy to apply. For each geophone station an arc of a circle is constructed, such that the envelope of the series of arcs represents the surface of the refractor. While the method is not quite exact, especially when the dips are large, it is of particular value in allowing for the effects of varying dips upon the offset distance. The method treats the overburden above the refractor as if it were of uniform velocity.

Introduction

Methods of interpreting refraction line observations can be divided into two broad classifications.

One group is typified by the method described by Slotnick (1950), where the time-distance graphs are drawn as short segments with characteristic apparent velocities. These segments are paired off in opposite directions of shooting so that the two apparent velocities, together with the reciprocal time, serve to define a short segment of the refractor.

The other type of method uses the arrival times at each observation point, and from each direction, separately, and attempts to depict the surface of the refractor by plotting the corresponding points of emergence from the refractor. The profiles from the opposite directions are then matched together and combined into an average profile.

While the Slotnick method, and those like it, deal best with difficulties arising from an unconformable multilayer overburden, the second type of method is best suited to cases where the complexity of the problem arises from the shape of the refractor. This is because when the dips are moderate, and vary considerably, the offset distance is also very variable, so that it is difficult

---

* Presented at the ninth Meeting of the European Association of Exploration Geophysicists, held in London, 7-9 December 1955.

** The British Petroleum Co. Ltd.

to select apparent velocity segments in the forward and reverse directions which really correspond to the same part of the refractor. This selection, or matching, in these cases is best left until after the profiles have been drawn.

The construction to be described below belongs to the second group of methods. It deals with the uncertainty regarding the precise point of emergence by plotting instead the locus of all permissible points of emergence corresponding to each observation station.

THEORY OF THE METHOD

It is first necessary to simplify the general seismic problem by treating the overburden above the refractor as if it were a uniform medium of velocity V_1.

Secondly, we make the approximation of regarding the seismic disturbance as travelling along the refracting medium with a constant *horizontal* velocity V_2. This is not strictly true, even if the refractor is uniform in velocity, since the disturbance will tend to follow the undulations of the refractor surface. Because the error is that of taking the cosine of the angle of dip as unity, it is negligible for small dips. However, for moderate dips this effect is the main source of error in the method, as will be discussed under another heading.

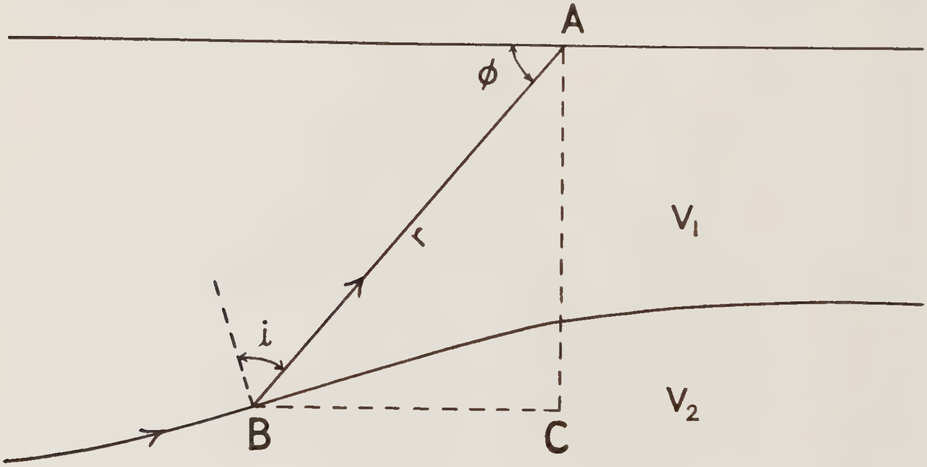

Fig. 1. Geometry of Emergent Refraction Ray.

Referring now to Fig. 1, the point A represents an observing station on the refraction line and B the corresponding point of emergence from the refractor r and φ are the polar co-ordinates of B relative to A. The overburden delay-time, T, is given by:

$$T = t_{BA} - t_{BC} = r/V_1 - (r \cos \varphi)/V_2$$

whence,

$$r = V_1 T / (1 - \sin i \cos \varphi) \quad \ldots\ldots\ldots\ldots (1)$$

This is the equation of an ellipse with one focus at the origin, the standard form being:

$$r = p/\,(1 - e\cos\varphi)$$

This ellipse is shown in Fig. 2, its dimensions being:

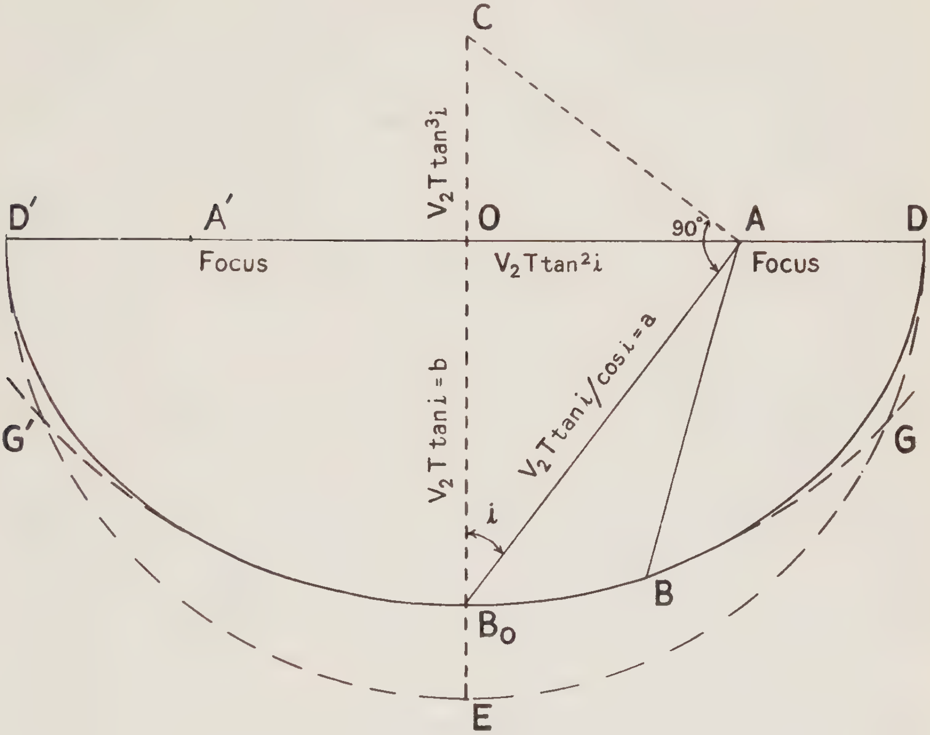

Fig. 2. Elliptical Locus of Point of Emergence.

semi-minor axis, $b = V_2T\tan i$ . . . . (2)

semi-major axis, $a = V_1T/\cos^2 i$ . . . . (3)

The position of the centre of the ellipse relative to the focus A is given by:

$$OA = V_2T\tan^2 i \quad (4)$$

Equation 1 indicates that for varying dip of the refractor the point of emergence, B, moves on a locus which is an ellipse with one focus at A. When the refractor surface is horizontal, B_0 is at the end of the minor axis of the ellipse.

A good approximation to the lower part of the ellipse near B_0, that is for low dips, is the circle which has a radius equal to the radius of curvature of the ellipse in that region.

This radius is given by:

$$R = a^2/b = V_1T/\cos^3 i = V_2T\ (\tan i + \tan^3 i) \quad . \quad . \quad . \quad . \quad . \quad (5)$$

The centre of this circle GB_0G' is the point C of Fig. 2, the angle CAB_0 being a right-angle.

DETAILS OF THE METHOD

It will be assumed that the refractor velocity V_2 has been determined by some appropriate method, for example by reverse observations over a flat portion of the refractor. It is also assumed that the equivalent average overburden velocity V_1 has been obtained, either by computation from the refraction observations, or even better from borehole control if available.

It would be out of place to describe here the various methods by which refraction arrival times may be converted into delay-times, but to avoid possible confusion the following equation will serve to define the particular meaning of "delay-time" intended:

Delay-time $T = t - L/V_2 - T_{SP}$ . . . . (6)

where t is the overall time

L is the distance from shot-point to observation station, and T_{SP} is the delay-time for the shot point.

The delay-time for each station is multiplied by the "conversion factor", $V_2 \tan i$, to give the various semi-minor axes, OB_0, of the ellipses. The various centres, C, from which to describe the circular arcs, are then obtained by a simple construction. AB_0 is drawn at an angle i to the vertical, and such that B_0 is at the correct depth below the datum. Then a vertical through B_0 is made to cut a perpendicular to B_0A from A at C.

At most points it will be found that the circular arc centred on C is a close enough approximation to the arc of the ellipse. However, when the dip is large, it may be necessary to draw the true ellipse. This is conveniently done by drawing the auxiliary circle, DED' in Fig. 2, and reducing the ordinates by the ratio of the minor to the major axis, which in our case is $\cos i$.

The envelope of the series of circular or elliptical arcs, constructed in the above way, will represent very nearly the profile of the refractor surface.

An alternative procedure, in cases where it would be necessary to draw the true ellipses for many points, is to draw only the auxiliary circles. The envelope of these circles will give the shape of the refractor, as if plotted with the vertical scale exaggerated in the ratio $1/\cos i$. The profile can then be completed by reducing the vertical scale by a factor $\cos i$.

EXAMPLE OF THE METHOD

Fig. 3 shows a theoretical example for one direction of shooting only. The calculated time-distance graph is at the top of the figure .Below this is shown the theoretical structural shape, and underneath is the reconstructed refractor.

It will be seen that the general shape of the refractor is reproduced fairly well and that the construction may be helpful in identifying the source of later arrivals as at stations 13 to 17. On the other hand the reconstructed depths are only exact at the 7,000 feet level, and owing to the time lost by the seismic pulse in travelling obliquely up the slope shown, the depth of the top of the structure is too great as reconstructed by about 150 feet.

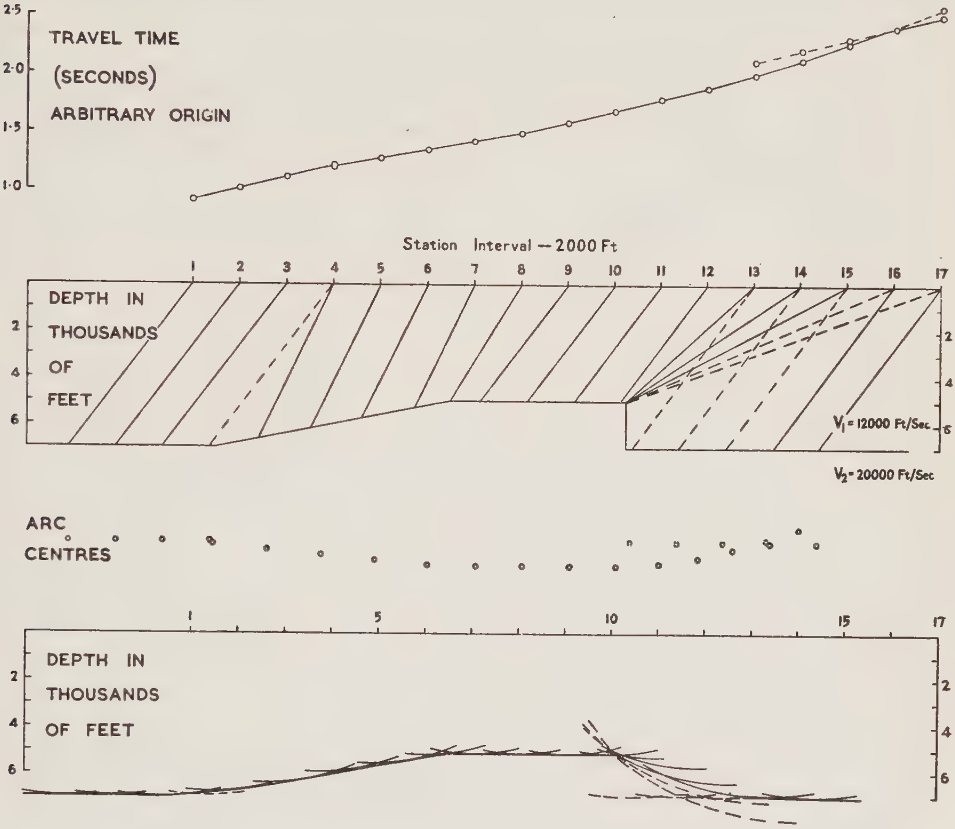

Fig. 3. Reconstruction of Theoretical Refractor Shape from Travel Times.

This error will be discussed in more detail in the next section. In practise it can be more or less eliminated in one of two ways. The travel paths may be constructed and the times computed, giving corrections to be applied to the delay-times. This is the only way if the times are available for one direction of shooting only. The alternative is to average the profile with that obtained from the opposite direction of shooting. The errors are of opposite sign and almost equal, wherever the dip is not too great, so that approximate cancellation takes place.

DISCUSSION OF ERRORS

There are certain possibilities of errors which are common to all methods of this type, and which therefore will only be mentioned. The assumptions of constant overburden and refractor velocities, and of isotropy in the overburden, will be near or far from the truth depending upon the natural circumstances. Of an entirely different nature, but nevertheless important, are the errors which can arise in graphical methods through undue reliance upon squared paper, which is rarely accurate enough.

Three separate sources of error are peculiar to the method under discussion, as follows:

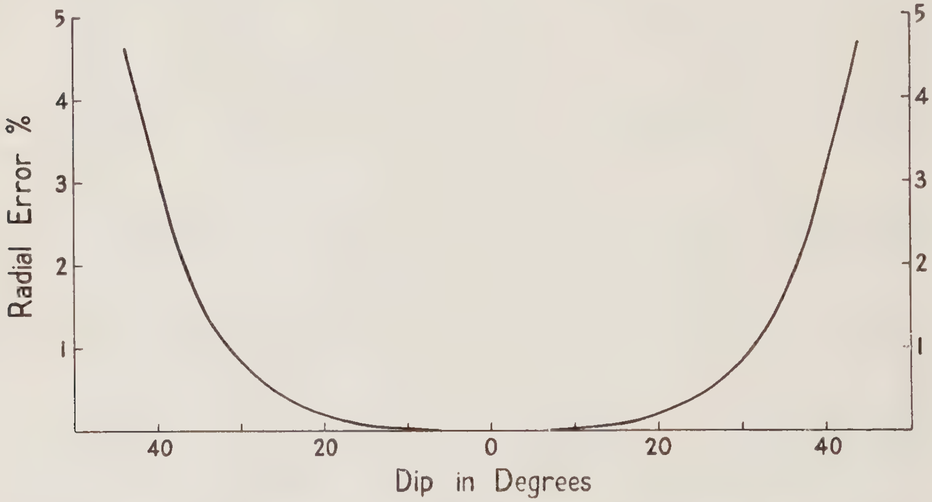

Fig. 4. Departure of Circular Arc from Ellipse as Percentage of Semi-minor Axis.

(i) the departure of the circular arc from the true ellipse,
(ii) the effects of oblique travel along the refractor surface,
(iii) errors due to the fact that the tangent to the ellipse does not quite make the correct angle with the radius vector representing the emergent ray.

The first of these errors is easily avoidable, either by drawing the true ellipses, or by employing the auxiliary circles as described above. However, it is useful to know the magnitude of the errors involved in using the approximation, and these have been calculated for the case of $\sin i = 3/5$. The error curve shown in Fig. 4, represents the amount by which the circular arc lies outside the ellipse measured along the radius, and expressed as a percentage of the semi-minor axis of the ellipse. For most purposes the error is quite negligible for dips up to 20 degrees, and only becomes serious at over 30 degrees.

The errors due to assuming a constant horizontal component of velocity in the refractor can be readily computed for a constant incline. It is found that the true dip, θ, is related to the erroneous dip, θ', by the following equation:

$$\sin(i \pm \theta) = \sin i \pm \sin\theta'/\cos i \mp \sin\theta' \sin(i \pm \theta') \tan i \quad . \quad . \quad . \quad (7)$$

The alternative signs depend upon whether θ and θ' are counted as positive in the down dip or the up dip sense.

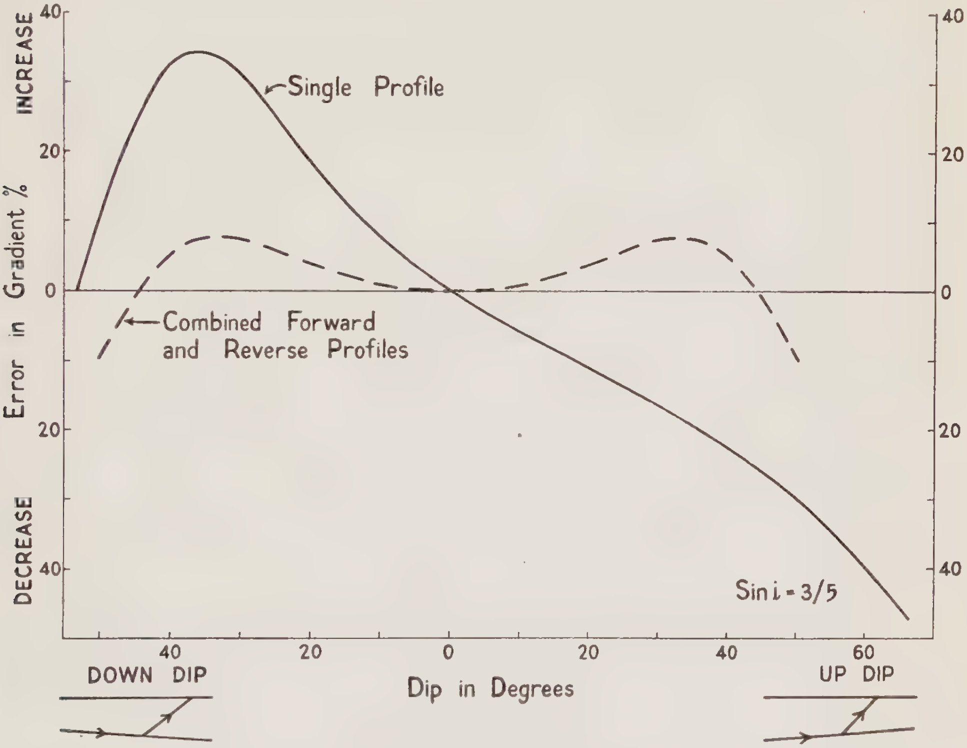

Fig. 5. Percentage Error in Gradient.

Figure 5 is arranged to show the percentage error in gradient due to this effect, that is, $100(\tan\theta'/\tan\theta - 1)$. It is again calculated for the case of $\sin i = 3/5$. It will be seen that the dip is overestimated when it is down towards the observing station, and underestimated when it is upwards. For the case illustrated in Fig. 3 where the slope is a little over 11 degrees we would expect a gradient error of $6\frac{1}{2}$ per cent, that is an overall reduction of the height of the structure by 130 feet in 2,000 feet. This corresponds more or less to the result obtained.

Also shown in Fig. 5 is the error to be expected after forward and reverse profiles have been averaged. Due to the asymmetry of the single profile curve, we do not get complete cancellation, but an error of up to 7½ per cent remains, this maximum being at 33 degrees of dip. For dips of up to 45 degrees the mean profile errs on the side of exaggerating the true gradient.

It should be pointed out here that natural features do not usually have uniform slopes from crest to trough as in Fig. 3. The maximum dip on a flank is often 50 per cent more than the average dip. It is the average dip which will control the percentage of error in the amplitude of the structure.

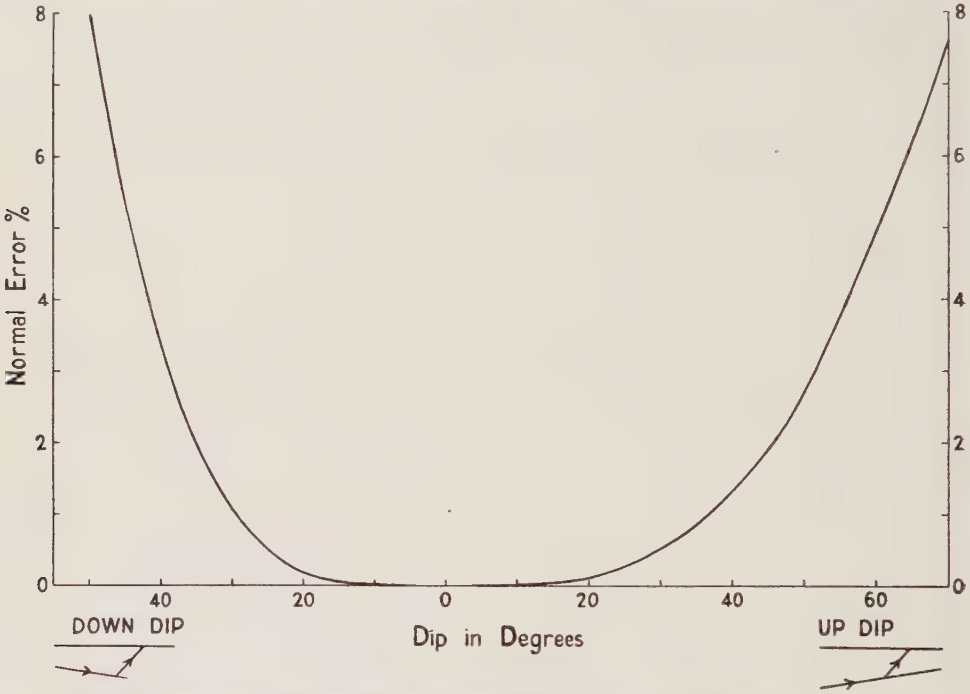

Fig. 6. Percentage Normal Displacement of Tangent of Ellipse from Chord.

The final source of error arises from assuming that the envelope of the series of ellipses is the correct refractor position. Now, although the ellipse is the true locus of points of emergence giving the same delay-time, the tangent to the ellipse is not in general the true refractor position. The normal to the refractor has to make an angle i with the emergent ray so that Snell's law is obeyed. The normal to the ellipse does this only at the end of the minor axis, B_0 of Fig. 2. Elsewhere the angle is smaller than i. Other than at B_0, therefore, the true refractor position should be a chord of the ellipse. The displacement between this chord and the tangent having the same slope, can easily be calculated from the properties of the ellipse. In Fig. 6 this error is shown, expressed as a percentage of the length of the normal from the observing station to the refractor.

This error is negligible for dips less than 20 degrees, and does not begin to increase rapidly until we reach 30 degrees of down dip or 40 degrees of up dip. It will be understood that this error applies only where the envelope of a series of arcs or ellipses is used. When the arcs intersect to define a point source, such as the upper edge of the step of Fig. 3, we are only interested in the travel time considerations, and not in the angle of emergence.

Uses of the Method

The method will be found particularly useful where a refractor has moderate dips and rather complex shape. It has no advantages to recommend it in cases where the dips do not exceed 5 degrees, or where the dips, if larger, vary slowly and regularly along the profile. Other methods are superior in these circumstances, especially as greater accuracy is often both necessary and attainable under these simpler conditions.

The inaccuracies of the method, provided they are understood and where possible allowed for, will be found to be generally unimportant compared with the uncertainties which inevitably arise in dealing with strongly folded structures. With such structures it is important, of course, to bear in mind the third dimension. It will rarely be possible to locate a line so that all the travel paths remain in the vertical plane. The diagrams and profiles must be generalised by rotating them about the surface trace of the line of observations, so that the family of ellipses described in this method, is really a family of ellipsoids of revolution. The solution of this problem in three dimensions must depend, of course, upon information from lines or arc traverses running at right-angles to the profile under consideration.

Acknowledgements

The author wishes to express his thanks to the Chairman, Board of Directors, and Chief Geophysicist of The British Petroleum Co. Ltd., for permission to publish this paper.

Discussion

Mr. Goguel: I have studied refraction profiles over buried valleys in the Alps, and I think that Mr. Tarrant's method should be very useful in such a case. We cannot expect such a high precision in the determination of the buried topography that the approximation involved in the method would be important.

To take into account the variation of velocity with depth in the overburden, it may be enough to take out a fixed part of the time delay, corresponding to the influence of the weathered zone.

Reference

Slotnick M. M., 1950, "A Graphical Method for the Interpretation of Refraction Profile Data", Geophysics, XV, 163-180.

SOME PROBLEMS OF SHALLOW REFRACTION INVESTIGATIONS *

BY

W. DOMZALSKI **

ABSTRACT

The term shallow refraction, as used in this paper, refers to investigations confined to the superficial layer of rocks, composed primarily of unconsolidated material. To define the scope of the discussion it will be assumed that the term shallow refraction applies to work of which the lower limit is approximately 300 feet and the upper of the order of a few feet. The consideration of the small magnitude of quantities measured (distances and times) determines the perspective of the problems involved, since difficulties encountered in the interpretation, although equally disturbing whether in deep or shallow work, will cause a greater percentage of error in the latter case. The purpose of this paper is to discuss and illustrate these problems. The factors considered include the location of the geophone spread in relation to the topography of the site, influence of the ground conditions in the vicinity of geophones on recorded times, consideration of the shallow uphole shots and problems arising from the repeated use of the same shothole. The rapid variation in the vertical velocity of the overburden and errors due to it are discussed together with the effects of a non homogeneous unconsolidated material and velocity reversal. The effects of the ill-defined solid rock surface are also considered. It appears that as the depth of investigations becomes shallower, the limits of the practical capabilities of the method are approached, because the differences between the theoretical assumptions and the actual conditions become more pronounced.

I. INTRODUCTION

1. *Definition*

The term shallow refraction is used in this paper to describe investigations confined to the superficial layer of rocks, composed primarily of unconsolidated material. In practical application, investigations of this type aim at (1) the determination of the depth to the boundary between the solid rock and the overlying unconsolidated deposits, (2) the estimation of the thickness of the weathered rock above the sound rock, (3) the estimation of the thickness of the different unconsolidated strata composing the mantle which overlies the solid rock.

The range of depth which will fall into the conception of shallow refraction work will depend on local conditions, and any statement of the limits must be of a somewhat arbitrary nature. Nevertheless, to be explicit it will be assumed that the shallow refraction applies to work of which the greatest depth is approximately 300 feet and the smallest of the order of a few feet. This statement may cause some controversy, but it is made in order to provide a proper perspective of the magnitude of the quantities involved. This is of great importance, because the difficulties involved in the interpretation, although equally disturbing whether in the deep or shallow investigations, will cause a much greater percentage of error in the latter case. To illustrate this point let it be assumed that the average vertical velocity along a refraction profile changed by 1,000′/sec. say from 4,500′/sec. to 5,500′/sec. This might have taken place without any indication being available, and assuming (say) a time of 10 milliseconds for the ray travelling from the refractor up to the surface the depth will be about 10 feet in error, which is approximately 20%. If the investigation concerns a deep refractor at say 2,000 feet the above figures will pertain to the error which is known as weathering and although its magnitude is the same, it is a small percentage only of the total investigated depth.

---

* Presented at the Ninth Meeting of the European Association of Exploration Geophysicists, held in London, 7-9 December 1955.

** Mining and Geophysical Services, London.

2. *The Scope of the Shallow Refraction*

It may be useful at this stage to consider in general the application of the seismic refraction method to problems of shallow investigations. Although the information which is required may ultimately serve different purposes, the problem fundamentally consists of the determination of the depth to the solid rock. Such investigations are undertaken mostly for civil and mining engineering projects but, adopting a broader point of view, they may also be required in connection with shallow structural investigations. Also, seismic measurements in the superficial rock layers and overburden are of great importance in the determination of the low velocity zone correction, to be applied in large scale seismic investigations.

In the application to civil engineering projects, the most common aim is the determination of the depth to the bedrock on dam sites and along high pressure tunnel routes. Such information may also be required when building large structures requiring deep foundations (power stations) or when estimating the amount of fill for some dam project, available within a certain area.

In mining (Domzalski 1954), determination of the thickness of the superficial deposits may be required in order to plan safely the underground operations, which require a certain thickness of the rock head. Another application would be to determine the thickness of the overburden to be stripped if opencast operations are considered.

3. *Statement of Purpose*

The purpose of this paper is to discuss and illustrate the problems commonly encountered in shallow seismic refraction investigations. It must be stressed that although these problems are present in any type of seismic work their relative importance becomes overbearing and their correct treatment vital, when dealing with relatively short times and shallow depths. The literature dealing with this subject is unfortunately limited, and consists mainly of case histories or, to be more exact, successful case histories. It is the strong belief of the author that anybody engaged in this type of work, must be aware of the various difficulties that cannot be overcome by considering the easy and straightforward cases only. It is hoped therefore that the present communication may induce discussion and sitmulate the exchange of information.

II. Discussion

From what has been said it may be seen that as the depth of investigations becomes shallower, the limits of the practical capabilities of the method are approached, the differences between theoretical assumptions and actual conditions become more pronounced, and the disturbing effects of the near surface inhomogeneities increasingly affect the results. There is one aspect of shallow investigations which may well be counted as advantageous, i.e. the comparative ease with which the seismic results can be checked, or interpretation helped, by drilling which, in the case of the deep structural investigations, is extremely costly. Nevertheless, if the seismic survey is to be an economical proposition, the boring programme must be very limited.

The problems which are to be discussed will be classified into five major groups:

1. Record information.
2. Lay out of the spread and shot hole conditions.
3. Nature of the overburden.
4. Nature of the rock refractor.
5. Interpretation.

1. *Record Information*

It is not proposed to discuss the instrumentation of shallow refraction work because it would be beyond the scope of this paper. It must be stressed that before sufficient confidence can be placed in the field results it is necessay to obtain a reliable record of good quality. Assuming that this has been achieved the next task is to read accurately times of the first breaks. It is necessary to bear in mind that a large proportion of the shallow refraction work involves investigations to the average depth of 50 feet or so, with total times of the order of 40 to 50 milliseconds; a millisecond becomes consequently a relatively large unit. With the velocity of the overburden, say, about 6,000 feet per second, an error of a millisecond in reading of the time may result in about 10% error in the estimation of depth, even without allowing for other factors which may adversely affect the accuracy. It is recommended that arrival times be estimated to the nearest ½ of a millisecond and for this fast paper speeds, of the order of 14″ to 18″ per second are required. The accuracy of this estimate will depend on the quality of the break, which in turn is influenced by the size, depth and tamping of charge, type of ground and amplifier gain. As the operations are often conducted in populated areas and on farm lands, the amount of charge has to be limited frequently. If due to extraneous conditions, gains have to be kept down, a rounded break occurs. With very rounded breaks, up to two milliseconds error can result from reading the record .Information about the amplitude and frequency of the pulse, which can be obtained from the record, should be used of course in the same manner as in any type of seismic work.

2. *Layout of the spread and shot hole conditions*

Apart from the usual considerations governing the choice of spread, such as the ratio of velocities and the depth to the deepest refractor about which information is sought, the topography of the site plays an all important role. This is especially true when planning work on proposed dam sites, where sudden changes in elevation frequently occur.

The usual procedure of reducing times to a datum cannot be employed successfully when dealing with very abrupt changes in the elevation where the average vertical velocity of the overburden changes along the line of traverse: the errors introduced during the reduction would cause a false picture of the bedrock profile. Before dealing, therefore, with the elevation changes during the interpretation, it is advisable to lay out the traverses so that major changes in elevation are avoided. This will often necessitate the laying out of traverses along the topographical contours. Although the amount of field work is thus increased, a reliable interpretation is made more probable. An even slope does not present so much difficulty.

Another problem consists of made up ground. This may occur on large sites where some sort of construction has been commenced, or in mining districts where the waste from underground mining operations has been accumulating for a long time. If other ground obstacles such as buildings or farmyards occur in the vicinity of the survey, the positioning of a spread requires some careful consideration.

In order to register the low velocities of the near surface layers, the first geophones have to be near to the shotpoint with the intervals between them gradually increasing, away from it. Adoption of such a procedure however is inconvenient for the shooting of the reverse shot, and it has been found that better field progress can be made by keeping the distances between the geophones constant, changing only the position of the end geophone for the reverse shot.

This is particularly convenient if a made up multi-core cable with evenly spaced take-outs is used. To obtain information about the low, near-surface velocities a short spread with small geophone spacing is shot at intervals. This short spread may have geophones arranged at 3 foot intervals or more, depending on the spacing of the main spread and on the velocity characteristics of the area.

Attention must be given to the positioning of the end geophone when shooting a reverse shot. To obtain the criterion of the reversed total times, the end geophone has to be removed from the old shotpoint because the disturbed ground near it causes a delay in the transmission of the seismic wave. This has been observed repeatedly, and to obtain some idea of the order of error introduced, a number of geophones were laid on an arc through a used shothole, at one foot spacings. The results indicated longer times for geophones near the crater, the maximum being 5 milliseconds for a geophone on the edge of the crater. This delay will naturally depend on the type of ground, but the possibility of such error occurring must be borne in mind. Under certain conditions it is possible to drive a pipe in the ground and explode the charge inside the pipe so as not to disturb the ground. Such a pipe could be used several times, though it may not always be convenient to appy this method.

The holes are usually augered to a depth of 3-10 feet. The use of a power drill capable of boring deeper holes would not be justified for shallow refraction work, where the total depth may be less than 50 feet. The disadvantage of using an auger is seen particularly in the case of an overburden containing many boulders; under such conditions the augering time may be a factor controlling the progress of the field work.

The condition of a shothole and the placement of the charge, including its tamping, affect the quality of a record to a great extent. There is another aspect which may not be apparent, except in the case of very small spacing of the geophones, and this is the effect which the position of the charge in a hole has on times of arrivals to the very near geophones. On one occasion geophones were at a distance of 1 foot on each side of the shot hole and the arrivals differed by 1 millisecond. The charge was placed at the bottom of an eight foot hole, of 4″ diameter, and pressed against the side of the hole nearest to the geophone which registered shorter time. (The times were 4 milliseconds and 5 milliseconds indicating velocities of 2,000 ft. per sec. and 1,600 ft. per sec. where boulder clay constituted the overburden.) This implies that the charge should be placed in the centre and tamped around evenly. On another occasion the geophones were spaced on the circumference of a circle of 10 feet diameter, with the shot placed at the interface between the overburden, composed of silty clay and sand, and rock in the borehole at a depth of 28 feet. The arrival times differed by 2 milliseconds (corresponding to velocities of 4,900 feet per second and 3,700 feet per second). In the latter example, however, the time discrepancies can be due in part to the disturbed conditions caused by boring and circulating fluid, which could have penetrated the walls of the borehole to a different extent.

In the case of geophones placed further away from the shothole it is difficult to offer conclusive evidence of the above findings because, as the distance increases, the different arrival times may be caused by the anisotropy of the medium (Uhrig and Van Melle 1955), or by refraction from a very shallow interface. It is believed however that the above effect may persist for distances of the order of 20 feet.

To complete the discussion of the field lay-out it is necessary to refer to the placement of the geophones. The necessity for the firm planting of geophones is widely recognised, and it is often desirable to put them in small holes in order to minimize the wind effects; this is, however, the limit of possible control of the geophone placement. On the other hand the elastic, transmitting characteristics of the material immediately underneath the geophone have direct influence on the arrival times. This fact has been demonstrated by Koefoed (1954) and the present experiments are in agreement with his results.

Five geophones were placed side by side at 200 feet from a shot point. One of them was on the ground surface as it would have been placed during a survey; the second geophone was resting on $3\frac{1}{2}$ inches of fine gravel filling a small hole dug previously; the third geophone was placed on top of a 7 inches thick layer of disturbed ground, consisting simply of the in situ soil turned over several times; the fourth geophone was placed on the top of a 3 foot steel rod driven into the ground flush with its surface; and the fifth one was placed on 6 inches of coarse sand. All geophones were on the same level. The velocity of the steel rod was determined in the laboratory by an ultrasonic pulse instrument and served as the gauging velocity in subsequent calculations. It must be realized that due to the short length and small cross-section of the rod compared with its high velocity, and due to the small thicknesses of the tested samples of material, the data are by no means accurate, but at least some quantitive analysis is possible. The difference in the arrival time, observed in the field experiment, is $t = \frac{l}{V_o} - \frac{l}{V_r}$; where l is the length of the rod and V_o and V_r velocities in the overburden and rod respectively. The change in the direction of the ray will not affect the result significantly. The velocity through the layers of sand and gravel and disturbed ground can be computed in the same manner. The calculated velocities are:

steel rod:	17,800	feet per second (measured).
overburden:	1,700	,, ,, ,,
loose sand:	630	,, ,, ,,
fine gravel	780	,, ,, ,,
disturbed ground	470	,, ,, ,,

These results show conclusively that the arrival times are influenced by even a small thickness of low velocity material. It is known that glacial and alluvial deposits may contain sand, or gravel lenses, and the longer times observed have therefore to be considered in the light of this possibility. It must be stressed again that when total times are of as low an order as 30 milliseconds, a two milliseconds delay caused by a pocket of low velocity medium, and attributed to some other cause, may have a very detrimental effect on the final interpretation. This aspect will be considered in further detail in the section discussing the nature of the overburden.

3. *Nature of the Overburden*

Horizontal and vertical variations in the composition of the overburden and variations in the thicknesses of its constituent layers are largely responsible for the uncertainties and errors in the interpretation of the shallow refraction data. The following discussion will concern:

a) the low velocity of the uppermost layer;
b) small near surface areas of abnormally low velocity;
c) horizontal and vertical variations in the velocity of the overburden;
d) comparison of some uphole velocities with velocities recorded by means of surface spread near the borehole.
e) reversal of velocity.

a) *Low velocity of the uppermost layer.* The uppermost layer of the overburden is frequently composed of a material of low velocity of the order of 1,000-1,500 feet per second, the lowest encountered in these investigations being 470 feet per second and registered on a spread of 52 feet, with the initial geophone spacings of 1,5 feet (fig 1); in this particular instance sand was overlying gravel resting on marl, the topmost layer consisting of dry aerated sand under desert conditions.

Topsoil, peat and sandy clay are commonly encountered materials of low velocity. The thickness of such a layer may be of the order of a few feet and may vary appreciable along the line of traverse within a short distance. It is quite impossible to predict the variations in thickness and impracticable to determine them. The change of thickness of say 3 feet at a velocity of 1.000 feet per second would cause a change of 3 milliseconds in the time of arrival. Also, slight topographical changes of the ground surface are often effectively composed of low velocity material. An illustration of this point is provided by the result of an experiment where two geophones were placed one at the foot and one at the top of a 3 foot rise on the ground surface. The horizontal displacement was 4 feet, though the shot, 200 feet away, was on a line at right angles to the line joining the geophones, so that the path along the refractor was approximately the same. The recorded difference in the time of arrival was 3 milliseconds, indicating the velocity of 1,000 feet per second in the surface top layer, whereas the velocity of the overburden was 5,000 feet per second.

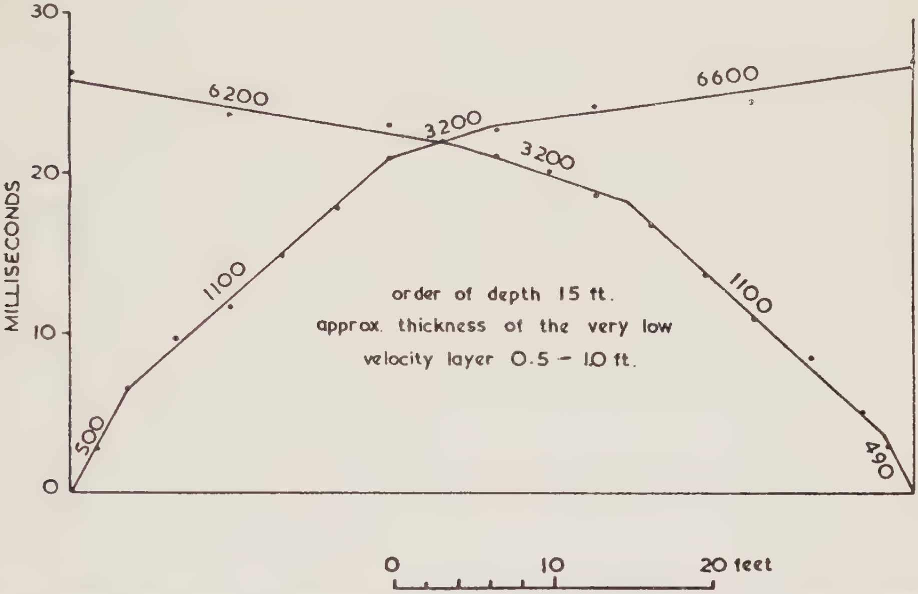

Fig. 1. Very low velocity of the top surface layer. Dry sand and gravel overlying marl.

It may be appreciated that it is impossible to apply a standard routine method for the reduction of times to a common datum, because the velocity between the datum and the surface will depend on the variation in the thickness of the topmost layer, even if the remainder of the overburden exhibits a uniform velocity. Errors incurred in such a way were known to amount to 10 per cent of the total times contained in the range of 30-50 milliseconds. The existence of this top, low velocity layer is confirmed in many cases by the fact that the first segment of the time distance curve does not pass through the origin, even with spacings of the order of 20 feet. It is not until the geophones are spaced very closely that this velocity can be recorded.

b) *Small, near surface areas of abnormally low velocity.* Very unusual results were obtained on some locations where patches with abnormally low velocity were encountered. Fig. 2a shows the time-distance curves obtained along a 1200 feet traverse with 50 feet spacing, with the abnormal area being subsequently checked by shooting a short spread with 5 and 10 feet spacings (Fig. 2b). Upon probing the ground with steel rods it appeared that under a comparatively firm surface there was an extensive pool of boggy peat.

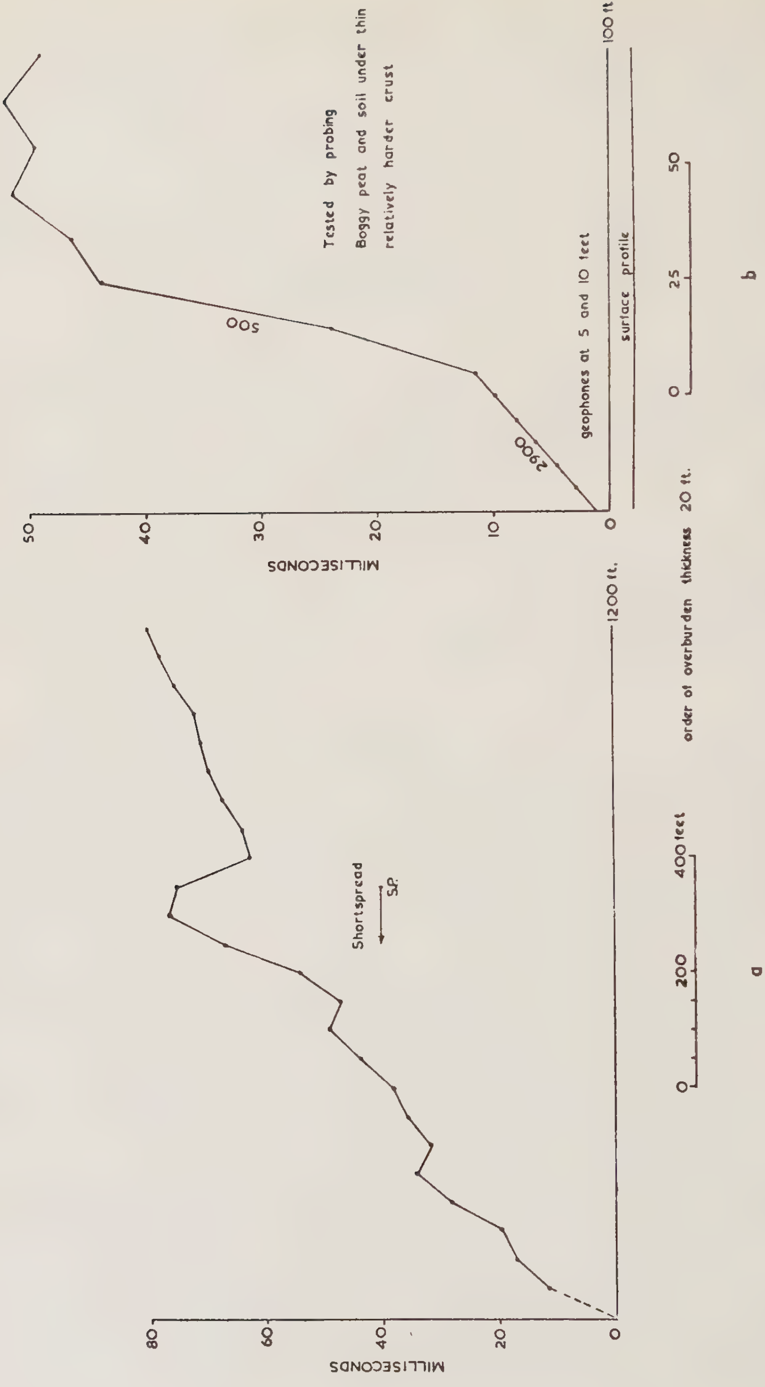

Fig. 2. Local, near surface area of the abnormally low velocity.

On another occasion, when operating under similar circumstances, an attempt was made to determine the velocity of such material. This was done by driving into the ground 9 feet of steel rod of known velocity, and placing one geophone on the top of it and another on the surface. The known rod velocity of 17,800 feet per second was used as a standard for the determination of the unknown velocity (using expression (1) which was of the order of 600 feet per second.

Although the presence of such abnormally long arrival times will naturally arouse the suspicion of the interpreter, it is still difficult to decide just how much of this delay is due to the very low velocity medium, and how much, if any is due to the fluctuation of the depth of the bedrock, without knowing the approximate thickness of the disturbing medium.

c) *Horizontal and vertical variations in the velocity of the overburden.* Examples of the variation in the horizontal velocity of an unconsolidated layer have been given in the past (Koefoed 1954, Evison 1952) and can be further emphasized here. Variations were encountered frequently in the low velocity top layer, and to quote a particular example a change of approximately 20% (2,500-3,000 feet per second) occurred within a distance of 100 feet. The material was sandy clay and samples from the 10 feet auger holes at the ends of the spread looked exactly the same. Another is an example of variation of the velocity of a deeper layer from 3,400 feet per second to 7,000 feet per second along a distance of some 400 feet in sandy boulder clay. These are probably extreme examples, but variations of 10% are commonly encountered. These variations are probably due to the changes in characteristics of the same layer, such as gradual transition from sandy clay to clayey sand, or from coarse sand to fine sand, although the simplest explanation would be that a definite change of material occurred such as boulder clay to sand etc.

These observations are confirmed by the results of uphole shots in shallow boreholes. Three boreholes were located at the corners of an approximately equilateral triangle with sides about 400 feet long. In each instance the shot was placed at the interface of the bedrock and overburden and the following velocities were recorded:

Depth of shot (in feet)		Veolcity ft. per sec.	Overburden	Rock
1.	14.	5,200	sandy clay,	schistose grit
2.	27.	4,300	stiff clay,	
3.	19.	8,700	sand	

Boreholes 1 and 3 were located at the bottom of a valley about 300 feet wide and the maximum difference in surface elevation was 40 feet (between boreholes 1 and 2). Many examples of this type could be cited, and thus it must be recognized that large variations in the velocity of the overburden do exist. Consequently the evaluation of seismic data in any area has to be made bearing this in mind.

In the examples above the overburden consisted of a non-stratified medium. The presence of well-defined, different layers in the overburden will further complicate the discussed phenomena, because, apart from the velocity fluctuations by virtue of the changing character of a single layer, the average vertical velocity will depend on the relative thicknesses of the layers along the line of traverse. To record in detail the variations of thickness of the upper layers would require a close spacing of shot points and might defeat the purpose which a seismic survey should fulfill, e.g. speed and economy.

d) *Comparison of some uphole velocities with velocities recorded by surface spreads at the boreholes.* In the course of tests to determine the velocities of the superficial layers in different areas, discrepancies were observed between the values obtained from uphole shots and those recorded on time-distance curves (fig. 3), and some examples are given below.

In one instance very coarse river gravel was overlying marl, the region being the flood plane of a river. The shot was placed at the depth of 16.5 feet at the contact of gravel and marl. The indicated uphole velocity was 3,600 feet per second, while two velocities corresponding to gravel were recorded, i.e. 1,500 feet per second and 4,300 feet per second, on time-distance curves (initial geophone spacing 3 feet). A pit in gravel was excavated near-by to see whether any change in the character of gravel was apparent, but the material was uniform throughout and the two velocities have to be explained as being representative of the upper loose layer and of the lower layer more compacted and containing moisture. Calculating the depth under the shot point from the time-distance curve, and using the time-distance curve velocities, the average vertical velocity is computed as 2,500 feet per second. This value is different from the directly observed uphole velocity.

On another occasion a shot was located at the contact of silty clay and rock (schistose grit) 19 feet below surface. The borehole was located in a shallow valley not far from a stream. The recorded uphole velocity was 8,700 feet per second, while the time-distance curve recorded a velocity of 7,500 feet per second. This segment of the time distance curve did not pass through the origin indicating the presence of another layer whose velocity was less than 3,800 feet per second (based on first observed time). Thus the average vertical velocity computed on the basis of the time-distance curve would be still less than 7,500 feet per second.

An example of the agreement between the velocity recorded from an uphole shot and indicated on the time distance curve was provided on another location. A charge was placed at 43 feet below surface at the contact of boulder clay and shale. Two velocities indicated on the time-distance curve were 2,500 ft/sec

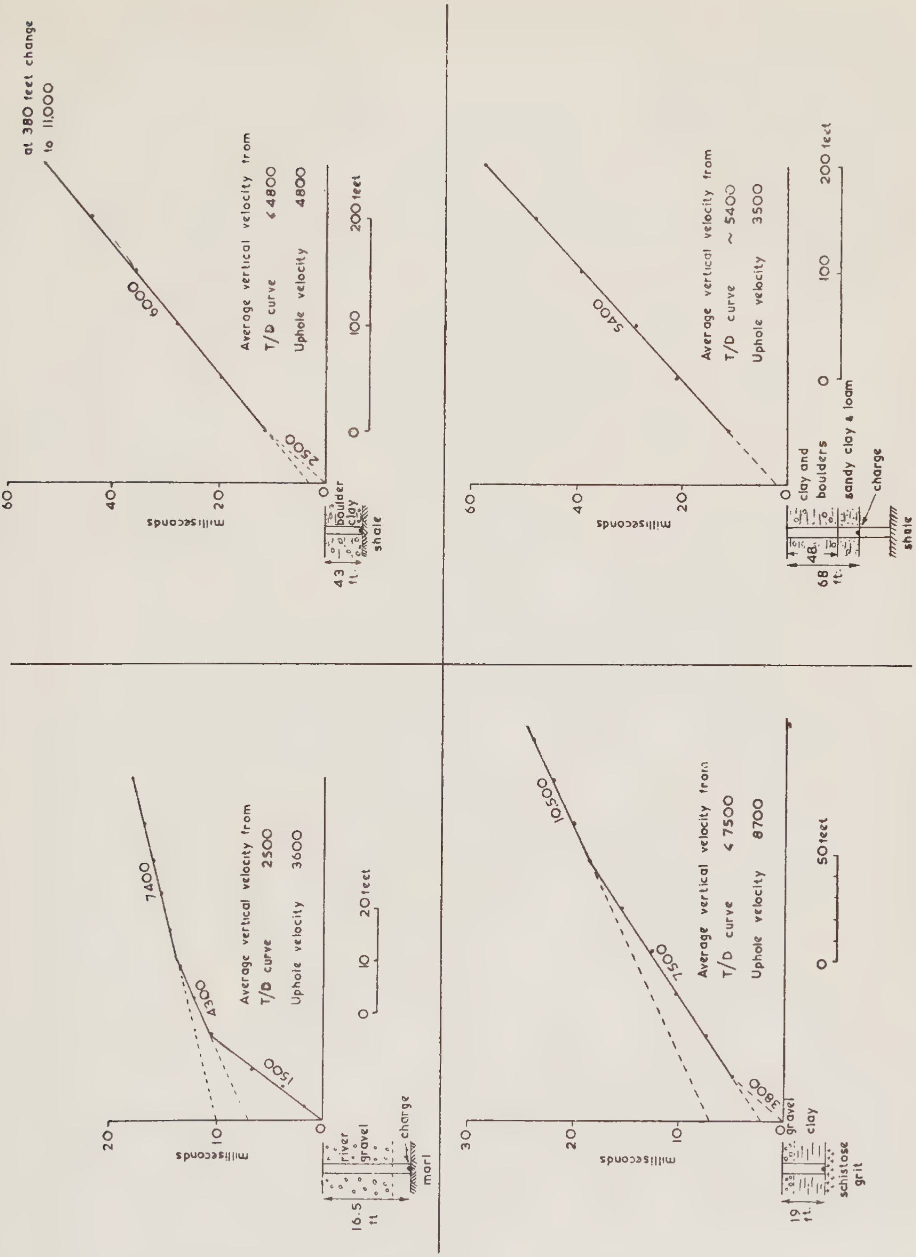

Fig. 3. Comparison of some uphole and T/D curve velocities. Velocities in ft./sec,

and 5,800 ft/sec giving an average vertical velocity of 4.800 ft/sec (on the assumption of depths calculated from the time-distance curve). The velocity observed by shooting an uphole shot was also 4,800 feet per second.

In the first two examples quoted here the velocities obtained from the uphole shots were higher than those indicated by the time-distance curves; the following is an example when the uphole velocity was lower. A charge was placed at 68 feet and the recorded uphole velocity was 3,500 feet per second. The velocity indicated by the time distance curve was 5,400 feet per second. It is obvious that this discrepancy must be caused by a layer of low velocity which underlies the higher velocity material, i.e. reversal of velocity. The borehole log indicated 47 feet of boulder clay underlain by 49 feet of sandy clay and loam. It is quite reasonable to assume that the sandy clay and loam represent the lower velocity medium. In this particular case as the shot was at 68 feet, the layer, whose vertical velocity was obtained, was composed of 47 feet of boulder clay and 21 feet of sandy clay and loam. Assuming that the velocity of the boulder clay was uniform throughout (5,400 feet per second), the velocity of sandy clay and loam would have to be about 2,000 feet per second to give an average vertical velocity of 3,500 feet per second. This value is of the right order but seems somewhat low. The possible explanation is that the velocity of 5,400 feet per second, indicated on the time distance curve, was that of the top layer of boulder clay, and masked a layer of lower velocity in the boulder clay as well as the layer of sandy clay and loam.

Whatever may be the actual distribution of velocities in this particular case, the uphole velocity lower than the time-distance curve velocity can be explained generally as being due to the presence of an underlying layer of low velocity which does not appear on the time-distance curve. On the other hand, no similar explanation can be offered in the case of the uphole velocity being higher than the time-distance curve velocity, and it is necessary to assume that the horizontal and vertical velocities of the unconsolidated strata may be different. Such an assumption would be in agreement with theoretical results derived by Gassmann (1951), who considered the propagation of elastic waves through a packing of spheres. In a numerical example quoted in his paper, velocities were calculated for a dry and wet packing of granitic spheres. For the dry packing the vertical velocity was higher than the horizontal velocity, the difference increasing rapidly with depth up to the depth of 3 feet, when the vertical velocity attained the value 100% higher than the horizontal velocity; below this depth the difference remained constant. For the wet packing the increase in the difference between the vertical and horizontal velocity was much less rapid, the vertical velocity attaining a value 15% higher than the horizontal velocity at the depth of 300 feet. (Diagrams on page 681 of the paper.) The differences observed experimentally by the present author were of the order of 40% and 20%. It would be too much to expect a numerical agreement, but both theoretical and experimental results seem to be generally in agreement.

e) *Reversal of velocity.* Although the interpretation of the time-distance curves is based on the assumption that each successive lower layer has a higher velocity, conditions occur when this is not true. The unconsolidated material overlying solid rock may consist of layers of glacial or alluvial origin and no definite sequence of higher velocity layers under those of lower velocity can always be expected, e.g. running sand may underlie firm boulder clay. If such conditions exist the low velocity layer will not be represented on the time-distance curve, and a gross overestimation of depth will occur. Unless there are facilities for an uphole shot the occurrence of the reversal of velocity may not become known at all. Under certain circumstances however, due to the phenomena connected with the propagation of the siesmic energy, this condition may become apparent on the time-distance curve. In the example which follows, the glacial drift was overlying the Coal Measures. Fig. 4 shows a time-distance curve obtained along 480 feet of traverse over practically flat ground. The unusual feature of this time-distance curve is a displacement of its first branch. This displacement amounts to 32 milliseconds (total time 102 milliseconds) and it may be seen that (a) the amount of the displacement is the same for the two

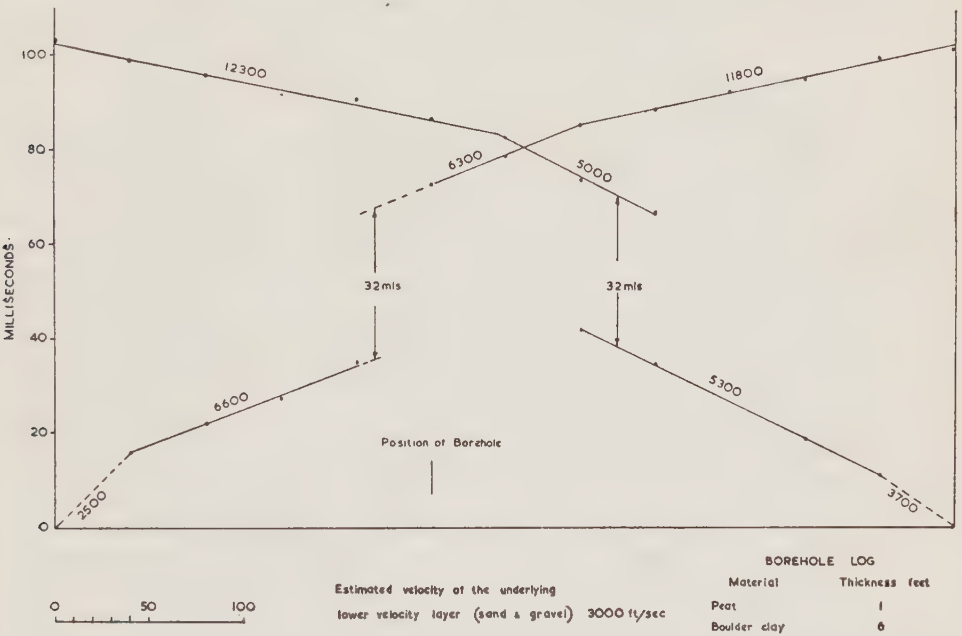

Estimated velocity of the underlying lower velocity layer (sand & gravel) 3000 ft/sec

BOREHOLE LOG

Material	Thickness feet	
Peat	1	
Boulder clay	6	
Running sand	6	61
Gravel	3	
Sand & Gravel	52	
Boulder clay	58	
Shale		

Fig. 4. Reversal of velocity in the overburden.

directions of shooting, (b) the displaced branches in each shot are almost parallel and (c) on some traces two breaks are present. It is not possible to show here all the results, but a similar picture was obtained over the whole area of this particular site. The depth to the rock was 126 feet and the overburden was composed of the following layers:

Material	*Thickness in feet.*	
Peat	1	
Boulder Clay	6	
Running Sand	6	61.
Gravel	3	
Sand and Gravel	52	
Boulder Clay	58	
Shale		

It is reasonable to suppose that the two displaced parts of the first branch of the time distance curve, indicating practically the same velocity, represent the upper and lower layers of boulder clay. If this is true, then the energy transmitted through the upper layer must have become very weak. This is quite possible because, if the top layer is absorbent for high frequencies and the initial pulse amplitude low, the pulse propagated along the first layer of the boulder clay may at a certain distance become unrecognizable. It may also be possible that there has been interference between the refracted and reflected waves at certain phase relationships (Bruckshaw 1952). A typical transition, as observed on the record, is shown on Fig. 5. The high frequency pulse registered by the near geophones, up to a distance of 160 feet, is of the order of 300 c.p.s. corresponding to a wavelength of about 17 feet at the observed velocity of 5,000 ft/sec. For a lower frequency pulse of 50-100 c.p.s. the corresponding wavelength would be 100 to 50 feet. Apart from the absorption of higher frequencies, therefore, another consideration is that the pulse of the lower frequency would not be refracted from the top layer of the boulder clay which is too thin. From the known velocities and thicknesses of the layers and observed times of arrival the velocity of the sand and gravel layer is of the order of 3.000 feet per second.

4. *Nature of the rock refractor*

The difficulties arising in the shallow refraction work which are due to the rock refractor may be considered from the point of view of its shape and physical condition.

The irregularities of the bedrock surface have a more pronounced effect on the shallow seismic results than irregularities of a deeply buried interface. A seismic profile is an average profile of the refracting horizon, and highs and lows of a very local character are necessarily smoothed out. Consequently the discrepancies between the true surface and seismically-determined surface may constitute a relatively large percentage of the total depth in shallow determinations. Also the steep dips of varying magnitude and direction near the surface are difficult to reproduce from the seismic data.

Another aspect of the effect due to irregularities is the scattering of the energy, or diffraction occurring when the curvature of the interface is large compared with the curvature of the incident wave front. If a selective scattering takes place, the high frequencies will be attenuated with an increase in distance. With normal dispersion the velocity will increase with wave lengths and, if the low frequencies are accentuated, an increase in velocity may occur.

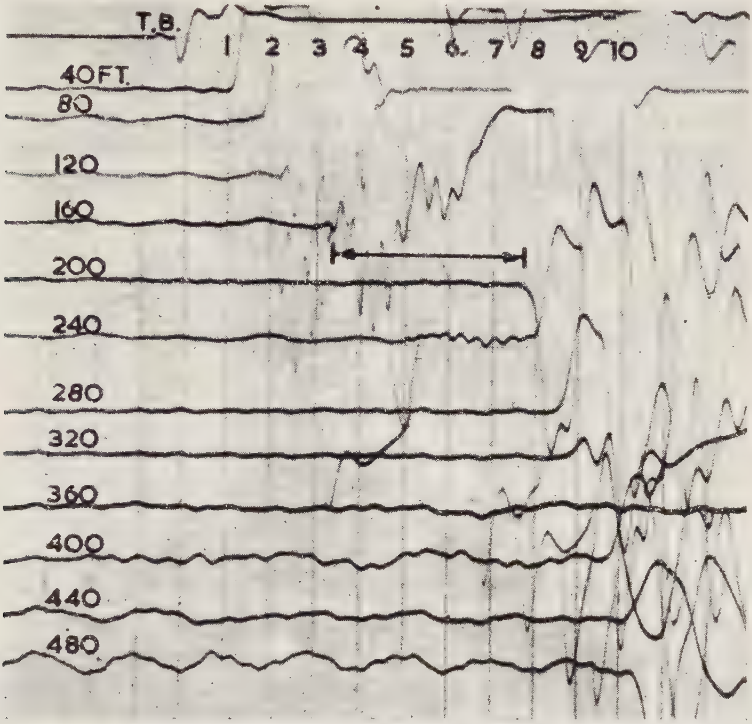

Fig. 5. Reversal of velocities (second events).

The effects of these phenomena will be further accentuated if the bedrock surface is not only eroded or irregular, but also weathered; in this case the interface will not be a reasonably well-defined plane but rather a transition zone. This unfortunately is often the case. Under such circumstances the difficulty is of a dual nature, i.e. in correlating the arrival pulses and in correlating the refractor, constructed from the seismic data, with some definite depth.

An ill-defined bedrock surface will occur in localities where the rock was exposed to erosion and weathering before a mantle of superficial deposits was laid down.

Another difficult condition arises when the geological interface is not sufficiently well defined in terms of the contrasting elastic properties. An example of this would be a layer of hard clay lying on soft shale, or sandstone. In a specific case of this type, velocities recorded were 7,200 feet per second and 7,300 feet per second. In consequence, the refracting horizon which was traced corresponded to a deeper, harder rock with a higher velocity and not to the required bedrock surface.

Finally, the rock underlying the unconsolidated strata may be composed of thin bands of various formations. This is typical of Coal Measures areas and is illustrated by a following borehole information:

Material	*Thickness* (*in feet*)
Unconsolidated deposits	85
Soft red sandstone	4
Grey sandstone	6
Shoft shale	1
Hard grey sandstone	5
Fireclay	4
Dark hard shale	2
Broken sandstone	11
Hard sandstone	2
Soft shale	10
Hard shale	10
Grey sandstone	15

In the case of thin layers of different material composing the upper section of the bedrock, the observed effect may be similar to that due to the increase of velocity with depth, i.e. there is a curving of the time-distance curve. It may also happen that some of these layers will be better media for the transmission of the seismic energy and at the same time, as the higher frequencies are absorbed, refraction will occur from progessively thicker beds.

Under any of these circumstances it is very difficult to determine, from the time-distance curve, the correct velocity of the refractor. The issue may be further complicated by the elastic anisotropy of the refractor resulting in the different velocities of propagation depending on the direction. This has been recorded on previous occasion (McCollum and Snell 1932, J. Cholet and H. Richard 1954) and observed by the present author. Two lines each about 2,000 feet long, and forming an angle of 98° with each other, were shot at regular intervals of 200 feet. Two definite and widely different refractor velocities of 7400 feet per second and 11.400 feet per second, (1,5 ratio), were recorded on each line. Each line was shot in reverse and there was no indication of substantial dip on either of them .The fact that the bedrock surface was virtually flat was confirmed by the results of three borings, one placed at each of the outer ends of the lines and one at the point where the lines crossed. The order of depth to the bedrock was 140 feet. The possibility that the two different velocities belonged to different refractors has to be ruled out because, (1). the computation of depth, based independently on each line ,yielded the same results which checked with the borehole information, and (2). the velocity of 7,400 feet per second did not appear on the time-distance curve which gave a velocity of 11,400 feet per second or vice versa. The underlying rock consisted of shale, and the higher velocity was recorded along the direction roughly parallel to the strike, as far as could be assessed from the available geological information in the area.

Owing to uncertainties in assessing the velocity of a refractor, an additional check is sometimes necessary. This can be effected in two ways either by shooting between boreholes, or by shooting on outcrops. In the first case, to avoid the lowering of geophones into the hole, a shot can be fired in each hole, at the interface between the overburden and the rock, with the geophones near each borehole. In this way the uphole times are determined and can be subtracted from the total times. The distance between the boreholes being known, the rock velocity can be calculated after some adjustment is made for the offset distance.

Determination of the rock velocity from the outcrop shots is less reliable as will be seen from the following experiments. A seismic survey was conducted in an area where an average thickness of 40 feet of glacial drift overlay conglomerate. The velocity indicated on time-distance curves was between 11,000-12,000 feet per second. It was decided to carry out measurements on the outcrops and two different localities were chosen. To the west of the surveyed area there was a ridge of conglomerate rising very steeply to a height of about 60 feet above the general level. This ridge was covered with a very thin layer of soil, 1-5 feet in thickness, and at places the conglomerate was exposed for varying distances, and very strongly weathered. Geophones were not placed in line, but on isolated outcrops, and the observed velocities varied between 6,500-7,000 feet per second.

In another place the rock was exposed for a distance of about 600 feet. The exposure was comparatively fresh, being due to a recent road cutting, and geophones were placed at an equal spacing of 50 feet. The points of the time-distance curve lie on one straight line (fig. 6a) which, however, does not pass through the origin. The indicated velocity is 14,000 feet per second. This example illustrates how the velocity of the same rock may fluctuate, depending on its degree of weathering, and, thus, that the outcrop measurements can not be conclusive.

An additional point of interest, with regard to the above measurements, is the fact that the time-distance curve does not pass through the origin. To investigate this point further, another test was made in a different locality on an outcrop of shale (fig. 6b). The velocity measured on the outcrop was 14,800 feet per second, while the indicated velocity of the refractor from the time — distance curves was 14,000 feet per second. In this case the agreement was much better, but obviously it can not be generalized. The time-distance curve again does not pass through the origin. The simplest explanation which can be offered is that there is a weathered surface layer of the rock and that the observed effect is due to refraction from the depth where weathering did not penetrate. Although visual inspection did not reveal any signs of weathering as implied by this term, the surface of the exposed rock must undergo certain changes due to the contact with air and moisture. It is possible however, that the observed facts have some connection with the phenomena of the propagation of the seismic energy near the free surface.

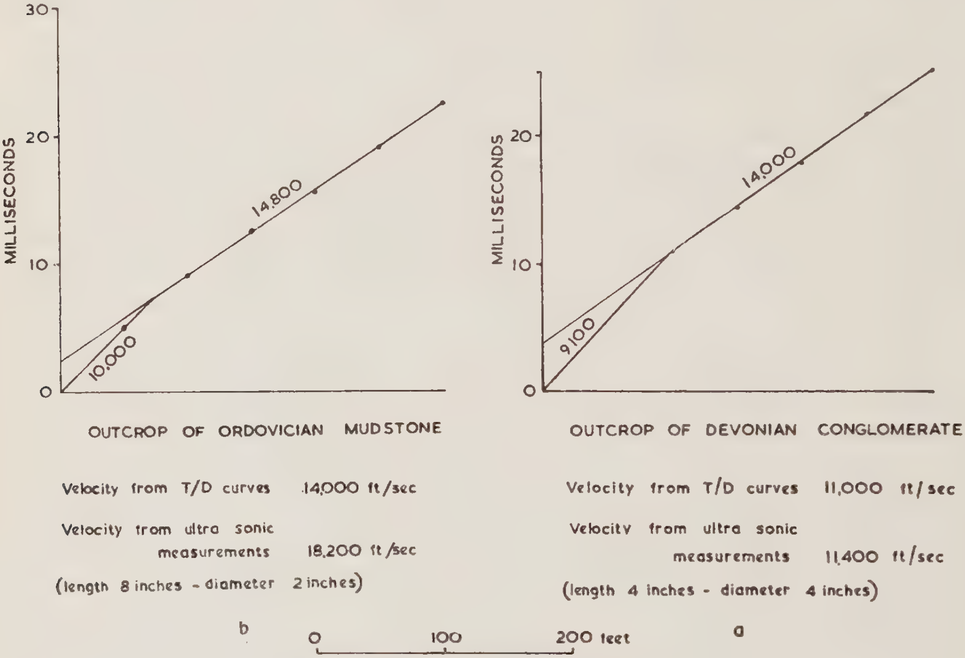

Fig. 6. Shots along rock outcrops. Velocities in ft./sec.

To complete the discussion of the means by which the rock velocity can be determined and compared with the velocity indicated on the time-distance curves, a mention should be made of the application of ultra-sonic pulse technique.

The method is based on measurements of the time of propagation of an ultra-sonic pulse, consisting of a train of longitudinal wave vibrations, through the tested specimen. This is achieved by placing two piezo-electric transducers in contact with the opposite ends of the specimen. The ultrasonic frequency is of the order of 200 kc/s, and the pulse repetition frequency 50 pulses per second; an instrument designed for testing concrete has been described in detail by Gatfield (1952). The accuracy of measurements is better than ± 1%. Some measurements were made on the core specimens from areas where seismic work had been carried out. The size of core was of the order of 7 inches long by 2.5 inches diameter. Velocities measured along the diameter were on the average 10% higher than velocities lengthwise. Also, velocities recorded by measurements on core specimens were higher than those registered on the time-distance curves. Not enough data have been accumulated, as yet, to offer an analysis of results. In any comparison however it must be borne in mind that (1) the source of vibrations is different, (2) the nature of the disturbance is different (intermittent pulse and continuous train of waves), (3) a single, much higher frequency is used when testing specimens and only one type of wave generated, (4) the dimensions of specimens are small (5), the physical properties of a small specimen do not indicate, the properties of the mass of the same rock in situ.

5. *Interpretation*

The basic difficulty in the interpretation of a shallow refraction survey consists not so much on the choice of a suitable method, on which to base the interpretation, as on the correct decision regarding the various aspects of the results. In other words, the information which is normally obtained from the examination of the time-distance curves can not be accepted entirely at its face value. This statement can be substantiated by theoretical and practical examples.

A theoretical example in Fig. 7 shows time-distance curves obtained from a reverse shot covering a distance of 360 feet. The assumed section consists of 5 feet of soil and peat which attains a thickness of 15 feet in the middle portion of the spread. This layer, which has velocity of 1,500 feet per second is underlain by boulder clay whose velocity is 5,000 feet per second. The rock below the boulder-clay has velocity of 10,000 feet per second, and the interface between the rock and boulder clay is at a uniform depth of 40 feet below the surface.

The first observation to be made about these results is that without the knowledge of the variation in thickness of the top layer, the observed lengthening of times can be erroneously taken as due to changes in the depth of the bedrock. The error thus committed would amount to about 13 feet or over 30% of the total depth.

Further, the position of the critical points on the time-distance curve is obscured by the change of its shape due to the change of dip of the interface between the top low velocity layer and clay. Consequently, both the apparent intercept time and the apparent critical distance are erroneous. It must be remembered that this is an idealised condition with no changes in the surface elevation, and that the actual curve based on field results would exhibit a greater scatter of points and increase the uncertainty.

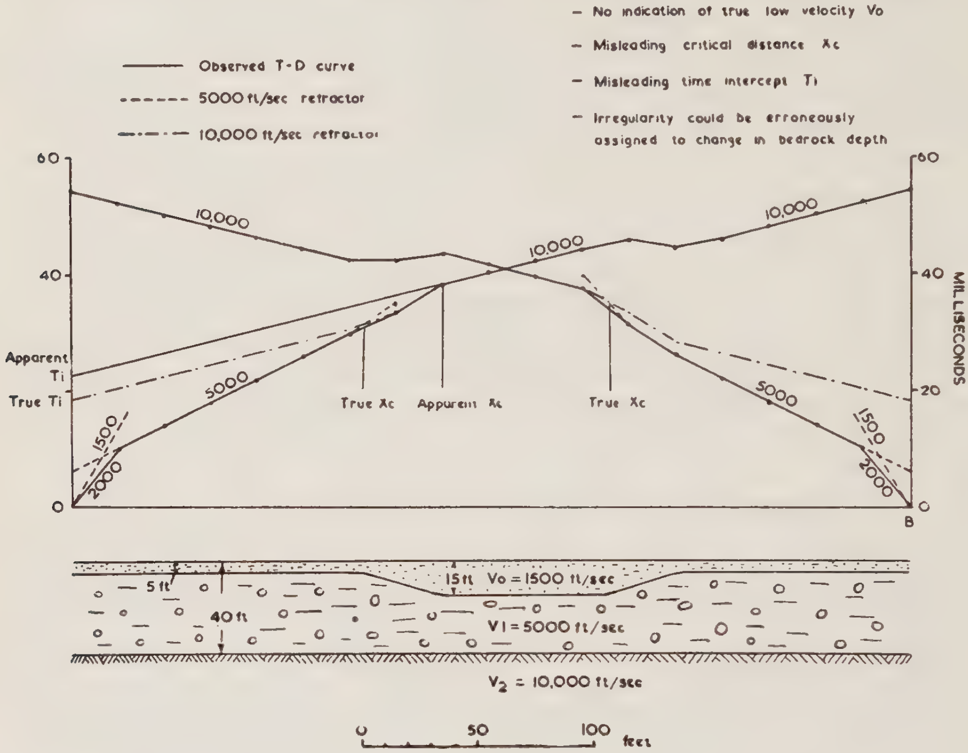

Fig. 7. Effect of variable thickness of top, low velocity layer.

Another example (fig. 8) shows the time-distance curves based on field results and the corresponding section based on borehole information. This illustration demonstrates the fallibility of interpretation based on the intercept, or critical distance methods when dealing with steep reversed dips. The points on the time-distance curve are not scattered but the picture is misleading.

It occurs sometimes that properties which qualify an horizon as "bedrock", from the geological or engineering point of view, do not correspond to its elastic properties from the seismic point of view. In this case the refracting horizon determined from the time-distance curvè does not correspond to the bedrock as determined by drilling. An example of such a discrepancy is shown in Fig. 9.

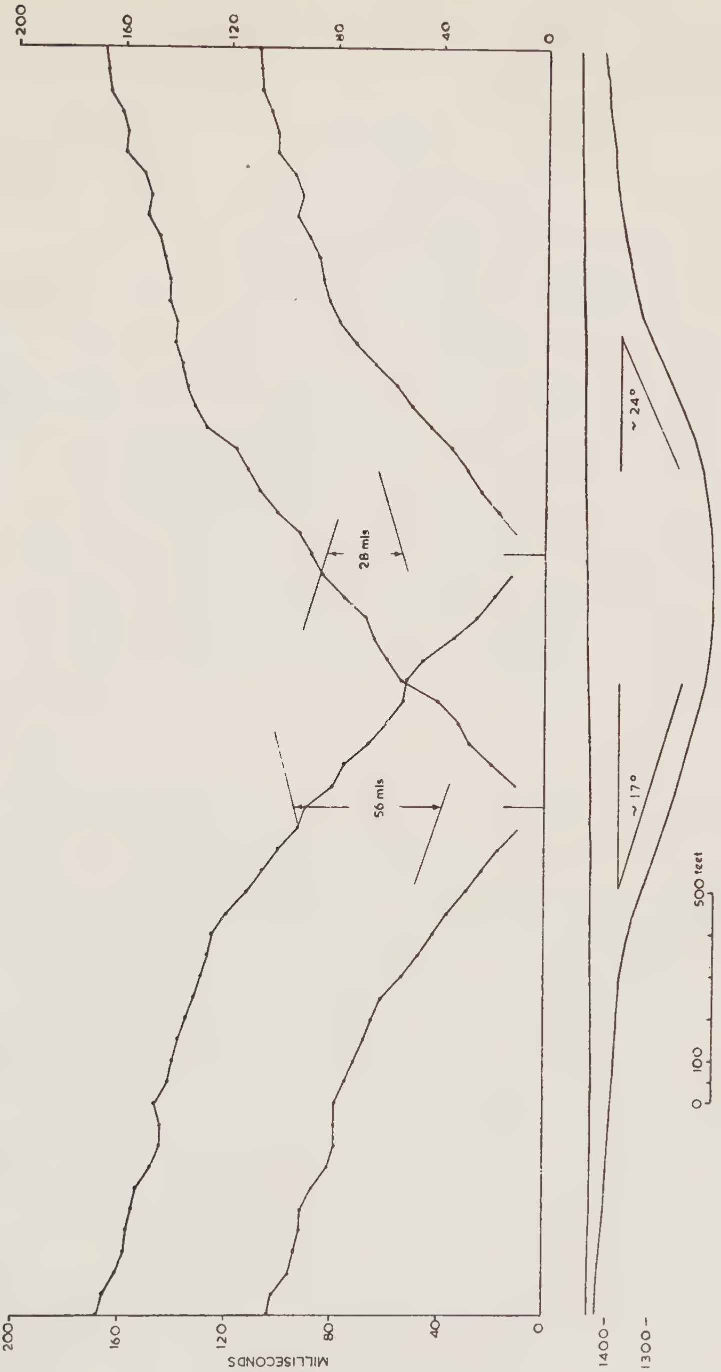

Fig. 8. Effect of steep and reversed dips.

where the rock (shale) was found by drilling at 14 feet, whereas the refractor exhibiting higher velocity, which would be attributed normally to rock, was much deeper.

It has been observed on occasions, when shooting two reserve shots into the same spread, that (1) the quality of the breaks depended on the direction of shooting, (2) the total times were different (up to 10% of the total times).

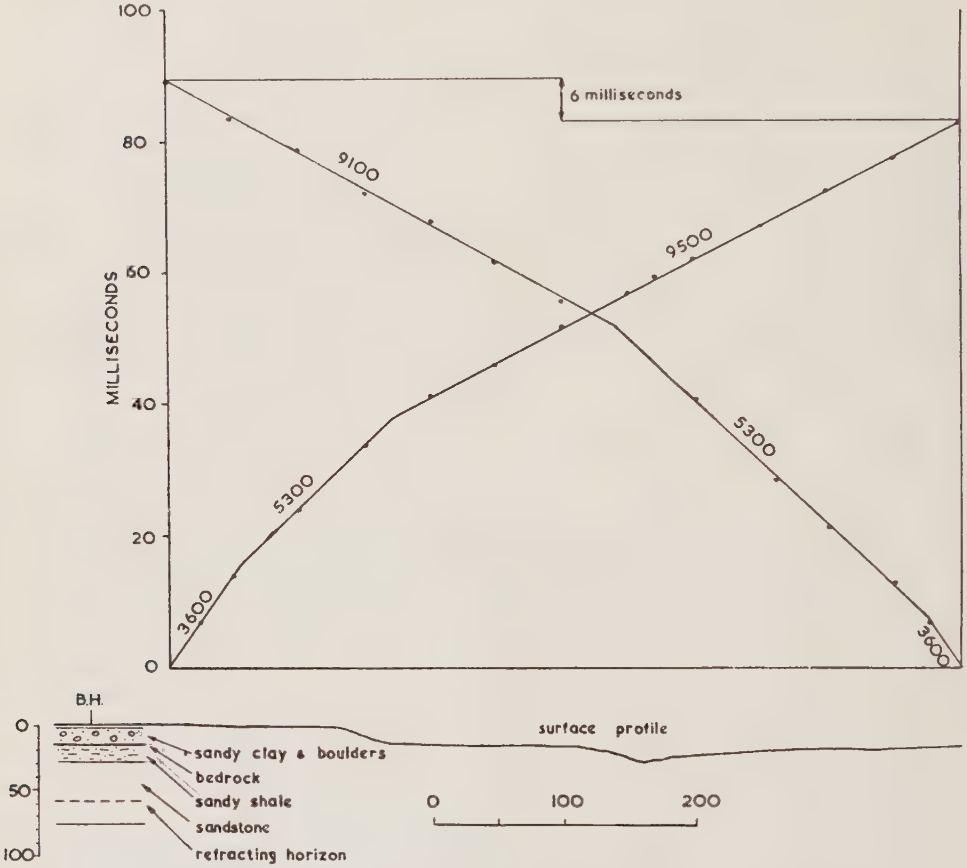

Fig. 9. Refractor not coinciding with bedrock. Total times different.

Concerning the quality of breaks, the possibility that the condition of the borehole, or the type of overburden around it was responsible for this phenomenon, has to be ruled out, because it was observed along the whole length of traverse and for the spreads shot from the same shothole. Two records shown on fig. 10, and representing reverse shots, are typical of a series obtained along a whole profile over a section of Coal Measures overlain by boulder clay; charges and amplifier setting were the same for both shots. A similar difference in the quality of breaks was observed during a survey over a section composed of schistose grit overlain by glacial drift. This seems to indicate the directional properties of the transmission of seismic energy.

The different total times, after allowing for the possible observational errors, could be due to two factors. Firstly, the refraction could possibly occur from different refractors. Secondly, it is necessary to bear in mind that the wavelength becomes a significant factor when the refractor is of a limited thickness. The results of seismic model experiments have shown that the phenomena associated with the propagation of seismic energy, under such circumstances, may have disturbing effects. Press, Oliver and Ewing (1954) demonstrated that when the ratio of the wave length to the refracting layer thickness is too large, the interference effects, created by multiple reflected pulses, cause resulting disturbance to travel at a velocity different from the refractor velocity. This is particularly so when the low frequencies are predominant. Also a composite refraction event, with a velocity depending on the elastic properties of the considered thin refractor and the refractor immediately below, may be considered erroneously as the continuation of the events due to the thin refractor.

Conclusions

As the depth of the seismic refraction investigations becomes shallower the differences between the theoretical assumptions and actual conditions become more pronounced, and the routine approach to the interpretation becomes more unreliable. Observational errors, errors due to assumptions and errors due to rapid changes of conditions within short horizontal and vertical distances, may result in a relatively large error in the estimation of the depth when dealing with short times and distances.

The disturbing effects are due to the method of generating the seismic wave, the shothole conditions, the configuration of the ground surface, the inhomogeneity, anisotropy and horizontal and vertical changes in the layering of the overburden, and the irregularity and weathering of the rock surface and thin stratification of the top portion of the underlying rock.

The amount of information which could be obtained in order to improve the accuracy has to be considered from the economical point of view. An inspection of the area where the survey is being conducted will help the interpreter in assessing the quality of the information available from time-distance curves.

Results obtained from shallow investigations are useful because they provide rapidly a picture of the bedrock configuration, and guide a subsequent drilling

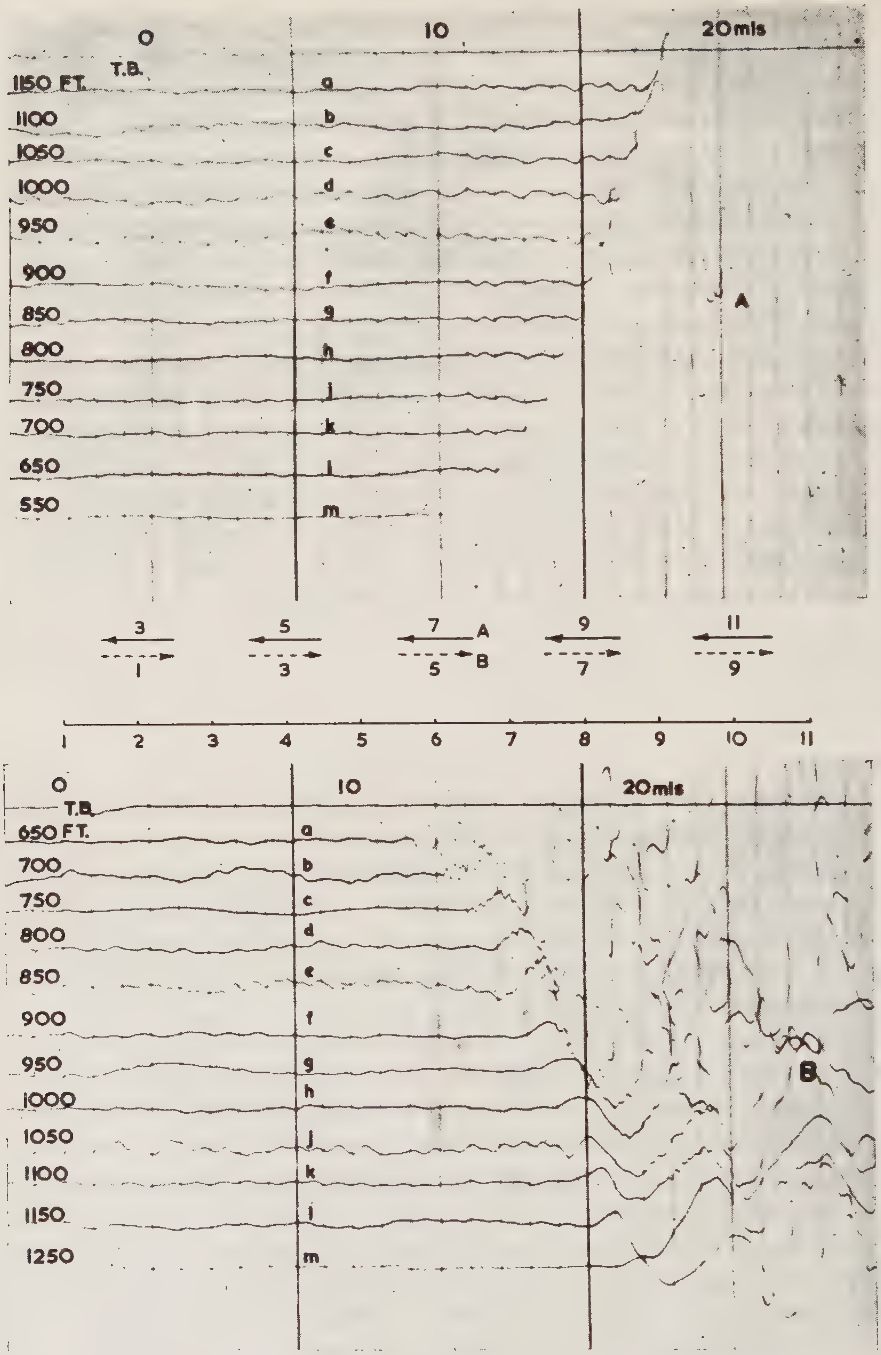

Fig. 10. Energy transmission dependent on direction of shooting.

programme. The accuracy of the depth determination will be improved generally if some preliminary borehole information is available, and this practise should be adopted whenever possible.

ACKNOWLEDGEMENTS

Thanks are due to the Directors of Mining & Geophysical Services Ltd. for permission to use the material published in this paper.

DISCUSSION

MR. WILSON: In similar work in N. Wales, we have found that certain surface layers, e.g. a glacial marine clay, a river alluvial deposit, and boulder clay transmit a wave of characteristically high frequency, 100-300 c/s. This wave can be seen as a second arrival, sometimes as far as one mile from the shot-point, and we feel that the picking of these late arrivals, well seen on account of their high frequency, is a necessary confirmation of the persistence of such a layer.

Concerning the low velocities often found in outcrop velocty determinations, our experience is that, at least with limestone, outcrops consist of blocks of high velocity, of the order of 100 ft. in size, separated by weathered zones or large joints which delay the wave, thus lowering the velocity when measured over a distance of about 400 ft.

MR. DOMZALSKI: In reply to the remarks of Dr. Wilson I would like to say that the registration and use of the second arrivals can undoubtedly give valuable information under certain circumstances.

I would like to stress however that

1) The presence of a layer of superficial deposits does not have to be confirmed by deductions from the study of the second arrivals because in normal survey this information is derived with certainty by spacing shot points along the line of traverse, along which this information is required, unless a reversal of velocity occurs. This spacing in shallow investigations has to be sometimes very close.

2) To give a reasonably accurate depth interpretation the velocity of the overburden has to be known as accurately as possible and although the frequency of transmission through, say, boulder clay and river alluvial deposit may be contained within the same broad band their velocities may be and in practice are different.

What is needed therefore is not a general indication of the persistence of a layer of superficial deposits, but an evaluation of the velocities which are an index of the vertical and horizontal changes in the overburden.

Concerning the rock velocities measured on the outcrops I agree that the most obvious explanation of the lower velocity is by the presence of the vertical joints if they exist. Apart however from the large scale weathering which can be assessed by visual inspection the exposed rock undergoes certain changes in its elastic characteristics, which are responsible for the observed effects.

REFERENCES

Bruckshaw J. Mc.G. 1952, Private Communication.

Chalet J. & Richard H, 1954, "A Test on Elastic Anisotropy Measurements at Berriane (North Sahara)". Geophysical Prospecting, 2, 232-246.

Domzalski W., 1954, "Seismic Investigations, their Application to Mining Problems", Mine & Quarry Engineering, 19, 151-159.

Evison, F. F., 1952, "The Inadequacy of the Standard Seismic Technique for Shallow Surveying", Geophysics, 17, 867-875.

Gassmann, F., 1951, "Elastic Waves through a Packing of Spheres", Geophysics, 16, 673-685.

Gatfield, E. N., 1952, "An Apparatus for Determining the Velocity of an Ultrasonic Pulse", Electronic Engineer, September.

Koefoed, O., 1954, "Some Observations on Seismic Weathering Corrections", Geophysical Prospecting, 2, 274-280.

McCallum & Snell, 1932, Physics 2 (3), March.

Press F., Oliver J., Ewing, M., 1954, "Seismic Model Study of Refraction from a Layer of Final Thickness", Geophysics, 19, 388-401.

Uhrig L. F. & Van Melle, F. A., 1955, "Velocity Anisotropy in Stratified Media", Geophysics, 20, 774-779.

SEISMIC EFFICIENCY OF EXPLOSIVES *

BY

Henri RICHARD **, Maurice PIEUCHOT **
Compagnie Française des Pétroles (Algérie)
and Société Nationale de Recherche et d'Exploitation
du Pétrole en Algérie

ABSTRACT

The parameters which characterize an explosive are derived from laboratory tests and none is directly usable for seismic purposes. Another one, derived from field experiments is proposed in this paper. It allows the comparison of two different explosives. The test must be conducted with care. Precautions concerning the equipment and the shot point detailed. The first available results suggest that the new parameter does not depend on the size of the charge nor on the shooting conditions, though the experimental data are not numerous enough to allow a general statement. It is shown how a coefficient of seismic efficiency can be used for selecting an explosive; and considerable amounts of money can be saved by the best choice. More studies on the generation of artificial seismic waves would be highly profitable.

THE SELECTION OF AN EXPLOSIVE = A PROBLEM

Seismologists do not always agree on the qualities of explosives they required most .Usually they are very particular about the physical characteristics of the charges (diameter, weight, density...) which affect the ease of handling in the field and determine the shooter's maximum production. Sometimes, they have a feeling that one explosive is better than another, but they cannot tell exactly why nor by how much. In an attempt to keep close to the realization of a point charge, it is customary to use high velocity, densely-packed, powerful explosives.

In the desire for power, one is limited by the cost, and the cost of explosives is a considerable part of the total-cost of a seismic exploration.

It is difficult here to present all the qualities of a seismic record; besides, the relationship between the quality of the records and the explosive has readily been discussed ***. So the present paper will be restricted to the dicussion of the minimum cost of explosive necessary to pick an energy arrival from a given horizon. Thus, only the energy carried by the seismic wave need be considered.

---

*) Presented at the Ninth Meeting of the European Association of Exploration Geophysicists, held in London, 7-9 December 1955.

**) Compagnie Générale de Géophysique.

***) V. Colledan and A. H. Selem "Seismic Response and Safety using different explosives"—5th E.A.E.G. meeting, Milano, dec. 1953.

USUAL CHARACTERISTICS OF EXPLOSIVES

The energy imparted to a seismic wave is related to 1) the internal energy of the explosive itself and 2) the mode of liberation of this energy. Each explosive may be characterised by certain parameters and these are defined by means of laboratory tests.

Some characteristics are directly related to the mode of ultilization and can be taken into consideration without discussion: such are the water resistance and the density. But difficulties arise with parameters which seem to have an influence on the seismic disturbance though we cannot measure this influence nor even see it directly on the records. These parameters are the velocity of detonation, the brisance, and the strength:

The Velocity of Detonation is measured by comparison with the velocity along a standard primacord. It is the well-known method of DAUTRICHE and is universally used so there is no necessity to describe it here. This velocity has a mathematical definition and it is easy to appreciate its significance.

The Brisance is measured by a small lead block test: a given weight of explosive is laid on a cylinder of lead with a steel plate interposed .After the explosion the reduction of height of the block measures the "brisance".

If this parameter is related to the ability to break rocks, it gives an idea of the proportion of energy lost in permanent deformations as opposed to the elastic deformations of seismic propagation. Thus, it would appear that brisance is undesirable in seismic studies. Actually, it measures the shock wave developed by the explosion under the experimental conditions. The relation between this shock wave and the elastic wave is not known but there might be a direct relation. If it had been called "shock wave test" instead of "brisance test" it is not unlikely that seismologists would have been interested in it and would have selected the explosives giving the greatest reduction of height of the lead block.

The coefficient of strength can be measured by different tests.

a) Firing the explosive in a manometric bomb corresponds to the explosion of the charge under a perfect tamping. It yields the maximum pressure and, the way in which this pressure develops.

Seismologists do not know the relation between the maximum pressure and the energy of the seismic wave. They do not know which is best for them, an initial pressure developing quickly or a pressure building up gradually.

b) The test with the ballistic pendulum consists of firing a certain weight of explosive placed in a gun fastened to a heavy pendulum and at right angles to its axis of rotation. When the charge explodes, the pendulum is swung by the reaction of the gases and its deviation is measured. This test is not common in France where the Government specifications are based on the results of the following test of TRAUZL.

c) This test makes use of a cylindrical lead block. A hole is bored in one end along the axis. The explosive is placed at the bottom of the hole and covered with loose sand up to the top of the lead block. The explosion widens the hole and the increase of volume is measured. The weight p grams of explosive which gives the same increase of volume as 15 gr of picric acid is used to calculate the "coefficient d'utilisation pratique" (CUP) from the formula:

$$CUP = \frac{1500}{p}$$

The TRAUZL test can be made only with explosives which detonate. With an explosive such as black powder which ignites, the gases expel the sand tamping and very little deformation is noticed. As DAVIS [1]), indicates it is essentially a brisance test, but it yields information on the relative strengths of explosives having the same brisance.

Cup and Seismic Efficiency

The CUP is the result of a laboratory test. It is a shot fired in a hole with poor tamping and it measures the dilatation of the cavity. So, it might be a very valuable piece of information when it is necessary to shoot a cavity in order to place a large charge in one hole. But this is not where the seismologist can make an appreciable economy.

He requires the type of explosive giving the stronger seismic waves .He may know which is the best for shooting cavities by using the strength parameter of the explosive and it is a temptation to take this "strength" for granted and to think that the seismic effects are directly related to it, but this not evident.

First, the different determinations of the strength parameter do not lead exactly to the same classification of explosives. Next, the CUP, as defined above is not independent of the brisance. Lastly the other parameters, which play a part in the way energy is liberated, may have considerable effects on the spectrum of the emitted wave and on the deflection of the galvanometers at the recording end.

CONCEPT OF "COEFFICIENT OF SEISMIC EFFICIENCY"

Only the galvanometer deflection is of interest to the seismologist and it is this that should be related to the quantity of explosive used.

---

[1]) Davis, V. L. 1950 "The Chemistry of Powder and Explosives." John Willey and Sons Inc. New-York.

It is obvious that this deflection will depend on the explosive, as well as on the field conditions .It is well known that the efficiency of an explosion varies from one point to another.

Now, if the deflection *DB* obtained with an explosive *B* is compared with the deflection *DA* obtained under the same conditions with an explosive *A*, the factor *DB/DA* should not depend upon the experimental conditions. If it can be proven that this factor depends on the explosives only, we have here a parameter giving the seismologist the percentage of additional energy he will record using explosive *B* instead of *A*. Putting it another way, this parameter will enable a calculation to be made of the weight of explosive *B* necessary to record the same galvanometer deflection as one pound of explosive *A*.

Such a factor establishing a comparison of the effects of two types of explosives is analogous to the "*CUP*". This analogy leads us to calling it: "coefficient of seismic efficiency". In French, it will be: "coefficient d'utilisation sismique' or "CUS".

The CUS is no longer the result of a laboratory test. It is derived from field experiments can be used to select the explosive which will be cheapest. But now we have to see how the CUS can be measured and to make sure that it does not depend on the size of the charge nor on the field conditions.

MEASUREMENT OF THE CUS

The measurement of the CUS is made by examining a galvanometer deflection This deflection comes from the combination of:

a) extraneous noise, apart of which is generated by the explosion, and b) reflected or refracted energy.

Evidently, only deflections related to the explosion are to be considered. The measurements necessary for determining the "CUS" can then be made using the explosive noise, and the reflected or refracted energy.

Attempts to Determine the CUS

The Compagnie Générale de Géophysique carried out two series of tests, one in Algeria for SNREPAL and CFPA.; and one in France during the same year.

These tests revealed several problems concerning the use of explosives in seismic work. They revealed the precautions to be taken for correct experimentation and suggested a suitable procedure.

Observed Signal and Instrument set up

In both series of lists the observed signal was a refraction arrival. For which Fig. 1 shows a specimen record. For the calculations, the deflections corresponding to the first maximum are measured and added.

The measured deflection should be proportional to the energy arriving at the geophone. For this purpose, the AGC is turned off and the filtering is reduced to a minimum. As well as this, it is necessary to ensure that the frequency of the signal is constant. Under these conditions, the gain will stay the same.

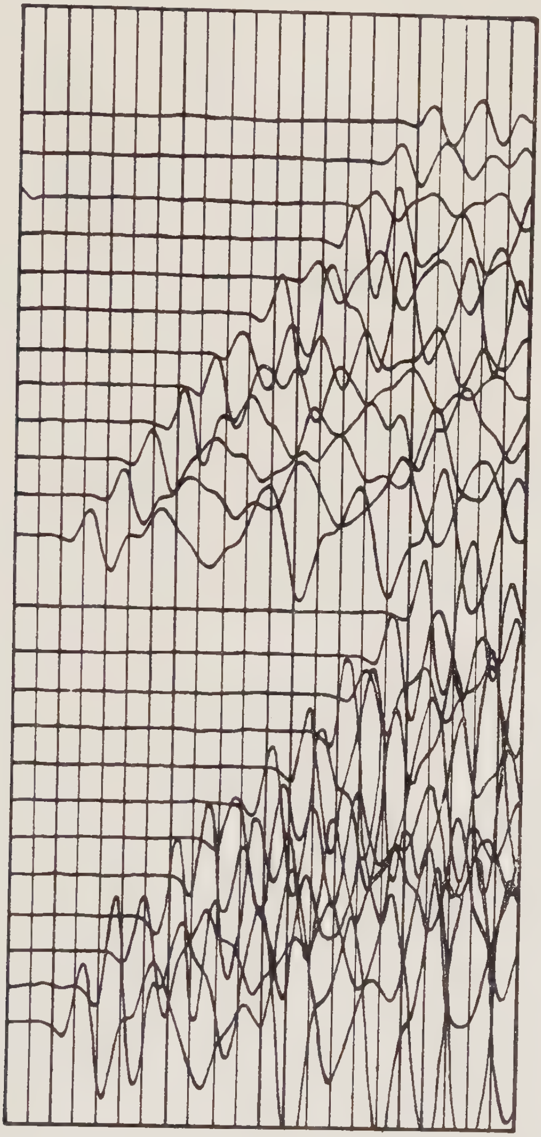

Fig. 1. Specimen of record used for seismic efficiency determinations.

Overloading of the amplifiers must be avoided and the measured deflections must be large enough for accurate readings. To guarantee this, two sets of amplifier with different gains have been used in parallel.

Necessity of Statistics

It would be very difficult to know accurately the slight variations of the sensitivity of the equipment over the complete period of the measurements. Besides, the energy output of the explosions is different for each particular shot, resulting in a scatter of observations. Random errors can be eliminated by averaging a certain number of measurements. Calculating the standard deviation will give an idea of the accuracy of the mathematical mean finally obtained. So, any determination of seismic efficiency must include the repetition of each individual experiment, and the number of repetitions depends on the accuracy required.

Constancy Checks

These can be used for checking the constancy of the equipment. Suppose, for instance, that we want a comparison between 6 explosives, 5 shots of each being necessary. This happened in a series of experiments which lasted for two days. The spread was left in the field during the night. 6 explosives were shot, three times on the first day and twice on the second. The mean deflections are tabulated in fig. 2.

Explosive used	1st day	2nd day
N 17	103.5	100.5
NIC	80.8	87.9
Kinsite	82.7	82.9
N 18	90.7	84.2
N 31	96.8	100.4
Hexolite Nitraté	106	97.5
Total deflections	560.5	553.4

Fig. 2. Constancy check.

The 2 or 3 measurements made each day with one particular explosive is too small a number for statistical analysis. But, when this number is multiplied by the number of explosives used, a total of 12 or 18 figures is reached and a statistical cancellation of errors occurs. The difference between the totals of these two days is 1.3%. It can be assumed that no gain correction has to be introduced in the computations of the second day as it would be smaller than the differences that are the object of the investigation.

Increasing the number of measurements leads to a better determination of the efficiency of each explosive and to a better overall average for constancy checking. So the statistical method of checking the constancy of the equipment allows any desired accuracy and this accuracy is automatically adapted to that required for the measurements themselves.

Variations of the Shot Conditions

After eliminating the influence of the equipment there remains the possibility of variations at the shot point. They may introduce systematical errors which must be accounted for four experimental examples are given below:

1) *Buried shots* .The shot point area was flat and the surface geology, as well as the drilling logs of the shot points, suggest uniform and constant conditions. The shot points were located at the intersections of perpendicular lines every 20 m.

Fig. 3 shows the results of 50 Kg shots for 3 explosives.

The scattering of the results is very large. By selecting one particular shot for each explosive, it is possible to obtain any previously established classification. The same scattering was observed with other buried shots, in spite of every precaution taken in loading and tamping. It was thought that the shot point area might have a variable output and, thus, the map of fig. 4 was plotted. It shows the position of each individual point with different signs indicating the energy recorded from the shot at this point, compared with the average energy level. It is very difficult to delineate areas of good or poor output, except, may be, for a zone around shot point 18.

The differences between individual measurements seem to be caused by slight variations in the tamping which cannot be perfectly constant.

2) *Surface shots.* Found types of explosives are compared by shooting 1 Kg of each .The load is laid simply on the surface of the ground. The determination includes 10 series of 4 explosions. The four types of explosives are used in sequence successive shot points distributed along an 80 m line perpendicular to the direction of the spread. On graph No. 5 the measured deflections have been plotted against the shot-point position on the line. This yields 4 curves, each one corresponding to one of the explosives and representing the variations of the deflection as a function of the shot point location. It is possible to obtain 4 curves which are almost identical. This similarity between the curves implies an influence of the shot point location. The overall variation is 30% whereas the local conditions seem to be invariable.

3) *Air-shots.* The variations from one shot to the other are presumably smaller if they are fired in the air or in water. There are no permanent deformations of the medium around the shot and it can be repeated at the same point. Actually, measurements made with air shooting show a much smaller scattering than with buried shots. The curves of graph No. 6 represent the variations

of the measured deflections, the shots being classified in the order in which they were fired. The double line represents the average deflection obtained

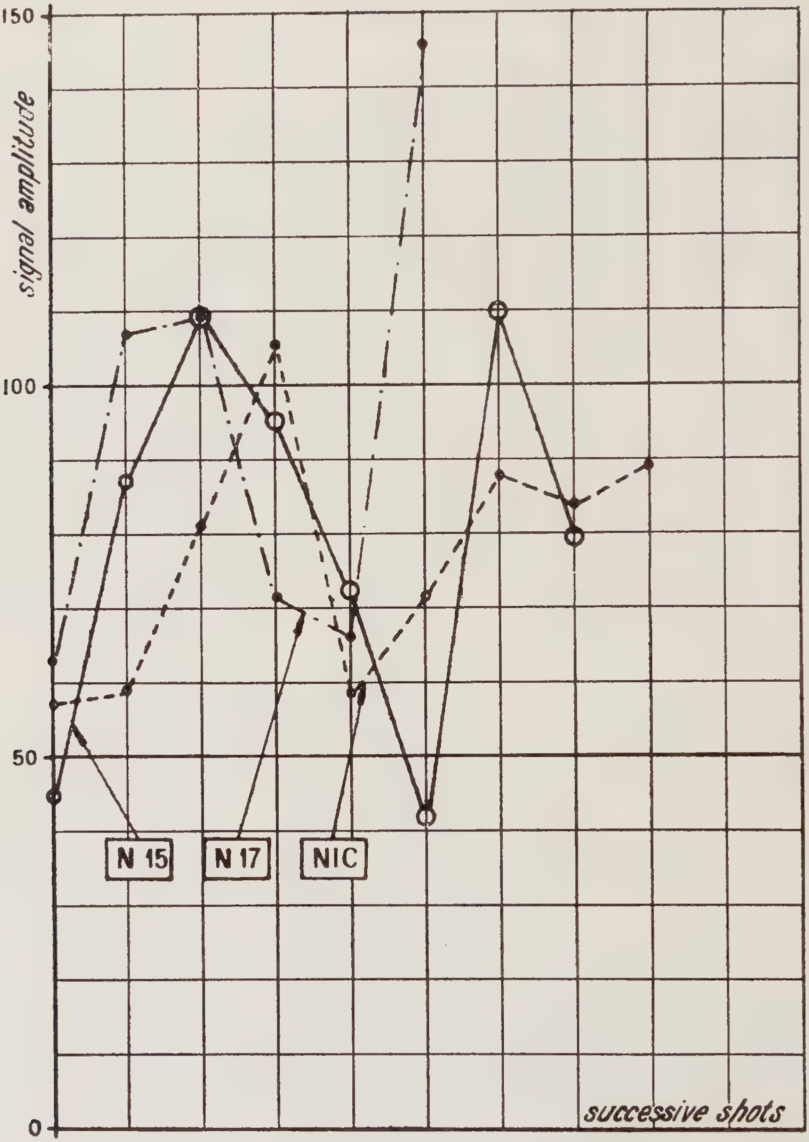

Fig. 3. Signal amplitudes for 50 kg buried charge.

with all 6 explosives of the series. The variations show only a normal deviation from a mean value.

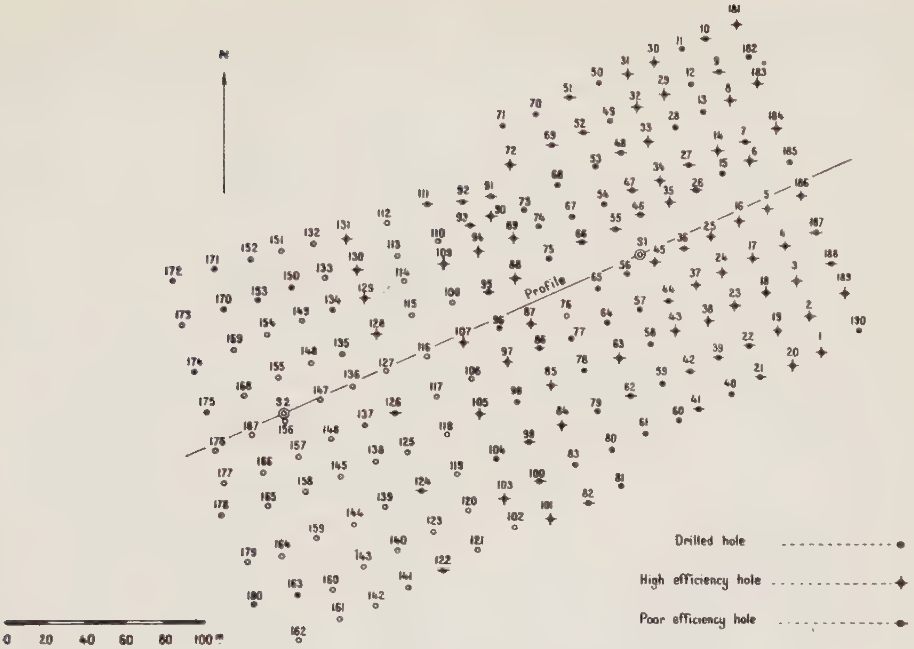

Fig. 4. Shot point location map

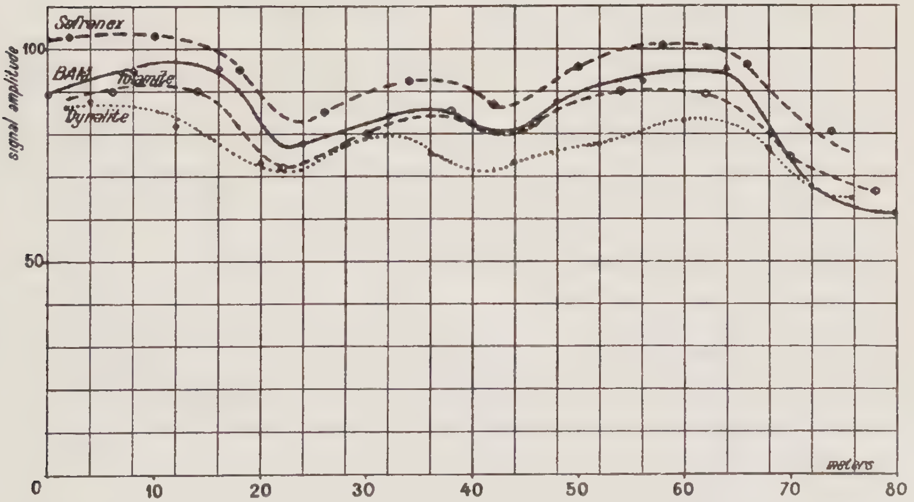

Fig. 5. Surface shot - Shot points in line.
Variations of the efficiency of individual shots according to their location along the line.

4) *Multiple air shots.* On the other hand, multiple shots fired in the air 200 m from this location revealed a progressive modification of the shot conditions. Figure 7 points out an improvement of 36% in one instance and of 16% in the other starting from the first shot. The bigger shots of 112.5 Kg were fired after the 56.25 Kg ones so that it may be admitted that the improvement of the energy output of the shot point area increases rapidly at first and then more slowly. This agrees with the general trend of the diagrams. The 3 curves correspond to 3 different spacings between individual charges.

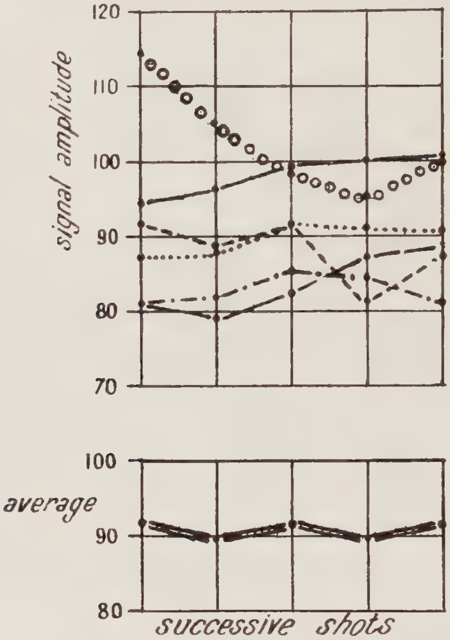

Fig. 6. Shots taken 2 m above the ground. Variations of efficiency for repeated shots.

Conclusion—Precautions to be Observed

To sum up, the output of the shot point may be very variable and has a considerable importance in the determination of the coefficient of seismic efficiency of an explosive. The experiment must be planned so that the variations can be known and, possibly, represented in a graphical form.

It can be seen too that the standard deviation is bigger for buried shots than for shots fired in the air or even at the surface of the ground. Thus, to obtain the same accuracy, in the comparing of explosives by buried shots more measurements are required than when shooting in the air. As each measurement requires a new hole, it is necessary to have a large area which is not always easy to find; also the drilling cost is high. It is much cheaper to make the comparison between explosives by air shots or surface shots.

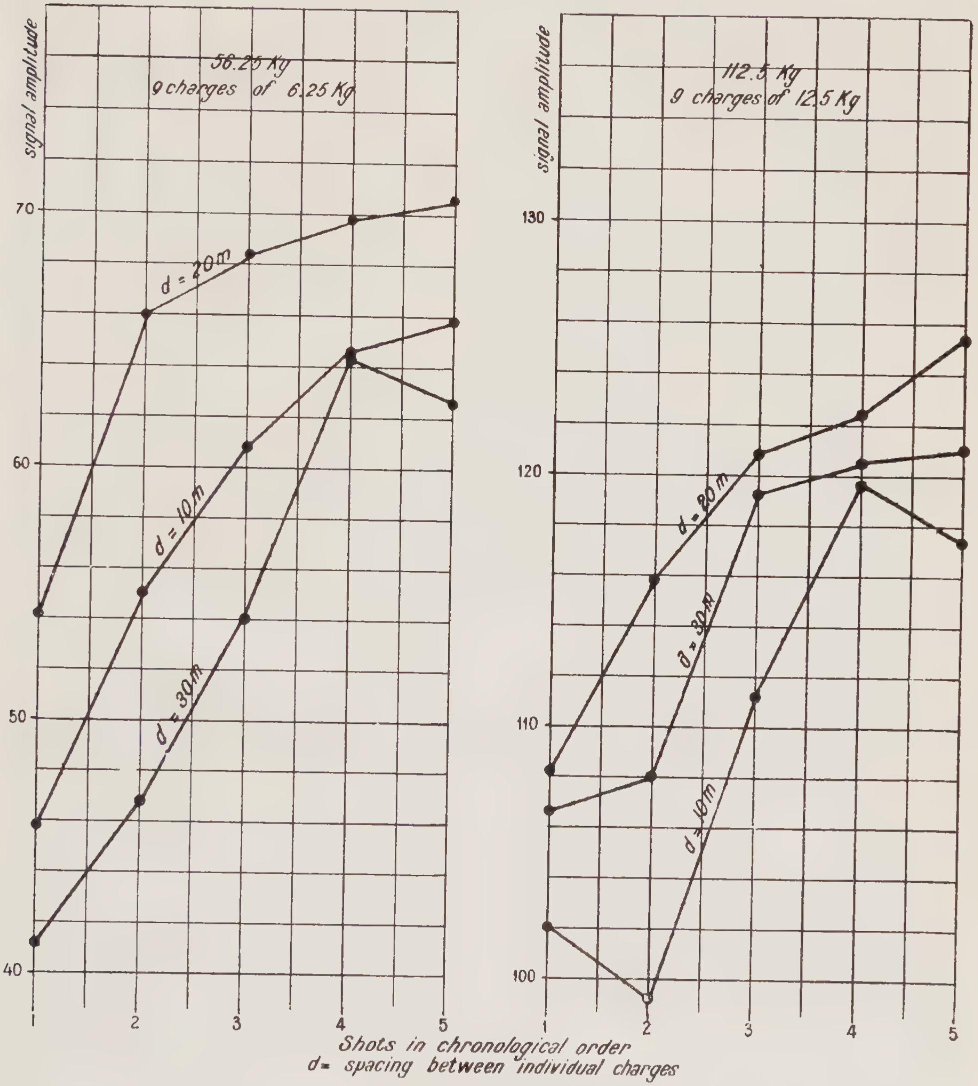

Fig. 7. Multiple air shots

Comparison of air Shooting and buried Shots

A comparison between air shots and buried shots was made in Algeria only. The number of determinations made with buried shots was small and in two instances only can they be compared with air shots.

1) The ratios between the seismic efficiencies of two nitrates turned out to be 1.17 and 1.20 in two different comparisons made with buried shots. With air shots, this ratio is 1.16.

With another pair of nitrates, the results are 1.04 for buried shots and 1.01 for air shots.

These figures differ from their averages by less than 2%. This difference is smaller than the standard deviations corresponding to each measurement. In these two instances the CUS does not depend on the mode of shooting.

Comparison of the results given by different charges

a) Buried shots.

In the first example above, the 1.17 ratio was obtained by comparing the results of 50 Kg buried shots. The 1.20 ratio corresponds to 200 Kg shots. The difference between these two factors is 13% whereas the standard deviation in each series of measurements range from 11% to 15%. It can be assumed that the ratios between the seismic efficiencies of these two explosives stay the same when the charge to increased from 50 to 200 Kg.

b) Shots in the air

More data is available concerning shots in air. As an example the following table shows the ratios of the seismic efficiencies of two explosives, for different magnitudes of charge, shot at 0.5 meters above the ground:

for 12.5 Kg	1.16
- 25 Kg	1.06
- 75 Kg	1.15
- 150 Kg	1.08

The maximum deviation from the average is smaller than 5% whereas the standard deviations on each set of measurements range from 2 to 3 %. But the accuracy of a ratio should be expected to be smaller than that of each term.

In every case, it was found that the relative seismic efficiency of two explosives could be assumed to stay the same whatever the charge used and even when the elastic limit of the ground was exceeded.

Comparison of the Results obtained in Algeria and in France

A comparison between the determinations made in Algeria and in France can be established on very few results only.

First by the composition of the nitrates are generally different in both countries due to legal specifications.

Second by the test made in Ageria was intended to make a selection among the nitrates used for refraction in the Sahara where the use of gelatines is prohibited by the hot climate. In France, on the contrary, the test was made mostly with gelatines.

Finally, two explosives only are common to the two series of experiments: the "gomme BAM" and the nitrate NIC. The nitrates N 17 of Algeria and N 30 of France have the same composition, but the N 30 is better mixed and this would account for their different denominations.

If the figures are reduced to the efficiency of the "gomme BAM" taken as unity, we find for the NIC the CUS is .79 in France and .77 in Algeria, for the N 30 the CUS is 1.0 in France and for the N 17 .9 in Algeria. There is no doubt that the proportionality between the seismic efficiencies of the NIC and of the "gomme BAM" is the same in Algeria and in France.

As for the N 30 or N 17 the 10% discrepancy is too big to be caused by the lack of accuracy. But it may be accounted for by the difference in manufacture.

CONCLUSIONS ABOUT THE "CUS"

The number of experiments is too small for a final decision. However, they all tend to show that the "coefficient of seismic efficiency" does not depend on the size of the charge, nor on the experimental conditions: it depends on the type of explosive only, and it is possible to speak of a "coefficient of seismic efficiency" just as well as of a "coefficient of strength". Using this "CUS", the seismologist may select one among all the explosives he can use and give definite and numerical reasons for his choice.

Example of Application to Refraction in the Sahara

The cost of explosives is an important part (up to 30%) of the total cost of a refraction crew in the Sahara. Because of this CFPA and SNREPAL asked CGG to carry out investigations on the type of explosive which would prove to be the cheapest to use.

A number of results and conclusions of this investigation has already been set forth, so we will limit ourselves to the comparisons between shots of 12.5 Kg fired 2 m high in the air.

Figure 8 shows how the different explosives can be classified according to their seismic efficiency. The dash represents the average deflection and the shadow zone is the limit within which the true value has 2 chances out of 3 of being located.

Firstly, it can be seen that the results are very close to each other, and more accurate measurements would be advisable.

Secondly the cost of the explosive necessary to get a given energy arrival

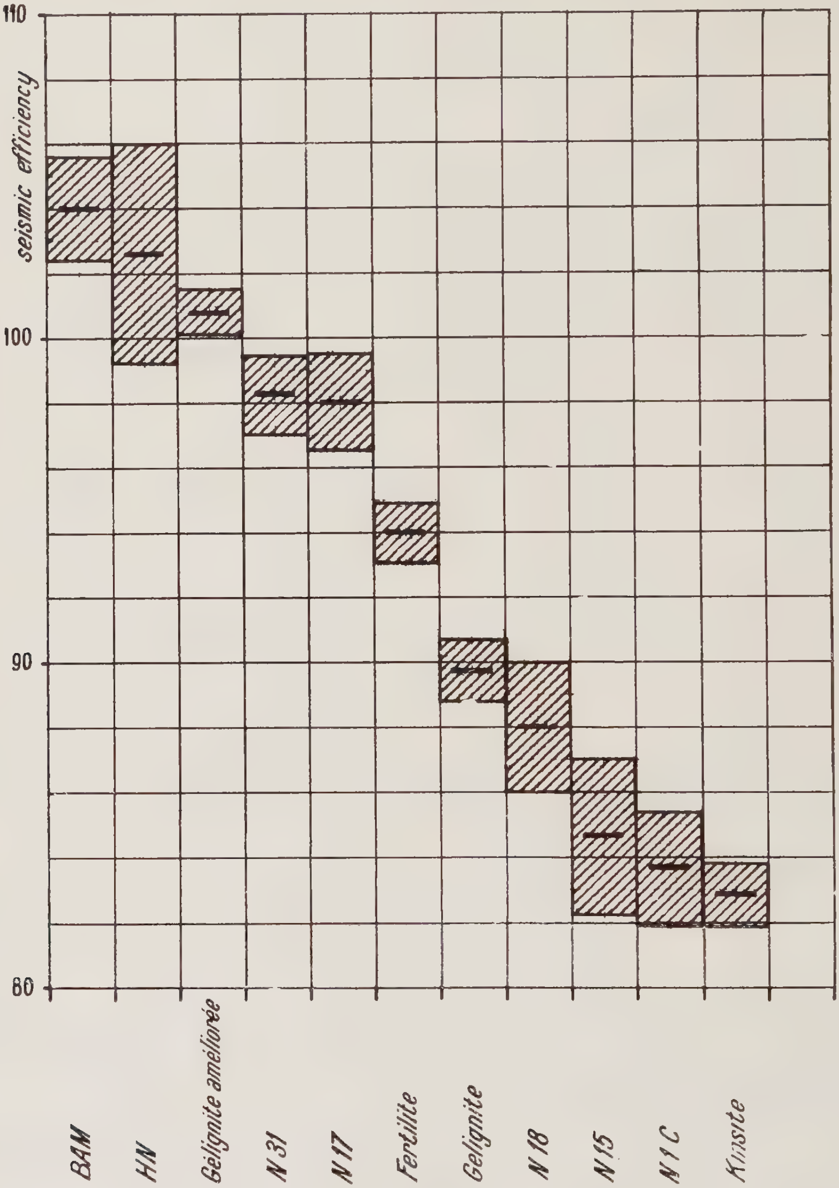

Fig. 8. Comparison of explosives by air shooting. 12.5 kg charges suspended 2 m

was computed. It was based on 100 for the N 15, the explosive normally used at that time by the refraction parties. These costs are plotted in fig. 9.

The selection which had been made of the N 15 was obviously satisfactory.

Even if the temperature conditions allowed the use of gelatines, it would be inadvisable to do so because of their high cost. To come back to what was said earlier, this is an example in which the higher strength coefficient derived from laboratory tests does not pay.

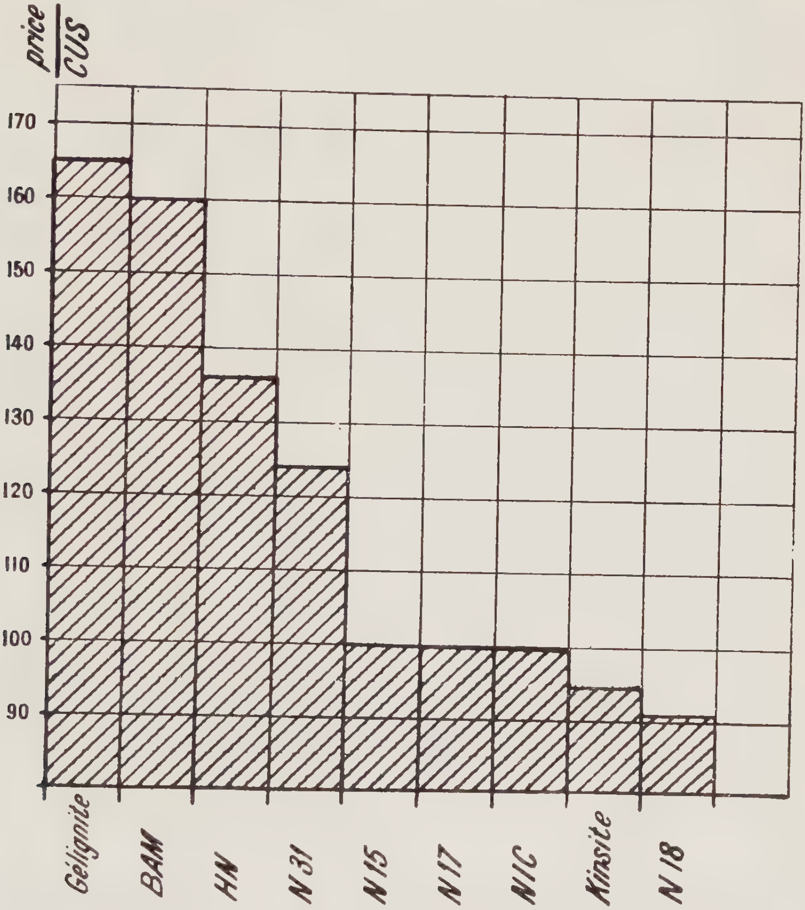

Fig. 9. Cost of the different explosives for the same seismic efficiency.

The N 18 is a composition developed during the experiments. Later it was brought on the market and was available for use by the refraction crews, resulting in an appreciable economy.

RELATION BETWEEN CUP AND CUS

It is not evident that the cost per unit of CUP could not be considered as well. On fig. 10 the measured deflections have been plotted against the CUP.

The correlation between CUP and CUS is very good and suggests a relationship, though it is possible that parameters other than the strength are involved in the determination of the seismic effects. This would account for the scattering of the experimental results around an average straight line, and for the abnormal positions of the points corresponding to the chlorate and the "Hexolite Nitraté".

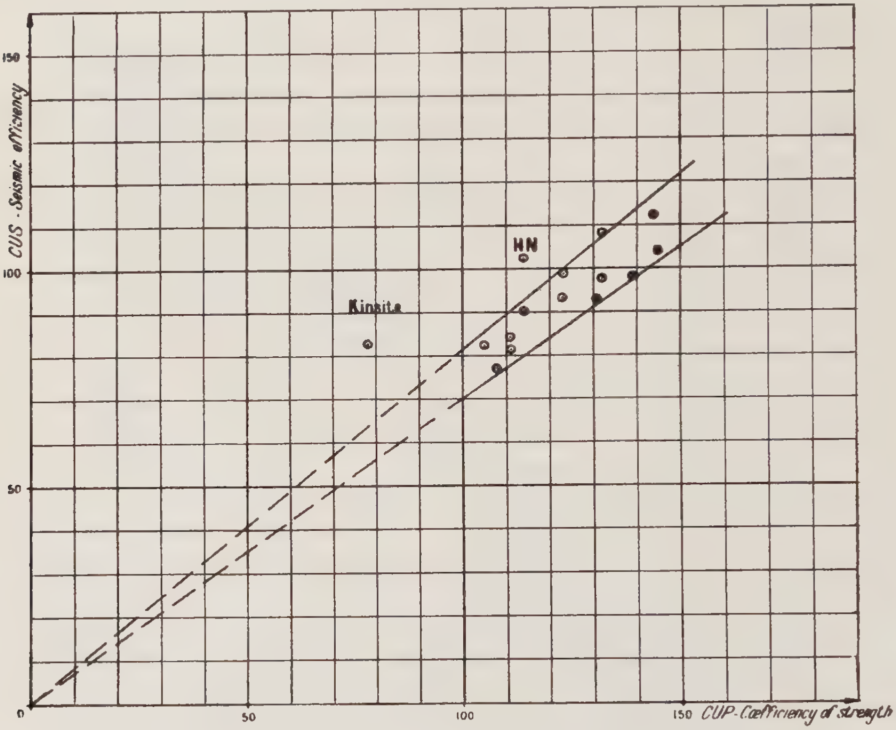

Fig. 10. Relation between the strength and the seismic efficiency.

No physical law can be derived from these few experiments. More points must be added to the diagram before trying to formulate a relationship between the coordinates, and before being able to show the influence of other specific parameters of the explosives.

CONCLUSIONS

The choice of an explosive may have an influence on the quality of the seismic records, particularly in reflection work. In most cases, the consideration of the amount of energy picked up by the equipment is of the utmost importance. A 10% economy means a lot of money for an oil company using several crews all the year round. Thus, it is highly economical to select the explosive which has the best seismic efficiency.

The experiments related here suggest that the concept of CUS, as defined here, depends on the explosive only and not on the size of the charge and on the conditions of uze. More experiments are necessary to establish this fact.

It is possible that the seismic efficiency can be derived from laboratory tests. So far, we have not accumulated enough data to show which of the physical properties of the explosive have an influence on the seismic efficiency or to develop a mathematical formula from which the CUS could be derived.

More investigations should be made on explosions and the transmission of seismic waves. A large number of experimental observations have to be statistically analysed before relations will appear and theories built up. In short, the problem of spending less money on explosives requires a logical treatment.

It is too early to apply the present results without precautions for they are based on relatively few measurements. But we hope we have shown how experiments on the seismic utilisation of explosives can be conducted. We have pointed out the difficulties and our aim will be realised if other experimentors can avoid a good deal of groping about. All along our investigations, problems arose and it is obvious that extensive research work lies ahead. We would like oil companies to become aware of the possible economies, and we are certain of the great utility of a serious investigation on explosives and the different ways to use them for seismic purposes.

Compositions and characteristics of the explosives experimented upon

Denomination	Chemical constituents %		Strength (CUP)	Velocity of detonation m/s	Brisance mm	Density
BAM	Nitroglycerine Nitrocotton Sodium nitrate Cellulose	60 3 3 6	145	2,000 or 7,000	13	1.5
Sofranex	Nitroglycerine Nitrocotten Ammonium nitrate Aluminium Dinitrotoluene	40 2 48 8 2	145	4,000	15	1.45
Tolamite	Nytroglycerine Nitrocotton Dinitrotoluene Ammonium nitrate Cellulose	27 1 9.5 61 1.5	131	3,000	11	1.45

Denomination	Chemical constituents %		Strength (CUP)	Velocity of detonation m/s	Brisance m/m	Density
Dynalite	Nitroglycérine Nitrocotton Dinitrotoluence Ammonium Nitrate Cellulose Aluminium	12 0.5 5 74.5 2 6	123	2,800	16	1.1
Gelignite D	Nitroglycerine Nitrocotton Sodium Nitrate Cellulose	57 3 27 13	114	2,800 to 4,400		
Gélignite améliorée	Same as Gelinite D plus some Barium sulphate		?	?	?	?
Hexolite nitraté or HN	Hexogen (or Penthrite) TNT Ammonium Nitrate	30 45 25	114	7,000	?	1.65
N 31	Pentolite Ammonium Nitrate Aluminium	12.3 78.5 9.2	138	4.200	12	1.1
N 17	TNT Ammonium nitrate Aluminium	11 80 9	132	3,400	?	?
N 18	TNT Ammonium nitrate Celluslose	12 82 6	110 ?	2,800 ?	?	?
N 15	TNT or DNT Ammonium Nitrate Cellulose	14 84 2	111	2,900	?	?
N 30	TNT Ammonium nitrate Alluminium	10.6 80.2 9.2	132	4,200	13	1
N 1 C	Dinitronaphtalene Ammonium nitrate	12.6 87.4	111	4,200	11	1
Kinsite	Chlorate ?	?	78	2,700	?	?
Fertilite	Recuperation of army explosives. For agricultural use only.		?	?	?	?

THE RELATION BETWEEN SIZE OF CHARGE AND AMPLITUDE OF REFRACTED WAVE *

BY

T. F. GASKELL **

ABSTRACT

Experiments carried out using charges of up to 200 lbs. at a distance of about 20,000 ft. from the geophones suggest that the amplitude of the refracted wave ground motion is roughly proportional to the weight of charge. Simple energy considerations lead one to expect a relation of a form in which velocity amplitude is proportional to $\sqrt{W}$.

An explanation of the observed relation may be based on a theory according to which the efficiency of the explosion increases with the source size, that is the distance from the source at which the pressure wave of the explosion ceases to cause permanent deformation of the surrounding medium.

The above theory was further confirmed by measurements of the radius of the cavity produced by explosions of charges of different size in clay. Also, explosion of charges in artificial water-filled cavities were found to give seismic wave amplitudes three or four times greater than those produced by the same charge in a narrow hole. It is possible that these observations explain in part why the charges required in marine refraction experiments are very much smaller than those needed in refraction work on land, but additional reasons for this difference are also discussed.

INTRODUCTION

Experiments have been made to determine the way in which shot size in seismic experiments affects the amplitude of refracted wave arrivals. The experiments were a preliminary to the study of use of amplitudes in refraction work. There is some possibility (Perkins 1952) that the decay of amplitude with distance may be consistently different for crystalline and sedimentary rocks, and in order to investigate refraction records it is desirable to know to what extent records from different shots can be compared. The first fact required is the relation between amplitude of refracted wave and charge size for similar shots. Information is also needed about the part played by the rock medium, shot depth and any other factors that make one shot different from another.

The conclusions drawn are that it is much better to rely on overlapping records than to assess efficiences of different shots, but that shots fired in similar conditions are repeatable to about ± 10%, and that refracted wave amplitude is roughly proportional to weight of charge. The experiments were

---

*) Presented at the Ninth Meeting of the European Association of Exploration Geophysicists, held in London, 7-9 December 1955.

**) The British Petroleum Co. L.td

useful in another respect, for although they could well be extended, they do suggest a useful working mechanism of seismic wave production which enables forecasts to be made of the effects of different shot point conditions.

The word amplitude is used in this report for the size of the first peak above zero line in a refraction record taken with a velocity instrument—that is, as the maximum velocity of the refracted wave pulse as normally measured.

AMPLITUDE/CHARGE WEIGHT RESULTS

Fig. 1 shows a plot of amplitude ratio to charge weight ratio for a series of repeat shots made in the course of refraction experiments in England. The ratios rather than actual charges and amplitudes have been used to remove as far as possible the scatter caused by changes in sensitivity of pick-ups and amplifiers. The scatter of the observations is still enormous, but the average amplitude values follow a direct proportionality between amplitude and charge more closely than for example an amplitude/square root charge relation. It was clear that controlled experiments rather than results from old records were needed and measurements of refracted waves at a distance of about 18,000 ft. were made for a series of charges from 20 to 200 lbs. The charges were all fired in Bunter Sandstone at depths of 120 ft. in holes within a few hundred feet of each other. The amplitudes of a conspicuous 2nd arrival wave as well as of the main first arrival refracted wave were measured in order to obtain a good reading for the 20 lb. charge. The results are shown in Table 1.

TABLE 1

Shots in Bunter Sandstone at 120 feet depth

Charge Weight	Amplitude of 1st Arrival	$\frac{\text{Amplitude}}{\text{Charge}}$	Amplitude of 2nd Arrival	$\frac{\text{Amplitude}}{\text{Charge}}$
200 lb.	252×10^{-6} cm/sec.	1.26	3840×10^{-6} cm/sec	19.2
100 ,,	114 ,, ,,	1.14	1420 ,, ,,	16.2
50 ,,	58 ,, ,,	1.16	630 ,, ,,	12.6
20 ,,			282 ,, ,,	14.1
		Mean 1.18		Mean 15.0

The ratio of amplitude to charge weight is nearly constant. Energy considerations would at first sight lead to a law of the form amplitude proportional to square root of charge weight, because energy is proportional both to square of ground velocity and to weight of explosive. The tendency of the results is in the direction of proportionality of amplitude to a power of W a little higher than one, rather than to $W^{\frac{1}{2}}$.

The result that amplitude is directly proportional to weight of charge implies that larger charges are more efficient than small ones in making the

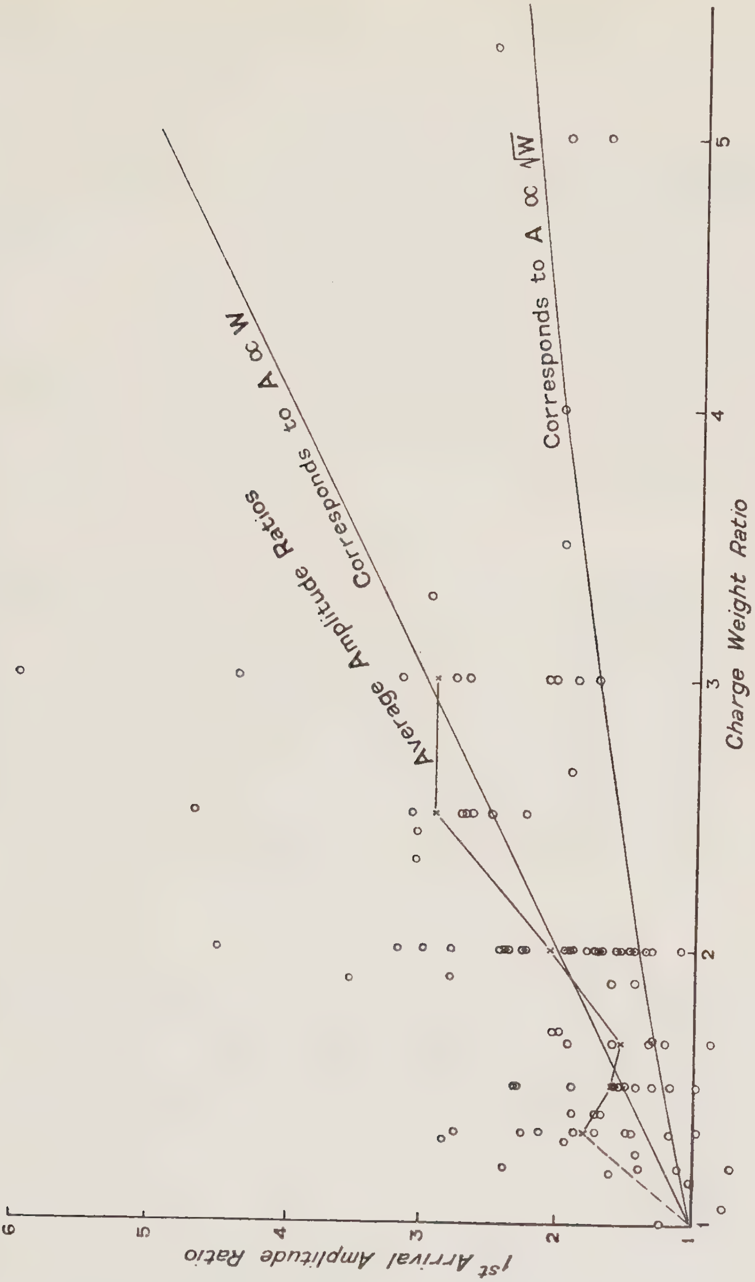
1st Arrival Amplitude Ratio
1
2
3
4
5
6
Charge Weight Ratio
1
2
3
4
5
Average Amplitude Ratios
Corresponds to A ∝ W
Corresponds to A ∝ √W

Fig. 1

seismic waves that are recorded at long distances. A possible reason for this may be found if the explosion is thought of as a radiator of energy. The wavelengths of refracted waves used in prospecting are normally of the order of hundreds of feet. The size of the explosive sources is very small compared with this wave length, and so the radiation efficiency will be nearly proportional to source size (Morse 1948). The source size will be determined by the distance from the centre of the explosion at which the pressure wave from the explosion ceases to cause permanent deformation of the medium surrounding the explosion, and this will vary as the linear dimensions of the explosive charge, that is as the cube root of the charge weight. For low frequency seismic waves, then, the amplitude will be proportional to the product of $W^{\frac{1}{2}}$ and $W^{\frac{1}{3}}$, that is to the five-sixth power of the charge weight. This is more nearly in agreement with the observed facts than is the simple root relation. When the source size approaches the wave length, that is for high frequency waves, the radiation efficiency will approach a constant value and the $W^{\frac{1}{2}}$ law should apply.

Source Size

Some measurements on the size of source were attempted, by firing a series of small ($\frac{1}{2}$ to 60 grams.) charges in clay, and subsequently digging out the cavities produced. The radius of the cavity was given by r (feet) = $W^{\frac{1}{3}}$ (W in lbs.), so that the expected cube root law was checked, and the small size of source was confirmed. The source cannot be much larger than the cavity because the clay was not permanently deformed at small distances outside the cavity walls. There must, of course, be some deformation outside the cavity in order to take up the material that was previously in cavity, but a small percentage increase of cavity size is adequate to look after this.

Tests with charges fired in large holes

If the efficiency of the source does depend on its size it should be possible to produce waves of increased amplitude by making an artificial source larger than the cavity that the charge makes for itself. There should be a limit to the increase of amplitude that is possible, because the diminution of the pressure wave spreading out from the explosion must eventually reduce the pressure below the elastic limit of the clay; after this, the inverse square spread (except for minor attenuations due to imperfect elasticity, scattering etc). will continue in the clay medium.

A series of small charges were fired in water filled holes of 1, 5, 8 and 14 inch diameter, and amplitudes of first arrivals were recorded with a flat response (1-100 cps.) velocity instrument at a distance of a few hundred feet The results are shown in Figure 2, and they are in agreement with the explo-

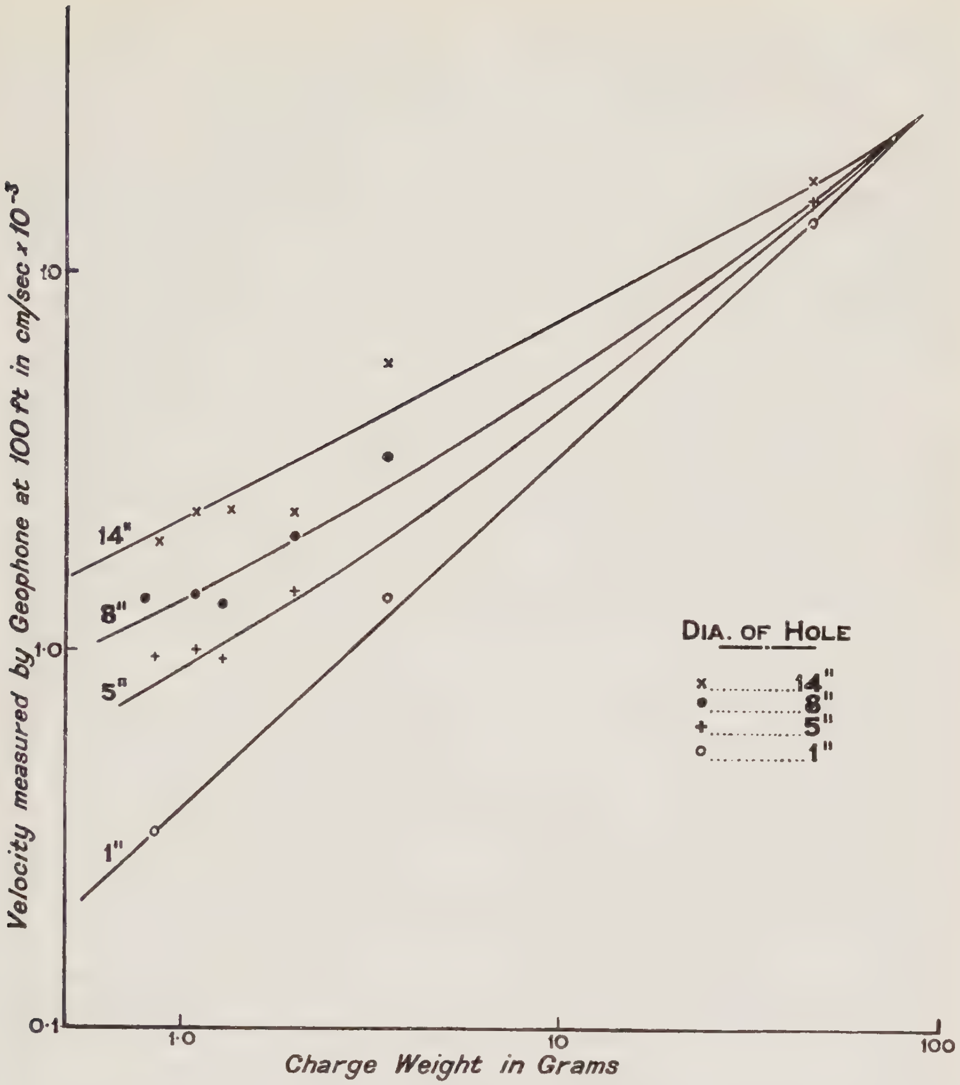

Fig. 2. Velocity of First Arrival Wave measured by Willmore Geophone at 100 ft. from Shot for different Charge Weights in Holes of Various Sizes.

sion mechanism given above. The observations are accurate only to about ± 20%, but are sufficient to show some general trends. At the small charge end of the diagram there is a linear increase of amplitude with size of hole. The cavity size for a one gram charge is about 4.5.inches diameter, and the progessive increase in amplitued for the 5, 8 and 14 inch holes follows the increase of the source size. If the only factor controlling amplitude is source size, then the amplitude would be expected to be the same for all holes less than 4.5 inches (for a 1 gm charge) in diameter because the source size would be the same, and equal to the cavity size, in each case. The 1 inch hole result is thus lower than expected and it must be that the theory outlined above is too simplified in that there is some effect of hole size on amplitude for hole size less than cavity size. However, the results at the big charge end show that the amplitudes are almost the same for 45 gram charge and will probably converge at a shot size of about 70 grams. For 70 grams the cavity size is 17.6 inches and therefore all the holes used in this case were smaller than the cavity.

The slopes of the lines of amplitude against charge weight for the different sized holes vary from the equivalent of amplitude proportional to $W^{0.9}$ for the 1 inch hole to $W^{0.6}$ for the 14 inch hole. This again is what is expected, on the one hand for hole smaller than cavity, and hence source size controlled by the charge itself, and on the other, for hole greater than cavity, and source size artificially constructed to be constant. It appears that the limit of increase of amplitude with hole size has not been reached in the result of Fig. 2. Either larger holes or smaller charges are needed. However, the fact that the 14 inch hole gives a slope corresponding to $W^{0.6}$ suggests that the limit is approaching, because $W^{0.5}$ should be obtained with a slightly larger hole for the range of charges used.

The gain in amplitude that can be achieved by exploding a charge in a water filled cavity appears to be nearly six to one in the region of 1 gram, but if the theoretical reasoning is correct there should not be much change between 1 inch and 5 inch holes because the cavity for a 1 gram charge is 4.5 inches diameter. It is probable that some further increase of amplitude would have occurred up to a 17½ inch hole, and the ratio of this source size to the cavity size of 4½ inches, that is about 4 to 1 is a more reasonable figure to claim for maximum gain of amplitude by using an artificial cavity. Beyond 17½ inches the amplitude of the pressure wave spreading out in water will fall below the elastic limit of clay and the source size will no longer be determined by the diameter of the water-clay boundary.

PRACTICAL CONSIDERATIONS

In order to make use of this 4 to 1 increase of amplitude in practice, large holes are needed, because the artificial hole must be of diameter four times that of the cavity, or for clay approximately 8W where the diameter is in feet and the charge weight (W) is in pounds. For a 100 lb. charge the hole will be 39 feet in diameter. It is no great advantage to use a preliminary shot to make a cavity for a subsequent one; for a charge of about three tons would be necessary to make a 39 ft. diameter hole. This explains the poor improvement in amplitude observed when shots are repeated in the same hole. An examination of 50 repeats from old records gave a mean ratio 1 to 1, with some considerable scatter. Three careful repeats made during the present series of experiments after cleaning out the shot hole by flushing with mud, gave values 1.08, 1.11 and 1.16 with a mean of 1.12. This increase is probably because at the second attempt the charge can enlarge the cavity slightly and therefore have an increased source size. The supposition that source size is completely independent of hole size for holes smaller than the cavity is obviously not quite correct. However, if we regard the process of reducing the pressure wave from the explosion to a value below the elastic limit of clay as one in which energy is dissipated in a volume of clay, we find that the repeat shot need only extend the destruction radius of the cavity by about 25% to embrace a volume as large as that of the original cavity.

Before doing these experiments we had hopes of making use of the expected amplitude proportional to $W^{\frac{1}{2}}$ law to economise on explosive, for if this law held it was clearly better to use several small charges instead of the same weight of charge in one unit. However, since the amplitude is proportional directly to weight of charge there is nothing to gain by such a method. In order to increase the effective size of source the holes must be placed close together so that the separate cavities join into each other. Furthermore, the separate charges must cover an area not a line to achieve this effect, and calculation shows that only a small advantage can be expected. It may be worthwhile using multiple shots to produce interference effects between various waves sent out by separate sources, but this is a different matter altogether.

COMPARISON OF LAND AND SEA SHOTS

It is possible that these observations explain in part why good refracted waves are recorded at distances of 50-80 miles during sea seismic experiments, when charges of the order of hundreds of pounds only are used, whereas thousands of pounds of explosive are needed on land to give refracted waves at about 60,000 ft. The experiments described above suggest a factor of improvement of 4 to 1 for water over clay, and other results demonstrate that clay is the best medium, sometimes by a factor of 3 or 4, of the rocks in which shots are fired in land seismic experiments. Many land shots, furthermore are fired in shallow holes, such that a crater is produced, and these may be expected to lose a proportion of their seismic wave producing efficiency, because the full source size needed for radiation of energy cannot be developed. In this respect, shots fired for blasting will have their source size controlled by the shortest path to a free surface, and not by the size of charge, so that a relation of the form amplitude proportional to $W^{\frac{1}{2}}$ will probably apply.

It can be argued that the solid basalt refractors beneath the deep oceans are better propagators of seismic waves than the usual limestone targets on land. The laboratory measurements of Hughes and Cross (1951) suggest that while crystalline rocks show an increase of velocity with depth, and hence a tendency to behaviour as a good refractor, some limestones and sandstones have the opposite properties; sedimentary rocks are often distributed in thin layers and this makes for poor propagation, and the general irregularity of the sedimentary formations will be expected to produce a great deal of loss of refracted wave energy by back reflection. The reported values of the attenuation that is dependent on wave length and is due to elastic imperfections of rocks is of the order of 0.05 db. per wave length for granite and about ten times this value for limestone (Bradfield 1947) (Nat. Coal Board), so that even on this count crystalline rocks should be better refractors than sedimentary ones. The fact that the amplitude attenuations for refracted waves in limestone are often much greater than 0.5 db. per wave length indicates however, that this last form of energy loss is not normally the main one. It is of interest in that it is probably the important factor controlling the change of frequency with distance. This change has been found to correspond to a much smaller attenuation than is given by the amplitude measurements, and it is probable that change of frequency with distance will provide a better means of distinguishing different rock types than changes in amplitude, because the amplitude is strongly affected by inhomogeneities in the rock. On the other hand, measurements of frequency of refracted wave arrivals must be treated with some reserve, because of the imposition of frequency character by waves multiply reflected.

These ideas and experiments are incomplete, but they were sufficient to provide some working rules in the amplitude investigations. I should like to express my thanks to Dr. G. Morris of I. C. I. Explosive research department and to Dr. G. Bradfield of the National Physical Laboratory, whose suggestions and previous work led to the source size concept, and to Mr. G. Pickering who ably assisted with the measurements.

This paper is published with the kind permission of the Chairman and Directors of The British Petroleum Company Limited to whom my thanks are most respectfully given.

DISCUSSION

MR. WRIGHT: Although one cannot disagree with the author's experimental results, there appear to be serious flaws in his theoretical explanations. For instance, it is just not true to expect that the amplitude (i.e. peak particle velocity in the author's notation) of the generated waves should vary as $W^{\frac{1}{2}}$ since the frequency also varies with charge size. Again, the concept of a source efficiency proportional to $W^{\frac{1}{3}}$ is in error since both source size and wavelength vary as $W^{\frac{1}{3}}$ and therefore the efficiency remains constant.

MR. GASKELL: I am afraid that I had assumed the frequency of the refracted wave pulses to be constant in my argument. At the distances we measure refracted waves in seismic prospecting, the high frequency components sent out by the source are removed by attenuation and scattering, and the refracted waves appear (on a velocity instrument) as a single cycle with a main frequency (if it can be said to have a frequency) of 5-25 c.p.s. If the frequency of the refracted wave pulse is dependent on source size (and therefore proportional to $\frac{1}{W^{\frac{1}{3}}}$) we should expect the peak velocity of the refracted wave to be proportional to $W^{\frac{1}{3}}$, which is far from the observed relation.

REFERENCES

BRADFIELD, G. 1947, 'Sonic Propagation and Ranging in Rock-like materials', T. R. E. Memorandum 2/M120/GB.

HUGHES, D. S. and CROSS, J. H. 1951, 'Elastic Wave Velocities in rocks at High Pressures and Temperatures', Geophysics 16, 577.

MORRIS, G. 1950, 'Some Considerations of the Mechanism of the Generation of Seismic Waves by Explosives', Geophysics 15, 61.

MORSE, P. M. 1948, "Vibration and Sound'. p. 243, Publ. McGraw-Hill, 2nd edition.

NAT. COAL BOARD, C.R.E. No. 88. 'An Appreciation of the Possibilities of Applying Sonic Energy to Problems of Exploration in Mines'.

PERKINS, B. 1952, Letter to the Editor, Geophysics, 17, 411.

GEOELECTRIC EXPLORATION OF INCLINED THIN BEDS AND ORE VEINS *

BY

F. ŠUMI **

ABSTRACTS

The equation for the deformation of the homogeneous electrical field caused by a long inclined thin plate, is given. By means of this equation a diagram is designed for the direct depth determination of the upper and the lower edge and for the inclination of the plate. The equation and the diagram are proved by small scale model measurements and applied in field exploration.

Introduction

In mining geophysics it is often necessary to determine the position of thin ore veins and beds. The choice of the most favourable geophysical method for such investigations depends on the contrast between the physical properties of the beds and of the surrounding media. In ore prospection on the mountainous regions in Yugoslavia, magnetic and electrical methods are frequently applied, and more rarely the gravimetrical method is used. Among the electrical methods the best results have been obtained by the self-potential, the potential-drop-ratio and the various electromagnetic methods.

When the position of the ore vein or deposit is known, the problem arises of the determination of the depth to the upper and the lower edges of the vein, together with its inclination. This can be determined by measuring the deformation of a homogeneous electrical field applied in a direction perpendicular to the strike of the bed.

Theoretical part

The theory of the method is based on the equation of the deformation of the electrical potential in a homogeneous electrical current in the earth, caused by the presence of an infinitely long horizontal cylinder of small circular cross section and whose resistivity differs from that of the surrounding medium. The deformation of the potential caused by the cylinder is

---

*) Presented at the Ninth Meeting of the European Association of Exploration Geophysicists, held in London, 7-9 December 1955.

**) Geological and Geophysical Research Institute, Beograd.

$$\varphi - \varphi_o = i_0 \rho_o \frac{\rho_0 - \rho}{\rho_0 + \rho} R^2 \left\{ (x/r^2) + (x/r'^2) \right\} \quad . \; . \; . \; . \; . \; . \quad (1)$$

where $\varphi - \varphi_0$ is the deformation of the potential, i_0 the current density, ρ and ρ_0 the resistivities of the cylinder and the surrounding medium respectively, R the radius of the cylinder, r the distance from the point of observation to the axis of the cylinder, and r' the distance to the axis of the image of the cylinder in the surface plane. For points in the surface plane (Fig. 1), the expression for the deformation of the potential becomes

$$\varphi - \varphi_0 = 2\, i_0\, \rho_0 \frac{\rho_0 - \rho}{\rho_0 + \rho} R^2 . \, (x/r^2) \quad . \; . \; . \; . \; . \; . \; . \; . \; . \quad (2)$$

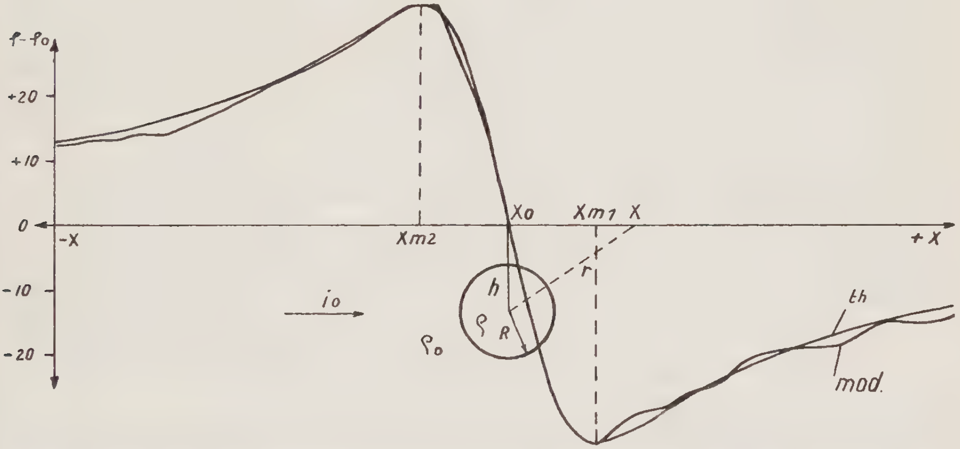

Fig. 1. Calculated and measured curves showing the deformation of the potential over a cylinder in the homogeneous electrical field.

To a cylinder having an infinitesimal cross section of arbitrary shape equation (2) may also be applied, substituting the area of the cross section for πR^2, provided that the assumption of a homogeneous electrical polarisation of the cylinder in a horizontal direction is valid. With this assumption, the deformation of the potential caused by a two dimensional body of arbitrary cross section may be obtained by integrating equation (2) over the cross section. This procedure involves the assumption of homogeneous polarisation in the direction of the original current. This assumption is commonly applied to the analogous problem in the interpretation of magnetic observations, although it is known not to be rigorously valid. The final justification of the application of this assumption in the present case will be obtained from the results of the model experiments described later in this paper.

With the above assumptions, the deformation of the potential over a long and thin inclined sheet can be determined by use of equation (2) and by integrating it throughout the inclined depth, from the upper (h_1) to the lower (h_2) edge of the bed. Thus:

$$\varphi - \varphi_0 = K \int_{h_1}^{h_2} \frac{x - h \cos \alpha}{x^2 - 2\,x\,h \cos \alpha + h^2}\, d\,h \quad . \; . \; . \; . \; . \; . \; . \quad (3)$$

$$\varphi - \varphi_0 = -\,K \left[\frac{\cos \alpha}{2}\, l\,n\,(h^2 - 2\,x\,h \cos \alpha + x^2) - \sin \alpha\, t\,g^{-1} \frac{h - x \cos \alpha}{x \sin \alpha} \right] \Bigg|_{h_1}^{h_2} \quad (4)$$

where K is the constant and depending on (I) the resistivity contrast of the bed and the surrounding media, (II) the thickness of the bed and (III) the current density. The thickness must be small in comparison with the depth (h_1) to the upper edge of the bed. The other quantities are defined in Fig. 2. The negative sign associated with K in equation (4), valid if a bed is of higher conductivity than the surrounding media, becomes positive for a bed of lower conductivity.

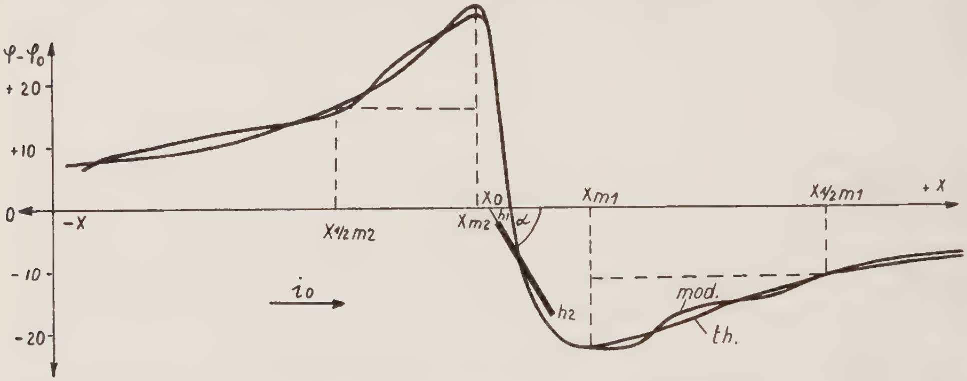

Fig. 2. Calculated and measured curves showing the deformation of the potential over an inclined thin bed in the homogeneous electrical field.

The position of the inclined plate can be defined, when four quantities are known, i.e. h_1, h_2, x_0 and α. For the calculation of these four quantities, four independent observations must be used, such as four characteristic points on the curve of the deformed potential. The most convenient for calculation are the positions x_{m1} and x_{m2} of the maximum and minimum values and the positions $x_{\frac{1}{2}m1}$ and $x_{\frac{1}{2}m2}$ when the function $\varphi - \varphi_0$ has values equal to a half of the extreme values. The positions of the half values remote from the sheet are most useful. The position of the extreme values of the function (4) are given by:

$$x_{m1,2} = \frac{h_1 + h_2}{2} \cos \alpha \pm \sqrt{(\frac{h_1 + h_2}{2} \cos \alpha)^2 - h_1 h_2 \cos 2\alpha} \quad . . (5)$$

Corresponding formulae for the abscissae of the half value points can also be developed.

The position of four characteristic points on the curve depend on the four characteristics of the plate i.e. the depths h_1 and h_2 of the upper and lower edges of the plate, the inclination (α) and the point x_0 where the extension of the plate intersects the surface. Using equations (4) and (5), a diagram of relations between the four known and the four unknown quantities, can be constructed (Fig. 3).

In order to make use of the diagram for arbitrary values h_1, h_2, α and x_0, relative quantities are introduced. Two ratios are calculated from the measured data: (I) the distance between the extremes, divided by the distance between the points of half value i.e. $(x_{m1} - x_{m2})/(x_{\frac{1}{2}m1} - x_{\frac{1}{2}m2})$, and (II) the distance between one extreme and the point of corresponding half value ,divided by the corresponding distance on the other side of x_0, i.e. $(x_{m2} - x_{\frac{1}{2}m2}) / (x_{\frac{1}{2}m1} - x_{m1})$. Relative quanlities h_2 / h_1, $h_1 / (x_{m1} - x_{m2})$, $x_{m1} / (x_{m1} - x_{m2})$ and the inclination α can be determined from the diagram, using the corresponding group of curves for each of these quantities. Since the absolute value of the distance $x_{m1} - x_{m2}$ between both extremes is known, it is possible to calculate the absolute values of h_1, h_2 and x_0. The diagram is constructed for vertical and steep beds. It can be used also for gently inclined beds, but in this case other geoelectrical methods are far better for the quantitative interpretation.

SMALL SCALE MODEL MEASUREMENTS

The equations and the curves were confirmed by measurements on a small scale model in a water tank. A homogeneous field in an electrolyte (water) was created by use of metal plate electrodes covering the two opposite walls of the tank. The model of the bed was either of metal ($\rho < \rho_0$), or of a plastic material ($\rho > \rho_0$). A long a traverse over the plate, the potential (φ) referred to a fixed point was measured. The potential (φ_0) measured in absence of the model was subtracted.

Equation (2) was tested by measurements over a cylinder of a radius $R =$ 3,5 cm at various depths h. In Fig. 1. the theoretical (th) and the measured (mod) curves at a depth of 5,5 cm are shown. Similar agreement between the curves was also obtained for deeper cylinders.

The model representing the inclined bed was made of a plate one milimetre thick. The relation h_2/h_1 varied from 3 to 20, and the inclination α from 90° to 30°. In Fig. 2. the theoretical (th) and measured (mod) curves for the case in which $h_1 = 1$ cm, $h_2 = 10$ cm and $\alpha = 60°$ are shown for a low conductivity plate.

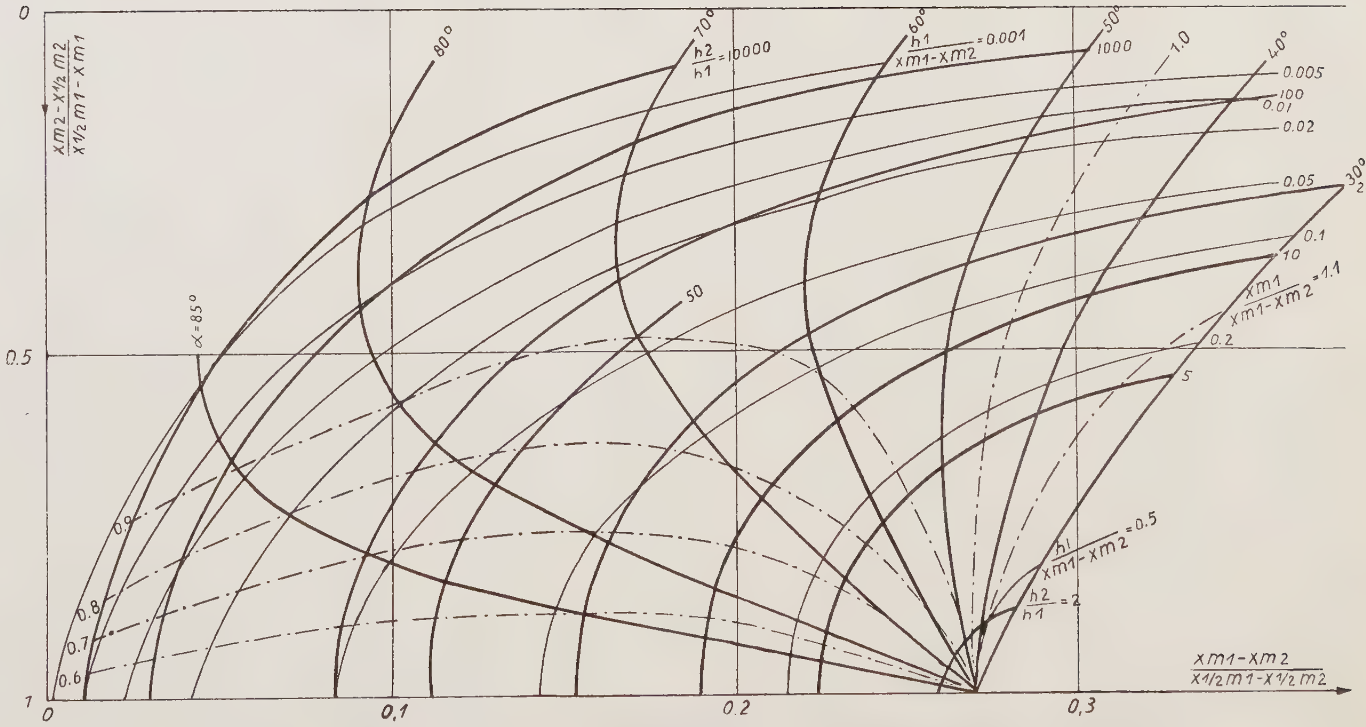

Fig. 3. The diagram for the direct determination of the depth of the upper and the lower edge and the inclination of the plate.

Practical Examples

At Goleš in south Serbia the geophysical exploration was carried out for the location of magnesite beds in serpentine. Serpentine is a relatively good conductor ($\rho_0 = 10.000\ \Omega\text{cm}$) but magnesite, on the other hand, is nearly an insulator.

Geologically it can be assumed that the parallel magnesite beds have a general north-south strike and a steep inclination towards the east. The upper edge of the bed near the surface is covered. The interesting zone is about 10 km long and a few km wide. Here and there the beds are interrupted and dislocated. They vary in depth extent from a few meters to some hundred meters. The geophysical problem consists of locating the beds and, if possible, of determining their inclination and the depth of the lower edge of the bed. The potential-drop-ratio method was chosen as the best one for the field investigation. The mineralized zone was covered with parallel east-west profiles. A section of these measurements is shown in Fig. 4. where two parallel beds have been located.

In order to obtain quantitative data, potential measurements on the electrical field were carried out over the eastern bed. The potential field was created between two point electrodes separated by 500 m with the bed in the centre. The calculated normal undisturbed potential was subtracted from the measured one. The results are shown in Fig. 5. The positions of the extreme value points (x_{m1} and x_{m2}) and the half value points ($x_{\frac{1}{2}m1}$ and $x_{\frac{1}{2}m2}$) were obtained. Using the diagram (Fig. 3.), both the depth to the upper ($h_1 = 0{,}2$ m) and to the lower ($h_2 = 100$ m) edge, the inclination ($\alpha = 65^\circ$) and the position ($x_0 \rightarrow x_{m2}$) of the bed were determined. The calculated position is shown in Fig. 5 as a thick dotted line. In a trench magnesite was found at the point x_{m2} while a bore hole east of the bed revealed, that the magnesite bed has an inclination of 60° towards the east. Taking into account the inclination of the surface, the difference between the geophysically determined and the actual inclination of the bed is 12°. The bore hole also confirmed that the depth extent of the bed is considerable.

The measurements on Golija, a mountain in central Serbia, form an example of geophysical explorations over ore veins of good conductivity. The electrical self-potential method has located some sulphide veins. In Fig. 6 part of the S.P. measurements on this terrain is shown. The trenches dug along the indications revealed a pyrrhotite vein with scheelite, i.e. tungsten ore. Magnetic and potential-drop-ratio methods have also given good results.

The problem of the depth extent and the inclination of the vein has also been solved geophysically. Along a line over the vein the deformation of the homogeneous electrical field was measured (Fig. 7). Resistivity measurements confirmed the homogeneity of the surrounding media. The potential, the

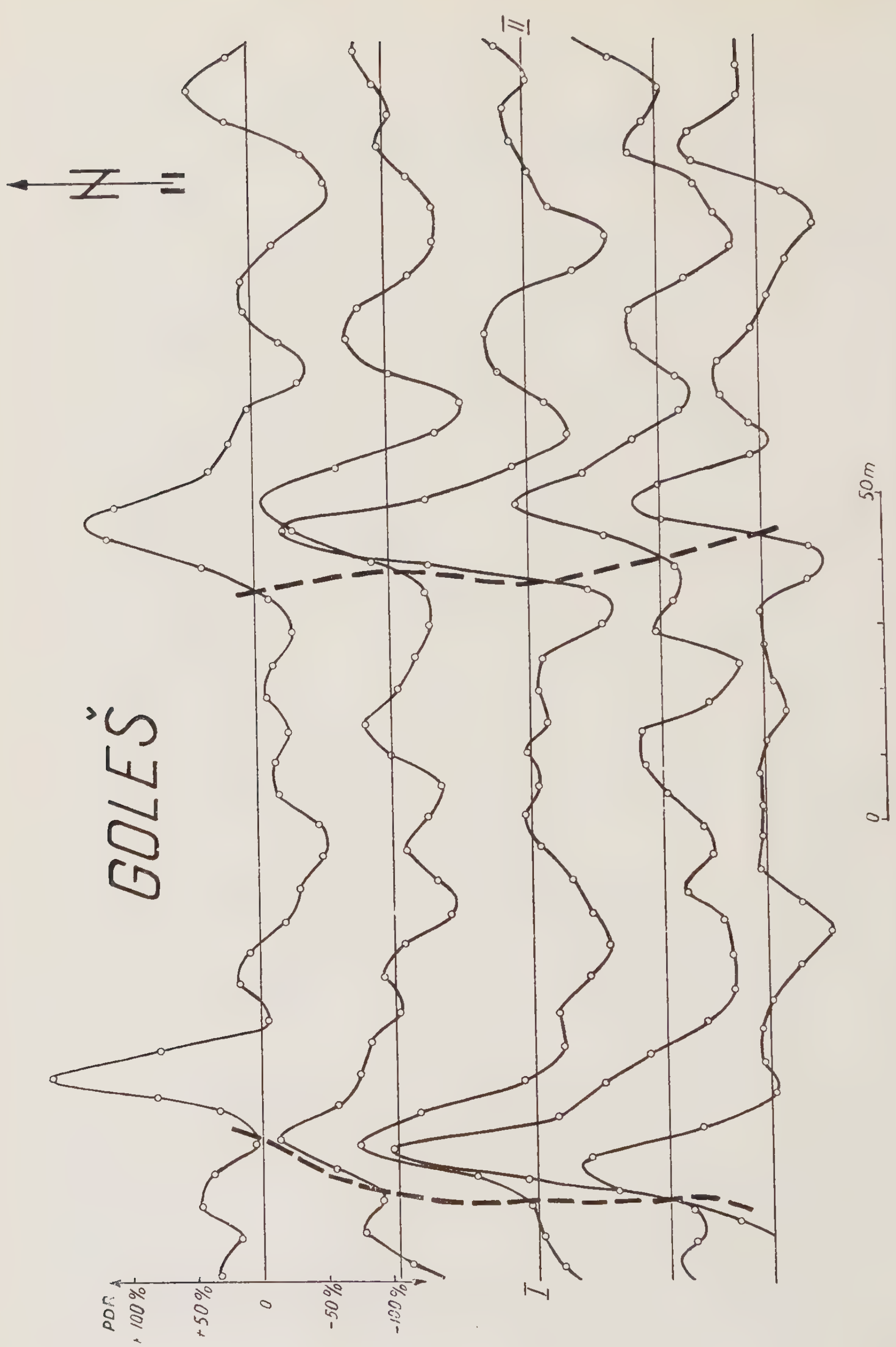

Fig. 4. Potential-drop-ratio measurements over magnesite beds at Goleš.

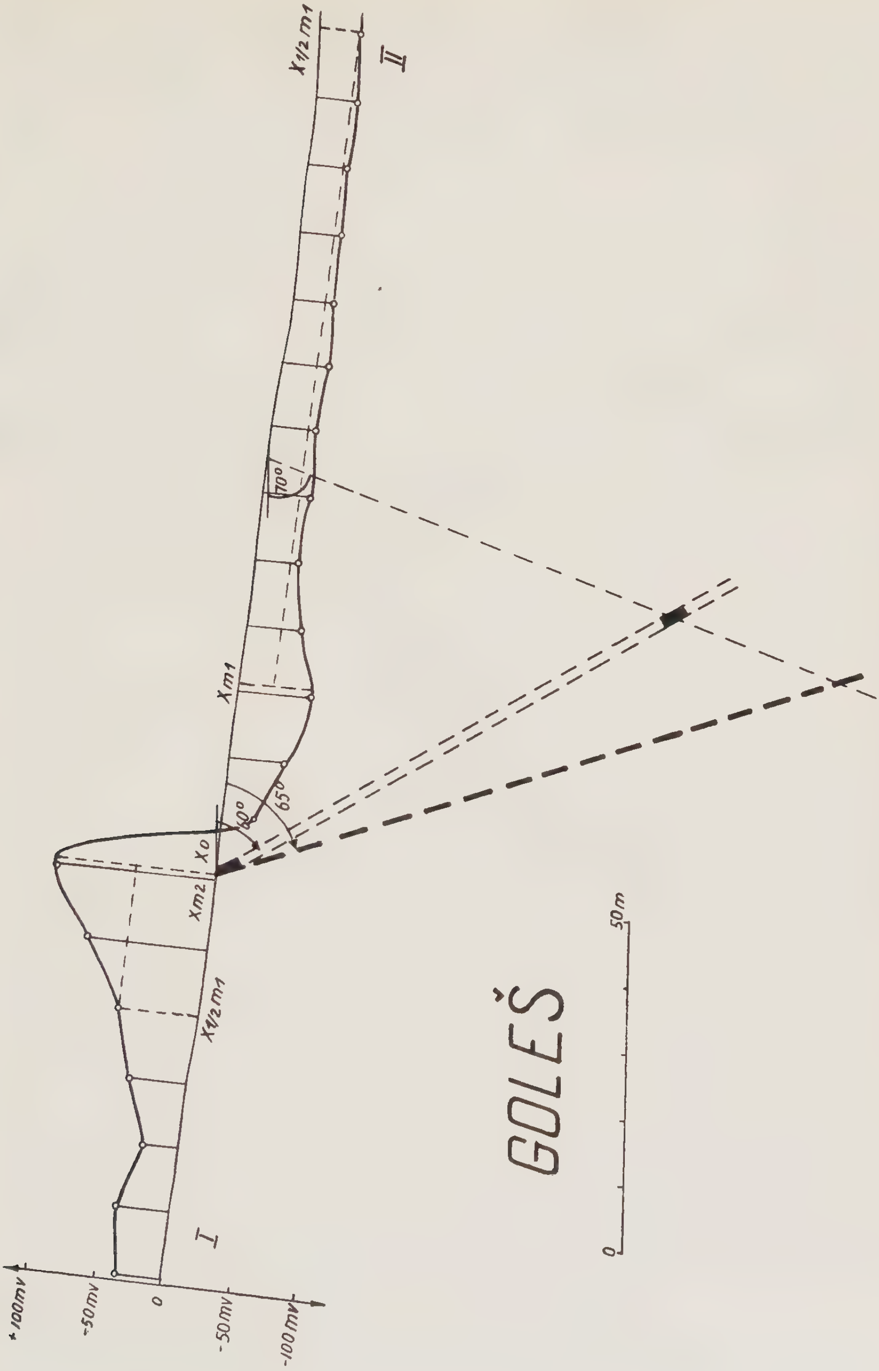

Fig. 5. Potential measurements over a magnesite bed at Goleš.

potential gradient and the potential-drop-ratio have been measured over the vein. All curves are consistent one with another. Using the diagram (Fig. 3), the

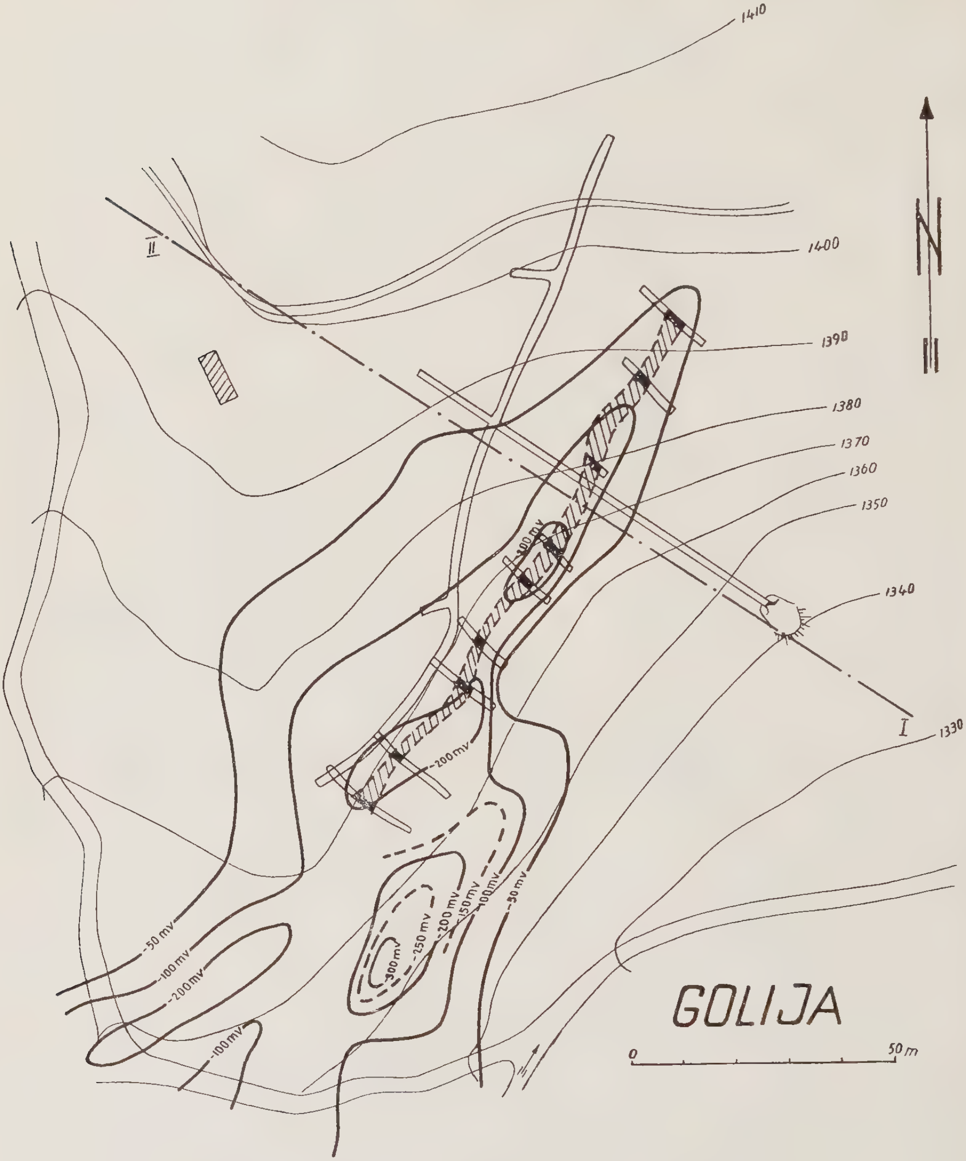

Fig. 6. Geoelectric exploration on Golija Mountain.

position, the inclination and the depth extent of the vein have been determined and the vein determined by geophysics is drawn as a thick dotted line in Fig. 7.

An adit intersected the vein at a point corresponding to the predicated posilicie. At this point the ore vein was only half as thick as at the surface. In the shaft the vein thins out an ceases at 29,5 m. The geophysically and geologically determined inclinations are in good accordance. The actual depth of the lower edge of the vein, however, is greater than that determinded geophysically. This fact can be explained by the thinning out of the vein with the depth, since the theoretical equation is only valid for a constant thickness of the vein.

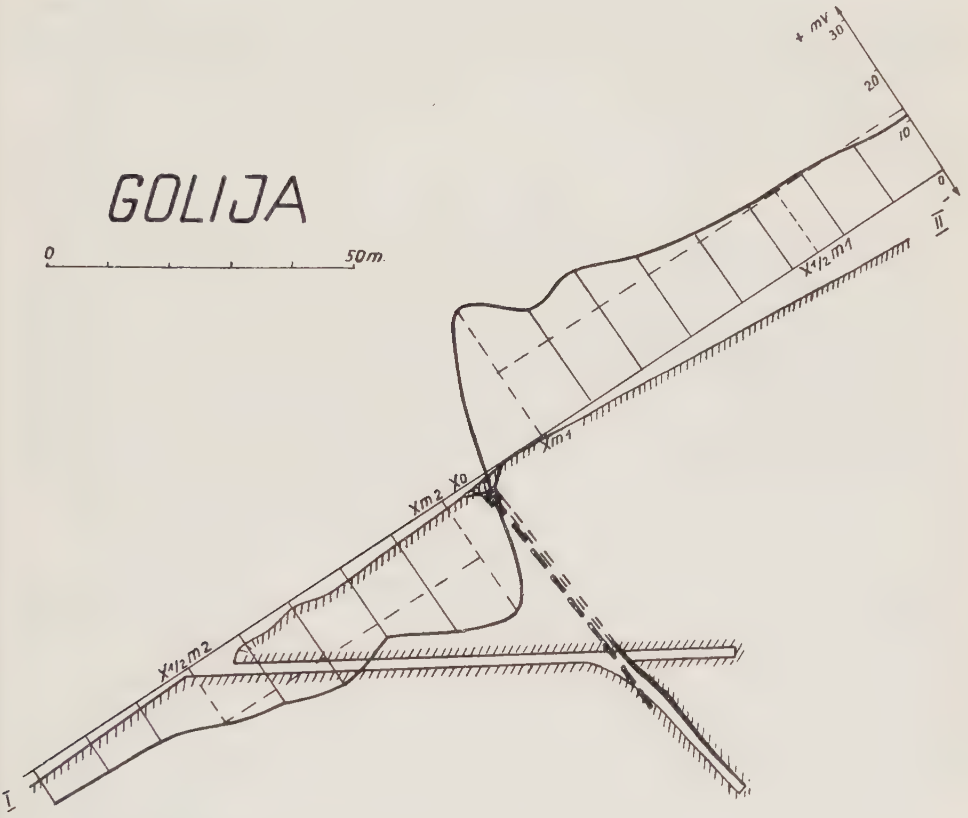

Fig. 7. Potential measurements over the sulphide vein on Golija Mountain.

Geophysical measurements to determine the inclination and the depth extent have been carried out elsewhere, but due to the lack of mining and bore hole data, an evaluation of the results has not yet been possible.

Conclusion

Geophysical determinations of the inclination and the depth extent of beds and veins can be only carried out in favourable geological and physical conditions. The bed must lie in a homogeneous medium, without any other layers. The ground surface may be steep, but the slope must be constant. In the majority of cases, the geophysically determined depth of the lower edge of the bed can only serve as a general guide, but this suffices for mining purposes where the most important factor is whether the mineralisation is superficial or of considerable depth extent.

Literature

Hedstrom, H., 1932, Electrical prospecting for auriferous veins and reefs, Mining Magazine, 46, p. 201-213.

Meisser, O., 1943, Praktische Geophysik, Verlag von Theodor Steinkopff, Dresden und Leipzig.

Šumi, F., 1953, Die Bestimmung des Einfallwinkels der Kontaktfläche, Bulletin du Service géologique et géophysique de la R. P. de Serbie, tome X, p. 277.

Logn, O., 1954, Mapping nearly vertical discontinuities by earth resistivities, Geophysics, 19, p. 739.

Cook, K. L. and Van Nostrand, R. G., 1954, Interpretation of resistivity data over filled sinks, Geophysics, 19, p. 761.

BOOK REVIEW

"Regional Gravity Investigations on the Eastern and Central Commonwealth of Australia", by C. E. Marshall and H. Narain; University of Sidney, Department of Geology and Geophysics, Memoir 1954/2, October 1st, 1954, 101 pp.

This publication gives the results of a reconnaissance gravimeter survey of the Eastern part of the Australian Continent, roughly between Alice Springs and the East Coast. The survey was executed with a Worden gravimeter which is very suitable for work of this nature.

Part A gives a description of the survey, the instrument, the reductions of the data and a good general discussion of "Bouguer anomalies and their interpretation".

Part B discusses the residual gravity anomalies on the various traverses. The residual anomaly is here defined as the difference between the observed curve and the regional curve drawn through the *minimum* values of the observed anomalies. The residual anomaly curve is then compared with the geological section. No quantitative studies could be made because no figures were available on rock densities. The authors express their feelings about this subject rather strongly: "investigation of rock densities and their variation is a field of study which is lamentably neglected by geologists. It would be a of great help if their attention could be directed to the importance of physical quantities which they could conveniently determine, together with the other physical characteristics of the various rocks which they study in field and laboratory investigations".

Part C discusses the regional curves and their relation to the crustal and tectonic structure of Central and Eastern Australia.

Part D is devoted to the discussion of the significance of negative gravity anomalies over batholiths. Most of these anomalies point to these batholiths having "roots" in the substratum formed by fusion at the bases of geosynclines. One traverse points to granitization taking place by metasomatism of the pre-existing rock in situ because no evidence of a root is present.

The book ends with a list of principal facts for about 900 gravity stations, giving all particulars including Free air- and Bouguer anomalies.

This survey is an important contribution to the mass of published gravity data. Next to nothing was known about the gravity field of this continent before its publication and apparently much more work is to be expected. The book is very carefully written and expresses the author's views and findings in a well-balanced way.

It is of particular interest to oil-geophysicists because most of the traverses run over what is usually called "basement" and it is quite revealing to see what large anomalies occur over this bare or thinly covered basement. What the authors call "residuals" are, for prospectors, still unwanted regional effects and even when we think of this type of basement being buried under thousands of meters of sediments, these effects will still be clearly visible on isogam maps.

J. W. de B.

E.A.E.G. ABSTRACT SERVICE

EXPLORATION — GENERAL

125. *E.A.E.G. Meeting at The Hague.*

A. T. Dennison, Nature, Vol. 175, No. 4457, pp. 583-584, 2nd April 1955.

At the 7th meeting of the E.A.E.G. held at the Hague during 8-10th December, 1954, twenty-two papers were read.

Y. d'Erceville (France) read a paper on the velocity of propagation of longitudinal waves in muds.

A. Stein (Germany) spoke on the application of the reflection seismic method to mining problems in Siegerland.

J. Baumgarte, H. Menzel, & O. Rosenbach (Germany) dealt with the reflection of longitudinal waves at a thin layer lying between media of different velocities.

W. Brauch (Germany) considered reflection travel-time curves and the possibility of determining velocity distribution.

W. M. Jones & A. T. Dennison (Great Britain) described a new, portable, low-frequency geophone.

J. Schoeffler & E. Diemer (Germany) demonstrated a protractor for facilitating refraction computations.

H. Richard & M. Rimbaut (France) gave the results of reflection experiments with multiple geophones in linear arrays.

A. M. Selem (Italy) described a coastal reflection survey at Southern Abruzzi, where the topography is heavily eroded.

M. Matschinski suggested a new prospecting method in which seismic ground unrest yields information on geologic structures.

G. C. Colley (G.B.) discussed variations in the elevation correction factor for gravity work.

F. Sumi (Yugoslavia) described the determination of the depth of an ore body whose shape is assumed.

K. Jung (Germany) derived a formula for numerical computations in gravity topographical corrections.

W. Domzalski (G.B.) reported gravity measurements taken in and over a mine.

S. K. Runcorn (G.B.) discussed the direction of magnetization of rocks in Great Britain.

J. T. Whetton, J. O. Myers & I. J. Watson (G.B.) described a gravity survey over a mining prospect in Carmarthenishire.

C. Monnet (Italy) presented an extended application of the vertical gravity-gradient-method, used in a survey in northern Italy.

J. W. de Bruyn (Holland) produced maps of Bouguer and isostatic isogals over most of Europe and N. Africa.

H. Closs (Germany) produced a furhter map of the magnetic Z-anomalies over Europe.

V. Baranov (France) provided charts which help in the interpretation of magnetic surveys.

J. L. Mathieu & C. Rosoff (France) gave a general account of current well-logging techniques.

O. Koefoed (Holland) proposed a modified method of calculating standard interpretation curves in surface electrical resistivity measurements.

A. Volker & E. O. Houtsma (Holland) described resistivity measurements in and near the Zuider Zee to determine the salinity of the subsoil.

126. *The Search for Australia's Uranium.*
H. J. Ward, Mining Engineering, Vol. 6, No. 12, pp. 1169-1173, 1954.
Airborne and ground radiometric, self-potential, and air-borne and ground magnetometer surveys are being used to locate uranium in Australia. Radioactivity logging of drill holes is also employed. The geophysical surveys are closely co-ordinated with geologic studies.

127. *General Review of Applied Geophysical Studies in Exploration for Oil in Northern Africa.* (In French).
L. Migaux, Convegno Naz. Metano e Petrolio, 7mo, Taormina 1952, Atti, Vol. 1, pp. 499-509, 1952.
A review is presented of geologic conditions and of the geophysical exploration for oil in northern Africa. The results are of interest to Italian geophysicists because of the geologic similarity of northern Africa and Sicily and of especially great interest in view of the proposed petroleum exploration in Sicily. Several seismic, electric and gravimetric maps of parts of northern Africa are shown and discussed, and detailed studies of telluric currents are described.
(From Geophysical Abstracts 159, U.S. Geol. Survey).

SEISMIC — GENERAL

128. *Examples of Geophysical Exploration for Uranium.*
D. Wantland, Mines Mag., Vol. 44, No. 9, pp. 26-33, 1954.
A buried Triassic channel system at Nokai Mesa, Navajo County, Arizona, was successfully mapped by the seismic refraction method.

129. *Seismic Prospecting at Onahama District in Joban Coal Field, Fukushima Prefecture.* (In Japanese with English Summary).
S. Kurihara, Geol. Survey Japan Bull., Vol. 4, No. 8, pp. 41-48, 1953.

130. *Continuous Velocity Logging Supplements Seismic Data.*
E. R. Denton, Oil in Canada, Vol. 7, No. 17, pp. 26-28, February 21, 1955.
In searching for stratigraphic traps, accurate interval velocity data is required. The well-geophone method is not accurate enough for this , therefore the continuous velocity logger was developed. The instrument described here develops a log of the formations penetrated by the well which is very readily correlatable and in some instances permits analytical evaluation of the formations. The log also provides overall velocity through any section. This, when used in conjunction with one or more well-geophone velocity shots, yields accurate average velocity information to the various horizons encountered.

131. *Deep Reflections from Southern California Blasts.*
G. G. Shor, Jr., Trans. Am. Geophys. Un., Vol. 36, No. 1, pp. 133-138, February 1955.
Two records showing reflections from the Mohorovicic discontinuity at normal incidence have been obtained from large quarry blasts in Southern California. Each record shows a strong reflection with corrected travel time near 10.6 seconds. An earlier reflection appears near 9.0 seconds. Strong reflections were also obtained at distances slightly beyond critical .Computations of the thickness of the crust near the quarries have been made using velocity data obtained from blast and earthquake refraction studies. The results using any crustal model that fits the refraction data or by assuming a single-layer crust agree closely. In this area the Mohorovicic discontinuity is 32km below sea level, and the mean velocity in the crust is 6.2 km/sec.

The data give additional evidence for the existence of a zone in which velocity decreases with depth.

SEISMIC INSTRUMENTAL

132. *Magnetic Tape Improves Geophysical Recordings.*

S. J. Begun, Electronics, Vol. 28, No. 1, pp. 152-155, Januari 1955.

A magnetic recording system presents a good solution for preserving and subsequently reproducing geophone signals. Frequencies in the range 20-500 c.p.s. within 1.5 db. may be recorded, with a signal/noise ratio of at least 40 db. and accuracy of time relationship between signals better than 1 millisecond. The truck-mounted recording equipment is described together with the reproducing equipment which is usually set up in the field office where the original signal is processed.

133. *High Resolution Reflection Seismograph.*

R. W. Olson, Oil & Gas J., Vol. 53, No. 36, pp. 84-86, January 10, 1955.

By using the higher frequency components existing in the pressure pulse from an exploding charge, a technique developed at Houston Technical Laboratories can record very shallow reflections, from about 50′ to 2500′ (implying a record length of approximately ½ second), and can also give useful information to depths of 10,000 ft. The method is particularly useful for the detection of small features; the detailed coverage of larger features at medium depth; and also for shallow geological engineering work. The equipment is completely portable.

134. *Performance of Resonant Seismometers.*

W. L. Donn, M. Ewing , & F. Press, Geophysics, Vol. 19, No. 4, pp. 802-819, October 1954.

A group of resonant vertical seismometers, each tuned to cover a part of the spectrum of microseism frequencies, has been operated for about one year.

These instruments (a) clearly distinguish between simultaneous microseisms from two separate sources; (b) show an improved signal-to-noise ratio for microseisms from a single storm, permitting earlier detection of storm onsets; (c) show clearly the increase in period of frontal microseisms as cold fronts move seaward from the east coast of North America; (d) record only the envelope of the oscillations, which greatly facilitates measurement of intensity as a function of time; and (e) appear to be very useful tools in continued attempts at hurricane location by means microseism amplitude studies.

The performance of the instruments is demonstrated by seven case histories in which microseismic readings of seismometers tuned to different frequencies are related to the meteorological conditions which are apparently responsible for the microseismic activity.

(Author's Abstract).

SEISMIC — FIELD TECHNIQUE

135. *Patents.* Abstracts in Geophysics, Vol. 19, No. 4, p. 826, October 1954.

U.S. 2, 675, 882. 20 April 1954.	Seismic shooting method in which a spiral of explosive cord is detonated on the surface to give a desired wave front.
U.S. 2, 679, 205. 25 May 1954.	Apparatus for generating and detonating an explosive gas in a seismic shot hole.

136. *Drilling Methods in Sand and Gravel Formations.*

G. Muratori, Geophysical Prospecting, Vol. 3, No. 1, pp. 56-64, March, 1955.

Different drilling systems are described that have been adapted to the different types of near-surface conditions in Northern Italy. In soft sands a high pressure water jet is used, a rotary table not being required in a great many cases. In medium consistency sand and small gravel, the drill rods are rotated by a special roller wrench equipment instead of the more usual kelly. In coarse formations, gravel and boulders, casing is driven by special pile driving equipment with collapsible mast for easy transport.

137. *Azimuthal Seismic Observations with Inclined Seismographs.* (In Russian).
G. A. Gamburtsev & Y. I. Galperin, Akad. Nauk SSSR Izv. Ser. Geofiz., No. 2, pp. 184-189, 1954.

A new arrangement of seismographs to be used in seismological investigations and in seismic prospecting consists of a set of eight seismographs installed in a circle and all inclined at the same angle to the vertical.

The relative amplitude on the seismogram of an inclined instrument is determined by the vector of the displacement of the ground and by the direction of the axis of the seismograph. Graphs are given of the complete record that is obtained for different values of these two vectors from all eight instruments. In the examples analyzed, the angle of inclination is made equal to 30°, 45°, and 60°. With an appropriate choice of this angle a record can be obtained that gives more accurate values of the amplitudes and makes possible the determination of the phase of the incoming wave.

Other applications of the proposed arrangement of seismographs are suggested, such as use of three mutually perpendicular seismographs.

(From Geophysical Abstracts 157, U.S. Geol. Survey).

SEISMIC — INTERPRETATION

138. *Better Seismic Reflection Computations.*
J. W. Flude, Oil & Gas J., Vol. 53, No. 33, pp. 146-149, December 20, 1954.

A new machine, the Reynolds Cross-Section Plotter, is described. By manual, electrical, optical, photographical and mechanical means, it corrects each used seismic trace for elevation or water depth, weathering and step-out; makes use of any desired velocity curve; and then plots these traces in their correct horizontally surveyed positions on paper on which the final interpretation is made. The cost of a seismic survey which employs this machine is no more than when conventional methods are used; but there method is much more speedy and the interpretation is considered more accurate. The speed of the method is especially important for offshore seismic surveys where large numbers of records are produced in a short time.

139. *Comparison of Break-Point and Time-Intercept Methods in Refraction Calculations.*
N. N. Zirbel, Geophysics, Vol. 19, No. 4, pp. 716-721, Oct., 1954.

This paper compares two methods of calculating depths from refraction data where the subsurface consists of a series of horizontal layers with velocities V_0, V_1, V_2, etc.

Equations are developed for calculating depths from the horizontal distances to the intersections of the various segments of the time-distance graph (the break-points). Examples are worked out to show that the error in depth due to an uncorrected change in thickness of the weathered layer is much less when the depths are calculated from break-points than when they are calculated from time-intercepts. In many areas weathering corrections should be unnecessary if the depths can be calculated from the break-points by the method outlined here.

(Author's Abstract)

140. *Some Observations on Seismic Weathering Corrections.*
O. Koefoed, Geophysical Prospecting, Vol. 2, No. 4, pp. 274-280, December 1954.

When a rather extensive network of short distance refraction profiles was shot the following two observations were made. Firstly, the wave velocity in the weathered layer showed a quite considerable fluctuation in horizontal direction, the extreme values being of the order of 300 and 700 m/sec. A practical result of this scattering of the velocities is that an uncertainty of about 10% is introduced in the computation of the weathering corrections. The second observation is that, in the majority of cases, the travel time curve does not pass through the origin. It could be ascertained that this observation was not caused by errors in the method of observation. A probable explanation of the phenomenon is found in a theory that has been developed by Gassmann, who derived the velocity distribution for a hexagonal packing of spherical solid bodies. According to this theory extremely low velocities would occur in the first few centimetres of the crust of the earth. Qualitatively, our observations are in agreement with the theory of Gassman.

(Author's Abstract).

141. *A Remark Concerning the Problem of How to Place the Reference Plane (Datum Level) in Reflection Seismic Prospecting.*
T. Krey, Geophysical Prospecting, Vol. 2, No. 4, pp. 281-284, December 1954.

It has been shown in a paper by L. Y. Faust that the wave velocity in rock depends on the depth below the ground surface according to a specified equation. It follows that the attitude of the planes of equal velocity is influenced by the topographic relief. Under these conditions the problems arises of how to place the reference plane in such a manner that the fluctuations of the planes of equal velocity, that result from the fluctuations in the topography, shall not affect the results of the depth computations. In the present paper an analytical solution of this problem is given.

(Author's Abstract).

142. *Determination of the Velocity of Propagating of Seismic Waves in Reflection Surveys.* (In Italian).
C. Contini, Convegno Naz. Metano e Petrolio, 7mo, Taormina 1952, Atti, Vol. 1, pp. 425-434, 1952.

Methods of determining the velocity of seismic waves are reviewed briefly, and a graphical means of determining the velocity is shown. The importance of considering the irregularity of the surface and the weathered layer, and the inclination and curvature of the reflecting surface is stressed. A practical example of the use of the graph in determining velocity in the Po valley is given.

(From Geophysical Abstracts 159, U.S. Geol. Survey)

SEISMIC — THEORY & RESEARCH

143. *Some Theoretical Considerations on the Use of Multiple Geophones Arranged Linearly along the Line of Traverse.*
F. W. Hales & T. E. Edwards, Geophysical Prospecting, Vol. 3, No. 1, pp. 65-73, March 1955.

An analytical treatment is given of the response of linear arrays of multiple geophones, as a function of the direction of incidence of the wave and of the wave frequency. The relation between the response and the direction of incidence may be quite complicated, the response being zero in several directions. As a function of wave frequency, the response may also have several zero values within the frequency band in which reflections are expectable. This would result in a serious modification of the filter characteristics of the amplifier. It is shown, however, how such a modification of the filter characteristics may be avoded by a judicious choice of the number and the spacing of the geophones in a multiple group.

(Author's Abstract)

144. *Recent Developments in Strong-Motion Analysis.*
J. Hershberger, Bull. Seismol. Soc. Amer. ,Vol. 45, No. 1, pp. 11-21, January 1955.

An improved accelerometer has eliminated the possibility of zero shifts: thus preventing the continued use of extra adjustments in the integration of accelerometer records to produce velocity and displacement curves. However, for obtaining displacement information of general engeneering significance, the Carder displacement meter has proved superior to the integration method and is being increasingly used.

145. *Screening Effect Produced by a Thin Elastic Layer.* (In Russian).
V. Babich & A. Alekseyev, Akad. Nauk SSSR Doklady, Tom 91, No. 4, pp. 763-765. 1953.

If a seismic wave propagating through a medium is incident upon an elastic layer of different elastic properties at an angle greater than the limiting angle, according to the laws of geometrical optics, total reflection takes place and no wave disturbance is propagated across the boundary. However, on the basis of dynamic relations of the theory of elasticity it is proved that for a sufficiently thin layer a certain portion of the energy involved in the oscillatory motion will pass over across the layer into the deeper part of the medium. Such propagation will be especially noticeable for long waves and for angles of incidence not too greatly exceeding the limiting value. Such a phenomenon was observed in the results of a seismic survey made by I.S. Berzon and A. M. Yepinat'yeva.

(From Geophysical Abstracts 159, U.S. Geol. Survey).

146. *The Multiple Refracted Waves in Vertically Stratified Media.* (In Russian).
I. S. Berzon, Akad. Nauk SSSR Izv. Ser. Geofiz. No. 5, pp. 424-442, 1954.

In vertically stratified refracting media, seismograms obtained over the sections of the wave path adjoining the boundary surface show changes in the shape of the multiple waves, which can cause interference of different multiple waves and in certain cases their complete disappearance. The travel times of the refracted-reflected wave (P_{1k1111}) and of the reflected-refracted wave (P_{111k11}) are different, but their travel-time graphs are both parallel to that of the simple wave. This is the main criterion for the identification of multiple waves. If the vertically stratified medium is composed of dissimilar and not too thick layers, the kinematic as well as dynamic conditions are not favourable for the creation of multiple waves. Seismic waves are said to be very seldom reflected more than twice. Experiments over a vertically stratified area gave results which are in good agreement with the theoretical data.

(From Geophysical Abstracts 159, U.S. Geol. Survey).

147. *Reflection of Waves from Varying Media.*
C. O. Hines, Quart. Appl. Maths., Vol. 11, No. 1, pp. 9-31, April 1953.

Formulae are found for the coefficient of reflection from varying media of a type encountered in physics. These are applied approximately for some general classes of media, and exactly for some specific cases. Many media which would normally be expected to be highly reflecting are shown to be completely transparent to certain waves at least and, in some cases, to a whole spectrum of waves. The results are considered both for electromagnetic (or other classical) waves and for mass waves.

(Author's Abstract).

148. *Synthesis of Seismograms from Well Log Data.*
C. A. Swartz, R. A. Peterson, & R. W. Fillippone, a paper read at the 48th meeting of the Acoust. Soc. of America at Texas, November 1954 (Not yet published).

Under certain highly simplified but realistic physical assumptions, the basic data from continuous velocity surveys in wells can be made to simulate the variations in aucoustic impedance in the ground which give rise to seismic reflections. An electrooptical analog device is described which makes use of the basic well data to produce synthetic seismic records which resemble actual seismograms from shot hole explosions. This provides an interesting insight into the requisite physical conditions as well as the physical processes whereby seismic reflections are set up in the earth.

149. *Seismic Waves from a Horizontal Force.*

J. E. White, S. N. Heaps & P. L. Lawrence, a paper read at the 48th Meeting of the Acoust. Soc. of America, at Texas, November 1954. (Not yet published).

As part of a program of fundamental research on seismic waves, a generator was built for applying a transient horizontal force at the surface of the ground, and the resulting seismic waves were observed in some detail. The force is applied when a mass swinging through an arc strikes a target anchored to the earth. Surface geophones along a line in the direction of the force register vertically polarized shear waves refracted back up to the surface, whereas geophones on a line perpendicular to the force register horizontally polarized shear waves. The speeds of the two types of shear waves are often different, indicating anisotropy. Buried geophones below the force show a down-going shear wave. Variation of amplitude with angle and other features are in qualitative agreement with the results given by Rayleigh and others for the waves caused by a force at a point in an infinite solid. Love waves and other surface waves were observed, which of course would not be expected from an interior force.

150. *Diffraction Problems in Elastic Wave Propagation in Solids.*

L. Knopoff, a paper read at the 48th meeting of the Acoust. Soc. of America, at Texas, November 1954. (Not yet published).

Integral solution to the differential equations of elastodynamics are given. The solutions for the displacement at any point in an isotropic, homogeneous, elastic medium are obtained in terms of the initial distribution of displacements and stresses within a given volume and over and over its bounding surface. These initial quantities appear in the solutions as retarded displacements and stresses with two types of retardation depending upon the velocities of longitudinal and transverse waves. Diffraction by rigid obstacles is discussed on the basis of these integral solutions. Examples are given of the diffraction of plane wave pulses of either compression or shear types of infinite or rigid slits. Rayleigh scattering by rigid spheres is also discussed.

151. *Application of Correlation Techniques to Geophysical Prospecting.*

C. W. Horton, a paper read at the 48th meeting of the Acoust. Soc. of Amer., at Texas, November 1954. (Not yet published).

A recent development in geophysical research is the application of auto- and cross-correlation techniques to geophysical data in the hopes of improving the signal-to-noise ratio. This work is summarized, and typical correlation functions for land and shallow water areas are presented. The relation between correlation techniques, filtering and direction patterns is reviewed and illustrated. A theory is developed to explain the shape of the autocorrelation function of a seismogram trace.

152. *Use of Models in the Study of Seismic Phenomena.*

D. Silverman, a paper read at the 48th meeting of the Acoust. Soc. of America, at Texas, November 1954. (Not yet published).

In the shallow crustal volume of the earth which is of no interest to the geophysicist, the seismic behaviour of the earth is adversely affected by the complexity of the earth's structure. In order to study seismic phenomena in the earth, recourse has been had to the use of acoustic models. These models are simplified idealized structures, generally scaled down in time and dimension, with which the basic action of seismic waves in the earth can be studied. Different types of models have been built, including single, two and three-dimensional solid models, multilayered liquid models, and optical models. All of these are essentially analog computers for solving the wave equations as applied to the specific structures. Model studies have been found quite useful in veryfying theoretical analyses, in explaining observed phenomena in the field, and in suggesting additional field experiments. The use of scale models in the study of the seismic process is becoming widespread both in universities and in industrial laboratories.

153. *On the Propagation of Elastic Waves in Aeolotropic Media.* I. *General Principles.* M. J. P. Musgrave, Proc. Roy. Soc., A, Vol. 226, No. 1166, pp. 339-355, 23 November 1954.

Using the principle of least action the equations of motion and momentum conditions for elastic disturbances in any continuous medium are derived. Consideration of energy flux defines the form of the wave surface as the first negative pedal of the surface of phase velocities for elastic plane waves in the medium. A general method for obtaining the forms of these surfaces and an associated inverse surface is given and general conclusions about the propagation of disturbances are drawn.

(Author's Abstract)

GRAVITY — GENERAL

154. *Geophysical Methods of Oil Prospecting — A Review.* II *Gravitational Methods.* D. Taylor Smith, Petroleum, Vol. 17, No. 12, pp. 426-429 ,December 1954.

This article describes briefly the various techniques employed in gravimetric prospecting and the general principles upon which they are based.

155. *Isogram Maps of Europe and North Africa.* J. W. De Bruyn, Geophysical Prospecting, Vol. 3, No. 1, pp. 1-14, March 1955.

Bouguer and Isostatic isogam maps of Europe and North Africa are presented. They are based on published data such as Bouguer isogam maps and lists of pendulum stations. Both are on the scale of 1:5,000,000 and have an isogam interval of 25 mgal with 5 mgal contours shown in parts. They provide a regional map of the gravity field in Europe. An appendix gives detail of the data used.

156. *Present State and Future Development of Gravity Measurements in Germany.* (In German) W. Grossmann, Deutsche Geod. Komm. Veröffentl., Reihe A, Heft 11, pp. 5-8, 1953.

By 1945 Germany had a gravity network of more than 100,000 stations, with the accuracy of some individual determinations as high as 0.2 mgal. The most important investigation project is the verification of the Potsdam absolute pendulum. The pendulum with the bob suspended on a string, and observation of a free falling rod will be used. Measurements will first be made at the three main observatiories in Potsdam, Harzburg, and Berchtesgaden, and later made at several secondary stations. At each place gravity determinations will be made by all three methods, and an accuracy of 0.02mgal is expected .The relative gravity network will be further extended, using chiefly the Graf-Askania and the Worden gravimeters.

(From Geophysical Abstracts 159, U.S. Geol. Survey).

157. *Detailed Gravimetric Survey of the Paris Basin.* (In French). J. Goguel, France Bur. Geol. Research Geophys. Pub., No. 15, 1954.

GRAVITY — INSTRUMENTAL

158. *Patents.* Abstracts in Geophysics, Vol. 19, No. 4, p. 825, October 1954.

U.S. 2, 674, 885 13 Apr. 1954.	A motion compensator for a gravimeter which has a motion detector.
U.S. 2, 674, 886 13 Apr. 1954.	A self-levelling gravimeter support.
U.S. 2, 674, 887 13 Apr. 1954.	A gravity meter with quartz suspended system.

159. *The Accuracy of a Modern Gravimeter* (In German).
F. Haalck, Zeitschr. Geophys., Sonderband, pp. 21-28, 1953.

Further improvement of the accuracy of gravimeters is certainly possible but hardly desirable because the limits of the attainable accuracy of a survey are now set by topographic data, knowledge of the density, and similar factors.

The new gravimeter "Gs9" manufactured by the Askania-Werke is a torsion instrument with its movable system supported by two pairs of twisted springs. The range of the gravimeter is about 4,000 mgals; the drift of the zero point is 0.003 mgal/hour; and the guaranteed accuracy is O. Olmgal. Ten graphs illustrate the properties of the instrument.

((From Geophysical Abstracts 159, U.S. Geol. Survey).

160. *Magnetic Perturbations of Invar Pendulums Used for Relative Gravity Measurements.*
A. H. Cook, Mon. Not. Roy. Astronom. Soc., Geophys. Suppl., Vol. 7, No. 1, pp. 1-21, October 1954.

Certain discrepancies in recent relative gravity measurements made with the Cambridge pendulum apparatus may be due to magnetic forces on the invar pendulums. In addition to effects that have been described previously, it is shown that disturbances may arise from a magnetic screen surrounding the pendulums and from the magnetic interaction of two pendulums swinging together. Theoretical estimates of these effects are compared with experiments. The behaviour of the pendulums is qualitatively as predicted but the numerical results are in poor agreement. This may be due in part to the difficulty of making calculations for pendulums with dimensions comparable to their distances from the magnetic screen and each other. The application of the results to gravity measurements is considered.

GRAVITY — INTERPRETATION

161. *On the Determination of Density by Nettleton's Method.* (In German).
K. Jung, Zeitschr. Geophys., Sonderband, pp. 54-58, 1953.

Nettleton's method for determining the density can be put into numerical form by equating to zero the coefficient of correlation between the Bouguer anomalies and the elevations. If σ is the density, σ_1 an assumed approximate density, and σ_2 the difference between them, then an equation may be written in which the Bouguer anomaly is the anomaly calculated assuming σ_1 minus two terms involving σ_2. The correlation coefficient between the Bouguer anomaly and the elevation is set equal to zero and an equation is obtained from which σ_2 may be determined. This procedure is compared with that developed by Parasnis for determining densities. Results are in good agreement.

(From Geophysidal Abstracts 159, U.S. Geol. Survey).

162. *Remarks on the Determination of Density by Nettleton.s Method.* (In German).
R. Bortfeld, Erdöl u Kohle, Jahrg-7, Heft 6, pp. 353-355, 1954.

In computing the Bouguer reduction it is necessary to assume the most probable value of the density of the upper layer of the ground. Nettleton has suggested a graphical method of finding this value, which was later expressed in mathematical form by Jung. Certain refinements are now introduced which make it unnecessary to assume that gravity has a constant value at all points of the reference horizon. The theoretical computations are presented and also applied to practical cases.

(From Geophysical Abstracts 159, U.S. Geol. Survey).

163. *A Procedure for the Computation of the Horizontal Gradient from the Gravity Values.* (In German).
O. Rosenbach, Zeitschr. Geophys., Sonderband, pp. 37-45, 1953.

Modern precise gravimeter measurements make possible the computation of horizontal gradients of gravitational anomalies from the Bouguer anomalies if a sufficiently dense network of stations is available. Approximate formulae of different accuracy are derived in the form of series by simple methods of potential theory, and applied to the several examples.

(From Geophysical Abstracts 159, U.S. Geol. Survey).

164. *Gravity Data Indicate Structural Conditions.*

W. R. Sype, World Oil, Vol. 140, No. 2, pp. 82-86, February 1, 1955.

The article illustrates some of the uses of residual gravity anomalies in developing a picture of the subsurface structure. There are three requisites for a correct interpretation: - a reliable survey, using properly corrected values; at least an approximate knowledge of subsurface densities; and an understanding of the local geology. Salt and non-salt structures capable of interpretation are discussed.

165. *Some Remarks on the Errors in the Calculation of the Vertical Gradient of Gravity.*

V. Baranov & J. Tassencourt, Geophysical Prospecting, Vol. 2, No. 4, pp. 285-289, Dec., 1954.

In a previous paper by the first author a method has been presented for computing the first vertical derivative of the gravity field or of the magnetic field. In the present paper an analysis is given of the errors in the first vertical derivative that result when the latter is computed by the above method. Two sorts of errors are considered. Firstly, the error in the first vertical derivative that results from the errors in interpolating between isogam lines on the Bouguer anomaly map. Secondly, the error in the first vertical derivative that results from the approximations upon which the computation method is based. The conclusion is reached that both sorts of error are only of minor importance.

(Author's Abstract)

166. *The Part Played by Luni-Solar Corrections in Gravimetric Prospecting.* (In French).

R. Neumann, Geophysical Prospecting, Vol. 2, No. 4, pp. 290-305, Dec., 1954.

The luni-solar corrections are considered under the three following aspects:

Quality of results: the application of tidal corrections to all stations is pointless as long as the operations do not substantially exceed two hours.

Working conditions: it seems possible to increase the duration of programmes without any loss of precision, but operating in such a way requires particular care.

Behaviour of gravity meters: the introduction of tidal corrections allows to separate three kinds of instrumental drifts; a good knowledge of the mean operational drift enables to appreciate the quality of a given set of measurements.

An example is given to show the possibility in some cases to detect small errors which are close to the limit of precision of the instrument.

(Author's Abstract)

167. *Tidal Gravity Corrections for* 1955.

J. Goguel & C. Morelli, Geophysical Prospecting, Vol. 3, Suppl., January, 1955.

Corrections for tidal gravity are provided in tabular form by J. Goguel and in graphical form by C. Morelli, for the whole of 1955. Both authors explain the compilation and use of the tables and graphs respectively.

168. *A New and Simple Method for Calculating the Deflections of the Vertical From Gravity Anomalies with the Aid of the Bessel Fourier Series.*

C. Tsuboi, Acad. Japan Proc., Vol. 30, No. 6, pp. 461-467, 1954.

This new method neglects the curvature of the earth, thus avoiding many complexities. It is based on a double Fourier expansion of the gravity potential for a plane surface, The deflections of the vertical are easily obtained by differentiating the potential function, and the unknown coefficients are determined by using the gravity data. After applying the method successfully to gravitational data for the entire U.S.A., it was felt that the method was not suitable for application at a particular station as this would involve too many terms in the series to be practicable. Instead, through the use of cylindrical co-ordinates, the gravity potential is expressed as a Bessel Fourier series. The formulae for the deflections of the vertical are derived and are conveniently expressed in the form of a radial integral which is graphically evaluated. An example shows agreement with the results of Rice.

(From Geophysical Abstracts 159, U.S. Geol. Survey).

169. *A Study of the Anomalies in the Vertical Gradient of Gravity with the Aid of the Bessel Fourier Series.*

C. Tsuboi, Acad. Japan Proc., Vol. 30, No. 6, pp. 453-461, 1954.

It is common practice to consider the free-air reduction of gravity as a constant. To be precise, however, the vertical gravity gradient at any point is a function of the variation of gravity in a horizontal plane. The vertical gravity gradient is more accurately determined by expanding the function in a double Fourier series. The coefficients are then determined by considering the gravity anomaly at the surface. The method was applied to gravity data covering almost the entire U.S.A. The largest calculated value of $\Delta\delta g/ \delta z\ (x)$ turned out to be approximately 10^{-8} c.g.s. units. However, shorter wavelengths were not considered in the series expansion as the calculations would become too difficult. The added terms would doubtless increase the correction.

To determine the gradient at a particular station, the Bessel Fourier representation of the potential was employed and the coefficients determined for a point in the southwestern U.S. The gradient was computed to be 37×10^{-9} c.g.s. units of 1% of the normal value.

(From Geophysical Abstracts 159, U.S. Geol. Survey).

GRAVITY — THEORY & RESEARCH

170. *Tides in the Solid Earth Body and the Corrections thereby Made Necessary for Very Precise Gravimeter Measurements.* (In German).

H. Haalck, Gerlands Beitr. Geophys., Band 64, Heft 1, pp. 1-15, 1954.

The basic relations of the theory of tides in the solid earth are derived in simplified form. These relations determine the amount of tidal deformation and the disturbances of the force of gravity in intensity and direction. From these relations are derived the numerical values of the corrections that are to be applied to very precise gravimeter measurements if the accuracy of the instruments is to be fully utilized. With the help of a practical example, the use of astronomical almanacs is explained for the practising geophysicist and the computations of the corrections shown.

171. *Three Dimensional Gravity Survey.*

W. Domzalski, Geophysical Prospecting, Vol. 3, No. 1, pp. 15-55, March. 1955.

An experimental gravity survey was conducted in which measurements were taken at different levels in a mine, in the mine shaft, and on the surface above the mine. Details are given of the various traverses run and comparisons are made between the theoretical results and observed data and known geology.

MAGNETIC — GENERAL

172. *The Magnetic Survey of Ireland for the Epoch* 1950-55.

T. Murphy, Dublin Inst. for Advanced Studies Geophys. Mem. 4, 1953.

173. *Total Intensity Aeromagnetic Maps of Minnesota.*

U.S. Geol. Survey, Geophys. Inv. Maps GP 97 and 101, 1954.

174. *Aeromagnetic Map of New Brunswick.*
Canada Geol. Survey, Deppt. of Mines and Tech. Surveys, Geophys, Paper 22, 1954.

175. *Aeromagnetic Maps of New Foundland.*
Canada Geol. Survey, Dept. of Mines and Tech. Surveys, Geophys. Papers 184-195, 198, 201-204, 207, 208, 210, 1954.

176. *Aeromagnetic Map of Northwest Territories.*
Canada Geol. Survey, Dept. of Mines and Tech. Surveys, Geophys. Paper 218, 1954.

177. *Aeromagnetic Maps of the Province of Ontario*
Canada Geol. Survey, Dept. of Mines and Tech. Surveys, Geophys. Papers 174 and 181, 1954.

178. *Aeromagnetic Maps of the Province of Quebec.*
Canada Geol. Survey, Dept. of Mines and Tech. Surveys, Geophys. Papers 161-163, 167-169, 171-173, 175, 182 and 183, 1954.

179. *Geophysical Methods of Oil Prospecting. A Review.* III. — *Magnetic Methods.*
D. Taylor Smith, Petroleum, Vol. 18, No. 3. pp. 86-90, March 1955.

Magnetic methods are used mainly for reconnaissance work. The airborne magnetometer can be used to cover very large areas at high speed with a relatively low cost. The nature of the geomagnetic field, magnetic properties of rocks, observation instruments, field techniques, and interpretation methods are briefly discussed.

180. *A Universal Torsion Magnetometer for Determination of D, H and Z.* (In German).
F. Haalck, Zeitschr. Geophys., Sonderband, pp. 1-7, 1953.

A universal magnetometer is described which measures D, H and Z directly. H and Z can be measured with an accuracy of 0,3 gammas, and angles with an error less than ±3 secs.

181. *Temperature Compensation of the Torsion Magnetometer.* (In German).
F. Werner, Zeitschr. Geophys., Sonderband, pp. 8-11, 1953.

It is impossible in constructing the torsion magnetometer to find material for the springs with the necessary thermo-elastic coefficient for good temperature compensation; hence two springs, which can be set either in series or in bifilar arrangement, must be used. In series, each spring produces an effect proportional to its length, and in the bifilar arrangement the springs are differently twisted. The diameter of the springs is about 30 μ. A theoretical analysis of instruments with vertical or horizontal twisted axis is given. The graphs shown indicate that variation of the temperature from 15°C to 25°C and back does not affect the readings of the variograph noticeably.

(From Geophysical Abstracts 159, U.S. Geol. Survey).

182. *Nol Vector Airborne Magnetometer Type 2A.*
E. O. Schonstedt & H. R. Irons, Trans. Am. Geophys. Un., Vol. 36, No. 1, pp. 25-41, February 1955.

The NOL vector airborne magnetometer type 2A (VAM-2A) measures the direction and intensity of the earth's magnetic field from aircraft. Like the earlier type 1A, it continuously records the total intensity of the field and the magnitudes of a number of angles which specify its direction, but the 2A can be used in all latitudes and requires fewer steps the the reduction of results. Electronic circuits are used to average continuously the always varying angular magnitudes over predetermined intervals of time so as to minimize errors arising from the deflection of the pendulously suspended magnetometer mechanism by acculerations of the aircraft. The total-field measuring system of the magnetometer has a temperature coefficient of about 0.5γ/°C. Drift due to causes other than temperature change is about one gamma in 12 hours. Magnetic compensation virtually eliminates the necessity for correcting the data for the field of the aircraft. In a region where the angle of dip is about 60°, F, H, Z, I, and D are measured under average conditions with estimated probable errors of 15, 40 and 30γ, and three and five minutes of arc, respectively.

MAGNETIC — THEORY & RESEARCH

183. *Calculation of the Components of the Magnetic Field of Masses of Any Shape.* (In Italian)
C. Contini, Geofis. Pura e Appl., Vol. 26, pp. 41-66, 1953.

A description is given of the diagrams for computing the components of the magnetic field generated by the magnetization of elementary masses of rotation round a vertical axis. It is further shown how such diagrams, in variable scale, make it possible to make rapid and fairly correct computations of the elements of the field of magnetized masses of any shape and size. An explanation is given of how the same diagrams can also be used for computing the Eötvössian elements. At the end some details are given on the computation of topographic influences.

(From Physics Abstracts, A, December 1954).

184. *Magnetic Studies of Rocks and Ores from the Bayerland Mine, in Connection with the ΔZ- and ΔH-Anomalies Found there.* (In German).
K. H. Seelis, Geol. Jahrb. Band 68, pp. 319-330, 1954.

The density, induced magnetism, remanent magnetism, and susceptibility of a large number of specimens are determined, and the geologic environment described. Owing to the complexity of the ore, one cannot readily recompute the magnetic effect of the whole ore body referred to the surface. The usual assumption of a uniform sheet, however, is not warranted here, because the intensity as well as the direction of magnetization differ greatly from place in the ore body. Furthermore, the magnetic properties of the phyllite country rock are such that they severely affect the anomaly at the surface.

(From Geophysical Abstracts 159, U.S. Geol. Survey).

185. *On the Reverse Natural Remanent Magnetism of Basalt at Cape Kawajiri, Yamaguchi Prefecture.*
E. Asami, Acad. Japan Proc., Vol. 30, No. 2, pp. 102-105, 1954.

The natural remanent magnetization of 52 specimens of basalt collected along the coast of Cape Kawajiri were measured. The cape is considered to be formed of one basalt eruption thought to be early Pleistocene. Along the western side of the cape the rocks are consistently normally magnetized and have generally a greater intensity of magnetization than the rocks along the northern and eastern side of the cape where the basalt is consistently reversely magnetized. Between these two areas eight specimens have mixed orientations.

(From Geophysical Abstracts 159, U.S. Geol. Survey).

ELECTRICAL

186. *Mapping Nearly-Vertical Discontinuities by Earth Resistivities.*
O. Logn, Geophysics, Vol. 19, No. 4, pp. 739-760, Oct., 1954.

Integral formulae are evaluated for the potential distribution around one current electrode placed in the neighbourhood of (a) one vertical plane of discontinuity and (b) two vertical planes of discontinuity. The apparent resistivity in the one-current-electrode configuration is defined, and integral formulae are given for planes of discontinuity.

187. *Patents.* Abstracts in Geophysics, Vol. 19, No. 4, p. 825, October 1954.

U.S. 2, 675, 521 13 April 1954.	A d-c electrical method where potential electrodes are placed in boreholes and current electrodes on the surface between the holes.
U.S. 2, 677, 801 4 May 1954.	An e.m. prospecting method in which telluric and magnetic fields for same area are simultaneously recorded.
U.S. 2, 680, 226 1 June 1954.	A pick-up circuit for an e.m. system in which the differerence between the generated e.m.f.s. of two coils is measured.

188. *The Dependence of the Apparent Resistivity on the Sonde Interval by the Four-Point Method.* (In German).
K. Deppermann, Geophysical Prospecting, Vol. 2, No. 4, pp. 262-273, December 1954.

The dependence of the apparent resistivity on the distance between the potential electrodes is examined and a numerical method is described permitting quantitative calculations. Such a numerical relation is also established for the transformation of Wenner graphs into Schlumberger graphs.

In addition it is shown in which manner the jumps in observed Schlumberger curves that result from changing the probe spacing, must be smoothed out.

(Author's Abstract).

189. *On the Direct Electromagnetic Effect of an A.C. Emitter on the Surface of a Homogeneous Earth.* (In Italian).
A. Belluigi, Ann. Geofis., Vol. 7, No. 3, pp. 415-440, July 1954.

A brief discussion of Sommerfeld's classical theory of a horizontal dipole is followed by a discussion of the Horton-Lewis theory. The theory is then extended to include the variation of the dielectric constant of the earth with frequency and finally generalized to include other types of oscillator. Graphs and tables are included to assist in the application of this theory to electrical prospecting.

190. *An Electrode Arrangement for Identification of Large Subsurface Anomalies in a Continuous Medium, by Spotting the Electrical Axis.* (In Italian).
F. Mosetti, Metano, Vol. 8, No. 10, October 1954.

191. *Geophysical Investigations and Hydrology in the Area of the Industrial Harbour of Trieste.* (In Italian).
F. Mosetti, Geophysical Observatory Pub., Trieste, 1955.

The results obtained with a great number of electrical soundings and some mechanical borings are explained. The work was carried out in order to determine the geological and hydrological structure in the zone of the industrial harbour of Trieste.

Of special interest with regard to electrical investigations is the treatment of the localisation of the ground water in a soil which is clayey to a great degree.

192. *The Inductive Absorption Method for Search for Good Extended Subsurface Conductors.* (In Italian).
A. Graf, Convegno Naz. Metano e Petrolio, 7mo, Taormina 1952, Atti, Vol. 1, pp 495-497, 1952.

A rigid frame supporting an electrical coil is suspended from three helipters at a height of some 20-25 m and is slowly moved parallel to the ground. If the coil is excited by alternating current, an alternating magnetic flux will be sent into the ground, generating in turn, currents in the underground bodies of an intensity determined by their conductivity. Graf's calculations show that this apparatus will have sufficient sensitivity so that an aquifer under even a thick layer of dry sand will cause a noticeable increase of the current in the coil, and a similar effect will be produced when the coil passes from an oil-bearing formation to another containing saline water.

(From Geophysical Abstracts 159, U.S. Geol. Survey).

GEOCHEMICAL

193. *Shallow (Surface) Geochemical Contour Maps.* (In Polish).
J. J. Glogoczowski, Bull. Polish Inst. Petr., Vol. 3, No. 11, 1953.

Samples from the area of the Potok anticline were tested for heavy and light hydrocarbons and for radioactivity. From the data obtained, geochemical contour maps were produced which were found to be in agreement with known sizes of crude oil reservoirs. Other work, in the area of the Carpathian fold, is described.

OTHER METHODS

194. *Many Factors Involved in Finding Oil by Airborne Scintillometers.*
H. Lundberg, Oil Forum, Vol. 9, No. 1, pp. 23-24, January 1955.

The mapping techniques and interpretation methods required in an airborne scintillometer survey are discussed. The characteristic fringe of high frequency round an oil-field is explained on the basis of upward seepage, at the edges of the field, of waters free of sulphates but with a high chloride content. Atmospheric waters percolating downwards will precipitate sulphates, including that of radium, and in dry seasons the high evaporation rates bring the sulphates to the surface, dissolved in the up-trending chloride waters.

195. *Gamma Ray Oil Exploration.*
D. S. Lobdell & E. F. Buckley, Petr. Eng., Vol. 26, No. 8, pp. B. 76-B. 83, August, 1954.

A question and answer interview. Gamma ray surveys are of value only if conducted with very sensitive and stable equipment, to map the changes in soil and topography in great detail. Continuous profile tape recording is essential, to determine the average background levels.

196. *Patents.* Abstracts in Geophysics, Vol. 19, No. 4, p. 825, October 1954.

U.S. 2, 675, 480	13 April 1954.	A radioactivity prospecting method in which time is measured for the same number of counts to accrue at each station.
U.S. 2, 677, 780	4 May 1954.	A multiple-plate radioactivity detector.
U.S. 2, 678, 398	11 May 1954.	An airborne radioactivity prospecting method.

197. *Geomicrobiological Prospecting.*
G. G. Soli, Bull. A. A.P.G., Vol. 38, No. 12, pp. 2555-2565, December 1954.

In a short essay the author lists and discusses the lines along which bacteriological and other microbiological research has been conducted, as an aid to locating oil and gas deposits. The appended bibliography includes some Russian papers.

APPLICATIONS OF THE REMANENT MAGNETIZATION OF ROCKS *

BY

S. K. RUNCORN **

ABSTRACT

The basic principles of remanent magnetization are stated, and possible applications are discussed in the fields of age determination of rocks, the study of relative movements of continents, and investigation of the thermal history of rocks.

BASIC PRINCIPLES

It is appropriate at the present stage of the development of the study of rock magnetism to attempt to set down its possible applications to geology and geophysical exploration. The application of a subject goes hand in hand with the deepening of knowledge of its fundamental principles. On the other hand technical advances enable data to be obtained faster and the possibilities of successful application provide an effective spur to basic research. The pure and applied aspects react with advantage on one another and this has been particularly true in palaeomagnetism.

The earliest recognition that sediments possess a remanent magnetization is that of Lynton (1937), who proposed that such measurements on borehole cores would be a powerful tool for their orientation. Similarly many geologists saw that the remanent magnetization of lavas might prove to be the tool for correlation, which is particularly needed in igneous geology. But, on the whole, limited success attended these efforts to make use of remanent magnetization because its mode of origin and retention was poorly understood. Because it was found to be technically possible to make a magnetometer, which can be used in an aeroplane, extensive use of aeromagnetic survey has been made. However, inferences from such surveys of the subsurface has been handicapped by lack of measurements of the magnetic properties of rocks.

---

* Based on a lecture to the Seventh Meeting of the European Association of Exploration Geophysicists, held in the Hague, 8/10 December 1954.

** Physics Dept., King's College, Newcastle upon Tyne.

The effective application of rock magnetism depends on the clear recognition of two factors:

(1) The ferromagnetic minerals in rocks can have varying degrees of magnetic stability. The extent to which they have acquired isothermal remanent magnetization by their long exposure to the present geomagnetic field, even at ordinary temperatures, depends on the chemical composition and texture of the minerals and the shape and size of the grains (Neel, 1955).

(2) It is now known broadly how the magnetic polarization of rocks in Great Britain and the U.S.A., varies in direction throughout geological time, see Runcorn (1955/6). Only during the Tertiary has the direction, when averaged over a geological period, coincided with the geocentric axial dipole field, from which the present field is a fluctuation of comparatively short time scale.

Sometime before late Pre-Cambrian times the magnetic pole was apparently in the North American continent, in late Pre-Cambrian times it was in the eastern Pacific near Hawaii, in Cambrian times it was in the western Pacific near the Marshall Islands, while in late Palaeozoic and early Mesozoic times it was near the east coast of Asia around Japan. Some evidence suggests that it had arrived near its present position by Cretaceous times. The palaeomagnetic evidence thus suggests that the pole has wandered at a mean rate of 20 km., or 0.2°, per million years, though it is as yet impossible to say how much this velocity fluctuated nor is it certain how smooth was the path followed. In addition to this slow wander of the pole, the magnetic polarity may alternate — in some geological periods a number of reversals occur in one series of rocks, perhaps at intervals of only a few hundred thousand years.

Such inferences on the history of the geomagnetic field are based in general on rocks, such as lavas and fine-grained red sandstones, for which evidence exists that they become magnetized along the direction of the field at their formation. Rock series are chosen which have stable magnetic minerals and which can be assumed not to have undergone chemical or physical changes likely to have caused remagnetization. Many rocks, e.g. cross-bedded sandstones in which stream action is important and metamorphosed rocks, in which magnetization may have been acquired at different times in their history, will be magnetized in directions not simply related to the geomagnetic field. Little study of such rocks has so far been made.

It is interesting to see how these results throw light on the earlier attempts to use rock magnetism in applied geophysics. Such success as attended the magnetic orientation of borehole cores, for which the assumption was commonly made that the polarization was similar to that of the present field, must be attributed to the fact that the sediments in question were magnetically unstable. Thus since the last reversal of the polarity of the field an isothermal remanent magnetization approximately in the direction of the present field had been built up which effectively masked whatever original magnetization was present.

Similarly, where the Koenigsberger ratio (remanent magnetic intensity divided by the intensity induced by the present earth's field) is of the order of one or greater, as is the case for most igneous rocks and probably for most metamorphic rocks, the interpretation of magnetic surveys in terms of an induced magnetization along the present earth's field is likely to be misleading.

Clearly the correct procedure in both these problems is to find outcrops of the rock series being investigated, on a representative selection of samples of which determinations of remanent magnetization, susceptibility and stability tests can be made.

USE OF ROCK MAGNETISM IN AGE DETERMINATIONS

The variation of the geomagnetic field in time makes possible a new method of dating rocks, in which the magnetization is their original one. The field apparently varies on three different time scales.

(1) The secular variation of which we are aware through measurements in historical time is, on a geological scale, a rapid one. It seems to consist of multipole magnetic components superposed on a dipole field orientated along the axis of rotation. It is probable that the field has no appreciable components of periods greater than a few thousand years but this cannot easily be examined. The dominant component at any place appears to be a roughly conical movement of the magnetic vector, clockwise when viewed along the vector towards its north seeking end, the path closing in about 500 years. This can be shown to be the result of the westward drift of the core relative to the mantle. We cannot be sure that this drift will always remain westward, only that the velocity of drift has an upper limit and therefore the precession of the magnetic vector cannot be too fast. Consequently the path traced out by the magnetic polarization vector in a continuous series of sediments may eventually be used to give some clue to its rate of deposition.

(2) The reversals of the geomagnetic field appear to occur very rapidly, perhaps in a few thousand years, the order of time required for the electric currents sustaining the field in the core to decay freely. Thus they may provide a stratigraphical horizon of value in correlation problems so far lacking in igneous rocks, see Hospers (1953 and 1954). The discussion of the interpretation of reversals of magnetization has not yet reached the stage where this can be used with confidence, for though the evidence for the occurrence of reversals of the geomagnetic field is very strong, the picture is complicated, to a degree not yet established, by the natural occurrence of self-reversal of magnetization in certain rocks (Nagata, 1951 and 1953).

(3) Comparison of the mean directions of magnetization of rocks of the same period in different continents will throw light on whether relative movements of the continents have occurred. This comparison has only so far been made between Europe and the south western U.S.A. The pole positions deduced for rocks of the same geological period in both places are sufficiently in accord for continental drift to be relatively unimportant in their interpretation (see Runcorn, 1956). This certainly does not exclude it being a major effect elsewhere in the world. There is a possibility of minor movements of continental masses of interest in connection with tectonic processes which need investigation. The Himalayan mountain building was possibly accompanied by a movement of India northwards relative to Asia by about 100 miles. To investigate this sufficient specimens must be taken to enable the mean direction to be determined with an error of less than a degree. At present this would involve the measurement of many hundreds of specimens and the investigation of the possibility of systematic deviation between the magnetization of rocks and the magnetizing field.

The value of palaeomagnetism in determining the age of non-fossiliferous rocks is evident. The fact that the polarization of the Pilansberg dykes is uniformly in a direction corresponding to poles in Abyssinia and Hawaii (Gough, 1956), would make this of the same age as the Torridonian sandstones of N.W. Scotland i.e. late Pre-Cambrian, supposing that there has been no relative movement of Great Britain and Africa. The geological age is post-Waterburg and pre-Karroo. Similarly Du Bois's pole position for the Keweenawan (du Bois, 1955) lies between the late Pre-Cambrian and Cambrian poles, deduced from English measurements and therefore puts them later, by say 50 million years, than the Torridonian (or the Grand Canyon series).

When any systematic differences between the direction of the field at the time of formation of a rock and the magnetization it acquires can be allowed for, the accuracy of the mean direction should be such that magnetic zoning is possible. The pole moves a degree in a few million years, so that zoning and correlation to a million years in most parts of the geological column should eventually be possible.

Applications to the thermal history of rocks

The magnetization of metamorphic rocks will be acquired at many stages in the history of the rock corresponding to the cycles of metamorphism. The Curie points of the iron oxide minerals range between 700°C and 200°C and any particular rock is not likely to have only one component (Nicholls, 1955). Thus if the rock is raised to different temperatures in different cycles of metamorphism different minerals will become magnetized at different times. If the time interval is sufficient, they will become magnetized in different directions. Consequently there is the possibility that the metamorphic history of rocks may be read in the different magnetic components present within it. In particular the origin of granites may be elucidated. If they have originated by being cooled from a magma, the stable and intense thermoremanent magnetization produced should be recognisable. If the granites have resulted from the metamorphism of sediments at comparatively low temperatures, only those minerals with low Curie points will have acquired the thermoremanent magnetization. Such developments await the construction of apparatus to study systematically the magnetization of rocks at different temperatures.

References

Du Bois, P. M. 1955, Nature, 176, 506.
Gough, D. I., 1956 M.N.R.A.S., Geophys. Suppl.
Hospers, J., 1953, Kon. Ned. Akad. Weten. 56, 467-476, 477-491.
Hospers, J., 1954, Kon. Ned. Akad. Weten. 57, 112-121.
Lynton, E. D., 1937 Bull. Amer. Assoc. Petroleum Geol., 21, 580-615.
Lynton, E. D., 1937, Geophysics, 3, 122-129.
Nagata, T., 1951, Nature 169, 704.
Nagata, T., 1953, Nature 172, 805.
Neel, L., 1955, Adv. in Phys. 4, 191-243.
Nicholls, G. D., 1955, Adv. in Phys. 4, 113-190.
Runcorn, S. K., 1955, Adv. in Phys. 4, 244-291.
Runcorn, S. K., 1956, Bull. Geol. Soc. Amer., 67, 301-316.

COMBINED ANALYSIS OF GRAVIMETRIC AND MAGNETIC ANOMALIES AND SOME PALAEOMAGNETIC RESULTS *

BY

ASGER LUNDBAK **)

ABSTRACT

An attempt is made to interpret some magnetic anomalies in Denmark and Northern Holland. As the thickness of the nonmagnetic sediments in the areas is large, the interpretation must depend mainly on computational procedures, i.e. a combined analysis of gravimetric and magnetic anomalies, assuming that the two kinds of anomalies originate in the same body.

The mathematic basis of these computations is presented, and from this conclusions are drawn about both direction and intensity of the magnetism in the underlying rocks.

On this basis, the magnetic declination in these rocks appears to be westerly for all the areas considered. This declination is, of course, a combined effect of induced and remanent magnetization. The corresponding magnetic inclination is smaller than the inclination existing at the surface, and in several cases the magnetic inclination in the rocks is clearly negative, i.e. directed upwards.

Both the declination and the inclination in the rocks vary considerally from one locality to another. However, if we assume that these varying results are caused mainly by different ratios of the strengths of induced and remanent magnetism, the directions of remanent magnetism group themselves around a fixed declination, about -160°, and a fixed inclination, about -60°.

Estimates of the magnitude of both induced and remanent intensities of magnetization are contained in these conclusions. In both cases the magnitude may be of the order 10^{-2} cgs units.

The hypothetical geomagnetic poles corresponding to this direction of natural remanence are situated near the central part of the northern Siberian coast and near that part of the Antarctic coast just south of South America.

INTRODUCTION

It is a wellknown fact that gravitational and magnetic effects are often caused by the same bodies (cf. S. Werner, 1945); in particular it may be emphasized that many ore-bodies possess a greater specific gravity as well as a greater intensity of magnetization than the surrounding sediments or rocks.

The basic principle of the combined analysis is founded on certain potential considerations. A fundamental point is that the same power of r — the distance from the source —can be obtained in both gravitational and magnetic effects by differentiating with respect to r, that is to say, by differentiating the gravitational potential one time more than the magnetic potential. Than it is possible to eliminate r and to obtain relations containing gravitational and magnetic properties of the rocks considered. On the other hand, no knowledge of r is obtained by such procedure, as r has been eliminated.

---

* Presented at the Ninth Meeting of the European Association of Exploration Geophysicists, held in London 7-9 December 1955.

**) Danish Meteorological Institute.

Concerning the magnetization of the rocks it is important to take into consideration that the direction of this magnetization is unknown initially. As a rule the magnetization is a resultant of two vectors, the induced and the remanent magnetism respectively.

It has been known for many years, at any rate since the end of the 19th century, that the directions of the remanent magnetizations frequenly differ from the directions of the induced magnetizations. Good reviews with many references have been given by J. G. Koenigsberger (1938) and T. Nagata (1943), who has also given a newer treatment of the problems involved (1953).

A connection between the axis of rotation and the geomagnetic axis is very probable, and various recent contributions have dealt with their displacements during the history of the Earth (A. Lundbak, 1954; J. Hospers and H. A. K. Charlesworth, 1954; J. M. Bruckshaw, 1954; J. A. Clegg, M. Almond and P. H. S. Stubbs, 1954; T. Einarsson and Th. Sigurgeirsson, 1955; S. K. Runcorn, 1955; A. A. Day and S. K. Runcorn, 1955; P. M. du Bois, 1955; J. W. Graham, 1955). Further contributions by several authors are to be found in a special number (Vol. VI. No. 4, Dec. 1954) of the Journal of Geomagnetism and Geoelectricity, Kyoto. The general view is, that the two axes have always been nearly parallel, i.e. sometimes directed in opposite or antiparallel directions, as in the present time, and sometimes directed along the same direction. The physical background of this is fully consistent with the dynamo theory of the geomagnetic field (cf. E. Bullard and H. Gellman, 1954).

PROCEDURE

Returning to the combined analysis of gravimetric and magnetic anomalies a possible procedure is outlined below (fig. 1). A buried volume element $\triangle v$ produces at a point P on the surface of the ground a gravimetric potential $\triangle V$, given by

$$\triangle V = -G\rho \triangle v/r,$$

G being the gravitational constant 6.668×10^{-8} cgs-units, ρ the density of $\triangle v$ and r the distance between $\triangle v$ and P.

In similar way the magnetic potential $\triangle U$ from the volume element $\triangle v$ can be written.

$$\triangle U = |M| \triangle v \cos\theta/r^2,$$

$|M|$ being the numerical or scalar value of the intensity of magnetization and θ the angle between the direction of this magnetization and the direction of r reckoned positive towards P.

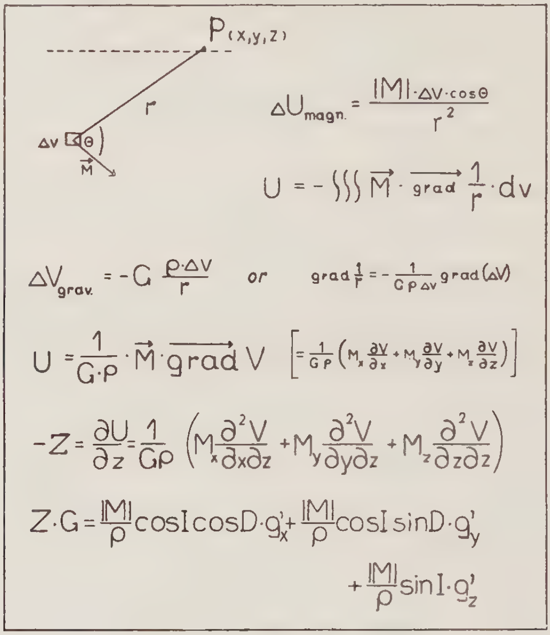
P(x,y,z)
r
Δv
θ
$\vec{M}$
$\Delta U_{magn.} = \frac{|M|\cdot\Delta v\cdot\cos\theta}{r^2}$
$U = -\iiint \vec{M}\cdot\overrightarrow{grad}\,\frac{1}{r}\cdot dv$
$\Delta V_{grav.} = -G\,\frac{\rho\cdot\Delta v}{r}$ or $grad\,\frac{1}{r} = -\frac{1}{G\rho\Delta v}\,grad(\Delta V)$
$U = \frac{1}{G\cdot\rho}\cdot\vec{M}\cdot\overrightarrow{grad}\,V \left[=\frac{1}{G\rho}\left(M_x\frac{\partial V}{\partial x}+M_y\frac{\partial V}{\partial y}+M_z\frac{\partial V}{\partial z}\right)\right]$
$-Z = \frac{\partial U}{\partial z} = \frac{1}{G\rho}\left(M_x\frac{\partial^2 V}{\partial x\partial z}+M_y\frac{\partial^2 V}{\partial y\partial z}+M_z\frac{\partial^2 V}{\partial z\partial z}\right)$
$Z\cdot G = \frac{|M|}{\rho}\cos I\cos D\cdot g'_x + \frac{|M|}{\rho}\cos I\sin D\cdot g'_y + \frac{|M|}{\rho}\sin I\cdot g'_z$

Fig. 1. Relation between the gravimetric and magnetic anomalies produced by the same body

If we use vectors for both gradient of $1/r$ and for intensity of magnetization (the scalar value of which will be designated by M solely in the following), and if we sum up the effects of several volume elements in integrating, we get

$$U = -\int\int\int \vec{M} . \overrightarrow{\mathrm{grad}}\,(1/r)\,dv.$$

It may be remarked that the potentials here considered are exclusively dealt with as potentials in the free space. As such they have partial derivatives of all orders, and all of these derivatives are continuous at all points of the free space. It means i.a. that Laplace's differential equation is valid.

The gradient of $1/r$ in the above scalar product can be transcribed by means of the first equation, where only $\triangle V$ and r are allowed to vary:

$$\overrightarrow{\mathrm{grad}}\,(1/r) = -\frac{1}{G\rho\,\triangle V}\,\overrightarrow{\mathrm{grad}}\,\triangle V.$$

Inserting in the expression for U and integrating we get (apart from an integration constant)

$$U = \frac{1}{G\rho} \vec{M} \cdot \overrightarrow{\text{grad}\, V}.$$

It is here supposed that $\vec{M}$ is constant in magnitude and direction, as also ρ is still supposed to be constant. In passing it may be mentioned that a similar formula has been used recently by *V.* Baranov for computation of socalled pseudo-gravimetric anomalies, i.e. magnetic anomalies translated to a form analogous to gravimetric anomalies (to be published).

Projecting $\vec{M}$ on Cartesian coordinate axes, getting M_x, M_y and M_z respectively, and using partial derivatives of V with respect to these coordinates, namely $\partial V/\partial x$, $\partial V/\partial y$ and $\partial V/\partial z$, the last equation and the enclosed scalar product can be written

$$U = \frac{1}{G\rho}\left(M_x \frac{\partial V}{\partial x} + M_y \frac{\partial V}{\partial y} + M_z \frac{\partial V}{\partial z}\right).$$

For convenience the direction of the X-axis is taken positive to the north‘ the direction of the Y-axis positive to the east and the direction of the Z-axis positive vertically downwards.

By differentiating once more, with respect to z, we get for the magnetic vertical intensity Z in P:

$$\begin{aligned} Z &= -\frac{\partial U}{\partial z} \\ &= -\frac{1}{G\rho}\left(M_x \frac{\partial^2 V}{\partial x\, \partial z} + M_y \frac{\partial^2 V}{\partial y\, \partial z} + M_z \frac{\partial^2 V}{\partial z\, \partial z}\right). \end{aligned}$$

Now, as shown by R. Eötvös (1907),

$$\begin{aligned} \frac{\partial^2 V}{\partial x\, \partial z} &= \frac{\partial^2 V}{\partial z\, \partial x} = -\frac{\partial g}{\partial x} = -g'_x, \\ \frac{\partial^2 V}{\partial y\, \partial z} &= \frac{\partial^2 V}{\partial z\, \partial y} = -\frac{\partial g}{\partial y} = -g'_y, \\ \frac{\partial^2 V}{\partial z\, \partial z} &= -\frac{\partial g}{\partial z} = -g'_z, \end{aligned}$$

g'_x, g'_y and g'_z indicating the gradients of gravity along the coordinate axes; further, introducing the magnetic inclination I and the magnetic declination D of $\vec{M}$, so that

$$\begin{aligned} M_x &= M \cos I \ \cos D, \\ M_y &= M \cos I \ \sin D \\ \text{and } M_z &= M \sin \ I, \end{aligned}$$

we get (when both sides of the equation are multiplied by G)

$$ZG = (M/\rho)\cos I \cos D\, g'_x + (M/\rho)\cos I \sin D\, g'_y + (M/\rho)\sin I\, g'_z.$$

In this final equation the gravity constant G and the magnetic vertical intensity Z are regarded as known quantities. The unknown quantities are the properties of the buried rock, namely the "buried" magnetic inclination I, the "buried" magnetic declination D and the proportion M/ρ. As to the gradients of gravity — g'_x to the north, g'_y to the east and g'_z downwards—, they are considered known quantities, as they can be computed on the basis of the gravity g in an area surrounding the point considered.

The computation of g'_x and g'_y offers no difficulty. g'_x f. inst. is the difference between two g-values on the meridian through the point considered divided by the corresponding distance, provided that the variation of g is sufficiantly smooth. Computation of g'_z is more difficult, but various authors (W. Hofmann, 1949; B. Kosbahn, 1949; V. Baranov, 1953; see also the discussion by V. Baranov and J. Tassencourt, 1954) have presented formulas well fitted for practical use. Further, this first vertical derivative g'_z can be computed from the second vertical derivative g''_z, which is more easily computed directly from g (H. A. Ackerman and C. H. Dix, 1955).

Before a presentation of some practical applications it can be mentioned, that a kindred procedure has been given by G. D. Garland (1951), and H. Haalck (1929) has made use of formulas like the above formula for Z, dealing with induced magnetization at Kursk and using results from torsion balance measurements in separate points.

APPLICATIONS

Four different areas in Denmark and one area in Northern Holland have been treated along the lines sketched. For computation of the vertical gradient g'_z of gravity the following formula has been employed:

$$g'_z = \frac{2}{d_1}\left(\overline{g_0} - \frac{7}{10}\overline{g_2} - \frac{2}{15}\overline{g_4} - \frac{2}{35}\overline{g_6} - \frac{1}{15}\overline{g_{10}} - \frac{1}{30}\overline{g_{18}}\right).$$

d_1 is the diameter of a circle with the point in question as centre, $\overline{g_0}$ is the mean value of the Bouguer-values within this circle, $\overline{g_2}$ is the Bouguer mean value in a circular belt between circles with diameters d_1 and $3d_1$ and with the point in question as centre. It is analogous for the mean values $\overline{g_4}$, $\overline{g_6}$, $\overline{g_{10}}$ and $\overline{g_{18}}$, so that f.inst. $\overline{g_{18}}$ is the mean value of the Bouguer-values in a circular belt, the diameters of which are respectively 17 d_1 and 19 d_1. As a convenient magnitude of d_1 a few kilometers has been chosen. This g'_z-formula is a modified form of formulas published elsewhere (cf. above); it is considered sufficiently accurate for the purpose.

In most of the areas dealt with 12 points are selected in a regular way, and for each of these 12 points the values of Z, g'_x, g'_z and g'_z are extracted. Further practical details—but only little theoretical basis—were given at an earlier occasion (A. Lundbak, 1954), when also some prerequisites were dealt with. Only, about Z it shall be mentioned, that Z in this respect is the departure from some conveniently chosen normal value of magnetic vertical force.

Under the given circumstances $\vec{M}$ and ρ are not the real magnitudes of magnetic intensity and density in the buried rocks dealt with, but they are the contributions, by which these two qualities exceed those of the surroundings. It is reasonable to think that $\vec{M}$ is rather near the real magnetic intensity in the rocks, as the magnetic intensity of the surroundings is often insignificant. ρ may in the cases dealt with be estimated at about 0.3—0.5 cgs-units.

The first table shows the results obtained. The values in the uppermost line indicate the numbers of points used in each selected area. 12 points f. inst. yield 12 equations, and these can be solved by the method of the least squares. Hereby the values in the following three lines of the table have been obtained. We get, as already mentioned, no information about M and ρ separately, only about their mutual proportion, and it should be remembered, that the vector $\vec{M}$ is the sum of induced magnetization $\vec{M}_i$ and remanent magnetization $\vec{M}_r$.

TABLE I

	Central Jutland	SW-Jutland	North-Holland	Central Seeland	SW-Seeland
Numb. of points	12	12	18	12	12
M/ρ	$1.2 \times 10^{-2} \pm 0.6 \times 10^{-2}$	0.39×10^{-2}	0.42×10^{-2}	0.76×10^{-2}	0.75×10^{-2}
Resultant incl. I	-23° ± 10°	-7°	-1.5°	+28°	+44°
Result. decl. D	-149° ± 13°	-113°	-56.5°	-112°	-28°
D'(ind.-res.decl.)	143°	107°	50°	106°	22°

The units of the proportion M/ρ are cgs-units. The direction of $\vec{M}$ is stated in the two following lines, partially by I, the inclination of $\vec{M}$, and partially by D, the declination of $\vec{M}$. Negative values of I mean that the vectors have directions against the hemisphere over the horizontal plane. Negative values of D mean that the corresponding vectors are directed against the western halfpart of the horizon. In the areas considered the actual declination at the groundsurface is negative too, although it is numerically small. The differences between the actual declination and the computed D-values are entered in the last line of the table and named D'.

These D'-values are represented in fig. 2. The line N-S is the actual magnetic meridian, and the arrows are projections of the M/ρ-vectors on the horizontal plane. The figures at the arrows indicate their lengths in thousandth parts of cgs-units. Going from south to north the arrows indicate the D'-values of Central Jutland, SW-Jutland, Central Seeland, Northern Holland and SW-Seeland.

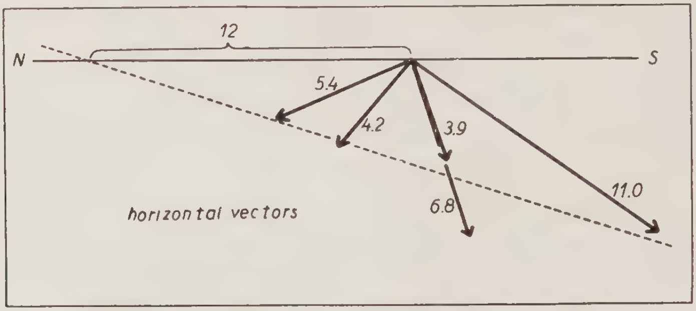

Fig. 2. Resultant declination of rock magnetization in Denmark and Holland

The probable errors are indicated for Central Jutland in the table. The same magnitudes of these errors are valid for SW-Jutland and SW-Seeland, whereas they are somewhat greater for North-Holland and Central Seeland.

DISCUSSION

It appears from fig. 2 that the drawn arrows have rather different directions. Nevertheless, they are all directed towards the western part of the horizon, and their endpoints are grouped along a straight line. Furthermore, the sequence of the arrows, which corresponds to the values of inclination, is almost the same as the sequence given by the values of declination; only Northern Holland and Central Seeland are interchanged.

It is difficult to decide, whether this tendency of regularity has a real basis. If we suppose that it really has, we can draw further conclusions. Such conclusions are supported by the fact that the areas of Northern Holland and Central Seeland have a lesser homogeneous character than the other areas.

Looking at fig. 3 it is to be seen by simple trigonometric considerations, how the following expressions can be computed for the tangent of respectively $D_i - D_r$ and I_r, D_i being the declination of induced magnetization, D_r the declination of remanent magnetization, I_r the inclination of remanent magnetization (and I_i the inclination of induced magnetization):

$$\tan(D_i - D_r) = - \frac{(M/\rho)\cos I \sin D'}{(M_i/\rho)\cos I_i - (M/\rho)\cos I \cos D'}$$

$$\tan I_r = - \frac{[(M/\rho)\sin I - (M_i/\rho)\sin I_i]\cos(D_i - D_r)}{(M_i/\rho)\cos I_i - (M/\rho)\cos I \cos D'}$$

If a fixed value of D_r in all the areas considered is chosen, the resting unknown quantity in the first equation, namely (M_i/ρ), can be computed. Further, substituting these values of D_r and M_i/ρ, respectively in the next equation, I_r can be determined. Finally, M_r/ρ can be computed in similar trigonometric way from these other quantities.

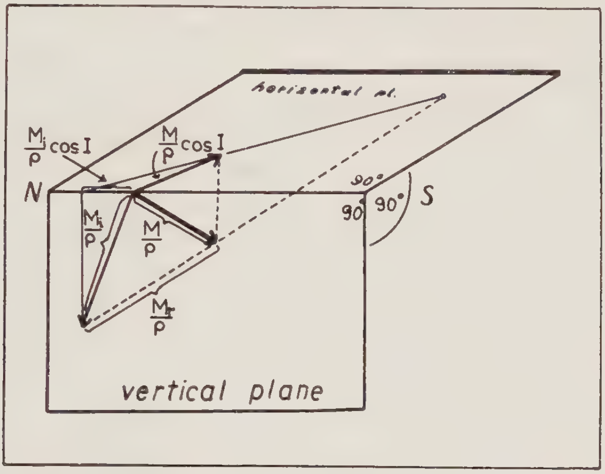

Fig. 3. Illustrating the relations between the components of the rock magnetization

In table II the such obtained values of (M_i/ρ), I_r and (M_r/ρ) are stated; in the uppermost part of the table is chosen the fixed value -166° of D_r, in the lower part -150°.

TABLE II

	Central Jutland	SE-Jutland	North-Holland	Central Seeland	SW-Seeland
M_i/ρ	2.7×10^{-2}	2.6×10^{-2}	3.0×10^{-2}	4.5×10^{-2}	3.0×10^{-2}
D_r	-166°	-166°	-166°	166-°	-166°
I_r	-57°	-66°	-72°	-64°	-76°
M_r/ρ	3.6×10^{-2}	2.7×10^{-2}	3.0×10^{-2}	4.3×10^{-2}	2.5×10^{-2}
M_i/ρ	0.1×10^{-2}	1.1×10^{-2}	1.9×10^{-2}	2.0×10^{-2}	2.2×10^{-2}
D_r	-150°	-150°	-150°	-150°	-150°
I_r	-26°	-60°	-73°	-54°	-78°
M_r/ρ	1.2×10^{-2}	1.3×10^{-2}	1.8×10^{-2}	1.9×10^{-2}	1.6×10^{-2}

It appears that the derived values are differing rather little from each other in the first part of the table, whereas in the second part they are more varying from one area to the other; especially the values of induced intensity of magnetization and the values of remanent inclination are variable.

So, if the remanent declinations from one cause or other have to be the same in all the areas dealt with (which is not proved), a fixed value about -160° or -165° is more probable than a numerical lesser value. The corresponding remanent inclination should then be about -60° or -65°, and both induced and remanent intensity of magnetization should be of the order of magnitude 10^{-2} cgs-units, when ρ is supposed to be about 0.3 cgs-units.

Two questions are still to be answered. The first question is: Do the magnetic and gravimetric effects originate from identical parts of the bedrock or primitive rock? The second question is: What is the depth of the rocks, which produce the anomalies in the areas considered?

The answer to the first of these questions is very decisive on the present assumptions Meantime, as the answers to both the first and second questions cannot be given with sufficient certainty here (the available material is insufficient), the author prefers to leave both unanswered. Thus these results must be considered rather tentative, until further evidence is obtained.

CONCLUSION

The gravimetric and magnetic anomalies at the surface of the ground in Denmark and Northern Holland are supposed to originate from the same deep-seated bodies. From a combined analysis of these anomalies it is concluded, that the intensity of magnetization in these bodies is of the order of magnitude 10^{-2} cgs of unit.

On the tentative assumption that the direction of remanent magnetization in these deep rocks is uniform, this direction is such, that it corresponds to an attracting magnetic pole (the southpole) near that part of the Antarctic coast which lies south of South America. Similarly the other pole (the northpole) may be situated somewhere in the neighbourhood of the central part of the Arctic Siberian coast. At the present time, the first of these poles is situated northwest of Greenland, and the other is situated south of Australia.

REFERENCES

Ackerman, H. A., and Dix, C. H., 1955, The First Vertical Derivative of Gravity, Geophysics, XX, 148-154.

Almond, M., see Clegg etc.

Baranov, V., 1953, Calcul du gradient vertical du champ de gravité ou du champ magnétique mesuré à la surface du sol, Geophys. Prosp., I, 171-191.

Baranov, V., and Tassencourt, J., 1954, Some Remarks on the Errors in Calculation of the Vertical Gradient of Gravity, Geophys. Prosp., II, 285-289.

Bois, P. M. du, 1955, Palaeomagnetic Measurements of the Keweenawan, Nature, 176, 506-507.

Bruckshaw, J.McG., 1954, Rock Magnetism — Some recent Developments, Science Progress, 42, No. 167, 406-418.

Bullard, E., and Gellman, H., 1954, Homogeneous Dynamos and Terrestrial Magnetism, Phil. Trans. Roy. Soc., Ser. A, Vol. 247, 213-278.

Charlesworth, H. A. K., see Hospers etc.

Clegg, J. A., Almond, M., and Stubbs, P.H.S., 1954, The Remanent Magnetism of some Sedimentary Rocks in Britain, Philos. Mag., 45, 583-598.
Day, A. A., and Runcorn, S. K., 1955, Polar Wandering: Some Geological, Dynamical and Palaeomagnetic Aspects, Nature, 176, 422-426.
Dix, C. H., see Ackerman etc.
Einarsson, T., and Sigurgeirsson, T. 1955, Rock Magnetism in Iceland, Nature, 175, p. 892.
Eötvös, R., 1907, Bestimmung der Gradienten der Schwerkraft und ihrer Niveauflächen mit Hilfe der Drehwage. Aus dem ersten Band der Abhandlungen der XV. Algemeinen Konferenz der Erdmessung in Budapest, 1906.
Garland, G. D., 1951, Combined Analysis of Gravity and Magnetic Anomalies, Geophysics, XVI, 51-62.
Gellman, H., see Bullard etc.
Graham, J. W., 1955, Evidence of Polar Shift since Triassic Time, Jour. Geophys. Research, 60, 329-348.
Haalck, H., 1929, Zur Frage der Erklärung der Kursker magnetischen und gravimetrischen Anomalie, Gerlands Beitr. Geophysik, 22, 241-255 & 385-399.
Hofmann, W., 1949, Uber Anvendungen einer Formel zur Berechnung der Vertikalgradienten der Schwere, Geofisica Pura e Appl., XIV, 145-162.
Hospers, J., 1954, Magnetic Correlation in Volcanic Districts, Geol. Mag., XCI, 352-360.
Hospers, J., and Charlesworth, H. A. K., 1954, The Natural Permanent Magnetization of the Lower Basalts of Northern Ireland, Royal Astron. Soc. Monthly Notices, Geophys. supp., 7, 32-43.
Koenigsberger, J. G., 1938, Natural Residual Magnetism of Eruptive Rocks, Terrestrial Magnetism and Atm. Elect., 43, 119-130 & 299-320.
Kosbahn, B., 1949, Uber die Berechnung sämtlicher Feldgrössen aus der Vertikalintensität und deren Anwendung auf die Auswertung von Schwerebildern, Geofisica Pura e Appl., XV, 27-36.
Lundbak, A., 1954, Magnetic Properties of Basement Rocks, Internat. Geol. Cong., Algiers, 19th sess., Comptes Rendus, Sec. 9, fasc. 9, 135-149.
Nagata, T., 1943, The Natural Remanent Magnetism of Volcanic Rocks and Its Relation to Geomagnetic Phenomena, Tokyo Univ. Earthquake Research Inst. Bull., XXI, 1-196.
Nagata, T., 1953, Rock-Magnetism 1rd Ed., Maruzen Co., Tokyo.
Runcorn S. K., 1955, Palaeomagnetism of Sediments from the Colerado Plateau, Nature, 176, 505-506.
Runcorn, S. M., see also Day etc.
Sigurgeirsson, T., see Einarsson etc.
Stubbs, P. H. S., see Clegg etc.
Tassencourt, J., see Baranov etc.
Werner, S., 1945, Determinations of the Magnetic Susceptibility of Ores and Rocks from Swedish Iron Ore Deposits, Sveriges Geologiska Undersökning, Ser. C, No. 472.

THE USE OF INTEGRATORS HELPS COMPUTING TERRAIN CORRECTIONS IN GRAVIMETRY *

BY

C. MONNET **)

ABSTRACT

A special method is described for calculating the terrain correction of the observed gravity data. The ground around each station is divided into a certain number of sectors and a special integral of the topographical section is calculated along each dividing radius.

A computation chart has been constructed, by means of which the integration is reduced to the measurement of an area or of the first moment of an area. A planimeter or alternatively an integrator have to be used for this measurement.

The article shows how to trace the computation chart for the use of the first moment method.

This method has been extensively tested by the author and on the basis of this experience it has been found that the method affords a considerable speeding up of the calculation and is, in this respect, superior to the other methods that have been used so far for calculating the terrain correction.

The problem of the accuracy of the integrator is also discussed in this paper.

INTRODUCTION

It is well-known to all geophysicists working in the gravimetric field that a very great time is expended in computing the terrain corrections to the measured data. The author feels sure that everybody who has been concerned with surveys covering a large area of rugged terrain will have tried at least once to find a way of eliminating or reducing this part of the treatment of data which is extremely tedious when done by the ordinary method.

This article illustrates a method that has been studied and thoroughly tested by the author in various parts of the Appennines and in Sicily with very good practical results due to the exceptional speed obtained in the calculations.

The methods usually adopted for calculating terrain correction require subdivision into zones and compartments of the ground around each station.

The average height of each compartment has to be measured and converted to a datum by means of tables.

---

* Presented as the Ninth Meeting of the European Association of Exploration Geophicists, held in London, 7-9 December 1955.

**) AGIP Mineraria. Milano, Italy.

The results for all compartments have to be added in order to obtain the total correction term for a station.

In the following method the subdivision is accomplished by means of equally spaced radial lines only, so providing a division into sectors instead of into compartments of the ground around each station.

An integral is calculated along each radial section in order to compute that part contributed by the corresponding topographical sector to the correction.

Since the number of sectors may be changed without involving any calculation it is possible to take into account any number of points on the ground. This cannot be done with the usual compartment method in which fixed radii are used for the zones because any change in the radial distances would require the preparation of new tables for the conversion of the data.

The possibility of calculating the integrals and the correction with the required accuracy, afforded by the sectors method, renders it distinctly superior to the old way.

The principal problem is to find a practical and rapid way of computing the integrals.

CALCULATION OF THE CORRECTION BY THE MEASUREMENT OF AN AREA

This system was the first to be put into practical use and has been employed in some companies for at least 20 years. A complete theory of the computation charts has been published (Ballarin 1939, Contini 1953). The use of these charts requires only the plotting of the altimetric section of each sector.

The scale used for the radial distances and the shape of the equal-height lines are so chosen that the areas lying under the topographical section are proportional to the gravitational effect of the corresponding volume elements.

Figure 1 shows a map arranged for computing the terrain correction. The area around the station has been divided into 12 sectors, up to a distance of 5 km. The contour lines are used for plotting the topographical sections on the computation chart. A similar map on a smaller scale is used for computing the terrain correction up to a distance of 20 km. The elevation profile of Fig. 2 corresponds to section 9 of Fig. 1 extended to 20 km.; the absolute difference between the real height of each point and the height of the station has to be used when computing the terrain correction.

The measurement of the areas may be made easily with a planimeter; it has been found useful to trace many sections, preferably in different colours, on the same computation chart.

The number of sectors is, within certain limits, arbitrary and should be fixed according to the topographical nature of the area around the station; however considerable experience in this field suggests that 12 sectors should always be sufficent, since only a very small difference is found when recomputing a station with all the dividing radii rotated through the same angle.

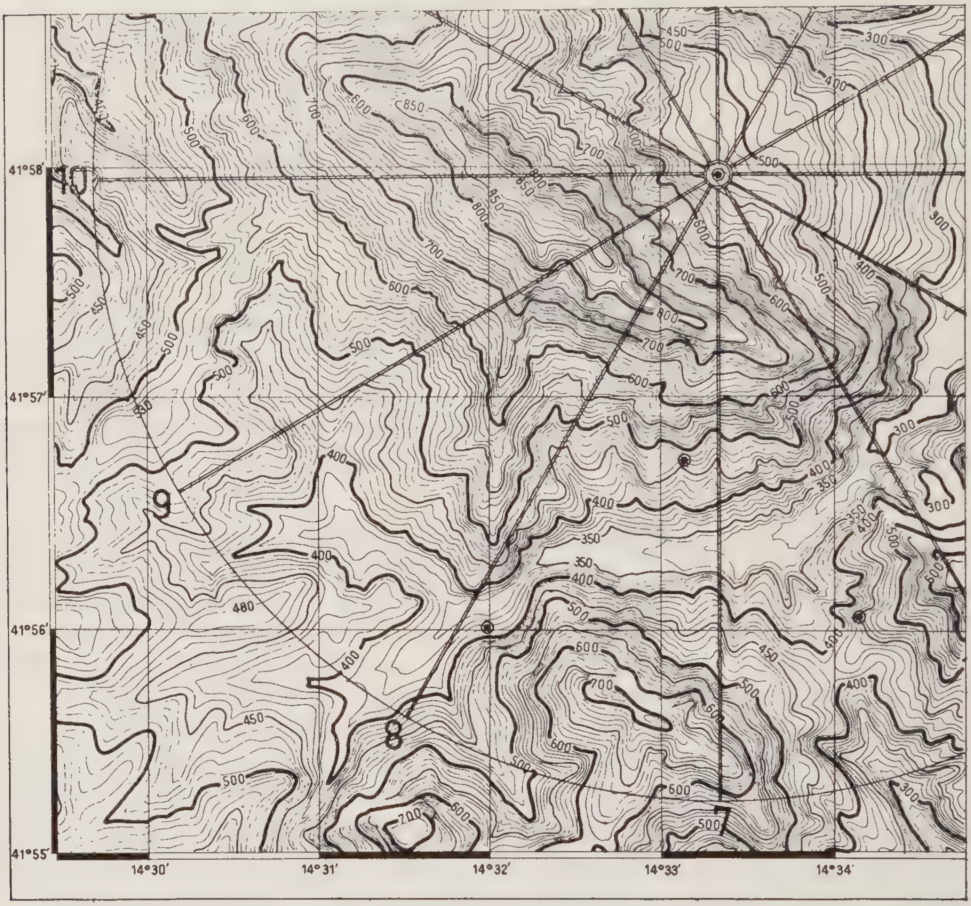

Fig. 1. Part of a map arranged for computing the terrain correction

This way of computation is still rather long and tedious; the following improvements were introduced in order to avoid the tabulation of the height data and the plotting of the altimetric sections:

1) Special maps were drawn, transferring to them from ordinary topographic maps only the contour lines and the stations. These special maps are simpler to use and the time required for drawing them is largely recovered in the subsequent operations.

2) The work is carried on by two operators, one working on the contour

lines map and the other one operating a planimeter on a computing chart of the kind shown in Fig. 2.

3) A certain number of points is fixed on each radius, starting from a station

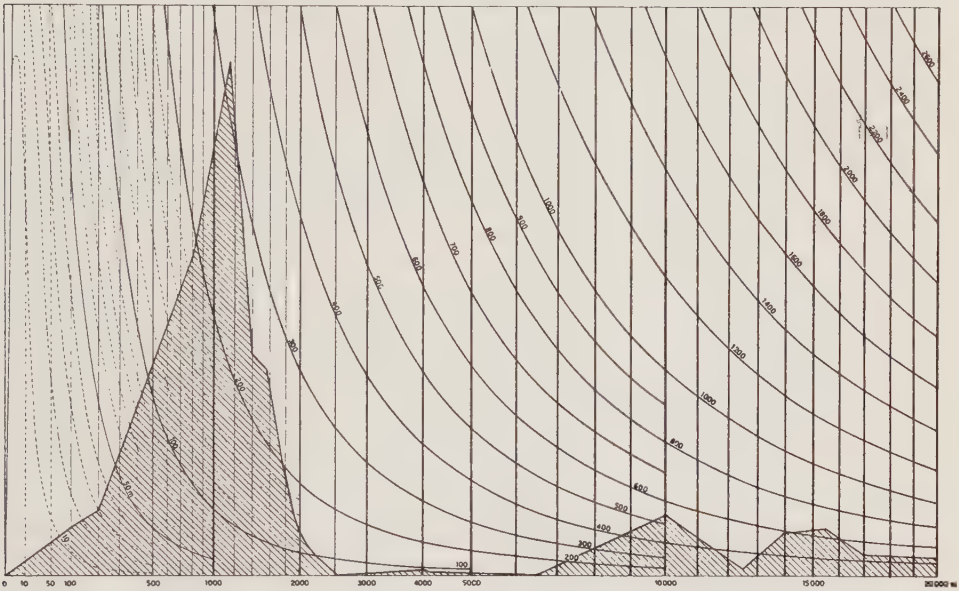

Fig. 2. The chart of computing the terrain correction with planimeter method. The shaded area corresponds to profile 9 of Fig. 1 and its extension

and the corresponding height differences are dictated, by the first, to the second operator, who simply follows the data with the tracing point of the planimeter on the computation chart, without having to plot the altimetric section.

Calculation of the correction by the measurements of a first moment

A reasonably satisfactory speed of work is achieved by the method shown previously; but the first operator has an extremely tedious task in reading the heights, computing the differences and dictating the data to the second operator.

Since this way of computing the differences lends itself to errors of calculation, we felt that a substantial improvement would be achieved if a method could be found to avoid them.

Several modifications of the computation chart were studied and in the end a solution was found satisfactory after thorough testing.

The practical work is carried out along the same general lines of the previous

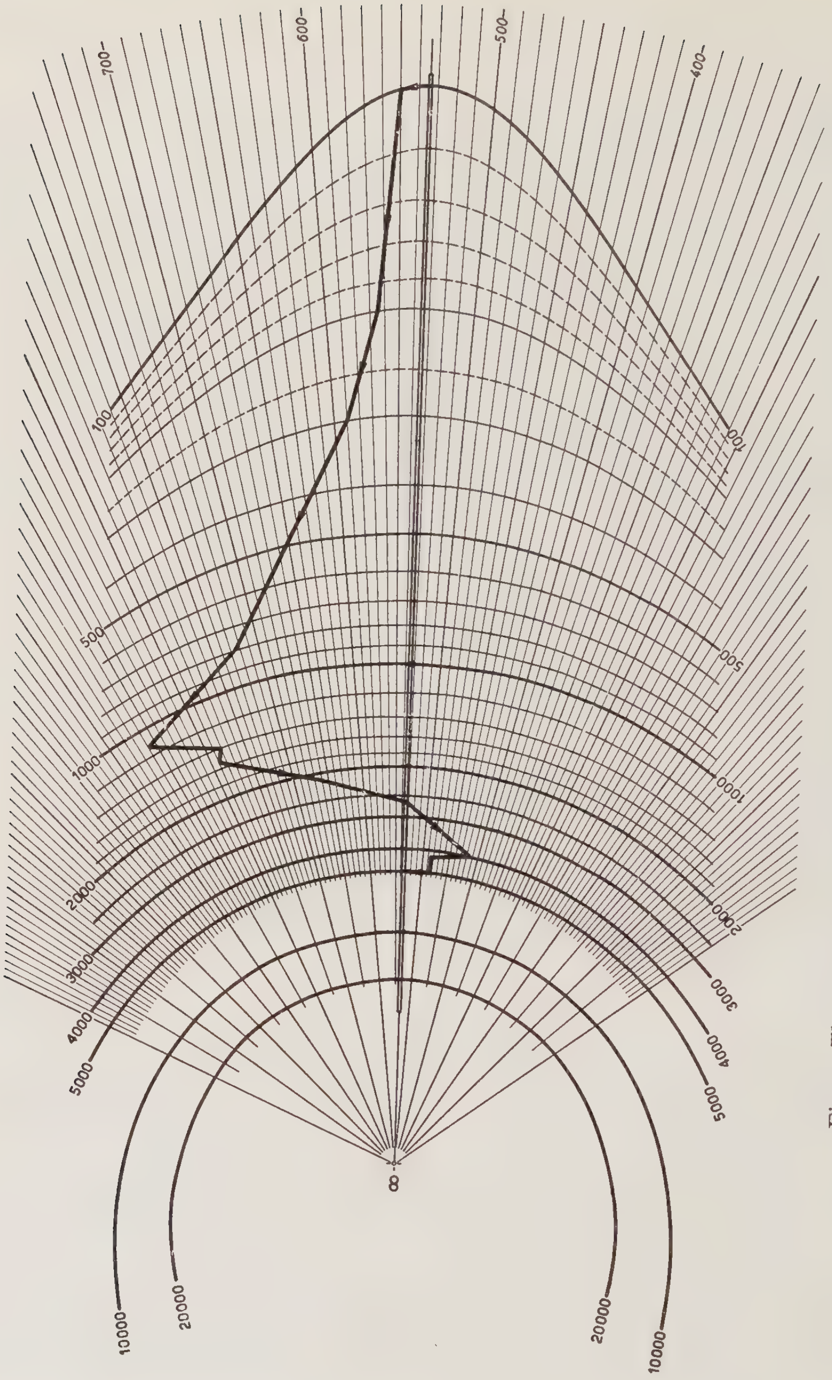

Fig. 3. The chart of computing terrain correction with first moment method. The line with the arrows corresponds to profile 9 of Fig. 1.

method, i.e. with two operators using the contour map, but a difference was introduced in the method of computing the integrals, the measurement of the first moment of an area being substituted for the measurement of the area.

Instead of a planimeter an integrator is used, the tracing point of which is guided over the topographic profile plotted on a special computation chart shown in fig. 3.

The chart is made of two sheets: the upper one is transparent and contains a system of curves (equi-distance lines) symmetrically arranged with respect to a central axis which must be coincident with the axis about which the instrument registers the moments. This axis will be referred to as the moment axis.

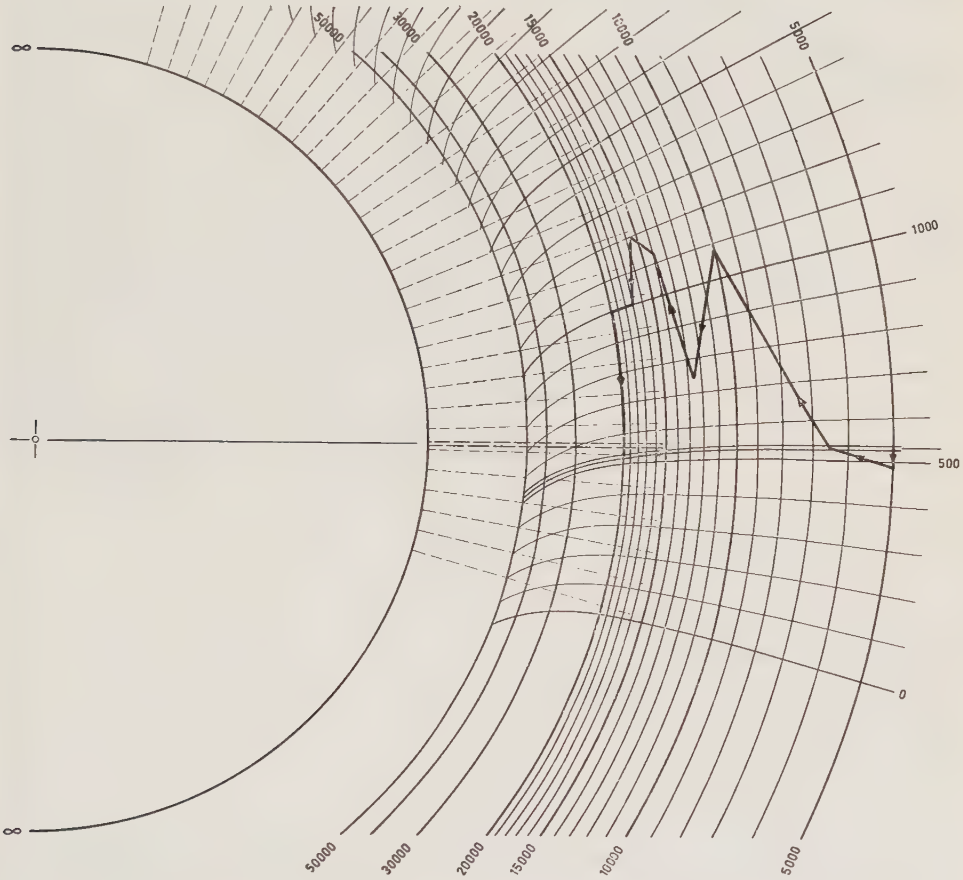

Fig. 4. The chart of computing terrain correction with first moment method for the zone beyond 5 km. from the station. The line with the arrows corresponds to the extension of profile 9 of fig. 1.

On the lower sheet are straight lines (equal height lines) radiating from a pole. This chart has the characteristic feature that a linear relation exists between the height and the corresponding angles. While the upper sheet is always kept fixed, the lower one is rotated when starting to compute the elevation correction for a new station and the line corresponding to the height of the station is brought to coincide with the moment axis on the upper sheet.

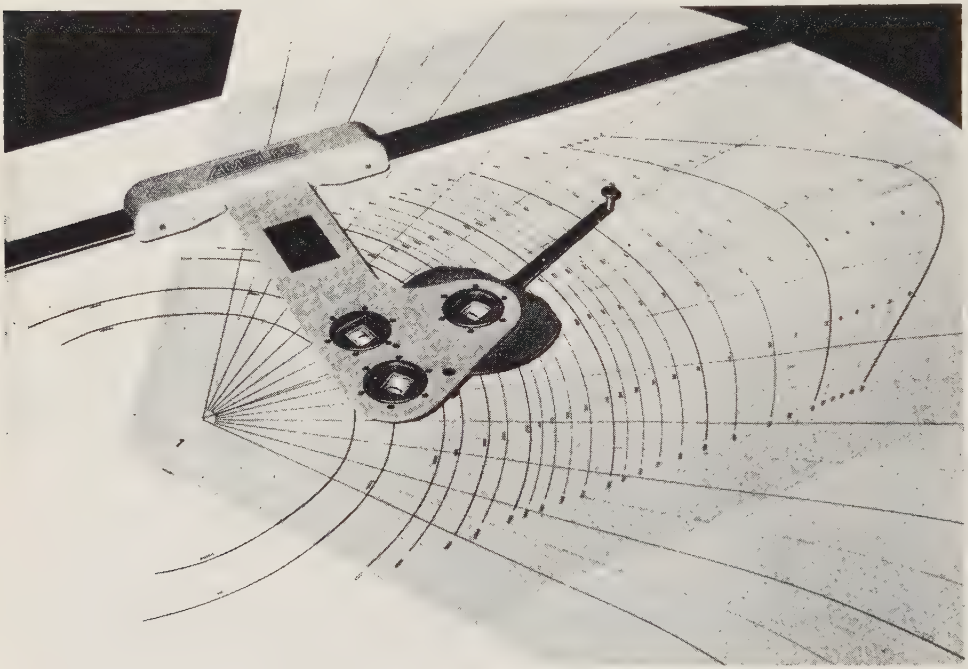

Fig. 5. The chart of Fig. 3 with the integrator in working position.

The actual heights are used when plotting the topographical section and there is no need to calculate the differences.

The first moments of the portions of the section both above and below the moment axis give a positive contribution to the terrain correction, each elementary moment being proportional to the respective gravitational effect.

This chart extends from a distance of 100 meters from the station to infinity. It will be shown further on that it is impossible to draw a chart of this nature starting at the station. The correction for the zone nearest to the station must be computed some other way. However it is easy to see that the contribution to the terrain correction by the circular zone inside a 100 meter radius around the station is quite small and may be calculated easily from the dip of the ground, only using the sectors planimetric method where very complex topography is involved.

Since topographic maps of two different scales are ordinarily used, another chart has been drawn (Fig. 4) which is more suited for computing the influence of zones beyond a 5 km radius from the station. The curvature of the earth is also taken into account in this chart.

On both Figures 3 and 4, section 9 of Fig. 1 and its extension have been plotted.

FORMULAE

Two conditions must be fulfilled when constructing computation charts of the type outlined above:

1) The equal-height lines must be straight lines and the angles between them proportional to the corresponding height differences.

2) The first moment of the areas of the topographical section must be proportional to the gravitational effect of the corresponding volume elements.

The first condition is necessary in order to divide the computation chart into two sheets and to avoid the calculation of the height differences.

Let α be the angle between an equal height line and the moment axis, Z the height and C a suitable proportionality constant. Then, to fulfil the first condition, necessarily

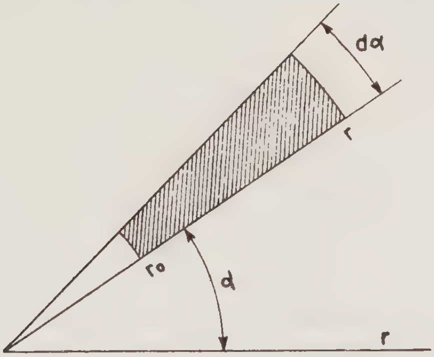

Fig. 6

$$\alpha = CZ \quad \ldots\ldots\ldots\ldots \quad (1)$$

The first moment of a surface element (Fig. 6), enclosed between angles α, $\alpha + d\alpha$ and radii r_0 and r is

$$dM = \frac{r^3 \sin\alpha}{3}\,\mathrm{d}\alpha - \frac{r_0{}^3 \sin\alpha}{3}\,d\alpha \quad \ldots\ldots\ldots \quad (2)$$

The terrain element corresponding to this geometrical surface element is the horizontal layer between the heights Z, $Z + dZ$ above the station O (Fig. 7), and lying within the sector of angular width $2\pi/n$.

The layer has no outer limit but is limited by the inner radius ρ measured from the vertical through the station O.

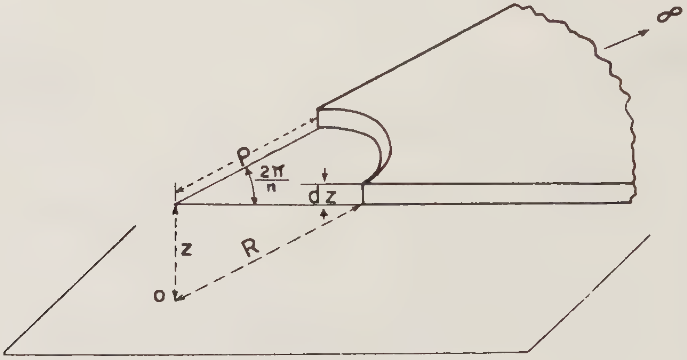

Fig. 7

Let n be the number of sectors, K of the constant of gravity, σ the density of the terrain, and $R = \sqrt{\rho^2 + Z^2}$.

Then the following expression gives the vertical component dg of the gravitational contribution of the terrain element:

$$dg = \frac{2\pi K \sigma}{n} \frac{Z}{R} dZ \quad . \; . \; . \; . \; . \; . \; . \; . \; . \; . \; . \; . \quad (3)$$

Since the computation chart has also to fulfil the second condition above, this requires that

$$AdM = dg, \quad . \; . \; . \; . \; . \; . \; . \; . \; . \; . \; . \; . \; . \; . \quad (4)$$

where A is a proportionality constant characteristic of the computation chart. Substituting in (4) from equations (1) (2) (3) it follows that

$$r = \sqrt[3]{\frac{6\pi K \sigma}{n\,AC^2} \frac{\alpha}{\sin\alpha} \frac{1}{R} + r_0^3}, \quad . \; . \; . \; . \; . \; . \; . \; . \; . \; . \quad (5)$$

where r_0 is an arbitrary function of α. For $\alpha = 0$ equation (5) becomes:

$$r_{\alpha=0} = \sqrt[3]{\frac{6\pi K \sigma}{n\,AC^2} \frac{1}{\rho} + r_0^3}, \quad . \; . \; . \; . \; . \; . \; . \; . \; . \; . \quad (5')$$

Equations (1), (5) and (5′) are used to plot the curves $\rho = \text{const}$ on the upper sheet of the computation chart. The lower sheet is much easier to construct once a suitable value for the constant C has been fixed.

It is obvious that $r_{\alpha=0} = \infty$ is the corresponding value for $\rho = 0$. This explains the impossibility of constructing a computation chart starting from zero. A minimum radius must be fixed at, say, 50 or 100 meters.

The charts shown in Figs. 3 and 4 have been extensively used for surveys in the Appennines and have been drawn for the following values:

Chart of Fig. 3:

$A = 0{,}0001$ mgal for cm^3 measured by the integrator (density $= 1$)
$n = 12$. However, if the number of sectors is changed, the same chart may be used, multiplying A by the fraction $12/x$ where x is the new number of sectors.
$C = 10 \dfrac{\pi}{180}$ for Z measured in hectometers.
$r_0 = 0$ The centre of rotation of the lower sheet corresponds to $\rho = \infty$.
$\rho_{min} = 100$ m.

Chart of Fig. 4:

$A = 0{,}0001$
$n = 12$
$C = 3 \dfrac{\pi}{180}$ for Z measured in hectometers.
$r_0 = 20$ cm.
$\rho_{min} = 5000$ m.

ACCURACY OF THE INTEGRATOR

When using the integrator we noticed that, although extreme care was used in centering and aligning the instrument and the most suitable kind of paper was selected for the contact with the integrating wheel, a regular error was still found in the measurements and an excessive figure was found for the moment of areas near to the moment axis, while the values for areas remote from axis was too small.

In order to understand the reasons for this difference it is advisable to look at the working principles of the instrument (Fig. 8).

A rod AB has a pivot in A and A may move only along a straight line x (moment axis).

The rod is fixed to a gear wheel d, centered on A, and which engages with another gear wheel e, this second gear carries the integrating wheel which rests on the paper. The transmission ratio between the first and the second gear is 2 : 1. Therefore if between the rod AB and the x axis the angle is α, then between the plane of the wheel and the axis the angle will be 2α.

Let us follow the contour of a rectangle with the tracing point B as in Fig. 8. Let x be the horizontal side of the rectangle, c the circumference of the integrating wheel and n the corresponding number of scale graduations; then the recorded difference for contouring the rectangle is

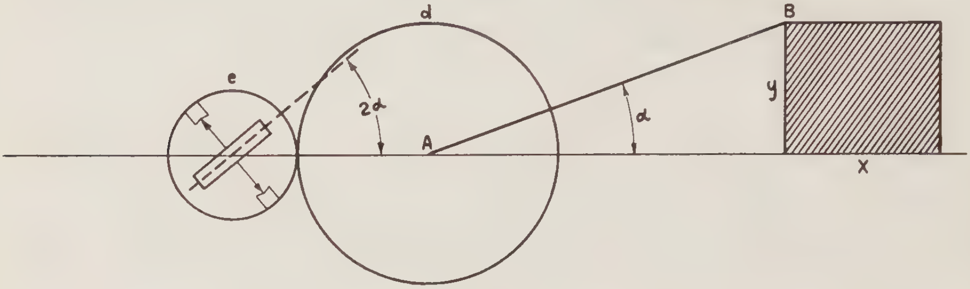

Fig. 8. Scheme of the integrator

$$l = \frac{n}{c}\, x \left(1 - \cos 2\alpha\right) \quad \ldots\ldots\ldots\ldots \quad (6)$$

The recorded difference agrees perfectly with the calculated difference when $2\alpha = 0$ because in this case the wheel doesn't slip on the paper. However if the angle α is different from zero then a certain amount of slip is present and this increases with α. A satisfactory experimental equation was found for the slip ε:

$$\varepsilon = \varepsilon_m \sin 2\alpha \quad \ldots\ldots\ldots\ldots \quad (7)$$

Where ε_m is the maximum slip for $2\alpha = 90°$. The absolute error found when contouring the rectangle is then:

$$e = + \frac{n\, x\, \varepsilon_m}{c} \sin 2\alpha \cos 2\alpha \quad \ldots\ldots\ldots\ldots \quad (8)$$

and the relative error is:

$$e_r = \varepsilon_m \frac{\sin 2\alpha \cos 2\alpha}{2 \sin^2 \alpha} \quad \ldots\ldots\ldots\ldots \quad (9)$$

Fig. 9 shows the curve of absolute and relative errors as a function of the ordinate y for an instrument with an arm AB of 20 cm. The absolute error is plotted as the ratio between the actual absolute error and the fraction $n\, x\, \varepsilon_m / c$. The relative error is plotted as the ratio between the actual relative error and ε_m.

In our case the absolute error is the most important and when tracing the computation chart we have to see that, even in the most unfavorable working conditions, the absolute error from the instrument doesn't exceed a negligible value.

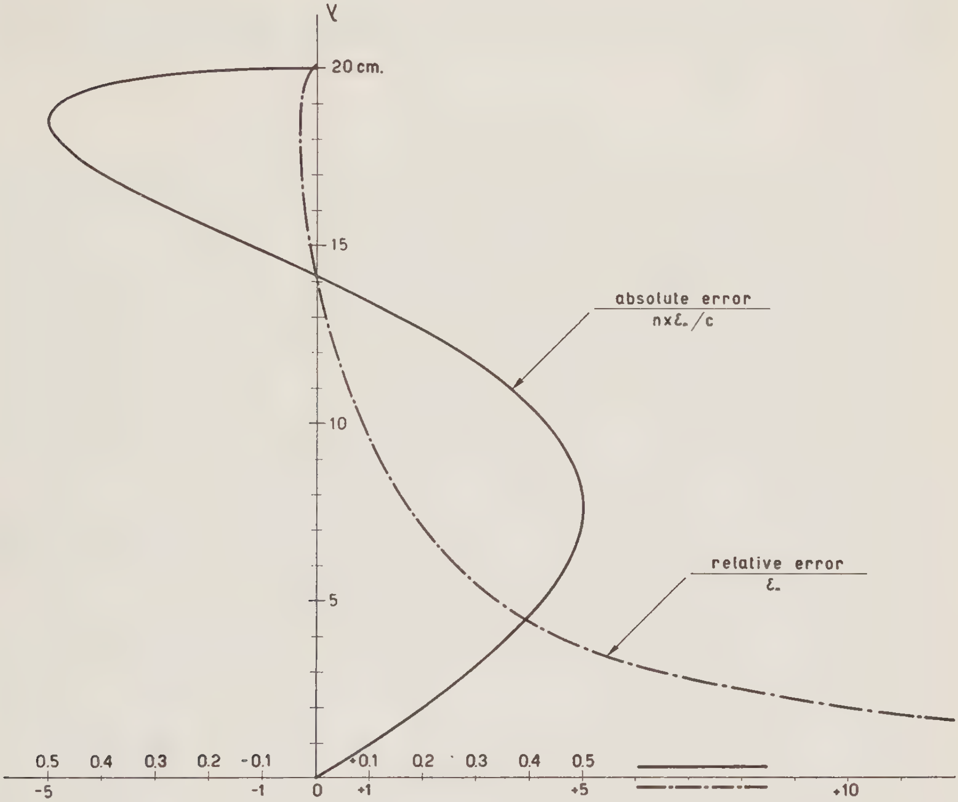

Fig. 9. Absolute and relative errors of an integrator with an arm of 20 cm.:

Y = height of the rectangular figure on the moment axis
x = length of the rectangular figure
ε_m = maximum slip of the wheel.
c = circumference of the wheel.
n = number of the scale graduation of the wheel.

For instance we have an instrument for which a relative error lower than 1,5 % is guaranteed when measuring a rectangular figure of 10 cm. in height; since Fig. 9 shows that the relative error for $y = 10$ is ε_m 0,86, ε_m will not exceed 1,75 %.

The maximum absolute error is 0,875 x for the ordinate $y = \pm 7{,}65$ cm, and $-0{,}875\,x$ for $y = \pm 18{,}48$ cm.

The error would have been zero for $y = \pm 14{,}14$ cm.

Our computation chart is 51 cm. in length and is divided into 12 sectors; the maximum absolute error is then ± 535 cm^3 and results in error of ± 0,053 mgal in the terrain correction.

It should be emphasized however that practical working conditions are usually quite far removed from those corresponding to the maximum absolute error.

REFERENCES

Ballarin S., 1940. Metodi grafici per il calcolo della riduzione topografica di zone vicino al punto di stazione. Memorie della Società Astronomica Italiana. Vol. XIII°, no. 2.

Baranov V., 1953 — Sur le calcul de l'influence gravimétrique des structures définies par les isobathes. Geophysical Prospecting, Vol. I°, n°. 1, p. 36-43.

Bickel H. C., 1948 — A note on terrain corrections. Geophysics, Vol. XIII, no. 2, p. 255.

Bollo R., Goguel J., 1955 — Un intégrateur pour le calcul des corrections topographiques. Geophysical Prospecting, Vol. III, n°. 3, p. 228-233.

Cassinis G., Dore P., Ballarin S., 1937 — Tavole fondamentali per le riduzioni dei valori osservati della gravità. Pubblicazione Nuova Serie n°. 13 della Commissione Geodetica Italiana.

Contini C., 1953 — Il calcolo dell'influenza topografica e la riduzione dei valori osservati nei rilievi gravimetrici di prospezione mineraria. Bollettino di Geodesia, Anno XII, no. 1, p. 31-71.

Hammer S., 1939 — Terrain corrections for gravimeter stations. Geophysics, Vol. IV, no. 3, pag. 184-194.

Hayford J. F., Bowie W., 1912 — The effect of topography and isostatic compensation upon the intensity of gravity. Department of Commerce and Labor — Special publication n°. 10, Government Printing Office, Washington.

Jung K., 1937 — Die Belov'sche Methode zur bestimmung der Wirkung gegeben Massen auf Krümmungsgrössen. Zeitschrift für Geophysik, Year 13, Vol. 2-3.

Schleusener A., 1940 — Nomogramme für Geländeverbesserung von Gravimetermessungen der angewandten Geophysik. Beitrage zur angewandten Geophysik, Vol. 8, n°. 4.

Siegert A. J. F., 1942 — A mechanical integrator for the computation of gravity anomalies. Geophysics, Vol. VII, n°. 4, p. 354-366.

Solaini L., 1943 — Sulla riduzione topografica delle misure di gravità. Rivista Geomineraria, Anno IV, n°. 2/3, pag. 55-67.

THE ELECTRICAL RESISTIVITY OF SOME SULPHIDE AND OXIDE MINERALS AND THEIR ORES *

BY

D. S. PARASNIS **

Abstract

The electrical resistivity of 60 pyrite, 31 chalcopyrite, 42 pyrrhotite, 8 arsenopyrite and löllingite, 6 cobaltite, 15 galena, 13 zincblende, 26 haematite, 46 magnetite, 16 various manganese minerals, 23 complex ores and 7 graphitic shale samples (mostly from Swedish localities) was measured by the four point method. The method and the precautions needed in its application are briefly discussed. The results are presented in the form of a table which also gives other relevant data on the samples (e.g. percentage of ore in a given sample). The results are believed to be of interest to geophysicists engaged in prospecting for ore by electrical methods.

The following can be mentioned among the main conclusions. The electrical resistivity of ore samples varies "locally" on a single sample often by factors of 10-100 but usually within about ± 30% and it often varies by much greater amounts (factors of 100-10000) from one sample to another. The possible causes of such variation are mentioned. The resistivity of pyrite, haematite and magnetite ore samples does not show any significant correlation with the ore content for the samples investigated. There is furthermore no correlation between the standard deviation of the resistivity on a single sample on the one hand and sample resistivity or ore content on the other hand. In the case of chalcopyrite and pyrrhotite the observations suggested the following relations:

For chalcopyrite:

$$\log_{10}\text{ (resistivity in ohmcm)} = (6.2 \pm 4.2)/(\text{vol. \% } CuFeS_2) - (1.39 \pm 0.38)$$

For pyrrhotite:

$$\log_{10}\text{ (resistivity in ohmcm)} = (73 \pm 19) / (\text{vol. \% } FeS) - (3.26 \pm 0.31)$$

The paper concludes by giving the approximate limits within which the electrical resistivity of the various ores investigated appreas to lie. The feasibility of detecting these ores by electrical operations is briefly discussed.

1. Introduction

The Research Board of Svenska Gruvföreningen in Stockholm resolved in February 1949 to investigate the electrical resistivity of the more important Swedish minerals and ores. This paper embodies the results of the investigations on the following minerals and their ores: (1) Pyrite (2) Chalcopyrite (3) Pyrrhotite (4) Arsenopyrite and Löllingite (5) Galena (6) Zincblende (7) Haematite (8) Magnetite (9) Psilomelane, Hollandite and Pyrolusite (10) Miscellaneous manganese minerals.

---

*) Presented at the Tenth Meeting of the European Association of Exploration Geophysicists, held in Hamburg, May 16-18 1956.

**) A/B Elektrisk Malmletning, Stockholm, Sweden.

Graphitic shales were also included in this series later.

From the point of view of the pure physicist the present results probably hold little of interest but it is believed that they may be of some importance to geophysicists engaged in prospecting for ores by electrical methods.

The purest forms in which the above named minerals abound are varied. Pyrite, galena and magnetite are frequently available as fairly large single crystals while chalcopyrite, pyrrhotite and arsenopyrite occur in compact, microcrystalline forms. Large crystals of these three minerals are extremely rare. Heamatite occurs in Sweden both in the form of single crystals (e.g. Malmberget or Långban) and as compact, microcrystalline mass (several localities). Psilomelane, hollandite and pyrolusite are amorphous.

The electrical resistivity of natural crystals of pyrite, galena and magnetite is treated in a separate paper (to be published) and therefore will not be dealt with here. The investigations on their ores, however, will be discussed in the present paper in detail.

2. METHODS OF MEASUREMENT

The electrical resistivity of a substance can be defined as the resistance between the opposite faces of a centimetre cube of that material. More generally, if l is the distance between two equipotential surfaces, s their cross-sectional area and R the resistance between them,

$$R = \rho\, l/s \text{ where } \rho \text{ is termed as the resistivity} \quad \ldots\ldots \quad (1)$$

The above relation can also be written as $E = \rho . j$ where E is the electric field and j the current density. From the theoretical stand-point, this latter definition of ρ is to be preferred. It shows the tensor character of ρ when E and j are treated as vectors. In isotropic media ρ can be represented by a single number (e.g. crystals of the cubic system) whereas in anisotropic media it is necessary to postulate different values of ρ depending upon the direction. It can nevertheless be shown that the tensor ρ has at most two independent components (See, for instance, Wilson 1953) so that two appropriate scalars give a complete representation of the resistivity of *any* anisotropic medium.

It is clear that if a regular specimen of uniform cross section is available the resistivity can be found by measuring the resistance between two plane parallel faces. By cutting the specimen in the appropriate way the resistivity in any desired direction can be determined. However, the labour involved in preparing a specimen of the required regularity is time consuming and prohibitive if a large number of samples is to be investigated. If the resistance across the end faces is to be measured it is absolutely necessary to ensure that contact resistances at the electrodes are negligible. As an alternative, two potential electrodes (probes) may be placed near the end faces but slightly towards the "inside" of the sample. The ratio of the potential drop across them to the current is the resistance R in the above relation but l is the distance between the probes instead of the entire length of the sample. For brevity, this will be refrered to as the definition method.

There is another and an equally direct method of finding the resistivity if a fairly large, homogeneous and isotropic specimen is available. Four point electrodes are placed on its surface in one straight line, the outer two being the current and the inner two the potential electrodes. Let a and c be the distances between a current electrode and the potential electrode nearest to it and b the distance between the two potential electrodes. Then, as is well-known,

$$\rho = 2\pi R/(1/a + 1/c - 1/a + b - 1/b + c)$$

where R is the ratio of the potential difference between the two inner electrodes to the current in the circuit. This is, of course, nothing but the four electrode configuration frequently used by geophysicists in electrical prospecting. Almost all the specimens in the present work were investigated by this method. If, in the above, $a = b = c = l$, say then

$$\rho = 2\pi R l \quad . \; . \; . \; . \; . \; . \; . \; . \; . \; . \; . \; . \; . \quad (2)$$

Strictly speaking the method is applicable to a homogeneous, isotropic and semi-infinite medium with a plane boundary. In practice, the assumptions regarding homogeneity and isotropy will be satisfied if we select our material properly while the specimen may be considered infinite with respect to the electrode configuration if a, b, c, are kept sufficiently small. When a, b, c become comparable to the linear dimensions of the specimen, corrections due to its finite size arise and also the resistivity depends upon the position of the configuration on the specimen. If we have a plate of thickness h extending to infinity in the x an y directions, the apparent resistivity calculated from (2) exceeds the real one by less than 10% for values of l/h and high as 1/2.

The additional error introduced in treating the specimen as infinite when its actual extent is limited in the x and y directions was investigated by measurements in small rectangular glass troughs filled with salt water. The results of these experiments show that as long as the total length of the electrode spread is smaller than the breadth of the sample at right angles to the spread, the error will be less than 10%. Similarly, if the legnth of the spread is kept smaller than 60% of the length of the sample, in the same direction as the spread, the error will be less than 10%. The electrode distances were always chosen with due regard to the above and to the dimensions of each particular sample ¹).

Resistivity values obtained with the definition method did not differ from those by the four point method by more than the experimental errors.

A resistivity meter manufactured by A/B Elektrisk Malmletning, Stockholm, for geophysical purposes was used for measuring the resistance R between the potential electrodes. This is a portable, compact instrument with a built-in low-frequency a.c. ($<$ 20 c.p.s.) generator operated by a handle and crankshaft. Its circuit, in principle, is shown in fig. 1. The meter M is first connected between P_1, P_2 and its deflection is noted. It is next switched to the dotted position and R is adjusted to give the same deflection. R is then evidently equal to the resistance between P_1, P_2. It is obvious that, in principle, the contact resistances at P_1, P_2, C_1 or C_2 do not affect the observations so long as the resistance P_1, P_2 is small compared with the input resistance of the meter (2 megohms). In practice, however, the meter becomes unstable due to stray currents when the contact resistances exceed 200,000 ohms. The instrument covers a total R-range from 10^{-3} to 10^{+4} ohms. Resistances as low as 10^{-4} ohm are measurable by sub-dividing the lowest scale division on the 10^{-3} ohm range but the calibration is not accurate in this part of the scale.

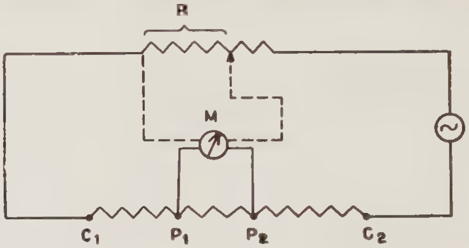

Fig. 1. Illustrating the principle of the ABEM resistivity meter.

The generator delivers an open-circuit voltage of 15, 150 or 250 volts. The current is independent of the variations in the cranking speed within reasonable limits. An older model of the instrument is operated on mains and is capable of measuring resistances from 10^{-4} to 10^{+7} ohms.

3. Previous Work

Most of the early work on the resistivity of minerals is concerned with classifying them as conductors or non-conductors of electricity and is of little quantitative value. The earliest work of any significance in the context of the present paper appears to be an investigation by Bäckström (1888)

---

[1] These experiments were done in the laboratory of A/B Elektrisk Malmletning, Stockholm.

of the electrical (and thermal) resistivities of haematite crystals from Langö in Norway. He obtained a value of about 0.6 ohmcm at room temperature, descreasing with a rise in temperature. Bäckström also mentions 0.0052 ohmcm as the electrical resistivity of a large magnetite crystal from Nordmarken, Sweden.

Beijerinck (1897) gives an extensive list of 380 minerals classified as conductors, or non-conductors but the paper is of limited quantitative value since only in a few cases does he mention the actual resistivity figure (in Siemen's units). He has discussed the observations of earlier workers since 1785 but it is evident that they are only of a qualitative nature except those of Bäckström.

Abt (1897) made determinations on some 17 ore samples among which were 9 fine grained magnetite and 3 haematite samples. The former showed a range of 7 to 4900 ohmcm despite the fact that the iron content was about the same in all. The haematite samples varied between 1430 and 6500 ohmcm. Two pyrrhotite samples gave values of the order of 0.01 ohmcm.

Mönch's measurements (1905) are obviously open to serious objections since they deal with compressed powders and not natural ores. Hayes (1911) came to the conclusion that proper electrical connection cannot be made between compressed Ag_2S powder and the electrodes.

Königsberger and Reichenheim (1906) made a systematic study of "the resistivity of some naturally crystallized oxides and sulphides and of graphite". The minerals investigated were haematite, cassiterite, molybdenite, pyrite, marcasite, galena and graphite.

Löwy (1911) published the resistivity values of 20 minerals samples which he had investigated by means of an a.c. Wheatstone bridge.

Sundberg, Lundberg and Eklund (1925) give a fairly extensvie list of the resistivities of the ore minerals common in Sweden. Details of the measurements are not given. [1])

Kerr and Cabeen's results (1925) are not of any quantitative use. They ordered a number of ore minerals according to the resistivity by means of a simple apparatus with glow lamps.

Harvey (1928) studied the resistivity of ores by means of "microelectrodes". A system of four electrodes separated from each other by small known fractions of a milimetre was placed on the relevent parts of an ore by looking through a microscope. Harvey presents the results in terms of the measured resistance between the potential electrodes although the resistivity in ohmcm can be calculated from the well-known formula of equation (2). His failure to eliminate the contact resistances by the use of liquid droplets under the electrodes is corroborated by the present writer's experience.

---

[1]) In this as well as most old papers the dimensions of electrical resistivity are incorrectly expressed as ohm per cm^3.

Jakosky, Anderson and Wilson (1932) published data on the "electrical properties of typical American ores, minerals and gouges". In the authors' words, "the studies described in this paper were made primarily to determine the variation of conductivity with frequency of pure minerals, and the influence of moisture content as exemplified by measurements upon typical fault gouges, clays and soft shales". Many of the minerals listed in their table 2 show no difference between the d.c. and the lowest a.c. resistivity although the frequency used was high as 20 kc/s.

Smith (1940) has studied the "variations in the electrical conductivity of pyrite". 35 crystals from various localities showed a variation from 0.021 to 246 ohmcm with modal values round 0.1—1.0 and 1.0—10 ohmcm. All these measurements were made on natural crystals [1]).

Most of the above workers have used a Wheatstone bridge to determine the resistance of a regular sample held between plane electrodes. In order to secure good contacts at the faces, resort has been taken to various methods. The faces were electroplated with gold, silver or copper and pressed between several layers of tinfol. Graphite and lead, mercury as well as its copper amalgam have also been used to obtain good contacts with the electrodes.

4. Results of the Present Work.

The results are collected in table I where other relevant data on the samples will also be found.

The selection of the samples has been very largely subjective inasmuch as no randomization procedure was used. The samples have been taken mostly from established mineralogical and geological collections. There is a natural tendency in such collections for rich and "interesting" ore samples to be represented to a greater extent than poorer ones.

The percentage of ore by volume in a sample has been estimated from its specific gravity. If g, g_0 and g_1 are respectively the specific gravities of the sample, the pure mineral and the gangue, then obviously,

$$\text{volume percentage of ore mineral} = 100\,\frac{g - g_1}{g_0 - g_1} \quad \ldots\ldots\ldots\ldots \quad (3)$$

Depending upon the size, shape etc. of the sample, the specific gravity was determined by 1) weighing in air and water or 2) weighing in air and carbon tetrachloride or 3) weighing in air and measuring the volume by displacement.

---

[1]) Smith's analysis has been reexamined in some respects by the present writer in a separate paper (Jernkontorets Annaler, Stockholm, vol. 140, 1956, pp. 494-511).

TABLE I

Electrical Resistivity of Minerals and Ores

The number of observations on a sample is given after the resistivity value in brackets. In column 2 the references are to Swedish places unless some other country is mentioned.

No. 1	Locality 2	Resistivity ohmcm 3	Sp. gr. 4	vol. % ore 5	gangue sp.gr. 6	Prin. gangue min. 7	Remarks 8
	1. PYRITE						
	*Västerbotten**						
	Bjurfors						
1)	östra	3-300 (5)	3.61	40	2.7	quartz	some ZnS
2)	jordrymning 11-v. del	0.44 ± 0.12 (5)	4.72	87	2.9	qu.+ZnS	some PbS
3)	östra	0.24 ± 0.05 (4)	3.72	44	2.75	various	polished
4)		60-260 (8)	4.09	56	2.75	various	polished
	Boliden						
5)		1.88 ± 0.70 (7)	4.4	74	2.7	quartz	
6)		2.88 ± 1.14 (5)	4.0	58	2.7	quartz	
	Rävliden						
7)		1.60 ± 0.34 (8)	4.6	77	3.3	amphibole	
8)		2.00 ± 0.51 (12)	4.54	79	2.8	qu.+amph.	polished
9)	Bh. 21.36 m	2.2 ± 1.5 (16)	4.29	42	3.8	qu.+ZnS	
10)	Rävlidengruva (banded)	ca 35 (2) ca 200 (2)	2.88	9	2.7	quartz	parallel bands across bands
11)	Ö. Högkulla	0.051 ± 0.022 (15)	4.35	35	4.0	ZnS	polished
12)	Rudtjebäcken	0.4-8.0 (10)	4.64	84	2.7	quartz	
13)	Rudtjebäcken	3.98 ± 1.47 (10)	4.68	86	2.75	various	polished
14)	Rudtjebäcken	0.2-4.5 (6)	4.69	86	2.75	various	polished
15)	Malå	7.4 ± 2.0 (6)	4.16	63	2.75	various	polished FeS, $CuFeS_2$ pr.
16)	Udden Bh. 21.05 m	845 ± 230 (3) 3190 ± 1460 (4)	3.48	34	2.7	quartzite	parallel bands across bands
	Ö. Akulla						
17)	Bh. 4.21 m	0.68 ± 0.22 (5)	3.31	25	2.85	qu.+cordierite, FeS pr.	
18)	Bh. 9.48 m	0.18 (0.03-0.4) (6)	3.88	49	2.8	chlorite, FeS, $CuFeS_2$ pr.	
19)	Bh. 1.49 m	285 ± 185 (5)	3.44	33	2.7	sericite qu.	
20)	Mensträsk, Bh. 57.68 m	1-23 (4) 180-600 (3)	3.25	24	2.7	chlo. ser. FeS pr.	
	Dalarna						
21)	Falun	2.50 ± 1.14 (5)	4.4	74	2.7	quartz	
22)	Falun	14 ± 4 (6)	4.1	61	2.7	quartz	
23)	Falun	30 (8-70) (8)	4.6	83	2.7	quartz	
24)	Åhlsgruva	0.7 ± 0.3 (7)	4.3	67	2.7	quartz	

---

* Names of Swedish provinces unless some other country is mentioned.

No.	Locality	Resistivity ohmcm	Sp. gr.	vol % ore	gan- gue sp.gr.	Prin. gangue min.	Remarks
1	2	3	4	5	6	7	8
	Västmanland						
25)	Ervalla	0.28 ± 0.08 (5)	4.0	57	2.7	quartz	
26)	Kaveltorp	0.037 ± 0.017 (8)	4.5	78	2.7	quartz	
27)	Kaveltorp	0.039 ± 0.010 (5)	4.5	78	2.7	quartz	
28)	Kaveltorp	0.098 ± 0.051 (9)	4.55	80	2.7	quartz	
29)	Kaveltorp	0.055 ± 0.018 (5)	4.4	74	2.7	quartz	
30)	Riddarhy.	0.055 ± 0.028 (15)	4.3	65	3.0	qu. + amph.	
31)	Guldsmedshy.	360-2300 (4)	3.90	35	3.3	amphibole	
	Upland						
32)	Dannemora	0.028 ± 0.20 (6)	4.4	74	2.7	quartz	
	Östergötland						
33)	Doverstorp	0.2-4.0 (6)	4.8	92	2.7	quartz	
	Småland						
34)	Kleva	0.013 ± 0.002 (5)	4.90	96	2.7	quartz	
35)	Slättåkra	0.66 ± 0.28 (5)	4.90	96	2.7	quartz	
36)	Ädelfors	0.3-300 (5)	4.4	74	2.7	quartz	
	Norway						
37)	Sulitelma	7 ± 5 (8)	4.8	92	2.7	quartz	
38)	Sulitelma	134 ± 41 (5)	4.6	83	2.7	quartz	
39)	Tromsö	2-10 (4)	4.1	61	2.7	quartz	
40)	Ytteröen	22.2 ± 5.5 (10)	4.2	65	2.7	quartz	
41)	Salten	0.5-33 (10)	4.8	92	2.7	quartz	
	Unknown						
42)	Västerbotten ?	0.2-2.0 (3) 14-60 (5)					

Pyrite crystal aggregates

All the following aggregates are estimated to contain between 95 and 100% FeS_2 by volume.

	Norbotten						
43)	Malmberget	0.006-26 (29)					
	Jämtland						
44)	Brunflo	38 ± 17 (10)					
	Gästrikland						
45)	Gävle	4.2 ± 1.3 (8)					
46)	Jonsåker	60 ± 21 (6)					
	Västmanland						
47)	Håkansboda	0.12 ± 0.07 (5)					
48)	Håkansboda	0.26 ± 0.04 (5)					
49)	Håkansboda	0.06-7.0 (6)					

No. 1	Locality 2	Resistivity ohmcm 3	Sp. gr. 4	vol % ore 5	gangue sp. gr. 6	Prin. gangue min. 7	Remarks 8
50)	Håkansboda	0.03-0.3 (5)					
51)	Håkansboda	0.12-10 (7)					
	Östergötland						
52)	Perstorp	7.2 ± 2.4 (5)					
53)	Perstorp	13.8 ± 6.1 (6)					
54)	Perstorp	8.9 ± 3.3 (5)					
55)	Vadstena-Skänninge	48 ± 23 (6)					
56)	Vadstena-Skänninge	122 ± 22 (5)					
57)	Vadstena-Skänninge	104 ± 11 (5)					
	Småland						
58)	Kleva	0.05-5.0 (16)					
59)	Kleva	0.003-0.04 (4)					
	Skåne						
60)	Börringe	31.2 ± 4.4 (5)					

Notes

43 —crystal size 3-10 mm

44 —crystal size 2-3 mm; interface resistances between crystals estimated to be of the order of hundreds of ohms

45 —crystal size 2-20 mm

46 —crystal size ca 10 mm

47 —crystal size ca 10 mm

48-50—weathered?, crystal size ca 5-10 mm

51 —crystal size ca 20 mm

52-54—three approximately spherical masses each about 25 mm in diameter. Crystals in 52, 53 rarely exceed 4 mms; in 54 several exceed 5 mms

55-57—three beautiful spherical concretions about 40 mms in diameter. Crystal sizes:

55 —fraction to a few mms

56 —fraction to 1 mm

57 —4 to 5 mms

58-59—Crystals vary in size between 6 and 12 mms. Interface resistances are of the order of a few ohms

60 —aggregate similar to 44

2. CHALCOPYRITE

	Norrbotten						
1)	Malmberget	0.30 ± 0.15 (25)	4.24	60		qu. + magnetite	
	Västerbotten						
2)	Rudtjebäcken	0.011 ± 0.002 (4)	4.21	80			ca 20% *FeS*
3)	Rudtjebäcken	0.13 (0.01-0.4)		ca 10			

No.	Locality	Resistivity ohmcm	Sp. gr.	vol % ore	gangue sp. gr.	Prin. gangue min.	Remarks
1	2	3	4	5	6	7	8
4)	Kuorbevarefältet	1-30 (5)	3.2	27	2.75	quartz	banded
5)	Lainijaur	0.022 ± 0.008 (4) 0.1-0.9 (3)	4.3	100	—	—	
6)	Granlunda	0.10 ± 0.05 (11)	4.02	88	2.75	quartz	polished
	Dalarna						
7)	Falun	0.015 ± 0.006 (8)	4.1	94	2.7	quartz	
8)	Falun	0.019 ± 0.011 (5)	3.8	73.5	2.7	quartz	
	Västmanland						
9)	Östanberg	0.012-0.14 (12)	3.7	64	2.8	qu. + basic rock	
10)	Förhoppningsgruva	0.6-5.0 (4)	3.18	30	2.75	qu. + basic rock	
11)	Yxsjögruva	0.089 ± 0.044 (5)	3.3	38	2.75	qu. + basic rock	
12)	Riddarhyttan	0.036 ± 0.010 (5)	4.5	70	5.2	magnetite pr.	
13)	Håkandboda	0.064 ± 0.028 (5)	3.3	40	2.7	quartz	
	Värmland						
14)	Rud	0.067 ± 0.022 (4)	3.7	67	2.7	quartz	
	Östergötland						
15)	Åtvidaberg	2.7 ± 1.1 (5)	4.14	96	2.7	quartz	fractured
16)	Åtvidaberg	0.064 ± 0.015 (5)	4.1	93.5	2.7	quartz	
17)	Åtvidaberg	0.068 ± 0.017 (5)	3.9	80	2.7	quartz	
18)	Bersbogruva	0.36 ± 0.19 (5)	4.05	90	2.7	quartz	
19)	Fångögruva	0.18 ± 0.06 (4)	4.0	84	2.7	quartz	
	Småland						
20)	Kleva	0.033 ± 0.008 (7)	4.24	100	—	—	
21)	Kleva	0.028 ± 0.013 (6)	4.2	100	—	—	
22)	Kleva	0.045 ± 0.017 (4)	4.3	100	—	—	
23)	Kleva	0.043 ± 0.002 (4)	4.3	100	—	—	
24)	Kleva	0.03-0.3 (6)	4.24	100	—	—	
	Norway						
25)	Storvuksgruva	0.017 ± 0.003 (5)	3.85	77	2.7	quartz	
26)	Storvartsgruva	0.031 ± 0.013 (6)	4.1	93.5	2.7	quartz	
27)	Kungsgruva	0.037 ± 0.010 (5)	3.9	80	2.7	quartz	
28)	Röraas	0.004-0.13 (5)	3.75	70	2.7	quartz	
	Germany						
29)	Neudorf	0.041 ± 0.006 (60)	4.2	100	2.7	quartz	
	Unknown						
30)		0.7-7.0 (5)	3.9	80	2.7	quartz	

No.	Locality	Resistivity ohm cm	Sp. gr.	vol % ore	gangue sp. gr.	Prin. gangue min.	Remarks
1	2	3	4	5	6	7	8
	Cubanite						
31)	Kaveltorp	0.13 ± 0.08 (5)	3.97	49	3.3	amphibole	
	3. PYRRHOTITE						
	Norrbotten						
1)	Nasafjäll	0.002-0.06 (55)	4.5				fractured
2)	Nasafjäll	0.003	4.7	96	7.5	galena	
3)	Kalix	0.40 ± 0.14 (8)	4.2	75	3.0	qu. + amph.	minute cracks present, polished samples
4)	Kalix	0.59 ± 0.11 (4)	3.92	58	3.0	qu. + amph.	
5)	Kalix	0.69 ± 0.15 (4)	3.81	51	3.0	qu. + amph.	
	Västerbotten						
6)	Vilhelmina	0.0066 ± 0.0012 (9)	4.18	78	2.75	quartz	polished
7)	Lainijaur	0.0014 ± 0.0003 (54)	4.5	95	2.7	quartz	
8)	Lainijaur	0.0014 ± 0.0004 (4)	4.5	95	2.7	quarz	
9)	Högkulla	0.001-0.03 (8)	4.32	83	3.0	qu. + ZnS	$CuFeS_2$ pr.
10)	Högkulla	0.022 ± 0.008 (6)	3.47	41	2.7	quartz	
11)	jordavrym. 4	0.006-0.2 (5) 0.3-2.0 (3)	4.3	81	3.0	qu. + ZnS	on rich part on poor part
12)	30 m level	0.0047 ± 0.0022 (4)	4.3	84	2.7	quartz	
13)	80 m level	0.0044 ± 0.0017 (4)	4.02	70	2.7	quartz	
14)	90 m level	0.0085 ± 0.0030 (4)	4.04	71	2.7	quartz	
15)	Högås level	0.12 ± 0.07 (8)	4.36	88	2.75		polished, many cracks
16)	Kuorbevare	0.02-0.3 (6)	4.0	65	2.9	qu. + amph.	$CuFeS_2$ pr.
17)	Rävliden	0.015 ± 0.004 (4)	4.28	84	2.7	quartz	
18)	Mensträsk	0.0057 ± 0.0029 (4)	4.1	74	2.7	quartz	
	Boliden						
19)	90 m level	0.0022 ± 0.0003 (4)	4.57	100	—	—	
20)	130 m level	0.0020 ± 0.0006 (4)	4.49	95	2.7	quartz	
21)	210 m level	0.0018 ± 0.0004 (4)	4.61	100	—	—	
22)		0.0076 ± 0.0026 (4)	4.7	74	2.7	quartz	FeS_2 pr.
	Renström						
23)	245 m level	0.0090 ± 0.0033 (3)	4.3	84.5	2.7	quartz	
24)	382 m level	0.0049 ± 0.0004 (4)	4.32	85	2.7	quartz	
	Dalarna						
25)	Slättberget	0.0014	4.2	79	2.7	quartz	
26)	V. Silvberget	0.031 ± 0.011 (5)	3.86	60.5	2.75	various	
	Västmanland						
27)	Håkansboda	0.0085 ± 0.0010 (4)	4.25	82	2.7	quartz	
28)	Kaveltorp	0.013 (0.007-0.09) (6)	3.95	66	2.7	quartz	
29)	Kaveltorp	0.023 ± 0.008 (5)	3.80	58	2.7	quartz	
30)	Kaveltorp	0.0004-0.001 (18) 0.0010-0.01 (61)	4.2	79	2.7	quartz	

No. 1	Locality 2	Resistivity ohmcm 3	Sp. gr. 4	vol % ore 5	gangue sp.gr. 6	Prin. gangue min. 7	Remarks 8
	Upland						
31)	Dannemora	0.0017	4.2	79	2.7	quartz	
32)	Ytterby	0.004-0.4 (7)	4.3	84	2.7	quartz	
	Småland						
33)	Kleva	0.0071 ± 0.0019 (4)	4.7	75	5.0	haematite	
34)	Kleva	0.033 ± 0.005 (3)	4.5	95	2.7	quartz	
35)	Carl XVgruva	0.0021	4.24	81	2.7	quartz	
	Östergötland						
36)	Ringarum	2.03 ± 0.20 (3)	3.24				polished
37)	Fångögruva	0.023 ± 0.011 (6)	4.4	90	2.7	quartz	*Co, Ni* pr
	Norway						
38)	Espedalen	0.0043 ± 0.0017 (4)	4.0	50	3.4	pyroxene	
39)	Ringerike	0.0057 ± 0.0030 (3)	4.4	100	—	—	
	Finland						
40)	Petsamo	0.00060 ± 0.00007 (48)					
	Bavaria						
41)		0.003-0.05 (7)	4.2	78	2.8	chlorite	
	Troilite						
42)	U.S.A.	0.008-0.08 (6)					much fractured

4. ARSENOPYRITE

No.	Locality	Resistivity ohmcm	Sp. gr.	vol % ore	gangue sp.gr.	Prin. gangue min.	Remarks
	Västerbotten						
1)	Boliden	0.060 ± 0.018 (23)	5.9	97	2.7	quartz	
2)	Lindsköld	0.017 ± 0.007 (6)					
3)	Lindsköld	0.011 (on ore) 0.26 (on ore + gangue) 1.43 (across gangue band)					
	Norway						
4)	Kongsberg	0.012 ± 0.005 (5)	6.2	100	—	—	Löllingite pr ?
5)	Sulitelma	0.0418 ± 0.0024 (12)		single crystal			
6)	Sulitelma	0.0285 ± 0.0027 (12)		single crystal			

5. LÖLLINGITE

No.	Locality	Resistivity ohmcm	Sp. gr.	vol % ore	gangue sp.gr.	Prin. gangue min.	Remarks
1)	Dalarna	0.0084 ± 0.0017 (5)	6.9		75% Löllingite, 25% *FeAsS*		
2)	Dalarna	0.0090 ± 0.0035 (4)	6.9		75% Löllingite, 25% *FeAsS*		

No. 1	Locality 2	Resistivity ohmcm 3	Sp. gr. 4	vol % ore 5	gangue sp. gr. 6	Prin. gangue min. 7	Remarks 8

6. Cobaltite

(All single crystals)

No. 1	Locality 2	Resistivity ohmcm 3	Sp. gr. 4	vol % ore 5	gangue sp. gr. 6	Prin. gangue min. 7	Remarks 8
	Västmanland						
1)	Håkansboda	5.1 ± 2.2 (7)					
2)	Smedsgruva	1.5-13.3 (16)					
3)	Smedsgruva	0.90 ± 0.27 (16)					
4)	Smedsgruva	0.65 ± 0.16 (12)					
	Södermanland						
5)	Tunaberg	0.1-4.0 (15)					
6)	Tunaberg	2.66 ± 0.66 (4)					

7. Galena

No. 1	Locality 2	Resistivity ohmcm 3	Sp. gr. 4	vol % ore 5	gangue sp. gr. 6	Prin. gangue min. 7	Remarks 8
	Norrbotten						
1)	Laisvall	300 ± 100 (5)	3.4	15	2.7	quartz	
2)	Laisvall	327 ± 150 (3)	3.4	15	2.7	quartz	
3)	Laisvall	364 ± 88 (4)	3.2	10.5	2.7	quartz	
4)	Laisvall	2000-6000 (3)	3.1	8 .5	2.7	quartz	
5)	Laisvall	70-250 (4)	3.35	14	2.7	quartz	
6)	Laisvall	2760 ± 600 (3)	3.0	6.5	2.7	quartz	
7)	Laisvall	2000 ± 50%	3.1	8.5	2.7	quartz	
8)	Laisvall	4000-7000 (4)	2.95	5.5	2.7	quartz	
9)	Laisvall	5000-20000 (3)	2.9	4.0	2.7	quartz	
	Västmanland						
10)	Norberg	3.6 (1-6) (5)	5.8	66	2.7	quartz	
11)	Guldsmedshyttan	18 (4-40) (4)	6.65	83	2.7	quartz	
12)	Guldsmedshyttan	28.6 ± 9.3 (4)	5.2	53	2.7	quartz	
	Upland						
13)	Dannemora	15.8 ± 1.6 (5)	5.9	67.5	2.7	qyartz	
	Värmland						
14)	Wegeboda	2.6 ± 0.6 (16)	6.8	86	2.7	quartz	
	Austria						
15)	Salzburg	15-80 (4) ca 0.5	4.7	42	2.7	quartz	on poor part on rich part

8. Zinc blende

a) containing galena

No. 1	Locality 2	Resistivity ohmcm 3	Sp. gr. 4	vol % ore 5	gangue sp. gr. 6	Prin. gangue min. 7	Remarks 8
1)	Granlunda	6-90 (13)	3.88				polished
2)	Falun	2.54 ± 0.35 (4)	3.94				

No. 1	Locality 2	Resistivity ohmcm 3	Sp. gr. 4	vol % ore 5	gangue sp. gr. 6	Prin. gangue min. 7	Remarks 8
3)	Kaveltorp	0.27 ± 0.14 (4)	4.5	Owing to the very fine distribution of *PbS* and FeS_2 it is not possible to estimate the *ZnS* content simply from the specific gravity in any of these samples.			
4)	Kaveltorp	6.3 ± 3.0 (4)	4.07				
5)	Kaveltorp	0.01-0.1 (5)	4.85				
6)	Kaveltorp	150-1500 (4)					
	b) containing pyrite						
7)	Rudtjebäcken	130 ± 60 (8)	3.60				
8)	Pänninge	36 (8-90) (3)	4.02				
9)	Saxberget	5.74 ± 1.92 (4)	3.98				
10)	N.Ö.Homträsk	5-300 (4)					
	c) complex zinc ores						
11)	Rävliden	200-400 (3)	3.81	*ZnS*, *PbS*, *FeS*, $CuFeS_2$, FeS_2 and quartz in a complex mixture			
12)	Rävliden	ca 850 (2) ca 0.7 (3)	3.53				
13)	Nasafjäll	0.34 ± 0.14	3.60	*ZnS*, *FeS*, *PbS* in a complex mixture			
	9. Haematite						
	Norrbotten						
1)	Malmberget	40-12000 (3)	5.1	100	—	—	
2)	Malmberget	0.40 ± 0.23 (5)	5.15	100	—	—	magnetite pr.
3)	Malmberget	60-500 (5)	5.3	100	—	—	
4)	Malmberget	10-300 (6)	5.1	100	—	—	magnetite pr.
5)	Gällivare	greater than 60000	5.2	100	—	—	
	Hälsingland						
6)	Mansjöbergsgr.	1070 ± 180 (4)	3.4	30	2.7	quartz	magnetite pr.
	Dalarna						
7)	Grängesberg	640 ± 150 (10)	4.9	91	2.7	quartz	
8)	Grängesberg	46 ± 19 (10)	4.55	74	3.0	various	
9)	Klenshyttebr.	45000	4.5	75	2.7	quartz	
	Västmanland						
10)	Hellefors	3400 (900-7000) (15)	4.1	59	2.7	quartz	magnetite pr.
11)	Kilgruvan	ca 1000 (15)	4.3	67	2.7	quartz	
12)	Kittlegruvan	12000 ± 2000 (3)	5.2	100	—	—	shaly
13)	Stripa	820 ± 125 (4)	5.3	100	—	—	
14)	Bondgruvan	2000-9000 (4) 4000-24000 (2)	4.2	63	2.7	quartz	parallel bands across bands
	Närke						
15)	St. Blanka-gruva	1800 (800-4000) (4)	4.9	92	2.7	quartz	
16)	St. Blankagr.	180 (35-300) (5)	4.6	79	2.7	quartz	magnetite pr.

No.	Locality	Resistivity ohmcm	Sp. gr.	vol % ore	gangue sp. gr.	Prin. gangue min.	Remarks
1	2	3	4	5	6	7	8
17)	Striberg	1500-15000 (5) 19000-43000 (4)	4.35	69			parallel bands across bands
18)	Striberg	660(100-2000) (6)	4.72	84	2.7 (W)	quartz	see below for "W"
	Värmland						
19)	Långban	3620 ± 950 (4)	4.9	91	2.9	qu.+magn.	dispersed magnetite crystals
20)	Långban	1-20 (6)	5.2	80	20-30% magn.		
	Småland						
21)	Gladhammer	1260 ± 510 (9)	4.7	83.5	2.7	quartz	magn ?, Co pr.
	Miscellaneous						
22)	Cumberland, England	17200 ± 7500 (5)	4.64	81	2.7	quartz	
23)	Madagascar	800-6000 (5)	4.87	92	2.7	quartz	
24)	Pilot Knob, U.S.A.	17200 ± 7500 (8)	3.9	50	2.7	quartz	
	Unknown						
25)		420 ± 130 (5)	4.5	75	2.7	quartz	magnetite pr.
26)		700-10000 (4)	5.1	100	—	—	

10. MAGNETITE

Note on magnetite samples:

"W" in the 6th column denotes that the ore contents in these samples have been determined by S. Werner (1945).

	Norrbotten						
1)	Malmberget	47 (4-125) (6)	4.82	83	W		
2)	"Baron"	0.005-0.10 (8)	5.1	96	2.7	quartz	
3)	"Ridderstolpe"	50-2000 (13)	5.1	96	2.7	quartz	
4)	"Dennewitz"	33 ± 12 (5) 8 ± 2 (5)	4.95	90	2.7	quartz	
5)	"Fredrika"	21 ± 9 (5) 3.1 ± 1.6 (3)	4.90	88	2.7	quartz	
6)	"Hertigen" av Östergötland"	165 ± 50 (10)	4.9	88	2.7	quartz	
7)	Sjangeli	0.038 ± 0.002 (5)	4.46	71	2.7	quartz	
8)	Kiirunavaara	132 ± 51 (5)	4.63	73	W		
8)	Kiirunavaara (layered)	55 ± 11 (11) 300-2000 (3)	3.95	50	2.7	quartz	par. layers across layers
10)	Luossavaara	42 (4-90) (6)	4.74	78	W		
11)	Kiruna	1500 ± 300 (5)	4.64	74.5	3.3	basic rock	polished
	Västerbotten						
12)	Näsberget	1-70 (8)	5.0	92	2.7	quartz	

No.	Locality	Resistivity ohmcm	Sp. gr.	vol % ore	gangue sp.gr.	Prin. gangue min.	Remarks
1	2	3	4	5	6	7	8
	Dalarna						
13)	N. Silvberget	0.3-12 (5)	4.3	64	2.7	quartz	
14)	Hemgruvan	600-3000 (4)	4.5	61	3.4	pyroxene	
15)	Olsängsgruva	40-300 (7)	4.4	56	3.4	pyroxene	
16)	Rättvik	20 ± 8 (5)	4.8	84	2.7	quartz	bits of the same sample
17)	Rättvik	48 ±14 (5)	4.7	80	2.7	quartz	
18)	Kalvgruvan	0.17 (0.03-0.4) (7)	4.95	90	2.7	quartz	
19)	Morgruvan	8.7 ± 4.8 (6)	4.61	77	2.7	quartz	
20)	Grängesberg	0.76 ± 0.13 (7)	5.01	92	W		
21)	Intrånget	6000 (300-26000) (6)	4.48	63	W		
	Närke						
22)	St.Lerbergsgr.	152 (60-250) (4)	4.95	90	2.7	quartz	
23)	Stråssa	1950 ± 1000 (3) 24000-56000 (4)	4.02	53	2.7	quartz	parallelbands across bands
24)	Stråssa	60-600 (5)	3.89		3.0	basic rock	polished
25)	Häggruvan	1.14 ± 0.48 (5)	4.07	49	W		
	Värmland						
26)	Nordmark	4300 (1000-13000) (4)	4.2	45	3.4	pyroxene	
27)	Nordmark	7100 (1000-12000) (5)	3.62	23	W		
28)	Kogruvan	54 ± 24 (5)	4.85	86	2.8	basic rock	
29)	Persberg	1660 (900-2300 (5)	3.90	48	2.8	calc.+serpentine	
30)	Persberg	0.45 ± 0.21 (5)	4.80	81	W		
31)	Persberg	436 (200-900) (5)	4.58	69	W		
32)	Finnmossen	3.54 (0.5-10) (9)	4.58	68	W		
33)	Getö koppargr.	92 (17-170) (4)	3.3	14	3.0	skarn minerals	
	Upland						
34)	Dannemora	13 ± 6 (6)	4.4	67	2.8	chlorite	"spegelmalm"
35)	Dannemora	2.0 (0.2-4.0) (9)	4.47	70	2.8	chlorite	"spegelmalm"
36)	Dannemora	2.6 (0.3-8.0) (13)	4.85	86	2.8	chlorite	"spegelmalm"
37)	Dannemora	1.7 (0.2-4.3) (10)	4.95	90	2.8	chlorite	"spegelmalm"
38)	Dannemora	35 (9-70) (8)	4.0	50	2.8	chlorite	"spegelmalm"
39)	Dannemora	0.6 (0.02-1.8) (6)	3.78	42	2.8	chlorite	slaty
40)	Dannemora	10 ± 5 (5)	4.3	63	2.8	chlorite	slaty
41)	Dannemora	8.0 (1.4-15) (8)	4.05	52	2.8	chlorite	"spegelmalm"
42)	Dannemora	1.1 ± 0.5 (14)	4.2	59	2.8	chlorite	"spegelmalm"
43)	Storrym.	10-300 (5)	4.5	71	2.8	chlorite	"spegelmalm"
	Södermanland						
44)	Ehrendalsgruva	260 ± 70 (5)	4.7	80	2.7	quartz	
	Östergötland						
45)	Godegård	0.2-20 (5)	4.9	87.5	2.8	chlorite	

No. 1	Locality 2	Resistivity ohmcm 3	Sp. gr. 4	vol % ore 5	gangue sp. gr. 6	Prin. gangue min. 7	Remarks 8
	Småland						
46)	Kronoberg	9.8 ± 3.8 (5)	3.8	21	3.4	hypersthene	
	12. Psilomelane						
1)	Skedberget, Dalarna	4.1 ± 1.2 (4)	3.96	All these samples are probably 100% pure. The specific gravity of psilomelane varies from 3.3 to 4.7			
2)	Orkney Is., Scotland	8.8 ± 4.3 (8)	3.98				
3)	Orkney Is., Scotland	31 ± 14 (4)	4.41				
4)	Elgersburg, Germany	127 ± 44 (4)	4.11				
5)	Morocco	40 (10-90) (4)	4.60				
6)	Brazil	140 ± 32 (4)	3.54				
7)	Brazil	11 (5-30) (10)					
	13. Hollandite						
1)	Ultevis, Norrbotten	10 (2-20) (9)	4.7				
2)	Ultevis, Norrbotten	2.1 ±0.7 (10)	4.7	All these samples are probably over 90% pure			
3)	Ultevis, Norrbotten	1.90 ± 0.4 (5)	4.7				
4)	Thabua, Central India	1.7 (0.2-6) (5)	4.6				
	14. Pyrolusite						
	Västergötland						
1)	Bölet	5.4 (2-13) (5)		These samples are too porous for density measurements. They appear to be rather pure			
2)	Bölet	1.2 (2)					
3)	Bölet	0.72 ± 0.17 (11)					
4)	Munkebacka	4.3 ± 0.9 (10)					
	Russia						
5)	Donetz-land	3180 ±530 (5)					

No.	Locality	Resistivity & No. of obsvns.	Sp. gr.	Remarks about resis.	General remarks
	15. Complex Ore Samples				
	a) Pyrite + Chalcopyrite				
1)	Rudtjebäcken	0.30 ± 0.10 (6)	4.05	—	very complex mixture of FeS_2 & $CuFeS_2$

No.	Locality	Resistivity & No. of obsvns.	Sp. gr.	Remarks abt. resis.	General remarks
2)	Rudtjebäcken	0.02-2.0 (7)			very complex mixture of FeS_2 & $CuFeS_2$ ZnS also present
3)	Bjurfors	4.10 ± 2.05 (4)	4.15		
	Ö. Åkulla				
4)	Bh3, 24.82 m	4-50 (5)	3.33		
5)	Bh3, 69.08 m	7-136 (5)	3.14		
6)	Bh3, 22.42 m	1.05 (0.5-2) (5)	3.49		
7)	Bh8, 25.82 m	5-60 (4)	3.46		FeS_2 crystals and $CuFeS_2$ in chloritic shales
	Udden				
8)	Bh2, 98.40 m	3-150 (5)	3.31		
		b) Pyrrhotite + Chalcopyrite			
9)	Lavergruvan	0.025 ± 0.015 (73)		on $CuFeS_2$ part	
10)	Rudtjebäcken	0.015 ± 0.006 (3) 0.062 ± 0.008 (2)		on FeS part on $CuFeS_2$ part	
11)	Lainijaur	0.067 ± 0.032 (5)	3.96		complex mixture of about 1/3 FeS, 1/3 $CuFeS_2$ & 1/3 chlorite. Polished
12)	Bjurfors	0.042 ± 0.014 (25) 0.0024 ± 0.0008 (15)	4.40	on $CuFeS_2$ part on FeS part	70% $CuFeS_2$ 30% FeS more or less distinctly separated
13)	Bjurfors	0.042 ± 0.014 (4) 0.0021 ± 0.0010 (3)		on $CuFeS_2$ on FeS	
14)	Rävliden	0.022 ± 0.012 (21)	4.11		complex mixture of about 40% $CuFeS_2$, 40% FeS & 20% amphibole. polished
15)	Rävliden	0.082 ± 0.028 (7)	4.11		
16)	Adak	0.38 ± 0.02 (3) 0.016 ± 0.0008 (5)	4.30	on $CuFeS_2$ part on FeS part	polished
17)	Adak	0.33 ± 0.09 (15) 0.0063 ± 0.0019 (16)	4.30	on $CuFeS_2$ on FeS	$CuFeS_2$ and FeS more or less distinctly separated
18)	Lindsköld	0.026 ± 0.008 (3) 0.009 ± 0.003 (3)	3.2	on $CuFeS_2$ on FeS	lean sample with local concentrations of $CuFeS_2$ & FeS
19)	Västmanland	0.008-0.08 (5)	3.9		
		c) Arsenopyrite + Pyrite or chalcopyrite			
20)	Adak	0.007-0.08 (5) 0.01-0.10 (4)	4.2	on $FeAsS$ part on $CuFeS_2$ part	rich ore with local concentrations of $FeAsS$

No.	Locality	Resistivity & No. of obsvns.	Sp. gr.	Remarks abt. resis.	General remarks
21)	Adak	0.06-0.30 (5)	4.2	on $FeAsS$ part	rich ore with local concentrations of $FeAsS$
		0.01-0.14 (7)		on $CuFeS_2$ part	
22)	Boliden	0.060 ± 0.021 (6)	4.9		complex mixture of $FeAsS$ & FeS_2 crystals
23)	Boliden	0.025 ± 0.008 (5)	4.8		complex mixture of ca 60% $FeAsS$ and 40% FeS_2; some $CuFeS_2$ pr.
		0.0068 (1)		on a single crystal of $FeAsS$	

16. GRAPHITIC SHALES

No.	Locality	Resistivity & No. of obsvns.	Sp. gr.	Remarks abt. resis.	General remarks
	Norrbotten				
1)	Ristimela	0.21 ± 0.07 (5)		parallel layering	
		0.21 ± 0.04 (3)		parallel layering	
		0.082 ± 0.015 (3)		across layering	
2)	Tväråkölen	0.64 (0.3-1.2) (7)	2.7		impregn. of pyrite minerals
3)	Aijärova	0.016 ± 0.008 (6)			almost pure graphite
	Västerbotten				
4)	Mensträsk	39 ± 11 (4)	2.80		banded shales with weak FeS_2 & FeS impregnation
		500-13000 (3)			
5)	Mensträsk	3.5 ± 2.5 (6)	2.95		
6)	Mensträsk	5-80 (6)	2.97_5		weak FeS impr.
7)	Mensträsk	690 ± 86 (3)	2.81		FeS impregnation

The specific gravity figures in column 4, table I are accurate to half a unit in the last place mentioned. Thus a specific gravity of 4.0 would mean a possible variation between 3.95 and 4.05. The accuracy to which the volume percentage of ore can be given depends upon the accuracy in g_0 and g_1 more than that in g. It will be noticed that most of the samples have only one principal gangue mineral. In such cases g_1 can be estimated with an accuracy comparable to that in g once the gangue is identified. When two or more gangue minerals were present their relative proportions were estimated by surface examination and a "mean" g_1 was assigned.

An uncertainty in g_1 in lean samples is proportionately of much greater significance for the accuracy in the volume percentage of ore than the same uncertainty in rich samples. This is easily seen from equation (3) and is easier to comprehend when one observes that the plot of volume percentage against g for different g_1's is a group of straight lines which all emanate from the point (100, g_0) and cut the g-axis at the respective g_1 values (pure gangue, 0% ore).

The values adopted for g_0 and g_1 in the present work are as follows:

Specific gravities

Ore minerals (g_0):

Pyrite	5.0	Galena	7.5
Chalcopyrite	4.2	Zincblende	4.0
Pyrrhotite	4.6	Haematite	5.1
Graphite	2.1	Magnetite	5.2

Gangue minerals (g_1):

Amphibole	3.3	Pyroxene	3.4
Quartz	2.7	Hypersthene	3.45
Calcite	2.7	Chlorite	2.8

The accuracy of the volume percentage figures in table I is estimated to be ± 5—10% for most cases.

The most striking feature of the resistivity values in table I is the large variation from sample to sample. Even on a single sample the resistivity frequently varies between wide limits.

Cracks, sometimes of microscopic size, play a dominant role in determining the resistivity. For example, pyrrhotite samples 3, 4, 5 from Kalix and 15 from Högås are relatively pure; their high resistivity is actually due to minute cracks. Inter-granular resistances are also an important factor. If the grains are isolated from each other by thin, more or less non-conducting films, the sample resistivity can be very high or even infinite although the percentage of conducting grains may be quite high (e.g. pyrite samples no. 52-57). Furthermore, if the intergranular resistances are very variable (depending, for instance, on the contact area or the thickness of the poorly conducting film) the resistivity values will show great variations on different parts of the sample. This is believed to be the cause of the variability of the resistivity values on many haematite and magnetite samples.

Samples are sometimes layered or banded. In such cases the resistivity depends on the interlayer resistances. Also the measured value across the layers depends on the number of layers included between the potential electrodes i.e. on the electrode separation.

The presence of holes or a porous or loose structure (e.g. in weathered samples) leads also to variable and usually high resistivity values.

It is self-evident that the mode of distribution of the conducting minerals should have a great influence on the resistivity.

When two or more conducting minerals are dispersed homogeneously in a sample then, in general, a resistivity intermediate between the resistivities of all the minerals present is to be expected for the whole sample. If, however, there are places where one or the other mineral is concentrated locally, the resistivity obtained will be very near to that of this mineral if the electrodes are placed on the concentrated "pocket". Examples of this will be found in the complex ores list in table I.

In the analysis of the results which is given in the next section, anomalous results (such as produced by cracks, weathering etc.) are neglected where the cause could be traced.

5. ANALYSIS OF THE RESULTS

a. Pyrite (FeS_2)

The resistivity of pyrite ore is very variable, but no correlation is found between ore content and the resistivity for the samples investigated. There is likewise no correlation between the percent standard deviation of the resistivity of a single sample on the one hand and ore content or the resistivity value on the other hand. The mean standard deviation of the resistivity of a single sample is ±38%. The experimental uncertainties are expected to be generally less than 10—15%. This indicates the extent to which the samples depart from homogeneity. Occasionally samples are encountered on which the ratio of the highest to the lowest measured value of the resistivity is of the order 100! The distribution of the mean resistivity values in table I is roughly as follows:

Range ohmcm	Number of samples
0.01—0.1	10
0.1—1.0	10
1—10	19
10—100	13
100—1000	8

Some samples cannot be adequately classified in the ranges adopted above.

b. Chalcopyrite ($CuFeS_2$)

The resistivity of chalcopyrite ore is apparently not as variable as that of pyrite.

Fig. 2 shows a plot of the mean resistivity of a sample against the reciprocal of its estimated chalcopyrite content by volume. The samples in table I exhibiting irregular values due to cracks, banding etc. are neglected. The equation of the best straight line through the points in fig. 2 can be written as:

$$\log_{10} (\text{resistivity in ohmcm}) = (6.2 \pm 4.2)/(\text{vol. } \% \; CuFeS_2) - (1.39 \pm 0.38) \quad (4)$$

The "correlation coefficient" which estimates the statistical significance of such a correlation is fund to be 0.29. The probability that it would arise by chance in 23 pairs of numbers is much greater than 5%. A 5% limit is generally adopted as showing significant correlation. It can be concluded, therefore, that, on the available data, the above linear relation between log (resistivity) and the reciprocal of volume percent chalcopyrite is statistically not of great significance.

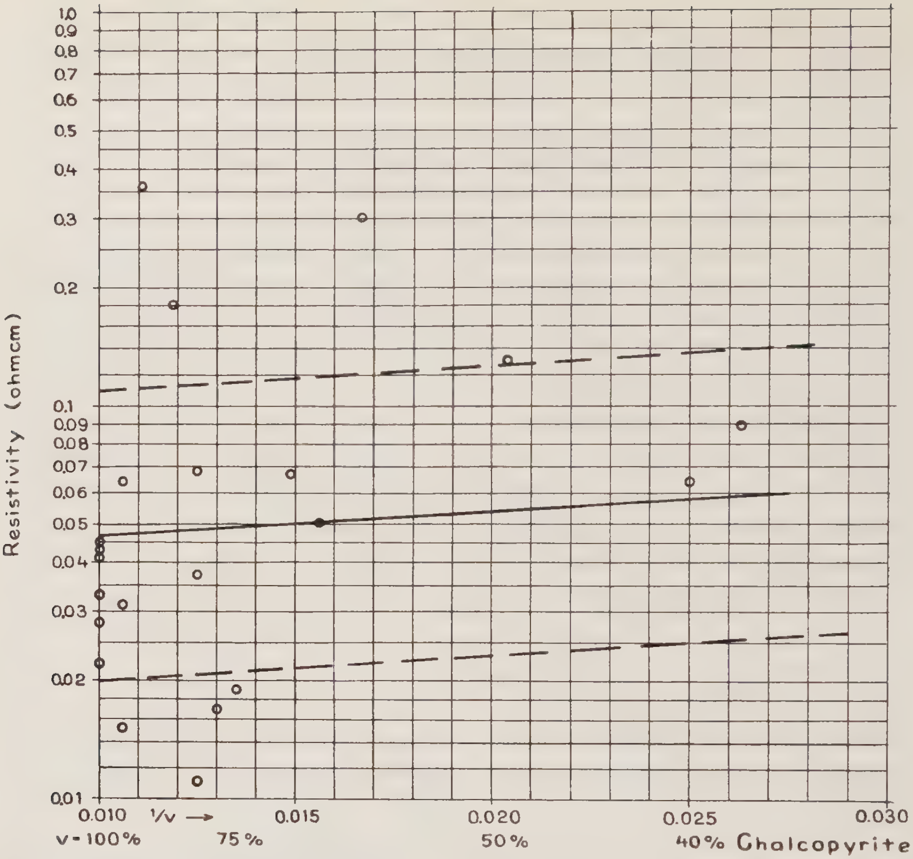

Fig. 2. Relation between chalcopyrite ore resistivity and vol. percent chalcopyrite (v) (Resistivity on logarithmic scale)

The two dashed straight lines in fig. 2 mark the region of the graph within which 2/3 of the observed points are (theoretically) expected to lie. In reality, the limiting lines are parabolic curves but in the present case their curvature is very small.

Each point in fig. 2 represents a mean of several (usually between 5 and 10) observations of resistivity with an average observed standard deviation of about ±25%. There is no correlation of the percent standard deviation of the resistivity value with the ore content.

The resistivity of pure chalcopyrite is estimated (by extrapolation from equation 4) to be 0.047 ohmcm with a "standard range" of 0.020—0.11 ohmcm.

c. Pyrrhotite (*FeS*)

The resistivity of pyrrhotite shows a distinct correlation with ore content (fig. 3), which it is possible to express as:

$$\log_{10} \text{(resistivity in ohmcm)} = (73 \pm 10)/\text{vol. \% } FeS) - (3.26 \pm 0.31) \quad . \quad . \quad (5)$$

Samples in table I owing their high resistivity to cracks or other imperfections have been neglected.

The correlation coefficient is 0.61 and the probability of its arising by chance of 24 degrees of freedom (the actual number) is less than 1% which means that the correlation given in equation (5) must be judged to be highly significant. The lines between which 2/3 of the samples are expected to lie are also shown in fig. 3.

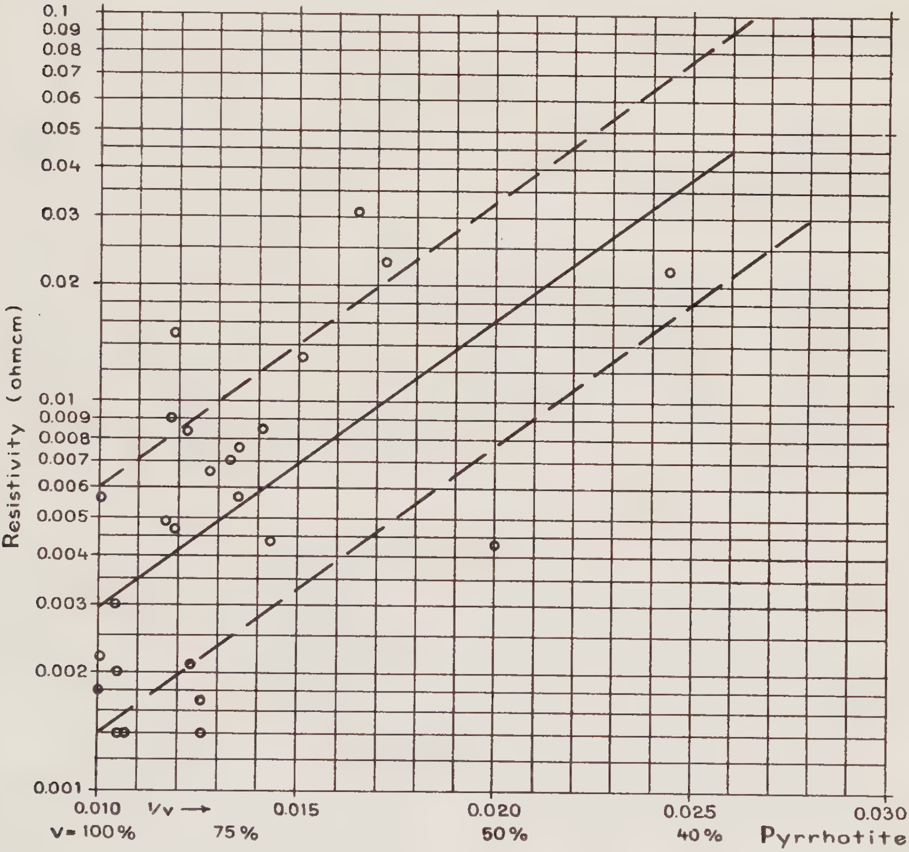

Fig. 3. Relation between pyrrhotite ore resistivity and vol. percent pyrrhotite (v) (Resistivity on logarithmic scale)

The resistivity of pure pyrrhotite is found to be 0.0030 ohmcm (by extrapolation) with a "standard range" of 0.0014—0.0060 ohmcm.

The resistivity of pure pyrrhotite is comparable to that of polycrystalline graphite. An interesting fact may be noted here. Samples of pyrrhotite with less than about 10% ore content were usually found to be non conductors. It was evident that the pyrrhotite grains were isolated from each other. On the other hand, graphite "ore" samples with less than 1% graphite were frequently very conductive.

There is no correlation between the standard deviation of the resistivity value on a pyrrhotite sample and ore content.

d. Arsenopyrite ($FeAsS$) and Löllingite ($FeAs_2$)

Pure arsenopyrite probably has a resistivity of the order of 0.03 ohmcm. Löllingite appears to have a resistivity of 0.005 ohmcm.

e. Cobaltite ($CoAsS$)

The crystals from Smedgruvan seem to have a resistivity not far removed from 1 ohmcm, but on the whole the data are insufficient for any definite conclusions to be reached.

f. Galena (PbS)

The samples in table I fall in two groups, one with an ore content less than about 10% and the other with about 50—80%. The former group shows a mean resistivity that varies between 300 and 30000 ohmcm while the latter varies between 1 and 30 ohmcm. Quartz is the only principal gangue mineral in all these samples. It is remarkable that when galena is present in small amounts (less than 10—20% by volume) in a zincblende matrix the resistivity can be as low as 1 ohmcm. (See table I, 8).

g. Zinc blende (ZnS)

Zinc blende is, for all practical purposes, an insulator. The observations recorded here must be looked upon as giving the resistivity of the particular distribution of conductive minerals in the ore sample. They could have been included in the pyrite or the galena list, the zincblende being then treated as gangue.

h. Haematite (Fe_2O_3)

The resistivity of haematite ore is characterized by a high value and a large scatter. As mentioned earlier (section 4) the large scatter is believed to be due to very variable intergranular contact resistances.

Pure stoichiometric Fe_2O_3 is known to be a non-conductor of electricity at ordinary temperatures. Small impurities (frequently as small as 1 or 2%) increase its conductivity enormously. Among such impurities is TiO_2. The explanation of this fact involves quantum mechanics and will not be pursued here.

Red haematite is an insulator.

It is apparent from table I that haematite samples containing magnetite (e.g. nos. 2, 4, 16) have low resistivities. Owing to the almost equal specific gravities of haematite and magnetite, the estimated percentage of haematite in the magnetite-bearing samples is uncertain.

Of special interest are the values parallel to and across the banding in samples 14, 17.

The samples are distributed as follows:

Range ohmcm	Number of samples
less than 100	3
100—1000	8
1000—10000	9
greater than 10000	6

i. Magnetite (Fe_3O_4)

The resistivity of magnetite ore is distinguished by its relatively low value and large variation from sample to sample. No significant correlation between resistivity and ore content is evident.

The "spegelmalm" group from Dannemora (Nos. 34-43) is a rather homogeneous group with a mean resistivity not far removed from 10 ohmcm. In contrast to this the Malmberget samples (Nos. 1-6) present a very wide scatter. These findings are in keeping with the mineralogical character of either group. The Dannemora group is a fine grained, colloidal deposit of remarkable uniformity while the Malmlberget samples are coarse grained with grain size varying much from sample to sample.

The distribution of the 50 resistivity values observed on 46 samples in table I is as follows:

Range ohmcm	Number of values
0.01—1.0	6
1—10	14
10—100	14
100—1000	7
1000—10000	8
greater than 10.000	1

j. Manganese minerals

Psilomalane, hollandite and pyrolusite have resistivities measurable in some tens of ohmcm. Hausmannite, bixbyite, manganite, piemontite and braunite are insulators.

k. Complex ore samples.

Ore samples in which two or more conducting minerals are present in nearly equal proportions cannot be properly classified under one of the constituents. They are therefore here listed as complex. The complexity nevertheless varies considerably. It often happens that the constituent minerals are distinctly separated especially in the case of pyrrhotite and chalcopyrite samples. If the electrodes are placed on one or the other mineral the resistivity appropriate to that mineral will be obtained (for instance, samples 12, 17, 18).

1. Graphitic shales.

It has already been remarked that a graphite content of less than, say, 2% is capable of making a sample conductive in certain cases. This is evident from table I. The behaviour is to be contrasted with that of pyrrhotite samples.

5. COMPARISON WITH PUBLISHED RESULTS.

The following table reproduces some of the published results. It is apparent from the study of the literature that, in general, only a few (sometimes only one or two) samples of a particular ore have been investigated by the authors concerned. A quantitative estimate of the ore content is very seldom available. Since the electrical resistivity of ores varies so enormously from sample to sample it is necessary to have a fairly large number of samples for significant conclusions to be drawn.

TABLE II

Comparison of electrical resistivity values

Ore and investigator	Resitivity ohmcm	Resistivity of pure mineral ohmcm	Nature of pure mineral
Pyrite			
Abt	—	9.20 (1)	Single crystal
Königsberger and Reichenheim	—	0.25 (1), 4.77 (1)	Single crystal
Löwy	—	0.1 (1)	Single crystal
Sundberg et al.	0.1—10^4 (8)	0.02	?
Harvey	0.001—10	—	—
Jakosky et al.	0.3—11.3 (3)	—	—
Smith	—	0.1—10 (25)	Single crystals
Present work	0.01—1000 (60)	0.005—5 (44)	Single crystals
Chalcopyrite			
Abt	1.0 (1)	—	—
Löwy	0.2 (1)	—	—
Sundberg et al.	0.1—10 (4)	1.0	Polycrystalline
Harvey	0.001—10	—	—
Jakosky et al.	0.3—4.4 (6)	—	—
Present work	0.01—10 (30)	0.012—0.069	Polycrystalline
Pyrrhotite			
Abt	0.01 (2)	—	—
Löwy	0.05 (1)	—	—
Sundberg et al.	7.0 (1)	0.01	Polycrystalline
Harvey	0.1—10	—	—
Present work	0.001—0.1 (37)	0.0011—0.0046	Polycrystalline

Ore and investigator	Resistivity ohmcm	Resistivity of pure mineral ohmcm	Nature of pure mineral
Arsenopyrite			
Harvey	0.001—0.01	—	—
Jakosky et al.	0.15—18 (3)	—	—
Present work	—	0.03 (2)	Single crystals
Galena			
Königsberger and Reichenheim	—	0.00265 (1)	Single crystal
Mönch	—	0.23	,,
Löwy	0.5—5 (2)	—	—
Sundberg et al.	0.1—1 (3)	0.003	?
Harvey	0.001—10	—	—
Jakosky et al.	17.66 (1)	—	—
Present work	1—30 (6) 300—30000 (9)	0.003—0.03 (9)	Single crystals
Zinc blende			
Löwy	$1.4\ 10^8$ (1)	—	—
Sundberg et al.	$>50\ 10^6$ (2)	—	—
Harvey	$>10^6$	—	—
Haematite			
Bäckström	—	0.6 (// c-axis) 0.4 (⊥ c-axis)	Single crystal from Langö, Norway
Abt	1400—6500 (3)	—	—
Königsberger	—	1.39 (// c-axis) 0.54 (⊥ c-axis)	Single crystal from Brazil
Löwy	200 (1)	—	—
Sundberg et al.	10—100	0.4—0.8	?
Harvey	$>10^6$	—	—
Present work	10—> 10000 (26)	—	—
Magnetite			
Abt	7—4900 (9)	—	—
Bäckström	—	0.0052 (1)	Single crystal
Löwy	1—10 (2)	—	—
Sundberg et al.	1—100	—	—
Harvey	0.001—10	—	—
Jakosky et al.	0.7—5.58 (3)	—	—
Present work	1—1000 (35)	0.01	Single crystals
Graphite			
Muraoka *	—	0.0012 (1)	Polycrystalline
Königsberger and Reichenheim	—	0.0029 (1)	,,
Sundberg et al.	—	0.03	?
Present work	0.1—1000 (7)	0.0020 (1)	Polycrystalline

1) Harvey's observations were taken by means of microelectrodes and probably represent the resistivity of pure mineral in question rather than that of the ore sample in bulk.

2) The observations on pyrite, galena and magnetite crystals recorded in the table

---

* Cited by Königsberger and Reichenheim (1906).

under "present work" are taken from a paper by the present author, see footnote p. 254.

3) The resistivity of single crystals of graphite can be found at several places in physical literature. It is anisotropic and has the following values (A. K. Dutta, 1953)

10^{-4} ohmcm along the basal plane
1 ohmcm perpendicular to the basal plane.

4) The single crystals investigated by all the authors are natural.

6. CONCLUSIONS.

It is necessary here to summarize only the most important conclusions reached in the present study of the electrical resistivity of ores and minerals.

a) The four point method enables one to investigate the resistivity of a given sample in a quick and detailed way. Approrpiate precautions must, however, be taken.

b) The electrical resistivity of ore and mineral samples has a twofold scatter. It varies "locally" on a single sample often by factors of 10-100 but usually within about ±30% and it varies by much greater amounts (factors of 100-10000) from one sample to another. Among the causes that contribute to the variability on a single sample are cracks, variable intergranular resistances, presence of a porous structure, mode of grain distribution etc. The variation from sample to sample depends in addition on the percentage of ore conetnt.

c) It would seem appropriate to indicate the approximate limits within which the ores and minerals of the present investigation seem to vary in their electrical resistivity.

TABLE III

The Electrical Resistivity of ores and minerals

Material	Resistivity (ohm cm)	
	Ore	Pure mineral
Pyrite	0.01—1000	0.005—5
Chalcopyrite	0.01—10	0.01—0.07
Pyrrhotite	0.001—0.1	0.001—0.005
Arsenopyrite	0.1—10	0.03
Löllingite	—	0.003
Cobaltite	—	1—5
Galena	1—30000	0.003—0.03
Zinc blende	—	Insulator at ordinary temperatures
Haematite	10—10000	,,
Magnetite	1—1100	0.01
Psilomelane Hollandite Pyrolusite	1—10	— —
Bixbyite Braunite Hausmannite Manganite Piemontite	—	Insulators
Graphite	0.1—1000 (Shales)	0.002 (Polycrystalline)

d) We may now discuss in short the feasibility of electrical prospecting for the above mentioned ores. The actual detection of an ore body is beset with many problems but it is evident that other circumstances being equal, pyrite, chalcopyrite, pyrrhotite, arsenopyrite, magnetite and graphite ore bodies make excellent objects for electrical prospecting. The suitability of haematite bodies for detection by electrical methods would depend very much upon the surrounding rock. Red haematite, being an insulator, is hardly likely to be detected electrically. Inasmuch as specular haematite with certain impurities (e.g. TiO_2) has low resistivity, under certain favourable conditions, it may give electrical indications. Galena, psilomelane, hollandite and pyolusite are also suitable objects for electrical prospecing. We can safely say that zinc blende and the manganese minerals bixbyite, braunite, hausmannite, manganite and piemontite would be almost indetectable by electrical prospecting.

The above remarks are, of course, of a very general and rough nature. It is not unthinkable that a badly conducting ore body, say haematite, may be more easily detectable in certain circumstances than, say, pyrite.

7. Acknowledgements

The work described above was undertaken at the instance of Svenska Gruvföreningien (The Swedish Mining Association) at Stockholm and was broadly directed through a committee appointed by it. The writer wishes to thank the members of the committee, namely Prof. N. H. Magnusson (Chairman), Mr. H. Hedström, Dr. D. Malmquist and Mr. A. Nordström for their interest and advice in the work. A few of the measurements described herein were made by Dr. P. Trotzig (since deceased) in 1949-50.

The samples for the investigation were made available by Prof. F. .E Wickman (Director, Mineralogical Department of the Swedish Natural History Museum), Prof. N. H. Magnusson (Director-general, Swedish Geological Survey) and Dr. D. Malmquist (Boliden Mining Company, Boliden, Sweden). The apparatus was supplied by Mr. H. Hedström (Chief Engineer, A/B Elektrisk Malmletning, Stockholm). To all of them, the author offers his thanks.

References

Abt A., 1897, Leitungswiderstand und specifische Wärme einiger Eisenoxyde und Eisensulfide, Ann. d. Phys. u. Chem., 62, p. 474-481.

Beijerinck F., 1897, Ueber das Leitungsvermögen der Mineralien für Elektricität, Neues Jahrb. f. Min. Geol. u. Pal., BBXI, p. 403-474.

Bäckström, H., 1888, Elektrisches u. thermisches Leitungsvermögen des Eisenglanzes, Öfv. af Kongl. Vet.-Akad. Förh., 8, p. 533-551.

Dutta A. K., 1953, Electrical conductivity of single crystals of graphite, Phys. Rev., 90, p. 187-192.

Harvey R. D., 1928, Electrical conductivity of polished mineral surfaces, Econ. Geol., 23, p. 778-803.

Hayes H. V., 1911, Notes on the electric conductivity of argentic sulphide, Proc. Amer. Acad. Arts & Sci., XLVI, p. 613-621.

Jakosky J. J., Anderson R. N., and Wilson C. H., 1932, Meeting of Am. Inst. Min. Met. Eng., February 15 (Private circular).

Kerr P. F. and Cabeen C. K., 1925, Electrical conductivity of ore minerals, Econ. Geol., 20, p. 729-737.

Königsberger J. and Reichenheim O,. 1906, Ueber die Elektrizitätsleitiung einiger natürlich kristallisierten Oxyde und Sulfide und des Graphits, Neues Jahrb. f. Min. Geol. u. Pal., 1906, II, p. 20-49.

Löwy H., 1911, Die Elektrizitätskonstante und Leitfähigkeit der Gesteine, Ann. d. Phys., 36, p. 125-133.

Mönch W., 1905, Ueber die Elektrische Leitfähigkeit von Kuppersulfür, Silber-, Blei-, und schwarzen Quecksilbersulfid, Neues Jahrb. f. Min. Geol. u. Pal., BB XX, p. 365-435.

Smith F. G., 1940, Variation in the electrical conductvity of pyrite, University of Toronto Studies, Geol. Ser., 44, p. 83-93.

Sundberg K., Lundberg., and Eklund J., 1925, Electrical prospecting in Sweden, Sv. Geol. Undersökning, Årsbok 17 (1923), Ser. C., No. 327, p. 1-74.

Werner, S., 1945, Determination of the magnetic susceptibility of ores and rocks from Swedish iron ore deposits, Sv. Geol. Unders., Årsbok 39 (1945), Ser. C, No. 472.

Wilson A. H., 1953, The Theory of Metals, Cambridge Univ. Press, Cambridge.

DESIGN PRINCIPLES FOR SEISMIC REFLECTION AMPLIFIERS*

BY

A. J. HERMONT **

ABSTRACT

During the last two years the Exploration and Production Research Laboratory, Shell Development Company, Houston, Texas, had occasion to evaluate a number of seismic amplifier channels submitted by various seismic contractors and manufacturers. From this study, material for the present paper has been collected.

The modern trends to be found in the electrical design of up-to-date equipment are reviewed, and opinions of the E & P Research Laboratory, not necessarily shared by the industry, are expressed. No specific designs are mentioned, the material being presented in a general way.

The over-all elementary channel is discussed briefly and the various components are described functionally.

Filtering is mentioned from a point of view of minimum requirements for an average reflection survey, and absolute sensitivity, minimum useful signal voltage from a geophone, and noise are discussed.

Gain control is treated in two regions—the automatic control region and the initial control region. For the former, static and dynamic control characteristics are discussed, and the factors influencing the control range are brought out. For the latter, it is pointed out when a system is said to require obligatory or optional initial suppression.

Harmonic distortion, originating in the inductive components of the input circuit due to low-frequency roller energy, is presented in a manner facilitating understanding of the distribution of low-frequency filtering along the channel.

INTRODUCTION

The evolution of the over-all system linking the geophone to the galvanometer, i.e., the seismic amplifier used in the reflection seismic technique, has taken a definite course from the first practical application of the physical principles involved to the present-day arrangement.

During the last two years we have had occasion to look, rather critically, into the performance of quite a number of instruments developed by various seismic contractors and manufacturers. From this study, as well as from a revaluation of our own instrument, material for the present paper has been collected.

---

* Presented at the Symposium on Seismic Instrumentation of the Fort Worth Geophysical Society, 16 November 1955.

** Shell Development Co., Houston, Texas.

It is proposed to outline, without too much detail, the modern trends to be found in the electrical design of today's equipment. The trends in the mechanical design will not be discussed, although the latter are the more spectacular ones, since general miniaturizing has brought about not only esthetic appeal but also considerable improvement in the ease of operation. Neither the geophone nor the galvanometer is considered here, except as a source of power and a detector, respectively.

The views disclosed in this paper are those held by a group of people, including the author, engaged in seismic work at the Exploration and Production Research Laboratory of the Shell Development Company, and are not necessarily shared by the entire industry. Out of this group, it is with pleasure that the author singles out Dr. E. Merten, whose basic philosophy formed the foundation on which rests the set of guiding principles governing this work.

THE OVER-ALL SYSTEM

As a matter of orientation, a typical elementary seismic channel is illustrated in Figure 1, and the function of the various components should be clearly understood if full benefit from the following discussion is to be derived.

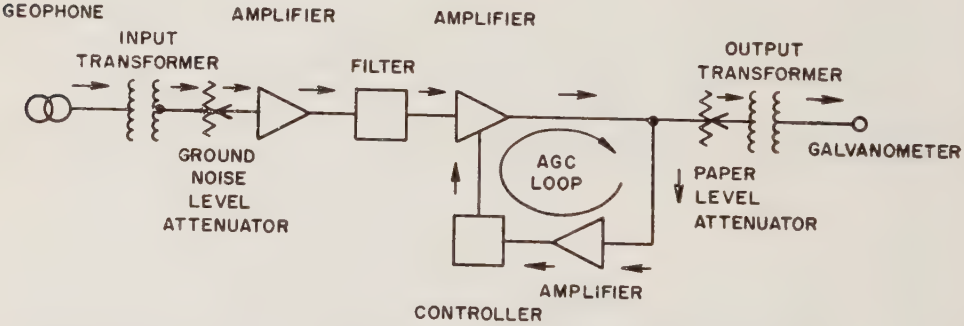

Fig. 1. Basic Block-Schematic of a Typical Seismic Channel

The power from the geophone, which is usually a low impedance device, is matched to the inherently high input impedance of the first amplifier stage by means of an input transformer. Voltagewise, a step-up has been achieved in an effort to keep the unavoidable amplifier noise to a minimum during the process of raising the voltage (and power) level. This increase of level is demanded by the weak but still useful signals appearing after a somewhat long time-interval following the initial arrival of energy; during the major time interval, however, when the signal is strong, only little amplification, if any, is required. A further function of the input transformer is to reduce interchannel coupling derived from leaky cables, etc., by providing a resistance with a variable or fixed tap-to-ground arrangement. It is understood that the geophone is properly damped, either by a resistor forming a part of the latter, or by a resistor forming a part of the input circuit.

If the galvanometer deflection is observed with only the natural ground unrest influencing the geophone, and if a predetermined paper level is maintained, it is easy to adjust the ground noise level attenuator: for example, if the ,,normal'' peak-to-peak galvanometer signal deflection is to be kept at 1 cm., then the ground unrest should amount to, say, 1 mm. Experience teaches that the maximum amount of this attenuation need not exceed 60 db. With multichannel operation in mind, it is well to arrange this attenuator as a tapped potentiometer, the steps between the taps ranging between 6 and 10 db. This is preferable to the continuous (marked) potentiometer sometimes found. The indicated location of this attenuator is a preferred one, i.e., it should precede most nonlinear elements (tubes, filter chokes) so as to keep the signal level reaching those elements at a minimum; from this point of view, the best location is directly across the geophone. Placing the attenuator after the first amplification stage has, however, the advantage of reducing the tube noise from that stage. Often, a combination of the above is the best practical solution.

The geophone signal is amplified and appropriately filtered, and the gain of the amplifier is automatically controlled so that the output level of the channel tends to remain constant as the input level varies over a certain range (Automatic Gain Control, AGC).

The purpose of the Paper Level Attenuator is twofold: first, it serves to equalize the outputs, which is important in a multichannel arrangement, and second, it permits us to select judiciously the recording level, since the contrast between rapid local ,,bursts'' and ,,collapses'' varies with the nature of the subsurface. Usually a total control of 12 db is sufficient.

Finally, the output power of the channel (usually at a relatively high source impedance) is transferred to the low impedance galvanometer element by means of an output transformer, this transfer being accomplished substantially without power loss.

The channel shown in Figure 1 indicates that all filtering is concentrated between the two amplifier sections and that a single AGC loop, consisting of amplifier and controller, the output of which acts in some manner upon the gain of the second amplifier section, is being used. Deviations from this elementary form will be discussed later.

As to the total number of tubes used, various arrangements have been encountered. Four physical tubes represent a minimum: 3 Duo-Triodes and 1 Duo-Diode (5 main channel amplifier stages, 1 control amplifier stage, and 1 Losser stage). The maximum number of tubes seems to be 12.

The most common source of B-supply is a 90-volt electronically controlled Vibrapack unit. The highest voltage encountered was 330 volts from either a Dynamotor or a Vibrapack. The lowest voltage was 24 volts derived from a small storage battery unit.

Filtering

Although the filter topic does not come within the bounds of this paper, it is not possible to omit filter considerations entirely, since the filter is regarded as an integral part of the amplifier channel.

Experience teaches that a filter system contained within the shaded area of Figure 2 will produce satisfactory results in most reflection shooting situations. Cutoff frequency is arbitrarily taken as the point at which the response has dropped to a value 50 percent of that at the peak frequency. Cutoff slopes may be defined as the chords drawn between cutoff frequency and a frequency one octave removed from the latter. On this basis the required low-frequency cutoff slope becomes 24 db/octave (not including the geophone) and the high-frequency slope becomes 18 db/octave (including the galvanometer). Selectivity of cutoff frequency may be achieved by appropriately subdividing the shaded area (say, 5 selections of low-frequency cutoff and 3 selections of high-frequency cutoff).

Gentler low-frequency cutoff slopes, such as 12 db/octave and steeper ones, such as 48 db/octave, as well as high-frequency slopes of 36 db/octave are certainly also useful in some areas.

As to the location of the filter along the amplifier channel, it is best to accomplish all the major filtering before the controlled portion of the amplifier. Some systems utilize low-frequency filtering within the AGC loop for stability reasons. High-frequency filtering in most systems is accomplished by one or more **L** sections, involving L, C, and R components; other systems utilize shunting condensers at various points of the channel. Low-frequency filtering is done by **L** or **T** sections. There are systems which utilize active filter sections (inverse feedback) in addition to the above passive types and some use active filters only. Others systems are derived from the general lattice structure and exhibit attenuation maxima for some low or high frequencies, accompanied by very steep attenuation slopes in the neighbourhood of the latter.

It will be shown later, in the discussion of harmonic distortions, that it is imperative to put a portion of the low-frequency filter at a different location than the one indicated in Figure 1.

A complete reflection channel should also include a refraction filter for weathering correction shots. Such a filter is satisfactory if it has an approximate slope of 2 db/octave, attenuation starting at about 20 cps, cf. Figure 2.

An important design quantity is the "absolute voltage sensitivity" of the channel at any filter setting. It is defined as the voltage at the input terminals of the channel required to produce a 1-mm peak-to-peak galvanometer deflection for a frequency in the transmission region and is expressed in db relative 1 volt RMS. This is given for zero attenuation introduced in the channel. On this basis -120 db/mm is considered average, -140 db/mm is good and -100 db/ mm is weak.

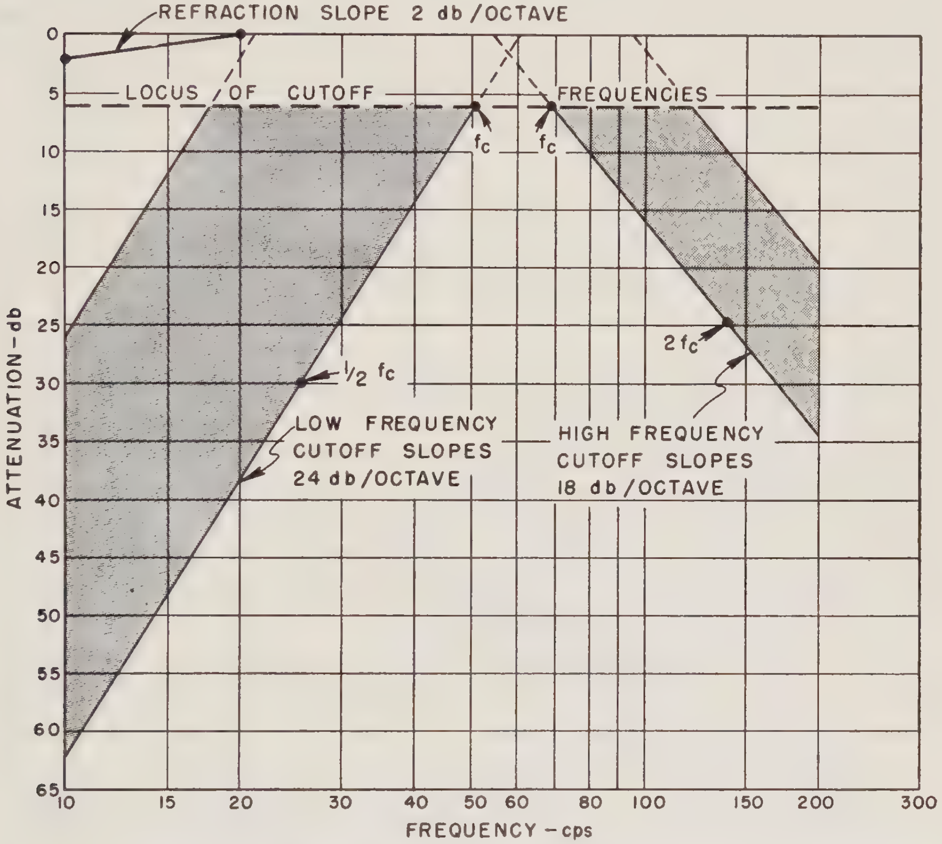

Fig. 2. Idealized Frequency Response of Filter System Satisfactory for Average Survey

SENSITIVITY AND NOISE

Another quantity pertains to noise referred to the input. It is measured by observing the noise deflection of an amplifier which is properly terminated at the input. Feeding-in a measurable signal at a frequency in the transmission region the strength of which is varied until the original deflection is doubled, amounts to a determination of the equivalent noise voltage, referred to the input. This noise voltage can be expressed in volt or in db relative 1 volt RMS or in watt (noise power). Another form of expressing the noise quality of an amplifier is even better, viz., the "noise figure". The latter is the ratio of the noise power to the noise power of an *ideal* generator having the same frequency response as the amplifier. This ratio indicates the excess of the amplifier noise over the absolute minimum noise produced by thermal agitation in the input resistor.

Noise figures provide clues whether attempts toward improvement are likely to be successful. Thermal agitation noise is known from theory and is computed from the relation $4KTB$ (watt) where K = Boltzmann constant = 1.37×10^{-23} joules/°C; T = absolute temperature in degrees Kelvin; B = effective bandwidth in cps. The latter is usually taken from the frequency response of the amplifier, between frequencies at which the attenuation has been reduced by 3 db. (half power points).

A word of caution at this point is appropriate, referring to the measurement of noise by means of a specific signal frequency. When a filter having appreciable insertion loss is incorporated in the circuit, it will take a relatively large (measuring) voltage at the input to produce twice the noise deflection at the output; therefore, an extremely high noise figure reflects not only poor noise quality, but also poor filter efficiency.

It has been found by experience that a noise figure of 20 corresponds to about an average noise quality in seismic channels. Excellent noise figures of about 4 also have been encountered in some systems.

GAIN CONTROL

As mentioned previously, maximum amplifier gain is required only after a sufficiently long time has elapsed following the arrival of initial energy. Before that time, amplification must somehow be reduced as a function of input level if the galvanometer deflection is to remain substantially at a constant level. The range of maximum to ,,normal" input signals (i.e., requiring full amplification to produce a desired galvanometer deflection, say, 1 cm peak-to-peak) may reach 90 db and normal level may be attained in 0.5 sec. If to these conditions are added the additional stipulations that abrupt amplitude change must be preserved, that only negligible phase shift is tolerable, and that distortion must be kept exceedingly low, it becomes clear that gain control presents a formidable problem.

The statement concerning "range" should be qualified by means of a numerical example.

Let it be assumed that the first geophone is 100 feet away from the shotpoint, that the lowest wave velocity is 5000 feet per second, and that the first reflection arrives at 0.1 second after the initial impetus.

Then the path for the reflected wave is 500 feet, while it is 100 feet for the direct wave. Since the amplitude is inversely proportional to the distance, the reflection would suffer an attenuation of 14 db for geometric reasons. Assuming further that the wave velocity in the reflecting layer is 7500 feet per second, and that the densities remain alike, then the ratio of reflection to incident amplitude corresponds to another 14 db.

Thus the first reflection is 28 db below the initial impetus. By experience, the reflection from the deepest horizon is seldom weaker than 60 db compared to the reflection from the shallowest horizon. Hence, if the control range is restricted to about 90 db, it ought to be satisfactory for most shooting conditions *).

The total recording time may be subdivided into three periods: the initial control period, the automatic control period, and the uncontrolled period.

Work on automatic gain control (AGC) was first conceived about 20 years ago and is still in progress. A very large number of control systems has been devised, all of them based on the fundamental recognition that the gain vs. output level relation must be a falling nonlinear function, i.e., that a nonlinear resistance must become part of the amplifier circuit. Of all proposed schemes, the one which has crystallized out and is by far the most popular today is the system disclosed by S. A. Scherbatskoy (U.S. Patent No. 2, 329, 558 of Sept. 14, 1943, Application Sept. 7, 1937). Basically, the idea is illustrated in Figure 3.

The seismic signal is amplified in A_1 and transferred to the input of amplifier A_2 as a variable voltage developed across (1) and (2) of a potentiometer containing a high resistor (megohm range) R. This voltage depends on the resistance of the parallel combination of branches (1) (3) (2) and (1) (4) (2). Each branch contains a thermionic diode D, a bias battery developing an emf E_b and an RC branch consisting of R_1 and C_1 in parallel.

The signal is further amplified in A_2 and (9) feeds the output of the channel and also another (control) amplifier A_3, the output of which is terminated in an isolation transformer; the latter feeds a full wave rectifier (usually of the semiconductor type (5) (6) (7) (8), the positive terminal (8) of which feeds (4) and the negative terminal (7) feeds (3) in the manner shown: R_2, C_2 (together with R_1, C_1) represent the rectification ripple filter and the time delay network, the required condensers usually being of the order of 10×10^{-6} farad (electrolytic).

---

* This line of reasoning originally was proposed by Dr. F. A. van Melle, Technical Service Department, Shell Oil Co, Houston, Tex.

Assuming the voltage at (9) to be below a certain threshold, the rectifier charges condenser C_1 to a potential $|E_s| < |E_b|$ and hence conduction current $i \cong 0$. As the signal at (9) increases above a threshold value, conduction current (i) flows in the direction shown through the diodes in series, reducing the dynamic resistance of each diode. Since this is a backward-acting (feedback) control system, the dynamic resistance between points (1) and (2) adjusts itself in accordance with the potential at (9) which is also a function of the input level; hence the system tends to keep the output potential constant provided that the nonlinear resistors possess sufficient range to do so. It should also be realized that, since (1) (2) (3) (4) is a bridge, any potential across (3) (4) (such as transients and ripple) does not appear across (1) (2) if all components are well-balanced.

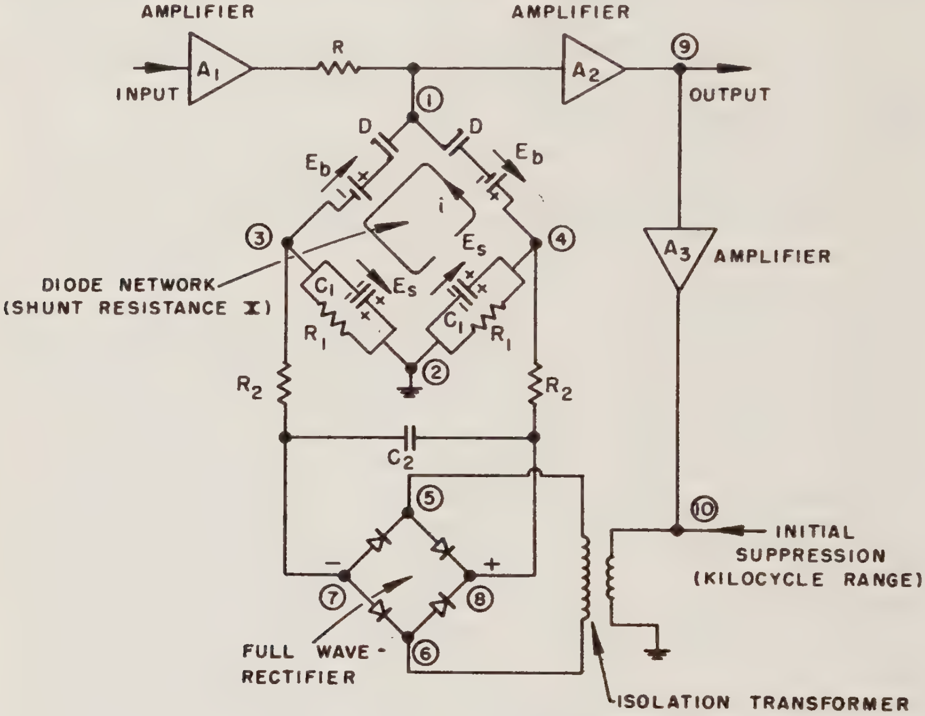

Fig. 3. Diode Type AGC System

In order to increase the range, two such sections are frequently used, so that two AGC loops are operative which may, or may not, be fed from independent control points.

Another modification of this scheme is to make the rectified signal (control dc) influence a modulator which transmits high-frequency conduction current through the diodes.

To mention but a few other systems, various semiconductor bridges (varistors) may be used to produce the variable potentiometer effect; pentodes whose gain is adjusted by applying rectified signal to control-and-suppressor grids may constitute the nonlinear resistance; the resistance temperature effect of metals may be utilized, and a forward-acting manner of control may replace the backward-acting mode of operation just discussed.

Those familiar with the general problem of automatic control realize that any backward-acting system represents a compromise between control accuracy (taper), reaction rate, and stability (hunting) considerations. It is *stability* which must at all cost be maintained, and usually the designer has to accept the remaining characteristics as they come. Forward-acting control is inherently stable. The difficulty here however is to find a nonlinear resistance whose characteristic is compatible with the desired control accuracy. Thus far all examined systems were of the backward-acting type.

The initial control period is usually taken care of by injection of high-frequency energy (kilocycle range) into the isolation transformer prior to the shot (initial suppression); the high frequency is tripped-off upon arrival of initial energy. Initial suppression may also be based on dc injection into the control network.

The AGC characteristics are illustrated in the qualitative Figure 4. Under static conditions, as the input level rises the output level first is uncontrolled, points (1′) (2′). At (3′) normal output level (corresponding to, say, 1 cm) has been reached and the control period is reckoned to start at this point [AGC threshold input level (3)]. From (3′) to (4′) the output level is held essentially constant, this range constituting the AGC range.

It is instructive to study the situation in the uncontrolled period, i.e., when the incoming energy is below the one resulting in the AGC threshold level (3). The previously mentioned amplifier noise level is represented by (1) and should be about 20 db below (3). Another signal level may be termed the ,,minimum useful'' signal from an ,,average'' geophone. This is based on the experimental observation that the minimum useful earth velocity is about 1.5×10^{-6} cm/sec. If, for example, the power sensitivity of an average geophone is assumed to be about 1.7×10^{-4} watt/(cm/sec)^2 and the geophone resistance is taken as 500 ohm, the corresponding signal level would compute to $1.5 \times 10^{-6} \times (1.7 \times 10^{-4} \times 5 \times 10^{2})^{\frac{1}{2}} = 0.44 \times 10^{-6}$ volt $=$ - 127 db relative 1 volt RMS. This level is indicated as (2) on the diagram of Figure 4 and should be located between (1) and (3). The advantage of a low (1) is now seen to imply a low (3), which is very hard to realize in practice: if it could be achieved it would indicate that operation with less powerful (smaller) geophones is justified.

An average value for (3) is -110 db relative 1 volt RMS.

There are several considerations which determine the correct location of (4), i.e., the static AGC range. One requirement is that distortion should not be apparent in that range; the distortion level (5) in the figure is seen not to constitute the determining factor. Another requirement is that the ,,control taper," i.e., the output level variation, is not excessive—usually 6 db is permissible. The majority of systems are satisfactory in this regard. The third requirement is governed by the dynamic control characteristics. Experimentally, the latter are taken as the response to a step-function change of level of 10 db at a midband frequency, from which the reaction rates in db/sec are computed (this is an arbitrary procedure). These are special ,,dynamic" characteristics, since the system is permitted to reach its final state after each

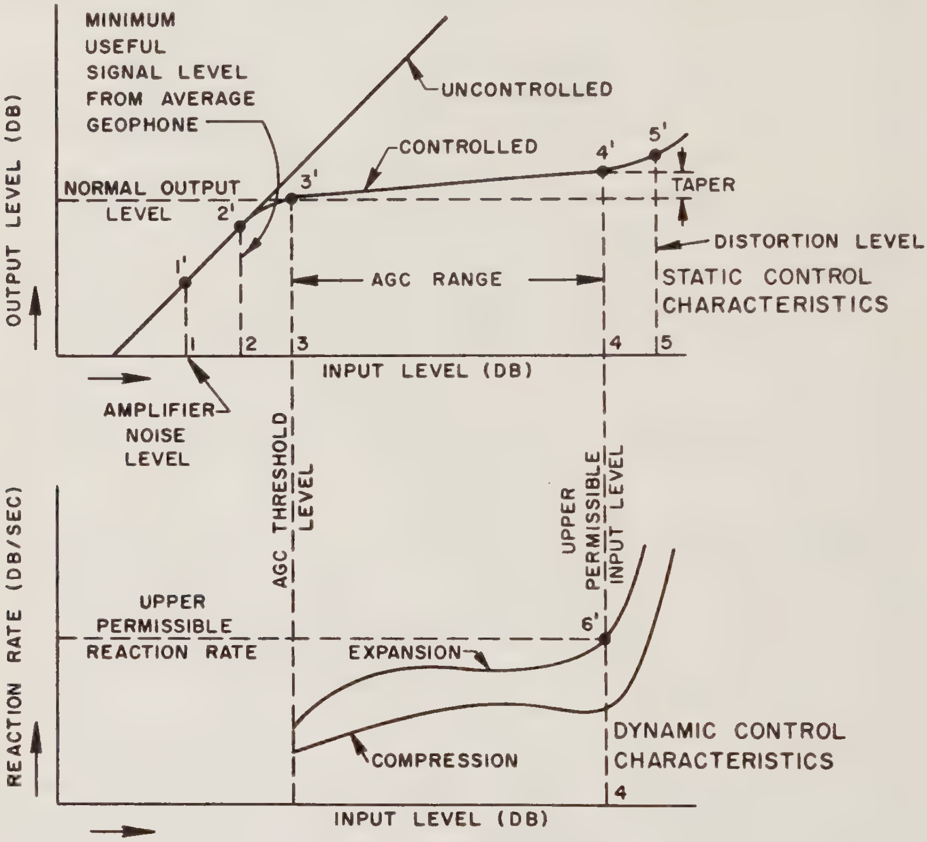

Fig. 4. AGC Characteristics

input change. Under actual conditions ,,effective dynamic characteristics", much more difficult to specify, obtain. Incidentally, an unbalance condition in the controlled network [(1) (2) (3) (4) of Figure 3] is indicated during the recording of the dynamic characteristics as a low-frequency ,,unbalance swing".

AGC implies gain expansion when the input level is falling and gain compression when the input level is rising. Normally, during the automatic control period, the former mode of operation prevails; however, areas exist in which gain compression is required. Ideally, it is felt that within the control range the rates should be constant and that the *expansion* rate should *exceed* the compression rate since, above everything else, a burst of energy should be well recognizable. Qualitative characteristics such as those shown in Figure 4 are considered excellent. The majority of systems, however, produce compression rates which exceed expansion rates.

What should the maximum permissible reaction rate be? It is believed that it should not exceed 150 db/sec. While input energy as a whole seldom decays at such a high rate, it may do so locally. If the expansion rate exceeds the decay rate, a diagnostically important ,,collapse" of energy would be interpreted as a ,,burst" of energy.

In Figure 4 the point (6′) on the expansion rate characteristic determines (4) and (4′) and hence the static AGC range. An average value for the latter is 70 db. Some of the systems have as low a range as 40 db, some as high a range as 110 db (cf. statement previously made with reference to maximum practical range).

What rate of signal level decay should the AGC be capable of following satisfactorily? This is mainly determined by observing the recorded signal at a time corresponding to the AGC threshold value of a suitable calibrated repetitive input signal. The output should be ,,well-developed" rather than more or less severely ,,depressed". An average requirement here is about 80 db/sec. Most systems are capable of such decay rates, some of them accommodating rates as high as 200 db/sec.

Another characteristic quantity may be termed the ,,attack time"; it is the time the system requires to come sufficiently under control without the aid of presuppression. This definition is obviously ambiguous, for it depends on the initial impetus and the decay rate of the input signal as well as on the meaning of the word ,,sufficiently". We assume, arbitrarily, an initial level of 0.1 volt peak, a slow input signal decay rate of 40 db/sec and an undistorted output signal not in excess of 3 cm. On this basis 0.4 sec is an average value; some systems have as low an attack time as 0.15 sec; others come under control very slowly, e.g., at 0.7 sec. The above definition implies that the signal at the ,,attack time" has decayed sufficiently to come within the AGC range.

Assuming, for example, a threshold level of -110 db and an AGC range of 70 db, the maximum signal which the system can accommodate becomes -40 db; starting with 0.1 volt (-20 db) and decaying at a rate of 40 db/sec, the level will have come down by 16 db in 0.4 sec. Thus, at the attack time, the level is -36 db, i.e., almost maximum, and the output signal would probably be undistorted. Whenever conditions require it, the peak input voltage is reduced to an appropriate value.

The attack time determines whether presuppression (initial suppression) as an aid during the initial control period is *obligatory* or *optional*. It is felt that for attack times exceeding 0.25 sec initial suppression is mandatory; if the attack time is short, the main reason for using initial suppression is to quiet the traces before the shot in order to recognize clearly the shape of the initial event. Initial suppression should provide variable means for attenuation of at least 60 db. The combined performance of initial suppression and AGC should not be too critical as to the selection of initial suppression and should be capable of reducing the attack time to zero. It is precisely because of an effort to develop a system with very short attack time, that the compression rate usually not only exceeds the expansion rate but also rises rapidly for higher levels. The requirements for the automatic control period and the initial control period are incompatible as far as the demands on the reaction rates are concerned: for the automatic period the expansion rate should appreciably exceed the compression rate, while for the initial period the reverse should be true. Hence, a compromise in the design is inherent.

Phase distortion due to AGC seldom exceeds 2 milliseconds. For relatively low signal frequencies, such as 10 cps, AGC does not act as effectively as for medium frequencies, such as 40 cps, so that (refraction filter assumed) a frequency discrimination characteristic, due to AGC, for constant input level usually is observed. This has the effect of boosting the output level at low frequencies and counteracts the effect of the filter. This becomes serious only if low frequency is deliberately permitted to appear in the output. The discrimination frequently amounts to an excess of 10 db at 10 cps relative to 40 cps.

At low frequencies a second harmonic distortion due to AGC is unavoidable. As an average value, it may vary between 2 percent and 4 percent of the signal, depending on the input level.

Harmonic distortion

Neither the above-mentioned AGC distortion nor the distortion due to the nonlinear tube characteristics, both of an inherent nature, are considered here. The present concern is with another distortion which is implied by the nonlinear flux vs. exciting current relation existing in iron core inductors and transformers. In particular, the input transformer shall be regarded as the source of distortion. It is best to develop a few basic equations and to study them numerically in order to get at the core of the problem.

In the following, all voltages (relative 1 volt RMS) and ratios will be expressed in db.

The total filter attenuation (α) is assumed composed of prefiltering ahead of the input transformer (α_p) and of additional filtering at some point past the input transformer (a_a):

$$\alpha = \alpha_p + \alpha_a \qquad (1)$$

The roller (ground roll) voltage at the output (R_o) in terms of the roller voltage at the input (R_i) and filter attenuation becomes

$$R_o = R_i - \alpha_p - \alpha_a \qquad (2)$$

if all losses are assumed to be in the filters and if gain is ignored.

The additional filter attenuation in terms of the roller voltage at the primary of the input transformer (R_t) and (R_o) is:

$$\alpha_a = R_t - R_o \qquad (3)$$

The harmonic distortion ratio (ρ_H) is defined in terms of (R_t) and the harmonic voltage (H) developed at the transformer:

$$\rho_H = H - R_t \qquad (4)$$

A marginal factor ($\varkappa_H$) is now introduced which describes the magnitude relation between the signal voltage (S) and the harmonic voltage (H), it being understood that (S) and (H) do not suffer attenuation:

$$\varkappa_H = S - H \qquad (5)$$

Finally, another marginal factor ($\varkappa_R$) is introduced which describes the magnitude relation between (R_o) and (S), viz:

$$\varkappa_R = R_o - S \qquad (6)$$

Figure 5 illustrates transformer harmonic distortion by indicating (ρ_H) in db or percent as a function of (R_t) in db, and in the following the characteristic of an „average" transformer will be assumed. Since it is well known that the magnetic flux varies inversely with frequency, this characteristic is taken at $f = 10$ cps which represents approximately the lowest roller frequency. The harmonics are odd frequencies thereof, with the third harmonic dominant ($f = 30$ cps). To distinguish this from signal energy, the latter is assumed at $f = 45$ cps. It is believed that $\varkappa_H = \varkappa_R = +10$ db are realistic values for the marginal factors: $K_H =$ 10 db means that the harmonic distortion is not permitted to be in excess of about 32 percent of the signal; $\varkappa_R =$ 10 db implies that the roller voltage in the output is not required to exceed about 320 percent of the signal (more low-frequency filtering should be used if the roller becomes too large). With these values fixed and assuming $R_i = O$ (i.e., 1 volt RMS), various values of (R_t) are assigned and the corresponding (ρ_H) obtained from Figure 5. Then (H) is computed from equation (4), (S) from equation (5), and (R_o) from equation (6). Next, (α_a) is computed from equation (3), while, of course, (α_p) is numerically $= -(R_t)$. The resultant characteristic, (α_a) vs. (α_p), represents the maximum permissible additional filtering corresponding to a certain prefiltering. It is illustrated in Figure 6. What happens if (α_a) is chosen larger than the values indicated in Figure 6? If the margin $(\varkappa_H)$ is preserved, computation shows that $(\varkappa_R)$ is decreased, i.e., the output roller may not be developed to its maximum strength. If the margin $(\varkappa_R)$ is preserved, then $(\varkappa_H)$ decreases, i.e., the harmonic distortion voltage interferes too much with the signal voltage. Above all, Figure 6 brings out the striking fact that, *without prefiltering*, almost *no additional* filtering is permissible, but that with

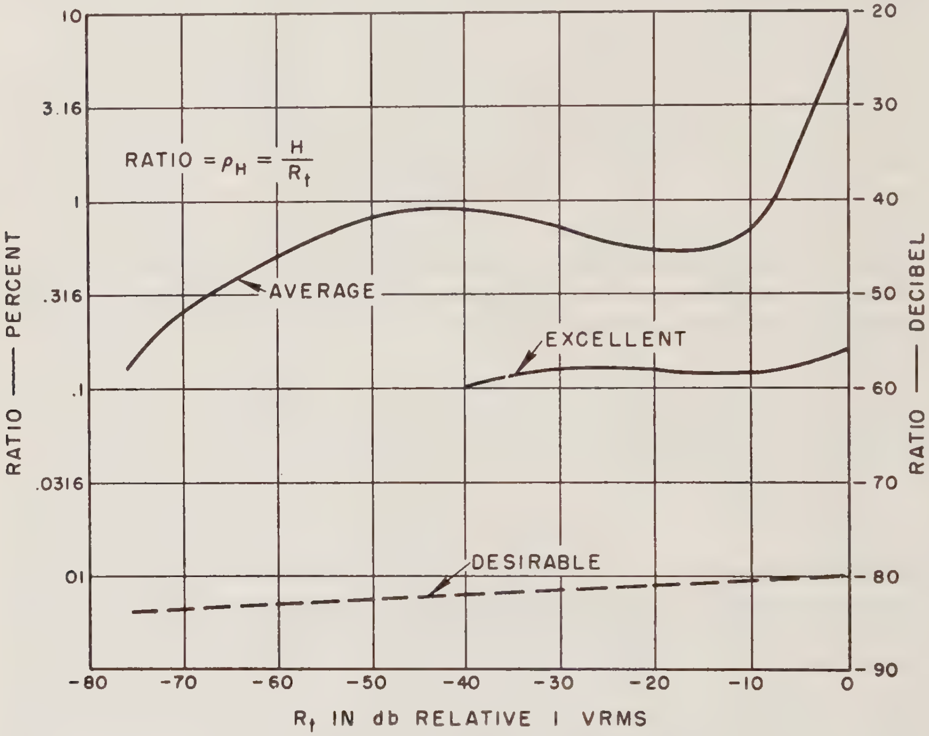

Fig. 5. Harmonic Distortion of Transformers.

as little as 10 db prefiltering, about 25 db of additional filtering is permissible.

Assuming finally that it is required to utilize a total filtering of $\alpha = 60$ db and that zero prefiltering is used, $\alpha_p = O$, and assuming further that, as previously, $R_i = O$, $\varkappa_H = \varkappa_R = 10$, the question arises: What is the required harmonic distortion (ρ_H)? By equation (2) $R_o = -60$ db, by equation (6) $S = -70$ db, by equation (5) $H = -80$ db, and by equation (4) $\rho_H = -80$ db, which is equivalent to 0.01 percent. The best transformer thus far investigated has a maximum distortion of about 0.16 percent and is still a long way from the desirable transformer (see Figure 5).

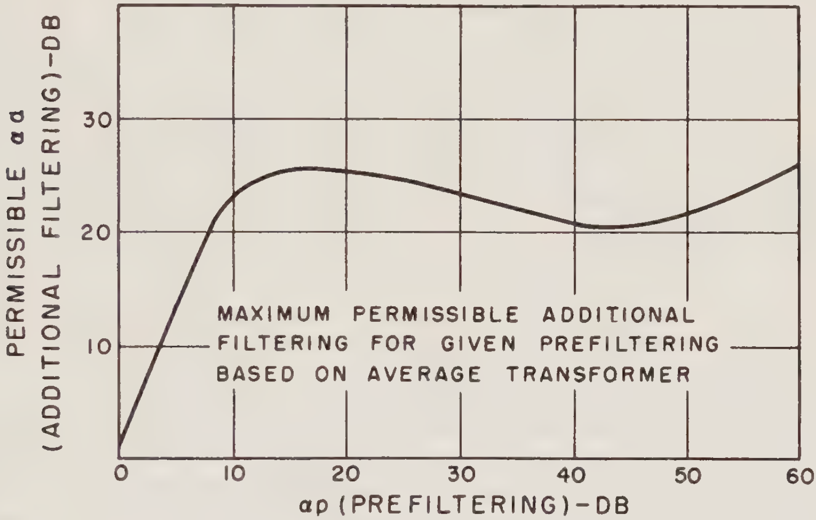

Fig. 6. Effect of Prefiltering

It is believed that this discussion sufficiently emphasizes the necessity of placing part of the low-frequency filter ahead of the input transformer. If the filter contains an inductor, its harmonic distortion, of course, contributes to the total distortion and must be taken into account.

Conclusion

Some of the fundamental design aspects of seismic reflection amplifier channels have been reviewed in this paper. The over-all system has been described functionally. Filtering, in terms of minimum requirements, sensitivity, and noise, has been briefly discussed. Gain control and harmonic distortion have been treated.

Acknowledgement

The author wishes to express his gratitude to the Shell Development Company for permission to publish this material. The excellent and reliable experimental work of Mr. J. C. Toups is also greatly appreciated.

A THEOREM CONCERNING ANISOTROPY OF STRATIFIED MEDIA AND ITS SIGNIFICANCE FOR REFLECTION SEISMICS *

BY

Th. KREY** and K. HELBIG**

Abstract

It is proved that horizontally stratified media, the various materials of which do not differ in their Poisson number, can be considered as isotropic for reflections of a small dip when taking into account quasi-longitudinal waves which have to be reckoned with in practice. Approximating the surface of the wave by an ellipsoid would, however, result in considerable errors.

Moreover, curves are presented allowing practical calculations for steeper dips to be made.

PART 1 BY Th. KREY

Introduction

Quite recently the problem of elastic anisotropy has attracted attention and has been discussed frequently at meetings and in periodicals. In particular, the work of Postma and Helbig may be mentioned who, independently of each other, have developed from the first principles the theory of the anisotropy of stratified media which in itself had already been dealt with in older literature. In so doing they have produced very interesting examples and enriched our knowledge. Since both papers give a complete reference to the literature, this is not repeated here.

In many papers attention is drawn to the fact that, in nature, anisotropy is frequently observed. Thus, the question arises concerning the significance of anisotropy in applied seismics, especially in reflection seismics, and how it may be taken into account. This is frequently done on the assumption (Uhrig and van Melle, Kleyn) that the wave surfaces of longitudinal or, more precisely, of quasi-longitudinal waves are ellipsoids of revolution. It will be shown in the following that in general, this assumption leads to considerable errors. In addition, it will be proved that in the case of reflections from small to moderate dipping boundaries, it is better to ignore anisotropy completely rather than to replace the wave surface by an ellipsoid of revolution.

---

*) Presented at the Tenth Meeting of the European Association of Exploration Geophysicists, held in Hamburg, May 16-18, 1956.

**) Seismos G.m.b.H., Hannover.

CALCULATION OF THE CURVATURE OF THE WAVE SURFACE AT THE INTERSECTION WITH THE AXIS OF SYMMETRY

The definitions and notations employed by Postma (1955) are used here with little alterations. From equations (17) and (18) in the paper cited it follows that

$$x = v \sin\beta + \dot{v} \cos\beta \qquad (1)$$

$$z = v \cos\beta - \dot{v} \sin\beta \qquad (2)$$

x and z being the coordinates of the wave surface, v the associated phase velocity or normal velocity and β the angle between the wave normal and the axis of symmetry. (Postma uses $\varphi = 90 - \beta$ instead of β.)

A dot over a symbol indicates a derivative with respect to β. Restricting ourselves to a quasi-longitudinal wave, v will have the greater value of the two positive roots of Postma's equation (13) which may be written in the following manner (φ is replaced by β):

$$\begin{vmatrix} c_{11} \sin^2\beta + c_{44} \cos^2\beta - \rho v^2 & (c_{13} + c_{44}) \sin\beta \cos\beta \\ (c_{13} + c_{44}) \cos\beta \sin\beta & c_{44} \sin^2\beta + c_{33} \cos^2\beta - \rho v^2 \end{vmatrix} = 0 \qquad (3)$$

(1), (2), and (3) together, give a parametric representation of the wave surface.

A formula will now be derived for the curvature of this wave surface at its intersection with the positive z-axis, an axis identical with the axis of symmetry. Considering v, according to (3), as a function of β, then x and y, by (1) and (2), will be also functions of β. Then

$$\dot{x} = + (v + \ddot{v}) \cos\beta \qquad (4)$$

$$\dot{z} = - (v + \ddot{v}) \sin\beta.$$

By differentiating (3) once or by considerations of symmetry it follows, that: $\dot{v} = 0$, $x = 0$ and $\dot{z} = 0$ for $\beta = 0°$ and that : $\dot{v} = 0$, $z = 0$ and $\dot{x} =$; 0 for $\beta = 90°$.

For the curvature k at $\beta = 0°$ which, according to the preceding note, will correspond to the intersection with the positive z-axis, we have therefore

$$k = \pm \frac{\ddot{z}\dot{x} - \ddot{x}\dot{z}}{(\sqrt{\dot{x}^2 + \dot{z}^2})^3} = \pm \frac{1}{v + \ddot{v}} \qquad (5)$$

With regard to the quasi-longitudinal wave considered we will have $v = \sqrt{\frac{c_{33}}{\rho}}$ for $\beta = 0°$. By differentiating (3) twice, $\ddot{v}$ will also be obtained for $\beta = 0°$, and from this we finally obtain

$$k = \pm \frac{\sqrt{\rho}\,\sqrt{c_{33}}}{c_{44} + \dfrac{(c_{13} + c_{44})^2}{c_{33} - c_{44}}} \qquad (6)$$

The sign in (6) is now fixed in such a way that k will be positive when the curve is concave towards the origin of the coordinates. Thus the positive sign is valid in (6).

AN INEQUALITY CONCERNING THE CURVATURE

According to the last but one formula on the bottom of page 787 in Postma's paper it is

$$c_{11} \geqq c_{44} + \frac{(c_{13}+c_{44})^2}{c_{33}-c_{44}} \quad . \quad . \quad . \quad . \quad . \quad . \quad . \quad . \quad . \quad . \qquad (7)$$

so that

$$k \geqq \frac{\sqrt{\rho}\ \sqrt{c_{33}}}{c_{11}} = \frac{\sqrt{\dfrac{c_{33}}{\rho}}}{\dfrac{c_{11}}{\rho}} = \frac{v\ (\beta = 0^\circ)}{v^2\,(\beta = 90^\circ)} = \frac{v_\perp}{v_{/\!/}{}^2}. \quad . \quad . \quad . \qquad (8)$$

Here $v_{/\!/}$ and $v_\perp$ are the normal velocities parallel to the stratification and perpendicular to the stratification.

Now, according to (1) and the preceding remarks, $v_{/\!/}$ and $v_\perp$ represent the semi-axes of the wave surface. To put is more clearly

$$\begin{aligned} v_\perp &= z_{(x=0)}, \\ v_{/\!/} &= x_{(z=0)}. \end{aligned} \quad . \quad . \quad . \quad . \quad . \quad . \quad . \quad . \quad . \quad . \quad . \quad . \quad . \qquad (9)$$

Since the curvature of an ellipse at the end of the b-axis, is equal to b/a^2 where a and b are the axes, eq. (8) states that the curvature of the wave surface belonging to the quasi-longitudinal waves, at the point of intersection with the z-axis, is greater or equal to the curvature that is obtained for an ellipse of the same length of axes.

THE PRINCIPLE THEOREM

Now, the case $\lambda_1/\mu_1 = \lambda_2/\mu_2$ may be considered, λ and μ being Lame's constants.

This means that both the substances making the stratified medium have the same Poisson's ratio ν. In this case, after some mathematical manipulations, not given here, we have

$$k = \sqrt{\frac{\rho}{c_{33}}} = \frac{1}{z_{x=0}} = \frac{1}{v_\perp}. \quad . \quad . \quad . \quad . \quad . \quad . \quad . \quad . \quad . \quad . \qquad (10)$$

This implies that the origin of the coordinate system is the center of curvature. Neglecting the terms of the fourth and higher powers in β

or x, the wave surface in the vicinity of the axis of symmetry will be a sphere the center of which is the origin of coordinates.

Consequently, for the ray velocity v_{ray}

$$v^2_{ray} = x^2 + z^2 = v_{\perp}^2 + o\,(x^4). \qquad \text{(11)}$$

Now, it is a well known fact that there is only a small variation in Poisson's ratio for the different types of rock occuring in nature. In the majority of practical cases eq. (11) may therefore be considered valid. This means that in reflection seismics it is permissible to base the computations in the case of smaller dips on the assumption of the existence of an isotropic medium with the effective velocity equal to the vertical velocity.

The question of what may be considered a smaller dip will here not be scrutinized. An approximate idea may be gained from Fig. 10 of Postma's paper. In the example, illustrated in this figure, Poisson's ratios of the media forming the stratification are only approximately equal. Their values are 0.273 and 0,286. Nevertheless relation (11) appears to be satisfied rather well, so it seems that, up to about 25°, it will not be necessary to take into account anisotropy. Evidently a relatively large error would arise from basing the calculation on the ellipse plotted in Postma's Figure 10. In the second part of this paper, this question will be discussed more rigorously by K. Helbig.

In the following a short discussion of the errors will be given for the case of small dips:

Let ψ be the angle made by a reflected ray with the vertical ina homogeneous medium, and op t the time of reflection. Then, in the case of isotropy the following well known relation holds

$$\sin \psi_{isotrop} = v \,.\, dt/dx.$$

When the wave surface is based on an ellipsoid of revolution the section by the x-z plane is:

$$\frac{x^2}{v_{/\!/}^2} + \frac{z^2}{v_{\perp}^2} = t^2 \qquad \text{(12)}$$

then, by differentiation of (12). with z constant, and eliminating z and t, we obtain

$$\tan^2 \psi_{ellipse} = \left(\frac{x}{z}\right)^2 = \frac{v_{/\!/}^2}{v_{\perp}^2} \frac{v_{/\!/}^2 \,.\left(\dfrac{dt}{dx}\right)^2}{1 - v_{/\!/}^2 \,.\left(\dfrac{dt}{dx}\right)^2} = \left(\frac{v_{/\!/}}{v_{\perp}}\right)^2 \tan^2 \psi_{isotrop\, v_{/\!/}} \qquad \text{(13)}$$

where $\psi_{isotrop\ v_{/\!/}}$ is the angle which would be obtained when isotropy is taken into account, the velocity being $v_{/\!/}$.

Assuming ψ to be so small that we can put $\psi = \sin\psi = \tan\psi$ we get

$$\psi_{ellipse} = \left(\frac{v_{\shortparallel}}{v_{\perp}}\right)^2 \psi_{isotrop\; v_{\perp}}. \qquad (14)$$

On the other hand, when proceding from the wave surface (11), it follows from a similar operation that

$$\psi = \psi_{isotrop\; v_{\perp}} + o\,(\psi^3) \qquad (15)$$

(14) and (15), together, give an idea of the positional errors arising from replacing the wave surface by an ellipsoid of revolution for small angles in the case of anisotropy. Equ. (15) states that, for a constant Poisson's ratio, the true ψ must be approximately equal to $\psi_{isotrop\; v_{\perp}}$. When, for instance, $v_{\shortparallel} = 1.2\, v_{\perp}$, then according to (14) a positional error of $(1.2^2 - 1) = 44\%$ will arise in the horizontal coordinate.

SOME FURTHER REMARKS CONCERNING THE CURVATURE

Another problem investigated was whether the curvature k can attain greater values than those given by (10). This question must be answered positively. Thus, for instance if $\mu_2 \longrightarrow 0$

then $c_{44} \longrightarrow 0$,

whence $k \rightarrow (\sqrt{\rho} \,.\, c_{33}{}^{3/2})/c_{13}^2$.

Now, in the general case $(\sqrt{\rho} \,.\, c_{33}{}^{3/2})/c_{13}^2 > \sqrt{\rho/c_{33}}$

for, when $\mu_2 \rightarrow 0$ then

$$c_{13} \rightarrow c_{33} - \frac{2}{D}\,(d_1 + d_2) \,.\, d_1 \,.\, \lambda_2 \,.\, \mu_1 < c_{33}.$$

Arbitrarily great values may be reached for k when, in addition to $\mu_2 \rightarrow 0$, $\lambda_1 \ll \mu_1$ and $d_2 \ll d_1$.

With reference to this, also see Figures 7 and 11 in Postma's paper!

It is easy to find examples where

$$\frac{\sqrt{\rho}\,\sqrt{c_{33}}}{c_{11}} < k < \sqrt{\frac{\rho}{c_{33}}}.$$

Inequality (8) cannot be improved further. This is easily proved by considering that in the last but one formula on the bottom of page 787 of Postma's paper, the factor $(\mu_1 - \mu_2)$ occurs in the second power whereas in the expression for $(c_{11} - c_{33})$ this factor is linear. See page 786 of Postma's paper!

PART 2 BY K. HELBIG

THE MAGNITUDE OF THE ERRORS AND THE COMPUTATION OF CORRECTIONS FOR GREATER DIPS.

To get a more exact impression of the nature and the magnitude of the errors involved in neglecting anisotropy, some further mathematics are necessary, which include the computation of corrections for greater dips.

The position and orientation of a reflecting element can be described by three coordinates:

1. the length l of the perpendicular dropped from the shotpoint upon the plane of the reflector,
2. the angle β between the perpendicular and the axis of symmetry (β is the dip of the reflecting plane against the plane of stratification),
3. the angle ψ between the ray (shotpoint—reflector—shotpoint) and the axis of symmetry.

Between these coordinates and the observed or proposed data there exist three equations which are generalisation of well known formulae:

$$l = v(\beta) \,.\, t_0/2, \qquad \sin\beta = v(\beta) \,.\, dt/dx, \qquad \psi = \psi(\beta) \,.$$

Calculating the position and the orientation of a reflector means solving this set of equations with regard to the assumed relations between the normal velocity v and the angle β on the one hand and between ψ and β on the other hand. One has to compare three cases:

a) the true wave surface,
b) the assumption of an elliptic wave surface,
c) the assumption of a spherical wave surface, i.e. assuming the medium to be isotropic.

We then get the following formulae:

a) *true wave surface* b) *ellipsoid* c) *sphere*

$$\tan^2\beta = \frac{w + w^2}{1 + (P - 1)\,w} \quad (16)$$

$$\frac{v(\beta)}{v_{\perp}} = \sqrt{\frac{1 + Pw + Qw^2}{1 + Pw + w^2}} \; (17) \qquad \frac{v(\beta)}{v_{\perp}} = \sqrt{1 + (Q - 1)\sin^2\beta} \; (19) \qquad v(\beta) \equiv v_{\perp} \; (21)$$

$$\tan\psi = \tan\beta \, \frac{1 + 2Qw + (P - 1)\,Qw^2}{1 + 2w + (P - Q)\,w^2} \; (18) \qquad \tan\psi = Q \,.\, \tan\beta \; (20) \qquad \psi \equiv \beta \; (22)$$

Here the following abbreviations are used:

(23) $Q = v_{\parallel}^2/v_{\perp}^2$; (24) $P = [Q\,(1 - \nu) + \nu]$, ν being Poissons ratio.

It may easily be seen, that for a small dip, implying a small value of the parameter w, which is defined by (16), the assumption of a spherical wave surface agrees much better with the exact case than that of an elliptic wave surface.

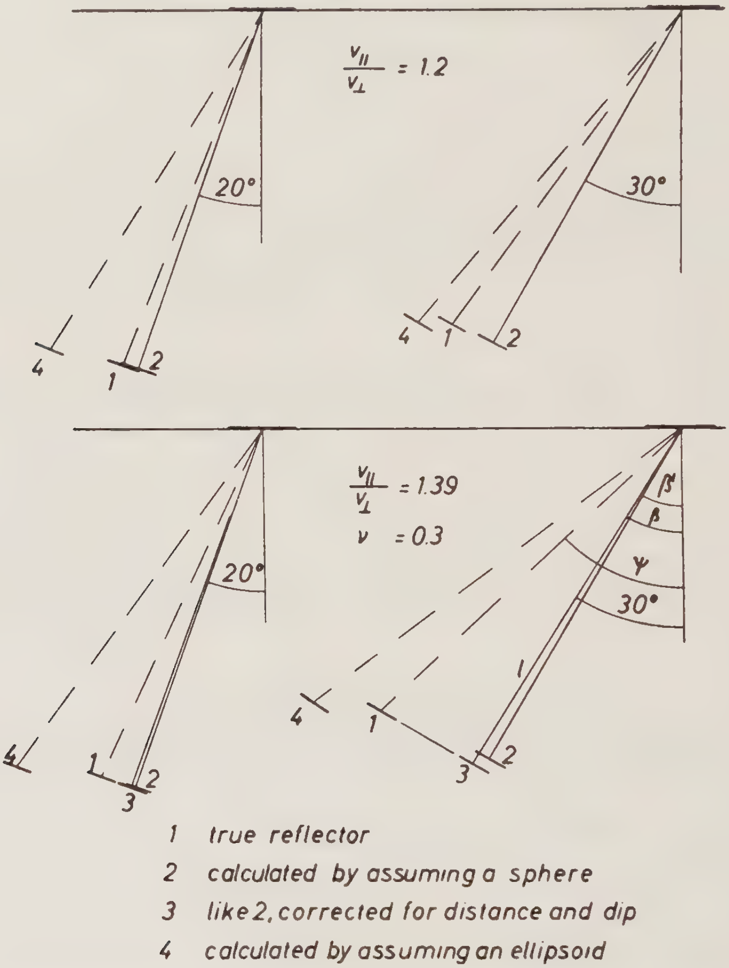
$\frac{v_{\parallel}}{v_{\perp}} = 1.2$
20°
30°
4
1
2
4
1
2
$\frac{v_{\parallel}}{v_{\perp}} = 1.39$
$\nu = 0.3$
20°
β'
β
ψ
30°
4
1
3
2
4
1
3
2
1 true reflector
2 calculated by assuming a sphere
3 like 2, corrected for distance and dip
4 calculated by assuming an ellipsoid

Fig. 1. Positions of reflectors, computed with different assumptions regarding the anisotropy.

In Figure 1 there are four examples showing the true position of the reflector (no. 1) and those positions calculated on one or the other assumption (no. 2 for a spherical wave surface and no. 4 for an elliptic one.)

For small dips no. 1 and no. 2 nearly coincide, whilst no. 4 differs from the true reflector by a considerable amount. In cases of strong anisotropy and steeper dip the errors in l and β remain relatively small, whereas those in lateral position now become considerable. But it is quite easily possible to get from no. 2 to no. 1 by using the corrections which are shown in figure 2 and which are derived from (16) to (22).

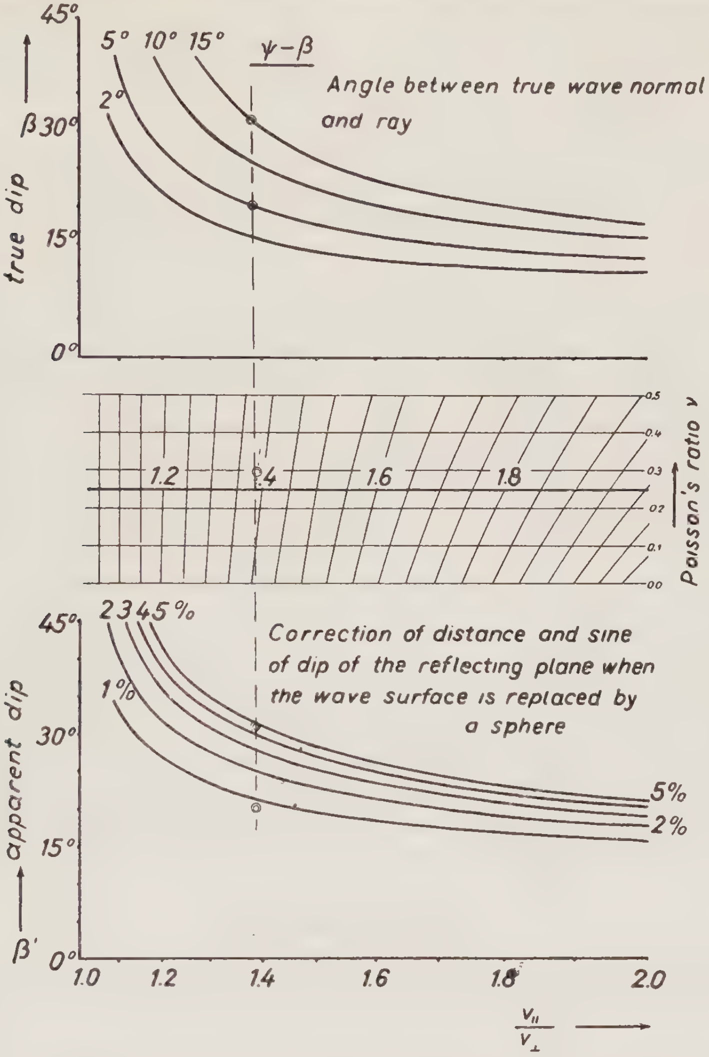

Fig. 2. Correction curves for the effect of anisotropy.

In the lower part of figure 2 the corrections in l and $\sin\beta$ are plotted as functions of the anisotropy factor and the apparent dip β'-that is the dip obtained when using $v_{\perp}$ instead of v (β). For example, for an anisotropy factor of 1.4 and an apparent dip of 30° the normal velocity will be about 4% higher than assumed. Therefore l and sin β must be enlarged by about 4%. This leads to a true fip of 31.3°.

In the upper part of figure 2 the angle between true wave normal and true ray is plotted against the anisotropy factor and the true dip.

In the example mentioned above $(\psi - \beta)$ is 15° and therefore $\psi = 46.3°$.

All these corrections are valid for Poisson's ration $\nu = 0.25$. "Lines of equal corrections" for different values of ν are drawn in the middle part of figure 2. By this all cases with arbitrary values of Poisson's ratio are reduced to the case $\nu = 0.25$. This means, that a stratified medium with an anisotropy factor of 2, the constituents of which have the common Poisson's ratio $\nu = 0.5$, has the same corrections as one with an anisotropy factor of 1.9 and $\nu = 0.25$ or as one with an anisotropy factor of 1.85 and $\nu = 0.1$. For media with relatively small anisotropy factors (up to about 1.6) the value of the common Poisson's ratio has nearly no influence.

By the different curves of corrections of figure 2 one is enabled to find the true reflector up to dips of 45°.

The double circled points represent the two media, for which the examples in figure 1 had been calculated. The way of calculating the true position and orientation is as follows:

The first approximation is the element no. 2 (by assuming the medium to be isotropic). By applying the lower part of figure 2 l and β are enlarged, and the element no. 3 will be obtained. Thus the plane of the reflector is known. To get the lateral position of the reflector within this plane, one needs only draw the ray, whose direction is known from the upper part of figure. 2

On the other hand, if there is a certain admissible error one can see from figure 2 up to which dip it is possible to disregard anisotropy completely.

ACKNOWLEDGEMENTS

The authors wish to thank the Seismos G.m.b.H. for the permission to publish these papers.

REFERENCES

HELBIG K., 1956, Die Ausbreitung elastischer Wellen in anisotropen Medien, Geophysical Prospecting 4 no. 1.

KLEYN A. H., 1956, On Seismic Wave Propagation in Anisotropic Media with Applications in the Betun Area, South Sumatra, Geophysical Prospecting 4 no. 1.

POSTMA G. W., 1955, Wave Propagation in a Stratified Medium, Geophysics 20 no. 4.

UHRIG L. F. and VAN MELLE F. A. V., 1955, Velocity Anisotropy in Stratified Media, Geophysics 20 no. 4.

ON THE RELIABILITY OF HARMONIC ANALYSIS OF SEISMOGRAMS

BY

A. KORSCHUNOW *)

ABSTRACT

Since harmonic analysis of seismograms seems to become more familiar in the interpretation of seismic data, the author presents the results of a thorough check analysis. Following a fixed scheme, one seismogram is analysed by means of a mechanical analyser (system MADER-OTT). Standard deviation of Fourier coefficients is examined, and scattering in phase values is discussed. At the best, in the range of maximum amplitudes of the spectrum, the method yields 6% in phase scattering. At the worst, on either side of the spectrum, 13 % are obtained. Generally 8 % have to be taken in account. (Percentages in periods of partial-waves of the analysis!). The results are in accordance with former routine analysis (Korschunow, 1955).

GENERAL REMARKS

In a previous paper (Korschunow, 1955) the author presented investigations on the dispersion of surface waves in loose materials of the soil. These investigations were based on thorough harmonic analysis of seismograms by means of an usual mechanical analyser (system MADER-OTT).

The method of mechanical analysis, as derived from Fourier's theorem, is established in theory. The well known base-relations of Fourier-analysis are:

$$\sum_n (a_n \cos nt + b_n \sin nt) = \sum_n c_n \sin (nt + e_n)$$

$$\sum_n (a_n \sin nt + b_n \cos nt) = \sum_n c_n \cos (nt - e_n) \quad \text{respectively,}$$

where: $a_n = c_n \sin e_n$; $b_n = c_n \cos e_n$; $c_n = (a_n^2 + b_u^2)^{1/2}$; and $\tan e_n = a_n/b_n$.

The application of harmonic analysis, however, is handicapped by mere technical difficulties, i.e.: continuous traversing of the outlines of the seismogram by hand, the reading of the vernier scale, and the uncertainty of the mechanical linkages of the apparatus. Principally the traversing of the outlines of the seismogram by hand with the pointer of the apparatus will in any case give the greatest uncertainty. The effect of reading the vernier scale and the limitations of the machine have already been discussed by H. Baer (1937).

---

*) Institut für angewandte Geophysik der Universität München.

Practically, it is not possible to analyse the exact shape of the seismogram, but deviations from it of an approximately random character will occur. The influence of these deviations still represents an unknown factor in the reliability of the method. The present investigations may be regarded as a contribution to this problem.

TECHNICAL PROCEDURES

For check analysis a seismogram from former measurements in a loampit near Emmering (Korschunow, 1955) was selected. Fig. 1 shows the seismogram over its whole length. It represents the vertical component (Z) of a complete three component set of mechanical seismographs. The ground motion resulted from a blast of 125 g of explosive at a distance of 200 m.

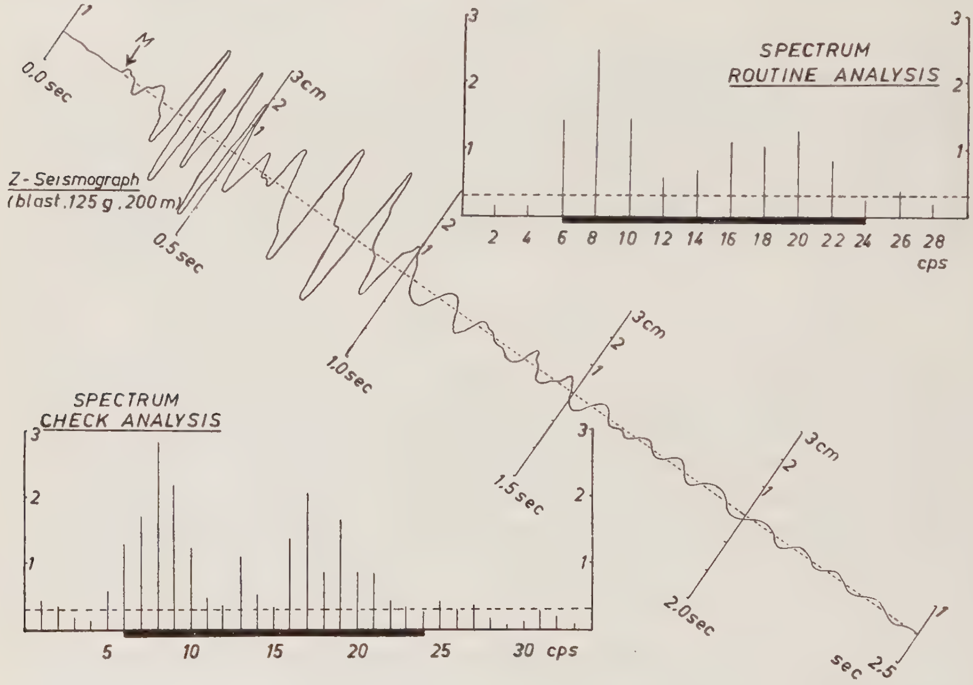

Fig. 1. Seismogram, with spectra obtained in routine analysis and in check analysis

The check analysis was extended over a total time of 2.5 seconds (from the time break of the explosion to the end of the motion). The original seismogram showed very small movements of high frequencies at about 105 milliseconds after the timebreak and which, as they would not have influenced the harmonic analysis, have been omitted in the present copy. At 168 milliseconds from the time break strong motions, with superposition of higher frequencies, are to be seen. This instant has been marked by an arrow (*M*).

The general check analysis of the present seismogram covers the interval from O.O seconds to 2.5 seconds. This will be referred to as the ,,total analysis''. Additional check analyses were carried out, omitting the first part of the seismogram, over intervals of 2.240 and 2.280 seconds, in both cases beginning at the time marked by the arrow (*M*.). These additional check analyses will be referred to as the ,,partial analysis''. The choice of intervals of 2.240 and 2.280 seconds for the ,,partial analysis'' is connected with the reproduction of integral frequencies (*cps*) and will be discussed later.

In the ,,total analysis'' a number of independent determinations of the Fourier coefficients a_n, b_n and c_n and phase angles e_n were obtained by using different settings of the analyser. The statistical comparison of these values provides a measure of the reliability of the mechanical analysis.

RESULTS OF THE CHECK-ANALYSIS

On Fig. 2 the results of the ,,total analysis'' are concentrated graphically on so called ,,periodograms'', as formerly introduced for the characterization

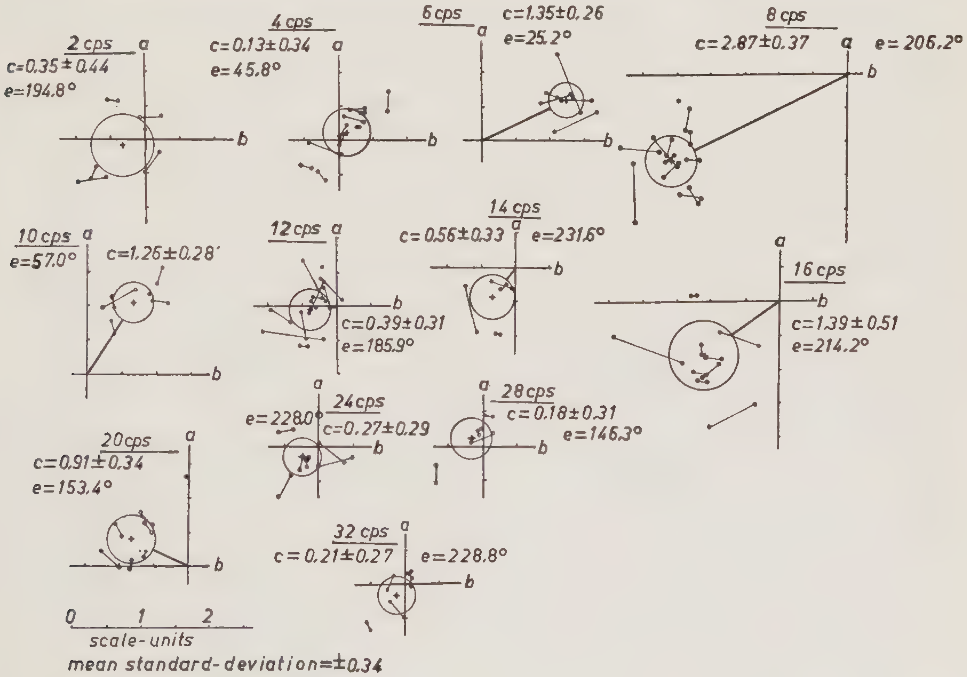

Fig. 2. — Periodograms of check analysis (including Fourier coeff. and phase angles of different frequencies)

of geophysical data by J. Bartels (1927). In these periodograms the values of a_n and b_n are plotted along the vertical and horizontal axis respectively, so that the distance from each point to the origin represents the value of c_n, and the angle between the horizontal axis and the line connecting each point with the origin represents e_n.

A cross (+) marks the statistical mean value as centre of a circle, giving the standard deviation as calculated from all reduced values a_n and b_n. The phase angles (e_n) and the length of the rotating vector of the periodogram are indicated separately for each frequency. The mean standard deviation of the whole material gives the value ± 0.34 scale units. As the ,,total analysis'' for every harmonic has been done twice for direct control of each traversing of the outline of the seismogram, repeated values on the periodogram are linked, so that the reproducibility of values can be estimated. Any single value on the periodogram relates to the routine analysis, dealt with in the previous paper (Korschunow 1955).

Before a critical discussion of the periodograms in Fig. 2, the resulting frequency spectra, shown in Fig. 1, must be considered. The spectrum of the routine analysis (see paper 1955) is compared with the spectrum of the check analysis. The amplitudes of the latter spectrum are mean values resulting from a number of determinations for each frequency. The amplitude scale of the spectra is twice the scale of the amplitudes in the seismogram. Formerly (Korschunow 1955), the ,,dispersion interval'' has been defined, as the ,,active part of the spectrum''. This ,,dispersion interval'' was the basis for the construction of experimental dispersion curves. The ,,dispersion interval'' was found to be typical for various measurements. Phase values lying outside the ,,dispersion interval'' could not be utilized for further treatment of a specific ,,Rayleigh wave mechanism''. On Fig. 1 of the present paper the ,,dispersion interval'' (6 to 24 cps) has been specially underlined. Moreover, a dashed line gives the amount of the mean standard deviation of all reduced Fourier coefficients which take part in the ,,total analysis'', thus demonstrating a ,,noise level'' of the spectra. Very important with regard to the reliability of harmonic analysis is the fact that amplitudes of the spectra beyond the ,,dispersion interval'' scarcely rise above the ,,noise level'', given by the mean standard deviation of the check analysis. In spite of the above mentioned technical shortcomings in the procedure of harmonic analysis, the spectrum of the routine analysis is very similar to that of a thorough check analysis.

Concerning the coordination of phases and amplitudes of Fourier analysis the periodograms (Fig. 2) reveal the following general relation:

> the larger the amplitudes, the less the scattering in phases.

The above mentioned mean standard deviation of Fourier coefficients of

0.34 scale units does not express uniform reliability of phases. Principally, phase data are reliable only in connection with larger amplitudes. Therefore, the reliability of phase data for the construction of dispersion curves is maximum in the active part of the spectrum, the so called ,,dispersion interval". Amplitudes lying beneath the ,,noise level" of a spectrum will yield scattering in phases throughout the four quadrants of the periodogram. Thus scattering in phases, more than standard deviation of Fourier coefficients, will give an objective mode of reliability.

The sensitiveness of phases, depending on the position of the frequency they belong to in the spectrum, may be demonstrated by the degree of their reproducibility, if double traversing of one and the same harmonic is carried through. The scattering of the so called ,,twin values", given in differences $\triangle\ c_n$ and $\triangle\ e_n$, accentuate their slope from the spectrum. The following table gives the characteristics:

mean values:	$\triangle c_n$			$\triangle e_n$	
entire range of ,,total analysis"	0.15	28.5°	=	0.079	periods
inside the ,,dispersion interval"	0.17	20.9°	=	0.058	,,
outside the ,,dispersion interval	0.13	47.4°	=	0.132	,,

The best reliability of phases is shown inside the ,,dispersion interval" by a scattering in phases of 0.058 periods.

The "partial analysis" of the seismogram, omitting the range between time break and arrow (M) (see Fig. 1), produced another proof of phase reliability. The space between time break and arrow (M) covers a time of 168 milliseconds. For different frequencies these 168 milliseconds represent different "phase shifts", that means: for different frequencies the same length of time is covered with different numbers of periods, and, consequently, different phase values will occur. For instance: 168 milliseconds, if distributed to 12 *cps*, make 2 full periods plus 0.025; the same time, distributed to 3 *cps*, makes 0.505 periods. The check of the "phase shift" is working on the fact that for an interval of 2.280 seconds the 7-th, 16-th, 23-rd, and 32-nd harmonic, within the limit of statistic approximation yield 3, 7, 10, and 14 integer *cps* respectively. An interval of 2.240 seconds with the harmonics 9, 18, and 27 gives with high accuracy 4, 8, and 12 integer *cps*.

On these principles "total and partial analysis" may be compared. The result of such comparison will be a scattering in phase, calculated in the following manner:

1. actual phase (total)
   minus theoretical "phase shift" = *theoretical phase (partial)*
2. actual phase (partial)
   minus theoretical phase (partial) = *scattering in phase.*

With neglection of 3 and 4 cps, the phase angles of which were not reliable (outside the ,,dispersion interval''!), the results of the comparison on "phase shift" are shown in the following table:

cps	actual phase (total)	theor. ,,phase shift"	theor. phase (partial)	actual phase (partial)	scatter
7	0,732	1,175	0,557	0,611	0,054
8	0,572	1,346	0,226	0,282	0,056
10	0,158	1,680	0,478	0,548	0,070
12	0,517	2,025	0,492	0,538	0,046
14	0,642	2,356	0,277	0,346	0,069

phases given in periods

Analysis does only provide fractions of full periods, therefore full periods have to be added respectively! The mean value of the scattering in phase is 0,059 periods. This quantity is in accordance with the scattering of "twin values" of the "total analysis" inside the "dispersion interval" (0.058).

CONCLUSION

The results of the present check analysis numerically demonstrated the functional connection between reliability of phase values and magnitude of Fourier coefficients. Frequency spectra of seismograms have to be divided into important and less important parts, as far as the reliability of the phase values is concerned. According to the scattering in phase of "twin values" and of "phase shift" a measure of the reliability of phase values may be given in percentages of periods of the partial waves. At the best, the method of harmonic analysis yields 6 % in phase scattering, at the worst 13 %. Generally approximately 8 % have to be taken in account.

Whenever carrying through harmonic analysis of seismograms, it will be of great use to design a spectrum as broad as possible. Thus it will be possible to discern important and less important parts of the spectrum, and, consequently, to fix more or less reliable harmonic elements. The spectrum of the check analysis, resulting from the present investigations, as well as that of a formerly (Korschunow 1955) carried through routine analysis (Fig. 1), demonstrates that on either side of the maximum amplitudes a range of more of less uniform small amplitudes extends. Obviously these minor amplitudes give an average ,,noise level" of the spectrum. Following the results of the present check analysis, it may be assumed that the ,,noise level" of any routine spectrum gives the order of magnitude of the standard deviation of Fourier coefficients. Consequently phase values of such parts of the spectrum are not reliable and have to be excluded from further treatment. Former experiences of the author in designing phase velocities for the construction of dispersion curves from experimental data (1955) led to the definition of "dispersion intervals" of the spectra. These "dispersion intervals" evidently are identical to the important parts of a spectrum, where elements of the harmonic analysis are reliable.

REFERENCES

Baer H., 1937 Genauigkeitsuntersuchungen am harmonischen Analysator Mader-Ott, Zeitschr. f. Instrumentenkunde, 57. Jahrgg. 6. Heft, S. 225-235.

Bartels J., 1927 Veranschaulichung beobachteter Perioden und ihre Genauigkeit, Zeitschr. f. Geophys., Bd. 3, S. 389-397.

Korschunow A., 1955 On surface waves in loose materials of the soil, Geophys. Prospect. III, pp. 359-380.

ABSTRACTS OF PAPERS PRESENTED AT THE TENTH MEETING OF THE EUROPEAN ASSOCIATION OF EXPLORATION GEOPHYSICISTS, HELD IN HAMBURG, 16-18 MAY 1956.

H. Lundberg, *The Latest Developments In Air-borne Geophysics.*

The most recent equipments and methods for radiometric, magnetometric and electromagnetic air-borne surveys are reviewed. The method of resolution in gamma radiation spectrometry is outlined, with a special reference to the separation between uranium and thorium effects.

R. Giret, *Etude d'un groupe de filons radioactifs par scintillomètre aeroporté à differentes altitudes.*

The results are described of airborne scintillometer observations at different flight levels over a group of thoriferous dykes. It was found that at a flight level of 100 m. it was just possible to distinguish the effects of two veins a distance of 500 m. apart; at a flight level of 150 m. a single anomaly was observed, caused by the entire mineralised zone. A quantitative analysis is given of the relation between the flight level and the intensity of the observed anomaly.

R. W. Olson, *The Technical-Economic Aspects of Automatic Data Reduction.*

Automatic processing can contribute to the increasing utility of seismic data. Reduction in the amount of routine work will permit talented people to utilize their time creatively on the more difficult problems. At the same time automatic reduction will provide for a greater volume of work. These two aspects will probably provide the first effective pressure for a high degree of automation. It is to be expected, however, that the ultimate and greatest value will be better interpretation. Time concepts in the processing of seismic data are, of course, vital; either in simple time corrections of either static or dynamic nature or in treatment of signals in the time domain. Much development work is needed before these advantages can be realized. Principal development needed is an increase in dynamic range in the overall system.

N. A. Anstey, *Modern Technique in Seismic Reflection Recording.*

The technique of taking seismic records has remained little changed for many years, being based on precepts established in the early years of reflection prospecting. The aim of this paper is to summarise those features of the technique which have withstood the test of time, to describe some new developments of technique allowed by modern instruments, and to investigate whether any changes of outlook, in the field, are required by recent clarifications of the fundamental seismic process. Aspects of recording technique covered in the discussion include: Instrumental sensitivity settings; Size and type of charge; Charge depth, choise of formation, and tamping; Patterns of shots and patterns of geophones; Type and length of spread; Filtering; Speed of A.g.c.; Mixing. The manner in which the recording problem is changed by the advent of magnetic recording is also discussed.

G. Pommier and H. Richard, *Supermultiplication des charges et des sismographes au Sahara.*

In dry and open country, reflection seismic often meets with considerable difficulties caused by bad surface conditions leading to poor reflections. From the beginning, the Northern Sahara proved particularly unfavourable. In 1954, systematical tests allowed to set up a procedure yielding good results. This procedure is based on high multiplicity of the shots up to one hundred per shot point combined with a similar high multiplicity of the geophones up to one hundred and more per trace. Suitable devices allowed to overcome drilling and other problems. This method has proved to be effective and relatively economical since 1954. The evident conclusion is that, under special conditions, high multiplicity can be very helpful.

F. J. Kuepper, *A Contribution to the Theory of Multiple Geophones.*

Layouts of multiple geophones are described by merely considering effective resistances by means of a system of coupled differential equations. For so-called symmetrical connections, which are the most frequent ones in practice, a method for the solution of this system can be given.

Effects of interference occurring with multiple geophones are investigated by means of a measure of superposition which is also applicable for any desired pulse-shaped excitation of the geophones. A numerical calculation was carried out for the special case of a group of 3 geophones connected in parallel, the exciting pulse being a damped oscillation. The effect of superposition and its directional characteristic are discussed.

On principle all considerations take into account the building-up transcient oscillation at the geophones.

A. Celmins, *Theoretische Fragen über Bündelung von Geophonen bei Untertage-Messungen.*

The number of multiple geophones in an array in underground seismic prospecting is limited. Therefore other possibilities must be found if a certain directional sensitivity of the array is required. In a linear array there are 3 free parameters in addition to the number of geophones: the geophone spacing, the sensitivity of the geophones, and a time shift. If the "best" values of these parameters are chosen, a favourable directional sensitivity of an array of only a few geophones can be reached, even if the regarded frequency band is wide.

W. Lode, *Die Darstellung von Tiefenlinienplänen beliebig gekrümmter Reflexionshorizonte unter Einschluss der Strahlenbrechung im Raume.*

A method for the construction of depth contour maps of curved reflection horizons of any kind obtained from reflection seismic surveys is discussed. This method includes refraction in three dimensional space avoiding the construction of seismic cross sections of any kind. It requires little work even if spacial refraction at several horizons is taken into account.

A calculated example is given for which the cross section was drawn according to the method used hitherto as well as according to the purely spacial method under discussion. The results obtained by the two methods show considerable differences which must necessarily lead to quite different geological conceptions regarding the surveyed area.

Th. Krey and K. Helbig, *A Theorem Concerning Anisotropy of Stratified Media and its significance for Reflection Seismics.*

Published in full length in the present issue of Geophysical Prospecting.

H. Braekken, *Organization of a Mining Prospecting Group.*

General problems and principles of organization are discussed. The functions of a mining prospecting group, aspiring to a reasonable degree of completeness, falls into three main sections: 1) Field Operations, 2) Development-Service, 3) Administration. The organization of the group will comprise the corresponding three main divisions. Each of these divisions will be subdivided. The general lines along which these subdivisions will be made, are discussed in the paper.

C. R. Collin and H. Sanselme, *Exemple d'utilisation de méthodes géophysiques dans la recherche en mine métallique.*

The uranium deposit at "Ecarpière" near Clisson, province of Vendée, was discovered by a reconnaissance team of the French Atomic Energy Commission using Geiger-Muller counters.

After some surface work is done, the study of the extension of the orebody is directed and helped by the use of geophysical methods along with the geological survey. The methods either used or tested are: isorad map, resistivity map, electrical sounding, potential maps, magnetometric study, seismic refraction.

The results obtained by these methods are discussed. The conclusion points out that the electric methods are specially suitable to this kind of investigation since the tectonics, on which they supply information, are directly connected with the ore occurence. If we consider the information obtained, these studies are rather inexpensive.

O. Kappelmayer, *Near-Surface Temperature Measurements for Discovering Anomalies Due to Causes in Greater Depths.*

The temperatures at shallow depth in the soil are subject to seasonal variations and irregular fluctuations, which tend to mask the temperature anomalies due to causes at greater depth. It is therefore not possible to detect temperature anomalies related to tectonic structure or to concentrations of radioactive elements. However, the following applications of temperature measurements seem to be feasible: detection of temperature anomalies caused by chemical reactions in the subsurface, in particular in the weathering zone of sulphide ore bodies; detection of leakages in dams; detection of subsurface steam reservoirs in volcanic area.

F. Haalck: *A Torsion-Magnetometer for Measuring the Vertical Component of the Earth's Magnetic Field.*

The paper describes a novel type of instrument for field work whose magnet system is provided with a torsion wire and in which torsion serves as a standard of measurement. Each time a measurement is made the magnetic axis of the magnet system is brought back into the horizontal position by altering the angle of twist (null-method). The measurements thus become practically independent of the position of the magnet system with respect to the magnetic meridian.Variations in the vertical intensity may be measured directly by the amount the angle of twist has been altered. With a scale value of 25 gammas per scale division the range of the torsion magnetometer for direct measurements is 65 000 gammas.

G. Fanselau, *Einige Neuerungen an der Geomagnetischen Feldwaage.*

At the Niemegk Observatory geomagnetic balances with torsion ribbons have been constructed since a few years. They have well known advantages over balances resting on knife edges: greater stability of the zero position, ease of enlarging the measuring range by torsion, no serious damage when the instrument is not clamped. Both H- and Z-balances have proved higly satisfactory. Also a combined H- and Z-balance has been developed. To a certain extent, the torsion ribbon balances can be made insensitive to levelling errors. Torsion wire balances used as zero instruments have not been considered for field measurements for reasons of time saving. They are however being made for laboratory measurements.

A. Brynjólfsson, *Studies of Remanent Magnetism in the Basalts of Iceland.*

Recent studies by Th. Sigurgeirsson and T. Einarsson have revealed that in Iceland inversely magnetized basalts occur just as frequently as normally magnetized basalts. Further studies have now been carried out to investigate: a) the homogeneity of the magnetization of the lava flows; b) the constancy of the magnetization in the lava-flows; c) viscose magnetization; d) the manner in which the direction of the magnetization changes in a section between inversely and normally magnetized lava-flows.

The experiments are described and the results of the investigation are discussed.

J. Homilius, *Über reflektierte Refraktionsimpulse.*

The n-layer problem for seismic refraction is treated for the case that the seismic energy is reflected several times at the boundaries of the (n-1)st layer. The exact numerical solution is given under the assumption that there are homogeneous and isotropic layers having longitudinal velocities of $V_1 < \ldots V_{n-3} < V_{n-1} < V_{n-2} < V_n$, and that there occurs only one reflection within the (n-1)st layer. A graphical procedure is described to determine the angle of inclination of the (n-1)st boundary.

R. Bortfeld, *Multiple Reflections in N.W.-Germany.*

In N.W.-Germany multiple reflections are observed in many areas. In many cases these multiples are recognizable by t-Δt analysis with routine records. Most of the multiples observed are of type AB (a multiple caused by reflections at two different reflectors A and B and at the surface or the groundwater table). Starting from this fact, it is shown that the preference for this type is also to be expected theoretically. Finally it is shown that interferences between both the components of AB (one multiple being first reflected at A and then at B, and the other being first reflected at B and then at A) are to be anticipated and what they look like.

H. Dürbaum, *On the Influence of rough Surfaces and Interfaces on seismic Waves.*

The influence of rough planar boundaries on the propagation of seismic waves is discussed. Approximation methods have to be used for this purpose whereas studying the corresponding problems for regular surfaces always leads to a discussion of eigenfunction properties. Methods are applied which have been used for studying the problem of non-specular reflection of electro-magnetic waves at rough fluid-surfaces. Studying the problem of reflection of seismic waves for non-periodic surfaces leads to integral equations which can be solved approximately only. The first approximation is given for some problems of reflection and refraction of seismic waves at planar boundaries.

P. Laurent, *The Rana, a System of Radiotopographie Surveying in Applied Geophysics.*

Considering its basic principle, the Rana belongs to a group of radiolocation systems which might be called "audio frequency phase comparison systems". The principle and the technical aspects of the system are described in detail. The opereation of the fixed stations is entirely automatic. They are started and stopped by timing divices actuated by clocks and do not require the presence of any crew, operator or watch. These stations may be set in buoys which can be disposed according to the foreseen exploration programme.

V. Fritsch, *Geoelektrische Untersuchungen im Strassenbau.*

In Vienna geo-electrical methods are in regular use in connection with building and maintenance of roads. One important field of application is the detection of old channels and cellars before a new road is built. Another application is the detection of cavities underneath the concrete plates of existing roads.

H. Rische, *Experimental Density Determination in solid Rock.*

For the determination of the density from gravity measurements, the requirements regarding accuracy are discussed. The necessary corrections for gravimetric underground measurements are presented in a manner suitable for practical purposes. A detailed description is given of the density determination results obtained from 65 mineshafts in Central Germany, which clearly prove the adaptibility of the procedure. The density values obtained for sediments result in regionally different depth-density functions. Density values for metamorphic and crystalline rocks were found to be independent of depth.

For underground torsion balance survey a new method of density determination in solid rock is described, and the results of the measurements are presented.

D. S. Parasnis, *Electrical Resistivity of some Sulphide and Oxide Minerals and their Ores.*

Published in full length in the present issue of Geophysical Prospecting.

E.A.E.G. ABSTRACT SERVICE

EXPLORATION — GENERAL

198. *The Applicability of Geophysical Methods in Prospecting for Hydrocarbons.* (In Italian).
G. Petrucci, Convegno Naz. Metano e Petrolio, 7^{mo}, Taormina 1952, Atti, Vol. 1, pp. 465-474, 1952.

In determining the most efficient methods of exploration for oil in Sicily, topographic conditions, as well as geologic conditions, must be taken into account. Thus magnetic methods are better than gravimetric, expecially when combined with airborne transportation for rapid reconnaissance. To delineate particular structures, seismic reflection surveys are needed and logging studies are used for depth, thickness, and correlation of layers. Several gravimetric and magnetic maps and tables of related physical constants are included.

(From Geophysical Abstracts 159, U.S. Geol. Survey).

199. *How Continental Trains its Geophysicists.*
H. R. Prescott, Oil & Gas J., Vol. 53, No. 38, pp. 91, January 24, 1955.

Continental Oil Company adopted a formal training programme for personnel in 1948. In the initial phase, college recruits follow a 12 to 18-month course which includes field work, instrumentation, computation, administration and theoretical research. After suitable experience, young geophysicists are promoted to party chief. This gives them the complete background to all branches of survey work. After a successful assignment as party chief, there follows a period in a regional office where planning experience is gained.

200. *Oil Exploration in the Persian Gulf.*
V. A. Swaminathan, Petr. Eng., Vol. 26, No. 10, pp. B. 36, September, 1954.

Submarine exploration in the Persian Gulf started actively in 1953. The Shell group, surveying off the cost of Qatar, are using both gravimetric and seismic methods. Techniques and equipment for both methods are described.

Anglo-Iranian have carried out a geological survey off the coast of Abu Dhabi to select a site for more detailed investigation.

201. *Geophysics and the Universities.*
Petroleum Times, Vol. 59, No. 1504, pp. 325-327, April 1, 1955.

The training of geophysicists in the U.K. lags well behind that of the U.S.A. This is mainly because of the poor facilities, with one or two exceptions, at the Universities. One of the exceptions is Cambridge, to which Sir Edward Bullard has recently returned since resigning from the directorship of the National Physical Laboratory. His move should stimulate an increase in research and the teaching of geophysics in Britain.

It is generally agreed that geophysics should not become a degree subject, but rather should form a course of post-graduate study. The first post-graduate year would lead to a diploma, the second and third years to M.Sc. and Ph. D. degrees. Also, a series of compulsory lectures on geophysics should be introduced into the courses for geology and pure physics.

202. *Geophysical Case History. Hastings Field, Brazoria and Galveston Cos., Texas.*
R. A. Weingartner, Oil & Gas J., Vol. 53, No. 48, pp. 190-194, April 4, 1955.
This case history is of a typical salt dome structure.

203. *Geophysical Case History. Vealmoor Field, Borden and Howard Counties, Texas.*
H. C. McCarver, Oil & Gas J., Vol. 53, No. 48, pp. 195-198, April 4, 1955.
This case history is of a typical reef structure.

204. *Geophysical Case History. Sandusky Area, Grayson County, Texas.*
P. E. M. Purcell, Oil & Gas J., Vol. 53, No. 48, pp. 200-206, April 4, 1955.
This case history is of a typical faulted anticline structure.

205. *Planning a Geophysical Programme for an Unexplored Basin.*
T. J. O'Donnell, Oil & Gas J., Vol. 53, No. 48, p. 210, April 4, 1955.
(Abstract only of paper read at the Annual Meeting of the S.E.G., New York, March, 1955).

The ideal geophysical programme for an unexplored basin would use magnetics, gravity and seismograph to provide an orderly flow of information leading successively to the determination of the overall form of the basin and its chief structural elements, to the delimiting of areas worthy of detailed study, and ultimately to the selection of drilling locations.

Examples are presented which suggest that these objectives can be obtained most efficiently by planning the programme to obtain data of adequate density and precision to permit quantitative interpretation. Geological data and speculation should be made immediately available to the geophysicists so that interpretations can be constantly re-examined in the light of new information and the programme modified accordingly.

206. *Geophysical History of Sharon Ridge Canyon Field, Scurry County, Texas.*
R. C. Stone, Oil & Gas J., Vol. 53, No. 48, p. 210.
April 4, 1955. (Abstract only of paper read at the Annual Meeting of the S.E.G., New York, March, 1955).
Gravity and seismic reflection methods were used to find this reef structure.

207. *Geophysical Contracting abroad a Complex Job.*
D. Kliewer, World Oil, Vol. 140, No. 5, pp. 140-141, April ,1955.
A general article outlining the problems that face a geophysical company taking on foreign contracts.

SEISMIC-GENERAL

208. *Geophysical History of the Good Field, Borden County, Texas.*
H. C. McCarver, Geophysics, Vol. 19, No. 4, pp. 791-801, Oct., 1954.
The discovery well of the Good oilfield was drilled subsequent to a seismic programme along a suspected reef trend. The discovery was made without benefit of reef reflections, and was based only on maps showing Permian draping. This technique offers interesting comparisons between seismic and subsurface data.

209. *The Development of Seismic Exploration.* (In German).
L. Mintrop, Zeitschr. Geophys., Sonderband, pp. 101-122, 1953.
A historical review of the development of seismic methods of exploration, including an extensive bibliography.

210. *Geophysical Investigations in the Emerged and Submerged Atlantic Coastal Plain: Part IX. Gulf of Maine.*
C. L. Drake, J. L. Worzel & W.C. Beckmann, Geol. Soc. Am. Bull., Vol. 65, No. 10, pp. 957-970, 1954.

211. *Seismic Measurements of the French Polar Expedition in Greenland and Iceland.* (In German).
P. Stahl, Zeitschr. Geophys., Sonderband, pp. 68-75, 1953.

212. *Observations of Reflections from Great Depths, Originating from the Large Quarry Blasts of Blaubeuren on March 4 and May 10, 1952, Registered by the Prakla Seismograph* (In German).
H. Reich, Geol. Jahrb., Band 68, pp. 225-240, 1954.

213. *A. Seismic Survey in the Canadian Shield.*
J. H. Hodgson, Pacific Sci. Assoc., 7th Cong., Proc., Vol. 2, pp. 637-8, 1949 (1953).

An account of the crustal study, by means of seismic investigation of rock bursts, in the vicinity of the gold mines at Kirkland Lake, Ontario.

214. *Seismic Prospecting at Nopporo, Ebetsu-Machi, Sapporo-Gun, Hokkaido.* (In Japanese with English summary).
H. Muraoka, S. Magumo & T. Kawashima, Geol. Surv. Japan Bull., Vol. 4, No. 11, pp. 15-20, 1953.

215. $ 2,000,000,000 *Worth of Seismic Records.*
H. B. Peacock, Oil & Gas J., Vol. 53, No. 45, pp. 180-182, 1955.

There is two thousand million dollars invested in seismic records stored in the U.S. Review and reinterpretation of the records, better co-ordination of geology and geophysics, and trading of seismic data can increase the value of this investment.

(From Geophysical Abstracts 160, U.S. Geol. Survey).

216. *The Seismic Reflection Method in Germany.* (In Italian).
H. Closs, Rev. Geofis., Vol. 13, No. 49, pp. 77-103, 1954.

A review of the development of the geophysical methods of exploration, primarily of the seismic reflection method, in Germany since the last World War.

(From Geophysical Abstracts 160, U.S. Geol. Survey).

217. *How Seismic Refraction Locates Uranium.*
D. Wantland, Oil & Gas J., Vol. 53, No. 48, pp. 149-156, April 4, 1955.

Locating uranium deposits on the Colorado Plateau has proved very expensive using the normal geological methods, since a large amount of drilling is involved. Interest has now turned to geophysical methods. The seismic refraction method proved to be applicable, with advantages, to the problem of tracing the path of buried channels that commence at the edge of a mesa. An investigation of this nature at Nokai Mesa, on the Colorado Plateau, is described.

SEISMIC INSTRUMENTAL

218. *Patents.* Abstracts in Geophysics, Vol. 19, No. 4, p. 826, October 1954.

U.S. 2,675,086 13 April 1954.	A continuous-wave ground vibrator forseismic prospecting.
U.S. 2,675,525 13 April 1954.	A variable-air-gap magnetic-bridge-type seismometer.
U.S. 2,675,533 13 April 1954.	A moving-coil electrodynamic seismometer.
U.S. 2,676,206 20 April 1954.	Apparatus for making a correlation analysis of a signal recorded on magnetic tape.

U.S. 2,678,107 11 May 1954. A seismograph mixing system for eliminating horizontally travelling waves.
U.S. 2,679,636 25 May 1954. Apparatus for comparing two series of seismic waves.

219. *Mapping Shallow Horizons with Reflection Seismograph.*
L. C. Pakiser, D. R. Mabey & R. E. Warrick, Bull. A.A.P.G., Vol. 38, No. 11, pp. 2382-2394, November 1954.

Instruments are described with which shallow-reflection seismic mapping can be carried out over a depth range of 50-1000 feet. This may even be extended to 4000 feet or more. Tests are described where beds 100-200 feet in depth were successfully mapped in Oklahoma and Kansas.

The instruments have high frequency response, high oscillograph paper speeds, fast-acting automatic gain control, and variable presuppression control. In principle they are straightforward modifications of conventional seismic reflection equipment.

220. *Magnetic Recording ... New Seismic Exploration Tool.*
M. J. Stolaroff, Oil & Gas J., Vol. 52, No. 34, pp. 95-98, December 28, 1954.

An F. M. recording system is described which meets the accuracy requirements for geophysical exploration. Having excellent low-frequency response, negligible low-frequency phase shift, and good amplitude accuracy, this system makes available a recording system having improved frequency response and dynamic range to geophysical users. The provision of an electrical signal makes possible many analysis techniques never before possible, such as post-recording filtering, variations in gain and mixing, and transposition of traces. Also made possible with such an electrical output is the use of correlation techniques, which if properly exploited, promise to greatly enhance the amount of information resulting from seismic records.

221. *Mapping Shallow Horizons with the Reflection Seismograph.*
L. C. Pakiser & D. R. Mabey, Science, Vol. 119, No. 3099, p. 740, 1954.

In successful tests of specially constructed reflection seismic instruments, the Neva limestone has been mapped at a depth of about 200 feet in Osage County, Okla., and the Stone Corral dolomite has been mapped at depths of 150 to 200 feet in Rice County, Kansas. In some places in the Kansas test areas, the base of the overburden at a depth of less than 100 feet has been mapped. Reflecting horizons have been mapped continuously from 200 feet to depths as great as 4,000 feet in the Oklahoma area.

The instruments do not differ radically from conventional equipment. The amplifiers have a frequency range of 75 to 300 c/s, the avc time constant has been reduced to about one-third its usual value, and a variable presuppression control has been installed to permit a sharp reduction of the first energy arrivals; the oscillograph paper speed is about 25 inches/sec; high frequency galvanometers have been installed; and the timing-line interval has been reduced from 10 to 2 millisecs.

(From Geophysical Abstracts 157, U.S. Geol. Survey).

222. *Optical Seismo-Clinometer.* (In Russian).
G. A. Gamburtsev, Izv. Akad. Nauk SSR, Moskau, Ser. Geofiz., Vol. 4, pp. 305-311, 1954.

The theory of a new kind of optical seismo-clinometer is given, with which small vibrations of the earth's crust in a given frequency range are determined. The seismo-clinometer here described is composed of a vertical pendulum and a horizontal torsion pendulum forming a single system. The vertical pendulum acts as a mass that is considered in a vessel with a viscous fluid. The suspended fibre of the vertical pendulum shares the same axis with the horizontal pendulum which consists of a balance arm. The balance arm is loaded to the limit with a mass which is small compared with the mass of the vertical pendulum.

The sensitivity of the seismo-clinometer is not so good by the usual optical registering method as by the simple optical inclination meter. The sensitivity may be increased simply by photoelectrical enlargement.

The sensitivity of a double seismo-clinometer is 50-100 times that of the simpler instruments. The frequency characteristics of both types differ only slightly. Precise numerical calculations for the period and for the sensitivity are not made in this paper.

223. *Patents.* Abstracts in Geophysics, Vol. 20, No. 1, p. 164, January, 1955.

U.S. 2,688,124	31 Aug. 1954.	A seismic prospecting system using a varying-frequency source wave which is picked up, multiplied and integrated.

224. *Magnetic Recording Seismometer by means of Moving Magnet* (In Japanese with English summary).
Y. Tomoda & K. Aki, Zisin, Vol. 5, No. 4, pp. 13-16, 1952.

A description of a seismograph in which the displacement of the seismometer is recorded on magnetic tape by a small magnet attached to the seismometer arm.

(From Geophysical Abstracts 160, U.S. Geol. Survey).

225. *On the Frequency Response of the Seismometer with Air Damper.* (In Japanese with English summary).
Z. Suzuki, Zisin, Vol. 5, No. 4 pp. 46-51, 1952.

Frequency-response curves have been calculated for a seismometer with air damping. Numerical results are given for the Ishimoto instrument.

(From Geophysical Abstracts 160, U.S. Geol. Survey).

226. *Some Experiments on the A.G.C. — Using Amplifier for Seismic Prospecting.* (In Japanese with English summary).
K. Mori & S. Nagumo, Geol Surv. Japan Bull., Vol. 4, No. 11, pp. 21-34, 1953.

Experiments on the transient characteristics of the automatic gain control amplifier and their influence on the detection of reflections are described.

(From Geophysical Abstracts 160, U.S. Geol. Survey).

227. *Patents.* Abstracts in Geophysics, Vol. 20, No. 2, p. 336, April 1955.

U.S. 2,692,306	19 Oct. 1954.	An audio amplifier with plural A.G.C.
U.S. 2,693,862	9 Nov. 1954.	A system for portraying seismic reflections in which the beam of a c.r. tube is modulated.
U.S. 2,693,908	9 Nov. 1954.	Apparatus for analysing records and indicating the correlation factor.
U.S. 2,695,211	23 Nov. 1954.	A direct-recording mechanical accelerometer.
U.S. 2,697,648	21 Dec. 1954.	A vibrating-reed seismic timing system.

228. *Some Problems of Standardization in Recording Seismic Data on Magnetic Tape.*
R. F. Beers & C. F. Casey, Geophysics, Vol. 19, No. 3, p. 629, July, 1954. (Abstract only of paper read at the Annual Meeting of the S.E.G., St. Louis, April, 1954).

It is believed that eventually a very large amount of seismic data will be recorded directly on magnetic tape. In this form many improvements in signal-to-noise ratio resolution and accuracy may be achieved. While magnetic recording systems are in the early stage of development it may be wise to consider some of the problems which will arise in establishing standards for the equipment and procedures required by the geophysical industry.

This paper recognizes the need for standardization, states some of the current problems and recommends precedures for studies of the problem to be continued. A compilation of existing equipment is included, derived from an illustrated brochure which will be distributed to all who may request it.

229. *The Shallow Reflection Seismograph in Mining, Engineering and Ground-Water Investigation.*
L. C. Pakiser & R. E. Warrick, Geophysics, Vol. 20, No. 2, p. 376, April, 1955. (Abstract only of paper read at the Annual Meeting of the S.E.G., New York, March, 1955).

A report on experimental work on the Colorado Plateau, the Upper Mississippi Valley & Portage Co., Ohio, using a specially constructed shallow-reflection seismograph.

230. *Seismic Applications of Some New Filtering Techniques.*
H. J. Jones, Geophysics, Vol. 20, No. 2, p. 381, April, 1955. (Abstract only of paper read at the Annual Meeting of the S.E.G., New York, March, 1955).

Modern communications theory and information theory have placed considerable emphasis upon the problem of detection and extraction of signals in noise backgrounds. Some of the methods and equipment developed have possible seismic applications. This paper presents a discussion of the delay-line method of filtering. Magnetic delay-line equipment which permits approximation of a wide variety of linear filters is described in detail. The fundamental theory of delay-line filtering is outlined briefly. Use of non-linear decision-making filters in seismic recording is discussed both from the standpoint of theory and of suitable equipment. The possibility of incorporating these types of filtering equipment in an automatic or semi-automatic seismic data processing system is outlined.

SEISMIC — FIELD TECHNIQUE

231. *Patents.* Abstracts in Geophysics, Vol. 20, No. 1, p. 164, January 1955.

U.S. 2,683,414. 13 July 1954.	Explosive charge arrangement that ensures complete detonation in seismic prospecting.
U.S. 2,687,092. 24 Aug. 1954.	Protective device for shot-hole loaders.
U.S. 2,687,093. 24 Aug. 1954.	Explosive charges that screw together.

232. *How to Reap the Maximum Magnetic recording benefits.*
F. B. Coker, World Oil, Vol. 140, No. 5, pp. 120-129, April 1955.

This article gives general background information on magnetic recording, and then deals, in question and answer form, with a number of questions that arise relating to field experience and application of magnetic tape recording. The author stresses that, for full benefit to be gained from the technique, all other phases of the seismic operation should be up-graded, — this particularly applies to the sizing and placement of shots, and the accuracy of interpretation.

233. *Air Shooting Useful as Reconnaissance Tool.*
L. V. Manry & W. Sax, World Oil, Vol. 140, No. 5, pp. 150-154, April, 1955.

Because of a very restricted time limit, a special geophysical exploration programme conducted recently employed air shooting as a means to speed up the survey. The Poulter method was used, the charges being mounted on tubular steel stakes approximately seven feet in height. It was found that the method was well suited to the high velocity sediments and sparsely settled areas of West Texas and Western Canada, but less suitable for the soft, low velocity sediments of the Gulf Coast.

234. *The Long Interval Method of Measuring Seismic Velocity.*
F. P. Kokesh, Geophysics, Vol. 20, No. 2, p. 378, April, 1955.
(Abstract only of paper read at the Annual Meeting of the S.E.G., New York, March 1955).

The method of seismic velocity determination, wherein the shot is detonated in the borehole and energy is detected at the surface, has been extended to operate in deep holes. This has been accomplished by the use of a long interval arrangement of a multi-shot selective firing sound source gun and one or more geophones separated vertically by a cable several hundred feet long.

Comparisons with conventional geophone surveys show that the long interval method has the advantages of substantial savings in cost, increased convenience, and more reliable results. The paper describes in a general way, the necessary field equipment. Field examples of surveys are presented.

SEISMIC — INTERPRETATION

235. *Procedure for the Determination of the True Position and the Dip of Seismically Detected Layers.* (In German).
G. Schenkel, Geol. Jahrb., Band 68, pp. 659-669, 1954.

The interpretation of seismic reflection recordings in steep-dip areas often becomes erroneous by the introduction of the average vertical seismic velocity $\overline{V}$ (t_0) instead of the actual $\overline{V}$-figure, referring to the inclined wave path. The actual figure, however, cannot be stated until the position of the reflecting element is determined. The difficulty is overcome by the described method, using the reflection times recorded at the ends of a cross-spread for the construction of a circle $K = 2h'' (\overline{V})$, whose intersection with a modified reference curve $TAB - 2h' (\overline{V})$ gives the true coordinates of the reflecting element, provided refraction of the wave paths can be neglected. (Author's Abstract)

236. *The Determination of the Weathered Layer in Seismic Reflection Prospecting.* (In Italian).
M. Signini, Convegno Naz. Metano e Petrolio, 7^{mo}, Taormina 1952, Atti, Vol. 1, pp. 417-423, 1952.

In the valley of the Po the weathered layer is in some places 20 to 25 m thick. The velocity in this layer is about 600 m/sec, and the velocity in the layer immediately below ranges from 1,500 to 2,000 m/sec. Where the upper layer is covered with peat, it presents a great obstacle to the propagation of seismic waves and it is necessary to place explosive charges in deep wells reaching the second layer. To avoid errors caused by the weathered layer Signini suggests a grapho-analytic method of determining its thickness and the corresponding velocity. Several possible configurations are discussed and the necessary formulae derived.
(From Geophysical Abstracts 159, U.S. Geol. Survey).

237. *Probability Distribution of Reflections on Seismic Records.*
L. Masse, Geophysics, Vol. 20, No. 2, pp. 243-253, April, 1955.

A modification of the theory of radar information is proposed for the analysis of noisy seismic records by means of the cross-correlation function. The method is applied to a synthetic record, and the amount of information provided by the method is evaluated by means of Shannon's formula. (Author's Abstract)

238. *Detection of Reflections on Seismic Records by Linear Operators.*
G. P. Wadsworth, E. A. Robinson, J. G. Bryan & P. M. Hurley, Geophysics, Vol. 18, No. 3, pp. 539-586, July, 1953.

Linear operators are used as a statistical tool in the analysis of seismic records. It was found that when an operator is chosen for a non-reflection interval and applied to regions during which reflections occur, the effectiveness of the operator is disturbed and large errors of prediction result. This effect provides a method for the discrimination of reflections. The technique used has its basis in the theory

of time series, relevant concepts of which are reviewed. The mechanics of application are given, and illustrative examples on ten seismograms are presented.
(Author's Abstract)

239. *Similarity of Output Traces as a Seismic Operator Criterion.*
S. M. Simpson, Jr., Geophysics, Vol. 20, No. 2, pp. 254-269, April, 1955.

The problem of emphasizing signals on multiple trace seismograms is approached by considering a relationship between the input and output records. It is proposed that the transformation to output record be one which causes the output traces to be most "similar" or "in phase" according to a certain definition of this property. If the noise and signal are "properly behaved", it may be demonstrated that a linear transformation chosen by this criterion must have a response emphasizing frequency ranges of high input signal-to-noise ratio. The determination of such a transformation from the input data alone is carried out for discrete linear operators. The numerical work involved in computing such operators is formidable. As an example the computations were carried out for a mixture of an artificial signal introduced into a noise record. The results are about as good as those obtained with conventional filtering techniques depending on prior knowledge of input signal-to-noise ratios. (Author's Abstract).

240. *The Effect of Topography on Near-Surface Velocities.*
W. Baillie, Geophysics, Vol. 20, No. 2, p. 378, April, 1955.
(Abstract only of paper read at the Annual Meeting of the S.E.G., New York, March, 1955).

Fictitious seismic anomalies often result from the use of improper velocities in making the elevation correction in seismic interpretation. The frequent coincidence of apparent seismic highs with topographic highs indicates a possible relationship between surface load and velocity. The importance of the load-factor is illustrated by an actual example in which a series of core hole velocity measurements were made over an apparent anomaly.

241. *Certain Questions of the More Precise Interpretation of Data Obtained from Simultaneous Use of Reflected and Refracted Waves* (In Russian).
A. M. Yepinat'yeva, Akad. Nauk SSSR Izv. Ser. Geofiz., No. 4, pp. 331-348, 1954.

It is usual in analysing travel time curves to replace the actual structure by an assumed structure. Thus the real medium of a composite structure can be replaced either by a homogeneous medium with an intermediate velocity of propagation, a stratified medium with constant velocity in each layer, or a heterogeneous medium with velocity continuously varying with depth. Similarly for refracted waves the real medium is replaced either by a homogeneous medium with a constant velocity or by a stratified medium with the velocity constant in each layer, but varying from layer to layer. The best assumption will be the one that gives the travel time curve most nearly approaching the real one. The determination of different seismic velocities and the position of intermediate layers are given for different velocity ratios of velocities and various geometric conditions, including that of a thin layer of high velocity within a homogeneous medium. Similar problems are also discussed for the combined data when the waves are reflected and refracted.
(From Geophysical Abstracts 160, U.S. Geol. Survey.)

242. *Electronic Calculators Speed Up Analysis of Complex Geophysical Computations.*
W. O. Heap, Oil & Gas J., Vol. 53, No. 48, pp. 184-186, April 4, 1955.

A brief account is given of the way in which punched-card processing and calculating machines can help to compute time-depth conversion data, solve variable velocity problems, compute true depths and displacements of seismic reflection points for steeply dipping areas, calculate data for the construction of wave-front diagrams, solve multi-layer refraction problems, reduce gravity data, and integrate continuous velocity logs.

243. *Interpretation of a Geophysical Prospect.*
R. W. Mossman, Oil & Gas J., Vol. 53, No. 48, pp. 210, April 4, 1955.
(Abstract only of paper read at the Annual Meeting of the S.E.G., New York, March, 1955).

In interpreting geophysical data it is essential to incorporate information on the geologic conditions characteristic of the area of the prospect. An analysis of the data on a purely geophysical basis can lead to very erroneous conclusions. As an illustration, a case history of a seismic prospect in a faulted area is presented, showing successive changes in the interpretation as additional geologic information is introduced into the evaluation. From an economically attractive graben, the interpretation is developed to show that a horst of even greater apparent potential is actually present, which is finally shown to be a very undesirable drilling site.

244. *The Determination of the Wave Front Velocity in a Uniaxial Inhomogeneous Medium by Seismic Reflection Surveying.* (In German).
M. Weber, Geofis. Pura e Appl., Vol. 29, pp. 11-21, 1954.

A new direct method is developed for calculating the wave velocity $c(z)$ from recorded travel-time curves. Comparison of the average $c(z)$ with the exact average is also made. Finally, a typical example is given.

245. *A Method for the Direct Computation of the Velocity-Layer in Seismic Reflection.* (In German).
D. Pietsch, Zeitschr. für Geophys., Würzburg, Vol. 20, No. 1, pp. 25-46, 1954.

A seismic reflection method is described, by which one can determine directly from seismograms the velocity of seismic waves in the particular layer under consideration. The method is developed for the case of horizontal parallel layers and extended to parallel inclined layers.

The customary calculation of the so-called mean-velocity is avoided. An error-value indicates the method's range of applicability.

The velocity calculation is an analytical method of Prakla (Hanover).

246. *How Computers facilitate Stratigraphic Correlations.*
C. W. Oliphant & P. Fullerton, World Oil, Vol. 140, No. 5, pp. 132-138, April, 1955.

An improved method of stratigraphic correlation, from logs or otherwise, is described in detail, the objective being to match as well as possible two discordant sets of specialised data, specify a degree of confidence in the match, and finally to interpret the physical continuity of distinctive rock units. The method employs punched card calculations, or specially-designed computing machines.

SEISMIC — THEORY & RESEARCH

247. *On the Propagation of Elastic Waves in Aeolotropic Media.* II. *Media of Hexagonal Symmetry.*
M. J. P. Musgrave, Proc. Roy. Soc., A, Vol. 226, No. 1166, pp. 356-366, 23 November, 1954.

The general analysis presented in Part I is here adapted to obtain the velocity, inverse and wave surfaces of a medium of hexagonal symmetry. Values derived from the elastic constants of (a) zinc and (b) beryl are tabulated and graphs of sections of the surfaces have been drawn. The details of the propagation of elastic plane waves in a single crystal of either substance may be obtained from the data presented. (Author's Abstract)

248. *Propagation of Seismic Wavelets.*
N. Ricker, a paper read at the 48th meeting of the Acoust. Soc. of America, at Texas, November 1954 (Not yet published).

This is a survey paper covering the development of the Wavelet Theory of Seismogram Structure over the past 15 years. The paper discusses the failure of the classical wave equation in accounting for the nature of seismograms, shows that the absorption of the earth must be taken into consideration, and sketches the development of the theory based on Stoke's wave equation

$$\nabla^2 \left[\Phi + \frac{1}{w_0} \frac{\partial \Phi}{\partial t} \right] = \frac{1}{c^2} \frac{\partial^2 \Phi}{\partial t^2}$$

The results of an extensive series of experimental researches are reviewed, and it is shown that the form and laws of propagation of the seismic disturbance, predicted by the theory, are supported by the experimental evidence. Applications of the theory to practical improvements in seismic prospecting are discussed briefly.

249. *Graphical Representation of the Spherical Propagation of Explosive Pulses in Elastic Media.*
W. Goldsmith & W. A. Allen, J. Acoust. Soc. Am., Vol. 27, No. 1, pp. 47-55, January 1955.

The propagation of spherically symmetric waves in a homogeneous, isotropic elastic medium of infinite extent is here analysed and the displacements, velocities, and stresses occurring at each point of the medium are represented in graphical form.

250. *Experimental Studies on the Mechanism of Generation of Elastic Waves.*
K. Kasahara, Bull. Earthq. Res. Inst. Tokyo Univ., Vol. 32, Part I, pp. 67-77, March, 1954.

Experiments are described in which an iron sphere containing an accelerometer was dropped onto level ground. Vertical surface displacements were measured at various distances from the point of impact. Consideration is given to the following phenomena: (a) The variation of amplitude and form of initial motion at a given point with height from which ball is dropped; (b) The variation of amplitude and form of initial motion at a given point for a given height of drop when impact pads of different materials are used; (c) The motion of the weight during the process of impact and the conversion of its energy to that of elastic waves. This last topic is discussed in terms of a somewhat crude mechanical model.
(From Applied Mechanics Reviews, Vol. 8, No. 1, 1955).

251. *Surface and Near-Surface Waves in the Delaware Basin.*
M. B. Dobrin, P. L. Lawrence & R. L. Sengbush, Geophysics, Vol. 19, No. 4, pp. 695-715, October 1954.

Seismic propagation studies made in the Delaware basin of West Texas have disclosed several unusual kinds of travelling waves. The near-surface zone in this area is characterized by high- and low-velocity layers, with a thin high-velocity cap. Physical characteristics of the recorded waves have been correlated with this layering.

252. *The Method of Cagniard in Seismic Pulse Problems.*
C. H. Dix, Geophysics, Vol. 19, No. 4, pp. 722-738, October 1954.

The main procedures used by L. Cagniard to calculate seismic pulse motion have been carried through for the case of a point source in an infinite medium. This relatively simple case serves as a basis for a simplified exposition of Cagniard's method. By using this case, we avoid cluttering the exposition with a large collection of algebraic details that tend to befog the main issues. (Author's Abstract)

253. *An Experimental Investigation of the Interaction between Shock Waves and Boundary Layers.*
G. E. Gadd, D. W. Holder, & J. D. Regan, Proc. Roy. Soc., A, Vol. 226, No 1165, pp. 227-253, 9 November, 1954.

An account is given of an investigation into the interaction between the boundary layer on a flat plate and a shock wave produced either externally, by a wedge in the supersonic mainstream, or from within the boundary layer, by a wedge held in contact with the plate. A wide range of free-stream Mach numbers, boundary-layer Reynolds numbers, and shock strengths has been covered, shock strength being defined as the ratio of the static pressure downstream of the shock to the static pressure upstream of it. Variations in these parameters can have large effects on the inter-action, and there are also large differences between cases with externally generated shocks and cases where the shock is generated from within the boundary layer. The investigation has thrown light on the physical mechanisms involved. It is found that many of the major features of the interaction arise because the boundary layer separates from the surface ahead of the shock wave. The conditions under which separation occurs and the behaviour of the separated boundary layer thus have important effects, in terms of which, for example, the differences between the interactions observed with laminar and with turbulent boundary layers may be explained. (Author's Abstract)

254. *Model Study of Air-Coupled Surface Waves.*
F. Press & J. Oliver, J. Acoust. Soc. Am., Vol. 27, No. 1, pp. 43-46, January 1955.

Flexural waves generated in a thin plate by a spark source are used to investigate properties of air-coupled surface waves. Both ground shots and air shots are simulated in the model. Effects of source elevation, fetch of air pulse, and cancellation by destructive interference are studied.

255. *Elastic Wave Velocities in Heterogeneous and Porous Media.*
M. R. J. Wyllie, A. R. Gregory & L. W. Gardner, Geophysics, Vol. 20, No. 2, p. 377, April, 1955. (Abstract only of paper read at the Annual Meeting of the S.E.G., New York, March, 1955).

Longitudinal wave velocities in numerous synthetic and natural porous media at room temperature and pressure have been measured. Basic characteristics of the measuring device are briefly described

Results of the measurements are graphically presented to show experimental relationships between wave velocity, porosity, pore content and matrix nature of sedimentary rocks. Some conclusions are drawn regarding general relationships between these factors based on the experimental results and on theoretical considerations. Through these relationships continuous velocity logs can be interpreted to furnish a measure of formation porosity. Some comparisons are given between porosities derived from continuous velocity logs and those found by core analysis.

256. *Seismic Wave Propagation in Porous Granular Media.*
N. R. Paterson, Geophysics, Vol. 20, No. 2, p. 378, April, 1955.
(Abstract only of paper read at the Annual Meeting of the S.E.G., New York, March, 1955).

Theoretical and experimental studies have been made of the manner in which sound waves are propagated in porous granular aggregates. Use is made of a radiating piezoelectric cylinder in order to simulate the explosion of a charge in a seismic shot hole.

It is found that in packings of un-cemented spherical grains the sound velocity is related to the stress in the frame and to the elastic constants of the grains and pore-filling material. Density and porosity are additional parameters in the dry system, while viscosity and permeability are important in liquid-filled aggregates.

257. *Seismic Wave Velocities in Westerly Granite.*

L Knopoff, Trans. Am. Geophys. Un., Vol. 35, No. 6, pp. 969-973, Dec. 1954.

A precision laboratory measurement of the principle wave velocities in a homogeneous material is presented as evidence that a closer agreement may be obtained between laboratory and field results than heretofore thought possible. The laboratory results differ from field quantities in a predictable direction. The method is an application of laboratory techniques in an imitation of field procedures to a scale model of field structures. (Author's Abstract)

258. *Seismic Model Studies.*

J. Oliver, F. Press & M. Ewing, Geophysics, Vol. 20, No. 2, p. 379, April, 1955. (Abstract only of paper read at the Annual Meeting of the S.E.G., New York, March 1955).

The seismic model technique, described in previous papers, has been applied to several new problems. One concerns the propagation of elastic waves in a medium in which the velocity varies continuously with depth. In such a configuration wave paths may become tangential to a horizontal discontinuity in which case boundary waves diffracted along the discontinuity are excited.

Similar waves may be excited in isotropic media when an incident S wave strikes a discontinuity at the critical angle. These waves have not to the author's knowledge been observed previously at the boundary between two different materials.

The effect of curvature of the surface on waves of the Rayleigh type has been also investigated experimentally. The dispersion is in good agreement with the theoretical results of Sezawa for Rayleigh waves travelling around a cylinder.

259. *Seismic Wave Attenuation Characteristics from Pulse Experiments.*

F. A. Collins & C. C. Lee, Geophysics, Vol. 20, No. 2, p. 380, April, 1955. (Abstract only of paper read at the Annual Meeting of the S.E.G., New York, March, 1955).

Stress wave attenuation, characteristics can be expressed by a stress-strain relation, which can be combined in a well-known manner with the strain-displacement relation and Newton's second law to deduce a wave equation applicable in an imperfectly elastic earth. A review of published data indicates that a stress-strain relation in which stress is a linear combination of strain and rates of change of strain is probably not adequate for all earth materials. It appears necessary to express the time-dependent properties of the material by using a memory function, which is incorporated in the stress-strain relation through a conventional integral. A method of obtaining the corresponding integro-differential wave equation by analysing seismic pulses recorded at several distances from a shot point is described, and applied to data obtained in a quarry sandstone. Although data from this experiment did not yield consistent results for different transmission distances, it is believed that data from additional experiments of this sort can be used to determine the wave propagation equation.

260. *The Moveout Filter.*

C. H. Savit, J. T. Brustad & J. Sider, Geophysics, Vol. 20, No. 2, p. 381, April, 1955. (Abstract only of paper read at the Annual Meeting of the S.E.G., New York, March, 1955).

The response of a seismometer array or "pattern" is a function of the wavelength (also of the moveout or phase velocity) of incident energy. Patterns are thus "moveout filters". Analyses of pattern behaviour in the literature has been confined to the calculation of the response characteristics of specific types of arrays. The present paper develops the general theory of arrays and gives an explicit solution for the design of an array having a predetermined moveout response.

It is further shown that the antenna theory approach to pattern design is inadequate in the seismic case by reason of the non-uniqueness of the velocity of incident energy.

An example of a pattern designed to meet specific requirements is exhibited. The case presented effects a calculated improvement of at least four to one in signal-to-noise ratio over conventional patterns. The output of the designed system for a horizontally-travelling, transient pulse input is shown to be greatly reduced in peak amplitude.

Results of preliminary field tests are in good agreement with theory.

261. *The Vertical-Time Curve in Seismic Reflection.* (In German).
W. Brauch, Erdöl u. Kohle, Vol. 8, No. 4, pp. 231-234, April, 1955.

First the concepts 'vertical-time curve' and 'vertical-time profile' are defined. Then the mathematical forms of the vertical-time curve for continuous faults are examined:

(a) With impact rays and underground paths straight,
(b) Impact rays straight, bent underground,
(c) Impact rays bent, straight underground.

This examination attempts to close a gap between theory and practice in seismic reflection evaluation. From the vertical-time curves a new continuous evaluation method may be conceived. It is considered that this may be adapted especially to the determination of wave velocities.

262. *The Mechanism of Generation of Long Waves from Explosions.*
C. H. Dix, Geophysics, Vol. 20, No. 1, pp. 87-103, January, 1955.

Cagniard's method is applied to the numerical calculation of the vertical displacement due to a point source in a semi-infinite elastic solic medium at three points on a vertical line through the source. The source is a step in the scalar displacement potential. From these calculated responses the response for any physically possible spherically symmetric source can be computed by application of the Duhamel integral.

Clear evidence of backward transmission of transverse wave energy is found along the vertical axis through the source. This, together with the energy of the longitudinal waves, also transmitted backwards, accounts for the mechanism by which energy is held near the source and near the free surface long enough to account for the generation of long period surface waves.

This mechanism of generation of long period surface waves is not restricted to the free surface case. Any good reflector, which also generates secondary transverse waves from longitudinal primary waves, will serve the purpose. It is suggested that this gives a clue to the mechanism of the formation of "ground roll" in many practical cases. (Author's Abstract).

263. *On Forms of Seismic Waves Generated by Explosion,* I.
Z. Suzuki & H. Sima, Tohoku Univ. Sci. Repts., 5th Ser., Vol. 6, No. 1, pp. 85-94, 1954.

Seismographic observations were made on the grounds of the Geological Survey of Japan at Kawasaki at intervals of 25 cm. from 11.25 to 25.25 meters. The source was a detonating cap fired at a depth of 74 cm. The ground motion generated consisted of some simple and regular wave groups and an irregular motion that is the apparent result of the superposition of wave groups. The period of the waves was constant within the range of observation. The amplitude ratio to the standard amplitude in a wave group varies linearly with distance. The "growing rate" of waves varies regularly in the order of the appearance in the group, the head of the group decaying with distance while the tail increases. Thus the initial motion of later phases is sometimes misread.

(From Geophysical Abstracts 160, U.S. Geol. Survey).

GRAVITY — GENERAL

264. *Notes on the Geophysical Exploration of the Structure of Bordolano.* (In Italian).
L. Solaini, Convegno Naz Metano e Petrolio, 7^{mo}, Taormina 1952, pp. 389-95, 1952.

265. *Gravimetric Survey of the Upper Adriatic.* (In Italian).
C. Morelli, Ann. Geofis., Vol. 7, No. 1, pp. 45-70, 1954.

266. *The Basic Gravimetric Network in Italy.* (In Italian).
C. Morelli, Convegno Naz. Metano e Petrolio, 7^{mo}, Taormina 1952, Vol. 1, pp. 451-460, 1952.

267. *Geophysical Features and Deep Geology of Sicily and Surrounding Areas.* (In Italian).
O. Vecchia, Riv. Geofis. Appl., Vol. 15, No. 1, pp. 15-46, 1954.

268. *Gravimetric Investigations on Madagascar. Techtonic Interpretation of the Southern and Western Parts.* (In French).
L. Cattala, Madagascar Bur. Geol. Travaux, No. 59, 1954.

269. *A Gravity Survey of the Rio Grande Trough near Socorro, New Mexico.*
R. C. Anderson, Trans. Am. Geophys. Un., Vol. 36, No. 1, pp. 144-148, February 1955.

270. *The Regular Parts of the Gravity Field, with an Application to Central Europe.* (In German).
A. Berroth, Geofis. Pura e Appl., Vol. 28, pp. 1-35, 1954.

The regular parts of the gravity field are the continental and regional terms; the local part is the remainder. The regional term always refers to a large area and cannot be defined by a datum. These component terms — the continental, the regional and the local —can be determined by two methods. The first consists of computing point by point the numerical value of a theoretical function. In the second method the derivation is computed area by area with an adjustment in terms of adjoining boundary values.

The second method is applied to the data of several surveys in Germany and France, and the corresponding expressions for the continental, regional and local anomalies are derived. Appropriate maps are included.

(From Geophysical Abstracts 160, U.S. Geol. Survey).

271. *A Survey of Gravity in Iceland.*
T. Einarsson, Visindefelag Islendinga, Vol. 30, 1954.

272. *Gravity Measurements along the Lines of Precise Levels over Whole Japan by means of a Worden Gravimeter. VII. Kyushu District.*
C. Tsuboi, Acad. Japan Proc., Vol. 30, No. 7, pp. 594-598, 1954.

273. *The Acceleration of Gravity at the Base Stations of Moscow: Geofian I, Geofian II, and Moscow-Initial.* (In Russian).
Yu. D. Bulanzhe, Akad. Nauk SSSR Geofiz. Inst. Trudy No. 20 (147), pp. 3-19, 1953.

274. *Gravity Meter Surveys at Steep Rock Iron Mines.*
G. R. Johnson, Geophysics, Vol. 19, No. 3, p. 635, July, 1954.
(Abstract only of paper read at the Annual Meeting of the S.E.G., St. Louis, April, 1954).

275. *Gravity Measurements at Sea, Part II, Southern Part of East Coast of U.S.*
G. L. Shurbet, J. L. Worzel & M. Ewing, Geophysics, Vol. 20, No. 2, p. 373, April, 1955.
(Abstract only of paper read at the Annual Meeting of the S.E.G., New York, March, 1955).

GRAVITY — INSTRUMENTAL

276. *The Modelling of the Anomalies in Magnetic and Gravitational Fields.* (In Russian).
A. G. Kalashnikov, Akad. Nauk SSSR Izv. Ser. Geofiz., No. 6, pp. 546-553, 1954.

This is a description of the special field meter used for measurement of field intensity in model experiments. The main element of this instrument is a very small rotating coil which can be placed at any point without disturbing the field pattern in the vicinity. Such a coil has been constructed using a wire of 25μ diameter, with the exterior diameter of the coil being only 0.8 mm. The field patterns produced by disturbing bodies of different forms and physical properties have been measured with such a field meter. The results are shown.

(From Geophysical Abstracts 160, U.S. Geol. Survey).

277. *New Era of Geodesy.*
W. A. Heiskanen, Science, Vol. 121, No. 3133, pp. 48-50, 1955.

This is an account of the symposium, the New Era in Geodesy, at Ohio State University in November 1954. New geodetic measuring instruments, the development of gravimeters, the process of recent gravity measurements on continents and at sea, and their significance for geodetic and geophysical purposes were discussed.

(From Geophysical Abstracts 160, U.S. Geol. Survey).

278. *Patents.* Abstracts in Geophysics, Vol. 20, No. 2, p. 335, April, 1955.
U.S. 2,695 165 23 Nov. 1954. Electromagnetic accelerometer.
U.S. 2,697,594 12 Dec. 1954. Electromagnetic accelerometer.

GRAVITY — INTERPRETATION

279. *Some Critical Notes on the Problem of the Analysis of Anomalous Gravity Fields.* (In German).
H. Haalck, Gerlands Beitr. Geophys., Vol. 64, No. 1, pp. 16-22, 1954.

The development and practical significance of the problem of analysis of local gravimetric disturbances are critically discussed. Representation by anomaly maps of *Wz*, *Wzz* and *Wzzz* in combination is most suitable, as the effect of the different disturbing masses is expressed with different intensities according to their depths. The computation of both *Wzz* and *Wzzz*, however, seems superfluous as the difference between them is not very essential. Determination of *Wzzz* is preferable, for this can be done with less work and with any practical accuracy. In conclusion the purpose of the calculations and the limits of their useful application are pointed out.

(From Geophysical Abstracts 159, U.S. Geol. Survey).

280. *The Computation of Wzzz from Gravimetric Measurements and Their Significance in Applied Geophysics.* (In German).
H. Haalck, Zeitschr. Geophys., Sonderband, pp. 46-53, 1953.

For the interpretation of the results of a gravity survey it is very important to have maps of the first three vertical differential quotients of the gravitational potential, that is of *Wz*, *Wzz* and *Wzzz*. In the expression for *Wz* the attraction of an elementary buried mass is proportional to the square of the distance, in *Wzz* to the cube, and in Wzzz to the fourth power; therefore the effect of the masses near the surface is more pronounced in the expression *Wzzz*, the effect of deep masses in *Wz*, and that of masses at intermediate depths in *Wzz*. Two procedures are given for the simple determination of *Wzzz*.

(From Geophysical Abstracts 159, U.S. Geol. Survey).

281. *The First Vertical Derivative of Gravity.*
H. A. Ackerman & C. H. Dix, Geophysics, Vol. 20, No. 1, pp. 148-154, January, 1955.

A formula is given which permits the relatively convenient calculation of the first vertical derivative of gravity in terms of the distribution of the second vertical derivative of gravity. The use of the formula is illustrated in a simple case. The formula is compared to Evjen's with respect to convenience of use.

(Author's Abstract)

282 *Orthogonal Polynomials: Their Use in Estimating the Regional Effect*
C. H. G. Oldham & D. B. Sutherland, Geophysics, Vol. 20, No. 2, pp. 295-306, April, 1955.

The examination of experimental data for significant trends by orthogonal polynomials is well known in statistics. The method is adapted here to the estimation of regional trends in potential field observations, and two characteristically-different gravity maps are analyzed.

The method is found to agree closely with a graphical solution in an area of fairly smooth contours, and to give a reasonable solution in an area where the graphical method would be difficult to apply. It is proposed that the orthogonal polynomials could also be adapted to evaluating total mass and to interpreting second derivative maps. (Author's Abstract)

283. *Two-Dimensional Smoothing, With Special Reference to Gravity.*
T. A. Elkins, Geophysics, Vol. 19, No. 3, p. 631, July, 1954. (Abstract only of paper read at the Annual Meeting of the S.E.G., St. Louis, April, 1954).

A brief discussion is given of known smoothing methods for one-dimensional data, that is, data along a profile. Next is reviewed the previously published work on smoothing two-dimensional data, that is, data over an area. Methods of two-dimensional smoothing using least squares polynomials are then developed and sets of smoothing coefficients derived for grid figures frequently occurring in practice. The application of these sets to gravity and second derivative values is then studied from the statistical viewpoint. Maps of practical field data before and after smoothing are included as illustrations.

MAGNETIC — INSTRUMENTAL

284. *Patents.* Abstracts in Geophysics, Vol. 20, No. 1, p. 163, January, 1955.

U.S. 2,684,465.	20 July 1954.	A detecting system for a flux-gate magnetometer.
U.S. 2,687,507.	24 Aug. 1954.	A self-oriented total-field airborne magnetometer.
U.S. 2,689,333.	14 Sept. 1954.	A stabilization system for a self-orienting airborne magnetometer.

285. *The Modelling of the Anomalies in Magnetic and Gravitational Fields.* (In Russian).
A. G. Kalshnikov, Akad. Nauk SSSR, Izv. Ser. Geofiz., No. 6, pp. 546-553, 1954.

This is a description of the special field meter used for measurement of field intensity in model experiments. The main element of this instrument is a very small rotating coil which can be placed at any point without disturbing the field pattern in the vicinity. Such a coil has been constructed using a wire of 25μ diameter, with the exterior diameter of the coil being only 0·8 mm. The field patterns produced by

disturbing bodies of different forms and physical properties have been measured with such a field meter. The results are shown.
(From Geophysical Abstracts 160, U.S. Geol. Survey).

286. *Hydrogen Atom Put to Work in Photo-Magnetometer Survey.*
Oil & Gas J., Vol. 53, No. 45, p. 88, 1955.
An airborne magnetometer based on nuclear physics has been developed. Changes in the rate of spin of oriented hydrogen atoms in a water sample are used to determine the absolute magnetic field.
(From Geophysical Abstracts 160, U.S. Geol. Survey).

287. *Patents.* Abstracts in Geophysics, Vol. 20, No. 2, p. 335, April, 1955.

U.S. 2,694,793.	16 Nov. 1954.	A non-oriented magnetometer with three mutually-perpendicular fluxvalves.
U.S. 2,695,384.	23 Nov. 1954.	Inductive device of saturable-core magnetometer having flux regeneration characteristics.
U.S. 2,696,602.	7 Dec. 1954.	A compensated flux-valve magnetometer for short-duration magnetic anomalies.

MAGNETIC — FIELD TECHNIQUE

288. *Micromagnetics — an Aid to Geological Investigation.* (In German).
R. Lauterbach, Karl Marx Univ. Leipzig Wiss. Zeitschr. Math.-Naturwiss. Reihe, Vol. 3, No. 4, pp. 224-238, 1953-54.
"Micromagnetics", as the term is used here, is a geophysical method based on the detailed mapping of small magnetic anomalies (less than 10^4 gammas in amplitude and less than 10 meters in extent). The principles and techniques, diagnostic criteria, and geological and mineralogical applications are discussed. The method is applied to selected test areas in a given region, and can be used not only on direct outcrops, but also for surfaces underlying younger layers or weathered zones a few meters thick. Microanomalies are influenced by rock structure and composition; analyzed statistically they can indicate, for instance, contacts between different formations, direction of flow structure in porphyry, or direction of sedimentation in young sediments. In a broad sense, the shapes of micromagnetic anomalies are "geological documents" which can lead to petrographic and geologic conclusions not obtainable by direct observation.
(From Geophysical Abstracts 160, U.S. Geol. Survey).

ELECTRICAL

289. *The Magnetic Field of a Rectilinear Alternating Current Conductor on Homogeneous Conducting Ground and the Measurement of the Electrical Conductivity of the Ground by Induction.* (In German).
W. Buchheim, Zeitschr. Geophys., Sonderband, pp. 123-135, 1953.
The physical relations between the primary alternating current flowing through a rectilinear conductor on the surface of the earth and the secondary electromagnetic field generated in the ground are discussed by starting from the Maxwell equations, and introducing imaginary functions to derive expressions for the components of electromagnetic field under the special conditions of the problem. These relations can be used for the determination of electrical conductivity of the ground replacing the old Wenner four-point method. The new method has the advantage of being free of galvanic effect. It is also applicable in the case of a parallel stratified medium even if the strata are inclined. In the latter case, the electrical conductivity parallel to stratification can be determined. The field procedure is summarized in the concluding section.
(From Geophysical Abstracts 159, U.S. Geol. Survey).

290. *Comparison of Rapid Variations of the Telluric Field at Stations Separated by Great Distances.* (In Italian).
G. Kunetz & H. Richard, Convegno Naz. Metano e Petrolio, 7mo Taormina 1952, Atti, Vol. 1, pp. 511-518, 1952.

Similarity of curves obtained in the course of exploration by the telluric method in Europe, Asia and Africa shows there are variations in telluric currents of a few seconds or minutes extending over vast regions. Examples are shown of observations in Italy and Madagascar on December 5, 1949, in which a relationship can be shown between variations of about a millivolt and period of a few minutes on which are superposed less intense rapid fluctuations of 10-20 second period; in Italy, Gabon and Madagascar on Sept. 9, 1950, in which there are quasi-sinusoidal variations of about 30-second period; and in Sicily at stations 160 km apart where variations of 0.5 millivolt with 15-second period are superposed on variations of about 1 millivolt and 1-3 minute period.

(From Geophysical Abstracts 159, U.S. Geol. Survey).

291. *Depth Determinations by Electrical Resistivity.*
H. M. Mooney, Mining Engineering, Vol. 6, No. 9, pp. 915-918, 1954.

A summary, with examples, of the empirical, theoretical-curve-matching, and direct methods of interpreting resistivity-depth curves.

(From Geophysical Abstracts 159, U.S. Geol. Survey.)

292. *Effect of a Variable Surface Layer on Apparent Resistivity Data.*
H. M. Mooney, Mining Engineering, Vol. 6, No. 12, pp. 1210-1212, 1954.

The variations in the resistivity of a surface layer may cause erroneous interpretations of resistivity-depth curves. Such errors in interpretation can sometimes be avoided if the effect of these variations can be recognised and taken into account.

(From Geophysical Abstracts 159, U.S. Geol. Survey).

293. *Geophysical Discovery and Development of the Pima Mine, Pima County, Arizona, a Successful Exploration Project.*
R. E. Thurmond, W. E. Heinrichs, & E. D. Spaulding, Mining Engineering, Vol. 6, No. 2, pp. 197-202, 1954.

The Pima ore deposit was discovered by a combination of electromagnetic and vertical intensity magnetometer surveys. Anomalies by both methods clearly indicated the presence of the ore body.

294. *Electrotelluric Survey of the Ferraran Ridge and Comparison with the Results Obtained by Other Methods.* (In Italian).
J. Y. Chereau & A. H. Roger, Convegno Naz. Metano e Petrolio, 7mo, Taormina 1952, Atti, Vol. 1, pp. 589-600, 1952.

295. *Three-Way Geophysical Method Points up Huge Pyrite Deposit.*
Y. Fujita, Eng. Min. J., Vol. 155, No. 12, pp. 84-88, 1954.

Apparent-resistivity, resistivity-gradient, and spontaneous-polarization surveys resulted in locating a large pyrite ore body at the Matsuo mine in Japan. A seismic survey also indicated the location of the ore body.

(From Geophysical Abstracts 159, U.S. Geol. Survey).

296. *Geophysical Prospectings at the Wagasennin Iron Mine, Iwate Prefecture.* (In Japanese with English Summary).
M. Murozumi, Geol. Survey Japan Bull., Vol. 4, No. 10, pp. 41-48, 1953.

Magnetic and electrical (resistivity, self-potential and equipotential line) surveys were made in 1952. The general structure was determined by the resistivity survey;

further prospecting was recommended on the basis of magnetic and self-potential anomalies.

(From Geophysical Abstracts 159, U.S. Geol. Survey)

297. *Geoelectrical Investigations of Underground Structures* (In German).
V. Fritsch, Die Bautechnik, Vol. 31, No. 10, October 1954.

Geoelectrical investigations of underground structures face many mechanical problems — especially in fractured areas—and have to determine the thickness, nature and hydrographical condition of the overburden.

Important advantages of the geoelectrical method are its economy and precision. Its employment makes possible a considerable saving in drilling and thereby provides a cheap and expeditious means of prospecting.

The geoelectrical method provides valuable information which, with careful planning, may be correlated with the data from surveys by other methods.

298. *Some Geoelectrical Problems of Soil Consolidation.* (In German).
V. Fritsch, a paper read at the second meeting of the Italian Soc. of Geophysics and Meteorology, in Genoa, April, 1954. (Not yet published).

Some problems of soil consolidation in geoelectrical prospecting are discussed. The electrical power is concentrated at the electrodes where also the resistance tends to rise quickly. A "critical resistance" is reached where soil consolidation by this method becomes too costly. This resistance is dependent on the number, form and configuration of the electrodes. Rollers and plates are preferable to sticks. Electrode voltage is determined by the specific resistance of the soil. Water content of the soil can be reduced electrically if it exceeds a certain minimum. The moisture-density relationship (Proctor diagram) is derived.

299 *Oscillations of the Earth's Electromagnetic Field and Its Daily Variation* (In Russian)
V. A. Troickaja, Dokl. Akad. Nauk SSSR, Vol. 93, No. 2, pp. 261-4, 1953.

The author refers to a former paper (Dokl., Vol. 91, No. 2, 1953) and treats the short-period oscillations of the electro-magnetic field along with earth currents and magnetic recordings in the Soviet Union. There are two distinct types: firstly, oscillation pulses of short duration; secondly, long permanent oscillations. The short oscillation impulses have a period of 40-63s. and an electrical component amplitude of 2-14 mV/km (or magnetic 0·6-5 γ). The long permanent oscillations have a period of 10-40s. and an electrical component amplitude of 0·5-3 mV/km (or magnetic 0·3-1·5 γ). In both cases GMT is used —resolved half-daily) The author assumes that the excitation of both oscillations depends on the orientation with the sun of the earth's magnetic axis.

OTHER METHODS

300 *Portable Scintillation Counters for Geologic Use.*
E. E. Wilson, V. C. Rhoden, W. W. Vaughn, & H. Faul, U.S. Geol. Survey Circ. 353, 1954.

A portable scintillation counter is described. It is small and light and was designed primarily for geological field work. However, it may be used in automobiles and light aircraft without modification. The basic circuit is also modified for gamma-ray logging of holes as deep as 1,000 ft.

301. *Prospecting with a Counter.*
R. J. Wright, Pub. of U.S. Atomic Energy Commission, Washington, 1954.

A booklet of 68 pages giving information on field counters covering their operation, use, abuse and application in prospecting, mining and geologic problems. A list of manufacturers and distributors of portable radiation detectors is included.

302. *Airborne Exploration for Uranium.*
R. S. Foote, Mines Mag., Vol. 44, No. 10, pp. 29-30, 1954.

Airborne radiation surveying, using a scintillation-type counter mounted in a light aircraft, is a rapid, cheap and effective method of exploration for uranium. The actual size and grade of deposits that can be detected depends upon the altitude of the survey, the speed at which the aircraft flies, and the type of instruments used. Some examples, with estimated costs, are given.

303. *How Geophysics Helps Find Uranium.*
R. S. Foote, Eng. Min. J., Vol. 155, No. 9, pp. 96-97, 1954.

Practical application of geophysics on the Colorado Plateau is restricted to radiation methods. These include airborne reconnaissance, ground reconnaissance, drill-hole logging, and carborne reconnaissance. Scintillation counters are in general use.

304. *Aerial Prospecting with Scintillation Counters.*
G. Cowper, Nucleonics, Vol. 12, No. 3, pp. 29-32, 1954.

Aerial prospecting for radioactive minerals is practicable when a sufficient fraction of the mineral deposit is exposed at the surface, the gamma-radiation detector is sufficiently sensitive to record unambiguously a significant change in the ground radioactivity from an altitude governed by aircraft safety, and the total weight of the detecting equipment is small enough to permit use of a small aircraft, making the method economically sound. To meet the second and third conditions a practical airborne detector using scintillation counters was developed at Chalk River (Atomic Energy of Canada Ltd.) in 1950. Two counters are used, with the crystal units in each containing two thallium-activated sodium iodide crystals 2 inches in diameter and 2 inches long placed end to end. A lucite cap on the cylinder containing the crystals fits over the end of the photo-multiplier tube. A conventional counting-rate meter with a modified integrating circuit and an additional circuit to cancel the contribution from large cosmic ray pulses is used and its output recorded continuously on a recording milliameter. The sensitivity was demonstrated by the detection of an 88-millicurie radium source in the centre of a frozen lake at altitudes of several hundred feet. The most difficult problem is one of interpretation, distinguishing between localised outcrops of high-grade ore and large areas of slightly abnormal radio-activity.

(From Geophysical Abstracts 160, U.S. Geol. Survey).

305. *Results of Airborne Radioactive, Electromagnetic and Magnetic Surveys.*
H. Lundberg, Oil & Gas J., Vol. 53, No. 48, p. 211, April 4, 1955.
(Abstract only of paper read at the Annual Meeting of the S.E.G., New York, March, 1955).

Airborne recording of radiation from the earth's surface is a new method of geological mapping. After eliminating effects from topography, surface waters and known geology, a pattern often remains that may enable the geologist (geo-physicist) to outline direct indications of oil and gas accumulations which apparently have a blocking effect upon upward trending movements. The position of radioactive mineral deposits may also be revealed directly in detail surveys, and it is also possible to distinguish the effect of uranium from that of thorium and potassium.

THE TECHNICAL-ECONOMIC ASPECTS OF AUTOMATIC DATA REDUCTION *

BY

ROBERT W. OLSON **)

Abstract

The background of automatic data processing as well as other improvements in prospecting methods is almost certainly economic. Consciously and intentionally or intuitively and even subconsciously, economic forces are the drive for improvements.

Automatic processing can contribute to the increasing utility of seismic data. Reduction in the amount of routine work will permit talented people to utilize their time creatively on the more difficult problems. At the same time automatic reduction will provide for a greater volume of work. These two aspects will probably provide the first effective pressure for a high degree of automation.

It is to be expected, however, that the ultimate and greatest value will be better interpretation; possibly more detail, possibly clearer more definitive interpretation, possibly both.

Time concepts in the processing of seismic data are, of course, vital; either in simple time corrections of either static or dynamic nature or in treatment of signals in the time domain.

Much development work is needed before these advantages can be realized. Principal development needed is an increase in dynamic range in the overall system.

Introduction

At the outset, let me state that this paper is based on as yet limited laboratory results. We have extended these results by purely synthetic estimates to explore practical applications.

The purpose of this paper is to stimulate thought and not to state proven results. The machine analysis of seismic data is an intensely complex business. It will be years, possibly decades, before dogmatic statements are justified.

We in the United States use an expression, the origin of which is unknown to me, but which might very well be the thesis of my paper. This expression is: "Necessity is the mother of invention".

All inventions in economic geophysics were most certainly mothered by necessity and they have been sired many generations back by the cost of locating a barrel of oil. These costs have been rising monotonously in the United States.

---

*) Presented at the Tenth Meeting of the European Association of Exploration Geophysicists, held in Hamburg, 16-18 May 1956.

**) Houston Technical Laboratories, Houston, U.S.A.

Costs are not the same everywhere, but in the long run costs of locating oil have no place to go but up, since each find reduces by one the remaining possibilities.

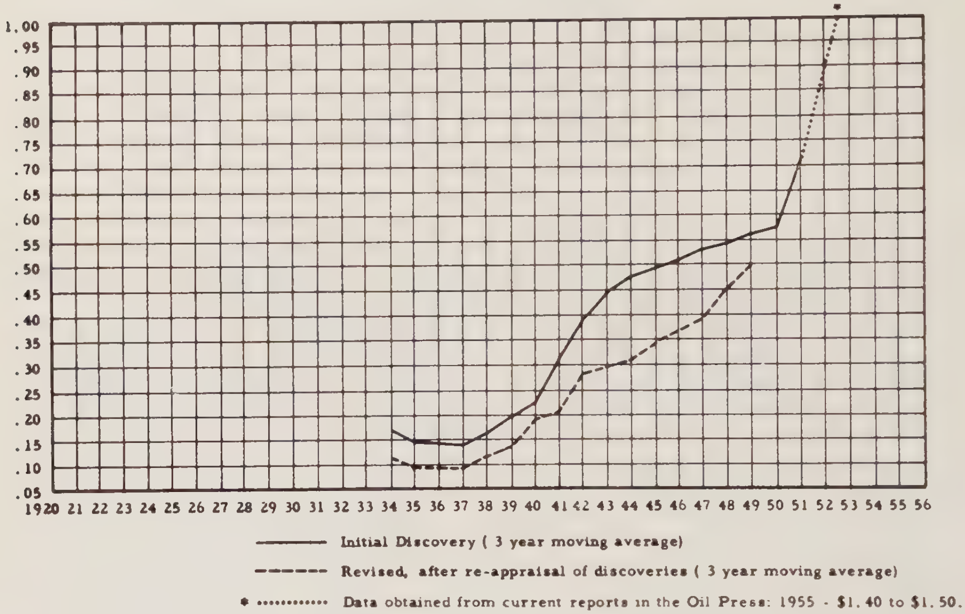

Fig. 1. Cost of Finding Oil in the United States (after H. J. Struth ,,Petroleum Engineer", May 1953

In the final analysis this — the cost of exploration measured in whatever terms one might wish — irrespective of economic systems or units of currency, is what is behind the lure of automatic processing of seismic data, or for that matter almost any geophysical development.

From the point of view of the scientist and the engineer, it is extremely discouraging that most new development must be "sold" to management on the basis of reducing operating costs for performing presently routine functions, rather than on the basis of the many new functions which might be performed. Unfortunately, there is not usually a demand for a service never heretofore performed.

I shall, therefore, attempt to: (1) demonstrate that machine processing of seismic records can become economic, (2) discuss the machine process in general, and (3) mention a very few of the future possibilities.

A high speed water crew (hypothetical) will be chosen for study. We will assume 2,000 24-trace records per month. This required at the time a computing crew of 24 men, at a daily cost of $ 350.

Water computing and data reduction are not in general done with the exquisite care and vivid imagination sometimes lavished on land jobs. Let us, therefore, set up a machine computing system that will provide picked records; the "picks" to be made to pre-set criteria. The end result will be a picked, corrected, plotted depth section. An attainable combination of machines mostly in existence is estimated to be able to compete with seventeen reasonably skilled junior computers.

If we can demonstrate economy on a routine job, we may have the opportunity to explore the fascinating possibility of a better, more complete job of analyzing seismic data.

TABLE I
Comparison of Total Costs per Record for High Production Seismic Computing; Manual versus Machine.

	Manual		Machine	
	2000 Rec/Mo One Shift	4000 Rec/Mo Two Shifts	2000 Rec/Mo One Shift	4000 Rec/Mo Two Shifts
Labor	$ 8,000 (24 men)	$ 16,000 (48 men)	$ 2,000 (5 men)	$ 4,000 (10 men)
Overhead				
Office rent	500	500	250	250
Depreciation	150	150	2,850*	2,850*
Misc. (utilities, supplies, etc.)	400	800	310	620
Supervision	700	700	700	700
Total	$ 9,750	$18,150	$ 6,110	$ 8,420
Cost per Record	$ 4.87	$ 4.54	$ 3.05	$ 2.10

* Assume $ 100,000 equipment cost - 36 months' depreciation

Now let us look at comparative costs. These are best shown in tabular form. (*Table* 1) Note that at a high volume level, machine processing can be cheaper in the near future.

The figures above are synthetic estimates. They illustrate, however, that machine processing has an early economic possibility. Let us, therefore, proceed to examine some of the basic technical concepts.

APPLICATION OF CORRECTIONS

All routine processing of seismic data (at the present state of the art) consists almost entirely of recognizing events, measuring their time, and applying time corrections. These corrections are either positive or negative.

Since there is no such thing as negative time, and since time corrections positive and negative are so important, all methods convert time to an analog and thereby acquire ability to introduce negative time.

The most common analog consists of recording the seismic signal so as to produce an analog having a single dimension in space, introducing an arbitrary analog delay, and then delaying (positive or negative) by means of changing the point of observation. This, of course, is done in manual working of records by searching for events advanced or retarded from the ideal position by the amount of weathering, elevation, normal move out correction, etc. (*Fig.* 2).

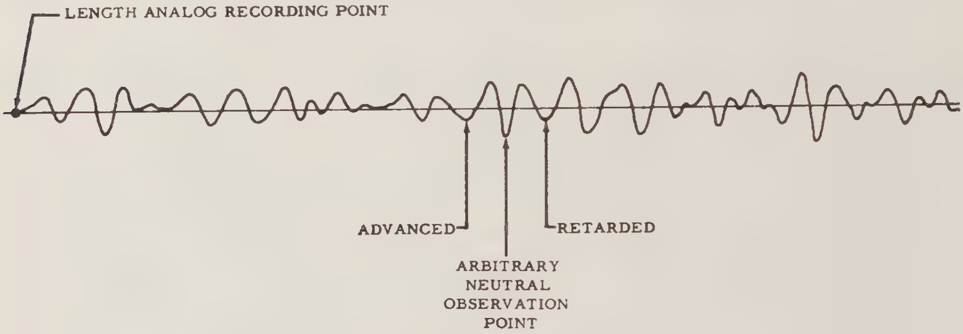
LENGTH ANALOG RECORDING POINT
ADVANCED
RETARDED
ARBITRARY NEUTRAL OBSERVATION POINT

Fig. 2. Length Time Analog

In general each point on each trace has a unique ideal time correction to be added or subtracted. Regardless of whether the signal is operated on in length analog or in time, a rather comprehensive program of corrections is required.

This has been programmed in a variety of mechanical ways having more or less flexibility plus a completely flexible computer type machine which constitutes the subject matter of much of this paper.

A research model of the machine for the automatic processing of seismic data is in operation and provides the basic framework for a complete seismic data processing system having flexibility of a high order to provide for techniques not yet conceived. The first practical approach and the least that it will do, is to make all of the time corrections and thus turn out a completely corrected record. *Figure* 3 shows a refined production model.

Functionally, this machine consists of a delay line with one millisecond or two millisecond increments, and a programmer to make a multitude of switching operations and specifically to connect in various amounts of delay. The programming is controlled digitally. In correcting time, any part of a seismic record is played without stretching or compressing. A selection might have been made either to gap the record or to replay part of it. We chose to replay part of the record.

The normal move out curve is approximated in a series of discrete steps. This is illustrated graphically in *Figure* 4. The traces in a seismic spread closest to the shot hole are played without correction; those farther away are played through the delay line and so scheduled that at various intervals of time short pieces of the record are replayed. The increments are'small enough and the frequencies resulting from the switching are high enough, that they are barely perceptible on the record.

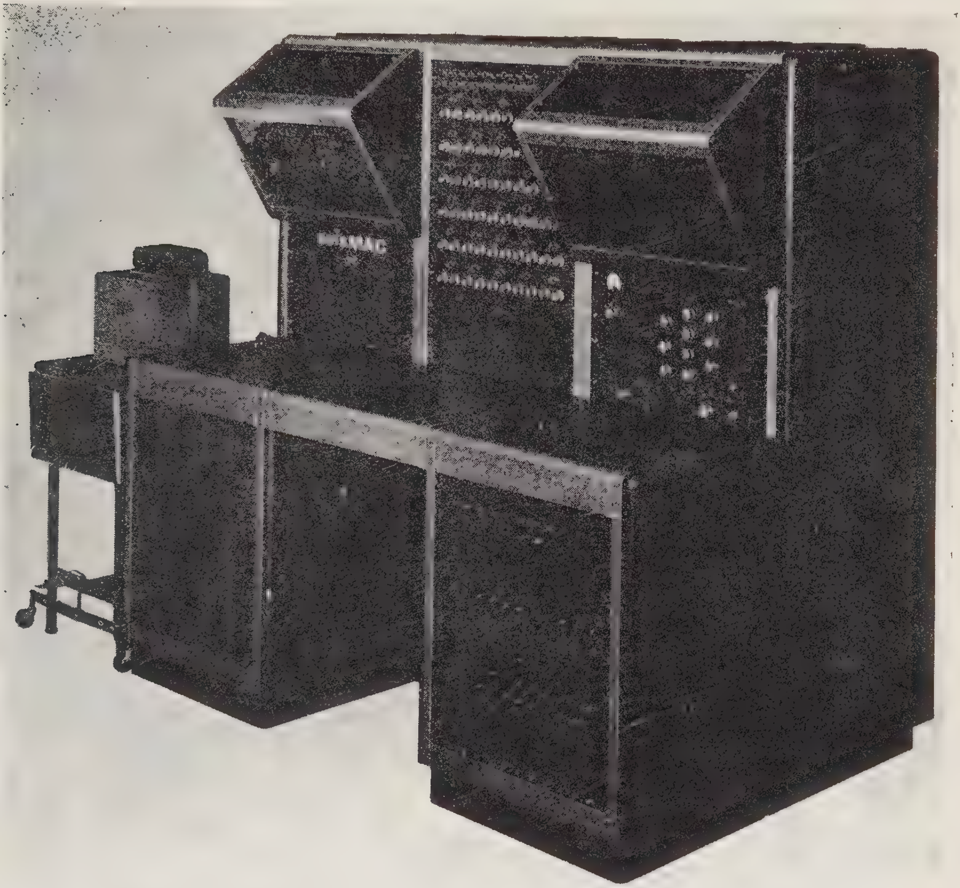

Fig. 3. Seismic Magnetic Automatic Computer

Constant time correction, that is, weathering and elevation, are pre-set into the machine by knobs shown on the front panel. These knobs control circuits which generate binary digital codes that are stored in a memory.

The variable time corrections are programmed into the machine by punched paper tape, and stored in the memory as a binary digital code. When the correction is to be applied to the seismic trace, the weathering and elevation correction and the normal move out correction are digitally added before being entered into the delay line switching operation.

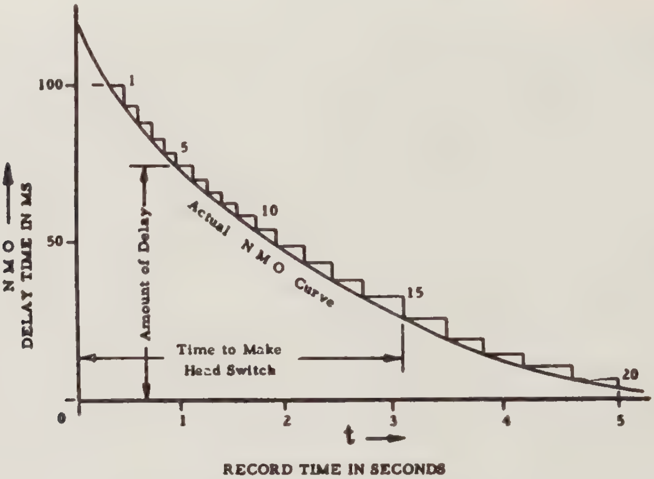

Fig. 4. Typical Approximation of Normal Moveout Curve for One Trace

The paper tape is typical of that used in modern high speed digital computing machines, as are the keyboard and tape punch and high speed photoelectric tape reader shown in *Figure* 5. The details of coding are well known and thoroughly covered in the literature so I will give no more explanation than is

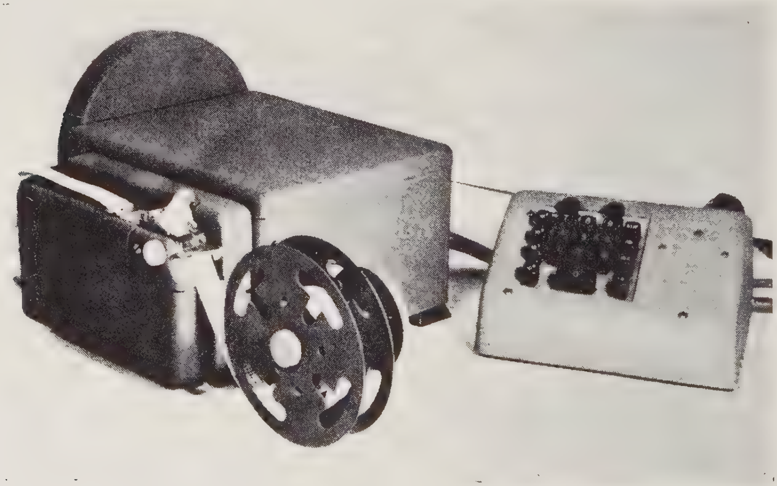

Fig. 5. Keyboard and Paper Tape Punch

shown on *Figure* 6. Note, however, that it is possible to punch into the tape the time at which a correction is to be made, the amount of correction, and in addition the control information necessary to have the data entered into the machine properly. Incidentally, approximately 1000 operations per second can be programmed.

The computing machine will then do all of the rest of the work. The processing time for a 24-trace record with four programming traces for time-break, etc., is about two and a half minutes. This incidentally provides adequate time for the operator to set up the next record. Note that 2,000 records per month require only 84 hours of operating time.

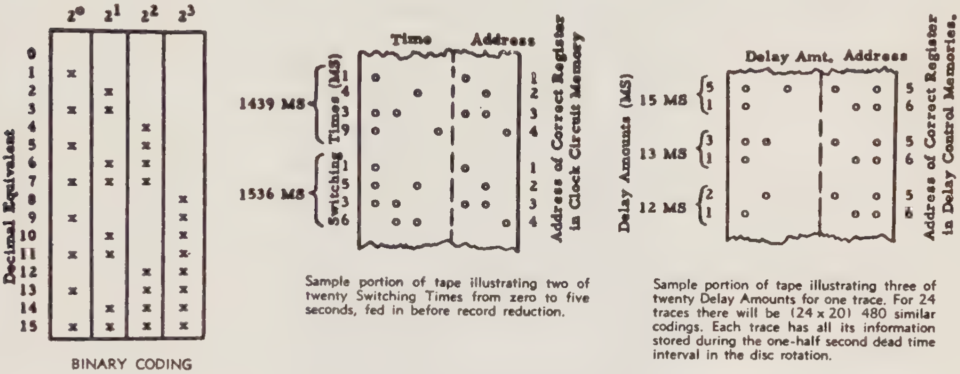

BINARY CODING

Sample portion of tape illustrating two of twenty Switching Times from zero to five seconds, fed in before record reduction.

Sample portion of tape illustrating three of twenty Delay Amounts for one trace. For 24 traces there will be (24 x 20) 480 similar codings. Each trace has all its information stored during the one-half second dead time interval in the disc rotation.

Fig. 6. Explanation of SeisMAC Tape Punch Coding

When all of the traces have been corrected and re-recorded, the corrected re-recorded data may be played off through a simple amplifier onto a section camera. At this point it is of course possible to composite (or stack or mix) to any extent desired, since the records are all time corrected, filtered, and levels adjusted after filtering.

Recognition of reflections

The other important part of processing seismic data consists of recognizing events. Here the human computer is at present aided by many circuit and mechanical tricks such as multiple seismometers, compositing, filtering, *AGC* treatment, and optical illusions. Finally, however, he picks a record by applying several criteria to each signal.

These criteria might be either singly or in combination (*a*) the number of channels having similar related signals, (*b*) time relation (presented in length analog) between signal peaks, (*c*) amplitude, (*d*) number of peaks, (*e*) period of oscillation, (*f*) phase angle of "harmonics", (*g*) "harmonics" content, (*h*) signal to noise ratio, (*i*) rise time, and (*j*) decay time. Most important, however, are usually (*a*), (*b*) and possibly (*c*). Machines can be built to comprehend and evaluate all of these criteria.

Such a machine, using only a few of the many possible criteria for automatic detection of signals is shown in block diagram form in *Figure* 7. It presents the early possibility of cost reduction in treatment of quantities of seismic records. This is really a decision-making filter.

As practiced now, the interpreter selects and filters or throws away all but two points of information from each discrete reflection on a seismic record, and plots these two points and establishes a line between them. This is regarded as the pertinent information of the particular reflection on the record.

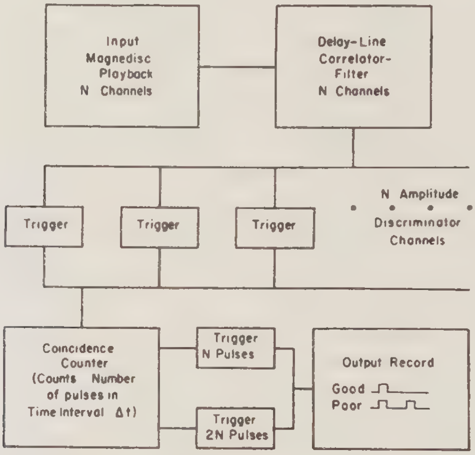

Fig. 7. Block Diagram of Simple Automatic Record Picker (Non-Linear Detection Filter)

Figure 8 shows an actual practical machine to do this job. The interpreter sets into such a machine the criteria which he demands in order for the machine to make a pick. Following this, the machine will make consistent and reliable picks.

The particular criteria, and they are very simple, which have been selected for this first machine are amplitude contrast, phase coincidence and persistence of the event from trace to trace. Various levels of confidence may be established, and if the record meets these criteria it puts out a single pulse. In describing this machine, I can do no better, perhaps not so well, as to quote my colleague, Dr Hal J. Jones:

"For example, in this equipment we might require that on a n-trace seismic record the positive peak amplitude must exceed a set value simultaneously within a small time interval Δt on r out of n traces, before we are willing to state that a reflection has occurred . . . The operation of the filter is such that if the amplitude discriminators on individual channels are set for a signal level A, the occurrence of an amplitude greater than or equal to A opens an electronic gate designed to open at the instant of peak amplitude. If then peaks greater than or equal to A are reached on r other traces during the time interval Δt, over which the gate is opened, a pulse output occurs. The value of r can be pre-selected. For detecting weak signals, A and r must be set relatively low and the 'false alarm' probability, that is the probability of mistaking noise for signal, is rather high although, of course, weak signals will be detected. Increased stringency on the requirements of the signal by increasing r and A will increase the probability of failing to detect actual weak signals."

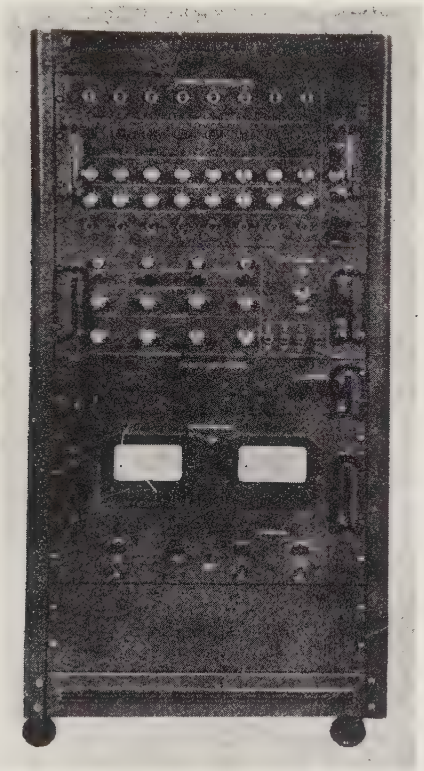

Fig. 8. Seismic Signal Detection Filter

Figure 9 shows the type of record and presentation obtained. Again quoting Dr Jones:

"For each analog seismic trace shown on this figure, there is a quantized trace (124) showing the output of the amplitude discriminator for that particular piece of data. At the bottom of the figure is a summary trace (119) showing the 'pick' (122) of the unit for each event. In this case, the equipment was set for eight out of twelve traces at a given negative peak level above background. Note that the strong events (123) are 'picked' without difficulty, but that high amplitude events (120, 121) which do not occur on the required number of traces do not have an output on the picked trace . . ."

A computing setup such as that being described herein has in addition to others, the advantage of freeing skilled personnel from "busy work" for more creative endeavors. Thus by forcing centralization of some functions it provides for more stable living conditions for professional geophysical interpreters. This makes possible the attraction of types of intellect who might contribute greatly but find nomadic existence abhorrent and hence stay out of the profession. This is thought to be an important advantage.

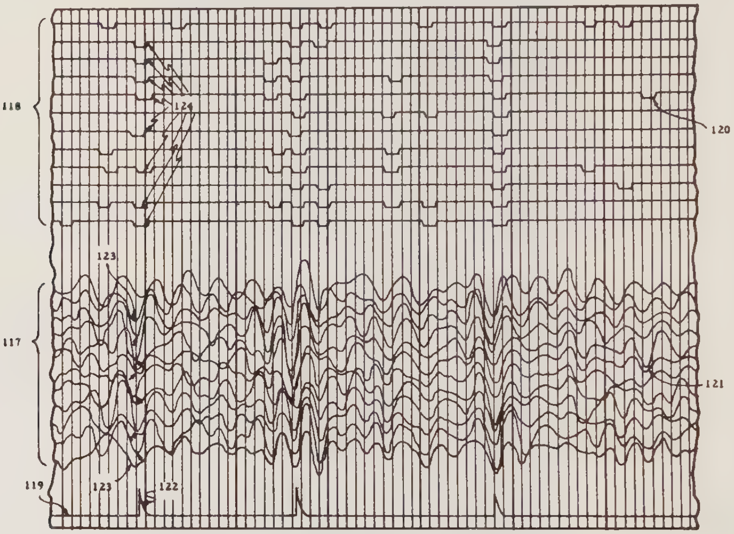

Fig. 9. Type of Record obtained with Automatic Signal Detection System

Further possibilities of automatic data reduction

However important, mere reduction of costs of doing the same old thing is not intensely attractive to the scientist. So let us take a look at those aspects of our data processing which might be more stimulating to the forward-looking geophysicist. What tools and what techniques can be tied to the automatic data processing machine?

Generally, the switching capacity of machines of this type is very great — about 1000/second allowing myriad processing functions to be introduced.

The use of the delay line is probably the most interesting specific tool that has come out of these investigations.

Let us look at a simple case of a delay line used as a time domain filter. Filtering has been done with LC filters for years; and so many variations are possible that from a straight filtering sense very little can be expected from time domain or delay line filters. However, if one takes the new point of view of treating the signal as a time series rather than as an electrical signal, many new avenues are open. Indeed, this provides the basis for thinking in terms of information theory.

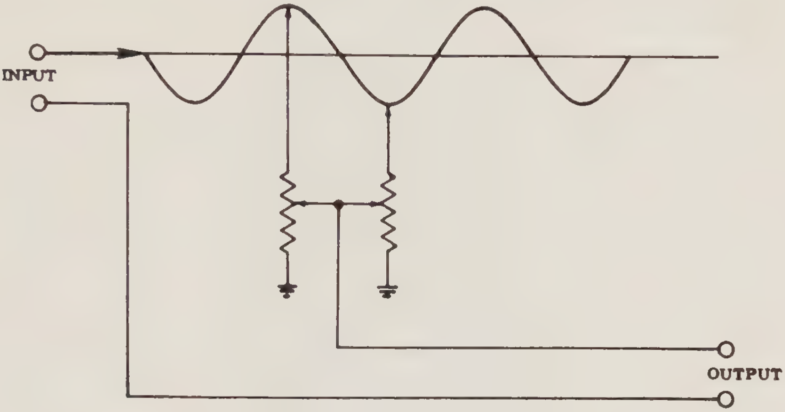

Fig. 10. Simple Analog of a Delay Line or Time Domain Filter

A simple analog of a delay line or time domain filter is shown in *Figure* 10. An electrical signal is represented by an analog, in this case let us assume a magnetic recording in a track, where the input is recorded as a track moves by and the output is sampled at several points. Let us assume that two output points are sampled, a half-wave length apart, and that the amplitudes of the two are adjusted to equality and added. Under this circumstance no output will result at that particular frequency but at other frequencies some output will result. Thus we have a filter with infinite attenuation at one frequency. It does not take a particularly vivid imagination to add more heads and sample different portions of the signal at the various pickup points. The variables at one's command are very great. A delay line filter can be made to perform very much like an LC filter. Some examples of delay line filtering are shown on *Figure* 11.

Figure 12 is a photograph of a research model of a magnetic delay line or time domain filter. It has a recording head, 18 reproducing heads, and an erasing magnet. The filter operator that is, the total length of time that a signal will be in the delay line before being erased, is 45 milliseconds. Thus with 18 reproducing heads, it is possible to sample every two and a half milliseconds along a record.

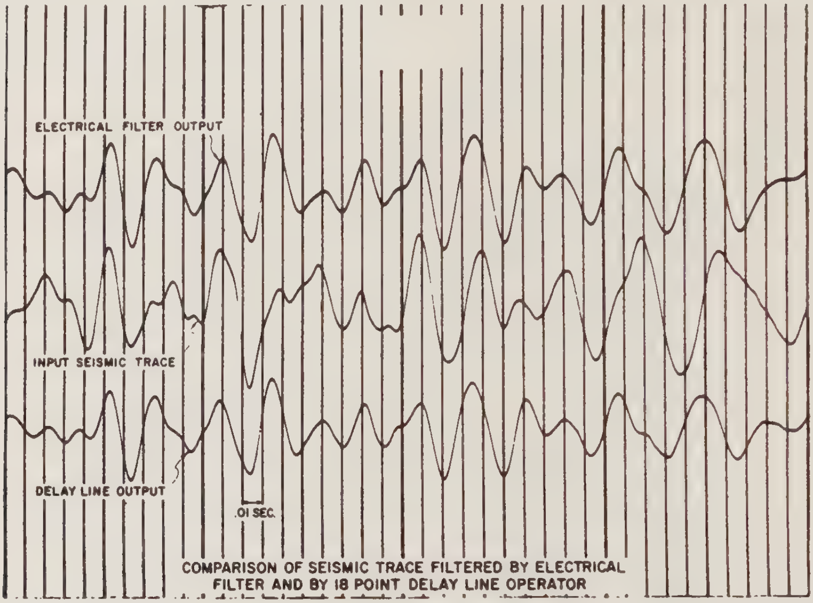

Fig. 11. Comparison of Seismic Trace Filtered by Electrical Filter and by 18 Point Delay Line Operator

Cross correlating, which can be done with a delay line having suitable properties, provides for a highly flexible filter. In simplest terms, a signal can be analyzed bit by bit in comparison with an ideal signal and all irrelevant material rejected. This is the very essence of filtering.

With flexible analysis equipment, that which may become important is reserved for the future but surely a way will be found to utilize more information from a record than mere time to a few events.

Some intriguing possibilities long contemplated are these:

a. What information about the reflecting boundary can be gotten by the frequency content, particularly by the change in the frequency content with change in location?

b. What detail can be gained by displaying reflections systematically at several widely different frequencies?

c. "Character" and changes in character have long been discussed but beyond using them for recognition and timing little has been done with them.

d. Phase breaks.

In summary, a simple pulse is introduced into the earth, a complex wave train returns. The wave properties displayed are the effect of the earth's section on the simple pulse. How is effect related to cause? In this is literally and figuratively a wealth of information.

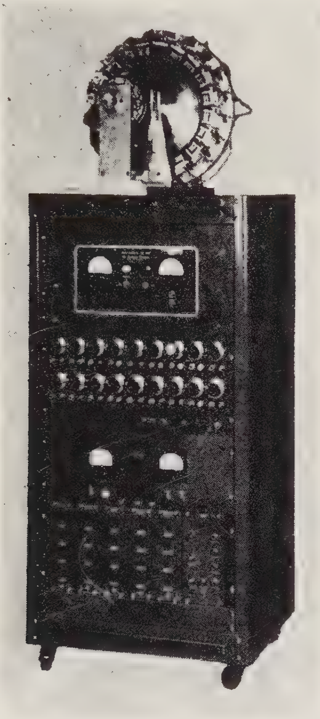

Fig. 12. Research Model of Time Domain Filter

REFERENCES

BUCY, J. F., et al. Oct. 1955 Patent Application No. 538,062

JONES, H. J., and MORRISON J. A., 1954, Cross-correlation Filtering, Geophysics, XIX, p. 660-683

JONES H. J., MORRISON, J. A., SARRAFIAN, G. P., and SPIEKER, L. J., 1955, Magnetic Delay Line Filtering, Geophysics, XX, p. 745-765

JONES, H. J., 1956, Application of Magnetic Recording to Seismic Data Processing, presented at meeting of Fort Worth (Texas) Geophysical Society, January 25.

SCALE MODEL SEISMIC EXPERIMENTS

BY

S. H. HALL*

ABSTRACT

An experimental arrangement is described using an electric spark as source and barium titanate as a detector. Model experiments were made in water with the source mounted above the surface. The effect on the pulse shape on transmission through the air-water interface and the change of pulse shape with depth were investigated. A number of profiles are presented of reflections from a slate slab immersed in the water with different arrangements of the model and detector.

INTRODUCTION

Model seismology provides a means of repeating the field situation within the bounds of the laboratory under simple conditions, for not only is the unknown quantity of the subsurface geologic structure eliminated but the investigator has greater control over his experimental conditions and arrangement. This control is perhaps the greatest virtue of model seismology, for the method facilitates investigation of the initial disturbance as well as providing complete freedom to adapt the model arrangement, and its nature, to any desired configuration or to any desired control in its elastic parameters. This versatility of the experiment makes it a tool for the geophysicist with virtually limitless applications which need not necessarily be confined to the study of fundamental propagation problems but also include problems of a direct geological nature. To achieve this reproduction in the laboratory it is of prime importance to retain the proportions as they occur in the field of wavelength to geological structure size e.g. the thickness of sedimentary layers or volcanic dykes, etc. A reasonable reduction ratio of 10^3 for structural dimensions thus requires a proportionate increase in working frequencies from the 5-100 cycles p. s. of prospecting seismology to 5-100 kilocycles p.s. in model work.

The corresponding reduction in time-scale for the passage of events has required the use of electronic techniques unlike those employed in the field. On the same basis of reduced time-scale the shortened intervals between successive arrivals of a disturbance demand a detector with a high damping factor or low Q. In the majority of papers published the type of detector used has been piezoelectric, with the exception of the first published paper by Kaufman and Roever (1951) who used a miniature displacement geophone. Others, notably Oliver, Press and Ewing (1954) have used the electrostrictive barium titanate as accelerometers. On the same grounds, a highly damped source pulse is necessary which can be obtained either by pulsing a piezoelectric transducer or by the discharge of an electric spark. Ewing et al., (1954) in an elegant two dimensional experiment periodically pulsed a barium titanate projector and produced a stationary recorded wave of the transient event.

---

*) Imperial College of Science and Technology, London.

To reduce extraneous effects such as scattering, selective absorption, or reflections and refractions from gradations in density within the model, workers have either avoided the issue as for example Oliver, Press & Ewing (1954) in their use of flexural waves in place of body waves, or attempted to manufacture fine grained media of wax or concrete. Tejada-Flores, Randolph and Howes (1953) have used water, which though opaque to shear waves permits the investigation of seismic phenomena in depth.

Experimental method

The experiments were made in a tank 1 metre square and 30.5 cms. deep filled with water in which the model was immersed. A three-electrode spark, similar to that of Kaufman and Roever (1951) was used as a source, discharging at 3000 volts. The general experimental arrangement is shown in Fig. 1.

The construction details of the detector are shown in Fig. 2. It consists of a piezoelectric disc of barium titanate 2 cms. in diameter and 3 mm. thick with a fundamental radial frequency of 143.5 kc. p.s. To the rear face of the disc is attached a conical mass of brass which has a characteristic impedance close to that of barium titanate. The metal sleeve on the front face of the disc has a narrow flange which is pressed against the disc perimeter to damp edge vibrations. A copper cylinder enclosed the complete detector which was then dipped in wax to make it waterproof.

It is a difficult problem to measure the frequency response of a detector over a wide frequency range, such as met with in model work. Some idea, however, of the behaviour of the detector can be gained from impedance measurements. This was done over the frequency range 0-180 kc. p.s. by the method illustrated in Fig. 3. The capacitance C_1 in series with the barium titanate disc C is of the order $C_0/50$ where C_0 is the clamped capacitance of the disc. The large reactance of the series capacitance ensured a capacitive load on the source generator at all frequencies. The impedance Z_e was then determined from the relation

$$Z_e = E_2/\omega C_1 (E_1 - E_2)$$

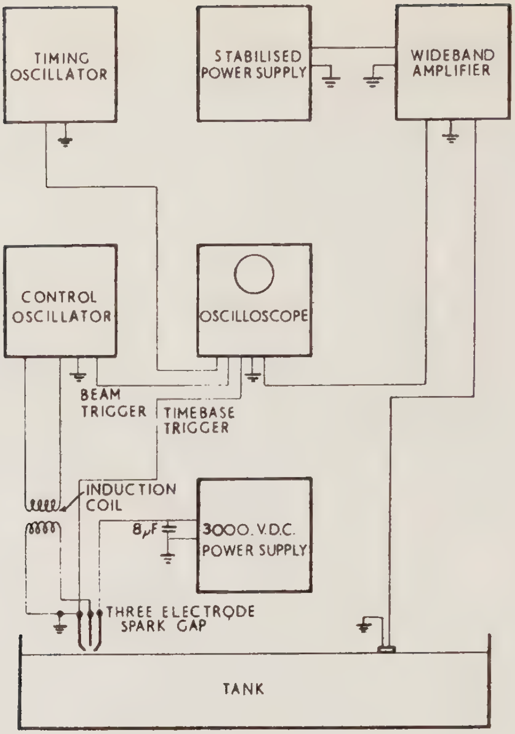

Fig. 1. Experimental arrangement

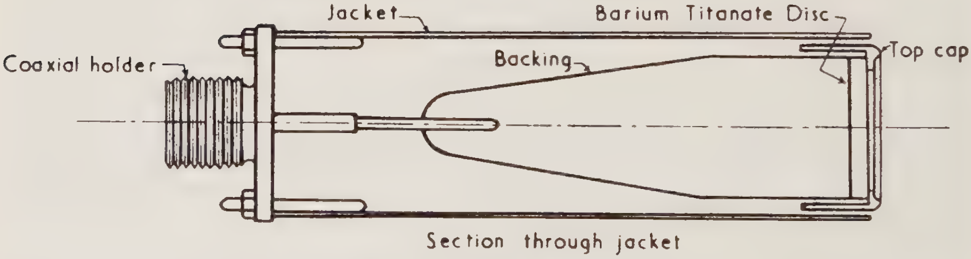

Fig. 2. Detector design

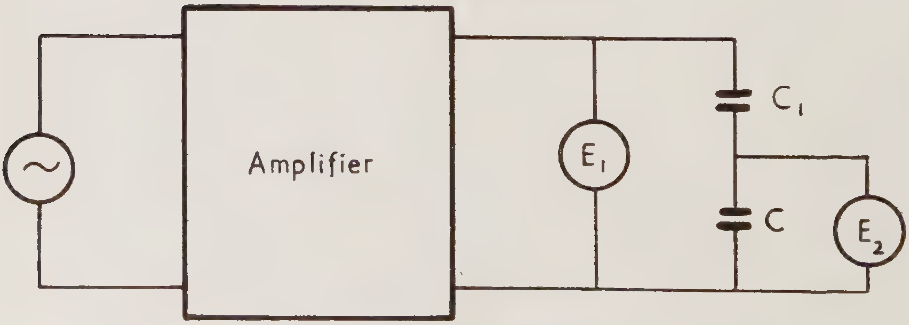

Fig. 3. The method of measuring Z_e

where E_1 is the voltage input and E_2 is the voltage drop across the transducer.

In Fig. 4 the curve of impedance for the disc in air exhibits the customary resonance and anti-resonance character of a piezoelectric transducer which

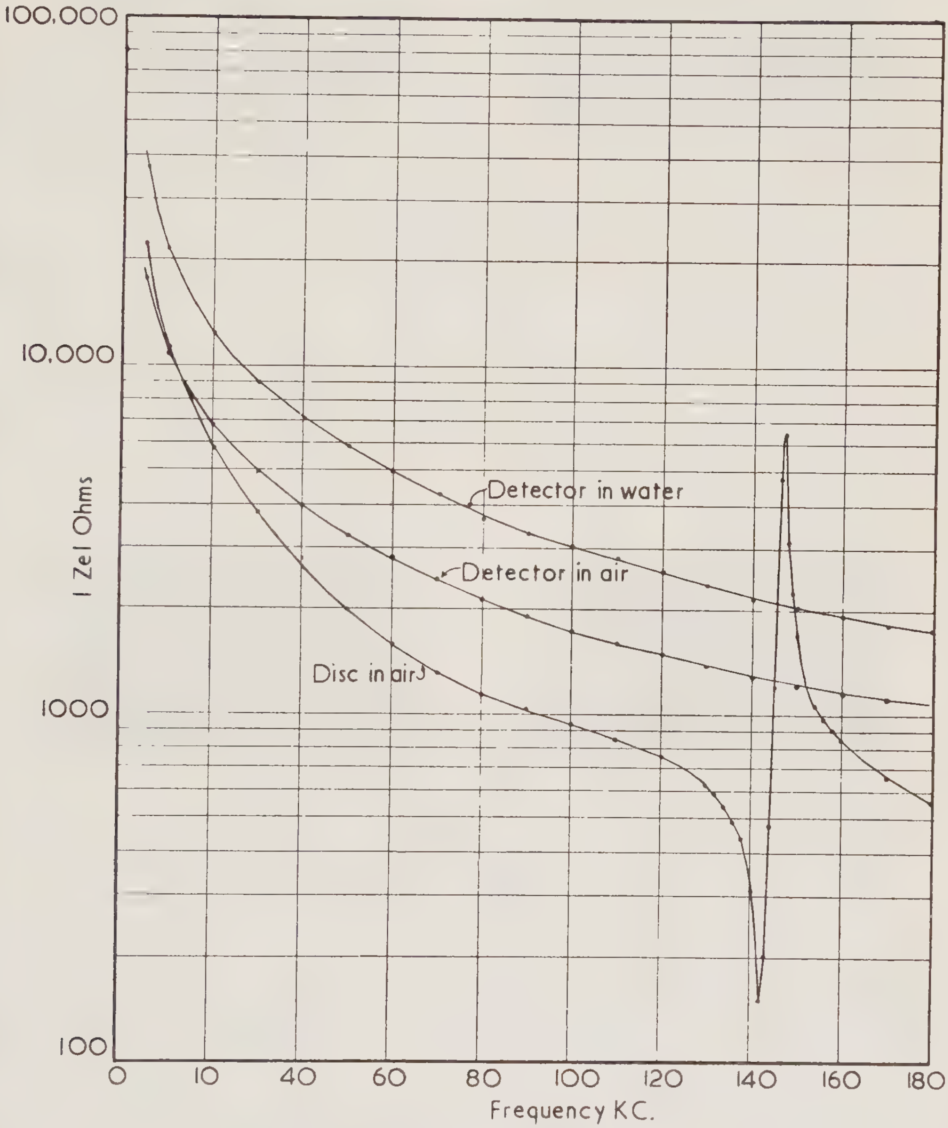

Fig. 4. Curves of the impedance Z_e

in the curve for the assembled detector with backing is completely suppressed. The third curve of Fig. 4 shows the effect on the impedance when the detector was immersed in water, the loading effect of the water giving higher values for the impedance particularly at low frequencies.

SOURCE PULSE

In the experimental arrangement the spark source was mounted in air above the water surface and hence it was desirable to know the character of the pulse front following transmission through the air-water interface. Care was necessary to exclude spurious reflections occurring between the interface and source that might mar the shape of the pulse. Fig. 5a shows the pulse shape in air with the detector at a distance of 8 cms. from the spark. From the 50 kc.p.s. timing wave in the upper part of the record it is seen that the duration of the initial compression is 20 μsecs. Considerable abbreviation of this duration was achieved by placing absorbent sponge rubber at the rear of the electrodes which had the added effect of damping the remainder of the pulse resulting from the air disturbance after the spark discharge. The result is illustrated in Fig. 5b where the timing wave is 100 kc.p.s. and the duration of the initial compression is shortened to 10 μsecs.

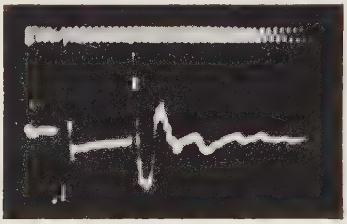

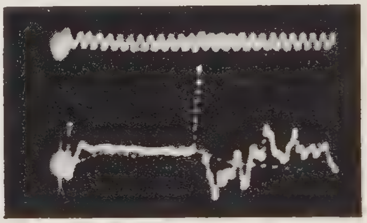

Fig. 5a. Pulse recorded in air at 8 cms. distance from the spark, timing wave 50 kc.p.s.

Fig. 5b. Pulse recorded in air at 6.4 cms. distance from the spark with sponge rubber behind the electrodes, timing wave 100 kc. p. s.

In examining the transmission through the air-water interface the pulse was first recorded in air, Fig. 6a and then in water Fig. 6b with the same source-receiver separation of 6.4 cms. but with the receiver immersed to a depth of 1.9 cms. In each case the same amplification was used. The ratio of the amplitudes of the initial compression in water and air is 0.8 indicating no great change in pressure amplitude, the only marked difference being the appearance in the record in water of a small rarefaction and compression following the main event. The close equality of the pressure amplitudes is to be expected from theoretical considerations. The transmission coefficient is

$$T = {}^{\text{Energy in Water}}/_{\text{Energy in air}} = 10^{-3}$$

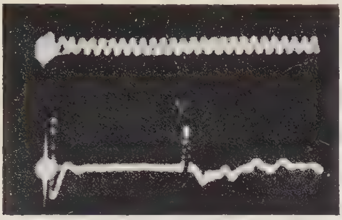

Fig. 6a. Pulse recorded in air at 6.4 cms. distance from the spark, timing wave 100 kc.p.s., amplification 3000

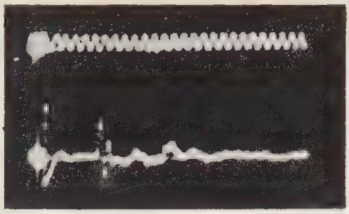

Fig. 6b. Pulse after transmission through air-water interface at a distance of 6.4 cms. from the spark and the detector, 1.9 cms. below the water surface, timing wave 100 kc.p.s., amplification 3000

But the energy is proportional to $\rho c \dot{\varepsilon}^2$ (Wood 1946) where $\dot{\varepsilon}$ is the particle velocity and ρc the characteristic impedance which for water and air is in the ration ρc water: ρc air $= 1.4 \times 10^5 : 40$ thus giving the ratio of the particle velocities

$$\dot{\varepsilon}_{\text{water}}/\dot{\varepsilon}_{\text{air}} = 5.3 \times 10^{-4}$$

Since the instantaneous pressure is proportional to $\rho c \dot{\varepsilon}$ we can derive the ratio

$$^{\text{Pressure in water}}/_{\text{Pressure in air}} = 1.9$$

Hence ideally for normal incidence of plane waves the pressure in water exceeds that in air by a factor of 1.9. This represents the instantaneous pressures at the interface and takes no account of the attenuation effects which would modify the observed result.

DEPTH PROFILE

Both source and detector were mounted at a fixed separation of 26 cms. in the same vertical plane with the face of the latter directed towards the base of the tank. Variation in depth was gained by increasing the water level, thus maintaining the detector at a constant height above the tank base. The records, Fig. 7, are shown with a 50 kc.p.s. timing wave and are arranged in order of increasing depth below the water surface, which is indicated on the right of each record together with the amplification.

The first arrival is the direct compressional wave (P) followed by the reflected wave (PP_1) and the doubly reflected wave ($PP_1{}^*$), whose paths are as shown in Fig. 8. The onset of P becomes an impulsive rarefaction at depth

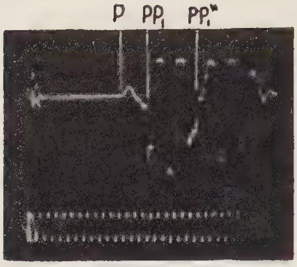

Depth Cms.
0
①
Gain 8700

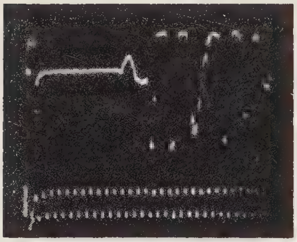

0·64
②
8700

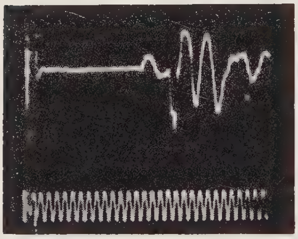

1·27
③
8700

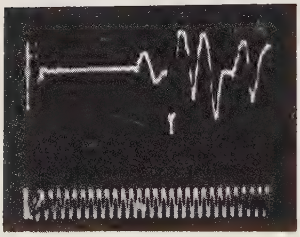

1·91
④
8700

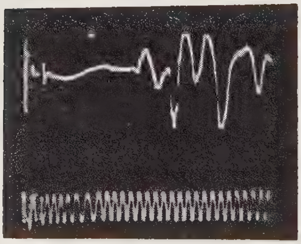

2·86
⑤
8700

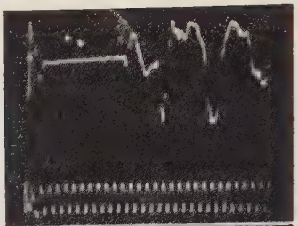

3·49
⑥
8700

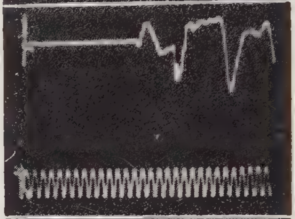

4·13
⑦
8700

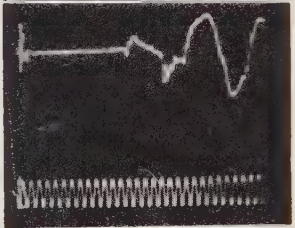

4·76
⑧
8700

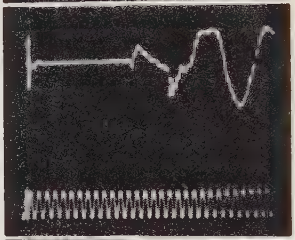

5·40
⑨
8700

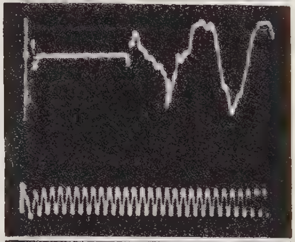

6·35
⑩
8700

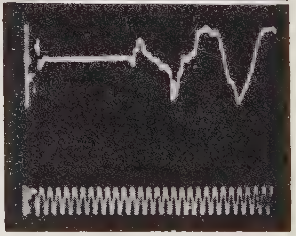

7·30
⑪
8700

Fig. 7

which is to be expected since at positions below the horizontal plane through the source the sensitive face of the detector becomes more and more oblique to the direct wave path. Because of its greater rigidity the detector can be regarded as a double source producing rarefactions on its side remote from the spark source as compressions are incident upon its near side. In record no. 1 it is evident that the amplitude of the direct wave compression is smaller than in the following records. This follows as the air-water interface is virtually a free surface which in the ideal case would not propagate any acoustic disturbance.

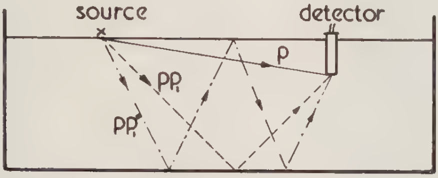

Fig. 8. Experimental arrangement for the profile of Fig. 7

The reflected wave in record no. 1 is incident upon the base of the tank at an angle of 45°. This bottom surface was sealed with a thin layer of pitch whose characteristic impedance is approximately half that of water. The critical angles were such that no energy was transmitted into the wooden base of the tank and the distinctive phase change in the onset of this arrival suggests that most of the energy was reflected at the water-pitch boundary.

The marked change in waveform that occurs as the depth of the detector increases below the water surface is produced in the PP_1 arrival by the steady decrease in amplitude of the second rarefaction which diminishes to the point where it is virtually non-existent in record no. 7. In addition the amplitude of the onset of this arrival deminishes with depth. The same effect is apparent in the waveform following the PP_1* arrival, but in this case the change takes place at a shallower depth, for in record No. 3 the characteristic period of 55 μsecs. appearing in (1) and (2) is absent. Some explanation for this might be expected from consideration of interference between PP_1 and PP_1* and their counterparts reflected from the water surface with change of phase. The path differences between PP_1 and PP_1* and their respective surface reflected ways is given in Table I. Also listed in this table are the time intervals required for the wave to travel over the path difference, computed from the velocity 1530 metres/sec. found from subsequent time-distance measurements.

The period of both PP_1 and PP_1* in record no. 1 is 55 μsecs. so that the effects of dispersion are negligible and the wavelength of 8.4 cms. can be assumed constant. With the change of phase at the water surface destructive

TABLE I

Record No.	1	2	3	4	5	6	7	8	9	10	11
Depth of detector (cms.)	0	0.64	1.27	1.91	2.86	3.49	4.13	4.76	5.40	6.35	7.3
Path difference (PP_1) (cms.)	0	0.9	1.9	2.9	4.4	5.5	6.5	7.6	8.8	10.5	12.2
Path difference (PP_1*) (cms.)	0	1.2	2.2	3.5	5.3	6.5	7.7	8.9	10.2	12.1	13.9
Time interval (PP_1) (μsecs.)	0	6	12	19	29	36	43	50	57	68	80
Time interval (PP_1*) (μsecs.)	0	8	14	23	35	42	50	58	66	79	91

interference will occur, by reference to Table I at depths between records numbers 8 and 9 for PP_1 and 7 and 8 for PP_1*. The arrival of the counterparts of PP_1 and PP_1* are not clearly distinct on these records and in the case of pp_1* it is seen that interference cannot account for the modification of the waveform between records 1 and 3. In records 10 and 11 the path difference is in the vicinity of λ/2 for both arrivals and their reflections from the water surface so that the constructive interference would produce results similar to that for a path difference of λ/2, i.e. records nos. 4 and 5, but there is no similarity in the waveforms of these records.

The PP_1 and PP_1* waves reflected from the water surface approach the detector at an angle sufficiently obtuse that their path to the sensitive face is blocked by the body of the detector. Thus, the indication of their arrival can only be secondary and most probably considerably weakened. A more plausible explanation lies in the relative importance of the direct and reflected waves. At the surface the PP_1 and PP_1* arrivals have the greatest energy whilst at depth the P wave is predominant and the superposition of these arrivals at intermediate depths where they have equal pressure amplitude could conceivably lead to the wave forms observed.

HORIZONTAL PROFILES

The experimental arrangement corresponding to each of the profiles figs. 9, 10, 11, 12, 13, is shown in Fig. 14. Against each record of the profiles is indicated the source-detector distance, the amplifier gain and the number. These records are arranged vertically to a scale corresponding to the horizontal distance between the source and the detector.

The profile of Fig. 9 was made with 12.7 cms. of water in the tank. The arrivals marked are the direct wave (P),, the reflected wave PP_1, the double reflected wave PP_1*, the air wave (A) and the refracted wave P_2 from the

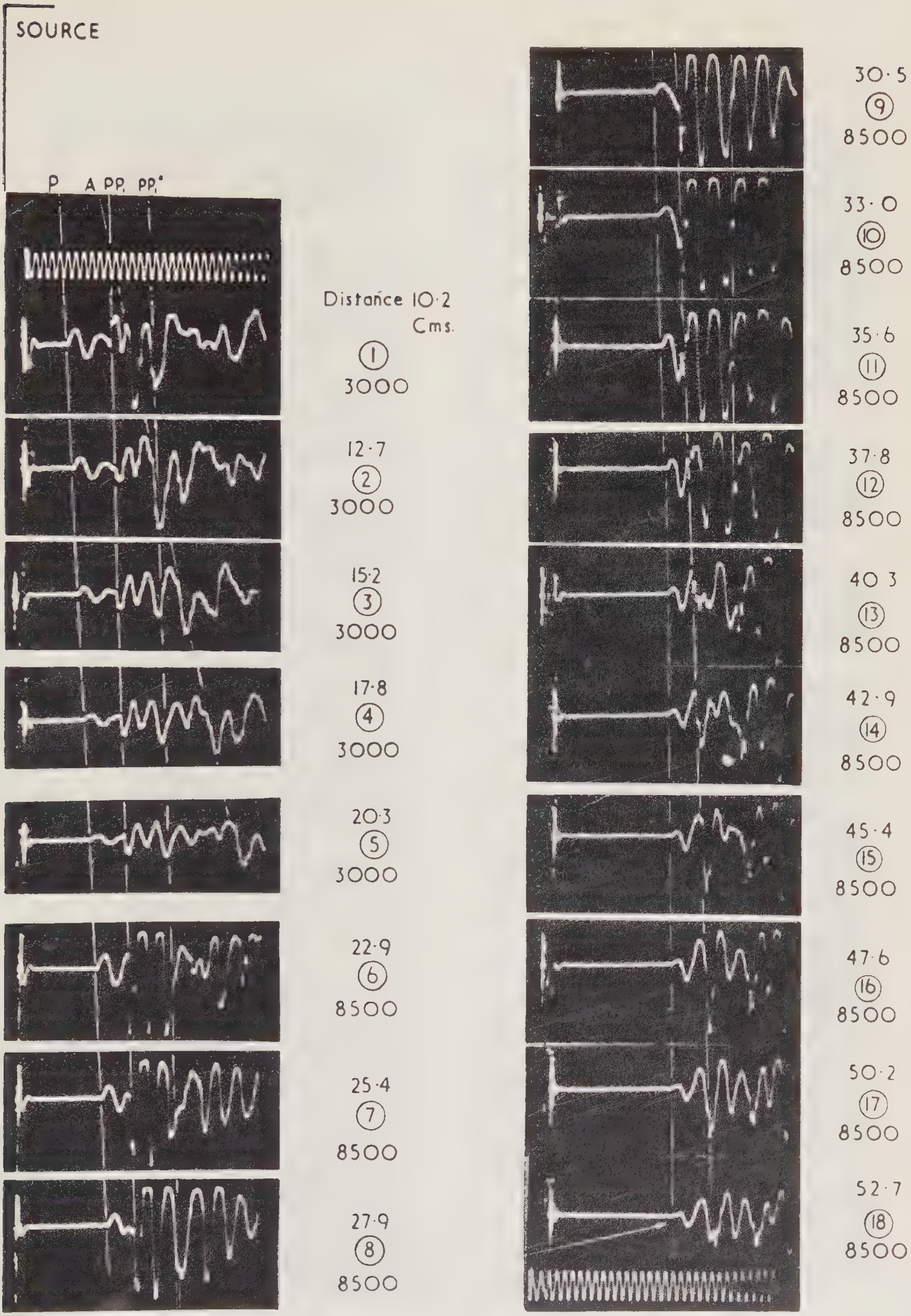
SOURCE
P
A
PP1
PP1'
Distance 10·2 Cms.
①
3000
12·7
②
3000
15·2
③
3000
17·8
④
3000
20·3
⑤
3000
22·9
⑥
8500
25·4
⑦
8500
27·9
⑧
8500
30·5
⑨
8500
33·0
⑩
8500
35·6
⑪
8500
37·8
⑫
8500
40·3
⑬
8500
42·9
⑭
8500
45·4
⑮
8500
47·6
⑯
8500
50·2
⑰
8500
52·7
⑱
8500

Fig. 9

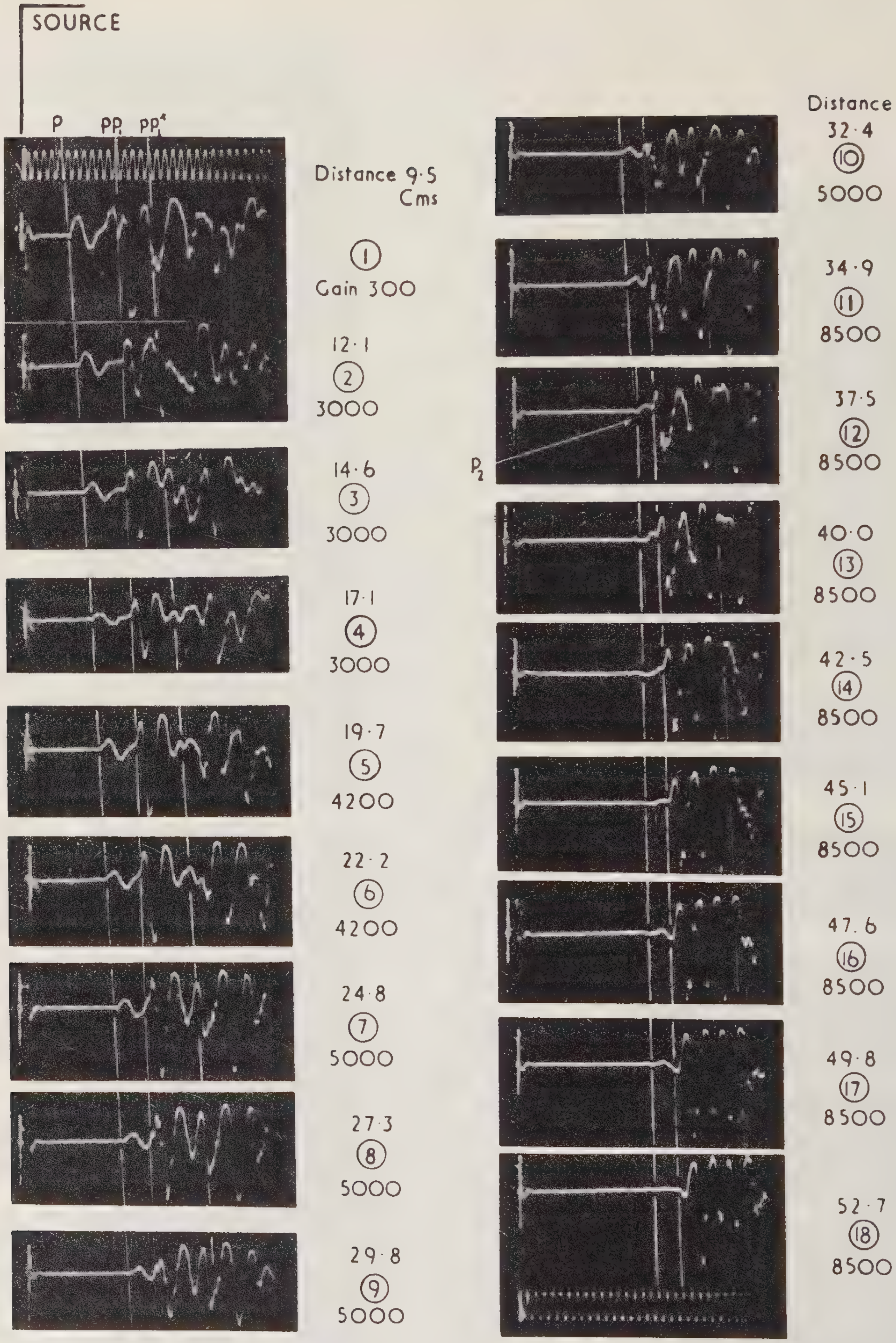
SOURCE
P
PP1
PP1'
Distance 9·5 Cms
① Gain 300
12·1 ② 3000
14·6 ③ 3000
17·1 ④ 3000
19·7 ⑤ 4200
22·2 ⑥ 4200
24·8 ⑦ 5000
27·3 ⑧ 5000
29·8 ⑨ 5000
Distance 32·4 ⑩ 5000
34·9 ⑪ 8500
37·5 ⑫ 8500
P2
40·0 ⑬ 8500
42·5 ⑭ 8500
45·1 ⑮ 8500
47.6 ⑯ 8500
49·8 ⑰ 8500
52·7 ⑱ 8500

Fig. 10

base of the tank appearing as the first arrival from record no. 12 onwards. Fig. 10 shows a similar profile across a slab of slate 48 cms. × 63.5 cms. × 3.8 cms. in 17.8 cms. of water. The records show the same arrivals as in Fig. 9 with the exception of the refracted wave from the slate which appears first in record no. 12 at a velocity of 4490 ± 170 metres p.s. The reflected wave in this case has an onset in the same direction as the direct P wave and differs also in being characterised by a single large rarefaction. In the first records of Figs. 9 and 10 the PP_1 onset is opposite in direction to those of the following records. In both these cases the angle of incidence of the PP_1 wave upon the bottom is close to the critical angle. In Fig. 9 the angle of incidence is 22° whilst the critical angle is 21.5° and in Fig. 5 the angle of incidence is 19° and the critical angle is 20°. The angle of incidence in both diagrams for record no. 2 is 26.5° and 23.5° for Figs. 9 and 10 respectively, which are larger than the respective critical angles.

Fig. 11 is the result of a traverse across the tank, with the same experimental arrangement as in Fig. 10 except that the detector is maintained at a depth of 8.6 cms. beneath the water surface. The P wave is characterised by a sharp negative (downward) onset which was observed in the depth profile, Fig. 7. As the source-detector distance increases this negative onset diminishes until, in record no. 11, it is superseded as first arrival by the refracted wave PP_2 from the slate with a velocity of 4090 ± 70 metres p.s.

A profile was also made, Fig. 12, with the slate supported at its corners 5.1 cms. above the floor of the tank in 14.9 cms. of water. In this case the refracted wave from the slate is the first arrival from record no. 5 onwards and at this point it is seen that the P wave is preceded by a high frequency wave which is most obvious in records nos. 8 and 9 and thereafter is practically undiscernable. The large rarefaction associated with PP_1 in Fig. 10 is absent in this profile and this arrival is instead here characterised by a number of short period rarefactions and compressions superposed upon the P wave train. The angle of approach of PP_1 to the detector is greater in this instance than in Fig. 10 so that its presence is not as noticeable.

With the model in the same position in the tank, the profile was repeated with the detector resting upon the slate slab, Fig. 13. The first arrival is the refracted wave in slate and it is again followed by a high frequency wave which appears first in record no. 4, reaches a maximum amplitude in record nos. 8 and 9 and becomes indistinct from record no. 13 onwards. Since in this profile and the preceeding one this effect occurs when the detector is traversing the centre of the slab it is possible that the slab is excited into a natural mode of vibration which, from the manner of its support, would lead to antinodal conditions at its centre. The relatively long period disturbance following PP_2 is identified as the Rayleigh wave (L.R.) of velocity 2340 ± 10 metres p.s. followed by the direct wave (P) of higher frequency.

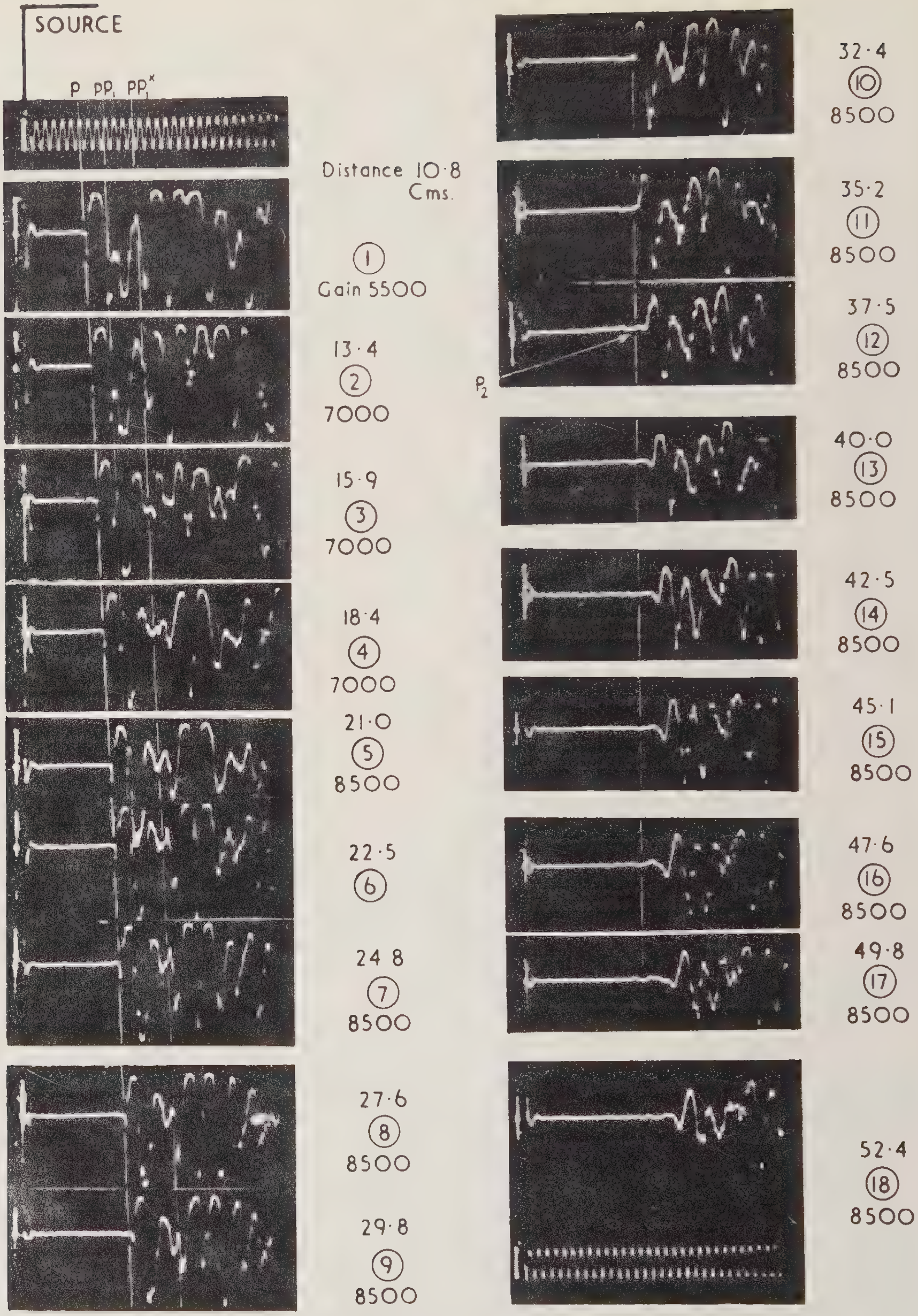
SOURCE
P PP₁ PP₁ˣ
Distance 10·8 Cms.
① Gain 5500
13·4 ② 7000
15·9 ③ 7000
18·4 ④ 7000
21·0 ⑤ 8500
22·5 ⑥
24 8 ⑦ 8500
27·6 ⑧ 8500
29·8 ⑨ 8500
32·4 ⑩ 8500
35·2 ⑪ 8500
37·5 ⑫ 8500
P₂
40·0 ⑬ 8500
42·5 ⑭ 8500
45·1 ⑮ 8500
47·6 ⑯ 8500
49·8 ⑰ 8500
52·4 ⑱ 8500

Fig. 11

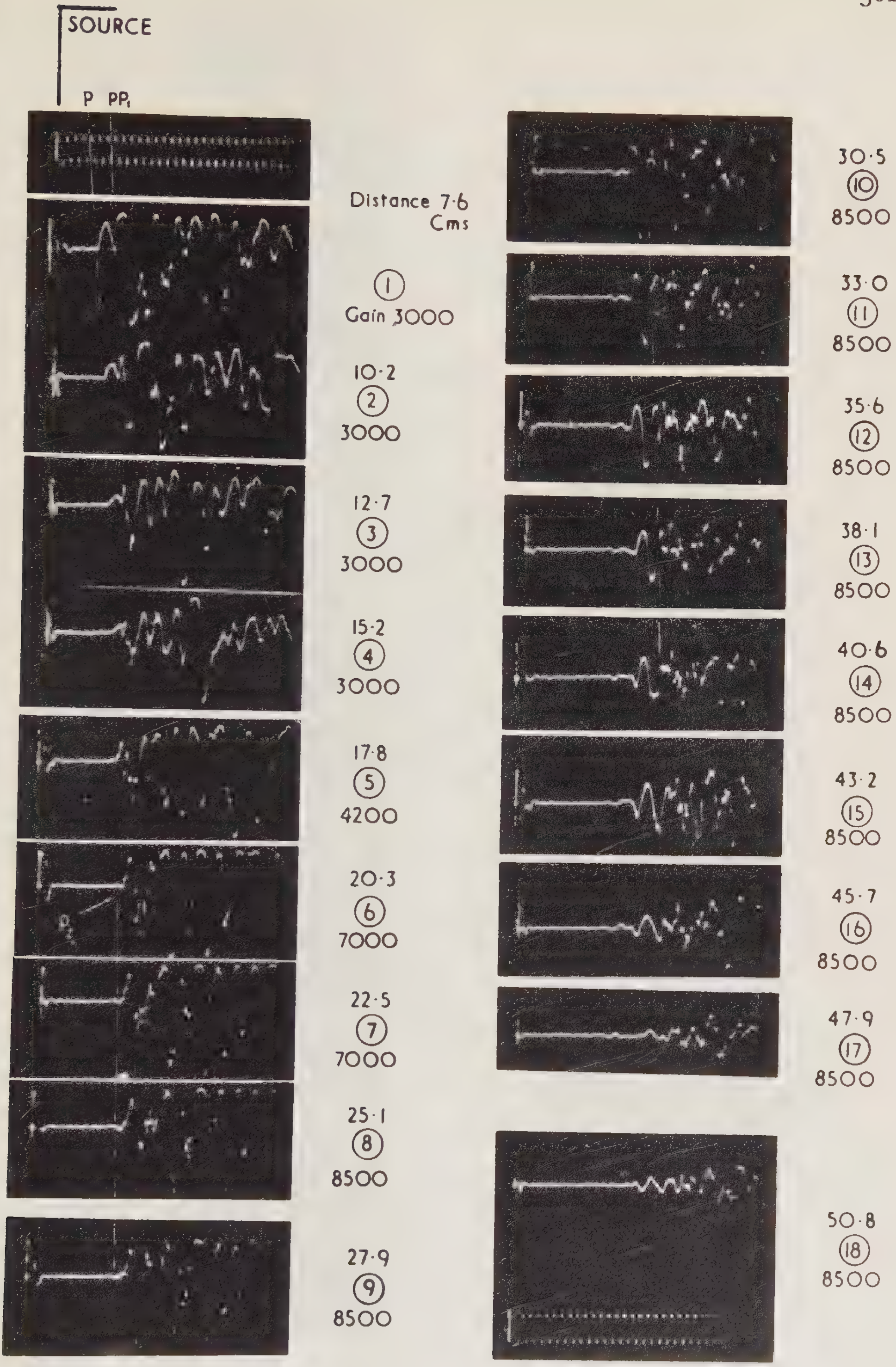
SOURCE
P PP₁
Distance 7·6 Cms
① Gain 3000
10·2 ② 3000
12·7 ③ 3000
15·2 ④ 3000
17·8 ⑤ 4200
P₂
20·3 ⑥ 7000
22·5 ⑦ 7000
25·1 ⑧ 8500
27·9 ⑨ 8500
30·5 ⑩ 8500
33·0 ⑪ 8500
35·6 ⑫ 8500
38·1 ⑬ 8500
40·6 ⑭ 8500
43·2 ⑮ 8500
45·7 ⑯ 8500
47·9 ⑰ 8500
50·8 ⑱ 8500

Fig. 12

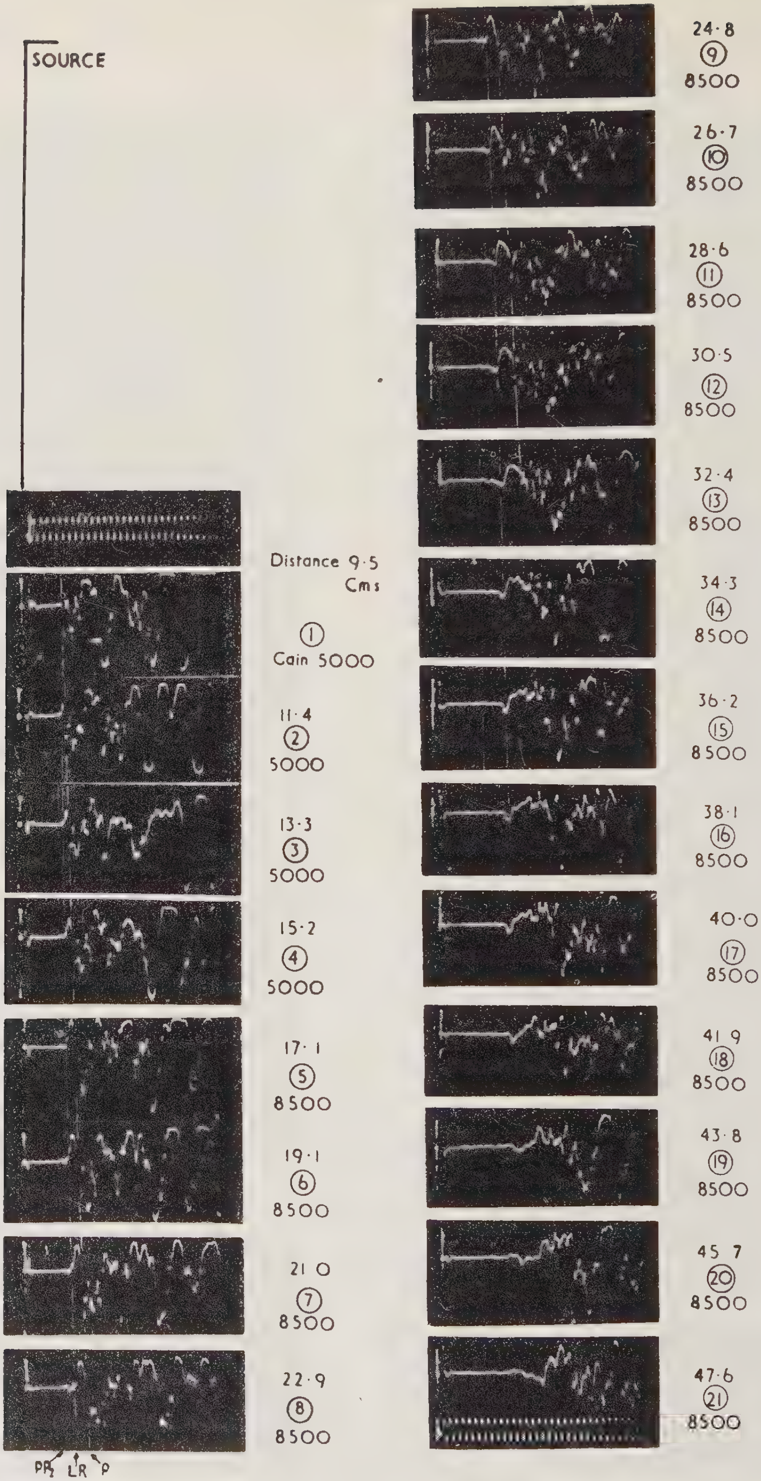
SOURCE
Distance 9·5 Cms
① Gain 5000
11·4 ② 5000
13·3 ③ 5000
15·2 ④ 5000
17·1 ⑤ 8500
19·1 ⑥ 8500
21 0 ⑦ 8500
22·9 ⑧ 8500
PR2 LR P
24·8 ⑨ 8500
26·7 ⑩ 8500
28·6 ⑪ 8500
30·5 ⑫ 8500
32·4 ⑬ 8500
34·3 ⑭ 8500
36·2 ⑮ 8500
38·1 ⑯ 8500
40·0 ⑰ 8500
41 9 ⑱ 8500
43·8 ⑲ 8500
45 7 ⑳ 8500
47·6 ㉑ 8500

Fig. 13

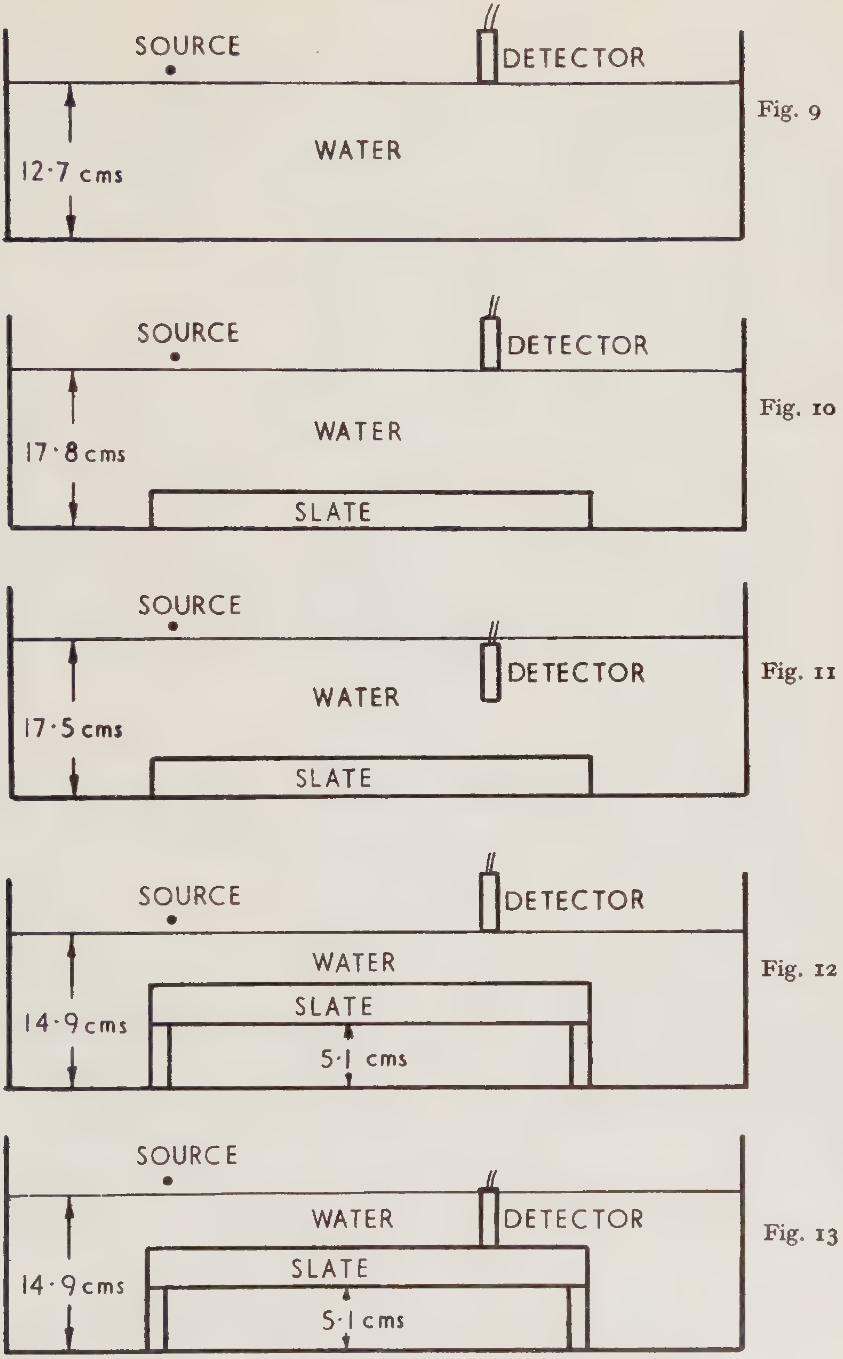

Fig. 14. Experimental arrangement for the profiles of Figs. 9, 10, 11, 12 and 13

CONCLUSIONS

The reduction of energy in the direct wave at the surface as found in the depth profile, together with the small pressure amplitude of the refracted wave in the horizontal traverses, enables comparisons to be made concerning the reflections. By replacing the reflecting surface of the tank bottom by a slab of slate, the waveform of the reflection on comparing Figs. 9 and 10 is altered to the extent that the number of rarefactions and compressions following the onset of PP_1 are not the same for equivalent source-detector distances. This is particularly noticeable on comparing PP_1 records nos. 4-8 in both Figs. 9 and 10. The single large rarefaction in PP_1, Fig. 10, in these records is replaced by a sinusoidal waveform in records nos. 14-18, whilst in Fig. 9, PP_1 is represented by a single large rarefaction. Thus, over the interval between these corresponding detector positions the situation is reversed. In Fig. 11 where the detector is immersed 8.6 cms. below the water surface the single rarefaction is again present in PP_1 but PP_1* develops a sinusoidal waveform as in Fig. 9 (records nos. 8 and 9), but is characterised by a single large rarefaction at shorter source-detector distances, records nos. 4-6. The high frequency wave superimposed on the PP_1 arrival in many of these records bears a resemblance to the water wave encountered in seismic investigations at sea, but there is no parallel occurrence in the direct wave in these records except in Fig. 13 where the detector is in contact with the slate.

ACKNOWLEDGEMENTS

Appreciation is expressed for the financial assistance given by British Petroleum for this work and to Professor Bruckshaw of Imperial College for his valuable guidance.

REFERENCES

HOWES E. T., TEJADA-FLORES L. H., RANDOLPH J., 1953, "Seismic Model Study", J. ACOUST. SOC. AMER. 25, 915-921.

KAUFMAN S., ROEVER W. L., 1951, "Laboratory Studies of Transient Elastic Waves", Proc. Third World Petroleum Congress, Section 1, 537-545, The Hague.

OLIVER J., PRESS F., EWING M., 1954, "Two-dimensional Model Seismology", Geophysics, 19, 202-219.

WOOD A. B., 1946, "A Textbook of Sound", G. Bell & Sons.

THEORETISCHE FRAGEN ÜBER BÜNDELUNG VON GEOPHONEN BEI UNTERTAGE-MESSUNGEN *)

VON

AIVARS CELMIŅŠ **)

ABSTRACT

The arrays of multiple geophones used in underground seismic prospecting must satisfy two conditions:

1) In each group only a few geophones can be used.

2) The array must work in a rather wide frequency band.

In the present paper the effect of the 3 parameters (geophone spacing, sensitivity and time shift) of a linear array is investigated in order to improve the directional sensitivity of the array.

Necessary conditions which are independent of the frequencies are found for the optimum sensitivities of the geophones in a linear array.

The optimum values of the parameters mentioned above are calculated for arrays of 2 and 3 geophones and for a frequency band width which may be used in underground seismic prospecting.

§ 1. EINLEITUNG

Bündelungen von Geophonen und Mehrfachschüsse sind in der angewandten Seismik schon lange bekannt und werden bei Messungen übertage mit Erfolg benutzt. Durch die Bündelung oder Mischung von Geophonen erreicht man zweierlei:

1) Durch Benutzung einer grösseren Anzahl von Geophonen auf jeder Spur werden aus statistischen Gründen zufällige Störungen im Seismogramm unterdrückt.

2) Die seismischen Wellen erreichen die einzelnen Geophone zu verschiedenen Zeiten. Durch Überlagerung der von den einzelnen Geophonen empfangenen Impulse kann die Amplitude des aufgezeichneten Impulses je nach den Zeitdifferenzen vergrössert oder verkleinert werden. Da die Zeitdifferenzen von der Einfallsrichtung der seismischen Welle abhängen, stellen die gebündelten Geophone eine Empfangsanordnung dar, deren Empfangseigenschaften von der Einfallsrichtung abhängen.

Im Hinblick auf die Bündelung von Geophonen sind die Untertage-Messungen durch zwei Eigenschaften charakterisiert. Auf der einen Seite hat man es mit dem Empfang in einem grossen Frequenzbereich (ca. 3 Oktaven) und hohen Frequenzen zu tun. Auf der anderen Seite ist die Anzahl der Geophone und die Möglichkeiten sie anzuordnen aus Platzgründen beschränkt.

---

*) Presented at the 10th Meeting of the European Association of Exploration Geophysicists, held in Hamburg, May 16/18, 1956.

**) Seismos G.m.b.H., Hannover.

Im folgenden wird gezeigt, dass trotz dieser erschwerenden Bedingungen die Bündelung von Geophonen bei Untertage-Messungen insofern erfolgversprechend ist, als Anordnungen hergestellt werden können, deren Empfindlichkeit merklich von der Einfallsrichtung der Welle abhängt. Eine nennenswerte Unterdrückung von zufälligen Störungen wird man dagegen bei Benutzung von nur wenig Geophonen nicht erwarten.

Die Geophone werden untertage im allgemeinen in einer Strecke angebracht. Dementsprechend werden hier nur Anordnungen von Geophonen auf einer Geraden betrachtet. Die Abstände zwischen den einzelnen Geophonen sollen untereinander gleich sein. Wie man sich leicht überlegen kann, bedeutet diese Bedingung keine wesentliche Einschränkung der Allgemeinheit. Ferner wird angenommen, dass die einzelnen Geophone beim Empfang der Wellen keine Richtung bevorzugen. Diese Voraussetzung entspricht nicht den Tatsachen. Man muss sie dennoch machen, wenn die Ergebnisse der Untersuchung unabhängig von der Art der zu empfangenden Welle sein sollen, denn die Richtcharakteristik der einzelnen Geophone hängt davon ab, ob Longitudinal- oder Transversalwellen empfangen werden. Wie man diese Richtcharakteristiken im einzelnen berücksichtigen kann, wird im § 3 angedeutet. Die Richtcharakteristik einer Anordnung der angeführten Art ist rotationssymmetrisch. Die Symmetrieachse ist die Gerade, auf der die Geophone angeordnet sind. Die Anordnung hat neben der Anzahl der Geophone 3 freie Parameter: Den Abstand zwischen den Geophonen, die Verstärkung der einzelnen Geophone und eine Zeitverschiebung von Geophon zu Geophon.

Die Ergebnisse der Untersuchung lassen sich sinngemäss auch auf Mehrfachschüsse übertragen. Nur muss in diesem Fall von den Verstärkungen vorausgesetzt werden, dass sie reell (keine Phasenverschiebung) und positiv sind.

§ 2. MATHEMATISCHE FORMULIERUNGEN UND DEFINITIONEN

Die ankommende (oder ausgestrahlte) Welle sei durch die Zeitfunktion $\Phi(t)$ gegeben. Die Funktion $\Phi(t)$ möge die Geschwindigkeit der Massenteilchen (die „Schnelle") bedeuten, doch lassen sich die Betrachtungen auch auf alle anderen Wellengrössen übertragen.

Die Zeitfunktion sei in ein Fourier-Integral entwickelt:

$$\Phi(t) = \int_{-\infty}^{\infty} A(f)\, e^{2\pi i f t}\, df. \tag{2.1}$$

Der durch die Zeitfunktion $\Phi(t)$ gegebene Wellenzug möge auf eine Empfangsanordnung fallen. Die Empfangsanordnung wird i. a. eine von der Einfallsrichtung abhängige Grösse anzeigen. Die Einfallsrichtung sei durch zwei Winkel φ und ϑ gegeben. Nach den Ausführungen in § 1. kann man annehmen, dass die angezeigte Grösse aus Symmetriegründen nicht von φ abhängt. Man kann dann diese Grösse $\Phi(t,\vartheta)$ auf folgende Weise in der Form eines Fourier-Integrals schreiben:

$$\Psi(t,\vartheta) = \int_{-\infty}^{\infty} A(f)\, R(f,\vartheta)\, e^{2\pi i f t}\, df. \tag{2.2}$$

Die Grösse $R(f, \vartheta)$ in (2.2), die die Vergrösserung einer aus der Richtung ϑ einfallenden harmonischen Welle von der Frequenz f angibt, nennt man den Richtfaktor. $|R|$ als Funktion des Einfallswinkels ϑ dargestellt nennt man die Richtcharakteristik der Empfangsanordnung bezüglich der Frequenz f.

Handelt es sich um den Empfang in einem grösseren Frequenzbereich, so eignet sich der durch (2.2) definierte Richtfaktor $R(f, \vartheta)$ wegen seiner Frequenzabhängigkeit nicht zur Charakterisierung der Empfangsanordnung. Man benutzt dann statt dessen die Grösse

$$E(\vartheta) = \frac{\int_{-\infty} \Psi^2(t,\vartheta)dt}{\int_{-\infty}^{\infty} \Phi^2(t,\vartheta)dt} \tag{2.3}$$

Sie gibt die Vergrösserung der aus der Richtung ϑ empfangenen Energie des Wellenzuges gegenüber der aus der Richtung ϑ einfallenden Energie an. Für harmonische Wellen geht $E(\vartheta)$ in $R^2(f, \vartheta)$ über. Die Grösse $E(\vartheta)$ sei hier die Empfindlichkeit der Anordnung genannt. Statt der Empfindlichkeit $E(\vartheta)$ benutzt man meist $\sqrt{E(\vartheta)}$ 1) und bezeichnet diese Grösse als Richtcharakteristik der Anordnung.

Nach der Parsevalschen Gleichung 2) ist

$$\int_{-\infty}^{\infty} \Phi^2(t)\, dt = \int_{-\infty}^{\infty} |A(f)|^2\, df \tag{2.4}$$

Beschränkt man sich auf gerade Funktionen $\Phi(t)$, so ist $A(f)$ gerade und reell und man erhält durch Anwendung der Parsevalschen Gleichung auch auf $\Psi(t, \vartheta)$ aus (2.3)

---

1) Stenzel 1939, S. 27.
2) Schmeidler 1950, S. 74.

$$E(\vartheta) = \frac{\int\limits_{-\infty}^{\infty} A^2(f)\,|R(f,\vartheta)|^2\,df}{\int\limits_{-\infty}^{\infty} A^2(f)\,df} \qquad (25.)$$

Die Richtcharakteristik $\sqrt{E(\vartheta)}$ ist also eine Art gewogenes Mittel des Richtfaktors $R(f, \vartheta)$. Sie hängt ausser von der Empfansanordnung auch noch von dem einfallenden Wellenzug, bzw. von dem Spektrum $A(f)$ des einfallenden Wellenzuges ab. Setzt man für $A(f)$ die Filtercharakteristik der Empfangsanordnung ein, so gibt $\sqrt{E(\vartheta)}$ ein gutes Bild von den Empfangseigenschaften der Anordnung.

Sucht man eine möglichst stark gerichtete Anordnung, so wird man von der Empfindlichkeit verlangen, dass ihr Maximum einerseits möglichst scharf und andrerseits gross gegen die gegebenenfalls auftretenden Nebenmaxima ist. Ein Mass für die mehr oder weniger gute Erfüllung dieser Bedingungen ist die Richtwirkung G. Sie ist definiert als das Verhältnis der maximalen Empfindlichkeit zu der mittleren Empfindlichkeit, wobei über die Einheitskugel gemittelt wird [1].

$$G = \frac{4\pi\, E_{\max}}{\int\int E\,d\Omega} = \frac{2\, E_{\max}}{\int\limits_{-\frac{\pi}{2}}^{\frac{\pi}{2}} E(\vartheta)\cos\vartheta\, d\vartheta} \qquad (2.6)$$

Man gibt $20 \lg_{10} \sqrt{G}$ in db an. Im Falle einer optimalen Richtwirkung nimmt G ein Maximum an.

§ 3. RICHTCHARAKTERISTIK EINER LINEAREN EMPFÄNGERANORDNUNG

Unter einer linearen Empfängeranordnung wird eine Anordnung von Empfängern (Geophonen) auf einer Geraden verstanden. Die einzelnen Empfänger können verschiedene Empfindlichkeiten haben und die Abstände zwischen den Empfängern brauchen nicht gleich zu sein. Bei einer allgemeinen linearen Empfängeranordnung können einzelne Empfänger auch noch über ein Zeitverzögerungsglied angeschlossen sein.

In diesem Paragraphen wird eine spezielle lineare Anordnung behandelt: Die Aufstellung sei äquidistant, der Abstand zwischen den einzelnen Geophonen sei d. Der ν-te Empfänger möge die Verstärkung c_ν bewirken. Die zu empfangende Welle falle aus der Richtung ϑ ein und habe die Geschwindigkeit v.

---

[1] Stenzel 1939, S. 38; Schelkunoff 1943, S. 104.

Die Zusammensetzung der $n + 1$ empfangenen und mit c_ν verstärkten Wellen ergibt die Empfangsfunktion

$$\Psi(t, \vartheta) = \sum_{\nu=0}^{n} c_\nu \, \Phi(t - \nu \frac{d}{v} \sin \vartheta) \tag{3.1}$$

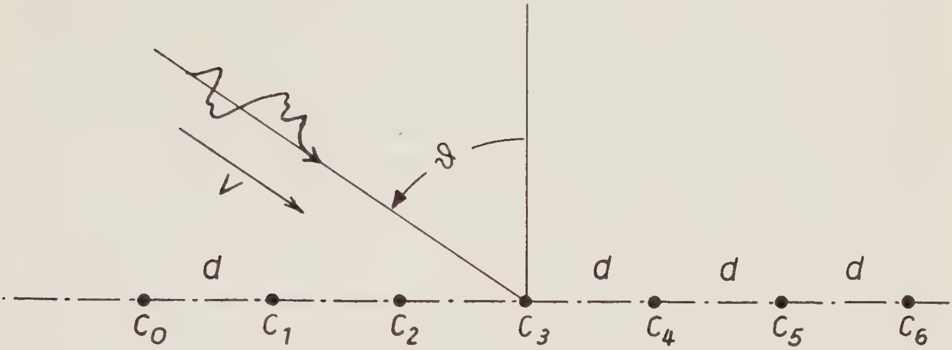

Fig. 1. Linear array of geophones

Nach (2.1) kann man hierfür auch schreiben

$$\Psi(t, \vartheta) = \int_{-\infty}^{\infty} A(f) \, e^{2\pi i f t} \left\{ \sum_{\nu=0}^{n} c_\nu e^{-2\pi i \nu d (f/v) \sin \vartheta} \right\} dl. \tag{3.2}$$

Falls die einzelnen Empfänger noch einen Richtfaktor $F_\nu(\vartheta, \varphi)$ haben, so ist das ν-te Glied der Summe mit F_ν zu multiplizieren. Meistens wird man annehmen können, dass die Richtungen der Geophonachsen gleich sind, so dass alle $F_\nu \equiv F$. Diesen gemeinsamen Faktor F kann man dann vor das Integralzeichen ziehen. — Hier wird angenommen, dass eine Richtempfindlichkeit der Geophone nicht vorliegt. Ein Vergleich von (3.2) mit (2.2) zeigt, dass der Richtfaktor der hier betrachteten linearen Anordnung durch die Summe

$$R(f, \vartheta) = \sum_{\nu=0}^{n} c_\nu e^{-2\pi i \nu d (f/v) \sin \vartheta} \tag{3.3}$$

gegeben ist. Es gilt offenbar

$$R(f, \vartheta) = \overline{R(-f, \vartheta)} \text{ also } |R(f, \vartheta)| = |R(-f, \vartheta)|$$

Man kann also beim Anschreiben des Ausdruckes (2.5) für die Empfindlichkeit $E(\vartheta)$ sich auf Integration von 0 bis ∞ beschränken:

$$E(\vartheta) = \frac{\int\limits_0^\infty A^2(f) \left| \sum\limits_{\nu=0}^{n} c_\nu \, e^{-2\pi i \nu d (f/v) \sin\vartheta} \right|^2 df}{\int\limits_0^\infty A^2(f)\, df} \tag{3.4}$$

Nach dieser Formel lässt sich die Empfindlichkeit einer linearen Empfängeranordnung berechnen, wenn das Spektrum $A(f)$ der zu empfangenden Welle bekannt ist. Nach den Ausführungen im § 2 wird man jedoch zur Charakterisierung der Empfängeranordnung für $A(f)$ die Filtercharakteristik der seismischen Apparatur einsetzen.

Führt man die Bezeichnung

$$z = e^{-2\pi i d (f/v) \sin\vartheta} \tag{3.5}$$

ein, so lautet der Richtfaktor nach (3.3)

$$R(f, \vartheta) = \sum_{\nu=0}^{n} c_\nu z^\nu = P(z) \tag{3.6}$$

$R(f, \vartheta)$ ist also ein Polynom n-ten Grades in z. Die Grösse z hat die Form e^{ia}, also ist der Betrag von z gleich 1. Das Argument von z hängt von der Einfalls-

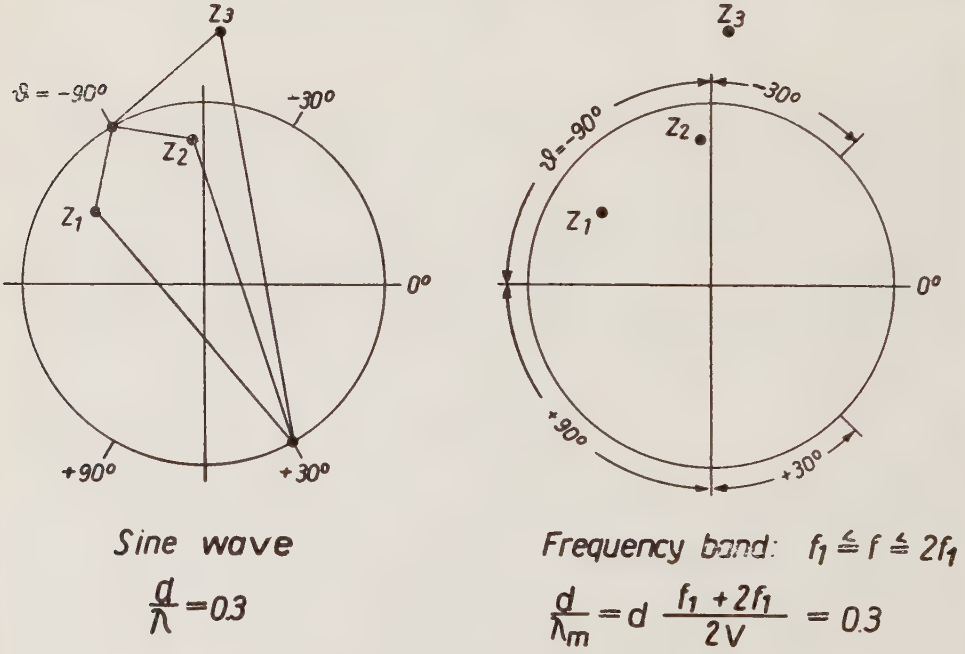

Fig. 2. The zeros z_μ of the polynomials $P(z)$

richtung ϑ der Welle und von dem Abstand d zwischen den Geophonen ab. Bei festem Abstand d bewegt man sich in der komplexen z-Ebene auf dem Einheitskreis, wenn der Einfallswinkel verändert wird. — Der Betrag des Polynoms $P(z)$ ist gleich dem Produkt der Abstände von den Nullstellen des Polynoms. Hat man z.B. eine Anordnung von 4 Geophonen, so ist das zugehörige Polynom nach (3.6) vom dritten Grade. In der Figur 2 sind in einem Beispiel die Lagen der drei Nullstellen eingezeichnet.

Wird eine harmonische Welle empfangen, so erhält man bei einem Abstand $d = 0{,}3\ v/f$ die in der Abbildung angegebene Zuordnung von Einfallswinkeln und Punkten auf dem Einheitskreis der z-Ebene. In diesem Fall würde man für $\vartheta = -90°$ einen wesentlich schlechteren Empfang haben. als für $\vartheta = +30°$. — Handelt es sich um den Empfang in einem Frequenzbereich zwischen den Frequenzen f_1 und f_2, so hat man jedem Einfallswinkel einen Abschnitt des Einheitskreises zuzuordnen. Aus dem zweiten in der Figur 2 gezeigten Beispiel sieht man, dass auch in diesem Fall eine merkliche Abhängigkeit des Richtfaktors von dem Einfallswinkel erreicht werden kann.

Die Abhängigkeit wird offensichtlich dann am stärksten, wenn die Nullstellen von $P(z)$ auf dem Einheitskreis liegen. Diese Forderung liefert notwendige Bedingungen für die Verstärkungen c_ν die nach (3.6) die Koeffizienten des Polynoms $P(z)$ sind. Man erhält sie auf folgende Weise: Setzt man Verstärkungen voraus, die keine Phasenverschiebung hervorrufen, so sind die c_ν reell. Dann gibt es zu jeder komplexen Nullstelle z_μ eine konjugierte komplexe Wurzel $\bar{z}_\mu$. Weil $|z_\mu| = 1$ sein soll, folgt daraus, dass mit z_μ auch $1/z_\mu = \bar{z}_\mu$ eine Wurzel von $P(z) = 0$ ist. Durch Übergang von z auf $1/z$ muss also die Gleichung $P(z) = 0$ in sich selbst übergehen. Daraus folgt, dass

$$|c_\nu| = |c_{n-\nu}|$$

sein muss.

> Die Verstärkungen von Geophonen, die gleich weit von der Mitte der Aufstellung stehen, müssen also dem Betrage nach gleich sein.

Eine zweite notwendige Bedingung für die c_ν folgt aus den Vieta'schen Wurzelsätzen. Danach sind die c_ν symmetrische homogene Funktionen der z_μ:

$$\begin{aligned} c_0 &= (-1)^n\, z_1 \cdot z_2 \cdots z_{n-1}\, z_n \\ c_1 &= (-1)^{n-1} \{ z_1 z_2 \cdots z_{n-1} + z_1 z_2 \cdots z_{n-2} z_n + \cdots \\ &\qquad \cdots + z_1 z_3 \cdots z_n + z_2 z_3 \cdots z_n \} \\ &\text{u. s. w.} \end{aligned}$$

Falls sämtliche $z_\mu = -1$ sind, so sind alle in den Ausdrücken für c_ν auftretenden Produkte reell, positiv und vom Betrage 1. Die c_ν sind in diesem Fall die Binomialkoeffizienten $\binom{n}{\nu}$. Für andere z_μ auf dem Einheitskreis sind die Beträge der Produkte zwar auch gleich 1, sie sind aber nicht mehr reell. Die Summe c_ν, die bei reellen Produkten ($z_\mu = \pm 1$) die Binomialkoeffizienten ergaben, können bei komplexen Produkten höchstens kleiner werden. — Die zweite notwendige Bedingung für die Verstärkungen c_ν lautet also:

> Die Verstärkungen c_ν bei einer Anordnung von $n + 1$ Geophonen müssen dem Betrage nach kleiner als die Binomialkoeffizienten $\binom{n}{\nu}$ sein. (In dieser Darstellung sind die beiden äussersten Verstärkungen zu 1 normiert: $c_0 = |c_n| = 1$).

Hinreichende Bedingungen für die c_ν lassen sich nur unter einschränkenden Annahmen über das zu empfangende Spektrum angeben.

Ein anschauliches Bild von den Eigenschaften der Empfängeranordnung erhält man, wenn man $|R(f, \vartheta)|$ als Relief in der $(\sin \vartheta, df/v)$—Ebene aufträgt. Die Figur 3 zeigt als Beispiel den Relief einer Empfängeranordnung von 4 Geophonen.

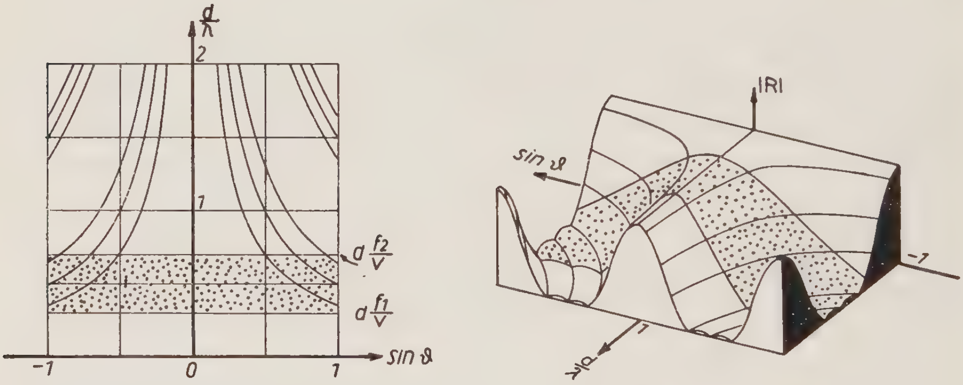

The zeros of |R|

The relief of |R|

Fig. 3. The function $|R(f, \vartheta)|$ for the array (1; 2.2; 2.2; 1)

Will man in einem beschränkten Frequenzbereich (f_1, f_2) aus der Richtung $\vartheta = \pm 90°$ möglichst wenig empfangen, so wird man d so wählen, dass der interessierende Bereich etwa in die eingezeichnete Lage in der $(\sin \vartheta, df/v)$—Ebene zu liegen kommt. — In den folgenden Paragraphen wird untersucht, wie man dem Relief eine möglichst vorteilhafte Gestalt verleiht und welchen Abstand d man zweckmässigerweise zu wählen hat.

§ 4. ZWEIFACHBÜNDELUNG

Der einfachste Fall einer linearen Empfängeranordnung ist die Zweifachbündelung, d.h. die Anordnung von zwei Geophonen im Abstand d von einander. Nach § 3 müssen die Verstärkungen der beiden Geophone den gleichen Betrag haben. Je nachdem, ob die Geophone gleichgepolt sind oder nicht, erhält man in der ($\sin \vartheta$, df/v)-Ebene eine der beiden Nullstellenverteilungen des Richtfaktors $R(f, \vartheta)$, die in der Figur 4 gezeigt werden.

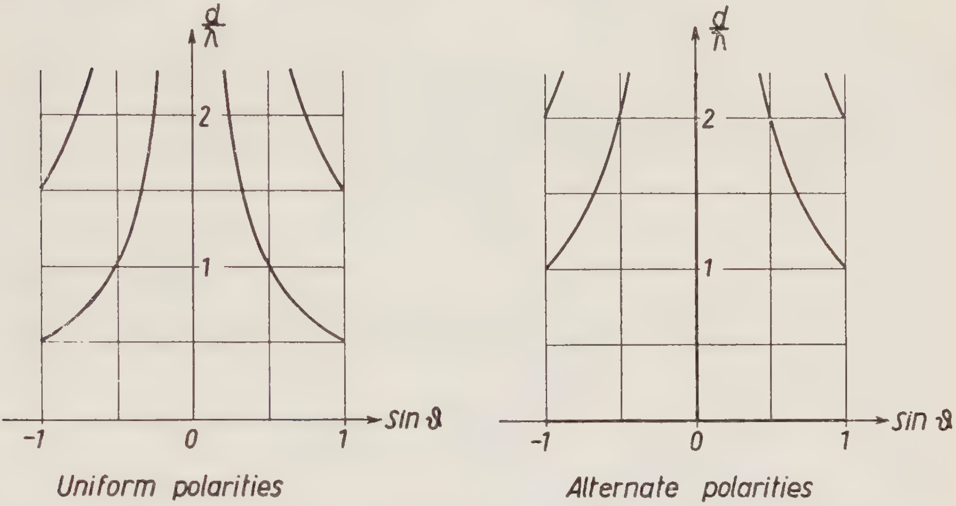

Fig. 4. The zeros of the function $R(f, \vartheta)$ for two geophone arrays

Man hat also in diesem Fall zur Erreichung einer möglichst günstigen Richtcharakteristik nur den Abstand d in der Hand.

Nach (3.3) ist

$$|R(f, \vartheta)| = |1 \pm z| = \\ = |e^{\pi i d (f/v) \sin \vartheta} \pm e^{-\pi i d (f/v) \sin \vartheta}| \tag{4.1}$$

also

$$|R(f, \vartheta)| = 2 \, |\cos \{\pi d (f/v) \sin \vartheta\}| \tag{4.2}$$

bei gleichgepolten Geophonen und

$$|R(f, \vartheta)| = 2 \, |\sin \{\pi d (f/v) \sin \vartheta\}| \tag{4.3}$$

bei umgepolten Geophonen.

Es sei hier zunächst der Fall mit gleichgepolten Geophonen behandelt. Die Empfindlichkeit lautet in diesem Fall nach (2.5) oder (3.4)

$$E(\vartheta) = \frac{4 \int_0^\infty A^2(f) \cos^2 \{\pi d (f/v) \sin \vartheta\} \, df}{\int_0^\infty A^2(f) \, df} \tag{4.4}$$

Um nun weiter rechnen zu können, müssen Annahmen über die Filtercharakteristik $A(f)$ gemacht werden. Es sei hier und im folgenden stets angenommen, dass die Filtercharakteristik durch die einfache Funktion

$$A(f) = \begin{cases} B = \text{const. für } f_1 \leqq f \leqq f_2. \\ 0 \text{ sonst} \end{cases} \tag{4.5}$$

genau genug angenähert werden kann. Berechnungen mit anderen Filtercharakteristiken haben gezeigt, dass selbst bei stärkeren Abweichungen der Filtercharakteristik von dieser einfachen Form der Wert des optimalen Abstandes d sich nur unwesentlich ändert. Mit den Abkürzungen

$$x = 2\ \pi f_1 d/v = 2\ \pi\, d/\lambda_1 \tag{4.6}$$

und

$$w = f_2/f_1 \tag{4.7}$$

(λ = Wellenlänge) erhält man mit einem $A(f)$ nach (4.5) für die Empfindlichkeit den Ausdruck

$$E(\vartheta) = 2 \left\{ 1 + \frac{\sin(w\,x \sin\vartheta) - \sin(x \sin\vartheta)}{(w\text{-}1)\,x \sin\vartheta} \right\} \tag{4.8}$$

Für die Richtwirkung erhält man nach (4.8) und 2.6)

$$G = \frac{E_{max}}{2\{1 + [Si\ (wx) - Si\ (x)]/[(w\text{-}1)\,x]\}} \tag{4.9}$$

Dabei bedeutet

$$Si(x) = \int_0^x \frac{\sin \xi}{\xi}\, d\,\xi \tag{4.10}$$

E_{max} ist im vorliegenden Fall unabhängig von $A(f)$: Nach (4.4) ist $E_{max} = E(0) = 4$.

Um den Geophonabstand d zu finden, für den die Empfängeranordnung für aus der Richtung $\vartheta = 90°$ einfallende Wellen am unempfindlichsten ist, wird der Ausdruck (4.8) für die Empfindlichkeit $E(90°)$ nach d abgeleitet und die Ableitung gleich Null gesetzt. Man erhält auf diese Weise die Gleichung

$$wx \cos wx - \sin wx - (x \cos x - \sin x) = 0 \tag{4.11}$$

Als Lösung dieser Gleichung erhält man Kurven $x(w)$, d.h. d/λ_1, als Funktion von w. Zweckmässiger ist es, nicht d/λ_1, sondern $d/\lambda_m = d(f_1 + f_2)/(2v)$ als Funktion des Verhältnisses $w = f_2/f_1$ darzustellen, denn es zeigt sich, dass diese Grösse für weite w-Bereiche praktisch konstant ist.

Den Abstand d für den die Anordnung die grösste Richtwirkung hat, erhält man als Lösung einer anderen Gleichung. Sie gewinnt man durch Differenzieren der Formel (4.9) und Nullsetzen der Ableitung. Sie lautet

$$\sin wx - Si(wx) - (\sin x - Si(x)) = 0 \tag{4.12}$$

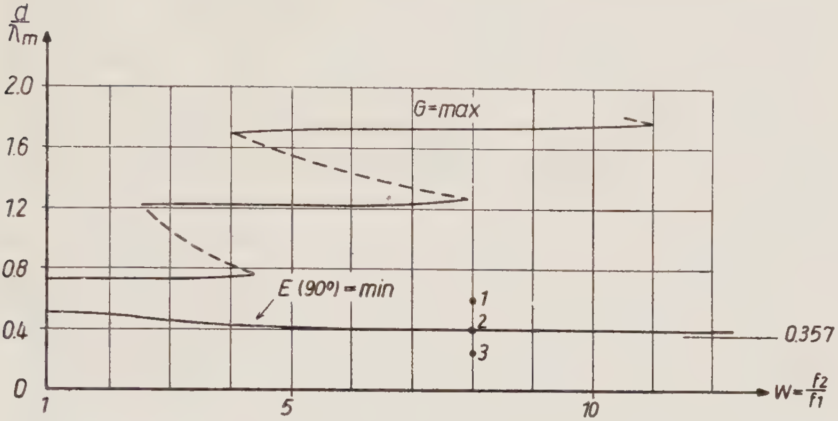

The optimum geophone spacing

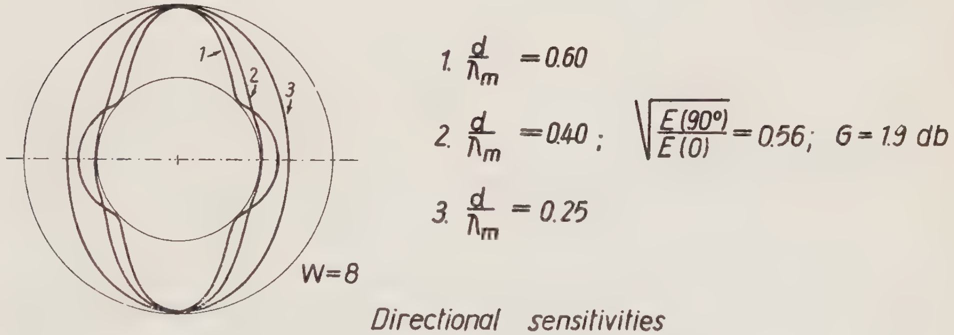
1
2
3
W=8
1. $\frac{d}{\lambda_m}=0.60$
2. $\frac{d}{\lambda_m}=0.40$; $\sqrt{\frac{E(90°)}{E(0)}}=0.56$; G = 1.9 db
3. $\frac{d}{\lambda_m}=0.25$

Directional sensitivities

Fig. 5. Array of two uniform polarized geophones

Die Lösungen von (4.11) und (4.12) sind in der Figur 5 dargestellt. — In der Untertageseismik kommen für das Verhältnis w Werte zwischen 6 und 10 in Frage. Man sieht aus der Abbildung 5, dass in diesem Bereich die optimalen Werte von d praktisch konstant sind. Ferner sieht man, dass zur Erreichung einer grösstmöglichen Richtwirkung der Abstand zwischen den Geophonen mehr als das 1,7-fache der mittleren Wellenlänge λ_m betragen muss. Das bedeutet Abstände von der Grössenordnung 20 bis 30 m. Solche Entfernungen werden im allgemeinen untertage nicht realisierbar sein. Man wird also auf eine Anordnung mit möglichst geringer Empfindlichkeit für $\vartheta = 90°$ beschränken müssen.

Im unteren Teil der Figur 5 sind als Beispiele drei Richtcharakteristiken in Polarkoordinaten aufgetragen. Diese drei Richtcharakteristiken gehören zu den entsprechenden Punkten der $(d/\lambda_m, w)$-Ebene, die im oberen Teil der Abbildung zu sehen sind. Die Kurve mit dem günstigsten Verhältnis $E(90°)/E(0)$ ist die Kurve 2. Für diese Kurve gilt $\sqrt{E(90°)/E(0)} = 0{,}56$. Die Richtwirkung beträgt dagegen nach (4.9) für diese Richtcharakteristik nur 1,9 *db*. Wird der optimale Wert von *d* überschritten, so treten in der Richtcharakteristik Nebenmaxima auf. Unterschreitet man den optimalen Wert, so wird das Verhältnis $\sqrt{E(90°)/E(0)}$ ungünstiger.

Die Anordnung mit umgepolten Geophonen unterscheidet sich wesentlich von der oben behandelten Anordnung mit gleichsinnig gepolten Geophonen. Während bei gleichsinnig gepolten Geophonen alle aus der Richtung $\vartheta = 0$ einfallenden Wellen unverzerrt empfangen werden, gibt es bei umgepolten Geophonen keine solche Richtung. Das bedeutet, dass jeder Wellenzug, selbst bei filterlosem Empfang, verzerrt wiedergegeben wird. Dagegen werden die aus der Richtung $\vartheta = 0$ einfallenden Wellen volkommen gelöscht. Bei umgepolten Geophonen ist darum eine bessere Richtwirkung zu erwarten.

Für die Empfindlichkeit einer Zweifachbündelung mit umgepolten Geophonen erhält man unter Zugrundelegung des Filters $A(f)$ nach (4.5) aus (4.3) und (2.5) den Ausdruck

$$E(\vartheta) = 2\left\{1 - \frac{\sin(wx \sin\vartheta) - \sin(x \sin\vartheta)}{(w\text{-}1)\, x \sin\vartheta}\right\} \tag{4.13}$$

Die Richtwerkung lautet

$$G = \frac{E_{max}}{2\left\{1 - [Si(wx) - Si(x)]/[(w-1)x]\right\}} \tag{4.14}$$

Aus der Figur 4 geht hervor, dass mindestens für schmale Spektra die Empfindlichkeit E (90°) mit wachsendem Abstand *d* zwischen den Geophonen zunächst wächst, aber dann wieder abnimmt. Es ist für die Anwendung der Bündelung von Interesse zu wissen, für welche *d* $E(90°)$ ihr Maximum annimmt. Dazu muss die Gleichung $\partial E(90°)/\partial d = 0$ gelöst werden. Ein Vergleich der beiden Formeln (4.8) und (4.13) für die Empfindlichkeit zeigt, dass diese Gleichung mit (4.11) identisch ist. Man erreicht also den grössten Wert für $E(90°)$ bei umgepolten Geophonen mit demselben Abstand *d*, mit dem man bei gleichsinnig gepolten Geophonen ein Minimum für $E(90°)$ erreichte. Überschreitet *d* diesen kritischen Wert, so liegt die maximale Empfindlichkeit nicht mehr bei $\vartheta = \pm 90°$. Man wird also bei der Anwendung der Bündelung mit *d* unter dem kritischen Abstand bleiben (vergl. Figur 6)

Rücken die Geophone näher aneinander, so verringert sich $E(90°)$. Als eine untere Grenze für *d* kann man z.B. den Abstand angeben, bei dem $E(90°)$

gleich der Empfindlichkeit eines einzelnen Geophons ist. Man erhält die Gleichung $E(90°) = 1$ oder

$$2 \sin wx - wx - (2 \sin x - x) = 0 \tag{4.15}$$

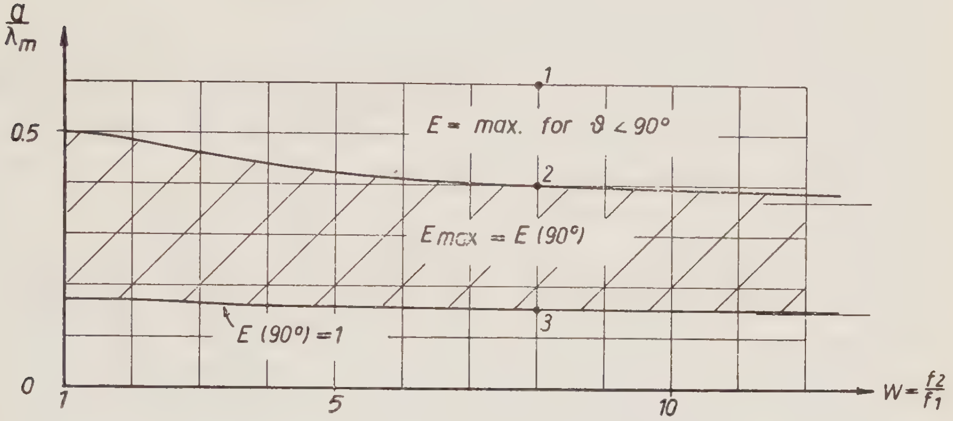

The optimum geophone spacing

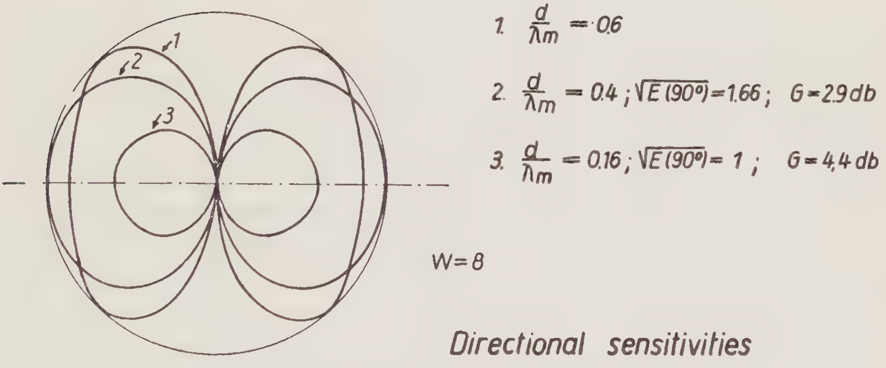

Directional sensitivities

Fig. 6. Array of two alternate polarized geophones

Die Lösung dieser Gleichung ist in der Figur 6 eingetragen. Für ein gegebenes w hat man danach ein festes Intervall, in dem d gewählt werden kann. — Eine Betrachtung der Richtwirkung (4.14) zeigt, dass G für kleiner werdende x (d.h. kleinere d) wächst. Man wird zur Erreichung einer möglichst grossen Richtwirkung also d/λ_m im unteren Teil des in der Figur 6 schraffierten Bereiches wählen. Im unteren Teil der Figur 6 sind wieder 3 Richtcharakteristiken aufgetragen, die den drei in der $(d/\lambda_m, w)$-Ebene eingezeichneten Punkten entsprechen. Die Kurve 2 hat ein Maximum von $\sqrt{E_{max}} = \sqrt{E(90^\circ)} = 1{,}66$, die zugehörige Richtwirkung beträgt 2,9 *db*. Die Richtcharakteristik 3 hat ein Maximum, das gleich 1 ist und eine Richtwirkung von 4,4 *db*.

§ 5. Dreifachbündelung

Unter einer Dreifachbündelung sei eine Empfängeranordnung verstanden, die aus drei Geophonen in gleichen Abständen besteht. Die Verstärkungen der beiden äusseren Geophone mögen zu 1 normiert sein. Sind sie beide gleichgepolt, so lautet das zugehörige Polynom nach (3.6)

$$P(z) = 1 + c\,z + z^2 \tag{5.1}$$

Die Nullstellen dieses Polynoms liegen auf dem Einheitskreis, wenn $-2 \leqq c \leqq +2$ ist. Sind die beiden äusseren Geophone umgepolt, so hat das zugehörige Polynom $z^2 + cz - 1$ nur dann beide Nullstellen auf dem Einheitskreis, wenn $c = 0$ ist. In diesem Fall geht die Dreifachbündelung aber in eine Zweifachbündelung über. Man kann sich also auf Dreifachbündelungen mit den Verstärkungen $(1, c, 1)$ beschränken. Der Betrag des Richtfaktors einer solchen Anordnung ist gleich

$$\begin{aligned} |R(f, \vartheta)| &= |P(z)| = |c + z + z^{-1}| = \\ &= |c + 2\cos(2\,\pi d\,(f/v)\sin\vartheta)| \end{aligned} \tag{5.2}$$

Mit dem Filter (4.5) erhält man aus (5.2) und (2.5) für die Empfindlichkeit den Ausdruck

$$\begin{aligned} E(\vartheta) = c^2 + 2 + 4c\,&\frac{\sin(wx\sin\vartheta) - \sin(x\sin\vartheta)}{(w-1)\,x\sin\vartheta} \\ &+ 2\,\frac{\sin(2\,wx\sin\vartheta) - \sin(2\,x\sin\vartheta)}{2\,(w-1)\,x\sin\vartheta} \end{aligned} \tag{5.3}$$

Die Richtwirkung lautet

$$\begin{aligned} G = E_{max} \Bigg\{ c^2 + 2 + 4c\,&\frac{Si(wx) - Si(x)}{(w-1)\,x} + \\ &+ 2\,\frac{Si(2wx) - Si(2x)}{2\,(w-1)\,x} \Bigg\}^{-1} \end{aligned} \tag{5.4}$$

Um einen Überblick über die Eigenschaften einer Dreifachbündelung zu erhalten, sei zunächst die am häufigsten benutzte Dreifachbündelung von drei gleich starken Geophonen betrachtet. — In diesem Fall ist in (5.3) und (5.4) $c = 1$ zu setzen. Als freier Parameter ist dann nur noch der Abstand d zwischen den Geophonen frei wählbar. Sucht man wieder die Anordnung, die möglichst unempfindlich für Wellen aus der Richtung $\vartheta = 90^\circ$ ist, so hat man die Gleichung $\partial E(90^\circ)/\partial d = 0$ zu lösen. Diese Gleichung lautet

$$\begin{aligned} wx \cos wx - \sin wx + 0.25\,(2\,wx \cos 2\,wx - \sin 2\,wx) &= \\ = x \cos x - \sin x + 0.25\,(2\,x \cos 2\,x - \sin 2\,x) & \qquad (5.5) \end{aligned}$$

Die Lösung dieser Gleichung ist in der Figur 7 als Kurve dargestellt. Wie bei der Zweifachbündelung so ist auch bei der Dreifachbündelung der optimale Wert des Abstandes in grossen w-Bereichen praktisch konstant.

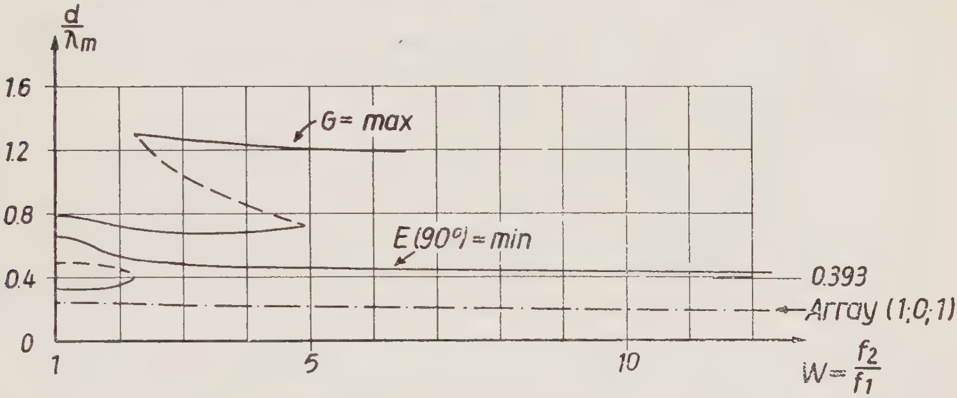

Fig. 7. The optimum geophone spacing for the array (1; 1; 1)

Bemerkenswert ist, dass für grössere w-Werte der optimale Abstand d sich nur wenig von dem entsprechenden optimalen Abstand der Zweifachbündelung unterscheidet. Um beide Fälle besser vergleichen zu können, ist in der Figur 7 strichpunktiert der optimale Abstand einer Dreifachbündelung mit $c = 0$ eingezeichnet. Man sieht, dass für grössere w-Werte beide Kurven sich praktisch nur um den Faktor 2 unterscheiden. Eine Abweichung ist lediglich bei kleineren Bandbreiten zu beobachten.

Der Abstand d, für den die Richtwirkung der Anordnung ihr Maximum erreicht, ist eine Wurzel der Gleichung $\partial G/\partial d = 0$. Diese Gleichung lautet

$$\begin{aligned} \sin wx - Si(wx) + 0.25\,[\sin 2\,wx - Si\,(2\,wx)] &= \\ = \sin x - Si(x) + 0.25\,[\sin 2\,x - Si\,(2\,x)] & \qquad (5.6) \end{aligned}$$

Auch die Lösung dieser Gleichung ist als Kurve in der Abbildung 7 dargestellt Wieder ist eine bemerkenswerte Ähnlichkeit des Kurvenverlaufes mit dem Verlauf der entsprechenden Kurve bei Zweifachbündelung festzustellen. Wie dort so sind auch hier die optimalen Abstände zu gross, um sie bei normalen Untertage-Messungen benutzen zu können.

Geht man nun zu Dreifachbündelungen mit variabler Verstärkung c des mittleren Geophons über, so muss man beachten, dass die maximale Empfindlichkeit, die bei $\vartheta = 0$ eintritt, nicht mehr konstant ist. Vielmehr gilt jetzt die Gleichung $E_{max} = E\ (0) = (c + 2)^2$. Anstatt nach der Anordnung zu fragen, bei der $E(90°)$ ein Minimum erreicht, muss man jetzt nach der Anordnung fragen, bei der das Verhältnis $E(90°)/E(0) = \text{Min.}$ wird. Dazu werden die partiellen Ableitungen des Verhältnisses nach c und d gebildet und gleich Null gesetzt. Man erhält auf diese Weise das Gleichungssystem

$$\left.\begin{aligned} c &= \frac{1 - 2\,S(x) + S\,(2x)}{1 - S(x)} \\ c &= -\ \frac{1}{2}\ \frac{S\,(2x) - C\,(2x)}{(Sx) - C\,(x)} \end{aligned}\right\} \tag{5.7}$$

mit $S(x) = \dfrac{\sin wx - \sin x}{(w - 1)\,x}$ und $C(x) = \dfrac{wx \cos wx - x \cos x}{(w - 1)x}$.

Die Lösung dieses Gleichungssystems ist in der Figur 8 dargestellt.

Für $w \to 1$ (harmonische Welle) strebt die Kurve dem Punkt $d/\lambda_m = 0{,}5$;

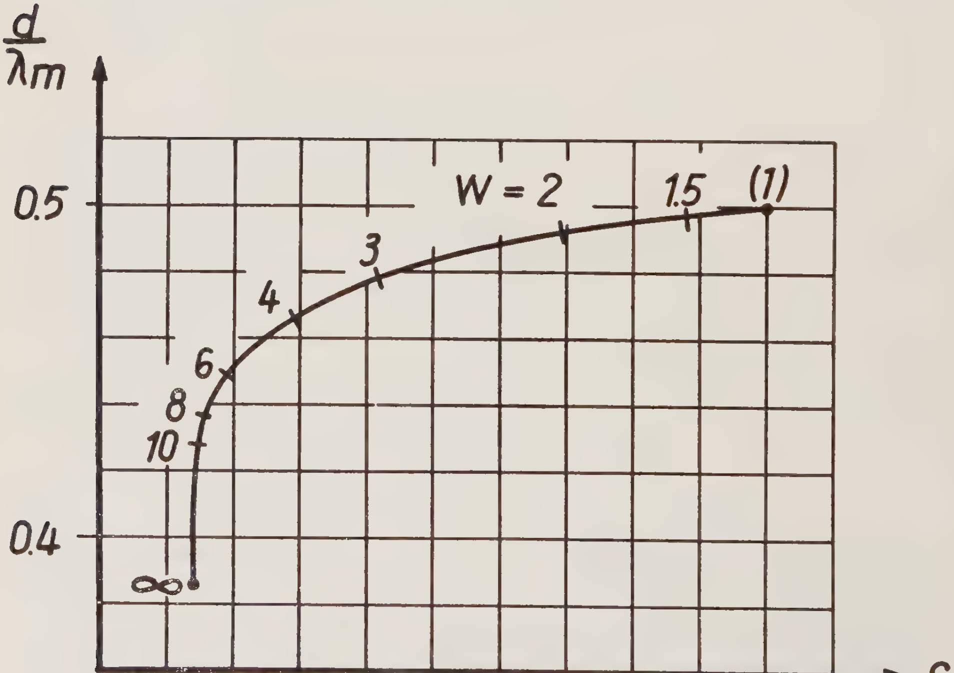

Fig. 8. The optimum geophone spacing d and the optimum sensitivity c of the array (1; c; 1)

$c = 2$ zu. Für den Wert $w = 1$ selbst besitzt das Gleichungssystem dagegen keine eindeutige Lösung, denn in diesem Fall kann man für jede Verstärkung c ein d/λ angeben, für den $E(90°) = 0$ wird. Mit wachsendem w nimmt zuerst der Wert von c ab, bleibt dann aber etwa für $w > 8$ praktisch konstant. Die zugehörigen Werte von d ändern sich in diesem Bereich nur unwesentlich. Die aus dieser Rechnung resultierende optimale Richtcharakteristik für $w = 8$ ist in der Figur 9 zu sehen.

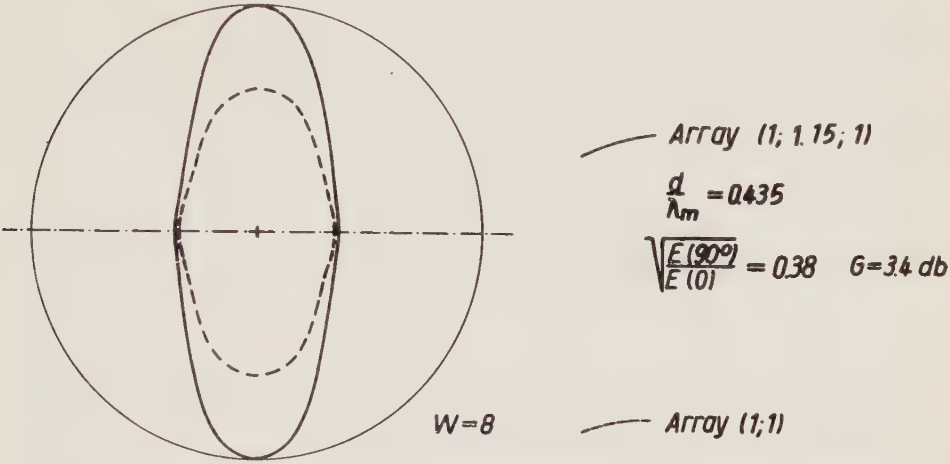

Fig. 9. The optimum directional sensitivities of arrays of two and three geophones.

Bei ihr ist $\sqrt{E(90°)/E(0)} = 0{,}38$, die Richtwirkung beträgt 3,4 *db*. Zum Vergleich ist die entsprechende optimale Richtcharakteristik bei Zweifachbündelung gestrichelt eingezeichnet.

Will man mit einer Dreifachbündelung aus der Richtung $\vartheta = 0$ möglichst wenig empfangen, so ist $c = -2$ zu wählen. In diesem Fall ist $E(0) = 0$ für alle Wellen. Ahnlich wie bei Zweifachbündelung mit umgepolten Geophonen wird man in diesem Fall die Wahl von d davon abhängig machen, ob eine grosse Richtwirkung erreicht werden soll, oder ob die Empfindlichkeit für $\vartheta = 90°$ möglichst gross werden soll. Im letzteren Fall ist die Gleichung $\partial E\,(90°)/\partial d = 0$ zu lösen. Diese Gleichung lautet

$$\begin{aligned} wx \cos wx - \sin wx - 0.125\,[2\,wx \cos 2\,wx - \sin 2\,wx] &= \\ = x \cos x - \sin x - 0.125\,[2\,x \cos 2\,x - \sin 2\,x]. & \qquad (5.8) \end{aligned}$$

Ihre Lösung ist in der Figur 10 zu sehen.

Beim Überschreiten des dort angegebenen Wertes von d tritt das Maximum der Empfindlichkeit nicht mehr bei $\vartheta = 90°$ auf. Bei Wahl eines kleineren Abstandes zwischen den Geophonen bleibt das Maximum der Empfindlichkeit bei $\vartheta = 90°$, es wird aber dem Betrage nach kleiner. Als untere Grenze ist wieder der Abstand angegeben, bei dem $E(90°) = 1$ wird. Die Richtwirkung der Anordnung wächst mit kleiner werdendem d. Man wird also wieder Abstände im unteren Teil des schraffierten Bereiches wählen. In der Figur 11 ist die Richtcharakteristik einer Anordnung mit $w = 8$ und $E(90°) = 1$ gezeigt. Die Richtwirkung der Anordnung beträgt 6,4 *db*.

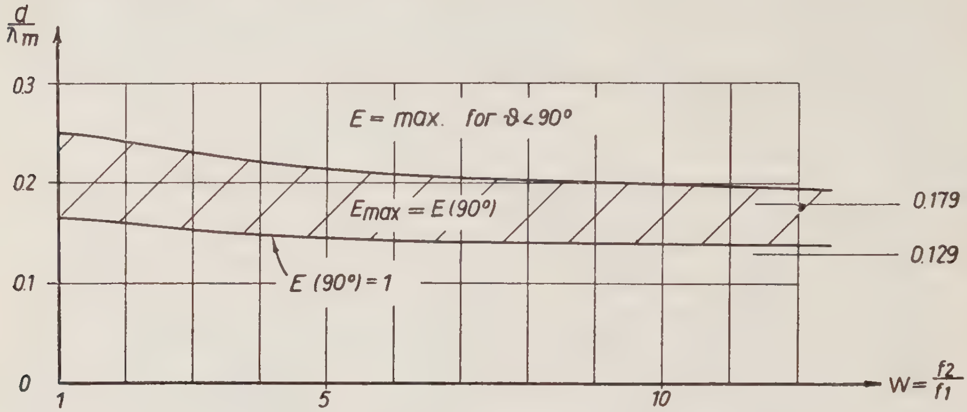

Fig. 10. The optimum geophone spacing for the array (1; -2; 1)

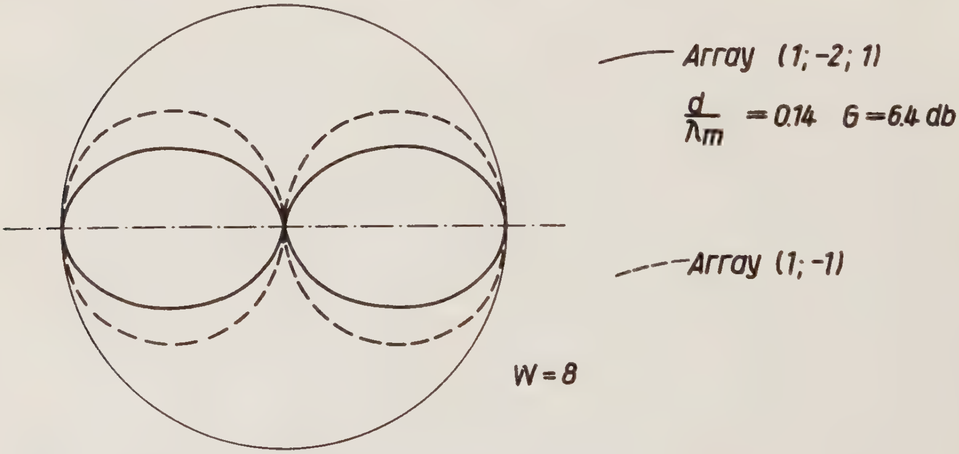

Fig. 11. The optimum directional sensitivities of the arrays (1; -2; 1) and (1; -1)

Zum Vergleich ist gestrichelt die entsprechende optimale Richtcharakteristik bei Zweifachbündelung mit umgepolten Geophonen eingezeichnet. — Auffallend sind bei der zuletzt behandelten Anordnung mit $c = -2$ die geringen Werte der optimalen Abstände. Sie lassen diese Art von Anordnungen für die Untertage-Messungen als besonders gut geeignet erscheinen. Allerdings ist der schraffierte Bereich in der Figur 10, in dem die Abstände zu wählen sind, kleiner als bei der entsprechenden Zweifachbündelung. Man muss also in Kauf nehmen, dass die Abstände zwischen den Geophonen genau eingehalten werden müssen.

§ 6. LINEARE EMPFÄNGERANORDNUNG MIT ZEITVERZÖGERUNG

In Erweiterung der bisher behandelten Empfängeranordnungen sei in diesem Paragraphen eine Empfängeranordnung mit Zeitverzögerung betrachtet. Man kann eine solche Anordnung etwa dadurch realisieren, dass man die einzelnen Geophone über elektrische Zeitverzögerungsglieder bündelt. Eine zweite Möglichkeit ist die Signale der einzelnen Geophone auf Magnetophonbändern aufzunehmen und sie anschliessend unter Anbringung einer Zeitverschiebung zu mischen. Bei Schüssen schliesslich lässt sich die Zeitverzögerung durch Benutzung von Zündschnüren einfach erreichen.

Mit t_ν sei die Zeitverzögerung bezeichnet, die das vom ν-ten Geophon empfangene Signal erleidet. Dann lautet die Empfangsfunktion

$$\Psi(t, \vartheta) = \sum_{\nu=0}^{n} c_\nu \, \Phi \left(t - \nu \frac{d}{v} \sin \vartheta - t_\nu\right) \tag{6.1}$$

Nach (2.1) kann man hierfür auch schreiben

$$\Psi(t, \vartheta) = \int_{-\infty}^{\infty} A\,(f)\, e^{2\pi i f t} \sum_{\nu=0}^{n} c_\nu \; e^{-2\pi i f (\nu\,(d/v) \sin \vartheta \,+\, t_\nu)} \tag{6.2}$$

Der Richtfaktor lautet dann

$$R(f, \vartheta) = \sum_{\nu=0}^{n} c_\nu \, e^{-2\pi i f (\nu (d/v) \sin \vartheta \,+\, t_\nu)} \tag{6.3}$$

Es sei zunächst der Fall mit frequenzunabhängigen Zeitverzögerungen betrachtet. Man kann in diesem Fall die Verzögerungen so wählen, dass sie von Geophon zu Geophon um einen konstanten Betrag wachsen. Ohne Einschränkung der Allgemeinheit kann man annehmen, dass das erste Geophon die Zeitverzögerung Null hat. Mit

$$t_\nu = \nu T \; d/v \tag{6.4}$$

erhält man dann für den Richtfaktor

$$R(f, \vartheta) = \sum_{\nu=0}^{n} c_\nu \, e^{-2\pi i \nu d \,(f/v)\, (\sin \vartheta \,+\, T)} \tag{6.5}$$

Diese Formel unterscheidet sich von (3.3) dadurch, dass statt $\sin\vartheta$ jetzt $\sin\vartheta + T$ auftritt. Mit der Bezeichnung

$$\mathfrak{z} = e^{-2\pi i d (f/v)(\sin\vartheta + T)} \tag{6.6}$$

erhält man analog zu (3.6)

$$R(f,\vartheta) = \sum_{\nu=0}^{n} c_\nu \mathfrak{z}^\nu = P(\mathfrak{z}) \tag{6.7}$$

$\mathfrak{z}$ unterscheidet sich von z nur durch einen Faktor vom Betrage 1. Alle Überlegungen in § 3, die zu notwendigen Bedingungen für die Verstärkungen c_ν führten, gelten daher auch jetzt. Geändert hat sich lediglich die Zuordnung der Einfallswinkel zu den Kreisabschnitten des Einheitskreises in der komplexen $\mathfrak{z}$-Ebene. Dem Einfallswinkel $\vartheta = 0$ entspricht jetzt ein Kreisabschnitt des Einheitskreises, dem Einfallswinkel $\vartheta = -\operatorname{arc}\sin T$ der Punkt $\mathfrak{z} = 1$. Die konjugiert komplexen Nullstellen des Polynoms $P(\mathfrak{z})$ bewirken jetzt eine unsymmetrische Richtcharakteristik.

Am besten übersieht man die Wirkung der Zeitverschiebung, wenn man den Betrag des Richtfaktors (6.5) als Relief in einer $(\sin\vartheta + T,\ df/v)$-Ebene aufgetragen denkt. Die Figur 12 zeigt diese Ebene mit den Nullstellen des Richtfaktors einer Anordnung von 4 Geophonen. Eine Änderung der Verzögerungskonstanten T bewirkt eine Verschiebung des interessierenden Bereiches in Richtung der Abszissenachse. Man hat also jetzt drei Möglichkeiten die Richtcharakteristik zu beeinflussen: Durch Wahl der Verstärkungen c_ν kann die Lage der Nullstellen des Richtfaktors bestimmt werden, durch Wahl des Abstandes d kann der interessierende Bereich in Richtung der Ordinatenachse verschoben werden und durch Wahl der Verzögerungskonstanten T kann der interessierende Bereich in Richtung der Abszissenachse verschoben werden. Für $T \neq 0$ erhält man unsymmetrische Richtcharakteristiken, wie sie in der Figur 12 zu sehen sind.

Es sei nun noch der Fall einer speziellen frequenzabhängigen Zeitverzögerung betrachtet. Die Zeitverzögerung sei durch die Formel.

$$t_\nu = A_\nu / |f| = A_\nu \lambda / v \tag{6.8}$$

gegeben. Die Zeitverzögerung soll also mit wachsender Frequenz geringer werden. Für die Empfangsfunktion erhält man dann statt (6.2)

$$\Psi(t,\vartheta) = \int_{-\infty}^{\infty} A(f)\, e^{2\pi i f t} \sum_{\nu=0}^{n} c_\nu\, e^{-2\pi i A_\nu \operatorname{sgn} f}\, e^{-2\pi i \nu d (f/v)\sin\vartheta} \tag{6.9}$$

Der Richtfaktor ist in diesem Fall

$$R(f,\vartheta)=\sum_{\nu=0}^{n} c_\nu\, e^{-2\pi i A_\nu \,\mathrm{sgn}\, f}\, e^{-2\pi i \nu d\,(f/v)\sin\vartheta} \tag{6.10}$$

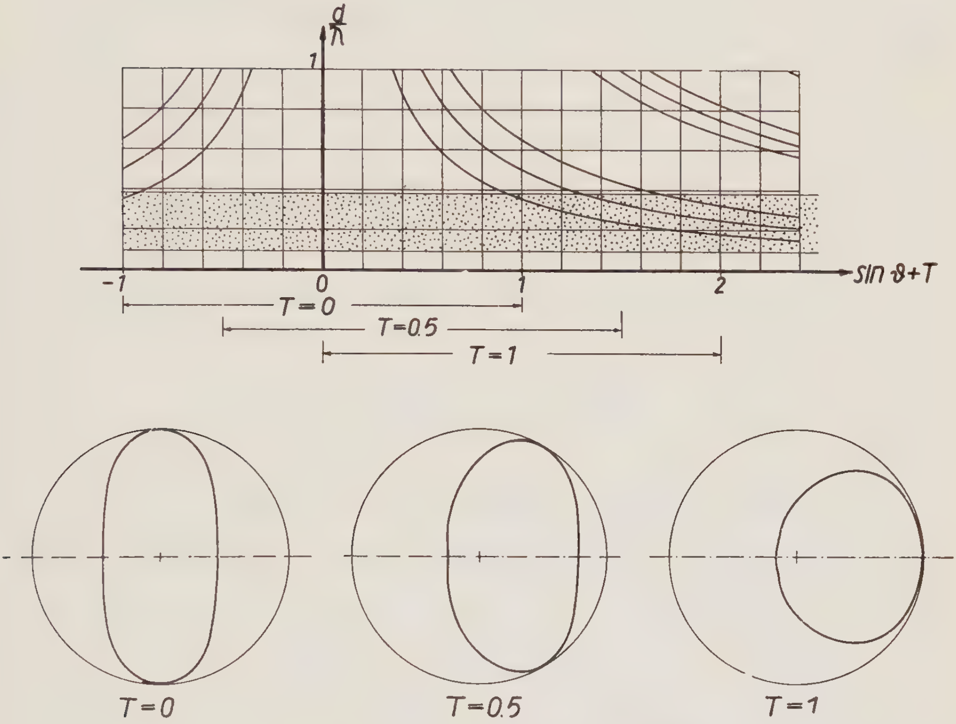

Fig. 12. The effect of the time shift.

Es gilt auch hier $|R(f,\vartheta)|=|R(-f,\vartheta)|$. Mit der Abkürzung (3.5) erhält man für positive f

$$R(f,\vartheta)=\sum_{\nu=0}^{n} c_\nu\, e^{-2\pi i A_\nu}\, z^\nu = P_1(z) \tag{6.11}$$

Dieses Polynom von z unterscheidet sich von (3.6) dadurch, dass die Koeffizienten auch komplex sein können. Es braucht also nicht nur konjugierte komplexe Nullstellen zu haben. Die Zuordnung der Einfallswinkel zu den Kreisabschnitten des Einheitskreises der z-Ebene ist dagegen die gleiche wie bei einer Anordnung ohne Zeitverzögerung. Durch geeignete Wahl der Nullstellen in der z-Ebene (unsymmetrische Lage) kann aber eine unsymmetrische Richtcharakteristik erreicht werden. — In der ($\sin\vartheta$, df/v)-Ebene drückt sich das so aus, dass die Nullstellen des Richtfaktors nicht mehr symmetrisch zu der Ordinatenachse zu liegen brauchen.

Die in § 3 abgeleiteten notwendigen Bedingungen gelten jetzt nicht mehr, weil die Koeffizienten des Polynoms $P_1(z)$ nicht reell zu sein brauchen. Die Verstärkungen brauchen daher nicht symmetrisch zu sein. Es gelten aber auch weiterhin die notwendigen Bedingungen

$$|c_0| = |c_n| \tag{6.12}$$

und

$$|c_\nu / c_0| \leqq \binom{n}{\nu} \tag{6.13}$$

§ 7. Zwei- und Dreifachbündelungen mit Zeitverzögerung

Es sei zunächst die Möglichkeit der Anwendung der Zeitverzögerung bei Zweifachbündelung untersucht. Die Zeitverzögerung sei frequenzunabhängig, das Signal des zweiten Geophons unterliege der Zeitverzögerung

$$t_1 = T \cdot d/v \cdot \tag{7.1}$$

Der Betrag des Richtfaktors ist dann für gleichsinnig gepolte Geophone nach (6.5) gleich

$$|R(f, \vartheta)| = |1 + 3| = |\, 2 \cos [\pi d\, (f/v)\, (\sin \vartheta + T)]|. \tag{7.2}$$

Mit der Filtercharakteristik (4.5) erhält man damit die zu (4.8) analoge Formel für die Empfindlichkeit

$$E(\vartheta) = 2 \left\{ 1 + \frac{\sin wx\, (\sin \vartheta + T) - \sin x\, (\sin \vartheta + T)}{(w-1)\, x\, (\sin \vartheta + T)} \right\} \tag{7.3}$$

Das Maximum der Empfindlichkeit verschiebt sich nach $\vartheta = -90°$ für $T = 1$, was an Hand der Figur 12 auch unmittelbar einleuchtet. Es gilt für $T = 1$ $E(-90°) = 4$ wieder unabhängig von der Form des Spektrums $A(f)$. $T = 1$ Für $\vartheta = +90°$ ist

$$E\,(+90°) = 2 \left\{ 1 + \frac{\sin 2\,wx - \sin 2x}{(w-1)\, 2x} \right\} \tag{7.4}$$

Um den Abstand d zwischen den Geophonen zu finden, für den $E(+90°)$ zum Minimum wird, ist wieder die Gleichung $\partial E(+90) / \partial d = 0$ zu lösen. Ein Vergleich von (7.4) mit (4.8) zeigt, dass der als Lösung dieser Gleichung bestimmte Abstand d genau halb so gross sein muss, wie der aus (4.11) bestimmte optimale Abstand d einer Zweifachbündelung ohne Zeitverzögerung. — Die Richtwirkung der Anordnung lautet

$$G = E_{max} \left\{ 2 + \frac{Si(wx\,[1+T]) - Si(x\,[1+T]) + Si\,(wx\,[1-T]) - Si\,(x[1-T])}{(w-1)\, x} \right\}^{-1} \tag{7.5}$$

Hält man sich an den Wert 1 für T fest, dann gilt für die Richtwirkung das Gleiche wie für die Empfindlichkeit. Man erhält die grösste Richtwirkung mit halb so grossen Abständen, wie bei Zweifachbündelung ohne Zeitverzögerung. Man kann sich leicht überlegen, dass der auf diese Weise erreichte Wert der Richtwirkung der gleiche ist wie der Wert der Richtwirkung ohne Zeitverzögerung.

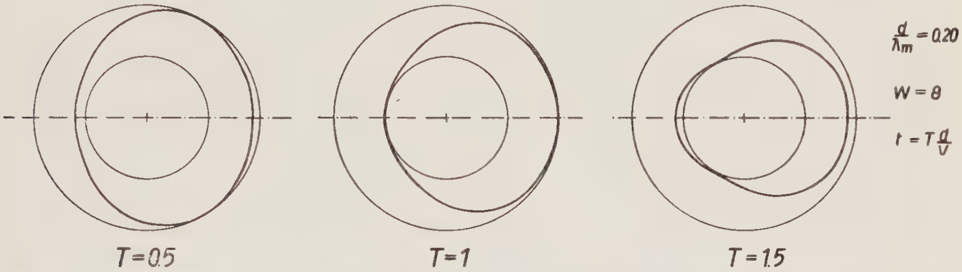

Fig. 13. Directional sensitivities of an array of two uniform polarized geophones with application of time shift.

In der Figur 13 sind Beispiele von Richtcharakteristiken für die Bandbreite $w = 8$ gezeigt. Die Richtwirkung der Anordnung mit $T = 1$ ist die gleiche wie bei der Anordnung $T = 0$, $d/\lambda_m = 0{,}40$ (Figur 5). Durch Vergrösserung von T kann man die Richtwirkung erhöhen, man muss dann allerdings eine Verringerung der maximalen Empfindlichkeit in Kauf nehmen. Durch eine Verkleinerung der Zeitverschiebung ($T < 1$), erhält man Richtcharakteristiken, deren Maxima nicht mehr bei $\vartheta = -90°$ liegen. In diesem Fall verringert sich die Richtwirkung der Anordnung.

Zu ähnlichen Ergebnissen führt die Anwendung der Zeitverzögerung bei Zweifachbündelungen mit umgepolten Geophonen. Mit der Zeitverzögerung (7.1) ist der Betrag des Richtfaktors nach (6.5) gleich

$$|R(f, \vartheta) = |1 - z| = |2 \sin\{\pi d(f/v)(\sin\vartheta + T)\}| \tag{7.6}$$

Mit der Filtercharakteristik (4.5) erhält man dann für die Empfindlichkeit den Ausdruck

$$E(\vartheta) = 2\left\{1 - \frac{\sin wx(\sin\vartheta + T) - \sin x(\sin\vartheta + T)}{(w-1)\,x\,(\sin\vartheta + T)}\right\} \tag{7.7}$$

Die Richtwirkung lautet schliesslich

$$G = E_{max} \cdot \left\{2 - \frac{Si(wx[1+T]) - Si(x[1+T]) + Si(wx[1-T]) - Si(x[1-T])}{(w-1)\,x}\right\}^{-1} \tag{7.8}$$

Mit $T = 1$ erhält man jetzt eine Empfängeranordnung, die aus einer Richtung überhaupt nichts empfängt — es ist für $T = 1\,E(-90^\circ) = 0$. Den Abstand zwischen den Geophonen wird man wieder so wählen, dass entweder $E(+90^\circ)$ möglichst gross wird oder die Richtwirkung der Anordnung möglichst gross wird. Die entsprechenden Abstände d sind halb so gross wie bei einer Zweifachbündelung ohne Zeitverschiebung. — Die Figur 14 zeigt einige Richtcharakteristiken für die Bandbreite $w = 8$.

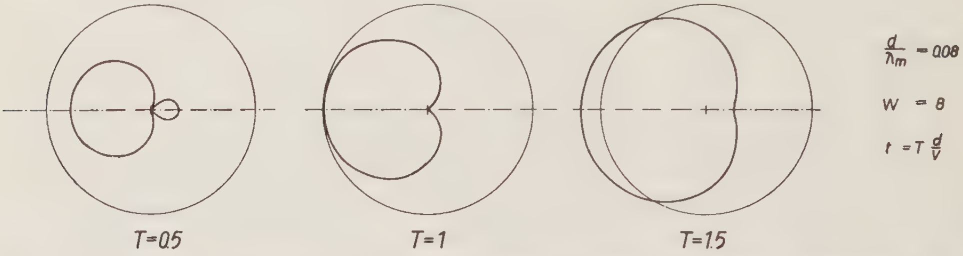

Fig. 14. Directional sensitivities of an array of two alternate polarized geophones with application of time shift

Der Abstand zwischen den Geophonen ist so gewählt, dass für $T = 1$ die maximale Empfindlichkeit $E(+90^\circ) = 1$ wird. Man ersieht aus der Abbildung den Einfluss der Zeitverzögerung auf die Form der Richtcharakteristik. Die Richtwirkung der Anordnung ist für $T = 1$ die gleiche wie bei der Anordnung $T = 0$ $d/\lambda_m = 0{,}16$ (Figur 6). Im Gegensatz zu der oben betrachteten Zweifachbündelung mit gleichsinnig gepolten Geophonen vergrössert sich die Richtwirkung mit Verringerung der Zeitverschiebung.

Bei der Anwendung der Zeitverzögerung auf Dreifachbündelung kann man wieder von den optimalen Werten der Verstärkung und des Abstandes bei einer Dreifachbündelung ohne Zeitverzögerung ausgehen. Für den'Betrag des Richtfaktors einer Dreifachbündelung mit den Verstärkungen 1, c, 1 und der Zeitverzögerung nach (6.4) erhält man nach (6.5)

$$|R(f,\vartheta)| = |c + 2\cos(2\pi d[f/v]\,[\sin\vartheta + T])| \tag{7.9}$$

Daraus erhält man mit der Filtercharakteristik (4.5) die Empfindlichkeit

$$E(\vartheta) = c^2 + 2 + 4c\,\frac{\sin(wx[\sin\vartheta + T]) - \sin(x[\sin\vartheta + T])}{(w-1)\,x\,(\sin\vartheta + T)} + \\ + 2\,\frac{\sin(2wx[\sin\vartheta + T]) - \sin(2x[\sin\vartheta + T])}{(w-1)\,2x\,(\sin\vartheta + T)} \tag{7.10}$$

Die Formel für die Richtwirkung lautet

$$G = E_{\max}\Big\{c^2 + 2 + 2c\,\frac{Si(wx[1+T]) - Si(x[1+T]) + Si(wx[1-T]) - Si(x[1-T])}{(w-1)\,x} +$$

$$+\left.\frac{Si(2\,wx[1+T])-Si(2x[1+T])+Si(2wx[1-T])-Si(2x[1-T])}{(w-1)\,2x}\right\}^{-1} \tag{7.11}$$

Sucht man eine Anordnung, deren Empfindlichkeit für $\vartheta = +90°$ möglichst gering sein soll, während die Empfindlichkeit für $\vartheta = -90°$ möglichst gross wird, so kann man hierfür die Ergebnisse des § 5 benutzen. Man erreicht offensichtlich für positives c die grösste Empfindlichkeit für $\vartheta = -90°$ mit $T = 1$. Es gilt unabhängig von $A(f)$ $E(-90°) = (c+2)^2$. Setzt man $T = 1$ in (7.10) ein, so zeigt ein Vergleich mit (5.3), dass $E(+90°)$ genau dann ihr Minimum erreicht, wenn man für den Abstand d den halben Wert nimmt, der aus dem Gleichungssystem (5.7) bestimmt wurde (Figur 8). Die zugehörige Verstärkung c des mittleren Geophons bleibt die gleiche.

Die Figur 15 zeigt einige mit diesen Werten erhaltene Richtcharakteristiken für die Bandbreite $w = 8$ und verschiedene Zeitverzögerungen T. Zum Vergleich ist die entsprechende optimale Richtcharakteristik bei Zweifachbündelung gestrichelt eingezeichnet.

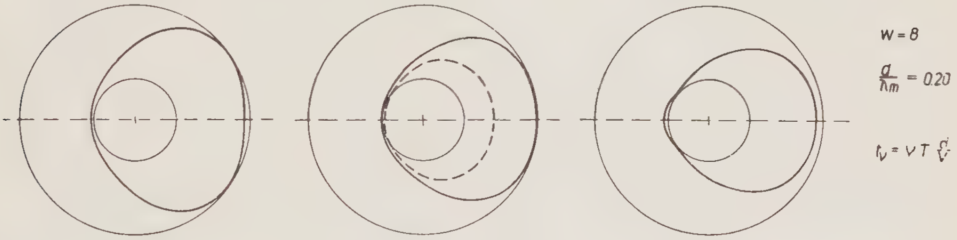

T=0.8 T=1 T=1.2

Fig. 15. Directional sensitivities of the array (1; 1.15; 1) with application of time shift

Die Abbildung zeigt den Einfluss einer nicht genau eingehaltenen Zeitverzögerung auf die Form der Richtcharakteristik. Wie bei der Zweifachbündelung ist die Richtwirkung der Empfängeranordnung mit $T = 1$ die gleiche wie bei der optimalen Anordnung in der Figur 9. Durch Vergrösserung der Zeitverschiebung kann man die Richtwirkung erhöhen, wenn man eine Verringerung der Empfindlichkeit $E(+90°)$ in Kauf nehmen will.

Durch Benutzung einer Dreifachbündelung mit den Verstärkungen 1, — 2,1 kann man mit Hilfe der Zeitverzögerung eine Empfängeranordnung herstellen, deren Empfindlichkeit für einen bestimmten Einfallswinkel gleich Null wird. Es sei hier wieder der Fall mit $T = 1$ betrachtet, in dem dieser Einfallswinkel gleich $-90°$ wird. Zur Erreichung einer möglichst grossen Richtwirkung wird man den Abstand zwischen den Geophonen wieder so wählen, dass die maximale Empfindlichkeit $E(+90°) = 1$ wird. (Vergleiche hierzu § 5.) Wie in dem oben betrachteten Fall mit positiver Verstärkung c des mittleren Geophons ist der zu wählende Abstand *d* halb so gross wie der in der Figur 10 angegebene Abstand für E (90°) = 1.

Die Figur 16 zeigt die auf diese Weise erhaltenen Richtcharakteristiken für die Bandbreite $w = 8$. Zum Vergleich ist gestrichelt die entsprechende optimale Richtcharakteristik für Zweifachbündelung eingezeichnet. $E(+90°)$ hängt bei dieser Art von Empfängeranordnungen offensichtlich sehr stark von der richtigen Wahl der Zeitverzögerung ab. Die Richtwirkung der Anordnung hat für $T = 1$ den gleichen Wert wie die in der Figur 11 gezeigte Richtcharakteristik. Wie bei der Zweifachbündelung mit umgepolten Geophonen wird die Richtwirkung grösser, wenn T vergrössert wird. Der sehr geringe Abstand zwischen den Geophonen und die Möglichkeit, störende Einflüsse aus einer gewünschten Richtung weitgehend auszuschliessen, machen diese Art von Empfängeranordnung recht brauchbar für die Untertage-Messungen.

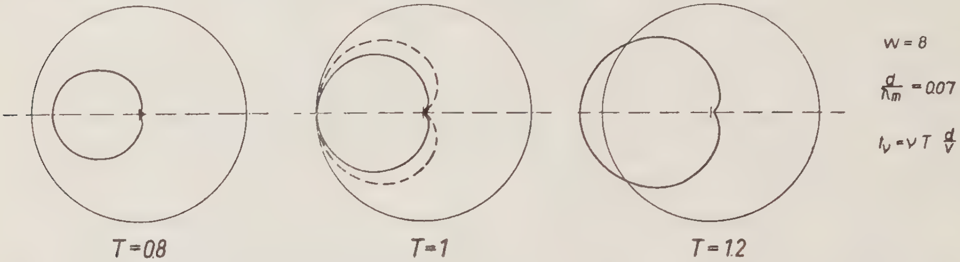

Fig. 16. Directional sensitivities of the array (1; -2; 1) with application of time shift

Zum Schluss sei ein Beispiel einer Empfängeranordnung mit frequenzabhängiger Zeitverzögerung angeführt. Die Anordnung bestehe aus drei Geophonen. Die Beträge der Verstärkungen seien 1, $\sqrt{2}$, 1. Das mittlere Geophon möge ausserdem umgepolt sein. Die Zeitverzögerungen seien nach dem Gesetz (6.8) von der Frequenz abhängig:

$$\left.\begin{aligned} t_0 &= 0 \\ t_1 &= 0{,}125/\,|f| \\ t_2 &= 0{,}25/\,|f| \end{aligned}\right| \qquad (7.12)$$

Dann hat das Polynom (6.11) die folgende Gestalt

$$P_1(z) = 1 - (1 - i)\,z - i\,z^2$$

Seine Nullstellen sind $z = 1$ und $z = i$.

Die Figur 17 zeigt die Nullstellen des Richtfaktors in der ($\sin\vartheta$, df/v)-Ebene. Der Abstand *d* zwischen den Geophonen sei so gewählt, dass für die

Bandbreite $w = 8$ der in der Figur 17 schraffierte Bereich für die Berechnung der Empfindlichkeit in Frage kommt. Man erhält für die Empfindlichkeit folgende Formel

$$E(\vartheta) = 4 - 4\,\frac{\cos(wx\sin\vartheta) - \cos(x\sin\vartheta)}{(w-1)\,x\sin\vartheta} - 4\,\frac{\sin(wx\sin\vartheta) - \sin(x\sin\vartheta)}{(w-1)\,x\sin\vartheta} + \qquad (7.13)$$
$$+ 2\,\frac{\cos(2\,wx\sin\vartheta) - \cos(2\,x\sin\vartheta)}{(w-1)\,2\,x\sin\vartheta}.$$

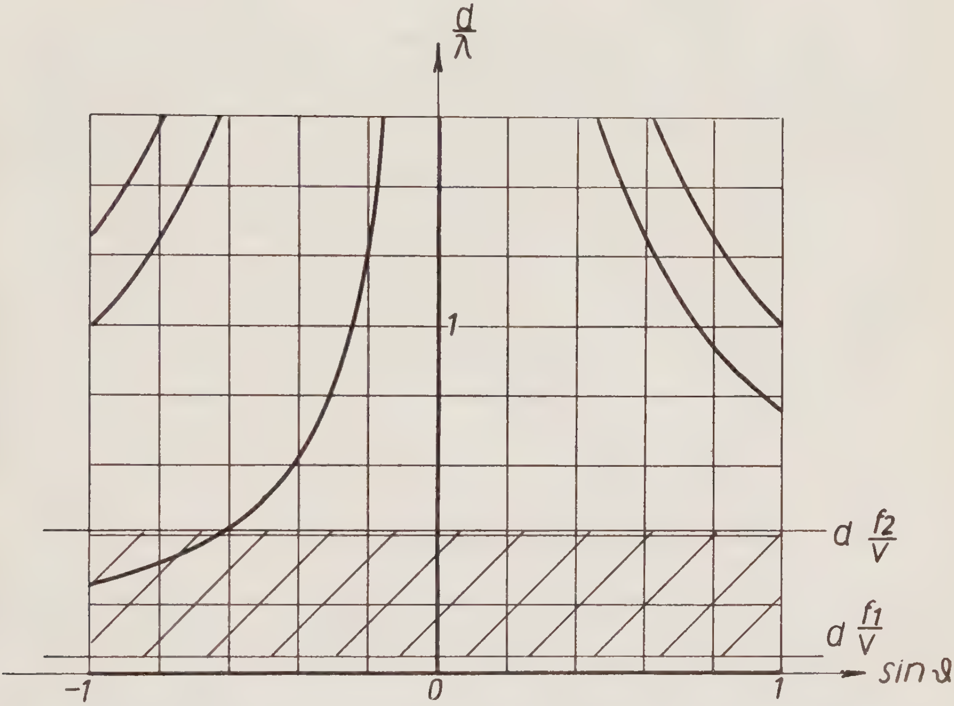

Fig. 17. The zeros of the function $R(f, \vartheta)$ of an array of three geophones with a time shift depending on the frequency

Die Richtwirkung wird dann berechnet nach der Formel

$$G = E_{max}\left\{4 - 4\,\frac{Si(wx) - Si(x)}{(w-1)\,x}\right\}^{-1}. \qquad (7.14)$$

Die Figur 18 zeigt die Richtcharakteristik der Anordnung.

Ihre Richtwirkung beträgt 4,0 *db*. — Nach der Richtcharakteristik hat die Anordnung für den Einfallswinkel 0 die Empfindlichkeit Null. Dies stimmt streng nur für harmonische Wellen. Hat man eine Welle von der Form $\Phi(t) = 0$ für $t < t_1$ und $\Phi(t) = \sin 2\pi\, tf$ für $t \geqq t_1$, so wirkt sich die Auslöschung der

Welle bei Benutzung nur eines schmalen Frequenzbereiches um f erst für $t \geqq 0{,}25/f$ voll aus, denn erst dann liefern alle Geophone einen Beitrag zum Seismogramm. Für die praktische Anwendung dürfte diese Abweichung keine Rolle spielen.

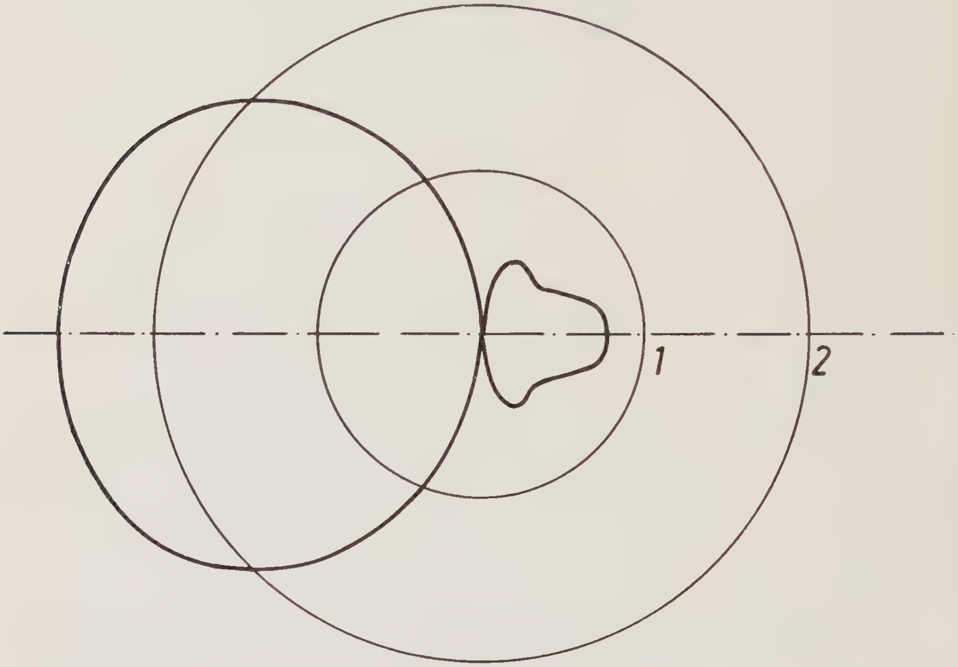

Fig. 18. Directional sensitivities of an array of three geophones with a time shift depending on the frequency

Die geschilderten Richtcharakteristiken können in der Praxis noch günstigere Ergebnisse liefern, als es nach dem bisherigen scheinen könnte: Weil die optimalen Abstände von der Geschwindigkeit v der Wellen abhängen, muss man sich bei der Herstellung einer Empfängeranordnung entscheiden, ob man die Geschwindigkeit der transversalen Wellen oder die der longitudinalen Wellen berücksichtigen will. Dadurch würde man immer nur eine Wellenart berücksichtigen können. Man kann aber die Anwendbarkeit der Anordnung auf beide Wellenarten ausdehnen, wenn man die Richtcharakteristik der Geophone selbst mit in Betracht zieht. So kann man z.B. sämtliche Wellen aus einer unerwünschten Richtung unterdrücken, indem man die Geophone so aufstellt, dass sie für die longitudinalen Wellen aus dieser Richtung möglichst unempfindlich sind und die Empfängeranordnung (Bündelung) gleichzeitig so wählt, dass die transversalen Wellen aus der gleichen Richtung unterdrückt werden.

Diese Untersuchung wurde im Auftrage der Forschungsgemeinschaft Seismik, e.V. durchgeführt. Der Forschungsgemeinschaft Seismik, e.V. und der Seismos G.m.b.H. danke ich für die Genehmigung zur Veröffentlichung der Ergebnisse. Ebenfalls danke ich Herrn Jost Schillemeit für wertvolle Anregungen.

LITERATUR:

STENZEL H., 1939, „Leitfaden zur Berechnung von Schallvorgängen", Berlin.

SCHELKUNOFF S. A., 1943, „A mathematical theory of linear arrays", The Bell System Technical Journal, 1, 80—107.

SCHMEIDLER W., 1950, „Integralgleichungen mit Anwendungen in Physik und Technik I", Leipzig.

MULTIPLE REFLEXIONEN IN NORDWESTDEUTSCHLAND *

VON

REINHARD BORTFELD **)

ABSTRACT

In N.W. Germany multiple reflections have been observed in numerous areas. They are not curiosities but represent true problems.

In many cases these multiples are recognizable by routine Δt analysis of the records. Sometimes the Δt anomalies are so great that multiples can be recognized without any computational work, merely by looking at the records. This is due to the great contrast between the interval velocities of the Tertiary and of the Upper Cretaceous. One example is discussed fully.

Most of the multiples are of the type AB (a multiple caused by reflections at two different reflectors A and B, and at the surface). It is also shown (by a rough estimate) that this type of multiple is theoretically the most probable. Finally, the interference between the two components of AB (one multiple being reflected first at A, then at B, and the other reflected first at B, then at A), and its appearance in constructed examples, are discussed.

EINLEITUNG

In grossen Teilen Nordwestdeutschlands treten multiple Reflexionen auf, oftmals sehr deutlich und in ziemlich grosser Anzahl. Sie sind hier bei allen reflexionsseismischen Messungen mit einiger Sicherheit zu erwarten und können das geologische Bild erheblich verwirren. Vielleicht aber verdienen diese multiplen Reflexionen über die praktische, lokale Bedeutung hinaus auch allgemeines Interesse — vor allem wegen ihrer Deutlichkeit und wegen des hohen Masses an Evidenz für die Art und Weise ihres Zustandekommens.

Es bestehen Anzeichen dafür, dass fast überall nördlich der gestrichelten Linie in Abb. 1 — was multiple Reflexionen anlangt — ganz ähnliche Verhältnisse vorherrschen wie bei dem Beispiel, das unten besprochen wird. Weitere Beispiele sind in einer Arbeit des Verfassers enthalten, die in Heft 9, September 1956, der "Erdöl-Zeitschrift" (Urban-Verlag GmbH., Wien-Hamburg) unter dem Titel "Beobachtungen multipler Reflexionen in Nordwestdeutschland" Dort wird ausführlicher über Beobachtungen und Erfahrungen erscheinen ist.

---

*) Part of a paper presented at the Tenth Meeting of the European Association of Exploration Geophysicists, held in Hamburg, May 16-18, 1956.

**) Mobil Oil AG., Celle, Germany.

mit multiplen Reflexionen im nördlichsten Teil Nordwestdeutschlands berichtet. Zur Abrundung und Ergänzung der in der vorliegenden Arbeit angeführten Fakten sei auf diese Veröffentlichung verwiesen.

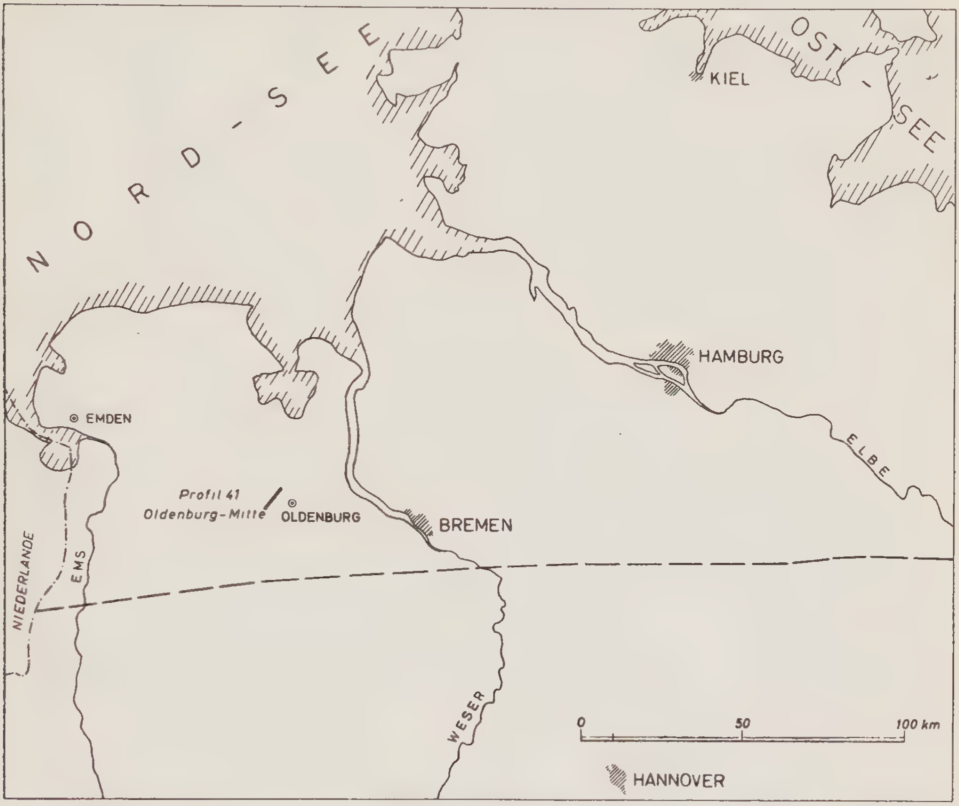

Abb. 1. Lageskizze
Map of NW-Germany; north of the dashed line multiple reflections of the type described in this paper may be expected

Der reflexionsseismische Profilschnitt Abb. 2 ist "typisch" für das nördlichste Nordwestdeutschland, und mit einer wohl vertretbaren Generaliesirung lässt sich dieses Gebiet folgendermassen beschreiben: Oberkreide, genauer: Alb, transgrediert über Jura; dabei ist es für das vorliegende Problem ohne Belang, um welche Stufen des Jura es sich jeweils handelt. Vom Alb an aufwärts hat man eine im wesentlichen ununterbrochene und auch — wenn man von Salzaufbrüchen und Salzaufbeulungen absieht — im wesentlichen ungestörte Sedimentationsfolge bis hinauf zum Quartär. Das Quartär ist ungefähr 100 m mächtig und vorwiegend sandig ausgebildet. Die Reflexionsseismik bringt hier recht gute Ergebnisse, und es treten kaum messtechnische

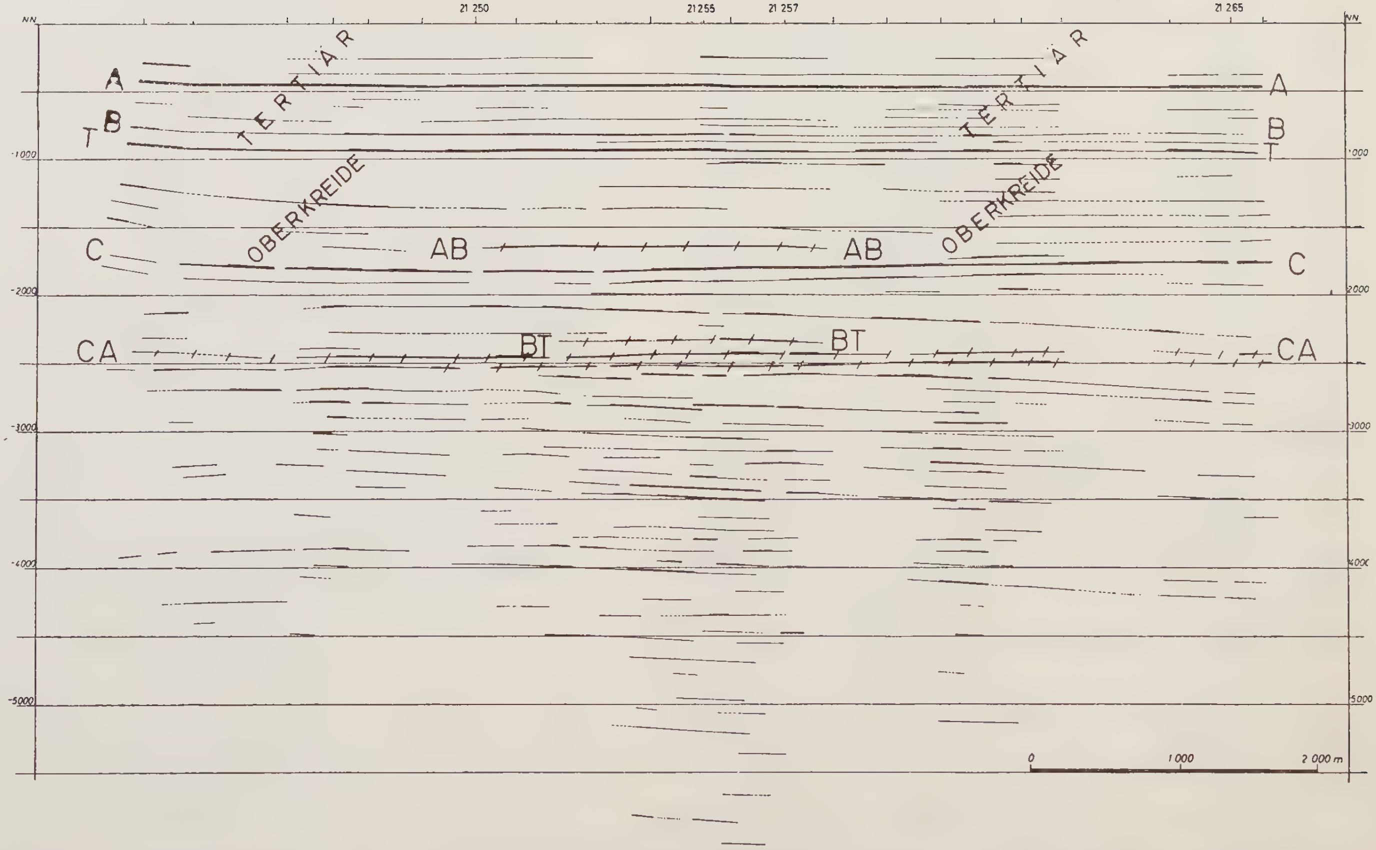

Abb. 2. Reflexionsseismischer Profilschnitt (Profil Oldenburg — Mitte 41). Seismic cross-section (profile Oldenburg — Mitte 41)

Schwierigkeiten auf. Meistens kommt man mit Einzelschüssen aus. Die erforderlichen Sprengladungen sind klein; sie liegen ungefähr zwischen 1 kg und 5 kg. Das Profil in Abb. 2 wurde mit Einzelschüssen und 6 Geophonen pro Spur aufgenommen (Geophongruppenlänge 15 m).

Das Gelände ist vorwiegend eben. Der (freie) Grundwasserspiegel steht einige Meter unter der Oberfläche. Die Schussbohrungen können heruntergespült werden und durchteufen fast nur Sand. Die Sprengladungen sind bei Schusstiefen zwischen ungefähr 7 *m* und 16 *m* im Grundwasser. So sind auch die Aufzeiten (up-hole time) klein; sie liegen (abgesehen von Ausnahmen bei Schlick oder Moor) bei 8 *m*sec bis 15 *m*sec. Diese Beschaffenheit der Oberflächenschicht passt gut zu den Beobachtungen von Ellsworth (1948) und Hansen (1948), die betonen, dass nach ihren Erfahrungen das Auftreten von multiplen Reflexionen wohl an eine dünne, gleichförmige Oberflächenschicht gebunden ist.

Einige der reellen Spiegel in Abb. 2 (und die Reflexionen davon) werden durch grosse lateinische Buchstaben, *A*, *B*, *T* und *C*, bezeichnet. *T* bedeutet die Tertiärbasis, *C* die Oberkreidebasis. (Die Oberkreide ist ziemlich reflexionsarm, was wohl hauptsächlich durch das Fehlen sandiger Partien bedingt ist). *AB*, *BT* und *CA* sind multiple Reflexionen. Diese Buchstabenpaare besagen nicht nur, dass es sich dabei um multiple Reflexionen handelt, sondern auch, auf welchem Wege sie wahrscheinlich zustande gekommen sind. *AB* bedeutet z. B., dass diese Multiple durch Reflexionen an *A* und *B* und an der Oberfläche entstanden ist. Es sind jeweils zwei Komponenten, aus denen sich eine multiple Reflexion vom Typ *AB* aufbaut (Abb. 3). Die eine Komponente läuft vom Schuss zum Spiegel *A*, dann zur Oberfläche, dann zum Spiegel *B*

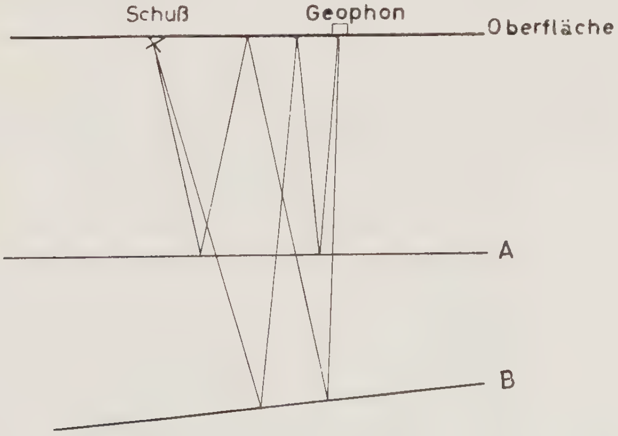

Abb. 3. Skizze der beiden Komponenten einer Multiplen vom Typ AB. Sketch of both the components of a multiple of type AB

und dann zu den Geophonen. Die andere Komponente läuft erst zum Spiegel *B*, dann zur Oberfläche, dann zum Spiegel *A* und dann zu den Geophonen. Beide Komponenten haben — jedenfalls soll das vorerst angenommen werden — dieselbe Laufzeit, überlagern sich also gleichphasig, mit konstruktiver Interferenz; und die Summe beider Komponenten soll als multiple Reflexion AB bezeichnet werden.

IDENTIFIZIERUNG DER MULTIPLEN REFLEXIONEN DURCH t- Δt-GESCHWINDIGKEITSBESTIMMUNG AUS ROUTINE-MESSUNGEN

Im nördlichsten Teil Nordwestdeutschlands liegt die Tertiärgeschwindigkeit bei 2000 *m*/sec. Die Oberkreide dagegen ist ziemlich schnell; ihre Intervallgeschwindigkeit liegt zwischen 3400 und 4200 *m*/sec. Beide Intervallgeschwindigkeiten treffen — mit nur unerheblichen Abweichungen — überall in diesen Gebieten zu (vgl. auch: von Zur Mühlen und Tuchel 1953). Dieser grosse Geschwindigkeitskontrast zwischen Tertiär und Oberkreide erleichtert das Erkennen von multiplen Reflexionen ganz erheblich.

Bei der t- Δt-Geschwindigkeitsbestimmung ergibt sich die Durchschnittsgeschwindigkeit auf dem von der Reflexion durchlaufenen Wege. Das gilt für primäre Reflexionen (Green 1938), aber auch für multiple Reflexionen (Dix 1948, 1952; Ellsworth 1948; Hansen 1948; Sloat 1948). Wenn z. B. die Reflexion *AB* in Abb. 2 primär wäre, so müsste sie eine t- Δt-Geschwindigkeit ergeben, die irgendwo zwischen der Tertiär- und der Oberkreidegeschwindigkeit liegt. Wenn *AB* aber multipel ist, wenn diese Reflexion nur durch das Tertiär gelaufen ist, so muss sich eine sehr viel kleinere, nämlich ungefähr die Tertiärgeschwindigkeit, ergeben. Wegen des grossen Kontrastes zwischen der Tertiär- und der Oberkreidegeschwindigkeit sind die zu erwartenden Unterschiede der t- Δt- Geschwindigkeiten ziemlich gross. Und das bedeutet, dass auch die Unterschiede der Δt ziemlich gross sein müssen. (Unter Δt soll — wie üblich — die Laufzeitdifferenz zwischen einer Aussenspur und den Innenspuren verstanden werden.) Abb. 4 soll die hier auftretenden Δt-Unterschiede zwischen primären und multiplen Reflexionen illustrieren.

Es ist der Ausschnitt von ungefähr 0,9 bis 2,2 sec aus dem Seismogramm von SP 21257 aus Abb. 2. Die Aufbaulänge beträgt nach oben 400 *m*, nach unten 360 *m*; die obere Hälfte der Abb. ist die gemischte Registrierung, die untere Hälfte die ungemischte. Das Intervall zwischen *T* und *C* ist das Oberkreideintervall. Die Reflexionen zwischen *T* und *C* müssen — sofern sie primär sind — eine kontinuierliche und zwar ziemlich schnelle Abnahme der Krümmung zeigen, denn diese Abnahme ist nicht nur durch die zunehmenden Laufzeiten, sondern auch durch die Zunahme der Durchschnittsgeschwindigkeit bedingt. Die Reflexion *AB* zeigt aber enorm starke Krümmung in grossem

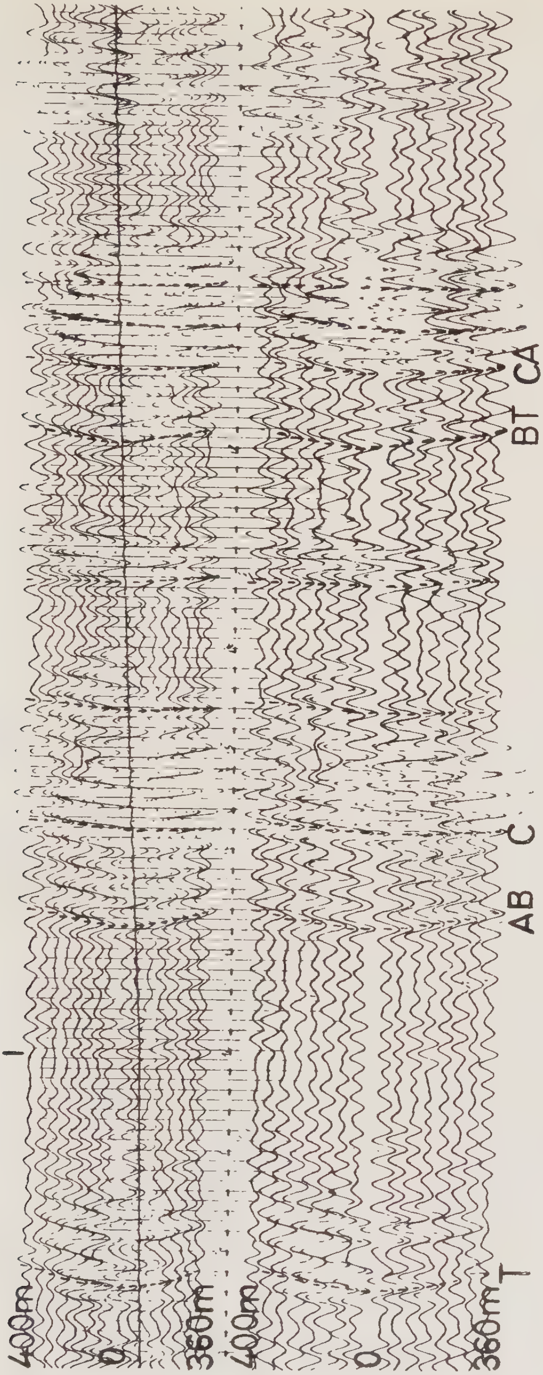

Abb. 4. Seismogramm von SP 21257 aus Abb. 2. Seismic record No. 21257 from Fig. 2

Kontrast zu der folgenden primären *C*-Reflexion, d.h. *AB* ist eine multiple Reflexion, die überhaupt nicht aus dem Tertiär herausgekommen ist. Hinter *C* sind zwei weitere primäre Reflexionen angerissen. Dann folgt die Multiple *BT*, wieder mit starker Krümmung, weil ihr Weg nicht in die Oberkreide geführt hat. Die Multiple *CA* hat kleinere Krümmung als *BT*, aber das muss ja so sein, weil sie durch die ganze Oberkreide gelaufen ist. Hinter *CA* folgen dann wieder primäre Reflexionen mit deutlich verschiedenem Δt. In der oberen Richtung finden sich bei den Aussenspuren Interferenzerscheinungen, verursacht durch die Überlagerung von *CA* mit einer primären Reflexion.

Im allgemeinen sind die multiplen Reflexionen nicht so gut zu erkennen wie bei diesem (ausgesuchten) Seismogramm. Aber oftmals genügt eine t-Δt- Geschwindigkeitsbestimmung mit den aus Routinemessungen vorliegenden Seismogrammen zur Identifizierung der Multiplen.

Es gibt einige Untersuchungen über die Genauigkeit der aus Routinemessungen, d.h. aus normal (200-400 *m*) langen Messstrecken, bestimmten Geschwindigkeiten (Romberg 1941, Steele Jr. 1941, Savit 1951, Swan and Becker 1952). Dabei stellt sich heraus, dass man zu verlässlichen Ergebnissen kommt, wenn man sehr viele Seismogramme verwenden kann — aber auch nur dann. Für das Erkennen von multiplen Reflexionen ist aber eine so hohe Genauigkeit gar nicht erforderlich — jedenfalls nicht hier bei den grossen Geschwindigkeitskontrasten und nicht sehr grossen Teufen der interessierenden Spiegel. Und deshalb reicht für diesen Zweck die meistens nur zur Verfügung stehende relativ kleine Zahl von Seismogrammen oftmals aus. (Die hier zu beschreibende Kennzeichnung der multiplen Reflexionen durch t- Δt-Analyse ist schon von Hansen (1948) in ähnlicher Weise vorgeschlagen und durchgeführt worden. Allerdings wurden in dem von ihm beschreibenen Beispiel (aus Argentinien) 800 m lange Strecken benötigt.)

Abb. 5 zeigt die über die t- Δt-Geschwindigkeitsbestimmung aus Routinemessungen gewonnene Laufzeit-Teufenkurve für das Profil Abb. 2 . Zur Berechnung der Geschwindigkeiten wurde eine Formel verwendet, die jetzt auch von Pflueger (1954) angegeben worden ist. Diese Formel berücksichtigt die Neigung der reflektierenden Grenzen und annulliert störende Effekte, die durch Änderungen der Oberflächenschicht verursacht werden. Die so erhaltenen, brauchbaren Geschwindigkeiten (Aufbaulängen $<$ 300 m sind nur bedingt brauchbar) wurden gemittelt und dazu der mittlere quadratische Fehler bestimmt. Durch Multiplikation mit der halben Laufzeit ergeben sich daraus die Teufenfehlergrenzen, die in Abb. 5 durch vertikale Striche dargestellt sind. An den Geschwindigkeiten könnte man noch Brechungskorrekturen anbringen (Krey 1951, 1954; Dürbaum 1954; Dix 1955), aber das ist hier nicht getan worden und für diesen Zweck eigentlich auch nicht nötig. Die Lotzeiten in Abb. 5 sind die Lotzeiten von SP 21255, abzüglich 20 msec als ungefähre Korrektur auf den wahren Einsatz der Reflexionen.

Man erkennt aus dieser Laufzeit-Teufenkurve wieder, dass *AB*, *BT* und *CA* multiple Reflexionen sind. Einmal lässt sich das an den Intervallgeschwindigkeiten sehen. Wenn man nämlich diese drei Reflexionen als primär ansehen will, kommt man zu ganz unsinnigen Werten. Zwischen *T* und *AB* hätte man eine Geschwindigkeit von 1700 m/sec.; was für diese Teufe nicht zutreffen kann und erst recht nicht, wenn man bedenkt, dass dieses Intervall schon in der Oberkreide liegt. Zwischen *AB* und *C* bekäme man eine Geschwindigkeit von 11440 m/sec, zwischen *C* und *BT* sogar eine negative Geschwindigkeit und zwischen *BT* und *CA* 10100 m/sec.

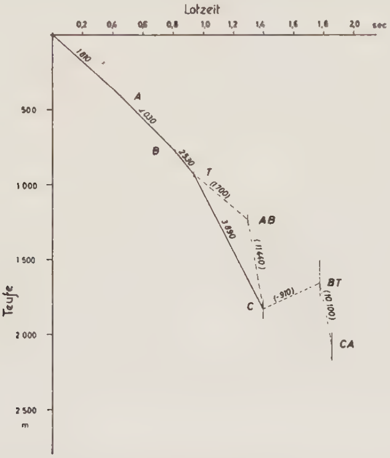

Abb. 5. Lotzeit-Teufenkurve aus Routine-Messungen zu Abb. 2. Time-depth curve from routine-records

Es lässt sich aber auch auf eine (formal) andere Art erkennen, dass *AB*, *BT* und *CA* multiple Reflexionen sind. Trägt man nämlich eine in einer benachbarten Tiefbohrung gemessene Laufzeit-Teufenkurve in Abb. 5 ein, so liegt diese dicht bei der ausgezogenen Kurve. Aber eine solche Bohrlochgeschwindigkeitsmessung ist nicht einmal nötig, denn man kennt ja im vorhinein die Tertiär- und die Oberkreidegeschwindigkeit ziemlich genau; weiss also ungefähr, wo die reelle Kurve verlaufen muss. Und die Abweichungen der Punkte *AB*, *BT* und *CA* von dieser reellen Kurve sind so gross, dass sie nicht durch Messfehler erklärt werden können.

Es lässt sich aber aus dieser Kurve nicht nur ablesen, dass *AB*, *BT* und *CA* multiple Reflexionen sind, sondern auch, auf welchem Wege sie wahrscheinlich zustande gekommen sind. Man kommt nämlich ungefähr zu dem Punkt *CA*, wenn man den Ast Anfangspunkt-*A* an *C* anlegt — wie es sein muss, wenn

CA auf die in der Einleitung beschriebene Art durch Reflexionen an *C* und *A* entsteht. Ebenso kommt man ungefähr zu dem Punkt *AB*, wenn man den Ast Anfangspunkt-*A* an *B* anlegt, und man kommt ungefähr zu dem Punkt *BT*, wenn man den Ast Anfangspunkt-*B* an *T* anlegt.

Die t- Δt-Geschwindigkeitsbestimmung aus Routine-Messungen gelingt hier mit für die Kennzeichnung von multiplen Reflexionen ausreichender Genauigkeit, weil der Geschwindigkeitskontrast zwischen Tertiär und Oberkreide grosse Δt-Anomalien verursacht, und weil der untersuchte Teufenbereich nicht viel tiefer als 2000 m reicht. In anderen Fällen reicht das Auflösungsvermögen nicht aus, und man muss dann Langstreckengeschwindigkeitsmessungen, insbesondere expanding spreads (Hansen 1947; Dix 1955), zur Geschwindigkeitsbestimmung verwenden.

ZUR IDENTIFIZIERUNG DER MULTIPLEN REFLEXIONEN DURCH LAUFZEITBEZIEHUNGEN

Es ist von den multiplen Reflexionen zu fordern, dass sich ihre Laufzeiten aus den Laufzeiten der zugehörigen primären Reflexionen zusammensetzen lassen müssen; und zwar nicht nur in einem Seismogramm, sondern in allen Seismogrammen, in denen die Multiplen vorhanden sind. Abb. 6 soll zur Demonstration dieser Laufzeitübereinstimmung für die Multiplen aus dem Profilschnitt Abb. 2 dienen. In diesem Bild werden die "Lotzeiten" der multiplen und der zugehörigen primären Reflexionen senkrecht unter den resp. Schusspunkten durch die Mitte der Striche dargestellt. Es sind die Lotzeiten für das ausgewertete, d.i. das erste deutliche Reflexionstal, und zwar auf das Schuss-

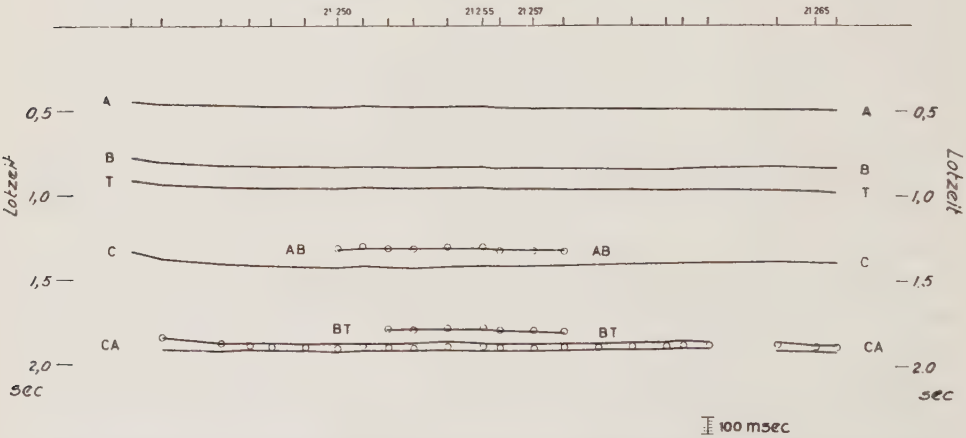

Abb. 6. Lotzeitplan (Auszug) zu Abb. 2. Reflection-time representation of some reflections from Fig. 2

niveau bezogen. Die Mittelpunkte der Kreise bedeuten die Summe dieser Lotzeiten für die zugehörigen primären Reflexionen, z.B. bei *AB* die Summe der Lotzeiten (des ersten deutlichen Tales, bezogen auf das Schussniveau) von *A* und *B*.

Die zu fordernde Laufzeitübereinstimmung ist recht gut erfüllt. Die „Lotzeiten" von *AB* weichen überall nur wenig, um weniger als 10 *m*sec, von der Summe der Lotzeiten von *A* und *B* ab. Ebenso ist es bei BT. Bei CA beträgt die Abweichung ungefähr 20 *m*sec, d. h. eine Periode.

Die Laufzeit einer Multiplen vom Typ *AB* ist im allgemeinen kürzer als die Summe der Laufzeiten von *A* und *B* (dasselbe gilt selbstverständlich auch für Multiple vom Typ *AA*). Der Laufweg von *AB* ist nämlich im allgemeinen kürzer als die doppelte Summe der Lote auf die Spiegel *A* und *B*. Man kann sich in jedem einzelnen Fall auf relativ einfache Weise ausrechnen (z.B. mit Hilfe der auf $x = 0$ spezialisierten Gleichung (13) bzw. (14), Seite 413, wie gross diese Verkürzungen zu erwarten sind; kann dementsprechende Korrekturen an den Laufzeiten der Reflexionen anbringen und nachsehen, ob die Laufzeitenübereinstimmung für die als multipel verdächtigte Reflexion dann besser oder schlechter wird. Die Unterschiede fallen allerdings erst bei grösseren Teufen und grösseren Neigungen ins Gewicht, und deshalb wird es nur selten nötig sein, solche Korrekturen anzubringen.

In der Literatur gehen die Meinungen auseinander, ob die Oberfläche oder der Grundwasserspiegel (bzw. die Basis der Verwitterungsschicht) bei der Entstehung der multiplen Reflexionen beteiligt ist. Es überwiegt zwar die Ansicht, dass es der Grundwasserspiegel ist, aber eigentlich ist die Entscheidung, auch regional, noch offen geblieben. Mit Hilfe der Laufzeitbeziehungen lässt sich für das Gebiet, aus dem dem Verfasser Beobachtungsmaterial vorliegt, eine gewisse Entscheidung treffen.

Mit der in Abb. 6 gewählten Art der Laufzeit-Darstellung, d.h. wenn man die auf das Schussniveau bezogenen Laufzeiten des ersten deutlichen Reflexionstales nimmt, bekommt man im nördlichsten Teil Nordwestdeutschlands recht gute Übereinstimmung der Laufzeiten der multiplen Reflexionen mit der Summe der Lotzeiten der zugehörigen primären Reflexionen. Bisweilen treten zwar Abweichungen auf, aber die sind ja auch durchaus zu erwarten; z.B. wegen der Phasenumkehr bei einer ungeraden Zahl von negativen Reflexionsprozessen oder überhaupt weil sehr verschiedene Schwingungsbilder vorkommen (bedingt durch die Frequenzselektion bei der Absorption und Streuung und durch Überlagerung von Störenergie), wodurch der zeitliche Abstand des ersten deutlichen Tales von dem Einsatz der Reflexion variabel wird.

Diese Laufzeitübereinstimmung (für das erste deutliche Tal, auf Schussniveau bezogen) wird durch (1) beschrieben:

$$t_{AB} \approx t_A + t_B \quad \ldots\ldots\ldots\ldots \quad (1)$$

Es soll nun angenommen werden, dass das erste deutliche Reflexionstal 20 msec hinter dem wahren Einsatz der Reflexion liegt:

$$t \approx \underset{w}{t} + 20\,m\text{sec} \quad . \; . \; . \; . \; . \; . \; . \; . \; . \; . \quad (2)$$

für A, B und AB.

Anstey (1956) zeigt experimentell, dass das eine ziemlich konservative Annahme ist, dass die Differenz tatsächlich noch grösser ist. Trägt man (2) in (1) ein, folgt (3) und schliesslich (4):

$$\underset{w}{t_{AB}} + 20\,m\text{sec} \approx \underset{w}{t_A} + 20\,m\text{sec} + \underset{w}{t_B} + 20\,m\text{sec} \quad . \; . \; . \; . \; . \quad (3)$$

$$\underset{w}{t_{AB}} \approx \underset{w}{t_A} + \underset{w}{t_B} + 20\,m\text{sec} \quad . \; . \; . \; . \; . \; . \; . \; . \; . \; . \quad (4)$$

Abb. 7 soll den Inhalt von (4) interpretieren. Bei der Skizze muss man sich Punkt 6 als mit S identisch denken, weil hier nur die Laufzeiten bei den schussnahen Geophonen betrachtet werden. $\underset{w}{t_A}$ ist die wahre Laufzeit für den Weg S-1-2, $\underset{w}{t_B}$ die wahre Laufzeit für den Weg 4-5-6; die wahre Laufzeit der multiplen Reflexion AB ist aber noch um 20 msec grösser als die Summe $\underset{w}{t_A} + \underset{w}{t_B}$, d. h. AB ist höchstwahrscheinlich noch zur Oberfläche und zurück gelaufen. Denn wie in der Einleitung erwähnt wurde, liegen die Aufzeiten im nördlichsten Nordwestdeutschland bei rund 10 *m*sec; die 20 *m*sec entsprechen also gerade dem Weg Schuss-Oberfläche-Schuss. Wenn man anstelle der 20 *m*sec für die Laufzeitdifferenz zwischen dem ersten deutlichen Tal und dem wahren Ein-

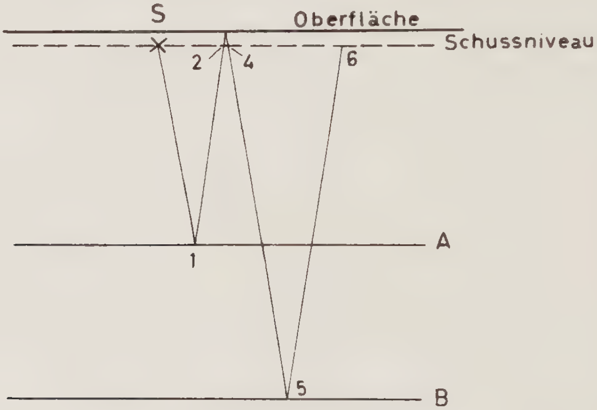

Abb. 7. Schematische Skizze der Laufzeitbeziehungen. Schematic diagram of travel-time relations

satz der Reflexion den wahrscheinlich richtigen grösseren Wert nimmt, wird die Beweiskraft hier noch erhöht.

Es ist also höchstwahrscheinlich so, dass die Oberfläche der obere Reflektor ist. Das schliesst aber nicht aus, dass auch der Grundwasserspiegel beteiligt sein könnte. Denn wegen der in der Einleitung beschriebenen Beschaffenheit der Oberflächenschicht ist in vielen Fällen konstruktive Interferenz zwischen der vom Grundwasserspiegel und der von der Oberfläche reflektierten Energie zu erwarten. Man hätte sich das so vorzustellen, dass zwar eine vom Grundwasserspiegel reflektierte Welle im Seismogramm vorhanden ist, dass sie aber erst sichtbar wird, wenn sich ihr die von der Oberfläche reflektierte Welle (im zeitlichen Abstand von ≈ 1 Periode) überlagert.

ÜBER DIE VERLÄSSLICHKEIT BEIM IDENTIFIZIEREN VOM MULTIPLEN REFLEXIONEN

Die Entscheidung, ob eine Reflexion multipel ist, kann sich auf 3 Kriterien stützen, die stichwortartig folgendermassen bezeichnet werden sollen:

a) Geschwindigkeiten
b) Laufzeitbeziehungen
c) Lage der Spiegel im Profilschnitt

Die Kriterien *a* und *b* sind im vorigen besprochen worden. Das Kriterium *c* bedeutet, dass man einen Spiegel als multipel, bzw. zunächst einmal als irreal, ansehen wird, wenn er eine geologisch irgendwie unwahrscheinliche Lage oder Neigung hat, wie z.B. der Spiegel *CA* in Abb. 2.

Gegen jedes der Kriterien können Einwände vorgebracht werden. Gegen a. z.B., dass Messfehler vorkommen, oder dass bei gekrümmten Reflektoren die t- Δt-Geschwindigkeiten verfälscht werden (bei nach oben konkaven Reflektoren resultieren im allgemeinen zu kleine Geschwindigkeiten, bei nach oben konvexen Reflektoren zu grosse Geschwindigkeiten). Gegen b kann eingewendet werden, dass sich manchmal auch die Laufzeiten einer *primären* Reflexion „zufällig" aus den Laufzeiten zweier anderer Reflexionen zusammensetzen lassen. Und gegen *c* kann man einwenden, dass ein der Lage nach „geologisch unwahrscheinlicher Spiegel" dennoch reell sein kann; dass z. B. „Kreuzschichtung im Grossen" vorkommen könnte, oder dass die als multipel angesprochene Reflexion in Wirklichkeit von einer Störzone kommt oder von einer Intrusion oder von einer quer durch die Formationsgrenzen laufenden (reflektierenden) lithologischen Grenzfläche.

So begründet diese Einwände im einzelnen sein mögen — wenn eine Reflexion durch alle 3 Kriterien als multipel ausgewiesen wird, wäre es eine an Unmöglichkeit grenzende Unwahrscheinlichkeit, dass diese Reflexion dennoch primär sein sollte, und man darf dann von einem lückenlosen und vollständigen Beweis der Multiplizität sprechen. Ein Beispiel dafür ist die Reflexion *CA* in Abb. 2.

Nachdem dann die Existenz multipler Reflexionen in Nordwestdeutschland durch mehrere solcher Beispiele unbezweifelbar belegt ist, erhöht sich die Wahrscheinlichkeit für Multiplizität auch für diejenigen Fälle, bei denen nicht alle 3 Kriterien herangezogen werden können, fast bis zur Gewissheit. So wird man z.B. mit voller Berechtigung von multiplen Reflexionen sprechen dürfen, wenn nur die Kriterien *b* und *c* herangezogen werden können, aber keine Geschwindigkeitsbestimmung vorliegt. Ebenso ist es, wenn Kriterium *c* ausfällt, wie z. B. bei der Reflexion *AB* in Abb. 2. Allerdings könnte in letzterem Fall evtl. noch eine — wenn vielleicht auch nur sehr schwache — primäre Reflexion auf der Multiplen liegen.

Während demnach unbezweifelbar feststeht, dass es in Nordwestdeutschland multiple Reflexionen gibt, ist die Gewissheit über den von den Multiplen durchlaufenen Weg nicht vollkommen. Denn man kann ja prinzipiell nicht ausschliessen, dass die Multiplen auch auf einem anderen als dem jeweils angenommenen Wege entstanden sein könnten. Andererseits aber dürften in den meisten Fällen die Annahmen über den von den Multiplen durchlaufenen Weg doch zutreffen, wenn sich die Beobachtungen mit diesen Annahmen gut erklären lassen, wie es hier der Fall ist. Und wenn es noch andere Wege gäbe, auf denen die Multiplen entstanden sein könnten, so müssten sich diese Wege ja jedenfalls irgendwie mal bemerkbar machen.

Unter diesem Vorbehalt können die bisher in Nordwestdeutschland deutlich beobachteten multiplen Reflexionen folgendermassen typisiert werden:

Sie entstehen auf die in Abb. 3 skizzierte Art durch Reflexionen an zwei beliebigen, im allgemeinen aber guten, Spiegeln und der Oberfläche. Die beiden Spiegel können verschieden (Typ *AB*) oder auch identisch (Typ *AA*) sein. Die Multiplen vom Typ *AB* sind aber — was die Häufigkeit anlangt — gegenüber den Multiplen vom Typ *AA* bevorzugt. Besonders gute Reflektoren sind auch besonders of bei der Erzeugung von multiplen Reflexionen beteiligt.

Die Tatsache, dass die in grossen Teilen Nordwestdeutschlands beobachteten multiplen Reflexionen einem so deutlich umrissenen Typ angehören, legt die Frage nahe, ob dieser Typ auch von der Theorie her zu erwarten ist, oder ob sich da Widersprüche ergeben. Damit beschäftigt sich das nächste Kapitel.

EINIGE ABSCHÄTZUNGEN ÜBER DIE WAHRSCHEINLICHKEIT VON MULTIPLEN REFLEXIONEN

Hier ist zunächst eine Vorbemerkung nötig. Prinzipiell sind zu irgendwelchen Reflektoren auch alle irgend denkbaren Kombinationen von multiplen Reflexionen „möglich", also z.B. alle Dreifach-, Vierfach- und Fünffach-Multiplen und auch solche Multiplen, bei denen die Energie mehrfach zwischen tiefen Reflektoren „pendelt". Ob diese Multiplen tatsächlich auftreten, d. h. ob sie im Seismogramm erkennbar sind, hängt vor allem davon ab, ob sie genügend grosse Amplituden haben, um sich von den primären Reflexionen und von der Störenergie abheben zu können. Und insofern sind alle theoretischen Aussagen über die Amplitudengrösse von multiplen Reflexionen gleichzeitig auch Aussagen über die Wahrscheinlichkeit für das Auftreten dieser multiplen Reflexionen.

Zur Herleitung solcher Aussagen wird man die Amplituden von multiplen Reflexionen mit den Amplituden von zeitgleichen primären Reflexionen bzw. den Amplituden von multiplen Reflexionen verschiedener Typen vergleichen müssen [1]. Das ist einfacher und hat sicher auch mehr allgemeine Gültigkeit als die Betrachtung der Absolutwerte der Amplituden.

Anhand von Abb. 8 wird zunächst die Amplitude einer Multiplen vom Typ *AA* mit der Amplitude einer ihr zeitgleichen primären Reflexion U verglichen. Es soll angenommen werden, dass das Geophon *G* dicht bei dem Schuss S steht, und dass die Reflektoren *A* und *U* horizontal sind; dass also alle Strahlen senkrecht auf den Schichtgrenzen stehen. Vom Schuss *S* möge eine Welle mit der Amplitude *W* ausstrahlen. Diese Welle erleidet auf ihrem Wege Amplitudenverluste, und zwar durch die kugelförmige Ausbreitung,

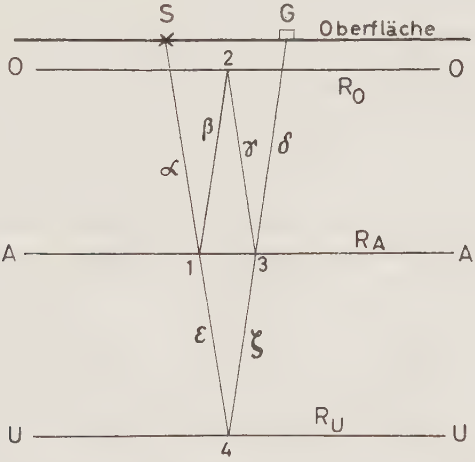

Abb. 8. Skizze zum Vergleich der Amplituden einer Multiplen vom Typ *AA* und einer ihr zeitgleichen primären Reflexion. Comparison of the amplitude of a multiple of type *AA* and of the amplitude of a primary reflection of equal travel-time; schematic diagram.

---

[1] Vgl. auch: Dix (1948)

durch Absorption, durch Streuung und durch Brechung (weil an Unstetigkeitsflächen reflektierte Energie verloren geht). Diese Verluste sollen hier „Laufweg-Amplitudenverluste" genannt und die Verlustfaktoren durch kleine griechische Buchstaben bezeichnet werden. Der Vergleich der Amplituden von AA und U lässt sich so ausführen, dass man zunächst die Laufweg-Amplitudenverluste von den Amplitudenverlusten durch Reflexion bzw. Brechung an den Spiegeln O, A und U trennt und dann die Laufweg-Amplitudenverluste bei der Quotientenbildung herauskürzt.

Auf dem Wege S-1 nimmt die Amplitude auf $W\cdot\alpha$ ab. In 1 erfolgt Reflexion mit dem Reflexionskoeffizienten R_A; die reflektierte Welle hat also über 1 nur noch die Amplitude $w\cdot\alpha\cdot R_A\cdot$ Auf dem Wege 1-2 treten wieder Laufweg-Amplitudenverluste auf, und deshalb beträgt die Amplitude unmittelbar unter 2 nur noch $w\cdot\alpha\cdot R_A\cdot\beta\cdot$ In 2 wird diese Welle mit dem Reflexionskoeffizienten R_O reflektiert, und die reflektierte Welle hat dann nur noch die Amplitude $w\cdot\alpha\cdot R_A\cdot\beta\cdot R_O\cdot$ Schliesslich ergibt sich für die Amplitude der Multiplen AA bei der Ankunft bei dem Geophon G

$$Ampl._{AA}: w\cdot\alpha\cdot R_A\cdot\beta\cdot R_O\cdot\gamma\cdot R_A\cdot\delta) \quad . \; . \; . \; . \; . \; . \; . \quad (5)$$

Analog hierzu ergibt sich für die Amplitude der primären Reflexion U

$$Ampl._U: w\cdot\alpha\cdot(1-R_A)\cdot\varepsilon\cdot R_U\cdot\zeta\cdot(1+R_A\cdot)\,\delta. \quad . \; . \; . \; . \quad (6)$$

Man hat dabei lediglich darauf zu achten, dass der Reflexionskoeffizient bei Spiegel A für die nach unten laufende Welle R_A, für die nach oben laufende Welle aber $-R_A$ beträgt, der Brechungskoeffizient also einmal (1-R_A), das andere Mal $(1+R_A)$. Nachdem man noch die Faktoren geordnet hat, bekommt man für das Verhältnis der Amplituden:

$$\frac{Ampl._{AA}}{Ampl._U} \approx \frac{w\cdot\alpha\cdot\beta\cdot\gamma\cdot\delta\cdot R_O\cdot R_A^2}{w\cdot\alpha\cdot\varepsilon\cdot\zeta\cdot\delta\cdot R_U\,(1-R_A^2)} \quad . \; . \; . \; . \; . \quad (7)$$

Es soll nun angenommen werden, dass die Laufweg-Amplitudenverluste auf dem Wege 1-2-3 ebensogross sind wie auf dem Wege 1-4-3, d. h. dass $\beta\cdot\gamma=\varepsilon\cdot\zeta$ ist. Diese Annahme ist jedenfalls als Erwartungswert (im Sinne der Wahrscheinlichkeitstheorie) berechtigt. Unter dieser Annahme lassen sich die Laufweg-Amplitudenverluste aus dem Quotienten (7) herauskürzen. Da ferner jedenfalls R_A^2 klein gegen 1 ist, darf man (1-R_A^2) durch 1 ersetzen, und damit folgt dann aus (7):

$$\frac{Ampl._{AA}}{Ampl._U} \approx \frac{R_O\cdot R_A^2}{R_U}. \quad . \; . \; . \; . \; . \; . \; . \; . \quad (8)$$

Weil die durch Absorption und Streuung verursachten Amplitudenverluste frequenzabhängig (Born 1941; Ricker 1953) sind, hätte man eigentlich eine Fourierzerlegung durchführen müssen und (7) würde dann nur für die Amplituden im Spektrum und nicht für die Reflexionsamplituden gelten. Dadurch aber, dass bei den hier getroffenen Annahmen die Laufweg-Amplitudenverluste bei der Quotientenbildung herausfallen, wird diese vereinfachte Behandlung hinterher gerechtfertigt.

(8) besagt, dass das Verhältnis der Amplituden von AA und U nur von den Reflexionskoeffizienten abhängt. Die Wahrscheinlichkeit für das Auftreten einer Multiplen AA ist demnach am grössten, wenn der Absolutbetrag von $R_O \cdot R_A$ möglichst gross ist, d. h. wenn $|R_O|$ und $|R_A|$ möglichst gross sind. Das aber bedeutet, dass diejenigen Multiplen AA am wahrscheinlichsten sind, bei denen O die Oberfläche ist und A ein möglichst guter Reflektor.

Es ist nützlich, in (8) für die Reflexionskoeffizienten in der Praxis vorkommende Werte einzusetzen. Mit $|R_O| = 1$ und $|R_A| = |R_U| = 0{,}1$ ergibt sich z.B., dass die Amplitude von AA ein Zehntel der Amplitude von U beträgt — ein Wert, der durchaus plausibel zu sein scheint.

Aber interessanter ist vielleicht die Erweiterung dieser Überlegungen auf Dreifach-, Vierfach- und Fünffach-Multiple. Vergleicht man nämlich die Amplitude einer Dreifach-Multiplen vom *Typ AAA* mit der Amplitude einer ihr zeitgleichen primären Reflexion U, so ergibt sich analog zu der oben durchgeführten Ableitung:

$$\frac{Ampl._{AAA}}{Ampl._{U}} \approx \frac{R_O \cdot R_A^3}{R_U} \quad \text{. . . . .} \quad (6)$$

Trägt man hier wieder die Werte $|R_O| = 1$ und $|R_A| = |R_U| = 0{,}1$ ein, so findet man, dass die Amplitude von AAA nur ein Hundertstel der Amplitude von U beträgt. Bei Vierfach-Multiplen hat man im Zähler von (9) noch mit $R_O \cdot R_A$ zu multiplizieren, und die Amplitude einer Multiplen vom Typ $AAAA$ beträgt nur ein Tausendstel der Amplitude von U. Bei Fünffach-Multiplen ist die entsprechende Zahl 1/10 000.

Daraus folgt, dass Dreifach-, und erst recht Vierfach- und Fünffach-Multiple vom Typ AAA usw. sehr unwahrscheinlich sind.

In Abb. 9 wird die Amplitude einer Multiplen vom Typ AB mit der Amplitude einer ihr ungefähr zeitgleichen Multiplen vom Typ AA verglichen. Dabei sind A und B zwei dicht übereinanderliegende Reflektoren. Hier (und auch im nächsten Kapitel) müssen die beiden Komponenten von AB getrennt behandelt werden. Unter der Komponente $\mathfrak{AB}$ der Multiplen AB soll diejenige Komponente verstanden werden, die erst nach A und dann nach B läuft, unter $\mathfrak{BA}$ diejenige Komponente, die erst nach B und dann nach A läuft.

Die Laufweg-Amplitudenverluste brauchen nicht berücksichtigt zu werden,

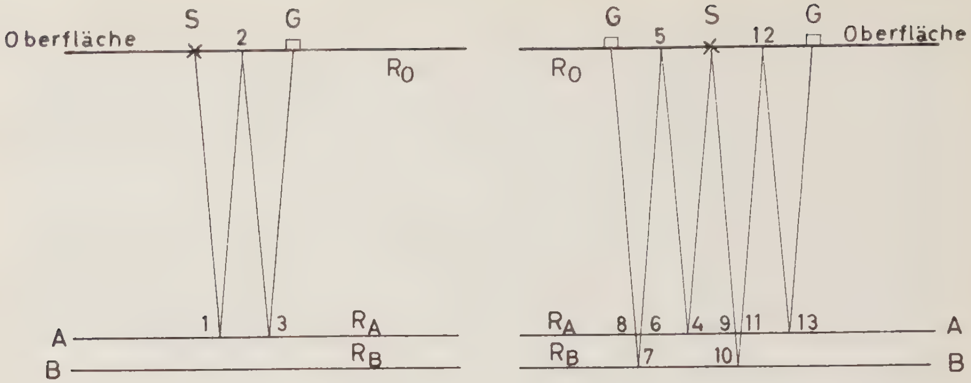

Abb. 9. Skizze zum Vergleich der Amplituden von Multiplen des Typs *AA* mit Multiplen des Typs *AB*. Comparison of the amplitudes of multiple reflections of type *AA* and of type *AB*; schematic diagram

weil sie bei der Quotientenbildung herausfallen. Für die Amplitude der Multiplen *AA* bekommt man dann:

$$Ampl._{AA}: W\cdot \overset{1}{R_A}\cdot \overset{2}{R_O}\cdot \overset{3}{R_A} \quad . \; . \; . \; . \; . \; . \; . \; . \; . \; . \quad (10)$$

(Die Zahlen über den Reflexionskoeffizienten beziehen sich auf die Zahlen in Abb. 9). Für die Amplituden der Komponenten $\mathfrak{AB}$ bzw. $\mathfrak{BA}$ erhält man:

$$Ampl._{\mathfrak{AB}}: W\cdot \overset{4}{R_A}\cdot \overset{5}{R_O}\cdot \overset{6}{(1-R_A)}\cdot \overset{7}{R_B}\overset{8}{(1+R_A)} \quad . \; . \; . \; . \; . \quad (11)$$

$$Ampl._{\mathfrak{BA}}: W\cdot \overset{9}{(1-R_A)}\cdot \overset{10}{R_B}\cdot \overset{11}{(1+R_A)}\cdot \overset{12}{R_O}\cdot \overset{13}{R_A}\,.$$

Die Multiple *AB* ist die Summe der Komponenten $\mathfrak{AB}$ und $\mathfrak{BA}$, und deshalb folgt schliesslich für das Verhältnis der Amplituden:

$$\frac{Ampl._{AB}}{Ampl._{AA}} \approx \frac{2\cdot W\cdot R_O\cdot R_A\cdot R_B\cdot (1-R_A^2)}{W\cdot R_O\cdot R_A\cdot R_A} \approx \frac{2R_B}{R_A}\,. \quad . \; . \quad (12)$$

Wenn die beiden Reflektoren *A* und *B* nicht dicht übereinanderliegen, sind zwar die Laufweg-Amplitudenverluste bei der Multiplen *AB* und der Multiplen *AA* verschieden gross, aber dieser Unterschied wird ja — ebenso wie das Absinken des Amplitudenpegels bei den primären Reflexionen — durch die Zunahme der Verstärkung in der seismischen Apparatur annähernd ausgeglichen. Diese einschränkende Voraussetzung darf man also fallen lassen. Weiter ist anzumerken, dass (12) auch dann gilt, wenn B über A liegt.

Wenn *B* ein halb so guter Reflektor ist wie *A*, wenn also gilt $R_B = \frac{1}{2} R_A$, ist nach (12) die Amplitude von *AB* ebenso gross wie die Amplitude von *AA*.

Weiter folgt aus (12) für alle Reflektoren X, für die gilt $R_X > \frac{1}{2} R_A$, dass die Amplitude der Multiplen AX grösser ist als die Amplitude der Multiplen AA. Betrachten wir nun irgendeinen reflexionsseismischen Profilschnitt, z. B. Abb. 2. Zu jedem der Reflektoren, z. B. zu A, gibt es im allgemeinen mehrere Reflektoren X, für die gilt $R_X > \frac{1}{2} R_A$. Nach dem Vorhergehenden gibt es also im allgemeinen zu jedem Reflektor A mehrere multiple Reflexionen AX, deren Amplitude grösser zu erwarten ist als die Amplitude von AA, d. h. deren Auftreten wahrscheinlicher ist als das Auftreten von AA. Das aber bedeutet, dass in der Häufigkeit ihres Auftretens eine Bevorzugung der Multiplen vom Typ AB gegenüber den Multiplen vom Typ AA zu erwarten ist.

Auch hier ist wieder eine Erweiterung dieser Überlegungen auf Dreifach-, Vierfach-, . . . -Multiple interessant. Bei *zwei* verschiedenen *gleich guten* Reflektoren A und B gibt es *zwei* verschiedene Wege für multiple Reflexionen an A und B. Die Multiple AB setzt sich aus *zwei* Komponenten zusammen (𝔄𝔅 und 𝔅𝔄), und ihre Amplitude ist nach (12) doppelt so gross wie die Amplitude von AA oder BB. Betrachtet man anstelle der zwei Reflektoren deren *drei*, so kann man sich überlegen, dass es dann *sechs* verschiedene Wege für Multiple an A, B und C gibt. Die Multiple ABC setzt sich aus *sechs* Komponenten zusammen (𝔄𝔅ℭ, 𝔄ℭ𝔅, 𝔅𝔄ℭ, 𝔅ℭ𝔄, ℭ𝔄𝔅 u. ℭ𝔅𝔄), und ihre Amplitude ist sechsmal so gross wie die Amplitude von AAA, BBB oder CCC. Bei vier verschiedenen Reflektoren tritt anstelle der Zahl 6 die Zahl 24, bei 5 Reflektoren die Zahl 120. Und daraus folgt dann wieder, dass Dreifach- und Vierfach-Multiple — falls sie überhaupt auftreten — wahrscheinlich bevorzugt dem „gemischten" Typ ABC bzw. $ABCD$ angehören werden. Ausserdem ist das eine, wenn auch nicht relevante, Abschwächung der oben besprochenen Unwahrscheinlichkeit von Dreifach-, Vierfach-, . . . Multiplen.

Aus diesen Abschätzungen geht hervor, dass 1. Zweifach-Multiple viel wahrscheinlicher sind als Dreifach-, Vierfach-, . . . -Multiple; dass 2. diejenigen Zweifach-Multiplen bevorzugt sind, bei denen die Oberfläche (oder evtl. auch die Basis der Verwitterungsschicht) der obere Reflektor ist; und dass 3.multiple Reflexionen vom Typ AB häufiger zu erwarten sind als multiple Reflexionen vom Typ AA. Das aber bedeutet, dass die in Nordwestdeutschland beobachteten, auf Seite 13 typisierten multiplen Reflexionen den nach der Theorie wahrscheinlichsten Typ darstellen.

Die Abschätzungen sind allerdings ziemlich grob. Z.B. bedeutet der Vergleich der Amplituden von multiplen Reflexionen mit den Amplituden von zeitgleichen primären Reflexionen eigenlich eine Beschränkung auf diejenigen multiplen Reflexionen, die in Teufenbereiche fallen, aus denen auch primäre Reflexionen kommen. Aber andererseits sind das ja auch wohl die interessantesten und wichtigsten Fälle. Ausserdem ist eigentlich nur von kleinen Reflexionskoeffizienten, wie sie normalerweise in Sedimenten vorkommen, die

Rede gewesen. Deshalb erfordern z.B. die in der Literatur bisweilen erwähnten multiplen Reflexionen von fossilen Basaltdecken eine gewisse Modifizierung dieser Überlegungen. Aber am einschneidendsten ist sicherlich die bei der Ableitung von (8) eingebaute Voraussetzung, dass die Laufweg-Amplitudenverluste in den verschiedenen Teufenbereichen identisch sind. Diese Annahme dürfte zwar als Erwartungswert zutreffen, aber die tatsächlichen Abweichungen von diesem Erwartungswert sind doch sicher ganz erheblich gross. Man muss sogar vermuten, dass diese Abweichungen – neben der Beschaffenheit der Oberflächenschicht und evtl. neben der Grösse der Reflexionskoeffizienten – einen wesentlichen bedingenden Faktor für das Auftreten von multiplen Reflexionen darstellen. Möglicherweise haben sie sogar ausschlaggebende Bedeutung. Wenn nämlich in einem Gebiet die relativen Amplitudenverluste durch Brechung, Absorption und Streuung (bezogen auf gleiche Laufzeit-Intervalle) mit der Tiefe zunehmen (d. h. wenn die spezifischen Verlustfaktoren α, β . . . mit zunehmender Tiefe kleiner werden, d. h. wenn im allgemeinen $\varepsilon \zeta < \beta \gamma$ ist), so folgt aus (7), dass dann multiple Reflexionen begünstigt werden. Wenn umgekehrt die spezifischen Amplitudenverluste mit der Tiefe abnehmen, resultiert eine gewisse Unterdrückung der multiplen Reflexionen. Aber ebenso wie danach aus der Verteilung der spezifischen Amplitudenverluste eine *regionale* Betonung oder Abschwächung der multiplen Reflexionen resultiert, können auch Besonderheiten in dem funktionalen Zusammenhang zwischen Teufe und spezifischem Amplitudenverlust in bestimmten *Teufenbereichen* eine Begünstigung oder Benachteiligung der multiplen Reflexionen verursachen. Während die spezifischen Amplitudenverluste evtl. eine ausschlaggebende Bedeutung für das *Auftreten* von multiplen Reflexionen haben können, ist nach Ansicht des Verfassers ihr Einfluss auf die Multiplen-*Typen* nicht so entscheidend. Aber diese Zusammenhänge müssten erst noch genauer untersucht werden.

ZUR GEOMETRIE DER MULTIPLEN VOM TYP AB

Angesichts des Überwiegens der Multiplen vom Typ *AB* in Nordwestdeutschland ist es naheliegend, dass man sich auch die „geometrischen" Zusammenhänge bei diesem Typ näher ansieht. Wie jetzt ausgeführt werden soll, stellt sich dabei heraus, dass man im allgemeinen mit Interferenzen zwischen den beiden Komponenten von *AB* rechnen muss.

Abb. 10 zeigt links die Konstruktion des Laufweges der Komponente 𝔅𝔄, rechts die Konstruktion des Laufweges der Komponente 𝔄𝔅. Es soll – wie bei solchen Konstruktionen üblich – vorausgesetzt werden, dass das Profil senkrecht zum Schichtstreichen verläuft, und dass eine gleichförmige Oberflächenschicht vorhanden ist; ferner sollen Brechungen vernachlässigt werden.

Zur Konstruktion des Laufweges der Komponente $\mathfrak{B}\mathfrak{A}$ muss man zunächst den Spiegel A an der Oberfläche spiegeln (A^x), dann muss man den Schuss S an B spiegeln (S^o) und das Geophon G an A^x (G^x). $\overline{G^x\text{-}S^o}$ ist die Länge des Laufweges der Komponente $\mathfrak{B}\mathfrak{A}$. Den Laufweg selbst bekommt man durch mehrfaches umklappen von Teilen der Strecke $\overline{G^x\text{-}S^o}$. Die Konstruktion des Laufweges der Komponente $\mathfrak{A}\mathfrak{B}$ verläuft ganz ähnlich; der Unterschied gegen die Konstruktion von $\mathfrak{B}\mathfrak{A}$ besteht lediglich darin, dass man jetzt den Schuss an A^x zu spiegeln hat und das Geophon an B. Aus dieser Konstruktion lässt sich die Differenz der Laufzeiten der Komponenten $\mathfrak{A}\mathfrak{B}$ und $\mathfrak{B}\mathfrak{A}$ herleiten. Dabei werden die Fallwinkel positiv gezählt, wenn die Spiegel in der (willkürlich gewählten) $+ x$ — Richtung fallen; negativ, wenn sie in der $+ x$ — Richtung steigen. Mit den Bezeichnungen aus Abb. 10 gilt dann für die Länge $S_{\mathfrak{A}\mathfrak{B}}$ des Laufweges der Komponente $\mathfrak{A}\mathfrak{B}$:

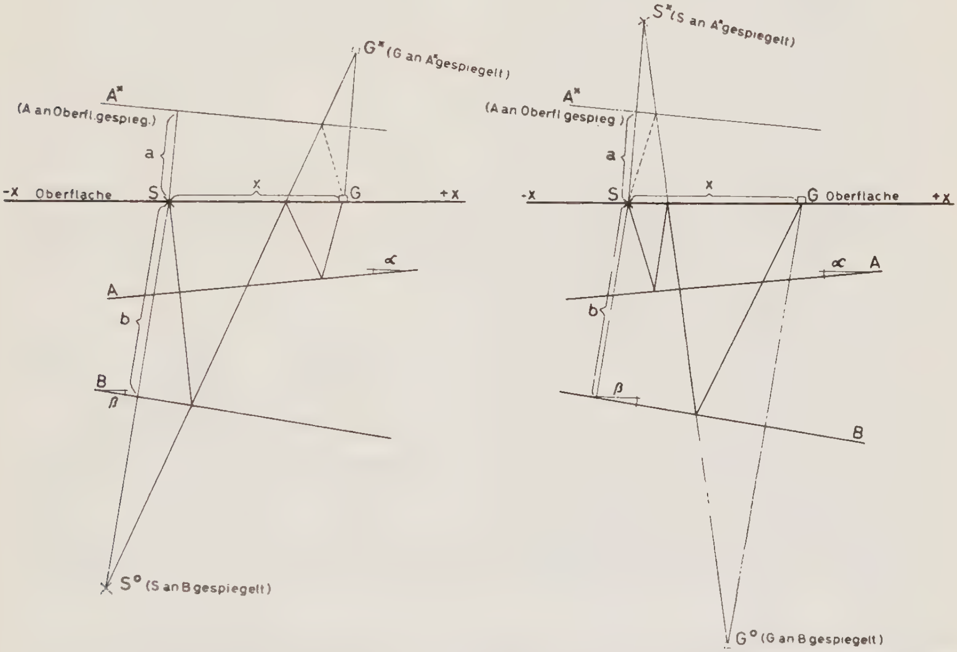

Abb. 10. Geometrische Konstruktion der Laufwege der Komponenten $\mathfrak{B}\mathfrak{A}$ (links) und $\mathfrak{A}\mathfrak{B}$ (rechts) Construction of ray paths for components $\mathfrak{B}\mathfrak{A}$ (left) and $\mathfrak{A}\mathfrak{B}$ (right).

$$S^2_{\mathfrak{A}\mathfrak{B}} = [2\,(b + x\sin\beta)\cos\beta + 2a\cos\alpha]^2 + [x - 2\,(b + x\sin\beta)\sin\beta + 2\,\alpha\sin\alpha]^2. \quad (13)$$

Für die Länge $S_{\mathfrak{B}\mathfrak{A}}$ des Laufweges der Komponente $\mathfrak{B}\mathfrak{A}$ ergibt sich:

$$S^2_{\mathfrak{B}\mathfrak{A}} = [2b\cos\beta + 2\,(a + x\sin\alpha)\cos\alpha]^2 + [\mathrm{x} + 2\,b\sin\beta - 2\,(a + x\sin\alpha)\sin\alpha]^2. \quad (14)$$

Nach einer Reihe von elementaren Umformungen folgt aus (13) und (14) für die Differenz der Laufweg-Quadrate:

$$S^2_{\mathfrak{A}\mathfrak{B}} - S^2_{\mathfrak{B}\mathfrak{A}} = 8\,x \cos(\alpha + \beta)\,[a \sin\beta - b \sin\alpha]\,. \quad . \quad . \quad . \quad (15)$$

Sei $S_{\mathfrak{A}\mathfrak{B}} = S_{\mathfrak{B}\mathfrak{A}} + \Delta S$. ΔS ist klein gegen $S_{\mathfrak{A}\mathfrak{B}}$ und $S_{\mathfrak{B}\mathfrak{A}}$, und deshalb gilt mit guter Näherung

$$S^2_{\mathfrak{A}\mathfrak{B}} - S^2_{\mathfrak{B}\mathfrak{A}} = 2\,\Delta S \cdot S_{\mathfrak{B}\mathfrak{A}} + \overset{2}{\Delta} S \approx 2\,\Delta S \cdot S_{\mathfrak{B}\mathfrak{A}}.$$

Damit folgt dann aus (15)

$$\Delta S \approx \frac{4\,x}{S_{\mathfrak{B}\mathfrak{A}}} \cos(\alpha + \beta)\,[\mathrm{a} \sin\beta - b \sin\alpha] \quad . \quad . \quad . \quad . \quad . \quad (16)$$

oder auch

$$\Delta S \approx \frac{2\,x}{(\mathrm{a} + \mathrm{b})} \cos(\alpha + \beta)\;[a \sin\beta - b \sin\alpha]. \quad . \quad . \quad . \quad . \quad . \quad (17)$$

Mit v als Durchschnittsgeschwindigkeit folgt schliesslich für die Differenz der Laufzeiten der Komponenten $\mathfrak{A}\mathfrak{B}$ und $\mathfrak{B}\mathfrak{A}$:

$$\Delta t_i = t_{\mathfrak{A}\mathfrak{B}} - t_{\mathfrak{B}\mathfrak{A}} \approx \frac{2\,x}{v\,(a + b)} \cos(\alpha + \beta)\,[a \sin\beta - b \sin\alpha]. \quad . \quad . \quad (18)$$

Das ist die Interferenzformel für multiple Reflexionen vom Typ *AB*. Ihr wichtigster Inhalt ist die Linearität in x, dem Abstand Schuss — Geophon. Mit zunehmender Entfernung vom Schuss wachsen die Laufzeitunterschiede. Für $x = 0$, d. h. bei den schussnahen Geophonen, ist die Laufzeitdifferenz Null; hier tritt also immer konstruktive Interferenz auf. Die Laufzeitdifferenzen sind besonders gross, wenn α und β verschiedene Vorzeichen haben, d. h. wenn die Spiegel *A* und *B* Gegenneigung haben. Bei horizontaler Lagerung, $\alpha = \beta = 0$, tritt immer konstruktive Interferenz auf.

Es kann hier darauf verzichtet werden, in die Beziehung (18) für die unbestimmten Grössen bestimmte Zahlen einzusetzen, weil die konstruierten Beispiele in den Abbildungen 11 — 14 schon einen Eindruck von der Grössenordnung der zu erwartenden Laufzeitdifferenzen vermitteln. In diesen Abbildungen werden (ausser den Profilschnitten mit je zwei Strahlengängen) die Laufzeiten und Schwingungsbilder so dargestellt, wie sie beim Gegenschiessen in den Seismogrammen aussehen müssten. Als Durchschnittsgeschwindigkeit wurden durchweg 2000 *m*/sec. verwendet. Als Schwingungsbild der Komponenten wurde das bei Anstey (1956, Abb. 2, 2.Zeile) abgebildete Schwingungsbild einer mit einem mässig breiten Filterband aufgenommenen symmetrischen Ricker-Wavelet (Ricker 1953) genommen. In Abb. 11 beträgt der Laufzeit-unterschied Δt_i, zwischen den beiden Komponenten bei den Aussenspuren 48 *m*sec, bei Abb. 12 24 *m*sec, bei Abb. 13 16 *m*sec und bei Abb. 14 8 *m*sec.

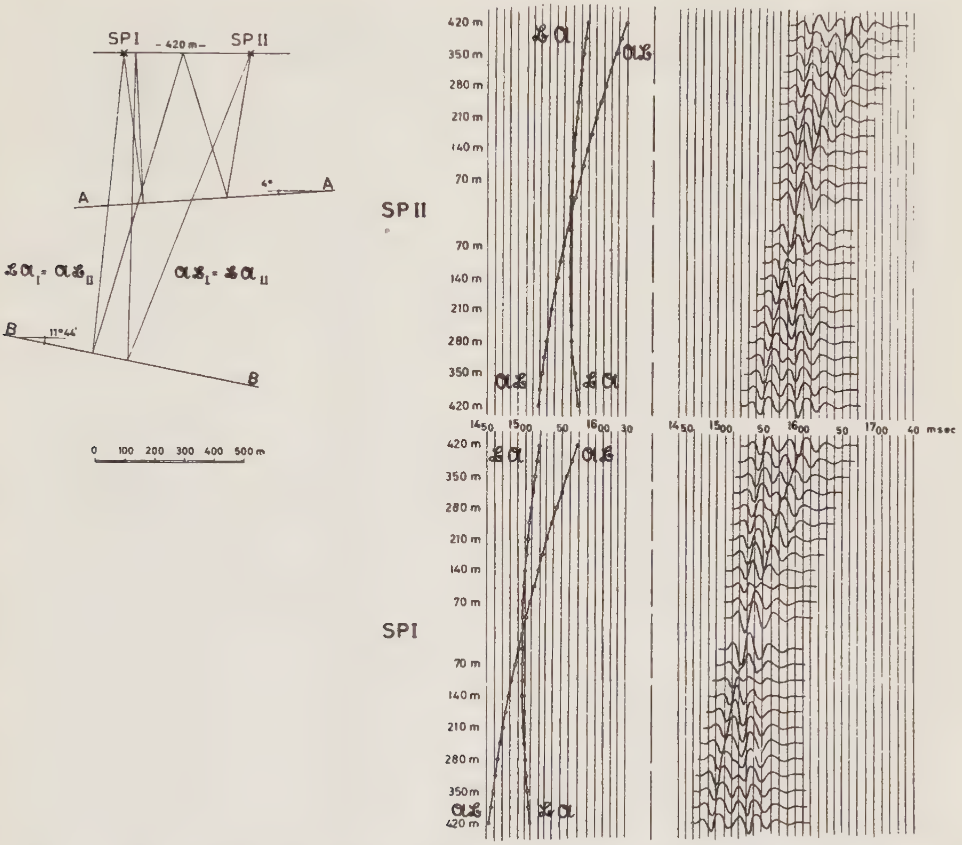

Abb. 11. Interferenzen der Komponenten 𝔄𝔅 und 𝔅𝔄. erstes (konstruiertes) Beispiel.
Interferences between components 𝔄𝔅 and 𝔅𝔄; first (constructed) example.

In den Laufzeitdarstellungen ist zu erkennen, wie die Laufzeiten der beiden Komponenten mit zunehmender Entfernung vom Schuss auseinanderspreizen. Weiter sieht man, dass immer die Komponente 𝔄𝔅 mit der Komponenten 𝔅𝔄 korreliert und die Komponente 𝔅𝔄 mit der Komponenten 𝔄𝔅. Die Laufzeiten der beiden Komponenten bilden also so etwas wie einen Reigen über die Seismogramme hin. Dasselbe ist auch an den Strahlengängen zu erkennen. Es ist nämlich immer der Laufweg der Komponente 𝔄𝔅 bei dem einen Schusspunkt mit dem Laufweg der Komponente 𝔅𝔄 des Nachbarschusspunktes identisch.

Die Schwingungsbilder zeigen destruktive Interferenz, wenn das Δt_i, ungefähr gleich der Hälfte der (vorherrschenden) Reflexionsperiode ist. In

Abb. 11 tritt das schon bei 105 m Entfernung vom Schuss ein; bei den Aussenspuren in dieser Abbildung ist das Δt_i so gross, dass die beiden Komponenten nahezu getrennt sind. In Abb. 12 tritt bei ungefähr 210 m Entfernung vom Schuss destruktive Interferenz, bei den schussfernen Spuren dann wieder

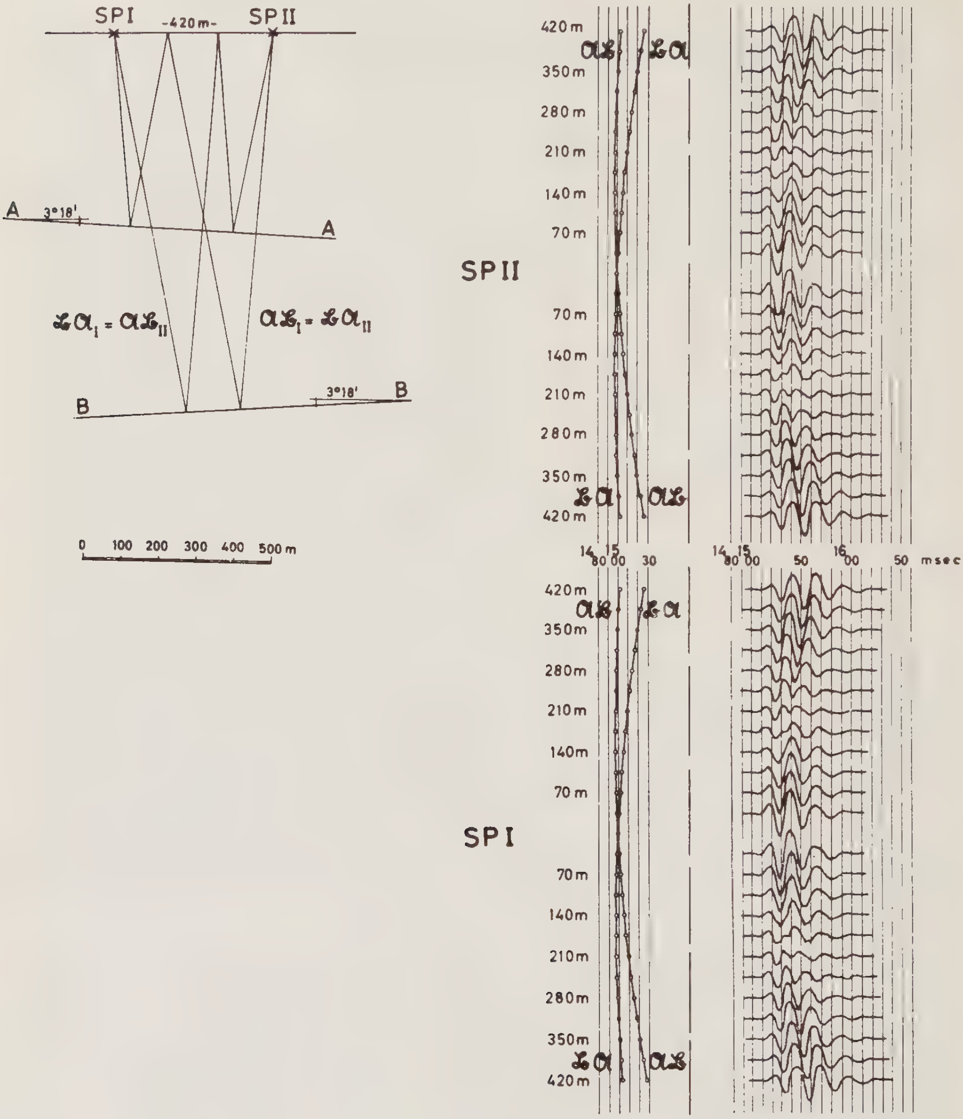

Abb. 12. Interferenzen der Komponenten 𝔄𝔅 und 𝔅𝔄, zweites (konstruiertes) Beispiel
Interferences between components 𝔄𝔅 and 𝔅𝔄, second (constructed) example

zunehmend konstruktive Interferenz auf. Ähnlich ist es in Abb. 13. In Abb. 14 kommt die destruktive Interferenz noch nicht richtig zur Entfaltung; hier

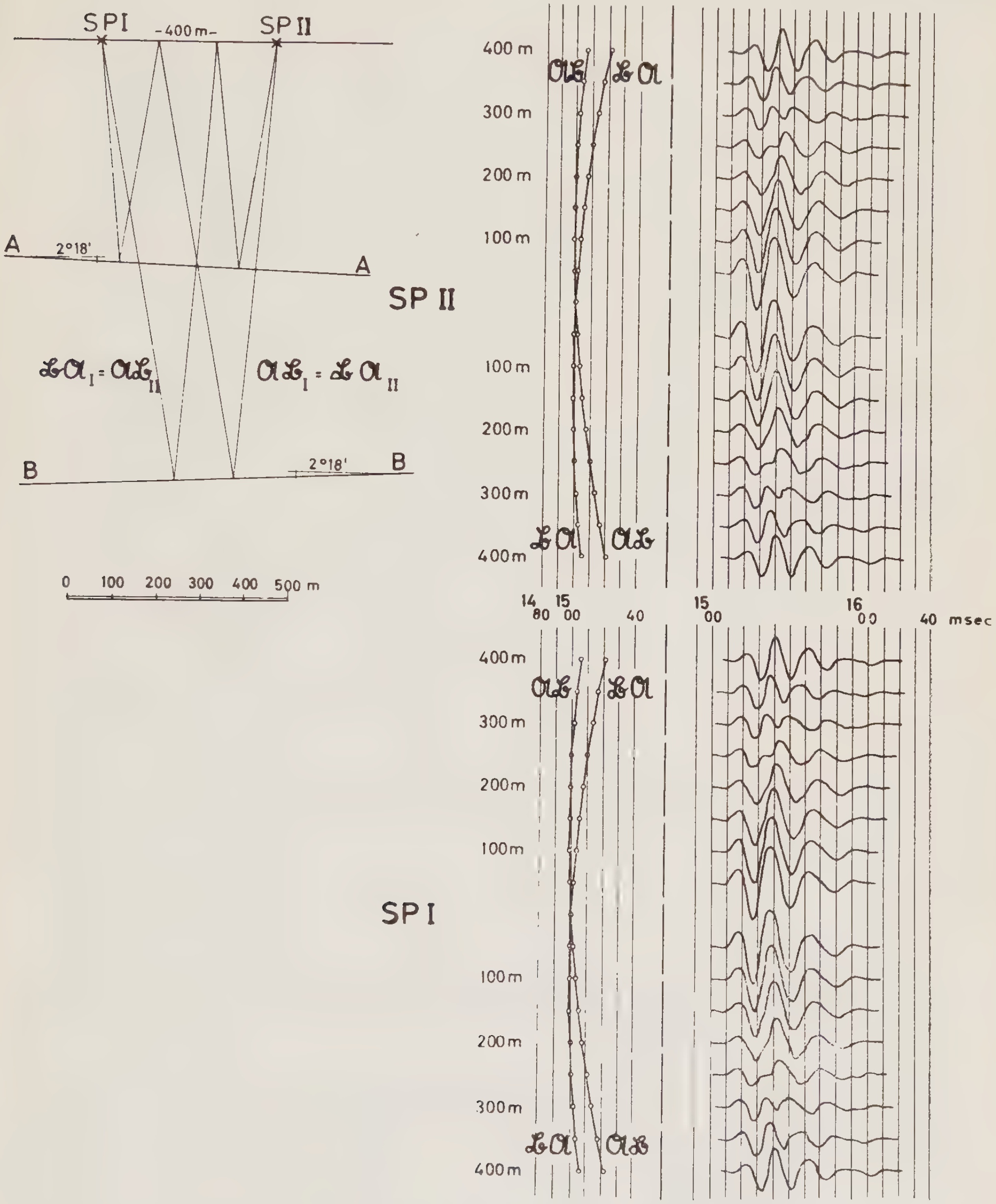

Abb. 13. Interferenzen der Komponenten 𝔄𝔅 und 𝔅𝔄, drittes (konstruiertes) Beispiel.
Interferences between components 𝔄𝔅 and 𝔅𝔄; third (constructed) example

ist bei den Aussenspuren lediglich eine Amplitudenverkleinerung vorhanden.

Die Interferenzen verursachen auch eine Mehrdeutigkeit bei der Verfolgung der einzelnen Phasen der Reflexionen. Verfolgt man in Abb. 12 die Reflexion von den Aussenspuren zu den schussnahen Spuren, so findet man, dass das erste kräftige Tal und auch das zweite in das erste grosse Tal bei den Innenspuren hineinlaufen. In Abb. 11 laufen sogar drei Täler der Aussenspuren in dasselbe Tal der Innenspuren hinein.

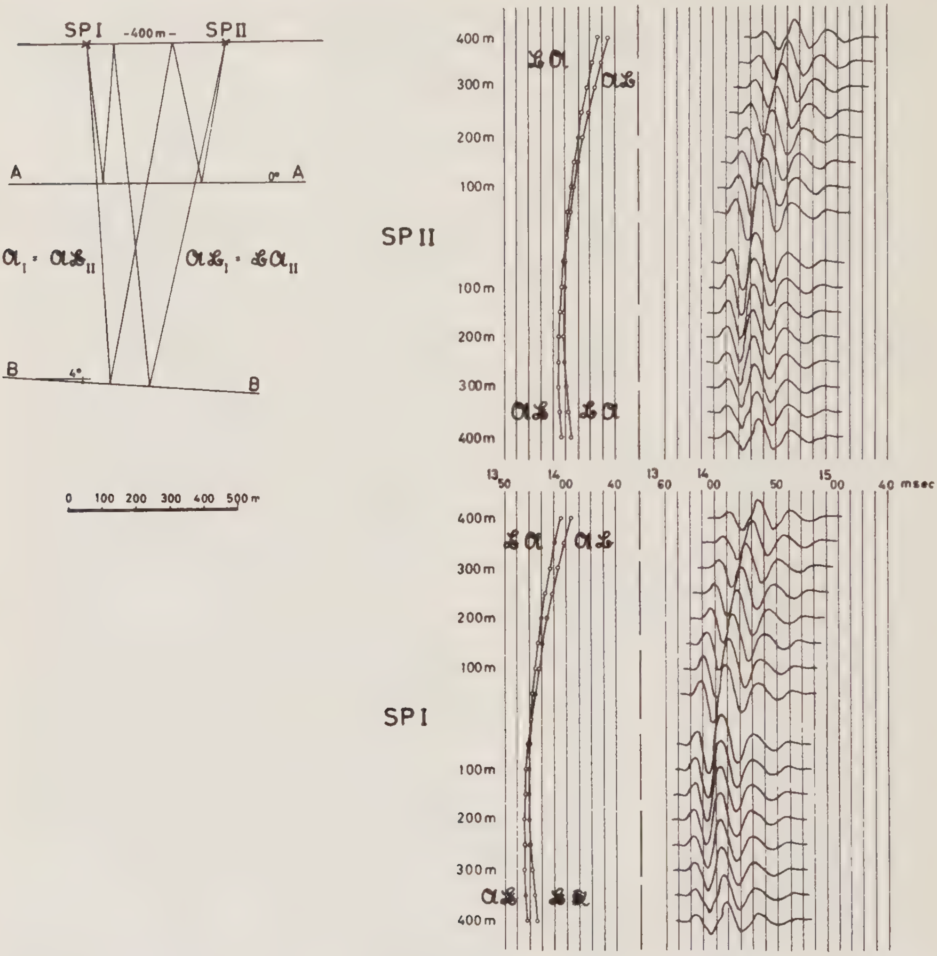

Abb. 14. Interferenzen der Komponenten 𝔄𝔅 und 𝔅𝔄, viertes (konstruiertes) Beispiel.
Interferences between components 𝔄𝔅 and 𝔅𝔄; fourth (constructed) example

Die Laufzeitunterschiede zwischen den beiden Komponenten der Multiplen vom Typ *AB* bedingen auch eine Problematik bei der Geschwindigkeitsbestimmung aus Reflexionsaufnahmen. Aus Abb. 10 ist zu erkennen, dass sich bei der t- Δt- Geschwindigkeitsbestimmung (und auch bei der x^2-t^2-Methode) bei der Verwendung von split spreads für *jede der beiden Komponenten* 𝔄𝔅 und 𝔅𝔄 die richtige Geschwindigkeit ergeben muss. Und zwar sieht man das, wenn man in Abb. 10 das Geophon ,,wandern'' lässt. Daraus folgt, dass man die richtige Geschwindigkeit bekommt, wenn man z. B. in Abb. 12 bei *SP* I die Laufzeiten der Komponente 𝔄𝔅 nimmt, d. h. wenn man bei der oberen Richtung das erste Reflexionstal nimmt, bei der unteren Richtung aber von dem ersten Reflexionstal bei den Innenspuren zu dem zweiten Tal bei der Aussenspur korreliert. Noch deutlicher ist das bei Abb. 11. Nimmt man dagegen durchweg das erste Tal, so resultiert eine viel zu grosse Geschwindigkeit.

Wenn man zur Geschwindigkeitsbestimmung aber nicht split spreads nimmt, sondern — wie allgemein üblich — gegengeschossene end shots, so werden die Schwierigkeiten noch grösser. Um annähernd die richtige Geschwindigkeit zu bekommen, müsste man z.B. in Abb. 12 bei SP I das Δt der Komponente 𝔄𝔅 nehmen und bei *SP* II ebenfalls das Δt der Komponente 𝔄𝔅. Diese Komponenten korrelieren aber nicht bei den Aussenspuren. Nimmt man in Abb. 12 durchweg das erste Tal, so resultiert eine viel zu grosse Geschwindigkeit; nimmt man dagegen bei *SP* I und *SP* II das Δt, das sich ergibt, wenn man von dem zweiten Tal bei den Aussenspuren zu dem ersten Tal bei den Innenspuren korreliert, so resultiert eine viel zu kleine Geschwindigkeit. Bei Abb. 11 resultiert sogar eine imaginäre Geschwindigkeit, wenn man durchweg das erste Tal zur t- Δt- Geschwindigkeitsbestimmung verwendet. Die annähernd richtige Geschwindigkeit ergibt sich auch dann, wenn man überall die Laufzeiten der beiden Komponenten mittelt. Das ist z. B. in Abb. 14 ,,automatisch'' verwirklicht. Denn hier ist das Δt_i der Aussenspuren kleiner als die Hälfte der Periode, und dabei überlagern sich die beiden Komponenten so, dass die resultierenden Berge und Täler gerade in der Mitte liegen. In anderen Fällen musste man sich in der Praxis so behelfen, dass man die Δt aus allen vorhandenen Bergen und Tälern mittelt.

Angesichts der beobachteten Häufigkeit der Multiplen vom Typ *AB* und angesichts des theoretischen Resultates, dass man in der Mehrzahl der in der Praxis vorkommenden Fälle mit merklichen Interferenzerscheinungen der beiden Komponenten der Multiplen *AB* rechnen muss, wird man denken, dass man diese Interferenzerscheinungen mit als Kriterium für das Erkennen von multiplen Reflexionen heranziehen könnte (und also auch die oben beschriebenen Geschwindigkeitsanomalien geradezu zur Identifizierung von multiplen Reflexionen ausnutzen könnte). Ausserdem legen diese Interferenzen noch eine andere Vermutung nahe. Es ist in vielen Gebieten beobachtet worden, dass die Seismogramme von kurzen ($\approx$ 200 m langen) Geophonaufbauten besser aussehen als die Seismogramme von längeren ($\approx$ 400 *m* langen) Geophonaufbauten. Es lässt sich eine ganze Reihe von Ursachen für diese Erschein ur aufzählen, aber man könnte nun denken, dass auch diese Interferenzen mit als Ursache infrage kommen. Denn nach (18) wachsen die Laufzeitunterschiede zwischen den beiden Komponenten von *AB* mit zunehmender Entfernung vom Schuss, d. h. mit zunehmender Entfernung ist immer mehr mit destruktiver Interferenz zu rechnen. Und es wäre nun möglich, dass oftmals das schlechtere Aussehen der Seismogramme von längeren Aufbauten mit dadurch bedingt ist, dass die Multiplen vom Typ *AB* zu den Aussenspuren hin durch destruktive Interferenz zerstört werden.

Aber mit diesen Vermutungen muss man doch wohl sehr vorsichtig sein. Denn die Interferenzen sind in der Praxis nicht so gut zu erkennen wie bei den konstruierten Beispielen, weil immer auch Interferenzen mit Störenergie oder mit primären Reflexionen vorkommen, die man schlecht von den Interferenzen der Multiplen-Komponenten unterscheiden kann. Und ausserdem sind die Interferenzerscheinungen vielleicht doch nicht so häufig wie man das zunächst erwarten möchte. Z. B. hat Verfasser unter den ihm bekannten Routine-Messungen noch kein *einwandfreies* Beispiel für diese Interferenzen finden können. Man möchte aber erwarten, dass die Interferenzerscheinungen bei sehr langen (> 800 m) Geophonaufbauten, also z.B. bei Langstreckengeschwindigkeitsmessungen, besser zu erkennen sind und dann evtl. auch zur Identifizierung von multiplen Reflexionen ausgenutzt werden können.

Verf. dankt der Gewerkschaft Brigitta für die freundliche Zurverfügungstellung der Abb. 2 und 4 und der Mobil Oil AG. für die Erlaubnis zur Veröffentlichung dieser Arbeit und für die Unterstützung bei ihrem Zustandekommen.

LITERATUR

ANSTEY, N. A., 1956, Instrumental Distortion and the Seismic Record, Geophysical Prospecting IV, 1, pp. 37-55.

BORN, W. T., 1941, The Attenuation Constant of Earth Materials, Geophysics VI, 2, pp. 132-148.

DIX, C. H., 1948, The Existence of Multiple Reflections, Geophysics XIII, 1, pp. 49-50.

——, 1952, Seismic Prospecting for Oil, New York, Harper and Brothers.

——, 1955, Seismic Velocities from Surface Measurements, Geophysics XX, 1, pp. 68-86.

DÜRBAUM, H., 1954, Zur Bestimmung der Wellengeschwindigkeiten aus reflexionsseismischen Messungen, Geophysical Prospecting II, 2, pp. 151-167.

ELLSWORTH, T. P., 1948, Multiple Reflections, Geophysics XIII, 1, pp. 1-18.

GARDNER, L. W., 1947, Vertical Velocities from Reflection Shooting, Geophysics XII, 2, pp. 221-228.

GREEN, C. H., 1938, Velocity Determinations by Means of Reflection Profiles, Geophysics III, 4, pp. 295-305.

HANSEN, R. F., 1947, A New System of Seismic Reflection Profiles, Boletin Inform. Petroleras, Buenos Aires, Vol. 24, pp. 237-247.

——, 1948, Multiple Reflections of Seismic Energy, Geophysics XIII, 1, pp. 58-85.

KREY, TH., 1951, An Approximate Correction Method for Refraction in Reflection Seismic Prospecting Geophysics, XVI, 3, pp. 468-485.

——, 1954, Bemerkung zu einer Formel für Geschwindigkeitsbestimmungen aus seismischen Messungen von C. A. Dix, Erdöl und Kohle 7, S. 8-9.

PFLUEGER, J. C., 1954, Delta-T Formula for Obtaining Average Seismic Velocity to a Dipping Reflecting Bed. Letter to the Editor, Geophysics XIX, 2, pp. 339-341.

RICKER, N., 1953, The Form and Laws of Propagation of Seismic Wavelets, Geophysics XVIII, 1, pp. 10-40.

ROMBERG, F., 1941, The Probable Errors of Delta-T Velocities, Geophysics VI, 4, pp. 356-369.

SAVIT, C. H., 1951, Routine Delta-T Analysis for Field Use, Geophysics XVI, 3, p. 562 (Abstract).

SLOAT, J., 1948, Identification of Echo Reflections, Geophysics XIII, 1, pp. 27-35.

STEELE, W. E., Jr., 1941, Comparison of Well Survey and Reflection "Time-Delta Time" Velocities, Geophysics VI, 4, pp. 370-377.

SWAN, B. G., and BECKER, A., 1952, Comparison of Velocities Obtained by Delta-Time Analysis and Well Velocity Surveys, Geophysics XVII, 3, pp. 575-585.

ZUR MÜHLEN, W. VON, and TUCHEL, G., 1953, A Study of Well Velocity Data in North West Germany, Geophysical Prospecting I, 3, pp. 159-170.

DISKUSSION

J. Lohr: Gilt die exakte Bestimmung von multiplen Reflexionen in gleichen Massen für geneigte Horizonte wie für horizontale?

R. Bortfeld: Ja, die Neigung der Schichtgrenzen bereitet keine Schwierigkeiten.

H. A. Rühmkorf: Haben Sie auch multiple Reflexionen vom W-Typ beobachtet?

R. Bortfeld: Nein.

H. A. Rühmkorf: Ich stellte diese Frage, weil wir in einer grossen Fülle von Material im nördlichen Belgien ebenfalls den AB-Typ als den vorherrschenden festgestellt haben. Der W-Typ wurde gesucht und nur in wenigen und vereinzelten Seismogrammen den Laufzeiten nach als möglich gefunden.

Als durchlaufend korrelierend wie der AB- oder AA-Typ wurde die W-Form nicht sicher erkannt.

Th. Krey: Zur Bezeichnungsweise möchte ich den Vorschlag machen, die Reflexion an der Erdoberfläche bzw. am Grundwasserspiegel ebenfalls mit anzudeuten, und zwar so, wie wir es bei meiner Firma machen, durch ein o. Statt *BC* würde es dann heissen: *BoC*, während mit *CBC* z. B. eine Reflexion gemeint wäre, die an *C* nach oben, an *B* wieder nach unten und an *C* endgültig nach oben reflektiert würde, und die von Herrn Rühmkorf soeben als Reflexion von der *W*-Form bezeichnet wurde. Diese Form scheint nach meinen Beobachtungen doch gelegentlich vorzukommen.

R. Bortfeld: Wir haben bei unserer Firma auch an eine solche Bezeichnung gedacht, sind aber wieder davon abgegangen, weil wir bisher noch keine

Reflexionen von der *W*-Form beobachtet haben. Deshalb schien uns eine solche Unterscheidung nicht nötig zu sein.

Herr R. Köhler: Haben Sie auch Frequenzbetrachtungen bei dem Versuch angestellt, multiple Reflexionen von „reellen" zu unterscheiden? Bei einem Teil unserer Feldmessungen hat es sich nämlich herausgestellt, dass die multiple Energie z. T. erheblich niederfrequenter ist als die reelle Energie, und dass sich bei der Auswahl eines günstigen Frequenzbereiches die multiple Energie zu Gunsten der reellen zurückdrängen lässt.

R. Bortfeld: Wir haben so etwas bisher nicht beobachtet. — Ich darf hier vielleicht noch eine Bemerkung anschliessen. In der älteren Literatur ist bisweilen auf die Ähnlichkeit der Schwingungsbilder der multiplen Reflexionen und der zugehörigen primären Reflexionen hingewiesen worden. Ich persönlich halte davon als Kriterium für das Erkennen von multiplen Reflexionen nicht viel. Denn einmal ist es nur eine qualitative Methode. Und dann ist ja doch durchaus zu erwarten, dass die Schwingungsbilder *verschieden* sind; denn wegen der Frequenzabhängigkeit von Absorption und Streuung ist die „Form" des Spektrums einer Multiplen *AA* sicher verschieden von der Form des Spektrums der primären Reflexion *A*.

Th. Krey: Ich möchte zunächst betonen, dass wir im Prinzip dieselben Beobachtungen gemacht haben wie Herr Bortfeld. Reflexionen vom Typ *CA* dürften nach meiner Ansicht nur äusserst schwer durch Geschwindigkeitsberechnungen zu erkennen sein, da man sehr oft unter der Oberkreide wieder niedrige Geschwindigkeiten hat, die denen des Tertiärs bereits ähneln.

R. Bortfeld: Ich danke Ihnen für die Bemerkung, dass Sie im Prinzip dieselben Beobachtungen gemacht haben wie wir. — Die Geschwindigkeitsbestimmung aus Routine-Messungen ist nur dann ausreichend, wenn starke Geschwindigkeitskontraste auftreten, und wenn die interessierenden Reflexionen nicht zu grosse Laufzeiten haben. Sonst muss man jedenfalls Langstrecken-Geschwindigkeitsmessungen verwenden; aber auch dann ist der Erfolg von dem Vorhandensein ausreichend grosser Geschwindigkeitskontraste abhängig.

Bei den erwähnten Multiplen *CA* ist der Geschwindigkeitskontrast zwischen dem Tertiär und dem Liegenden der Albtransgression entscheidend. Im nördlichsten Nordwestdeutschland sind das rund 2000 *m*/sec. gegen rund 3000 *m*/sec. Und dieser Kontrast reicht oftmals aus.

J. Lohr: Lassen sich durch Änderungen der Feldmethode Wege zeigen, wo die Erscheinung von multiplen Reflexionen unterdrückt wird?

R. Bortfeld: Mit den bisher in Deutschland üblichen Feldmethoden ist das nicht möglich.

Th. Krey: Zu der Frage, ob man multiple Reflexionen gegenüber den reellen durch besondere Messmethoden oder Messanordnungen unterdrücken kann, möchte ich bemerken, dass das nach meiner Ansicht und nach meinen Erfahrungen merklich wohl nur durch schräg gerichtetes Schiessen bzw. schräg gerichtetes Empfangen möglich ist, wobei vorausgesetzt ist, dass die Neigungen der multiplen und der reellen Reflexionen unterschiedlich sein müssen.

R. Bortfeld: Ich stimme Ihnen darin zu.

A TORSION-MAGNETOMETER FOR MEASURING THE VERTICAL COMPONENT OF THE EARTH'S MAGNETIC FIELD *

BY

F. HAALCK **)

Abstract

The paper describes a vertical component magnetometer for field work whose magnet system is provided with a torsion axis and in which torsion serves as a standard of measurement. When a measurement is taken the magnetic axis of the system is brought back into the horizontal position by altering the angle of twist (null-method). The angle of twist is thus a direct measure of the vertical intensity. The instrument is within wide limits independent of the magnetic north-south direction and may therefore be set up in practically any position. The magnet system is temperature compensated, well damped and provided with an automatic clamping device. With a scale value of 25 gammas per scale division the range of the instrument for direct measurements is 65000 gammas. A tripod of special design enables a measurement to be taken in about one minute. The weight of the torsion magnetometer inclusive of tripod is only 2.9 kg (6.4 lb).

Magnetic balances suitable for field work were first developed and used by Adolf Schmidt (1915). They quickly became very popular as soon as the Askania-Werke about 1920 succeeded in producing these delicate instruments in numbers. Since then magnetic balances of the Schmidt type have stood the test throughout the world. No other type has ever attained the same degree of accuracy and dependability.

Naturally, attempts to develop magnetic balances for field work based upon other principles of construction have not been lacking. Attempts were made by several investigators (Koenigsberger, 1925, Angenheister, 1926, Fanselau, 1948) to substitute a fibre for the knife edge as a mechanical axis of the system in order to be able to control the tilt of the magnet system from outside by applying a torque to the fibre. These investigators, especially Fanselau, indicate that it may be possible to use torsion not only for controlling the system, but also as a standard for the measurement itself. This would be the simplest procedure and might appear obvious. However, no suitable solution to this problem has, as yet, been published. In all instruments, variations in the vertical component of the earth's magnetic field are still measured by reading the tilt of the magnet system from the eyepiece scale. In this paper an instrument is described, which is equipped with a fibre axis and in which the torsion of the fibre is employed for measuring the vertical component of the earth's magnetic field.

---

*) Presented at the Tenth Meeting of the European Association of Exploration Geophisicists, held in Hamburg, 16/18 May 1956.

**) Askania-Werke AG, Berlin-Friedenau.

Fig. 1 shows the principle of construction: the magnet system (8) with the attached mirror is provided with two fine fibres (1) and (2), which when stretched form a fibre axis. The outer ends of both fibres are fastened to a U-shaped carrier (3), which is capable of being rotated in its bearings coaxially with the fibre axis. Rotation of the carrier by manipulating the knob (6) applies a torque to the magnet system through the fibres. At one end of the carrier is a disc (4), which is provided with a circular scale (5), whose centre lies on the fibre axis. By the autocollimating telescope (7) the position of the magnet system can be observed in the usual manner.

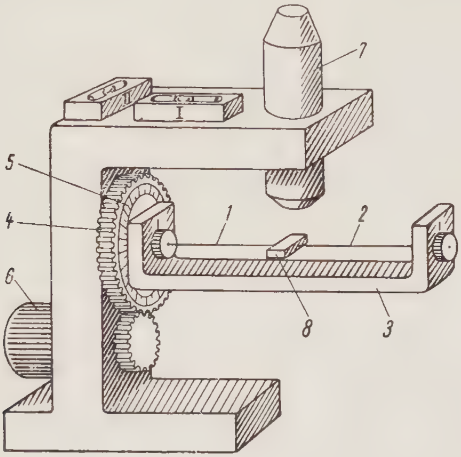

Fig. 1. Principle of the Torsion Magnetometer.
1 and 2 Torsion fibres; 3 U-shaped magnet-system carrier; 4 Torsion circle; 5 Circle graduation; 6 Setting knob; 7 Autocollimating telescope; 8 Magnet system.

In discussing the simple theoretical considerations which led to the development of the construction described above the following symbols will be used:

Z	Vertical intensity of the earth's magnetic field
H	Horizontal intensity of the earth's magnetic field
M	Magnetic moment of the magnet system
α	Angle between the magnetic axis of the system and a horizontal plane
λ	Angle between the magnetic meridian and the plane of oscillation of the magnet system

ϑ Angle between the axis of rotation of the magnet system and a horizontal plane
δ Angle between the magnetic axis of the system and the line connecting the centre of gravity and the axis of rotation of the system
m Mass of the magnet system
l Distance between the centre of gravity of the magnet system and the axis of rotation
g Acceleration of gravity
τ_1 and τ_2 torsion constants of the fibres ($\tau_1 + \tau_2 = \tau$)
a ratio of the two torsion constants ($\tau_1 = a \cdot \tau_2$)

In the absence of external torques it is possible for the two fibres to be twisted in opposite directions without the equilibrium being disturbed (see Fig. 2).

$$\omega \cdot \tau_1 - a \cdot \omega \cdot \tau_2 = 0$$

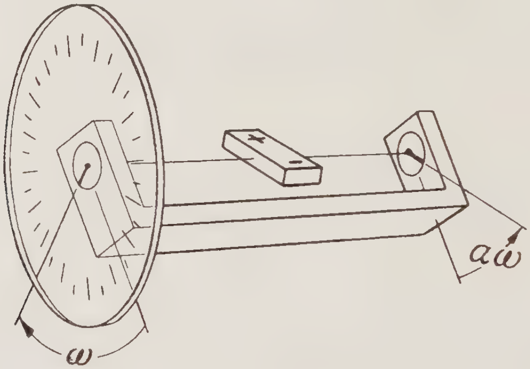

Fig. 2. Representation of the angles of twist ω and $a\ \omega$.

To balance the torque exerted by the magnetic field of the earth both fibres must be twisted over equal angles, φ, which is effected by rotating the carrier over this angle. Similarly, to balance the torque exerted by gravity, equal torsion angles, φ_0, must be applied to the two fibres. Thus the total torsion angles of the two fibres become $\varphi + \varphi_0 + \omega$ and $\varphi + \varphi_0 - a . \omega$ respectively.

Assuming that the magnetic axis of the system is at right angles to the torsion axis, the condition of static equilibrium of the magnet system having any orientation (Fig. 3) is

$$Z\cdot M\cdot\cos\alpha\cdot\cos\vartheta + H\cdot M\cdot\cos\lambda\cdot\sin\alpha - H\cdot M\cdot\sin\lambda\cdot\cos\alpha\cdot\sin\vartheta \qquad (1)$$

$$+ m\cdot g\cdot\cos\vartheta . l . \cos(\alpha+\delta) = \tau\cdot(\varphi+\varphi_0) + \omega\,(\tau_1 - a\cdot\tau_2).$$

The instrument is so constructed that both the magnetic axis and the axis of rotation of the magnet system are approximately horizontal, that is $\alpha \approx 0$ and $\vartheta \approx 0$. Equation (1) may then be simplified to

$$Z \cdot M + H \cdot M \cdot (\alpha \cdot \cos\lambda - \vartheta \cdot \sin\lambda) + m \cdot g \cdot l \cdot \cos\delta = \tau\,(\varphi + \varphi_0).$$

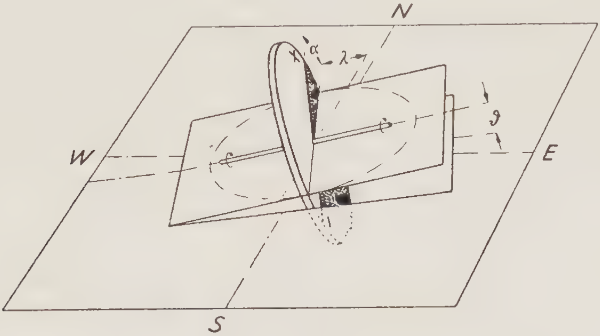

Fig. 3. Orientation of magnet system in space.

The accurate adjustment of the levels, $\alpha = 0$ and $\vartheta = 0$ is carried out in the following manner. First the instrument is placed in an approximately horizontal position by means of the levels which have been adjusted only in accordance with the constructional data. Readings are then taken with the rotation axis of the system oriented north-south ($\lambda = -\pi/2$) and south-north ($\lambda = +\pi/2$). In both orientations the magnet system must be in the same position, which is approximately horizontal. This position can be observed in the telescope, and is realised by applying appropriate torsion angles through the carrier. In the two orientations of the instrument the following equilibrium equations then obtain

$$\begin{array}{lcl} Z \cdot M + H \cdot M \cdot \vartheta + m \cdot g \cdot l \cdot \cos\delta & = & \tau \cdot (\varphi_1 + \varphi_0) \\ Z \cdot M - H \cdot M \cdot \vartheta + m \cdot g \cdot l \cdot \cos\delta & = & \tau \cdot (\varphi_2 + \varphi_0) \\ \hline 2 \cdot H \cdot M \cdot \vartheta & = & \tau \cdot (\varphi_1 - \varphi_2) \end{array}$$

Now the angle of twist $\varphi = (\varphi_1 + \varphi_0) - \frac{1}{2}(\varphi_1 - \varphi_2)$ is applied in the instrument orientation $\lambda = -\pi/2$. Equilibrium is re-established by tilting the instrument in the direction of the axis of rotation. When the index in the telescope coincides with the double line on the eyepiece scale, the level (I) is in the position for which the axis of rotation is horizontal ($\vartheta = 0$).

Under the condition of $\vartheta = 0$ the level II can be adjusted in the following way. First the coincidence must be realized in the azimuth $\lambda = \pi/2$ or $\lambda = -\pi/2$. The equilibrium condition is then

$$Z \cdot M + m \cdot g \cdot l \cdot \cos \delta = \tau\,(\varphi_3 + \varphi_0)$$

Then in the position $\lambda = 0$ the instrument has to be tilted in the direction of the plane of oscillation of the magnet system (i.e. in the direction of level II), without changing the angle of twist. If there is coincidence, the equilibrium is described by

$$Z \cdot M + H \cdot M \cdot \alpha + m \cdot g \cdot l \cdot \cos \delta = \tau\,(\varphi_3 + \varphi_0)$$

In this position of the level II, the magnetic axis of the system is horizontal ($\alpha = 0$).

If the instrument is levelled in accordance with the level readings obtained as described above the general condition of equilibrium (1) reduces to

$$Z \cdot M + m \cdot g \cdot l \cdot \cos \delta = \tau \cdot (\varphi + \varphi_0). \tag{2}$$

Therefore variations of the vertical component are given by

$$\Delta Z = \tau/M \cdot \Delta\varphi$$

because the influence of the acceleration of gravity g is practically equal at the stations in the same area. Equation (2) leads still to another result. The instrument can be set up in any direction, because no dependency on λ exists. This, however, does not hold under all circumstances since for $|\lambda| > 90°$, i.e. a southern orientation of the magnet system (north pole pointing south), the horizontal field will tend to upset the stability. No coincidence can be brought about at values of $|\lambda|$ approaching 180°.

The values of M, τ_1, τ_2 and $l \cdot \cos \delta$ depend on the temperature. However, the equilibrium will not be disturbed by variations in temperature if the following condition is fulfilled

$$Z \cdot dM + m \cdot g \cdot \cos \delta \cdot dl = (\varphi + \varphi_0)\, d\tau + \omega\,(d\tau_1 - a \cdot d\tau_2).$$

In the general case (any value of Z) this condition is necessary but not sufficient. The compensation of temperature is effective in all cases only if the following conditions are realized:

$$Z \cdot dM - \varphi \cdot d\tau = \varepsilon_1 = 0.$$
$$m \cdot g \cdot \cos \delta \cdot dl - \varphi_0 \cdot d\tau - \omega \cdot (d\tau_1 - a \cdot d\tau_2) = \varepsilon_2 = 0.$$

In practice, it is hardly possible to meet both these requirements at the same time. Attempts end in failure because the necessary materials either exhibit only a very small difference in their temperature coefficients and their choice is primarily determined by other properties. For instance, the material of the fibres has to be selected primarily in accordance with their elastic properties and not with respect to the value of the thermoelastic coefficient.

Despite all limitations a temperature compensation as shown schematically in Fig. 4 can be achieved. Within a range of approximately ± 10 000 gammas the temperature coefficient is $|\varepsilon| = |\varepsilon_1 + \varepsilon_2| < 1\ \gamma/°\mathrm{C}$.

In actual practice such a temperature compensation will be sufficient, if $Z_{\varepsilon=0}$ is the mean value of the vertical intensity in the surveyed area. However, $Z_{\varepsilon=0}$ is more or less an accidental result of manufacture which can

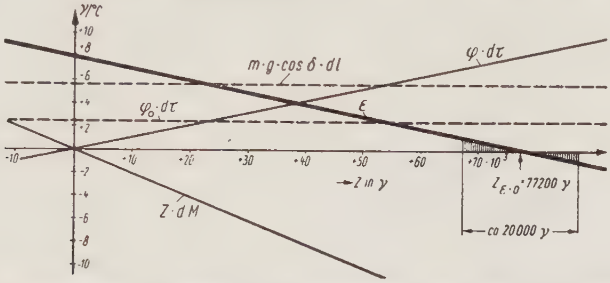

Fig. 4. Basic schematic diagram of temperature effect against vertical intensity.

only be modified if the two fibres are made of materials having different thermoelastic coefficients. Choice of ω allows adjustment of ε_2 and thereby also ε only if $(d\tau_1 - a \cdot d\tau_2)$ differs from zero. In such a manner $\varepsilon = 0$ can be adjusted for any value of Z.

Errors of tilt in the direction of the level I and II respectively are deviations of the angles α and ϑ from zero. This is the case because the torsion axis is coupled mechanically with the level I and the magnet system is coupled optically (since each measurement requires coincidence) with the level II. Whenever the instrument is improperly levelled, the conditions $(\alpha = 0, \vartheta = 0)$ under which the equation (2) holds, are no longer valid. The dependence of the angle of twist upon tilt must therefore be derived from the general condition of equilibrium (1).

Level I : $-H.M.\sin\lambda.d\vartheta = \tau.d\,(\varphi + \varphi_0)$.
Level II: $(H \cdot M \cdot \cos\lambda - m \cdot g \cdot l \cdot \sin\delta) \cdot d\alpha = \tau.d\,(\varphi + \varphi_0)$.

From this it may be deduced that the sensitivity of the instrument to tilt increases with the horizontal field, and in both directions depends to a high degree on the azimuth. At extreme values of λ one of the two levels must be levelled much more accurately than the other.

The scale value is defined by $dZ/d\varphi = \tau/M$.

Without great difficulty one scale division on the circular scale can be made equal to 0,1°. Therefore if we wish to have a scale value of about 25 γ/ s.d., it is necessary to choose the values of τ and M from

$$\frac{dZ}{d\varphi} = \frac{25 \cdot 10^{-5}}{\pi \cdot 1800^{-1}} \approx \frac{1}{7} = \frac{\tau}{M}$$

This ratio can only be realized if both the torsion constant τ and the magnetic moment M assume relatively small values. By a rough calculation it can be shown that the diameter of the fibres must be less than 100 microns and the total weight of the magnet system only about 100 milligramms.

The magnet, serving also as a metal mirror, is equipped with torsion fibres on both sides each about 5 cm long. The materials of these two fibres have unequal thermoelastic coefficients. The outer ends of these fibres are fastened to the carrier in such a manner as to form, when stretched, a torsion axis. This torsion axis is practically an extension of the axis of the carrier, which can be rotated in its bearing. Both fixing points of the fibres at the carrier are so designed that they may be rotated separately about an axis which likewise coincides with the axis of the carrier. So it is possible to give fibre (1) a setting of angle ω and fibre (2) a setting of angle $(-a\cdot\omega)$. When actual measurements are being taken the magnetic axis of the magnet system must be horizontal. This can be achieved by manipulating the knurled knob (6) whereby the U-shaped carrier is turned by means of a worm gear thus causing a change in the torque applied to the magnet. The magnet system is horizontal when the image of the index line, projected by the optical system, lies symmetrically in the double line in the eyepiece. The optical system for observation of coincidence and for reading the circular scale is shown in Fig. 5. The scale of the glass circle (5) and the index line located in the image plane (but outside the field of view) of the eyepiece (11) are illuminated by light reflected from the external mirror (9) and passed through the objective (10). The glass scale and index line are arranged in such a manner that their images lie in the image plane of the eyepiece. In the image plane of the eyepiece lies the surface of a glass plate carrying a double line to observe the coincidence, and a scale providing the subdivisions for the divisions of the glass circle (Fig. 6). The length of the scale is such that ten of its divisions are exactly equal to the interval between two optically projected divisions of the glass circle.

The torsion magnetometer is provided with a novel type of tripod on which the instrument remains fixed for most of the time. Only on longer transits or when shipping the instrument it is expedient to separate instrument and tripod. The novel type tripod is provided with two ballcups (Fig. 5) which are separately actuated. The first ball-cup (12) serves for rough levelling, the instrument being moved directly by hand. To find the correct position for reading, the instrument can be moved on the second ball-cup (13) by means of two screws (15). Each of them tilts the instrument only in the direction of the corresponding level, so the final levelling can be done in a very short time.

The instrument is fitted with an automatic clamping device. The magnet system is permanently pressed by a spring clip against two spring stops which are adjusted in such a manner that the index line appears in the field of view of

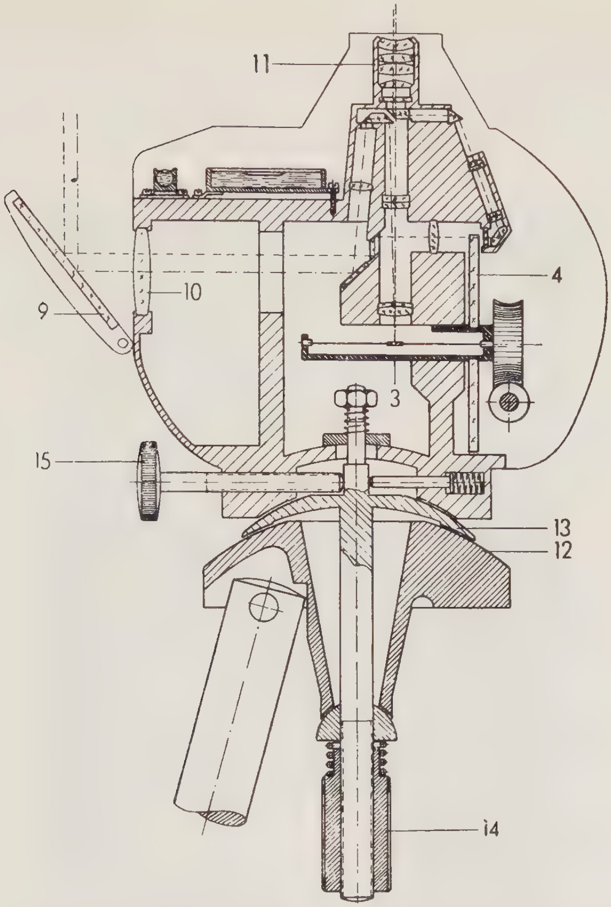

Fig. 5. Cross sectional view of torsion magnetometer
3 System carrier; 4 Torsion circle; 9 Illumination mirror; 10 Objective lens; 11 Eyepiece; 12 First ball-cup; 13 Second ball-cup; 14 Knurled screw for clamping when rough levelled; 15 Knurled screw for final levelling

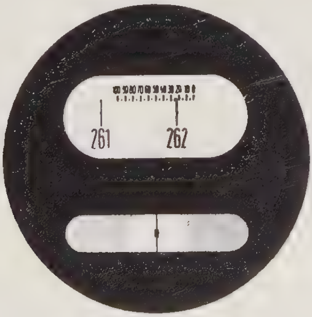

Fig. 6. View through eyepiece

the eyepiece. Only when measurements are actually taken, is the system released by slighly pressing the clamping button (16) with a finger. The spring clip is then displaced sufficiently for the magnet system to swing freely.

The normal measurement can be done in a simple way. The tripod, onto which the instrument remains fixed during a series of observations, is set up in such a manner that the marking "N" on the instrument is oriented approximately north. To insure stability of the set-up the 3 legs of the tripod are, as usual, driven a certain distance into the ground. After a rough levelling of the instrument the mirror (9) is swung out into a position ensuring that the index line and the circle graduation are fully illuminated. Thereafter, the final levelling is accomplished by means of the two knurled head screws (15). To bring the magnet system to zero the index mark is viewed through the telescope (7) while one of the fingers of the left hand depresses the clamping button (16). The angle of twist, having the value of the previous measuring point normally

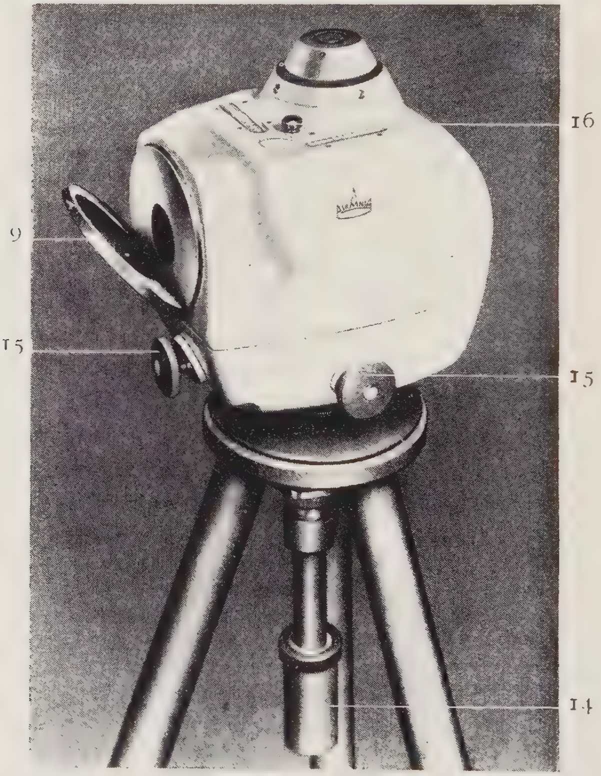

Fig. 7. Torsion magnetometer (model for test purposes)
9 Illumination mirror; 14 Knurled screw for clamping when rough levelled; 15 Knurled screw for final levelling; 16 Clamping knob

will not produce the right torque to balance the magnet system. Therefore it may happen, that the index line will move off the field of view after release. In this case the knurled screw (6) is rotated so that the figures marked on the scale come into the field of view of the eyepiece from that side on which the index line vanished when the system was released. Should this have escaped the observer's attention it is always possible to repeat the observation by pressing the arresting knob several times, i.e. by repeated clamping and unclamping the system. As soon as the index mark is brought into coincidence by manipulating the screw (6) the measurement is accomplished. The angle of twist is read and booked and the instrument can be removed without any further manipulation because the magnet system is automatically clamped when the clamping button is released. After some experience a skillful observer should be able to take a complete measurement in about 60 seconds.

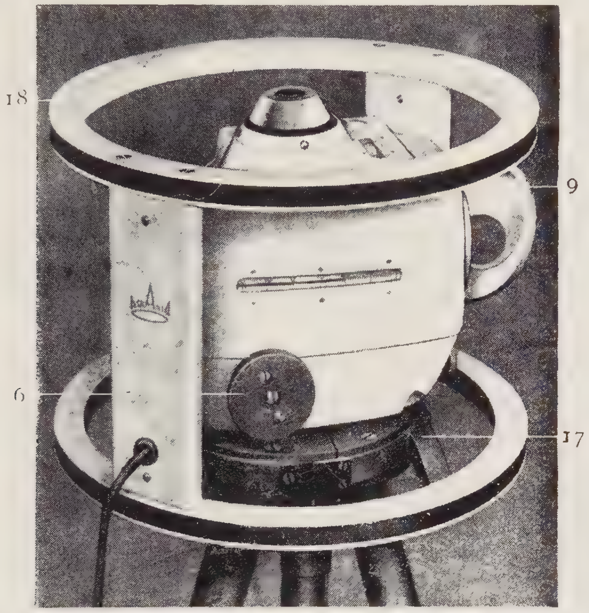

Fig. 8. Torsion magnetometer with attached calibrating coil.
6 Setting knob; 9 Illumination mirror; 17 Holder for calibrating coil; 18 Calibrating coil

The prototype of such a torsion-magnetometer was built by the Askania-Werke (Fig. 7 and 8). It was checked in the Fürstenfeldbruck ¹) and Wingst ²)

These tests were carried out by
¹) Dr. Anton Graf, Lochham near Munich
²) Dr. Reinhard Schulze, Askania-Werke AG, Berlin-Friedenau.

observatories. The field tests were carried out in the vicinity of these observatories so that the results could be checked continually on the magnetograms. No difficulties of any kind have been encountered. Pertinent information on the instrument and the results obtained in field work is given below.

Scale value

The torsion magnetometer is provided with a carrier (17) to support the coil system, thus permitting calibration coils (18) to be used. Size and design of the carrier are so chosen that the calibration device of the Askania Field Balance Gf 6 may be utilized. The instrument was calibrated (Table 1), and a scale value of 23.8 γ /s.d. was obtained.

Table 1

Calibration

September 15, 1955 at the Fürstenfeldbruck Observatory

mA	$(\varphi+\varphi_0)$	(coil constant: 4.67 γ /*mA*
0	267,96	
—60	266,78	1,18° = 11.8 s.d. / 60 *mA*
+60	269,13	
0	267,95	or 23.8 γ / *s.d.*

Measuring range

The carrier (3) of the magnet system cannot be rotated into every position because the telescope and the clamping and damping device do not allow it. Only an angular displacement of about 270° is possible. This angle corresponds to a range of roughly 65 000 gammas. Therefore the torsion-magnetometer can measure directly all the values which may be encountered in practice. Latitude adjustments which have continually to be made in knife-edge instruments no longer arise. Even great anomalies can be surveyed without reduction of sensitivity and use of auxiliary magnets. In addition, this range may readily be shifted simply by turning appropriately the fixing points of both torsion fibres.

Angle of twist φ_0

By the adjustment of the instrument the reading of the circle becomes zero if the magnet system is in the horizontal position without any torsion of the two fibres (i.e. $Z = 0$ and $m.g.l.\cos\delta = 0$). To balance the vertical component at the Observatory Wingst ($Z = 44500$ gammas) an angle of twist

$(\varphi + \varphi_0) = 275^\circ$ was necessary. If the scale value is taken into account, the result is: $\varphi = 190^\circ$ and $\varphi_0 = 85^\circ$.

INFLUENCE OF GRAVITY

The magnetic moment M and the mass of the magnet system m are measured before the instrument is assembled ($M = 2.1\ \Gamma\,\text{cm}^3$; $m = 0.06$ gr). Z and g of the measuring point are known also, so it is possible to find $l.\cos\delta = 0{,}007$ cm by equation (2). If these values are inserted in

$$dg = \frac{M \cdot Z}{m \cdot l \cos\delta \cdot \varphi} \,.\, d\,\varphi_0$$

a variation Δg in the acceleration of gravity of 100 mgal and a variation ΔZ in the vertical intensity of 0.6 gammas will produce approximately equal angles of twist. Therefore in practice, the influence of gravity may be neglected. Only in exceptional cases and when measurements to a very high accuracy are required should corrections be applied.

LINEARITY

In theory the torsion of the fibre depends linearly on the intensity of the

TABLE II

The Linearity Test

mA	Angle of twist Reading s.d.		for every 10 *mA*	deviation from the average s.d.	γ
—100		249,39			
+100	271,47 5		1,110	+0,006	+1,4
—90		250,50	1,105	+0,001	+0,2
+90	270,37		1,100	—0,004	—1,0
—80		251,60	1,090	—0,014	—3,3
+80	269,28		1,100	—0,004	—1,0
—70		252,70	1,100	—0,004	—1,0
+70	268,18		1,095	—0,009	—2,1
—60		253,80 5	1,110	+0,006	+1,4
+60	267,07		1,095	—0,009	—2,1
—50		254,90	1,120	+0,016	+3,8
+50	265,95		1,130	+0,026	+6,2
—40		256,03	1,115	+0,011	+2,6
+40	264,83 5		1,090	—0,014	—3,3
—30		257,12	1,110	+0,006	+1,4
+30	263,72 5		1,100	—0,004	—1,0
—20		258,22	1,105	+0,001	+0,2
+20	262,62		1,110	+0,006	+1,4
—10		259,33	1,105	+0,001	+0,2
+10	261,51 5		1,100	—0,004	—1,0
0		260,43	1,085	—0,019	—4,5
0	260,43				

magnetic vertical component. To check linearity the calibration device of the Askania Field Balance *Gf* 6 was used. The results presented in table 2 show that no systematic deviation from linearity up to ± 2630 γ exists. Only a few readings are not in line. Their deviation is about 3 γ and in one case even about 6 γ. This may be explained as resulting from the errors inherent in the measuring device. Also, an error of about 1 γ may be introduced in the results by the correction for diurnal variation.

COMPENSATION OF TEMPERATURE

First, the instrument was adjusted with the angle $\omega = 0$.

It was found $\varepsilon = +3{,}5\ \gamma/°C\ (Z = 44500\ \gamma)$ and

$\varepsilon = +8{,}0\ \gamma/°C\ (Z = 0\ \gamma)$

Now the fixing point of one torsion fibre was turned through an angle $\omega \approx 50°$. The fixing point of the other fibre was turned in the opposite direction, to make the magnet system horizontal. Then the instrument was checked again. From the result

$\varepsilon \approx +1{,}0\ \gamma/°C\ (Z \approx 44500\ \gamma)$ and

$\varepsilon \approx +5{,}5\ \gamma/°C\ (Z \approx 0\ \gamma)$, it was calculated, that the angle ω must be about 70° if compensation in central Germany ($Z = 43000\ \gamma$) is required. The result of this adjustment, illustrated in Fig. 9, was checked at the observatories Wingst and Fürstenfeldbruck[1]). At Wingst $\varepsilon = -0{,}12\ \gamma/°C$ was obtained. Without knowledge of this value a few weeks later at Fürstenfeldbruck observatory $\varepsilon = +0{,}15\ \gamma/°C$ was found. The same value could likewise have been taken from Fig. 9. It may further be seen from this diagram that

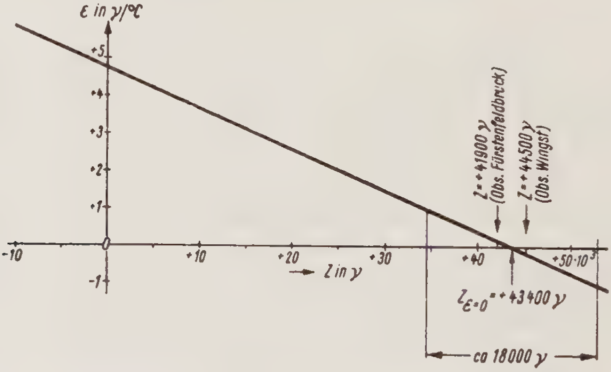

Fig. 9. Temperature coefficient of test model against vertical intensity of magnetic field

the temperature coefficient $|\varepsilon|$ is less than 1 $\gamma/°C$ over a range of ± 9 000 gammas. Such a compensation may be considered good. This is emphasized by the fact that the temperature coefficient within the boundaries of Germany does not exceed 0.2 $\gamma/°C$.

---

[1]) See footnote on page 433.

There are no difficulties in making the temperature coefficient of the instrument zero for any other value of Z. Only a single setting is necessary, because the angle ω which must be set for a predetermined value of $Z_{\varepsilon=0}$ can be calculated from the results of the first adjustment. In the instrument described a value of $\Delta\omega \approx + 10°$ corresponds to $\Delta Z_{\varepsilon=0} \approx - 4500\,\gamma$. The adjustment itself can be done in only a few minutes. No special ability over and above that normally available is required.

SENSITIVITY TO TILT

The theoretical considerations show that the sensitivity to tilt is strongly dependent upon the azimuth. In the subsequent considerations it will always be assumed that the orientation of the instrument will be such as to produce maximum sensitivity to tilt. For $\lambda = 0$ the torsion magnetometer is insensitive to tilt in the direction of level I due to the dependence upon $\sin\lambda$. In this azimuth no effect on the reading could be ascertained when the entire range of the level was utilized. Since values of $|\gamma| \leqq 45°$ are considered permissible, the maximum effect of the tilt occurs when $|\lambda| = 45°$. For this case a tilt of the instrument of one scale division of the level was found to produce a change of the angle of twist corresponding to $\Delta Z \approx 5.0$ gammas. Therefore, the bubble of level I must be centred with an accuracy of 0.1 division if the result is not to be in error by an amount exceeding 0.5 gammas.

For the level II the sensitivity to tilt is greatest at $\lambda = 0$. It was found by experiment that, in this most unfavourable azimuth, the error caused by tilt amounted to 5.6 gammas per level division. Within the range of the level this dependence is practically linear.

If λ differs from zero the sensitivity to tilt decreases due to the dependence on $\cos\lambda$.

ELASTIC AFTER-EFFECTS

The following procedure was used to check the elastic after-effects. After producing another value of Z, two readings were taken. The first value was obtained directly after the change of Z, the second, 5 minutes later. The difference between these two readings ($\Delta\gamma$) depends upon the change of Z as illustrated in the diagram (Fig. 10). Whenever the magnetic field was suddenly changed by about 1000 gammas no difference in the two readings could be observed. It was found that within a period of 5 minutes the elastic after-effects amounted to about 0.1 per cent of the change in the field. In practice, therefore, the elastic after-effects are of no importance.

When tested in the field the new type of magnetometer has proved its value in all respects. The results of measurements repeated several times at 5 different stations (Fig. 11, 12 and 13) may serve to illustrate this. The first and second series of measurements were made on one day following some other investigations, while the third series was started next morning. Each of the series of measurements was evaluated separately and independently of the others. The results obtained are summarized in table 3. Each reading was corrected for diurnal variations, which were taken from the magnetograms

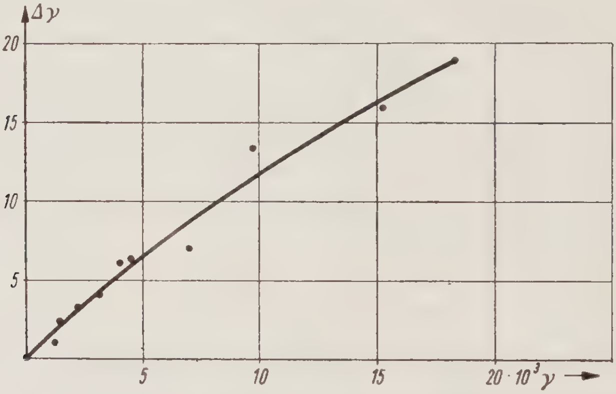

Fig. 10. Change in setting after a period of 5 minutes (elastic aftereffects) against the magnitude of a sudden field change

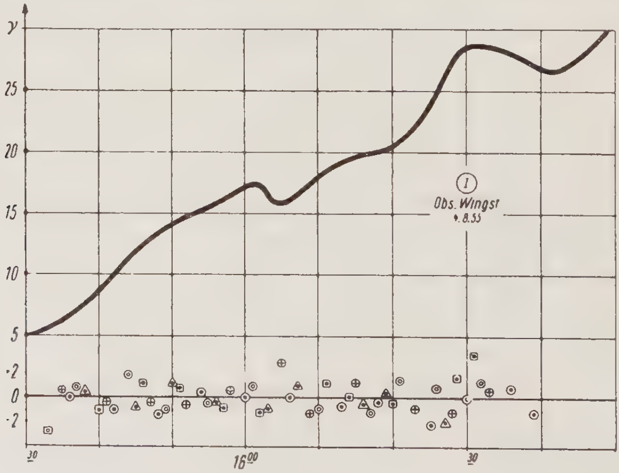

Fig. 11. I. set of readings at stations 1-5

of the Wingst observatory. No further corrections were applied. However, for the graphic representation the values obtained at stations 2 to 5 were

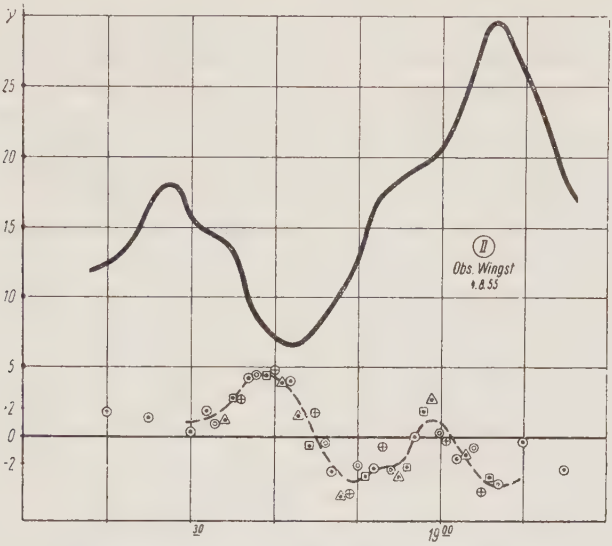

Fig. 12. II. set of readings at stations 1-5

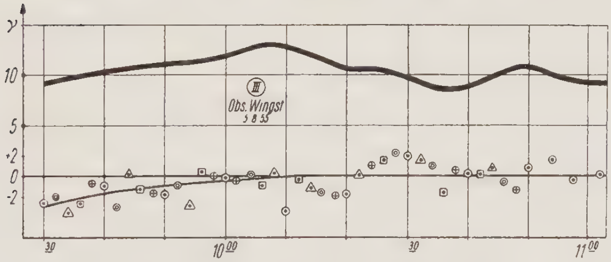

Fig. 13. III. set of readings at stations 1-5

TABLE III

Summary of Results

Station	I	II	III	Average
1	0	0	0	0
2	— 219,2	— 218,8	— 219,4	— 219,1
3	—1578,1	—1579,9	—1578,7	—1578,9
4	+ 862,5	+ 861,5	+ 861,8	+ 861,9
5	— 113,6	—113,4	— 113,6	— 113,5

altered by adding to each of them different constants. The constant for each station is equal to the difference between the readings there and those taken at station 1. By this means all the readings should have the same value, i.e. a horizontal line in the diagram should result.

It may be seen from the graphically represented results that the uncertainty of an individual reading is less than 2 gammas. The scattering reaches a maximum value of 3 gammas in only a few cases. These deviations can readily be accounted for by the inaccuracies of reading and by the uncertainties in the determination of the time variations. The solid curve shows the variations of the vertical component which were deducted from the readings. The time variations of Z for the second set of readings are especially large, and it is therefore somewhat difficult to correct them exactly. In such cases there is liable to be a considerable difference in the values obtained at different times. The results derived from this series of measurements make it evident that the variations have not been determined correctly. The third set of measurements shows a drift of about 3 gammas in a period of 40 minutes. Such a drift was observed several times when the instrument was not transported for some time, for instance overnight. It is, however, not difficult to determine this initial zero drift by a suitable arrangement of the measurements and to allow for it by corrections.

In general, the experience gained up to the present shows that the torsion magnetometer is not only an instrument with sufficient accuracy, but also with a number of marked advantages such as, light weight, speedy operation, extensive measuring range, simplicity of manipulation, automatic clamping, and convenient rough and final levelling.

Discussion

A. Hahn: Muss der Arretierungsknopf ständig heruntergedrückt werden, wenn das System frei schwingen soll?

F. Haalck: Ja. Es genügt jedoch schon ein Druck von 100 g, um den Arretierungsknopf herunterzudrücken. Eine Verstellung der Libelle kann dabei nicht eintreten, zumal die Einstellung der Koinzidenz in wenigen Sekunden durchgeführt werden kann.

A. Hahn: Kann man im Feldbetrieb einen zerrissenen Faden selbst ersetzen?

F. Haalck: Magnetsystem und Torsionsfaden sind so dimensioniert, dass ein Zerreissen der Fäden praktisch nicht vorkommt. Es wurden tagelange Versuche durchgeführt, die zeigen sollten, ob man auf eine Arretierung überhaupt verzichten könne. Dabei zeigte sich lediglich eine nicht tragbare Nullpunktsunsicherheit. Eine direkte Beschädigung der Fäden trat nicht ein. Also selbst dann, wenn die automatische Arretierung nicht funktionieren sollte und das Instrument unarretiert transportiert wird, ist eine Beschädigung

der Fäden nicht zu erwarten. Sollte durch besondere Umstände trotzdem ein Torsionsfaden zerreissen, so muss das Instrument zur Reparatur eingeschickt werden.

A. LUNDBAK: Darf ich fragen, aus welchem Material der Torsionsfaden hergestellt ist?

F. HAALCK: Es können Torsionsfäden benutzt werden, wie sie bei anderen magnetischen Instrumenten üblich sind. Leider ist es bis jetzt nicht gelungen, Torsionsfäden zu finden, die gegenüber anderen eindeutig bessere Eigenschaften aufweisen. Dieses hat seinen Grund darin, dass die Eigenschaften der Fäden sehr unterschiedlich sind, wenn das Material aus verschiedenen Lieferungen stammt.

A. LUNDBAK: Ferner möchte ich gern wissen, ob es in den Ablesungen einen Gang gibt, im Laufe einer Woche zum Beispiel; ist es möglicherweise bei längeren Serien von Feldmessungen am besten, eine oder mehrere Basisstationen anzuwenden?

F. HAALCK: Um diese Frage mit Sicherheit richtig beantworten zu können, müssen längere Felderfahrungen abgewartet werden. Bis jetzt scheint es so, als ob der Nullpunkt (drift) nur ünwesentlich pro Woche abwandert.

B. KUNZ: Kann in dem Torsionsmagnetometer auch ein H-System benutzt werden?

F. HAALCK: Nein. Das Instrument besitzt keine Einrichtung, die es ermöglicht, die magnetische Achse des Systems genau senkrecht zum H-Vektor einzustellen. Selbstverständlich ist es möglich, das Instrument so einzurichten, dass wahlweise ein Z- oder H-System benutzt werden kann. Auch die Konstruktion eines Kombinationsinstrumentes bringt keine unüberwindlichen Schwierigkeiten mit sich. Diese Wege sind aber bewusst nicht beschritten worden, da nur ein Z-Magnetometer, das nach der Nullmethode arbeitet, vom Azimut unabhängig ist. Die dadurch bedingten grossen Vorteile würde man aufgeben, wenn man das Instrument auch für Messungen der Horizontalkomponente einrichtet.

REFERENCES

ANGENHEISTER, G., "Magnetische Waage mit Fadenaufhängung". Zeitschrift für Geophysik, II. Jahrg., Heft 1, 1926.

FANSELAU, G., "Über eine neue magnetische Vertikalfadenwaage." Zeitschrift für Meteorologie, 1948, Bd. 2.

KOENIGSBERGER, J., "Vertikalvariometer für Feldmessungen." Zeitschrift für Geophysik, I. Jahrg., Heft 6, 1925.

SCHMIDT, A., "Ein Lokalvariometer für die Vertikalintensität." Tät.-Ber. d. Kgl. Pr. Meteor. Inst., 1914 u. 1915.

BOOK REVIEW

Harold M. Mooney and W. W. Wetzel: "The Potentials about a Point Electrode and Apparent Resistivity Curves for a Two-, Three- and Four-Layer Earth", The University of Minnesota Press, Minneapolis. Price $ 18.—.

In this very valuable book the results are presented of computations of potentials and apparent resistivities for 350 three-layer cases and about 2000 four-layer cases.

The method by which the potentials have been computed is described in detail. It is based on an evaluation of the Stefanescu integral, and the procedure involves certain refinements dealing with a convenient approximation to the integrand and the inclusion of a remainder term.

The most valuable part of the book, however, is the publication of the results of the computations for such a large number of cases. These results are presented in two different forms: numerical tables of potential data, and master curves of apparent resistivities for the Wenner electrode configuration.

It is regrettable—but of course beyond the responsibility of the authors of the present book—that two distinct methods of resistivity surveying (Wenner and Schlumberger) are in current use, and that of the two major collections of master curves now available, one is based on the Wenner configuration and the other (that published by the Compagnie Générale de Géophysique) on the Schlumberger configuration. For the majority of European geophysicists master curves for the Schlumberger configuration might have been more convenient. However, the tables of numerical values of potential data included in the present book, permit at least a reasonable approximation to the Schlumberger master curves to be drawn. Also, the availability of the present set of four-layer master curves may well induce European geophysicists in certain cases to switch over to the Wenner configuration.

The authors mention, as one of the functions of collections of master curves, that "an intuitive feel for the general behaviour of apparent resistivity curves in various situations . . . can be attained by a careful study of them". This function seems indeed to be equally important as that of the actual curve matching. For this function, in view of the general similarity in shape of Schlumberger and Wenner resistivity curves, the present set of master curves may be used, independent of whether the field curves have been obtained by the Schlumberger or by the Wenner method.

The authors must be complimented on carrying out and publishing the results of a tremendous work, which is of the greatest utility in the interpretation of resistivity measurements.

O. K.

E.A.E.G. ABSTRACT SERVICE

EXPLORATION — GENERAL

306. *The Use of Geophysical Methods for Base Metals Exploration in Northern New Brunswick.*
H. O. Seigel, Geophysics, Vol. 19, No. 3, p. 632, July, 1954. (Abstract only of paper read at the Annual Meeting of the S. E. G., St. Louis, April, 1954).
Various techniques of mining geophysics have proved very successful in the search for lead-zinc—silver-copper mineralization in the Bathurst area of northern New Brunswick. Some of the results are discussed.

307. *Geophysical Case History of the Anacon-Leadridge Base Metal Orebody in New Brunswick, Canada.*
S. H. Ward, Geophysics, Vol. 19, No. 3, p. 632, July, 1954.
(Abstract only of paper read at the Annual Meeting of the S.E.G., St. Louis, April, 1954).

308. *A Case History of the Geophysical Discovery of the Pima Mine, Pima County, Arizona.*
W. E. Heinrichs & R. E. Thurmond, Geophysics, Vol. 19, No. 3, p. 633, July, 1954.
(Abstract only of paper read at the Annual Meeting of the S.E.G., St. Louis, April, 1954).

309. *Geophysical Investigations in the Mojave Desert Area of California.*
D. R. Mabey, Geophysics, Vol. 19, No. 3, p. 633, July, 1954.
(Abstract only of paper read at the Annual Meeting of the S.E.G., St. Louis, April, 1954).

310. *Geophysical Prospecting in the Union of South Africa.*
J. F. Enslin, Geophysics, Vol. 19, No. 3, p. 634, July, 1954.
(Abstract only of paper read at the Annual Meeting of the S.E.G., St. Louis, April, 1954).

311. *Geophysical Prospecting for Iron Ore in the Lake Superior Region.*
L. L. O. Bacon, Geophysics, Vol. 19, No. 3, p. 634, July, 1954.
(Abstract only of paper read at the Annual Meeting of the S.E.G., St. Louis, April, 1954).

312. *Investigation of Mineral Deposits in Australia by Geophysical Methods.*
R. F. Thyer, Geophysics, Vol. 19, No. 3, p. 635, July, 1954.
(Abstract only of paper read at the Annual Meeting of the S.E.G., St. Louis, April, 1954).

313. *Geophysical History of Grand Isle, Block* 18, *Oil Field, Gulf of Mexico, Louisiana.*
L. A. Markley, Geophysics, Vol. 20, No. 2, p. 375, April, 1955.
(Abstract only of paper read at the Annual Meeting of the S.E.G., New York, March, 1955).

314. *Problems of Uranium Exploration.*
T. R. Shugart, Geophysics, Vol. 20, No. 2, p. 375, April, 1955.
(Abstract only of paper read at the Annual Meeting of the S.E.G., New York, March, 1955).

The present state of knowledge with regard to the geology of uranium occurrence is briefly outlined. Some of the geological problems of uranium exploration are stated. The application of various geophysical and geochemical techniques to the solution of these geological problems is discussed. A typical exploration programme is described in which geology and geophysics are combined to meet present day exploration requirements.

315. *On the Problem of Designing and Computing Magnetic Systems for Geophysical Instruments.* (In Russian).
G. V. Groshevoy, Akad. Nauk SSSR Geofis. Inst. Trudy, No. 20 (147), pp. 88-94, 1953.

A method is suggested for the improvement of the design of magnetic systems of some instruments such as galvanometers, oscillographs, and others, usable only when the magnetic flux within a similar instrument is known, by making magnetic field measurements. As a preliminary step, correlation must be established between the magnetic leakage of the system and the intensity of magnetization in the gap. In order to decrease the leakage a new magnet is designed with variable cross-section and proper length so that a maximum of magnetic energy is concentrated near the vicinity of the rotating element.

(From Geophysical Abstracts 160, U.S. Geol. Survey).

316. *Civil Engineering and Geophysical Prospecting, Part I.*
R. Hammond, Civil Engineering, Vol. 50, No. 584, pp. 191-193, 1955.

This is a brief review of the magnetic, gravitational, and seismic methods. It is said that a "torsion balance type" instrument is used in gravity surveys, and a Worden gravimeter is described. The first application of the seismic method in determining depth to bedrock is said to have been in Sweden in 1941. The seismic refraction method is described as that used by the Southwestern Industrial Electronics Co.

(From Geophysical Abstracts 160, U.S. Geol. Survey).

317. *Geophysics in an Expanding Economy.*
J. Boyd, Mines Mag., Vol. 45, No. 1, pp. 8-10, 1955.

A discussion of the role of geophysics in locating the raw materials required in our expanding economy.

(From Geophysical Abstracts 160, U.S. Geol. Survey).

318. *Future Exploration in Canada.*
F. Gardner, Oil & Gas J., Vol. 53, No. 45, pp. 76-79, March 14, 1955.

Canada faces a future of oil exploration that will have a vast scope and will take place over a great number of years. The most important areas are: the Arctic salt domes; the North Yukon; the Peace River; the Pembina-Cardium foothills; and the Williston Basin. A brief history of these areas is given and the future is discussed.

319. *Geophysical Activity in Western Canada,* 1954.
W. P. Ogilvie, World Petroleum, Vol. 26, No. 5, pp. 64-65, May 1955.

In 1954 there was a decline in geophysical activity of 15%, from 1953. Operations appear to be becoming more seasonal than previously. The ground magnetometer has been almost wholely replaced by airborne magnetometers which operate at less unit cost. The airborne scintillation counter was used experimentally, but its value as a prospecting tool has not yet been assessed. The gravimeter, though still primarily a reconnaissance tool, is being increasingly used for high station density detail work. The tendency for seasonal operation of seismic crews reflects the shift of the exploration effort from the plains areas to the more remote and inaccessible bush and muskeg country.

The cost of exploration during 1954 is estimated at \$ 35,000,000, which is \$ 2,000,000 less than the previous year, and \$ 5,000,000 less than 1952.

320. *Geophysical Activity off* 6.3 *Percent.*
S. Hammer, World Oil, Vol. 140, No. 6, pp. 98-101, May 1955.

Though geophysical activity in prospecting for petroleum showed an increase during 1954 in Europe, the Middle East and the Far East, this was not sufficient to offset the big decreases in the U.S.A. and Canada. Seismic operations showed the largest drop, with 8.4 per cent. Gravity, however, showed an increase of 7.1 per cent. Global charts show the distribution of the various activities by area and method. Tables of comparisons are also included.

321. *Geophysics Can Find More Oil for You.*
N. S. Morrisey, Oil & Gas J., Vol. 54, No. 7, pp. 95-99, June 1955.

Exploration successes are increased by more than one third when geophysics is coupled with geology. The various ways in which geophysics assists the geologist are discussed. For the future, the application of geophysics will increase as the remaining oil structures become smaller and more difficult to find.

322. *Atmospheric Electricity and Geophysical Operations.*
F. W. Fordham, Geophysics, Vol. 20, No. 3, pp. 638-653, July 1955.

Lightning is a danger to geophysical operations, especially where explosives are being used. This paper describes a system whereby potential lightning can be detected, using a point collector. This is a sharp metal point that picks up the corona-discharge current and records it on an oscillogram. With co-operation throughout the industry, data obtained could be used for forecasting lightning storms.

323. *Geophysical Prospecting over Continental Shelves.*
H. C. Cortes & R. N. Gsell, Proceedings of the 4th World Petroleum Congress, Section I, p. 575, June 1955.

Many difficult problems were encountered and solved in extending oil search offshore. The principal methods used, in order of increasing resolution and operating costs, have been magnetic, gravimetric and seismic. Major amounts of offshore geophysics have been done off California, Louisiana and Texas. Comparatively small areas have been covered offshore with the airborne magnetometer.

324. *Exploration for Reefs by Geophysical Methods.*
F. J. Agnich, Proceedings of the 4th World Petroleum Congress, Section I, p. 619, June 1955.

Methods used in geophysical exploration for limestone reefs are described. Where reefs are shallow and the density contrast with surrounding materials is relatively great, the gravity meter can be successfully employed. The seismic refraction method like the gravity method, is strictly limited to shallow reefs. Even then a favourable contrast in velocity must exist between the reef and the geologic section around and above it. The most effective geophysical method in reef location has been the reflection seismograph.

325. *Geophysical Technique Employed for Petroleum Exploration in Mexico.*
H. S. Figueroa, Proceedings of the 4th World Petroleum Congress, Section I, p. 647, June 1955.

By applying practically all available geophysical methods it has been possible to study a large part of the oil-bearing subsurface where conditions are extremely varied. In some cases special techniques have been employed in the investigation of reefs, high relief structures, salt domes, and fracture zones. As a result of the new exploration campaign, there has been a steady advance in the accumulation of information.

326. *Correlation of Geological and Geophysical Data.*
D. C. Skeels, Proceedings of the 4th World Petroleum Congress, Section I, p. 665, June 1955.

The importance is stressed of careful co-ordination of geological and geophysical data in both regional and local exploration. The application of geological information in guiding geophysical interpretations, and the use of seismic records in subsurface mapping of stratigraphic units is discussed and is illustrated by examples from several areas.

327. *Comparative Geological and Geophysical Study of the Po Basin.*
T. Rocco, Proceedings of the 4th World Petroleum Congress, Section I, p. 675, June 1955.

After a reference to the development of the oil exploration that has been carried out during the last few years, general and critical information is given on the gravitational and seismic surveys made by AGIP Mineraria in the Po Valley. The results obtained with these two geophysical methods and with extended stratigraphic studies on a large number of wildcats are then compared in the light of the knowledge of the principal structural features of the Po Basin.

328. *Development in Geophysical and Geological Exploration in Germany*, 1951-1954.
A. Bentz & H. Closs, Proceedings of the 4th World Petroleum Congress, Section I, p. 691, June 1955.

The type of geophysical and geological methods used in the three principal oil provinces of Germany depends on the type of geological structures. As yet the greatest success has been achieved in north-western Germany where salt domes, anticlines, deepseated domes, fault-structures and stratigraphical traps abound. Oil exploration in Germany is characterized by close co-operation between geology and geophysics.

329. *The Modern Planning of Regional Surveys for Petroleum.*
P. Leicester, J. Inst. Petrol., Vol. 41, No. 379, pp. 217-228, July 1955.

Improved knowledge of the possibilities for oil accumulation has increased the efficiency, intensity and cost of competent exploration. Before commencing in an area, a geological assessment is always necessary, together with a preliminary exploration programme and budget for the estimated time to prove the area. These should indicate the capital risk and also the potential profit in the event of discovering oil.

With normal geological conditions, exploration is straight-forward, but local petroleum laws might restrict and hamper operations. Some of the Shell Co.'s prominent present and recent regional ventures are reviewed.

Contributors to the discussion which followed the paper are: D. C. Ion, P. Evans, A. E. Gunther, S. E. Hollingworth, S. J. M. Auld, N. L. Falcon, J. H. G. Carlile, P. T. Cox and C. M. Pollock.

330. *Hunting for Oil.*

Petroleum Press Service, Vol. 22, No. 7, pp. 246-249, July 1955.

Material drawn from papers presented before the Geology and Geophysics section of the 4th World Petroleum Congress is condensed into a short, general account of the current techniques of oil exploration. An assessment is made of what such exploration has achieved so far, and of the possibilities of the discovery of future reserves.

331. *The Future of Geophysics.*

P. L. Lyons, Geophysics, Vol. 20, No. 3, pp. 503-515, July 1955, and Bull. A. A. P. G., Vol. 39, No. 7, pp. 1202-1213, July 1955.

A further decline in seismic prospecting throughout the world was recorded for the year of 1955. The trend indicates that the upper limit of activity has been passed. The peak was reached during a race of oil companies to be the first in the field with the most equipment, but now economies are being applied. There has by no means been a complete coverage of favourable prospects as yet; large areas remain virtually unexplored. In addition, there is immense scope for development of instruments, field techniques and interpretation methods, for solving the problems of very-small-relief structures and stratigraphic traps. The future of geophysics will be a changing one.

332. *An Educational Programme in Geophysics.*

G. P. Woolard, Geophysics, Vol. 20, No. 3, pp. 671-680, July 1955.

The ideal undergraduate curriculum for undergraduates in geophysics would include course coverage along the following lines; (a) basic geology with advanced work in stratigraphy, structural geology, mineral deposits and petrology, (b) basic physics with advanced work in electricity and magnetism, optics, light and sound and instrumentation techniques, and (c) basic mathematics with advanced work in calculus, differential equations, potential theory, and vector analysis.

Such a programme as the above is difficult to work out in the average technical school, because of the high number of technological courses required already. However, several U.S. colleges and universities have curriculums that approach the ideal. That of the University of Wisconsin is described as an example.

This paper is followed by a discussion by M. King Hubbert.

333. *Some Aspects of Exploration of the Offshore Gulf Coast.*

M. G. Frey & O. A. Poirier, Geophysics, Vol. 20, No. 3, p. 714, July 1955.
(Abstract only of paper read at the 10th Annual Gulf Coast Meeting of the S.E.G. at San Antonio, Texas, May 1955).

Since the first large scale geophysical exploration work in 1944 the offshore areas of Louisiana and Texas have seen an ever-increasing tempo of oil-finding activity. Geophysical methods have demonstrated that the water-covered areas out to at least 100 feet are underlain by a seaward continuation of the same type of structures that have been so prolific on-shore. The advantage of unrestricted movement and high production enjoyed by the seismograph is somewhat counterbalanced by special problems including surveys, weathering and regional velocity control. Stratigraphy and economic drilling and producing techniques are other all-important, and as yet unanswered, questions.

334. *Geophysical Accident Facts.*

B. W. Sorge, Geophysics, Vol. 20, No. 3, p. 714, July 1955.
(Abstract only of paper read at the 10th Annual Gulf Coast Meeting of the S.E.G. at San Antonio, Texas, May 1955.)

The work of the S.E.G. Safety Committee has continued during 1954. As a result of these efforts, more information is now known about geophysical accidents. This is useful in planning the prevention of future accidents and the continued improvement of the safety record of geophysical field parties. Much progress has been made since the inception of the Committee, but much still needs to be done to put the improvement on an industry-wide basis. Effective accident-prevention is not only a moral obligation, but can result in a drastic reduction of field operating expenses.

335. *Geophysical Data Reduction with Electronic Computers.*
S. M. Rock, Geophysics, Vol. 20, No. 3, p. 715, July 1955.
(Abstract only of paper read at the 10th Annual Gulf Coast Meeting of the S.E.G. at San Antonio, Texas, May 1955).

Digital computers are now available at a variety of prices and capacities, some of which are suitable for geophysical data reduction and research. A brief description is given of the types of operations which these machines perform, with special reference to the Electro-Data, or Datatron, systems. Several types of geophysical computations lending themselves to digital computation are briefly discussed.

SEISMIC — GENERAL

336. *Structural and Seismic Deformations along Faults in Eastern Venezuela.*
H. P. Laubscher, Geophysics, Vol. 20, No. 2, p. 373, April, 1955.
(Abstract only of paper read at the Annual Meeting of the S.E.G., New York, March, 1955).

337. *Seismic Operations in Saudi Arabia.*
C. G. Flittie, Geophysics, Vol. 20, No. 2, p. 375, April 1955.
(Abstract only of paper read at the Annual Meeting of the S.E.G., New York, March, 1955).

A discussion of seismic operations in Saudi Arabia, with particular emphasis on problems of logistics and equipment requirements for desert operations.

338. *Geophysical Methods of Oil Prospecting — A Review.* IV.—*Seismic Methods.*
D. Taylor Smith, Petroleum, Vol. 18, No. 6, pp. 211-217, June 1955.

With advances in instrumentation and interpretation, the seismic method of exploration has proved suitable for detecting most varieties of geological structures that are favourable for the accumulation of oil. A brief history of the various types of seismic technique is given and the general theory is discussed.

339. *New Developments in Seismic Methods.*
H. Salvatori, Proceedings of the 4th World Petroleum Congress, Section I, p. 605, June 1955.

Field equipment has seen several important improvements and new devices. Among these are the air and auger drills, specialized track vehicles and a cable handling device. Continuous control of velocities and moveouts of individual reflections removes an important source of interpretation errors. Research and development is proceeding apace from investigation of basic earth physics and information theory to new and improved instruments and techniques.

340. *Reflection-Seismic Exploration of Schleswig-Holstein.*
F. Hecht, H. Helms & W. Kehrer, Proceedings of the 4th World Petroleum Congress, Section I, p. 715, June 1955.

Detailed reflection-seismic surveys have been carried out all over Schleswig-Holstein. They have resulted in an accurate delineation of geological structures.

The geophysical results have furnished detailed stratigraphical, lithological and structural data on the most dominant structures, the flanks of salt domes and sedimentary basins. As a result, the main structural units of Schleswig-Holstein have been disclosed.

341. *Seismic Crustal Exploration, Colorado Plateau, and Wasatch-Uinta Mountains.*
M. A. Tuve & H. E. Tatel, Paper read at the 36th Annual Meeting of the Am. Geophys. Un., Washington, May 1955. (Not yet published).

The continental seismic survey of crustal structure has been extended to the southern part of the Colorado plateau and the eastern rim of the Great Salt Lake Basin. The average elevations were 4500-7000 ft. and 6500 ft. respectively. Shots in Santa Rita, New Mexico and Morenci, Arizona were observed along several radiants. Critical reflections were observed at 108 km. and total reflections beyond; the P_n were traced out to 300 km. with a cross over at 145 km. to the south and 175 km. to the north. The depth of the lower crustal (Mohorovicic) discontinuity is thus at 28 km. to the south and 34 km. to the north (10-15 pct greater if corrected for increase of velocity with depth). In Utah shots were recorded from Bingham Canyon but no reflections were observed. The shots were weak. The cross over is at about 135 km. and the discontinuity depth is about 29 km. Similar measurements in the east have shown the crustal depth to be at greater depth (40 km). with lesser surface height (2000 ft.). It is concluded that the Pratt-Airy Hypotheses while they may have limited regional applicability, are not in their present form descriptive of whole continental structures.

342. *Electrical Hazards in Seismic Prospecting.*
A. M. Selem & E. Merlini, Geophysical Prospecting, Vol. 3, No. 2, pp. 163-167, June 1955.

Hazards due to power lines, radio-transmitters and self-potentials, in connection with weather conditions, are considered. Voltage and current values are given for several measurements made under the most servere conditions of circuit arrangements. The necessity of general safety precautions is stressed.

(Author's Abstract).

343. *Safety Training for Seismic Units Operating in Foreign Fields.*
W. F. Rickards, Geophysics, Vol. 20, No. 3, p. 715, July 1955.
(Abstract only of paper read at the 10th Annual Gulf Coast Meeting of the S.E.G. at San Antonio, Texas, May 1955).

The author presents the problem of effective administration of a safety programme in foreign operations where the services of a full-time safety engineer are not justified. Some practical aspects of setting up and administering such a programme are also presented.

344. *The Geophysical Case History of the Good Hope Field, St.Charles Parish, Louisiana.*
G. A. Burton, Geophysics, Vol. 20, No. 3, p. 716, July 1955.
(Abstract only of paper read at the 10th Annual Gulf Coast Meeting of the S.E.G. at San Antonio, Texas, May 1955).

Comparisons of the seismic and subsurface maps of the field show that the major features of the structure were correctly predicted by continuous reflection profiles.

345. *Geophysics Scores in Western Canada.*
C. J. Chapman, Oil & Gas J., Vol. 54, No. 15, pp. 140-147, Aug. 15, 1955.

A short historical account of seismic work is given, with details of the numbers of crews operating each year from 1945 onwards. No complete information is available on the percentage of successes, but in the author's opinion almost all discoveries so far can be credited to the seismograph. Operational problems and hazards, and the more unusual techniques employed to overcome them, are described.

346. *Seismic Study of Crustal Structure in Pennsylvania and New York.*
S. Katz, Bull. Seismol. Soc. Am., Vol. 45, No. 4, pp. 303-325, October 1955.

347. *The Refraction Seismograph in the Alberta Foothills.*
G. J. Blundun, Geophysics, Vol. 21, No. 3, p. 828, July 1956.

The primary purpose in the use of the refraction seismograph in the Alberta foothills is the mapping of the Madison limestone together with the detection and definition of faults. This paper deals with the advantages and limitations of refraction, both in-line and broadside, initial programme, spread length, geophone separation, dynamite charges, system of survey and permissible tolerance, and other recommended field practices. Typical specimen seismograms and cross-sections are illustrated, as well as a gravity-refraction comparison of a typical limestone fault.

348. *Acoustic and Other Physical Properties of Shallow-Water Sediments off San Diego.*
E. L. Hamilton, G. Shumway, H. W. Menard & C. J. Shipek, J. Acoust. Soc. Am., Vol. 28, No. 1, pp. 1-15, January 1956.

The study of acoustic and other physical properties of shallow-water sediments off San Diego, California, is reported. Seismic velocity measurements at 100 kc. were made by pulsing between small transducers inserted into the sediment.

Samples of sediment were obtained by diver for laboratory tests. Measurements of velocity and attenuation at 25-35 kc. were made by a resonant-chamber method. The samples were also tested for density, porosity and particle size.

The results are tabulated and illustrated with graphs and diagrams.

SEISMIC — INSTRUMENTAL

349. *Magnetic Recording—New Tool in Seismic Prospecting. A Symposium.*
W. T. Born, H. R. Frank, C. F. Hadley & J. H. Hidy, Oil & Gas J., Vol. 53, No. 48, pp. 172-174, April 4, 1955.

The Geophysical Society of Tulsa recently held a symposium on the subject of Magnetic Tape Recording. The Moderator was W. T. Born. This article contains summaries of the three papers read which were entitled as follows:
"Magnetic Recording in Field Operations"—H. R. Frank.
"Display of Magnetically Recorded Seismic Data" — C. F. Hadley.
"Improving Signal to Noise Ratio by Compositing Magnetic Records"—J. H. Hidy.

350. *Geophysical-Type Magnetic Tape Recorders.*
J. D. Skelton, Oil & Gas J., Vol. 53, No. 48, pp. 176-183, April 4, 1955.

With the need for more information from seismic records, playback magnetic recording systems are becoming more important. This paper describes and compares seven magnetic recording units that are available for geophysical application. They are as follows:-

Ampex Model 700, a 24-channel drum-type recorder using F. M.
Brush Model BK 315, a 24-channel drum-type recorder using F.M.
Electro-Tech. Model DS-2, a 12-channel reel-type recorder using pulse-width modulation.
Magna-Disc Recorder, a disc-type using F.M.
Mirragraph Model TI-400A, a drum-type 24 or 48-channel recorder using bias-type recording.

S.I.E. Co. NR-4, a 24-channel recorder using F.M.
U.G.C., a 24-channel belt-type recorder using F.M.

351. *Geophysical Instrumentation is Making Rapid Progress.*
F. J. Agnich, World Oil, Vol. 140, No. 5, pp. 109-111, April 1955.

A general review is made of the recent modifications that have been made to geophysical instruments. Significant new techniques include magnetic recording, mechanical plotting, weight dropping for seismograph shock, single-ship method of marine shooting, and the expansion of frequency range in seismograph recordings. The instrumentation associated with these is briefly discussed.

352. *A Low-Frequency Refraction Geophone.*
W. M. Jones & A. T. Dennison, Geophysical Prospecting, Vol. 3, No. 2, pp. 168-176, June 1955.

This paper describes a highly portable geophone, designed for large scale refraction surveying, which uses a novel suspension system to obtain a natural frequency of about 1.85 c/s. The nominal output is 0.7 volts/cm./sec. into a 500 ohm load, the damping then being 0.7 of critical. Some typical recorded arrivals obtained with this geophone are illustrated. (Author's Abstract).

353. *Seismic Recorder for Monitoring Magnetic Tape.*
G. P. Loper, Geophysics, Vol. 20, No. 3, pp. 585-592, July 1955.

A new recorder utilizing Polaroid "picture-in-a-minute" film has been developed to monitor seismic data recorded on magnetic tape. Signals from 12 magnetic recording heads are applied through appropriate networks to conventional galvanometers in the monitor as the magnetic record is made. The optical system is arranged to make a miniature seismogram of conventional appearance on a standard 3″ × 4″ Polaroid print. The record is a satisfactory guide for the operator to evaluate the quality of the record on the magnetic tape without the need for playing it back. (Author's Abstract).

354. *Patents.* Abstracts in Geophysics, Vol. 20, No. 3, p. 689, July 1955.

U.S. 2,698,927.	4 Jan. 1955.	A seismograph mixing system.
U.S. 2,578,133. (Re. 23,919)	11 Jan. 1955.	A seismograph recording system using a geophone with a broad-frequency response, a h-f carrier, and magnetic tape for reproduction and playback.
U.S. 2,700,753.	25 Jan. 1955.	A multichannel radio seismograph recording system.
U.S. 2,703,150.	1 Mar. 1955.	A seismic reflection display system.

355. *Instruments for More Complete and Effective Coverage of the Seismic Spectrum.*
F. A. Brock, Geophysics, Vol. 20, No. 3, p. 716, July 1955.
(Abstract only of paper read at the 10th Annual Gulf Coast Meeting of the S.E.G. at San Antonio, Texas, May 1955).

The quest for more accurate and detailed structural information has led to the development of high-resolution reflection systems, to improvements in conventional reflection systems, and to the development of tailor-made refraction systems. These systems are described and other instrumentation advances discussed.

SEISMIC — FIELD TECHNIQUE

356. *Measurement of Noise and Multiple Geophones.* (In French).
H. Richard & M. Rimbaut, Geophysical Prospecting, Vol. 3, No. 2, pp. 177-194, June 1955.

Signal-to-noise ratio improvements have been obtained by the use of multiple geophones and longer spreads. Work was carried out in the difficult recording area of Landes to obtain a direct measurement of noise reduction as a function of the geophone pattern, etc.

Initial shots showed the noise to be of a random nature, so that many experiments were necessary. Two geophone patterns were employed, one of 12 in a straight line and the other of two parallel lines; directions of the lines being along the shot line, perpendicular to the shot line, or at any other angle.

Results from two locations were in agreement. A long 12-geophone line reduces noise by a factor of 0.36 and two 12-geophone lines, each 55 m. long and widely apart, reduce noise by a factor of 0.29. In general the noise reduction agrees with the factor $KN^{-\frac{1}{2}}$, where K is close to unity and N is the number of geophones per trace.

357. *Patents.* Abstracts in Geophysics, Vol. 20, No. 3, p. 689, July 1955.

U.S. 2,698,575.	4 Jan. 1955.	An explosive charge consisting of two superimposed explosives designed to produce a flat shock-wave downwards.
U.S. 2,704,031.	15 Mar. 1955.	A plastic anchor for retaining borehole explosive charges.
U.S. 2,704.514.	22 Mar. 1955.	A method of preparing an irregular shot hole with a plastic material and refrigerant.

358. *Seismic Exploration in Hard Rock Country.*
R. L. Palmer, Petroleum Engineer, Vol. 26, No. 8, pp. B. 85-B. 96, Aug. 1954.

This article describes the advantages of the McCollum weight-dropping ("Geograph") method in prospecting areas with hard rock on or near the surface, where conventional seismic shots would produce very large horizontal reverberations. The Geograph equipment and field techniques are described, and some typical logs shown.

359. *Star Patterns.*
Oil & Gas J., Vol. 54, No. 13, pp. 82 & 83, August 1, 1955.

This article describes a shooting technique employing multiple hot sholes and multiple geophones. The shot holes number 36 arranged in concentric circles, situated at the centre of the "spread". The geophones are arranged in star patterns. In a typical pattern there may be twelve "stars" at 200 foot intervals along two main cables extending in opposite directions from the shot-hole area.

The method involves some 40 % extra time in picking up and reassembling 432 geophones and cable after each shot, and in drilling the extra shot holes (low-pressure air-drilling is employed), but the expense is considered worthwhile. Advantages of the method are: better signal pick-up and better selectivity of signal.

360. *Patents.* Abstracts in Geophysics, Vol. 20, No. 2, p. 336, April 1955.

U.S. 2,691,939.	19 Oct. 1954.	Apparatus for planting an explosive charge below the surface of the earth beneath a body of water.
U.S. 2,693,245.	2 Nov. 1954.	An above-ground explosive array.

361. *Reflection Survey in Rough Topography.*
A. M. Selem, Geophysical Prospecting, Vol. 3, No. 3, pp. 246-257, Sept. 1955.

The problems connected with reflection surveys in areas of rough topography consist of choosing proper equipment and of making careful near-surface corrections. This paper illustrates some solutions to these problems that have been adopted in a survey which has recently started in a hilly coastal district, in southern Italy.

Details are given of the truck-mounted light equipment which was necessary to allow straight-line shooting.

The great differences in elevations, and in surface or near-surface materials, called for careful analysis before the thickness of the correction zone could be decided. The solution adopted for obtaining the reference base of the correction zone for the whole area is explained.

Velocity variations were checked by methods based on up-hole-time analyses and refraction 'first breaks'.

The final cross-sections indicate that topographic and near-surface velocity influences have been eliminated, though no deep holes are yet available for checking the seismic data.

SEISMIC — INTERPRETATION

362. *Seismic Velocities from Surface Measurements.*

C. H. Dix, Geophysics, Vol. 20, No. 1, pp. 68-86, January 1955.

The purpose of this paper is to discuss field and interpretative techniques which permit, in favourable cases, the quite accurate determination of seismic interval velocities prior to drilling. A simple but accurate formula is developed for the quick calculation of interval velocities from "average velocities" determined by the known x^2—T^2 technique. To secure accuracy a careful study of multiple reflections is necessary and this is discussed.

Although the principle objective in determining velocities is to allow an accurate structural interpretation to be made from seismic reflection data, an important secondary objective is to get some lithological information. This is obtained through a correlation of velocities with rock type and depth.

(Author's Abstract).

363. *Additional Notes on the Resolved-Time Computing Method.*

R. B. Rice, Geophysics. Vol. 20, No. 1, pp. 104-122, January 1955.

The basic elements of a time-resolution method of performing reflection seismograph computations have been published previously. The purpose of this paper is to present additional material to show how, by varying the spacing between shotpoints on the time cross-section, the method may be made to give results comparable to various standard techniques and to describe the corresponding time method of handling cross-spread data. An additional example showing actual cross-sections computed by the method is included. (Author's Abstract).

364. *The Reynolds Plotter.*

V. T. Reynolds & P. Farren, Oil & Gas J., Vol. 53, No. 48, p. 211., April 4, 1955. (Abstract only of paper read at the Annual Meeting of the S.E.G, New York, March 1955.)

A system of seismic data analysis is presented which mechanically identifies, times, computes, and plots in cros-section form (point plot) or record section form (full envelope of each trace) all events on a seismogram.

Velocity depth function, and normal moveout, weathering and elevation corrections, are applied to each trace individually as all traces are scanned and reproduced simultaneously by a mechanical process.

The system produces cross-sections and record sections with speed, thoroughness, and accuracy. Convenience in correlation of the sections expands the output of the interpreter, flexibility in handling the mass of data facilitates special projects such as velocity, isopach, and magnetic-tape studies; thoroughness of presentation of seismic evidence, especially segmental reflections, permits a more valid interpretation.

365. *New Computing Device Aids Seismic Interpretations.*
World Oil, Vol. 140, No. 5, pp. 142-148, April 1955.

This article, based on material supplied by S.I.E.—the manufacturers of the equipment, describes the operation of the Reynolds Plotter for identification of reflected events ('picking'), counting their time values, correcting these values for variables and plotting event depths on a graph representing an earth cross-section. Picking does not begin or end at a given shot point, but proceeds along the traverse; the interpreter is free to make his decisions without attempting to render the corrections applicable to each trace, and without interpolating "raw" trace times.

366. *The Treatment of Lateral Velocity Variation in Seismic Interpretation.*
L. W. Gardner, Geophysics, Vol. 20, No. 2, p. 378, April 1955.
(Abstract only of paper read at the Annual Meeting of the S.E.G., New York, March 1955).

Lateral velocity variations are associated with geologic structural, stratigraphic and lithologic conditions. The construction of the most suitable time-depth conversion chart applicable to a given area for seismic interpretation depends upon these conditions. A number of different cases are treated which typify sets of conditions present in different areas and basins.

Regional velocity corrections are necessary to account for facies change but may incorporate other factors either deliberately or inadvertently. Some comments are made with respect to sub-weathering velocity variation, reef influence, influence of overthrustings and topographic kinds of velocity corrections and the time depth chart which becomes increasingly binding with increase in amount of available vertical velocity information. Consequently, there is a pitfall that a poor assignment of one factor can induce a poor assignment of a second factor with deleterious effect upon mapped results.

367. *Templates for Fitting Smooth Velocity Functions to Seismic Refraction and Reflection Data.*
J. G. Hagedoorn, Geophysical Prospecting, Vol. 3, No. 4, pp. 325-338, December 1955.

Velocity functions can be grouped into families, any one of which results in seismic pictures differing among themselves only in their scales of time and distances but similar in all other respects. For any one of these families it follows that curves drawn on logarithmic scales of time and distances to represent a particular relationship between seismic quantities will be similar in shape. This leads to the use of templates with logarithmic scales for fitting a smooth velocity function to a set of seismic data. Suitable templates for fitting refraction and reflection data to velocity distributions, linear with either depth or vertical time are presented. An insight into the uncertainties involved is obtained with the aid of numerical examples.

(Author's Abstract).

368. *Reflection Survey in Rough Topography.*
A. M. Selem, Geophysical Prospecting, Vol. 3, No. 3, pp. 246-257, September 1955.

The problems connected with reflection surveys in areas of rough topography consist of choosing proper equipment and of making careful near-surface corrections. This paper illustrates some solutions to these problems that have been adopted in a survey which has recently started in a hilly coastal area in southern Italy.

Details are given of the truck-mounted light equipment that was necessary to allow straight-line shooting.

The great differences in elevations and in surface, or near surface, materials called for careful analysis before deciding the thickness of the correction zone.

The solution adopted for obtaining the reference base of the correction zone for the whole area is explained.

Velocity variations were checked by methods based on uphole-time analyses and refraction 'first breaks'.

The final cross-sections indicate that topographic and near-surface velocity influences have been eliminated, though no deep holes are yet available to check the seismic data.

SEISMIC — THEORY & RESAERCH

369. *Three-Dimensional Seismic Model Studies.*
F. K. Levin & H. C. Hibbard, Geophysics, Vol. 20, No. 1, pp. 19-32, January 1955.

Elastic wave propagation in a two-layer section has been studied with a solid two-bed model and records resembling seismograms obtained for the four possible source-detector configurations. Numerous events are identified. Among these, the shear waves are found to be surprisingly prominent. The amplitude of the ground roll falls off approximately as (distance)$^{-\frac{1}{2}}$. This is the amplitude range dependence expected for a surface wave. The ability of two in-line detectors to reduce surface waves has been demonstrated.

(Author's Abstract).

370. *The Initial Behaviour of a Spherical Explosion. I. Theoretical Analysis.*
M. Holt, Proc. Roy. Soc., A, Vol. 234, No. 1196, pp. 89-109, 24 January, 1956.

The analysis of the disturbance near the source of the spherical blast from a polytropic explosive in which $\gamma = 3$, given in Berry & Holt (1954), is generalised to apply to an explosive gas and a surrounding medium governed by any equations of state. Most of the properties established in the special case are found to be generally true. In particular, a second blast wave is shown to be a consequence of the breakdown of continuous gas flow in the neighbourhood of a singular characteristic. The complete field near the origin of blast can be determined from series expansions similar in type to those in Berry & Holt (1954). Except in the gas expansion zone the co-efficients in these expansions can be expressed in simple terms. The quantity defining the first departure of the second shock from the singular characteristic is given by an expression as simple as that in the polytropic case, although its derivation presents new difficulties.

The analysis shows that, for all types of explosive, the second shock is a second-order effect in terms of the square root of the time from the end of detonation. This contradicts the conclusion reached earlier by Wecken (1951) on the basis of less detailed analysis.

(Author's Abstract)

371. *The Initial Behaviour of a Spherical Explosion.* II. *Application to Petn Charges in Air and Water.*
M. Holt, Proc. Roy. Soc., A, Vol. 234, No. 1196, pp. 110-115, 24 January, 1956.

The initial fields of disturbance due to explosions of spherical charges of PETN in air and water are calculated, using the analysis developed in Part I. The results in air compare favourably with earlier calculations (Berry & Holt 1954). In water it is found that the second blast wave immediately moves towards the centre of the explosion, with very small initial strength.

(Author's Abstract)

372. *Model Seismology — The Critical Refraction of Elastic Waves.*
P. N. S. O'Brien, Geophysics, Vol. 20, No. 2, pp. 227-242, April 1955.

Model experiments on the head wave are described. Quantitative data are obtain-

ed for three different pairs of media: light lubricating oil on top of a saturated solution of calcium chloride, water on top of wax, and water on top of concrete. Within the limits of experimental error these data agree with the theoretical prediction that the head wave should decay with distance as $r^{-\frac{1}{2}} L^{-3/2}$ (Heelan, 1953).
(Author's Abstract).

373. *Some Velocity Measurements in Drill Holes in Northern Germany.* (In German).
T. Krey & G. Teudesmann, Erdöl u Kohle, Vol. 7, No. 9, pp. 548-550, 1954.

Measurements of seismic velocities in drill holes showed that when the charge is placed on the ground over the hole and the geophone suspended on a cable in the borehole, the wave propagating through the cable causes interference. It is necessary to place the charge at a certain lateral distance from the hole and make necessary corrections for the refracted waves. The velocity in the ground above the water table was very low, in some places only 200 m/sec. Below the water table, the velocity immediately increased to 1,600-2,000 m/sec. Data are given on several graphs.

(From Geophysical Abstracts 160, U.S. Geol. Survey).

374. *Elastic Wave Velocities in Laminated Media.*
J. E. White & F. A. Angona, J. Acoust. Soc. Am., Vol. 27, No. 2, pp. 310-317, March 1955.

Elastic wave velocities in a laminated medium have been determined by calculating the effective elastic parameters and densities. The media are assumed to be in static equilibrium and under stress. The stress generates strain that simulates elastic waves. An effective stiffness constant is obtained from application of Hooke's Law. The ratio of the effective stiffness to the effective density is the square of the elastic wave velocity. For a laminated medium of two materials where the densities are equal but the velocity contrast is 2, the compressional wave velocity is 20 % higher along the laminations than perpendicular to them. The SH shear wave velocity is 25 % higher than the SV shear wave for the same laminated medium.

375. *The Composition of Reflections.*
J. P. Woods, Oil & Gas J., Vol. 53, No. 48, p. 211, April 4, 1955.
(Abstract only of paper read at the Annual Meeting of the S.E.G., New York, March 1955).

The reflection seen on a seismic record is often a composite of several reflections. The interpreter thinks that he deals with a single interface, when in reality, he is dealing with a number of close-spaced, reflecting layers. If the arrangement of these layers changes, the composite reflection seen on the record will change in time of occurrence and in character. In consequence, the horizon carried by the interpreter will be in error. To demonstrate this composition of reflections, a simple acoustical model has been built and various records made with this model are shown.

376. *Reflection of Sound from a Continuous Stratum Containing a Velocity Extremum.*
E. O. Cook & H. S. Heaps, J. Appl. Phys., Vol. 26, No. 4, pp. 429-433, April 1955.

The reflection of a plane wave of sound from a layer separating regions of different sound velocities, the layer itself containing a velocity variation through an extremum, is considered in terms of its dependence upon the angle of incidence, the layer thickness, and the velocity variation through the layer. It is found that the power reflection coefficient may differ significantly from its value for the corresponding abrupt or montonic velocity transition. Numerical results are tabulated for various types of layers of thickness from zero to ten wavelengths and with a total velocity transition of ± 5 and ± 10 ft./sec.

377. *A Deep-Sea Seismic Reflection Profile.*
C. B. Officer, Geophysics, Vol. 20, No. 2, pp. 270-282, April 1955.

This paper presents a detailed seismic reflection profile taken over the deep ocean. Clear sub-bottom reflections and refractions are obtained which are interpretable to show the variation of velocity with depth. From the travel-time difference between the bottom reflection and a prominent sub-bottom reflection as a function of range and frequency and from the variation of the amplitudes of the bottom and sub-bottom reflections with frequency and angle of incidence, the conclusion is reached that the sediment is dispersive, i.e., that the velocity of sound propagation through it is a function of frequency. Further it is concluded that at lower frequencies the velocity in the sediment near the bottom is less than that in the adjacent ocean. This rather unexpected geophysical phenomenon is explained theoretically in terms of propagation in a porous media.

The low velocity sediment forms a wave guide between the higher velocity ocean above and the higher velocity sediment beneath. This resultant wave guide explains previously observed single-frequency arrivals.

(Author's Abstract).

378. *Channel Waves in the Earth's Crust.*
B. Gutenberg, Geophysics, Vol. 20, No. 2, pp. 283-294, April 1955.

Three major low-velocity layers seem to exist in the earth's crust, of which two, the lithosphere channels, are found respectively in the "granitic" and "basaltic" ("gabbro") layers of the continents; a third channel extends from the Mohorovicic discontinuity downward into the asthenosphere. Several types of waves are guided by these channels, especially Pa and Sa by the asthenosphere channel, Lg 1, Lg 2 and Rg by the lithosphere channels; waves guided by low-velocity layers in sediments must also be expected.

379. *Variations in Time Delay between Detonations as a Factor in Quarry Blast Vibrations.*
J. H. Wiggins, Paper read at the 36th Annual Meeting of the Am. Geophys. Un., Washington, May 1955. (Not yet published).

Certain seismic phases, produced by different millisecond dealy quarry blasts, were identified and compared by Fourier analysis and other, more conventional methods. The only variable between the test shots was time delay. The results of the investigation showed that compressional energy is increased, shear energy is possibly reduced, and surface waves are decreased in amplitude as the time delay is changed from 0.015 to 0.030 sec. Some possible conclusions affecting the results are discussed.

380. *Maximum Group Velocity of Rayleigh Waves between* 60 *and* 80 *Seconds.*
F. Press & M. Ewing, Paper read at the 36th Annual Meeting of the Am. Geophys. Un., Washington, May 1955. (Not yet published).

In the period range 15-60 secs., crustal Rayleigh waves show an increase of velocity with period. As the period increases between 80 and 225 secs., mantle Rayleigh waves decrease in velocity. The maximum value of group velocity found by combining both dispersion curves is about 3.9 km./sec. and falls between 60 and 80 secs. Neglect of the mantle velocity gradient in interpretation of crustal Rayleigh waves leads to a value of mantle shear velocity which is too small. The effect of the maximum group velocity on the initiation of crustal Rayleigh waves is illustrated with seismograms.

381. *Constructive Representation of Seismic Horizons Making Use of the Refraction Method.* (In German).

J. Baumgarte, Geophysical Prospecting, Vol. 3, No. 2, pp. 126-162, June 1955.

The paper describes a geometrical construction which allows the reflecting of refracting boundaries to be derived from seismic time observations.

In reflection work the construction makes use of the ray reflected from the boundary at normal incidence. For constant velocities of the beds, or for a linear increase of velocity with depth, the method leads to the construction of successive envelopes from which the reflecting interface and the rays are obtained. By using the idea of "stretching fictitious rays", the construction requires ruler and compasses only and is applicable to both plane and curved boundaries with any strike direction and in any number.

The same principles can be applied to refraction problems and again the construction of successive envelopes allows the indirect or Mintrop wave to be defined. The position of the refracting boundary and the velocity can be derived immediately. As in the reflecting method any number of plane boundaries with any strike can be dealt with.

An appendix discusses the use of the method in reflection work with any type of velocity distribution.

(Author's Abstract)

382. *Calculated Travel Times of Seismic Core Waves.*

R. D. Forester, Bull. Seismol. Soc. Am., Vol. 45, No. 3, pp. 187-195, July 1955.

Travel times for the seismic core waves, PKP, PKS, and SKS, were computed by integration along the travel paths. For this purpose the velocity distribution within the earth was broken into segments which were represented by continuous functions. Except for rays of grazing incidence to the outer core the times calculated for PKP and PKS are intermediate between the smoothed times given by Jeffreys and times based upon recent observed data. The times calculated for SKS are in fair agreement with the smoothed times given by Jeffreys.

(Author's Abstract).

383. *The Synthesis of Seismograms from Well Log Data.*

R. A. Peterson, W. R. Fillippone & R. B. Coker, Geophysics, Vol. 20, No. 3, pp. 516-538, July 1955.

Under certain simplified but realistic physical assumptions, the basic data from continuous velocity surveys in wells can be used to simulate the variations in acoustic impedance in the ground which give rise to seismic reflections. An analogue computer is described which makes use of the basic well data to produce synthetic seismic records which resemble actual seismograms from shothole explosions. This process provides an interesting insight into the requisite physical conditions, as well as the physical processes, whereby seismic reflections are set up in the earth. The close relationship between seismograms and well logs is brought out. Illustrations are given of field results. (Author's Abstract).

384. *Application of Correlation Techniques to Geophysical Prospecting.*

C. W. Horton, Geophysics, Vol. 20, No. 3, p. 715, July 1955.

(Abstract only of paper read at the 10th Annual Gulf Coast Meeting of the S.E.G. at San Antonio, Texas, May 1955).

A recent development in geophysical research is the application of auto- and cross-correlation techniques to geophysical data in the hope of improving the signal-to-noise ratio. This work is summarized, and typical correlation functions for land and shallow water areas are presented. The relation between correlation techniques, filtering and directional patterns is reviewed and illustrated. A theory is developed to explain the shape of the autocorrelation function of a seismogram trace.

385. *A New Method of Pattern Shooting.*
J. O. Parr & W. H. Mayne, Geophysics, Vol. 20, No. 3, pp. 539-564, July 1955.

In areas where reflection shooting is difficult, it is often necessary to attenuate the energy in a broad continuous band of disturbing wavelengths to less than a few hundredths of what would be recorded if all units were bunched together. The wavelength band of the attenuated energy should be adjacent to the band of reflection wavelengths received. Attenuation of the undesired energy is best accomplished with multiple detectors or charges. In many areas the pattern should attenuate energy horizontally propagated in all directions, not just in the direction of the detector line. Neither a finite number of uniformly effective, uniformly spaced units in line nor a uniformly effective sheet of finite length will accomplish this result. A system for gradation of effectiveness of the units described in this paper does produce this result (not only for in-line disturbances but also for disturbances coming in from the side of the line). The attenuation band can be made broad with good attenuation or narrower with still better attenuation, as desired. The variation of effectiveness can be applied to detectors or charges arranged in a horizontal line, over a horizontal area, in a vertical line, or over a vertical area. The principle of varying effectiveness can also be applied to reversed-polarity detectors in order to accentuate certain apparent wavelengths.

(Author's Abstract).

386. *The Structure of the Noise Background of a Seismogram.*
C. W. Horton, Geophysics, Vol. 20, No. 3, pp. 565-584, July 1955.

It is postulated that the noise background of a typical seismogram is the result of the arrival at random times of a large number of small reflections which are reflected from small scatterers distributed throughout the earth. It is shown on the basis of this assumption that if one knows the shape of a typical reflection, one can calculate the statistical parameters of the seismogram trace. Conversely, if one has the experimental autocorrelation function, the shape of the individual reflections can be determined. This analysis has been applied to a vertical spread of three geophones located 10, 75 and 125 feet below the surface. The shapes of the individual reflections were determined for the two deeper geophones. These curves show that the disturbances detected by the deeper geophone have a significantly smaller dominant frequency.

(Author's Abstract).

387. *Velocity Anisotropy in Stratified Media.*
L. F. Uhrig & F. A. Van Melle, Geophysics, Vol. 20, No. 3, p. 715, July 1955.
(Abstract only of paper read at the 10th Annual Gulf Coast Meeting of the S.E.G. at San Antonio, Texas, May 1955).

Velocity anisotropy has been reported in Texas, Oklahoma and Canada. The phenomenon includes anisotropy of the individual layers as well as an apparent anisotropy resulting from the time gain on oblique paths in a sequence of layers. The authors and other Shell personnel made time measurements on oblique paths to seismometers in wells and studied late arrival refraction data in sedimentary basins in Texas and Canada. The anisotropy factor (ratio of horizontal to vertical compressional speed) was found to vary from 1.05 to 1.24. At the present time the amount of statistical data on velocity anisotropy is limited, and it is therefore suggested that additional observations be made. The interpretation of seismic data would certainly gain from a knowledge of the degree of anisotropy, especially in wide angle reflection work and in refraction surveys, and this can be accomplished by adding offset shotpoints to routine well velocity surveys.

388. *Statistical Methods in Multiple Seismometer and Pattern Hole Shooting.*
M. K. Smith, Geophysics, Vol. 20, No. 3, p. 716, July 1955.
(Abstract only of paper read at the 10th Annual Gulf Coast Meeting of the S.E.G. at San Antonio, Texas, May 1955).

Much has been said and written about multiple seismometers and pattern hole shooting, including material based on empirical results, antenna theory and statistics. In the present paper is attempted a comprehensive treatment leading to nomograms suitable for field determination of optimum multiple seismometer and multiple shot patterns. Field measurements providing information essential to the application of the nomograms are discussed and statistical estimation is used to supplement the necessarily limited experimental information.

389. *Propagation of Rayleigh Waves in Transversely Isotropic Medium in Three Dimensions.*
S. C. Das Gupta, Trans. Am. Geophys. Un., Vol. 36, No. 4, pp. 675-678, August 1955.

The possibility of propagation of Rayleigh waves in a transversely isotropic medium is discussed. It is found that the frequency equation is the same as in the two-dimensional case. In the case of ordinary crystals, there is only one real root of the frequency equation which satisfies the necessary boundary conditions.

390. *The Determination of a Given Curved Surface by Seismic Reflection Measurements.* (In German).
M. Weber, Geofis. Pura e Appl., Vol. 32, No. 3, pp. 7-11, Sept. 1955.

Under the assumption that the measuring surface $z = \zeta\ (x, y)$, and the reflection horizon of a structure $z = f\ (x, y)$ have an arbitrary curvature a simple method is developed for calculating the surface 'f' from seismic reflection data measured along the surface ζ. In addition the general solution is discussed and some special cases are treated.

(Author's Abstract).

391. *The Travel-Time Surface for Multiple Reflections in a Inhomogeneous Medium with a Given Curved Surface.* (In German).
M. Weber, Geofis. Pura e Appl., Vol. 32, No. 3, pp. 12-18, Sept. 1955.

The travel-time surface for multiple reflections has been calculated, under the assumption that the wave-velocity 'c' is an arbitrary functions of the depth 'z' and that the surface of the elastic body has an arbitrary curvature.

392. *On the Theory of the so-called Headwaves with Infinitely Small Amplitudes.* (In German).
M. Matschinski, Geofis. Pura e Appl., Vol. 32, No. 3, pp. 19-30, Sept. 1955.

A paper on: the case of two reflected waves in seismology; four types of wave near to a surface; general properties of the concept 'wave'; thermic and geometric extinction of a wave; the conditions that an aggregate of waves has, or has not, the properties of a wave; and the interference of two waves and the impossibility of such interference of two wave ensembles.

393. *On the Focusing Effect of Reflection and Refraction in a Velocity Gradient.*
W. J. Noble, J. Acoust. Soc. Am., Vol. 27, No. 5, pp. 888-891, Sept. 1955.

The divergence factor, which is of importance in the reflection of waves from a convex spherical surface, is shown to have its counterpart in plane reflection and refraction in the presence of a velocity gradient. Within a small angle approximation, a linear velocity gradient gives the ordinary spherical spreading of a pencil of rays; any discontinuity of gradient causes a divergence or convergence of the pencil. Analytical expressions and tables of typical values are calculated for four different cases.

394. *Theoretical Study of the Velocity of Compression Waves in Silt.* (In French).
I. D'Erceville, Geophysical Prospecting, Vol. 3, No. 3, pp. 240-245, Sept., 1955.

It has been noted that in water-saturated silt, the velocity of propagation of longitudinal waves is very low. The purpose of this paper is to suggest a theoretical explanation for this phenomenon.

The medium under study is assumed to consist of identical solid spheres piled one upon the other in a regular array, with the fluid filling the interstices. First the velocity of propagation is calculated for the system of the solid particle alone; then, utilizing the results obtained for this case, the velocities for solid-fluid system are calculated. Two velocities are obtained, one of them being higher and the other lower than in the case where no fluid is present.

(Author's Abstract).

395. *Seismic Wave Propagation and Pressure Measurements near Explosions.*
G. R. Pickett, Q. Colorado School of Mines, Vol. 50, No. 4, pp. 1-77, October 1955.

Limitation of the seismic method to structural mapping seems at present to be due largely to a lack of knowledge about the phenomena of seismic wave generation and propagation and to the lack of means for arriving at an unambiguous interpretation of the records obtained.

With the object of finding relations between the recorded seismic waveforms and the physical properties of the medium through which the seismic waves have travelled, the following investigations were carried out:

1. An analytical investigation of several seismic wave theories. The object of this investigation was to arrive at results which may be proved or disproved by pressure-time measurements in the field.
2. A comparison of pressure waveforms with the waveforms recorded by shallow seismic reflection recording equipment.
3. Empirical determination of the pressure-time-distance relations surrounding the shot for several formations in situ.
4. Charge size-pressure peak relations for several formations.
5. Charge size-"hole fatigue" relations.
6. The effect of reflections and refractions on pressure—time records.

GRAVITY — GENERAL

396. *Gravity Measurements at Sea, 1950 and 1951.*
J. L. Worzel, G. L. Shurbet & M. Ewing, Trans. Am. Geophys. Un., Vol. 36, No. 2, pp. 335-338, April 1955.

397. *Gravity Measurements at Sea. 1952 and 1953.*
J. L. Worzel, G. L. Shurbet & M. Ewing, Trans. Am. Geophys. Un., Vol. 36, No. 2, pp. 326-334, April 1955.

398. *Underwater Gravity Survey in the Adriatic Sea.*
C. Morelli, Proceedings of the 4th World Petroleum Congress, Section I, p. 661, June 1955.

399. *Geological Implications of Gravity Anomalies over the Grenville and Northern Appalachian Regions of Quebec.*
G. D. Garland & L.G. D. Thompson, Paper read at the 36th Annual Meeting of the Am. Geophys. Un., Washington, May 1955. (Not yet published).

400. *Structural Prospecting with the Gravity Meter.*
W. F. Stackler, Oil in Canada, Vol. 7, No. 39, pp. 52-62, July 25, 1955.
This paper describes the progress made in structural prospecting with the gravimeter. The theory and experimental results over the Erskine (reef structure) and Turner Valley (Foothills structure) oil-fields are presented and discussed. It is concluded that gravimeters are very suitable for prospecting in such areas.

401. *A Review of the Factors Affecting the Accuracy of Long-Distance and Inter-Continental Gravimeter Measurements.*
G. P. Woolard & W. E. Bonini, Trans. Am. Geophys. Un., Vol. 36, No. 4, pp. 575-583, August 1955.
The problems associated with making gravity connections over large distances with gravimeters are reviewed and discussed. Comparative data are presented as obtained using various types of gravimeters. Discrepancies in results are discussed in terms of their probable sources. (Author's Abstract).

402. *The Geological Results of Measurements of Gravity in East Carmarthenshire.*
J. T. Whetton, J. O. Meyers & I. J. Watson, Geofis. Pura e Appl., Vol. 32, No. 3, pp. 43-53, Sept. 1955.

403. *Regional Geophysical Studies in the Uravan District, Colorado.*
H. R. Joesting & P. E. Byerly, A paper read at the Annual Meeting of the S.E.G. at Denver, Colorado, October 1955. (Not yet published).
Regional gravity and aeromagnetic surveys have been conducted in the Uravan district of southwest Colorado.

GRAVITY — INSTRUMENTAL

404. *Patents.* Abstracts in Geophysics, Vol. 20, No. 3, p. 688, July 1955.

U.S. 2,699,062. 11 Jan. 1955.	A sensitive control spring for a force measuring instrument.
U.S. 2,699,067. 11 Jan. 1955.	A gravimeter using a very sensitive coiled spring which is specially mounted.

405. *Gravimeters for Regional Surveys.* (In Italian).
F. Werner, Convegno Naz, Metano e Petrolio, 7mo, Taormina 1952, Atti, Vol. 1, pp. 371-5, 1952.
For regional surveys instruments of great precision with low drift constants and small temperature variations are needed. Werner considers gravimeters with metallic springs preferable to those with quartz springs, in spite of some possible effect of the geomagnetic field on magnetic springs. In the following discussion, Prof. Solaini pointed out that one important advantage of the astatic instrument is its low period of natural vibration, which eliminates the interference from microseismic disturbances.
(From Geophysical Abstracts 159, U.S. Geol. Survey).

406. *The Problem of Calibrating High-Range Geodetic-Type Gravimeters.*
G. P. Woolard, N. C. Harding & J. C. Rose, Trans. Am. Geophys. Un., Vol. 36, No. 1, pp. 12-24, Feb. 1955.
Various methods for the calibration of gravimeters are considered and discussed in terms of the potential and actual accuracy of calibration obtained. Comparative data are given for different types of gravimeters calibrated by the same method and for the same type of gravimeter calibrated by different methods. The uncertainties

in calibration are shown to be the major factor determining differences in gravimeter values reported by different investigators.

GRAVITY — INTERPRETATION

407. *An Integrator for the Calculation of Topographical Corrections.* (In French).
R. Bollo & J. Goguel, Geophysical Prospecting, Vol. 3, No. 3, pp. 228-233, Sept., 1955.

In areas of broken relief, the calculation of topographical corrections is very important. The classical method for these calculations is both lengthy and costly.

With the object of speeding up such calculations, a polar integrator has been designed. This instrument follows the contour lines of a map and plots a subsidiary graph which gives the value of the integrals in terms of the height. From this graph the correction values are obtained with a planimeter and a moment integrator. Thus the calculations are speeded up, made more exact, and also less laborious.

408. *Minimum Variance in Gravity Analysis. Part I: One-dimensional.*
W. F. Brown, Jr., Geophysics, Vol. 20, No. 4, pp. 807-828, October 1955.

To estimate a second derivative at a specified point in an area where the vertical intensity of gravity has been measured at 'n' points, one can interpolate and differentiate with a polynomial of degree $k - 1 < n - 1$. However, when experimental errors are present, the minimum variance principle says: adjust the $n - k$ arbitrary constants of the polynomial formula so as to minimise the mean square error (variance). Application of this principle gives 'best' estimation formulae of specified degree 'k'. 'Best' formulae are also given by a least-squares method, using a statistical theorem. This theorem facilitates estimation of the variance and a value for 'k'. Use of orthogonal polynomials shortens the calculations; tables of them are provided here together with tables of their derivatives. Illustrated examples of application to data with known errors are given.

409. *Minimum Variance in Gravity Analysis. Part* II: *Two-dimensional.*
W. F. Brown, Jr., Geophysics, Vol. 21, No. 1, pp. 107-141, January 1956.

The principles developed in Part I apply whether the data points are located on a line or distributed over a plane. The practical calculation problem, however, is more complicated in two dimensions than in one. There are two steps: (1) deciding what terms to keep in the polynomial approximation: (2) estimating second vertical derivatives and the like on the basis of the chosen approximation. For (1) two-dimensional orthogonal polynomials can be used: but complete tables of them would be bulky, and therefore several alternative procedures are outlined. For (2) 'best' estimation formulae can be easily derived by the minimum-variance method; but these usually involve many-digit multipliers, and therefore "near-best" coefficients, with fewer digits, are also derived. The specific problems solved here start with uncorrelated data at points of a square grid. In practice, data are taken at irregularly distributed stations: then the minimum-variance principle and orthogonalization still apply, but the calculations are more complex, and grid values computed from the station values are correlated.

(Author's Abstract).

GRAVITY — THEORY & RESEARCH

410. *Earth Tides: the Effect of Dephasing in the Analysis of Observations.* (In French).
J. Metzger, Geofis. Pura e Appl., Vol. 29, pp. 71-83, 1954.

The relative amplitude of earth tides is the ratio of the theoretical and observed variations of gravity. These values are compared hourly. The eventual dephasing of the earth tide over the generating forces is neglected. With a dephasing of one hour there is a negative error in the relative amplitude values of 11-14%, depending on whether extreme amplitudes or totality of hourly values are considered.

If dephasing has slight effect when the tidal value is high, it is possible that it introduces a noticeable relative error on the hourly readings corresponding to a low value. The computation shows nevertheless that the total result is little improved by systematic elimination of the latter.

411. *The Graphical Calculation of Total-Intensity Anomalies of Three-dimensional Bodies.*
R. G. Henderson, A paper read at the Annual Meeting of the S.E.G. at Denver, Colorado, October 1955. (Not yet published).

Calculation of the total-intensity anomaly of a three-dimensional body of arbitrary shape is greatly facilitated by the orthographic projection of a topographic map of the body on a plane normal to the inducing field. The graphical integration is then effected by means of a modified Gassmann integration process. Applications to theoretical and laboratory models establish the relative accuracy of the method. Examples are given of applications to observed anomalies over geologic structures.

MAGNETIC — GENERAL

412. *Contribution to the Structural Interpretation of the Geo-magnetic Survey Map of the German Democratic Republic.* (In German).
R. Lauterbach, Karl Marx Univ. Leipzig Wiss. Zeitschr. Math-Naturwiss. Reihe, Vol. 3, No. 3, pp. 271-279, 1953-54.

413. *A Magnetic Study of the Ardennes.* (In French).
L. Godard, Ann. Geophys., Vol. 10, No. 3, pp. 254-257, 1954.

414. *Results of Airborne Radioactive, Electromagnetic and Magnetic Surveys.*
H. Lundberg, Oil & Gas J., Vol. 53, No. 48, p. 211, April 4, 1955.
(Abstract only of paper read at the Annual Meeting of the S.E.G., New York, March 1955).

Airborne recording of the total magnetic field over very large areas greatly assists geological mapping. For detail studies the recording of the vertical component at low altitude is found to be an excellent method of outlining magnetic ore bodies and zones of mineralization, particularly in the pre-Cambrian formations.

415. *Geomagnetic Measurements in the Gulf of Mexico.*
M. Ewing & E. T. Miller, Geophysics, Vol. 20, No. 2, p. 374, April 1955.
(Abstract only of paper read at the Annual Meeting of the S.E.G., New York, March 1955).

MAGNETIC — INSTRUMENTAL

416. *A Resonance Type Magnetometer.*
N. Kumagai & N. Kawai, Kyoto Univ. Coll. Sci. Mem., Ser. B, Vol. 20, No. 4, pp. 307-309, 1953.

A sensitive astatic magnetometer has been designed to measure the natural remanent magnetic polarization of rocks and that of small single grains of rock-forming ferromagnetic material. Magnets are fixed in opposite magnetic direction on both ends of a hollow aluminium cylinder 25 cm. long and 0.2 cm. in diameter. The specimen is placed in front of the lower magnet and rotated around a vertical axis with an angular velocity whose period is equal to that of the free oscillation of the magnetometer until it acquires a resonance oscillation. In the resonance state the phase angle of the magnetometer oscillation is retarded $\pi/2$ from that of the rotation of the magnetic dipole of the specimen, and it is thus possible to find the direction of the horizontal projection of the dipole vector with respect to the co-ordinate axes fixed to the specimen. The magnitude of the polarization can be obtained by comparison of the observed amplitude of the resonance oscillation of the magnetometer with the amplitude caused by a standard sample of known

polarization. Polarizations as small as 10^{-8}cgs/cc. can be determined with a 5 cm. cube placed 10 cm. from the lower magnet. The smallest grain of natural magnetite measurable is 300 μ in diameter.
(From Geophysical Abstracts 160, U.S. Geol. Survey).

MAGNETIC — INTERPRETATION

417. *The Sudbury Aeromagnetic Map as a Test of Interpretation Methods.*
I. Zietz & R. G. Henderson, Geophysics, Vol. 20, No. 2, pp. 307-317, April 1955.

The method of interpretation of aeromagnetic maps described by Vacquier, Steenland, Henderson and Zietz (1951) is applied to several anomalies on the aeromagnetic map of part of Sudbury, Ontario. The resulting average computed depths deviate from the known depths by less than 10 %. The aeromagnetic map is described and compared with the known surface geology.

(Author's Abstract).

418. *Preliminary Report on Total-Intensity Magnetic Interpretations by Means of Model-field Studies.*
I. Ziets & R. G. Henderson, Geophysics, Vol. 20, No. 2, p. 376, April 1955.
(Abstract only of paper read at the Annual Meeting of the S.E.G., New York, March 1955).

A method is presented for interpreting total-intensity aeromagnetic anomalies of three-dimensional structures. The anomalous structure is approximated by prismatic rectangular slabs of constant thickness and varying horizontal dimensions. The magnetic field for any irregularly shaped magnetic mass may be approximated by superimposing the appropriate contoured maps and adding numerically the effects at each point. The contoured total-intensity fields of these slabs buried at different depths and for several magnetic inclinations will be published later.

419. *A New Method of Interpretation of Aeromagnetic Maps: Pseudo-Gravimetric Anomalies.*
V. Baranov, Geophysics. Vol. 20, No. 2, p. 379, April, 1955.
(Abstract only of paper read at the Annual Meeting of the S.E.G., New York, March 1955.)

This paper describes a method of interpretation based on a transformation of the total magnetic intensity anomalies into more simple anomalies. The result of this transformation is the elimination of the distortion due to the obliquity of the normal magnetic field, so that the resulting anomalies will be located on the vertical of the disturbing magnetized bodies.

MAGNETIC — THEORY & RESEARCH

420. *Micromagnetics — an Aid to Geological Investigation.* (In German).
R. Lauterbach, Karl Marx Univ. Leipzig Wiss. Zeitschr. Math. Naturwiss. Reihe, Vol. 3, No. 4, pp. 224-238, 1953-54.

"Micromagnetics," as the term is used here, is a geophysical method based on the detailed mapping of small magnetic anomalies (less than 10^4 gammas in amplitude and less than 10 meters in extent). The principles and techniques, diagnostic criteria and geological and mineralogical applications are discussed. The method is applied to selected test areas in a given region, and can be used not only on direct outcrops, but also for surfaces underlying younger layers or weathered zones a few meters thick. Microanomalies are influenced by rock structure and composition; analyzed statistically they can indicate, for instance, contacts between different formations, directions of flow structure in porphyry or direction of sedimentation in young sediments. In a broad sense, the shapes of micromagnetic anomalies are "geological documents" which can lead to petrographic and geologic conclusions not obtainable by direct observation.
(From Geophysical Abstracts 160, U.S. Geol. Survey).

421. *Determination of the Magnetic Susceptibility of Rocks in the Field* (In Russian).
A. G. Kalashnikov, Akad Nauk SSSR Izv. Ser. Geofiz., No. 5, pp. 415-423, 1954.

An apparatus for determination of susceptibility in the field gives an integration value of susceptibility for a certain portion of the formation rather than for a small sample. The instrument consists of four flat, concentrically-wound coils mounted in pairs, each pair consisting of a small coil placed inside a large coil. A current passed in opposite directions in the outer coils induces magnetic fluxes of opposite directions in the inner coils so balanced that the resulting flux approximates to zero. Formulae are derived for the case when direct current flows through the coils and also for alternating current susceptibility of the rock on which one pair of coils is placed. Errors of such determinations do not exceed 5%. Description of the instrument is given as well as severall graphs characterizing its operation.

(From Geophysical Abstracts 159, U.S. Geol. Survey).

422. *Rock Magnetism — Geophysical Aspect.*
S. K. Runcorn, Advances in Physics, Vol. 4, pp. 244-291, April 1955.

Rock magnetism, reversed magnetization, and polar wandering are discussed. Rock magnetism is considered a means of extending the knowledge of physical properties of the earth through geological time.

ELECTRICAL

423. *Instrumentation for a New Electromagnetic Geophysical Field Technique, as Applied in South Africa.*
G. Bellairs, Geophysics, Vol. 20, No. 1, pp. 155-162, January 1955.

The carrying out of rapid geophysical surveys by the electromagnetic method has been facilitated by the development of new apparatus, which enables the field intensity at any point to be read directly from the scale of a portable instrument.

(Author's Abstract).

424. *Apparent Resistivity for Dipping Beds.*
K. Maeda, Geophysics, Vol. 20, No. 1, pp. 123-139, January 1955.

The potential field of a point source of electric current, located on the surface of the earth above a dipping bed, is determined exactly by solving the appropriate differential equation. It is concluded that image theory is useful only in the two cases in which the reflection coefficient is plus one and the angle of dip is π/m and in which the reflection coefficient is minus one and the dip angle is $\pi/2\,m$, m being an integer. Computing methods are also developed for the cases in which the image theory is not applicable. Some numerical tables necessary for computation and several apparent resistivity curves are presented.

(Author's Abstract).

425. *Apparent Resistivity for Dipping Beds — A Discussion.*
R. G. Van Nostrand & K. L. Cook, Geophysics, Vol. 20, No. 1, pp. 140-147, January 1955.

This is a discussion of the paper by Maeda. The problem of interpretation of resistivity data over dipping beds has been attacked by two groups; the "image school" and the "harmonic school". The latter workers have been more successful recently. This discussion appraises the relative merits of various prior solutions to the dipping bed problem in the light of the exact solution to the problem, which is given by Maeda.

426. *Patents.* Abstracts in Geophysics, Vol. 20, No. 1, p. 163, January 1955.
U.S. 2,684,468. 20 July 1954. Apparatus for measuring a periodically recurring signal in the presence of random noise.

U.S. 2,685,058.	27 July 1954.	An electrical prospecting system using commutated rectangular pulses passed between electrodes.
U.S. 2,690,537.	28 Sept. 1954.	An electrical prospecting system using a-c of two frequencies and its modulation-frequency signal.
U.S. 2,683,563.	13 July 1954.	A method of operating potentiometric models.

427. *Electrical Resistivity Studies in the Kansas River Valley.*
D. F. Merriam, Kansas Geol. Surv. Bull. 109, Pt. 7, pp. 97-112, 1954.

428. *Geophysical Case History of a Commercial Gravel Deposit.*
R. P. Jacobson, Mining Engineering, Vol. 7, No. 2, pp. 158-161, 1955.

429. *Prospecting for Water in Karst and the Use of Applied Geophysics* (In Jugoslav).
Z. Zagorac, Geol. Vjesnik, Sv. 5-7, God 1951-53, pp. 201-216, 1954.

430. *Geoelectric Exploration for Water in Karst on Islands.* (In Jugoslav).
J. Sedlar, Geol. Vjesnik, Sv. 5-7, God 1951-53, pp. 217-224, 1954.

431. *Resistivity Methods Applied to Some Ground Water Studies.*
H. C. Spicer, Geophysics, Vol. 19, No. 3, p. 632, July 1954.
(Abstract only of paper read at the Annual Meeting of the S.E.G., St. Louis, April 1954).

Electrical resistivity studies in two different areas and some problems related to ground-water geophysics are described. Measurements taken near Marshfield, Wisconsin, indicated the presence of an aquifer that was later drilled and found to produce more than 200 gals. of water per min. Measurements taken near Columbus, Ohio, successfully traced the course of the preglacial buried channel of the Teays River.

432. *The Limitations of Resistivity Methods of Geophysical Prospecting in Mining Exploration.*
J. E. Blanchard, Geophysics, Vol. 20, No. 2, p. 376, April 1955.
(Abstract only of paper read at the Annual Meeting of the S.E.G., New York, March 1955).

Resistivity methods are limited by many factors. In order to determine these quantitatively it is helpful to assume ideal conditions of homogeneous overburden, country rock and ore. With these restrictions approximate expressions are given for calculating the anomalous field to be expected from spherical and cylindrical shaped ore bodies in rock beneath a layer of overburden. Various electrode configurations are discussed. Numerical values are given for several situations of practical importance.

433. *The Ore Contact Method of Electrical Exploration.*
J. E. Blanchard, Geophysics, Vol. 19, No. 3, p. 636, July 1954.
(Abstract only of paper read at the Annual Meeting of the S.E.G., St. Louis, April 1954).

A new method has been developed for determining the size and shape of ore bodies which have a lower resistivity than the surrounding country rock and which have been intersected by a diamond drill hole or underground working. A large number of boundary value problems approximating different shaped ore bodies have been worked out for the electrode configurations used. The quality of the interpretation is limited by the number of measurements which field conditions permit. However, even where only a few measurements can be made the order of magnitude of size can be determined.

434. *Electrical Prospecting at Kasuga Gold Mine, Kagoshima Prefecture.* (In Japanese with English summary).
J. Suyama & H. Kobayashi, Geol. Surv. Japan Bull., Vol. 4, No. 12, pp. 35-46, 1953.

435. *Electrical Prospecting at the Oguchi Gold Mine, Kagoshima Prefecture.* (In Japanese with English summary).
J. Suyama, Geol. Surv. Japan Bull., Vol. 4, No. 11, pp. 35-40, 1953.

436. *Geophysical Prospecting at Noda-Tamagawa Mine, Iwate Prefecture.* (In Japanese with English summary).
K. Shibato, Geol. Surv. Japan Bull., Vol. 4, No. 12, pp. 17-34, 1953.

437. *Electrical Prospectings on Sulphur Deposit at the Matsuo-Hachimantai District, Iwate Prefecture.* (In Japanese with English summary).
K. Shibato, Geol. Surv. Japan Bull., Vol. 5, No. 1, pp. 41-48, 1954.

438. *Results of Airborne Radioactive, Electromagnetic and Magnetic Surveys.*
H. Lundberg, Oil & Gas J., Vol. 53, No. 48, p. 211, April 4, 1955.
(Abstract only of paper read at the Annual Meeting of the S.E.G., New York, March 1955).

In sedimentary regions airborne electromagnetic surveys may reveal underlying structures down to 1,000 or 2,000 ft. by recording the effects of secondary fields created in good conducting layers by a transmitter in the plane. In order to outline deposits of conductive bodies of mineralization, current is supplied to the ground by means of very long cables with enough effect to directly outline the conducting bodies at depth from airborne recordings.

439. *A New Electromagnetic Field Technique.*
J. F. Enslin, Geophysics, Vol. 20, No. 2, pp. 318-334, April 1955.

A technique has been developed for accurate location of narrow vertical or inclined structures such as joints, fault planes, mineralized fissures and weathered dykes.

An alternating current of audio-frequency is introduced conductively into the ground at a centre-point. Relative or absolute measurements of the tangential component of the resultant horizontal electromagnetic field are made at stations on concentric circles around the centre-point. Curves of the amplitudes, in decibels, are plotted as ordinates against the station positions. These are called the H_T curves. The locations of peaks occurring vertically above current concentrations in narrow conducting zones are plotted on a map of the area and corresponding peaks are easily joined up to delineate such structures.

Phase measurements have proved to be of minor importance for the location of geologic structures.

(Author's Abstract).

440. *Electrical Methods of Oil Exploration.* (In French).
M. Migaux, Proceedings of the 4th World Petroleum Congress, Section I, p. 545, June 1955.

This paper aims at making more widely known the frequently ignored possiblities of applying electric methods to oil prospecting. After briefly recalling the peculiar characteristics which distinguish these methods from the traditional ones such as gravimetric and seismic, the paper furnishes a series of practical examples taken from prospecting carried out under varying conditions, and compared with the results of borings and other methods. It is shown that electric methods may be considered a fully efficient instrument which has already been of service in oil prospecting and deserves to be adopted more widely.

441. *Possibilities and Limitations in Applying Geoelectrical Methods to Hydrogeological Problems in the Coastal Areas of North West Germany.*

H. Flathe, Geophysical Prospecting, Vol. 3, No. 2, pp. 95-110, June 1955.

Results of geoelectrical investigations in East Frisia are presented to show how geoelectrics helps in finding water, or in enlarging existing water works, in coastal areas. Most important is the search for permeable beds, their delimitation and location of suitable well sites. Difficulties are presented by clays forming impervious layers which split the permeable beds into sections. Further difficulties arise from the occurrence of brine-bearing deposits near the coast and salt water rising from the deep salt domes. Examples from the Rheiderland illustrate these problems. Two of the most important problems are:

(a) The physical interpretation of the measurements with special regard to the principle of equivalence:

(b) The correlation of the physical data with the subsurface geology.

442. *Mutual Electromagnetic Coupling of Loops over a Homogeneous Ground.*

J. R. Wait, Geophysics, Vol. 20, No. 3, pp. 630-667, July 1955.

Computations are presented for the mutual impedance between small wire loops situated on or over a semi-infinite conductor. The results have application to electromagnetic methods of geophysical exploration.

(Author's Abstract).

443. *Electromagnetic Induction in a Two-layer Earth.*

B. K. Bhattacharyya, J. Geophys. Res., Vol. 60, No. 3, pp. 279-288, Sept. 1955.

The problem of determining the induced field components outside a horizontal two-layer earth has been tackled from the theoretical point of view. The expressions obtained have been applied to evaluate the induced magnetic field due to an oscillating magnetic dipole on the surface of the earth. Two separate cases have been considered, for example, (i) two layers of nearly equal conductivities, and (ii) a conducting layer over an insulating medium, and the formulae have been reduced to a form amenable to numerical integration.

(Author's Abstract).

444. *A Practical Method of Calculating Geoelectrical Model Graphs for Horizontally Stratified Media.*

H. Flathe, Geophysical Prospecting, Vol. 3, No. 3, pp. 268-294, Sept. 1955.

For the quantitative interpretation of field resistivity curves it is necessary to possess theoretically calculated standard graphs. The problem of calculating such graphs for certain parallel stratified media has been solved long ago. The methods developed so far, however, require facilities which are not normally available to the geophysicist in the field. It has been shown by experience, that the catalogues of graphs, which have been made available for practical use, are inadequate, when the number of layers exceeds three. For this reason endeavours are made to find a method, to allow the geophysicist to calculate model graphs suited to any given special geological situation, with ordinary field facilities and without too great an expenditure of time. The principle of equivalence implies that such a model graph be known with a high accuracy.

To this end, a method for the calculation of model graphs for a series of parallel beds is described. The importance of this method in practice is demonstrated with the help of examples.

445. *Resistivity Curves for a Conducting Layer of Finite Thickness Embedded in an Otherwise Homogeneous and Less Conducting Earth.*
O. Koefoed, Geophysical Prospecting, Vol. 3, No. 3, pp. 258-267, Sept. 1955.
A method is described for computing master resistivity curves. It is a modification of that devised by Ehrenburg and Watson, but is superior as a shorter time is required for the computations. A collection of 31 master curves for the three layer case is presented.
(Author's Abstract).

GEOCHEMICAL

446. *Water Study as Exploration Aid.*
G. V. Chilingar, Petroleum Engineer, Vol. 27, No. 4, pp. B-119-B-121, April 1955.
A study of spring waters in the Tartar republic of the U.S.S.R. has shown that a low Ca/Mg ratio may characterize a formation with abundant anaerobatic bacteria and high hydrocarbon content.

447. *Hydrochemical Studies in Oil Exploration.* (In Russian).
K. Szypula, Nafta (Krakow), Vol. 10, pp. 56-8 and 76-8, 1954.
Saline waters and H_2S have long been observed to occur with oil deposits and served thus as indicators. The reasons for this occurrence have been investigated. Many water samples have been analysed and classified by their composition and occurrence. 'Forecast Maps', based on the composition of water samples, have been prepared. These maps are compared with geological, geophysical and geochemical maps of the same area.

448. *Application of the Gauss Theory of Error in Probability Calculation for Interpretation of Geochemical investigations.* (In Polish).
J. Strzetelski, Bull. Polish Inst. Petrol., Vol. 4, pp. 3-4, 1954.
Technical improvements will not eliminate anomalous results and personal errors. Each result contains therefore a ± x' (true value ± error). Gauss' statistical analysis allows the correct interpretation of these results.
(From J. Inst. Petrol. Abstracts, July 1955).

449. *Patents.* Abstracts in Geophysics, Vol. 21, No. 1, p. 192, January 1956.

U.S. 2,712,986.	12 July 1955.	A method of analysing soil samples for concentration of paraffin hydrocarbons.
U.S. 2,715,450.	16 Aug. 1955.	Apparatus for detecting small quantities of gas in drilling mud.

450. *Geophysical-Geochemical Prospecting for Uranium.*
M. E. Denson, A paper read at the Annual Meeting of the S.E.G. at Denver, Colorado, October 1955. (Not yet published).
Physical and chemical properties of sedimentary rocks associated with uranium deposits have variations which indicate applicability of geophysical and geochemical exploration methods. Some of the variations in the properties can be attributed to geologic factors and phenomena connected with deposition of ore. Correlations between chemical and physical properties are used as a guide for sequencing of field techniques.

Geophysical field data are supplemented by geochemical data on trace quantities of uranium, thorium and potassium. These data are augmented by other chemical information on soils, waters and gases to serve as a guide for evaluation of prospective areas. Examples of such field data, including shallow seismic reflection, surface and in-hole resistivity, surface radiometric and geochemical, from areas in South Dakota, Wyoming and Colorado are presented to show the types of detectable physical and chemical variations found to be significant.

RADIOACTIVE

451. *Aerial Prospecting for Radioactive Materials.*
E. A. Godby, S. H. G. Connock, J. F. Steljes, G. Cowper & H. Carmichael.
Atomic Energy Canada Report No. 13, March 13, 1952.

Tests have been carried out over known radium-ore and pitchblende deposits in N. Saskatchewan and the N. W. Territories, using airborne ion chambers, Geiger-Muller counters and scintillation counters. The latter attained an optimum survey height of 550 feet compared with 200 feet for the G-M counter. It is concluded that a scintillation detector system is capable of economic and successful prospecting from the air.

452. *Patents.* Abstracts in Geophysics, Vol. 20, No. 3, p. 688-9, July 1955.

U.S. 2,699,513.	11 Jan. 1955.	A gamma-ray detector.
U.S. 2,700,108.	18 Jan. 1955.	A gamma-ray meter.
U.S. 2,700,110.	18 Jan. 1955.	A gamma-ray meter.
U.S. 2,701,175.	1 Feb. 1955.	A method of treating a gamma-ray detector to reduce its background counts.

453. *Airborne Scintillometer Surveys for Oil.*
J. C. Whitaker, Geophysics, Vol. 20, No. 3, p. 717, July 1955.
(Abstract only of paper read at the 10th Annual Gulf Coast Meeting of the S.E.G. at San Antonio, Texas, May 1955).

The instrumentation and flying technique with an hypothesis to explain the observed facts. This involves a discussion of (1) the radioactivity of marine sediments, (2) Their solution at depth, and the near-surface precipitation of radioactive materials, (3) The evidence (chemical, electrical and geological) bearing on vertical migration and the migration and accumulation of oil.

454. *A Mechanism to Account for Radiometric Anomalies in the Soil over Oilfields.*
R. M. Tripp, Geophysics, Vol. 20, No. 3, p. 717, July 1955.
(Abstract only of paper read at the 10th Annual Gulf Coast meeting of the S.E.G. at San Antonio, Texas, May 1955).

This paper attempts to account for the radioactivity-halo phenomenon that has been observed in the soil above petroleum accumulations. Briefly, migrating gases cause increased surface evaporation and geochemical changes occur, including the precipitation of gamma-emitting elements.

455. *How to Avoid Costly Errors in Gamma Ray Surveying.*
J. W. Merritt, World Oil, Vol. 141, No. 2, pp. 84-90, August 1, 1955.

The author summarises his experience in field surveying using radiation equipment.

The merits of the new crystal probe scintillometers and the older ionization chamber counters are compared and the proper techniques for sampling discussed. Different types of natural and artificial contamination are listed and the principles of interpretation set down.

456. *Multiple-Purpose Scintillation Counter.*

Petroleum, Vol. 18, No. 10, p. 380, October 1955.

A very brief description, with photograph, of the 'Super Fission Finder', a scintillation counter specifically designed for locating uranium ore and assisting in the detection of stratigraphic oil traps.

The instrument is suitable for use in the air, in a vehicle, on foot, or for radioactivity logging of drill holes.

OTHER METHODS

457. *Geophysical Prospection of Underground Water in the Desert by Means of Electromagnetic Interference Fringes.*

M. A. H. El-Said, Proc. I.R.E., Vol. 44, No. 1, pp. 24-30, January 1956.

Principles and techniques of prospecting for underground water in the desert, using electromagnetic interference fringes, are described.

Two methods, (1) the "Variable Frequency Interference Method" and (2) the "Variable Distance Interference Method" are formulated. Interference patterns from two desert locations are shown; the water table at one of these places is known from boring.

Interpretation of the interference patterns and calculation of the water table requires a knowledge of the average dielectric constant of the propagating medium together with a single interference pattern determined by method (1) or (2). Derived results and the known water table were in good agreement.

3 8198 313 763 904
THE UNIVERSITY OF ILLINOIS AT CHICAGO